The Dissertation Committee for Andrew Robert Waldeck Certifies that this is the approved version of the following dissertation:

Development and Application of Metal Catalyzed Transfer Hydrogenative C-C Bond Forming Reactions

Committee:

Michael J. Krische, Supervisor

Stephen F. Martin

Guangbin Dong

Jennifer S. Brodbelt

Sean M. Kerwin

Development and Application of Metal Catalyzed Transfer Hydrogenative C-C Bond Forming Reactions

by

Andrew Robert Waldeck, B.S.; B.S.

Dissertation

Presented to the Faculty of the Graduate School of

The University of Texas at Austin

in Partial Fulfillment

of the Requirements

for the Degree of

Doctor of Philosophy

The University of Texas at Austin

May 2016

Dedication

To my parents and to Erin:

Without your love and support, none of this would have been possible.

Acknowledgements

The work described in this document would not have been possible without the mentorship of Professor Krische and the collaboration of a number of talented individuals. Felix, Emma, Jeff, Anne-Marie, and Abbas: Working with each of you has made me a better chemist. Thank you for all of the help and guidance each of you has provided in the context of the projects on which we worked together. Thank you to rest of the Krische group for your insightful conversations. Victoria, Zach, and Stephen: Thank you for your help reviewing and editing this document and thank you for being a source of many laughs during my time here. John Ketcham: Thank you for your advice and insight regarding all things chemistry, but thank you especially for being a friend.

To Erin: Thank you for sharing in this adventure with me. Your love, support, and patience have carried me through challenging times. Thank you for always being there for me and for helping to make me a better person. You are my best friend and I love you.

To Matt and Laura: Your friendship has meant the world to me. You have always been a source of so much light, and without you two I would be lost. You have taught me so much about who I am and what it means to be happy. Thank you for your camaraderie and positivity. I love you both.

To my Dad: Your love, support, encouragement, and positive attitude have helped me through many hardships and without you I certainly would not be where I am today. You help ground me when I am overwhelmed and talking with you always brightens my day. Thank you for being a source of strength and comfort throughout my time here. I love you, Dad.

To my Mom: You inspire me to keep trying and to keep being better. You are the reason I have done so many great things and without you I would not be the person I am today. Thank you for teaching me, for guiding me, and for being the one in whom I could always confide. To lose you during the course of my graduate studies was incredibly difficult, but I know that you would be proud of me. I wish you could have seen me graduate. I love you and I miss you every day. This is for you most of all.

Development and Application of Metal Catalyzed Transfer Hydrogenative C-C Bond Forming Reactions

Andrew Robert Waldeck, Ph.D.

The University of Texas at Austin, 2016

Supervisor: Michael J. Krische

While polyketides display a diverse range of biological properties and are used extensively in human medicine, a lack of methods for the concise preparation of these complex structures still poses a significant challenge in the field of synthetic organic chemistry. To address this issue, metal catalyzed methods for transfer hydrogenative C-C bond formation have been developed. These methods construct products of carbonyl addition through direct C-H bond functionalization, which provides a more atom economic and efficient approach to carbonyl addition products and circumvents the need for stoichiometric use of chiral auxiliaries, premetallated *C*-nucleophiles, and discrete alcohol-to-carbonyl redox reactions. Efforts have been focused on the development of ruthenium-catalyzed coupling reactions of secondary alcohols to basic chemical feedstocks as well as the application of iridum-catalyzed couplings of primary alcohols with π-unsaturates in the context of the total syntheses of (–)-cyanolide A and (+)-cryptocaryol A. These total syntheses represent the most concise route reported to date for each natural product and illustrate the synthetic utility of transfer hydrogenative C-C bond forming methodology.

Table of Contents

List of Tables

List of Figures

List of Schemes

Chapter 1: Application of Two-Directional Allylation and Crotylation to the Total Synthesis of Natural Products

1.1 Brief Overview of Asymmetric Carbonyl Allylations

1.1.1 Introduction

Organic molecules are defined as compounds primarily composed of carbon and hydrogen. As such, dynamic methods for the construction of C-C bonds are of great importance in the field of synthetic organic chemistry. Carbonyl addition is one such method and encompasses a broad field of reactions that utilize the inherent electron deficient nature of the carbonyl carbon in conjunction with an electron rich *C*-nucleophile to forge a new C-C bond. Over the past century, a myriad of valuable methods for the construction of C-C bonds via carbonyl addition have been developed and applied in the context of total synthesis. While natural products are of considerable importance due to the extent to which they exhibit pharmacological or biological activity, synthesis of these structurally complex compounds is often quite challenging.

Polyketide natural products are a class of secondary metabolites produced by certain living organisms and are often composed of repeated polyacetetate or polypropionate substructures. As such, carbonyl addition chemistry has played an important role in the synthesis of polyketide natural products. The evolution of methods available for the construction of C-C bonds via carbonyl addition has facilitated the synthesis of polyketide natural products. Enantioselective carbonyl allylation ranks among the foremost methods used for the construction of chiral polyketide natural products. These methods typically transform aldehydes or ketones into chiral, homoallylic alcohols, which serve as useful synthetic building blocks as they contain C-O bond functionality as well as a pendant olefin. These functional groups can serve as synthetic handles for further synthetic manipulations.

Due to the significance of chirality in the context of biology, biochemistry, and pharmacology as well as the abundant representation of chirality in natural products, methods

that facilitate introduction of chirality into otherwise achiral molecules are of great importance. Over the past half-century, the development and application of asymmetric methods for carbonyl allylation has been extensive. These advancements can be differentiated by the strategy for chirality induction and includes stoichiometric, Lewis acid- or base-catalyzed, and Bronsted acid-catalyzed chirality transfer. The following chapter should serve as a brief overview of methods for enantioselective carbonyl allylation and crotylation as well as the application of two-directional variants to the total synthesis of complex natural products.

1.1.2 Enantioselective Allylation via Stoichiometric Chirality Transfer

The majority of methods for carbonyl allylation rely on the use of a preformed allyl metal reagent. Early examples of such reactions employed allyl boron reagents and allyl silanes.[1] While these methods were useful for the construction of homoallylic alcohols, conditions that would install the allyl moiety with high levels of stereoselectivity were more desirable. In 1978, Hoffmann and coworkers published the first method for the enantioselective allylation of simple aldehydes.[2] Stereoselectivity was induced through use of chirally modified allyl boronic ester **1.1** derived from camphor (Figure 1.1). Inspired by this initial success, increasingly effective methods for asymmetric carbonyl allylation using chirally modified allyl metal reagents were developed.

Figure 1.1 Methods for stoichiometric chirality transfer in carbonyl allylation reactions.

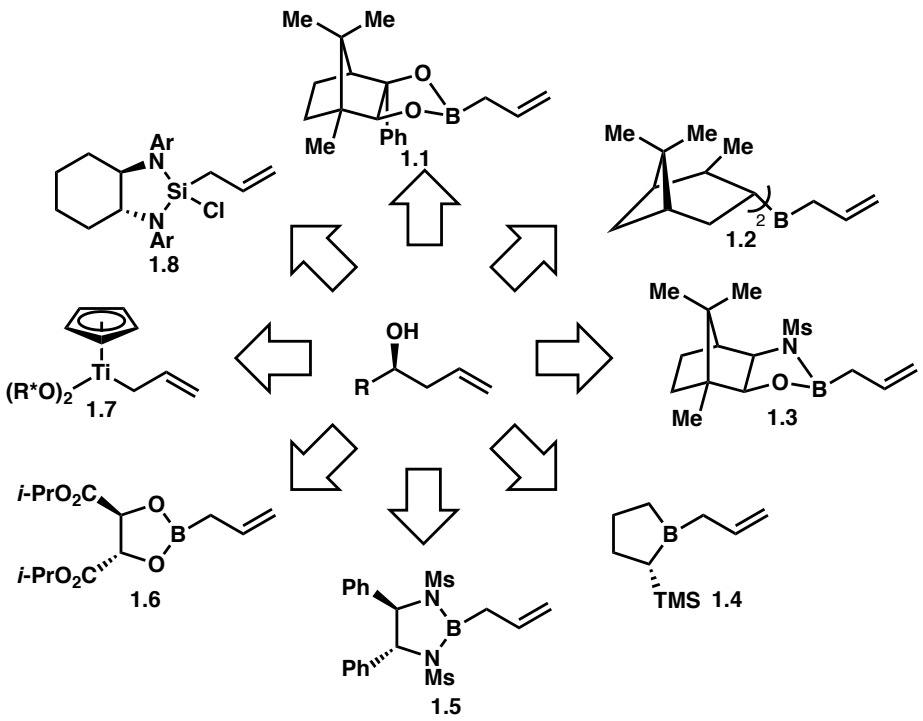

In 1983, Brown and coworkers found that allyldialkyborane **1.2** derived from (α)-pinene could be employed in carbonyl addition reactions to give products of allylation with remarkable levels of stereoselectivity.[3] Similarly high levels of stereoinduction were observed by Reetz and coworkers using their camphor-derived chiral auxiliary **1.3** in the allylation of aldehydes.[4] Interestingly, Masamune and coworkers found that the much less sterically encumbered borolane **1.4** engaged in enantioselective allylation reactions.[5] Corey and coworkers designed allylborane **1.5** that is modified with readily available chiral 1,2-diamino-1,2-diphenylethylene and observed enantioselective allylation upon exposure to aldehydes.[6] Roush and coworkers design allylboronic ester **1.6** derived from tartaric acid to effect allylation with high levels of selectivity.[7]

In a departure from using organoboron complexes, Duthaler and coworkers developed allyldialkoxytitanium **1.7** and found it to be a successful reagent for enantioselective allylation.[8] More than two decades after Hoffmann's first report, Leighton and coworkers synthesized

strained allylsilacycle **1.8** in an effort to develop a stable reagent that could be stored and used directly under mild conditions.[9]

A stereochemical model for the Brown allylation is presented in Figure 1.2. Coordination of the aldehyde to boron occurs in such a way as to keep the substituent attached to the aldehyde in a pseudo-equatorial position and the aldehydic hydrogen in the pseudo-axial position. This minimizes the steric 1,3-diaxial interactions between the pseudo-axial substituent and the bulky isopinocampheyl substituents on boron. The stereochemical models for selectivity in the other allylation reactions mentioned above that employ an allylboron reagent are presumably very similar.

Figure 1.2 Proposed stereochemical model for the Brown allylation.

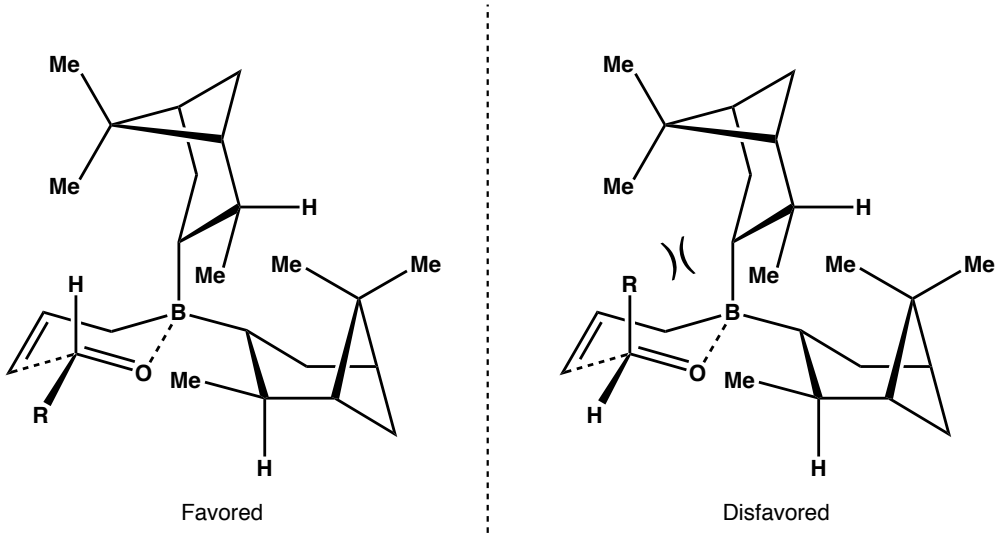

While all of the methods described above provide access to enantioenriched homoallylic alcohols, they also share a number of significant drawbacks that stem primarily from the stoichiometric use of allyl metal reagents. Generation of stoichiometric byproducts often detracts from the utility of most chirally modified allyl metal reagents due to the additional challenges and costs associated with separation and disposal of the byproducts. Additionally, multistep syntheses are required in order to obtain the reagents and, with the exception of Leighton's allylsilane, the substantial difficulty or inability to recover the chiral auxiliaries poses a

significant barrier to their use. For these reasons, methods for the introduction of chirality in a catalytic manner are valuable and much work has been done in developing catalytic methods for carbonyl allylation that exhibit high levels of reactivity and stereoselectivity.

1.1.3 Lewis Acid-Catalyzed Methods for Chirality Transfer

In 1991, Yamamoto and coworkers reported the first catalytic asymmetric carbonyl allylation reaction.[10] The catalyst employed was chiral (acyloxy)borane **1.9** derived from tartaric acid. Exposure of benzaldehyde and allyltrimethylsilane to catalytic **1.9** (20 mol%) afforded the corresponding homoallylic alcohol in modest yield and enantioselectivity (Scheme 1.1). Interestingly, higher levels of stereoinduction were observed in the case of 2-substituted allyltrimethylsilanes.

Scheme 1.1 The first catalytic enantioselective carbonyl allylation reaction.

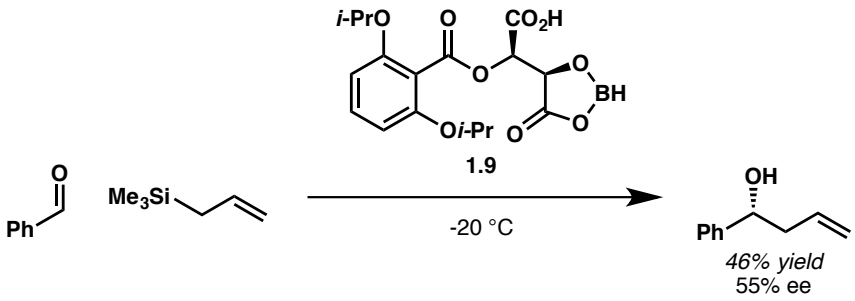

In 1993, Umani-Ronchi and Keck independently developed the first highly enantioselective catalytic method for carbonyl allylation.[11] Their method employed allyltributylstannane as the allyl donor and titanium(IV) catalyst **1.10** modified with a chiral BINOL ligand (Figure 1.3). While the mechanism is not fully understood, one plausible mechanistic pathway involves activation of the aldehyde with the catalyst to give intermediate **A**, which undergoes nucleophilic addition by allyltributylstannane to produce cationic species **B**. The cation is presumably stabilized through hyperconjugation with the adjacent C-Sn bond. Chloride attack on the Sn atom forms titanium alkoxide **C**, which likely undergoes transmetallation to afford tin alkoxide **D**, which releases the titanium catalyst. Hydrolysis of tin alkoxide would furnish the homoallylic alcohol product.

Figure 1.3 Proposed catalytic cycle for the titanium-catalyzed allylation of aldehydes with allylstannanes.

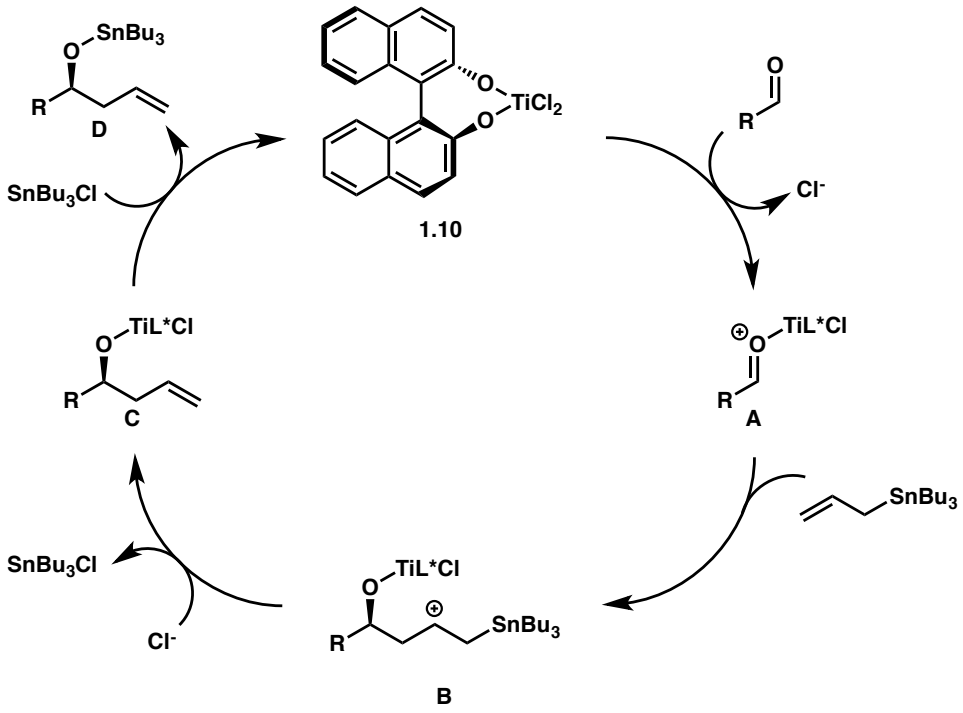

Lewis basic compounds have also been found to catalyze carbonyl allylation reactions with high levels of enantioselectivity. In 1994, Denmark and coworkers published a report detailing the development of chiral Lewis basic catalyst **1.11** capable of facilitating enantioselective carbonyl allylation using allyltrichlorosilane as the allyl donor (top, Figure 1.4).[12] It was proposed that these reactions proceed via a closed six-centered silconate transition state, which enhances the enantioselectivity. The nature of the silicon atom in the transition state could be either a cationic trigonal bypyamidal structure is which only one Lewis basic phosphoramide is bound to the silicon center (bottom left, Figure 1.4), or a cationic octahedral complex in which two phosphoramides are attached to the silicon center (bottom right, Figure 1.4).

Figure 1.4 Lewis basic catalyst **1.11** and two proposed transition states for the allylation of aldehydes with allyltrichlorosilane.

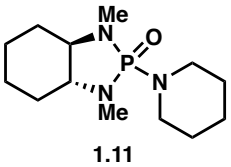

1.11

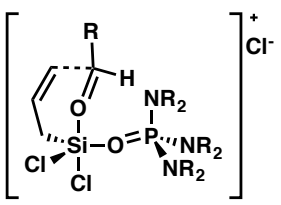

cationic
trigonal bypyramidal

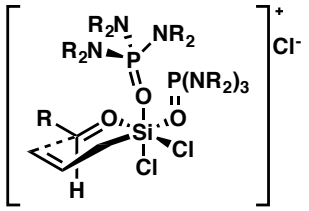

cationic
octahedral

Further development of tethered bisphosphoramide catalyst **1.12** afforded markedly higher levels of enantioselectivity and yield in the allylation of benzaldehyde (Scheme 1.2).[13] The strong cooperativity of dimeric catalyst **1.12** compared to monomeric catalyst **1.11** in conjunction with enhanced selectivity supports the hypothesis of a two-phosphoramide pathway.

Scheme 1.2 Comparison of catalysts **1.11** and **1.12** in the allylation of benzaldehyde with allyltrichlorosilane.

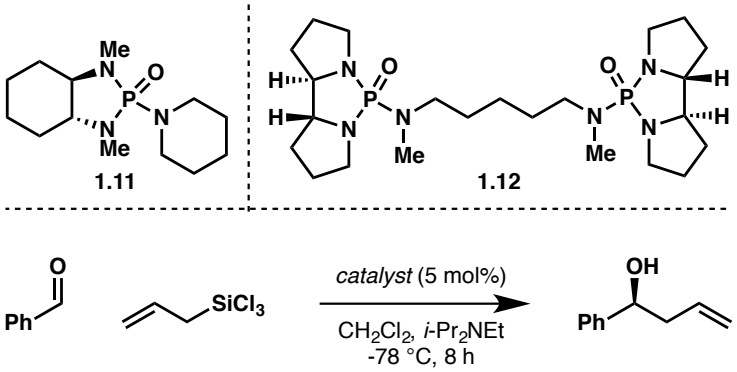

catalyst	er	% yield
1.11	78/22	56
1.12	93.5/6.5	85

While methods that employ Lewis acidic or Lewis basic catalysts in carbonyl allylation are very effective, the use of preformed allyl metal reagents is still required and can pose a

barrier to use due to the quantities of, and hazards associated with, the byproducts generated in these reactions. The allyl stannanes implemented in the Umani-Ronchi-Keck allylation generate stoichiometric quantities of tin byproducts and the trichlorosilanes used in the Denmark allylation are moisture sensitive and upon hydrolysis generate stoichiometric quantities of hydrochloric acid.

1.1.4 Brønsted Acid-Catalyzed Methods for Chirality Transfer

Chiral phosphoric acids with binaphthyl ligands have proven to be versatile and efficient catalysts that promote a number of enantioselective transformations, including C-C bond forming reactions as well as reduction and oxidation reactions.[14] In 2010, Antilla and coworkers reported the enantioselective allylation of aryl and heteroaryl aldehydes using chiral phosphoric acid catalyst **1.13** (Scheme 1.3). The allyl donor employed was allyl pinacol boronate, an inexpensive and commercially available reagent. Exceptionally high yields and enantioselectivities were observed in the coupling of allyl pinacol boronate with aryl and heteroaryl aldehydes; however, selectivity was diminished when primary or secondary aliphatic aldehydes were employed.

Scheme 1.3 Chiral phosphoric acid **1.13** and general reaction conditions for the Brønsted acid-catalyzed allylation.

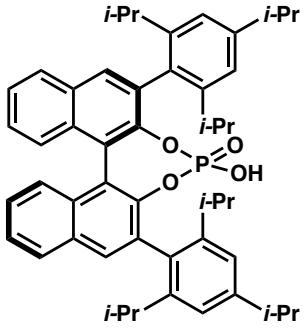

1.13

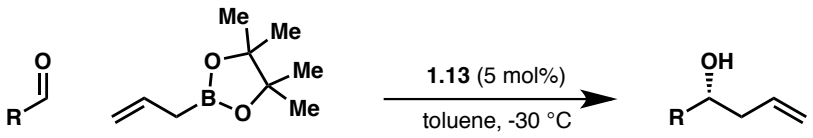

R = aryl, heteroaryl

> 90% yield
> 95% ee

A stereochemical model was proposed that invoked activation of the boronic ester via hydrogen bonding to the phosphoric acid. Computational studies performed by Goodman and coworkers indicated that in addition to activation of the boronic ester, hydrogen bonding between the phosphoryl oxygen and the aldehydic hydrogen atom.[15] This dual hydrogen bonding was proposed to both activate the boronic ester as well as enforce a more rigid transition structure, which would explain the remarkably high levels of stereoselectivity observed. The computational model for the observed stereoselectivity is shown in Figure 1.5. Transition structure **A** projects the bulky pinacol group towards an empty pocket of the catalyst; however, the aldehyde substituent projects into the bulky aromatic group of the catalyst. Transition structure **B** projects the bulky pinacol group into the bulky aromatic group of the catalyst, but the aldehyde substituent points to an empty pocket of the catalyst. Calculations show that transition structure **A** is favored over transition structure **B** by 6.7 kcal/mol when benzaldehyde is used as the model aldehyde. This indicates that the steric clash between the pinacol moiety and the aromatic group of the catalyst is significantly greater than that of the aldehyde substituent projecting into the aromatic group of the catalyst.

Figure 1.5 Comparison of two possible transition state structures in the chiral phosphoric acid-catalyzed allylation reaction.

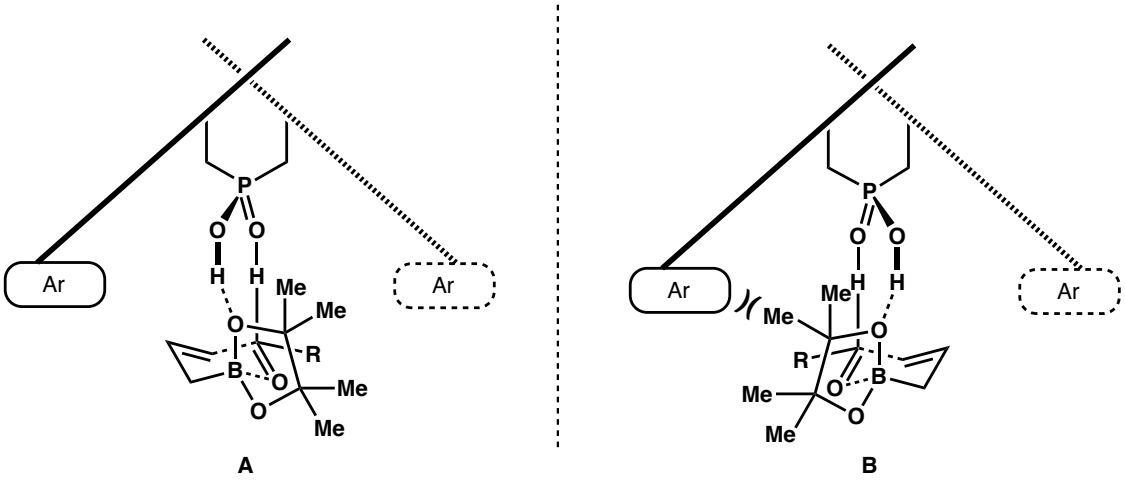

While this Brønsted acid-catalyzed carbonyl allylation is very effective, it does exhibit some major limitations. In addition to the reaction scope, which only tolerates aryl or heteroaryl

aldehydes, the reaction still employs stoichiometric quantities of the allyl metal reagent and therefore generates stoichiometric quantities of allyl metal byproducts. Challenges associated with the separation and disposal of the reaction byproducts can be significant and may preclude the use of such technology to industrial scale applications.

1.1.5 Redox-Triggered Transfer Hydrogenative Methods for Chirality Transfer

In 2008, Krische and coworkers reported an iridium-catalyzed method to construct products of carbonyl allylation employing allyl acetate as the allyl donor.[16] In this protocol, allyl acetate serves as a precursor to a transient allyl metal nucleophile, which upon carbonyl addition generates homoallylic alcohols with high levels of stereoselectivity. This nucleophilic behavior is a departure from that typically observed in allyliridium species, which most often exhibit electrophilic character and undergo addition by nucleophiles.[17]

The iridium catalyst is generated *in situ* upon mixture of $[Ir(cod)Cl]_2$, a chiral bidentate phosphine ligand, 3-nitrobenzoic acid, Cs_2CO_3, and allyl acetate and heating the mixture to 100 °C in THF. Upon addition of aldehydes and a terminal reductant, such as isopropanol, the corresponding homoallylic alcohols were obtained in typically high yields and high levels of enantioselectivity (Scheme 1.4). Both an acidic and a basic additive were found to be necessary to facilitate formation of the cyclometallated iridum catalyst **1.14** (Figure 1.8). The structural nature of an iridium complex modified with (*R*)-BINAP isolated from the reaction mixture was determined through single X-ray diffraction analysis.

Scheme 1.4 Enantioselective iridium-catalyzed transfer hydrogenative allylation.

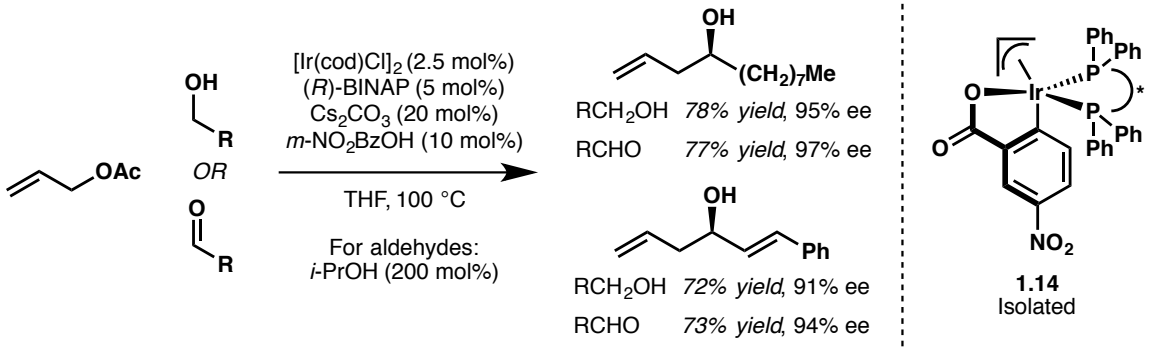

Most interestingly, it was found that primary alcohols would undergo allylation directly under the above conditions. The proposed mechanism begins with cyclometallated iridium catalyst **1.14**, which upon protonolysis of the π-allyl species affords iridium(III) alkoxide **A** (Figure 1.6). β-Hydride elimination generates iridium(III) hydride **B**, and subsequent dissociation of the newly formed aldehyde furnishes species **C**. Deprotonation of species **C** provides anionic iridium(I), which ionizes allyl acetate to regenerate catalyst **1.14**. The π-allyl haptomer of the iridium complex exists in equilibrium with the σ-allyl haptomer **E**, which possesses an open coordination site. Association of the aldehyde and coupling of the allyl fragment affords complex **F** and subsequent alcohol exchange releases the homoallylic alcohol product regenerating complex **A** and closing the catalytic cycle. The secondary alcohol products do not undergo further allylation since the pendant olefin occupies the coordination site that would be required for β-hydride elimination.

Figure 1.6 Proposed mechanism for the iridium-catalyzed allylation of primary alcohols.

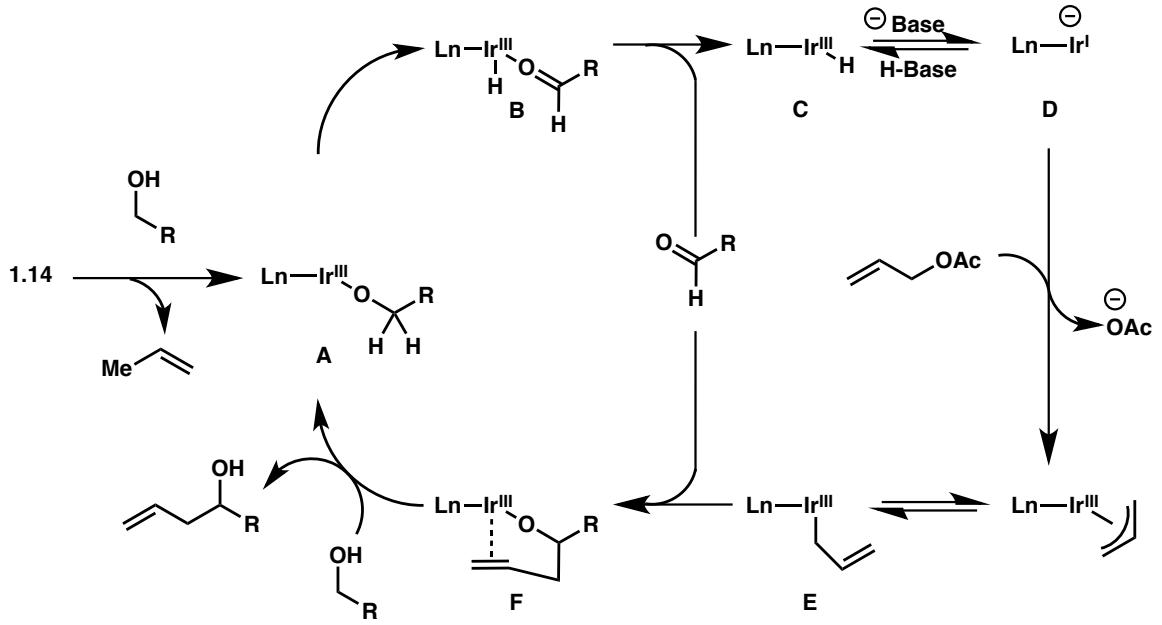

As this methodology allows for direct allylation of primary alcohols without the need for discrete alcohol-to-aldehyde oxidation, it has found use in systems in which discrete oxidation

would generate an unstable or intractable aldehyde. The scope of this methodology has recently expanded to include α-chiral alcohols, which show no loss of enantiopurity upon transfer hydrogenative allylation.[18] The ability to bypass stoichiometric pre-formation of aldehyde electrophiles enables allylation processes that cannot be performed efficiently from certain unstable aldehydes. Of particular note, 1,*n*-glycols were found to undergo two-directional allylation with high levels of enantioselectivity (Scheme 1.5). Under classical conditions for carbonyl allylation, in order to obtain product **1.15**, a 1,3-dialdehyde would need to be employed; however, these dialdehydes are often unstable and are susceptible to enolization, self-condensation, and trimerization.[19]

Scheme 1.5 Two-directional allylation of 1,*n*-glycols.

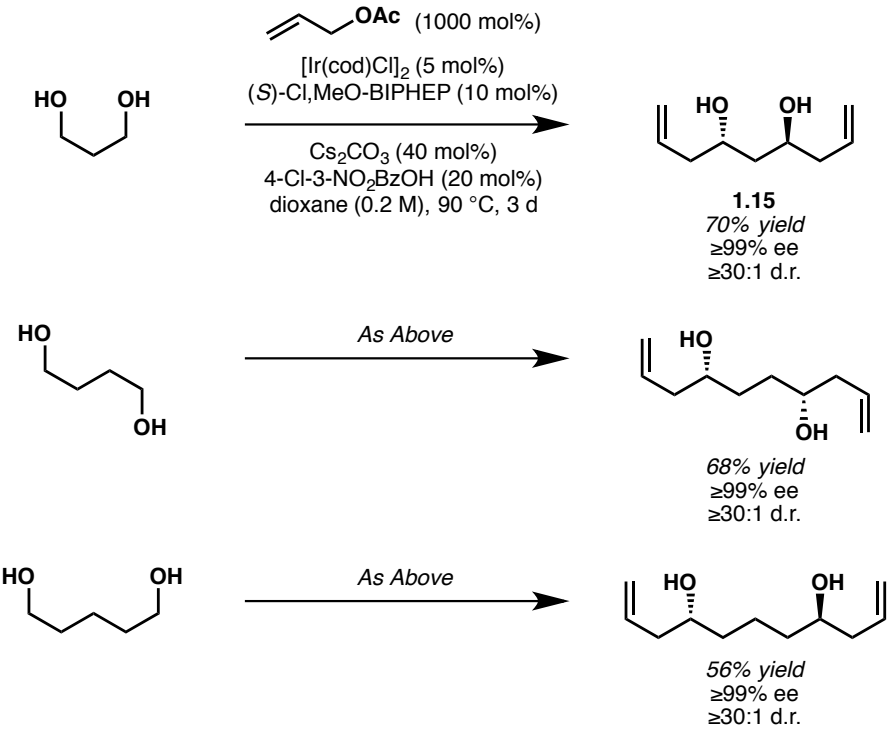

As such, synthetic routes for generating products like **1.15** are often significantly complicated and require many steps in order to bypass the 1,3-dialdehyde. One can envision two alternative routes to synthesize **1.15** via traditional methods for carbonyl allylation, the first of which is presented in Scheme 1.6. Generation of the unstable 1,3-dialdehyde is avoided by

selective monoprotection of one hydroxyl group followed by oxidation to afford the corresponding aldehyde, which upon allylation furnishes the product of monoallylation. Protection of the secondary alcohol and deprotection of the primary alcohol followed by oxidation afford another aldehyde, which upon allylation and deprotection affords **1.15**. This sequence requires eight steps to construct 2 C-C bonds and set two stereocenters.

Scheme 1.6 Theoretical route to **1.15** employing tradition carbonyl allylation methodology.

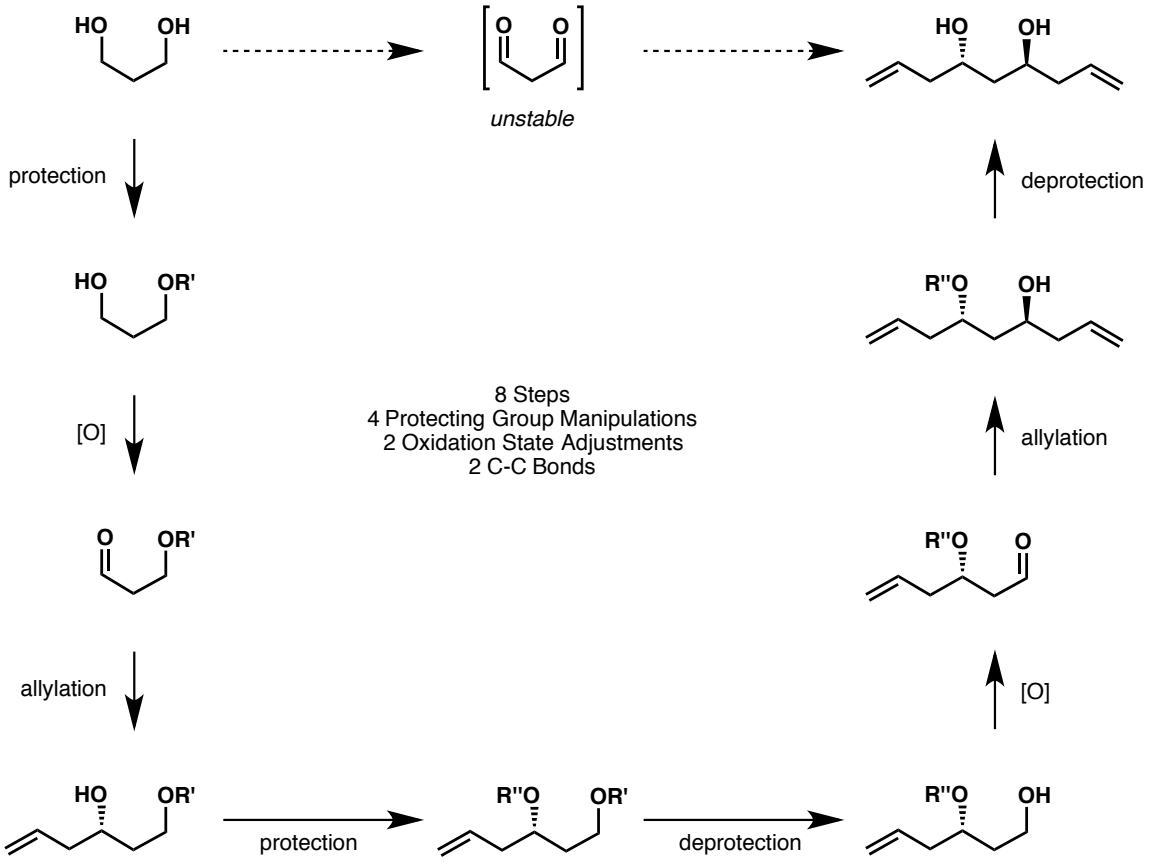

In an alternative route, **1.15** is prepared from 2,4-pentanedione (Scheme 1.7).[20] Copper-mediated bis-chlorination affords a dichloroketone, which is subjected to enantioselective ruthenium-catalyzed hydrogenation to give a diol. Deprotonation of the hydroxyl groups followed by S_N2 displacement of the adjacent chlorine atoms produces a chiral diepoxide. Epoxide ring-opening with vinyl lithium delivers **1.15** in a four step sequence. While both of the

aforementioned methods grant access to the desired 1,3-*anti* diol, both require multiple synthetic transformations.

Scheme 1.7 Alternative route to **1.15** via chiral ketone reduction, epoxidation, and ring-opening.

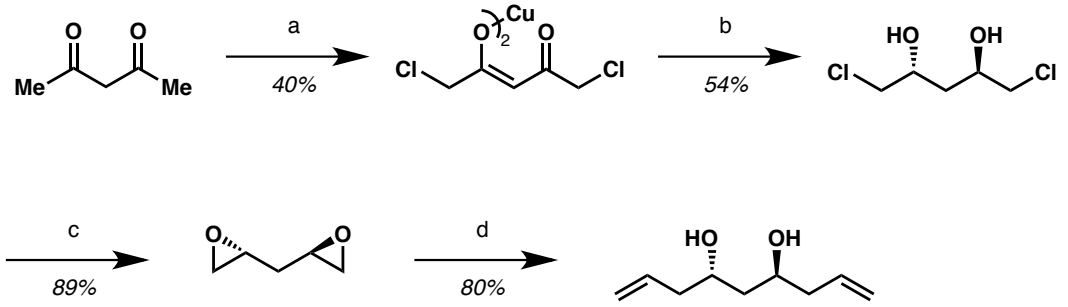

Key: (a) $AlCl_3$, $ClCH_2COCl$, 60 °C, then $Cu(OAc)_2$; (b) H_3O^+ then $[((S)\text{-BINAP})RuCl_2]_2$, Et_3N, H_2, 1200 psi, 102 °C, MeOH then recrystallize; (c) KOH, Et_2O; (d) $Ph_2CuCNLi_2$, THF, -78 to 0 °C.

1.2 Iridium-Catalyzed Two-Directional Allylation in Total Synthesis

Methods for the construction of the 1,3-*anti* diol substructure are important due to the prevalence of such motifs in polyketide natural products. Iridium-catalyzed two-directional allylation affords chiral C_2-symmetric 1,3-diols in a single transformation from inexpensive, highly tractable glycols. As such, this methodology has been applied to the total synthesis of a number of complex natural products. As a consequence of the simplicity with which the 1,3-*anti* diol substructure is assembled, each total synthesis that has implemented the iridium-catalyzed two-directional allylation represents the most concise route to that natural product to date. The following is a brief summary of the natural products constructed through application of this technology and will aim to demonstrate how the implementation of this methodology facilitated such concise syntheses.

1.2.1 Roxaticin

Roxaticin **1.16** is pentaene macrolide isolated from streptomycete X-14994, found in soil near Ecalante, Utah, USA (Figure 1.7).[21] It was found to exhibit antimicrobial activity that is selective for fungi over bacteria as is often the case with polyene macrolides. It was noted that the C14-C28 portion of the molecule is C_2-symmetric and contains six secondary alcohol

stereogenic centers. Due to this symmetry and as a means to challenge the utility of the newly developed iridum-catalyzed two-directional allylation methodolgy, roxaticin became a target of synthetic interest.

Figure 1.7 Molecular structure of the polyene macrolide roxaticin **1.16** and anticipated precursor **1.17**.

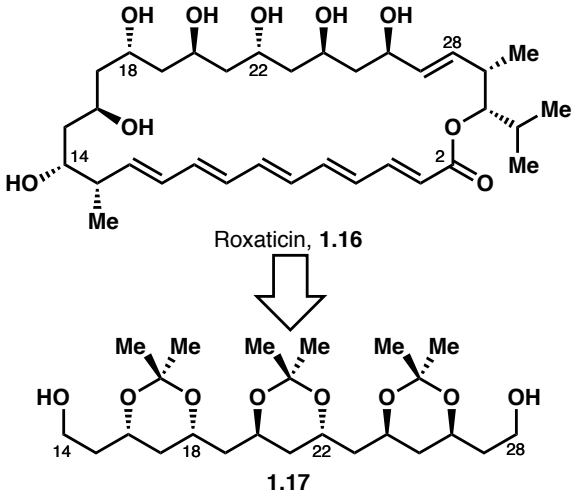

The synthesis began with the first of what would be three separate two-directional allylations (Scheme 1.8). Exposure of 1,3-propanediol to allyl acetate in the presence of $[Ir(cod)Cl]_2$, (*R*)-Cl,MeO-BIPHEP, 4-chloro-3-nitrobenzoic acid, and Cs_2CO_3 in dioxane furnished chiral C_2-symmetric diol **1.18**. Protection of the 1,3-*anti* diol as the 2,2-dimethyl acetal was achieved with PPTS and $(MeO)_2CMe_2$ in CH_2Cl_2, and subsequent oxidative cleavage of the terminal olefins reduction with $NaBH_4$ afforded **1.20**. A second two-directional allylation was accomplished using catalyst **1.19** in the presence of allyl acetate. Protection of the resulting diol as the corresponding TBS ethers followed by oxidative cleavage of the terminal olefins and reduction with $NaBH_4$ provided another primary diol. A third two-directional allylation, acetal protection, and oxidative cleavage and reduction produced **1.17**.

Scheme 1.8 Synthesis of the C14-C28 domain of roxaticin **1.16** using an iterative iridium-catalyzed two-directional allylation approach.

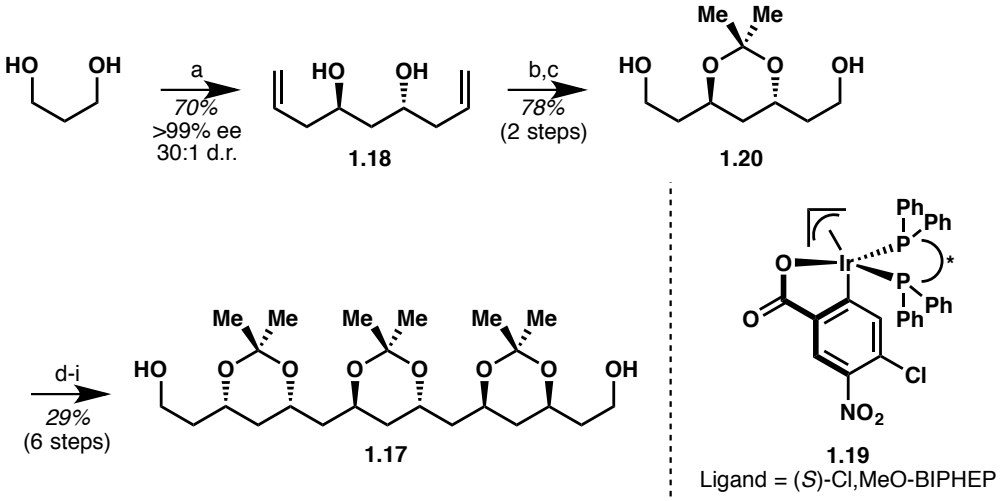

Key: (a) allyl acetate, $[Ir(cod)Cl]_2$, (*R*)-Cl,MeO-BIPHEP, Cs_2CO_3, 4-Cl-3-NO_2BzOH, dioxane, 110 °C; (b) PPTS, $(MeO)_2CMe_2$, CH_2Cl_2; (c) O_3, CH_2Cl_2:MeOH, -78 °C to rt; (d) **1.19**, allyl acetate; (e) TBSCl, imidazole, DMF; (f) O_3 then $NaBH_4$; (g) **1.19**, allyl acetate; (h) PPTS, $(MeO)_2CMe_2$, CH_2Cl_2; (i) O_3 then $NaBH_4$.

The total synthesis of roxaticin was completed in 20 steps (longest linear sequence, LLS) and 29 total steps and is the shortest total synthesis of the natural product to date.[22] Rapid assembly of the C14-C28 domain was accomplished in just 9 steps from 1,3-propanediol. Three iterations of iridium-catalyzed two-directional allylation were employed to construct six C-C bonds and set six stereocenters. This approach circumvents additional manipulations associated with the use of non-native functional groups or substructures to mediate bond construction, such as chiral auxiliaries, and minimizes refunctionalizations, especially redox manipulations.

1.2.2 Tetrafibricin C21-C40

Tetrafibricin **1.21** is a fibrogen receptor inhibitor that exhibtis a unique array of functionality, including alternating 1,3-diol and 1,5-ene-diol substructures, a tetraenoic acid moiety, and a primary amine (Figure 1.8).[23] Although biosynthetically related to oxo-polyene macrolide antibiotics such lienomycin,[24] tetrafibricin is not macrocylic and not exhibit activity against *Bacillus subtilis* and *Esherichia coli*. The structure of tetrafibricin also differs from all other naturally occurring fibrogen receptor antagonists. Tetrafibricin is of interest as a tool to

study fibrogen binding as well as platelet aggregation and as a potential therapeutic agent for the treatment of arterial thrombotic disease.[25] The total synthesis of tetrafibricin **1.21** remains an unmet challenge; however, Krische and workers have developed a strategy that enables rapid assembly of the C21-C40 fragment of the natural product.[26]

Figure 1.8 Molecular structure of tetrafibricin **1.21** and anticipated precursor **1.22**.

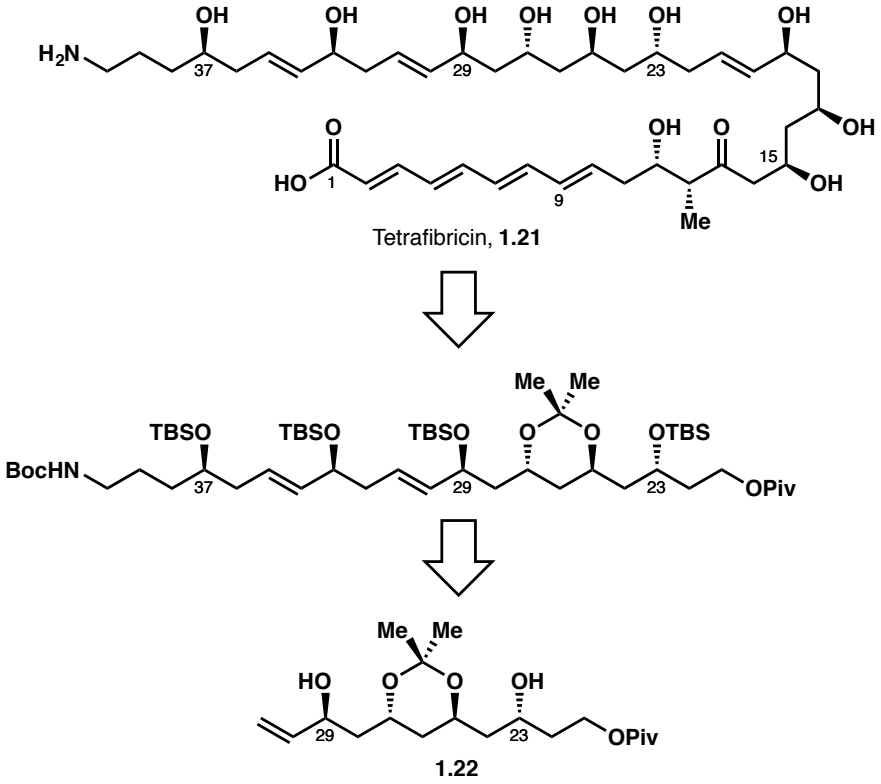

The synthesis began with iridium-catalyzed two-direction allylation of 1,3-propanediol and 2,2-dimethyl acetal protection of the resultant 1,3-diol to afford **1.23** (Scheme 1.9). Oxidative cleavage of the terminal olefins and reduction with $NaBH_4$ afforded another primary diol, which underwent a second iteration of two-directional allylation to give **1.24**. Protection of the secondary alcohols as silyl ethers and oxidative cleavage of the terminal olefins with ozone followed by reduction with $NaBH_4$ furnished diol **1.25**. Differentiation of the C_2-symmetric molecule was accomplished through monoprotection with pivaloyl chloride to generate alcohol **1.26**. Grieco's procedure for two-step primary alcohol dehydration followed by removal of the silyl ether protecting groups provided **1.22**. Thus, the synthesis of this fragment was completed

in 10 steps from 1,3-propanediol. Further elaboration of **1.22** to construct the C21-C40 domain (**1.22**) of tetrafibricin was accomplished. Unfortunately, fragment union and further manipulations were not successful; therefore, completion of a total synthesis of tetrafibricin **1.21** is still an outstanding challenge.

Scheme 1.9 Synthesis of **1.22**, a potential precursor to tetrafibricin **1.21**.

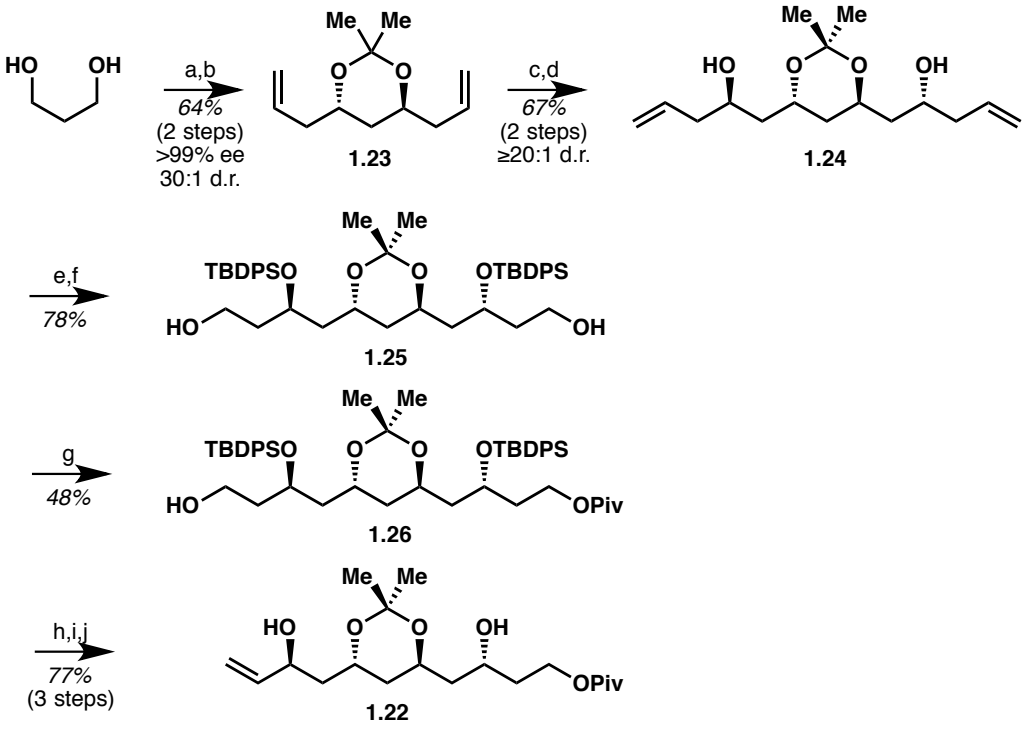

Key: (a) allyl acetate, $[Ir(cod)Cl]_2$, (*S*)-Cl,MeO-BIPHEP, Cs_2CO_3, 4-Cl-3-NO_2BzOH, dioxane, 110 °C; (b) PPTS, $(MeO)_2CMe_2$, CH_2Cl_2; (c) O_3, CH_2Cl_2:MeOH, -78 °C to rt; (d) allyl acetate, $[Ir(cod)Cl]_2$, (*R*)-Cl,MeO-BIPHEP, Cs_2CO_3, 4-Cl-3-NO_2BzOH, dioxane, 110 °C; (e) ^{t}BuPh$_2$SiCl, imidazole, CH_2Cl_2; (f) O_3, CH_2Cl_2:MeOH then $NaBH_4$, -78 °C to rt; (g) PivCl, pyridine, CH_2Cl_2; (h) *o*-(NO_2)PhSeNC, *n*-Bu_3P, THF; (i) H_2O_2, $NaHCO_3$, THF; (j) TBAF, THF.

1.2.3 Bryostatin 7

The bryostatins are a family of 20 marine natural products originally isolated from the bryozoan *Bugula neritina*.[27] Bryostatin 7 **1.27**, an illustrative representative of this family of natural products and a target of total synthesis performed by the Krische group, is presented in Figure 1.9. The bryostatins exhibit a wide array of biological effects, including antineoplastic activity, immunopotentiating activity, restoration of apoptotic function, and the ability to act synergistically with other chemotherapeutic agents.[28] They have also exhibited neurological

effects such as activity against Alzheimer's disease,[29] neural growth and repair, and the reversal of stroke damage, [30] as well as memory enhancement.[31] Given the challenges associated with finding a concise route to the bryostatins, bryostatin 7 **1.27** was deemed another ideal candidate to illustrate the utility of the C-C bond forming hydrogenations developed in the Krische laboratory.[32]

Figure 1.9 Molecular structure of bryostatin 7 **1.27** and anticipated precursor **1.28**.

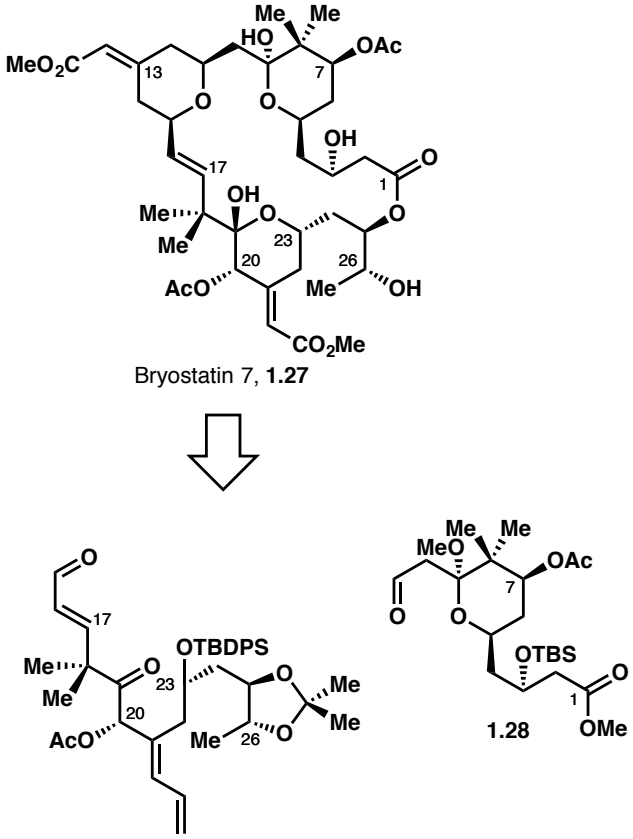

The synthesis of the pyran fragment **1.28** began with two-directional allylation of 1,3-propanediol to provide chiral C_2-symmetric diol **1.15** (Scheme 1.10). Oxidative cleavage of the terminal olefins followed by reductive workup with PPh_3 and then treatment with TBSCl furnished pyran **1.29**. Diastereoselective reverse prenylation of the aldehyde was performed via iridium-catalyzed transfer hydrogenative coupling with 1,1-dimethylallene using catalyst **1.30** to afford secondary neopentyl alcohol **1.31**. Acylation of the secondary alcohol followed by oxidative cleavage of the terminal olefin with ozone and reductive workup with PPh_3 provided

aldehyde **1.32**, which underwent allylation with catalyst **1.33** to generate **1.34**. Oxidation of the secondary alcohol afforded ketone **1.35.** Treatment with PPTS led to formation of pyran **1.36** and the terminal alkene was oxidatively cleaved to afford aldehyde fragment **1.28**.

Scheme 1.10 Synthesis of fragment **1.28**, a precursor to bryostatin 7 **1.27**.

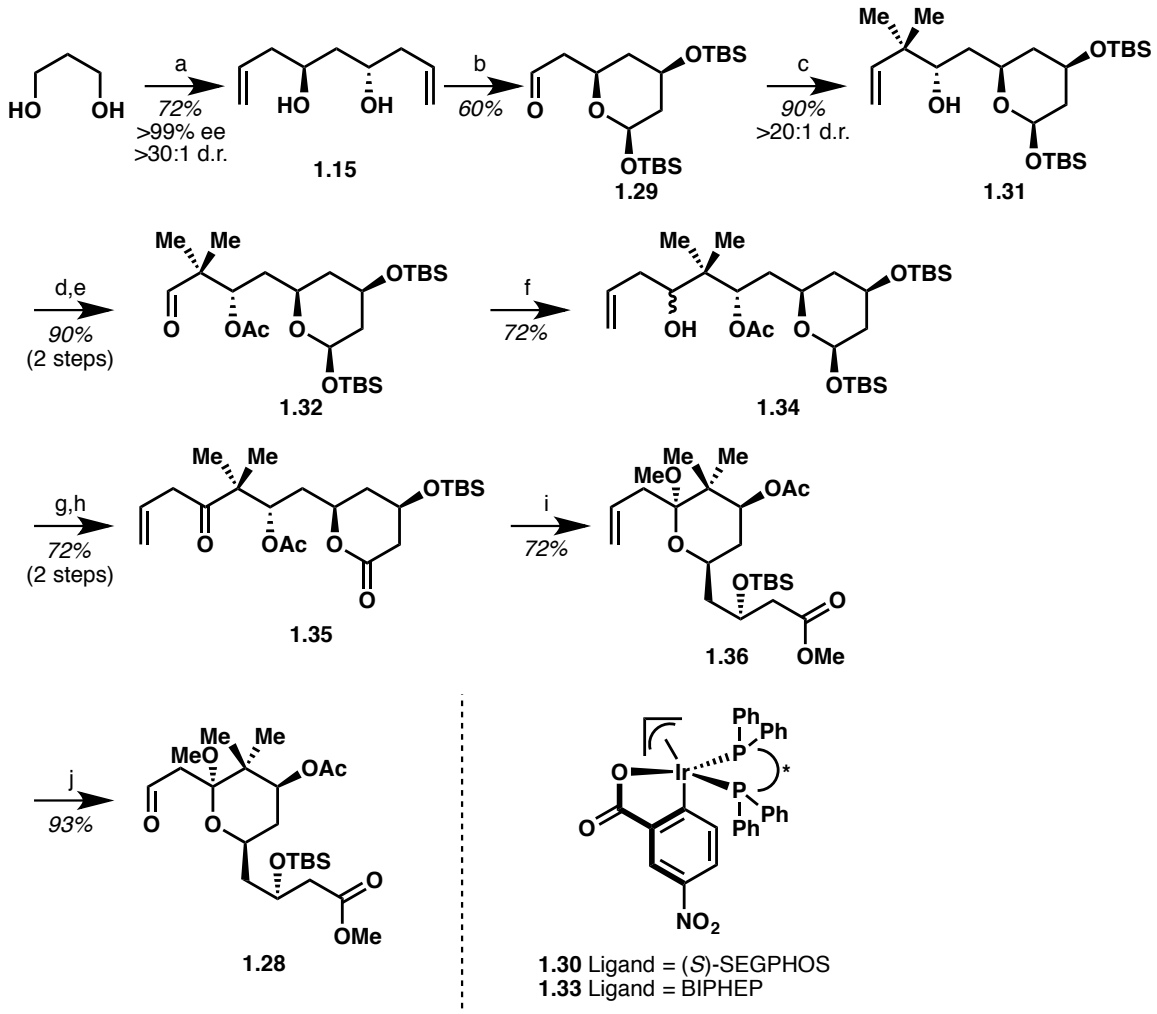

Key: (a) $[Ir(cod)Cl]_2$, (*S*)-Cl,MeO-BIPHEP, Cs_2CO_3, 4-Cl-3-NO_2BzOH, dioxane, 90 °C; (b) O_3, CH_2Cl_2, -78 °C, then PPh_3, TBSCl, imidazole; (c) **1.30**, *i*-PrOH, 1,1-dimethylallene, toluene, 60 °C; (d) Ac_2O, Et_3N, DMAP, THF; (e) O_3, CH_2Cl_2, then PPh_3; (f) **1.33**, *i*-PrOH, allyl acetate, Cs_2CO_3, THF, 90 °C; (g) TBAF, AcOH, THF; (h) DMP, $NaHCO_3$, CH_2Cl_2; (i) PPTS, MeOH; (j) O_3, CH_2Cl_2 -78 °C, then PPh_3.

In using the iridium-catalyzed two-directional allylation methodology, aldehyde fragment **1.28** was synthesized in 10 steps from 1,3-propanediol. This fragment was successful joined with the western half of the molecule (shown in Figure 1.9) and elaborated further to complete the total synthesis of bryostatin 7.[33] Transfer hydrogenative C-C bond forming reactions facilitated

the concise total synthesis of the natural product in just 20 steps LLS. This represents the most concise route to any of the members of the bryostatin family and illustrates the power and versatility of this new class of catalytic C-C bond forming reactions.

1.2.4 Neopeltolide

Neopeltolide **1.37** was isolated from a deep-water sponge of the family *Neopelidae* by Wright and coworkers in 2007 (Figure 1.10).[34] The natural product exhibited significantly potent *in vitro* cytotoxicity against a variety of different cancer cell lines, including A-549 human lung adenocarcinoma, NCI-ADR-RES human ovarian sarcoma, and P388 murine leukemia cell lines. Neopeltolide **1.37** demonstrated antifungal activity against the fungal pathogen *Candida albicans*, and also inhibited cell proliferation in the PANC-1 pancreatic cancer cell line, as well as the DLD-1 colorectal adenocarcinoma cell line. Structurally, neopeltolide **1.37** is composed of a 14-membered macrolactone with an embedded tetrahydropyran ring, and six stereogenic centers. As prior total syntheses had resulted in structural reassignment, She and coworkers designed a concise formal synthesis of the known intermediate **1.38**, which would be synthesized from pyran **1.39** and alcohol **1.40**.[35]

Figure 1.10 Molecular structure of (+)-neopeltolide **1.37**, known intermediate **1.38**, and proposed precursors **1.39** and **1.40**.

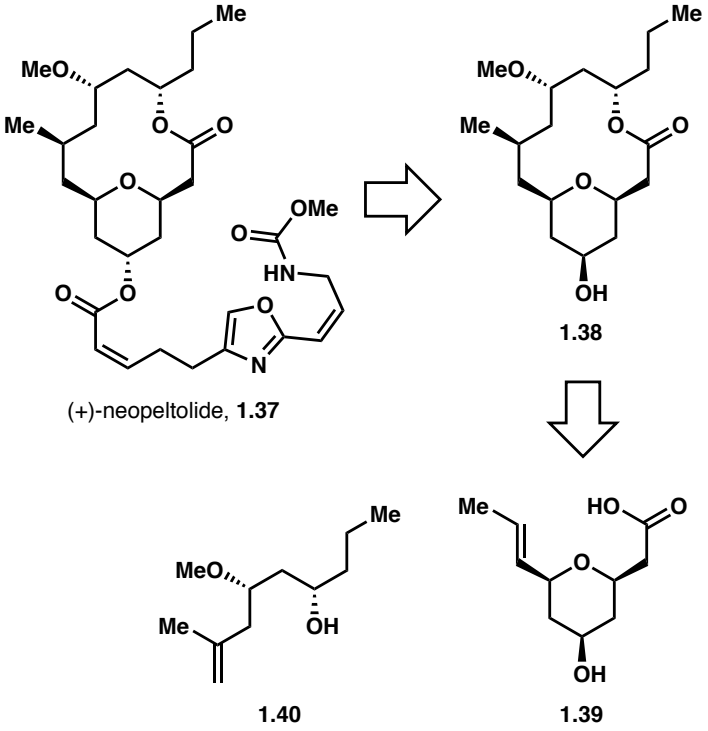

The synthesis of **1.38** began with construction of the pyran moiety **1.39**. Krische two-directional allylation of 1,3-propanediol furnished known C_2-symmetric, chiral diol **1.18** (Scheme 1.11). Palladium-catalyzed intramolecular alkoxycarboxylation reaction followed by protection of the resultant secondary alcohol as the corresponding benzyl ether afforded pyran **1.41**. Isomerization of the terminal olefin with Grubbs' 2nd generation catalyst in methanol followed by hydrolysis of the methyl ester provided carboxylic acid **1.39**. Coupling of fragment **1.39** with fragment **1.40**, which was prepared in nine steps from L-valinol, gave ester **1.42**. Ring-closing metathesis was achieved using Hoveyda-Grubbs' 2nd generation catalyst and provided macrolactone **1.43**. Diastereo-selective hydrogenation of the trisubstituted olefin and simultaneous cleavage of the benzyl ether furnished **1.38**, which completed the formal synthesis of neopeltolide **1.37**.

Scheme 1.11 Synthesis of **1.38**, a known intermediate in the total synthesis of neopeltolide **1.37**.

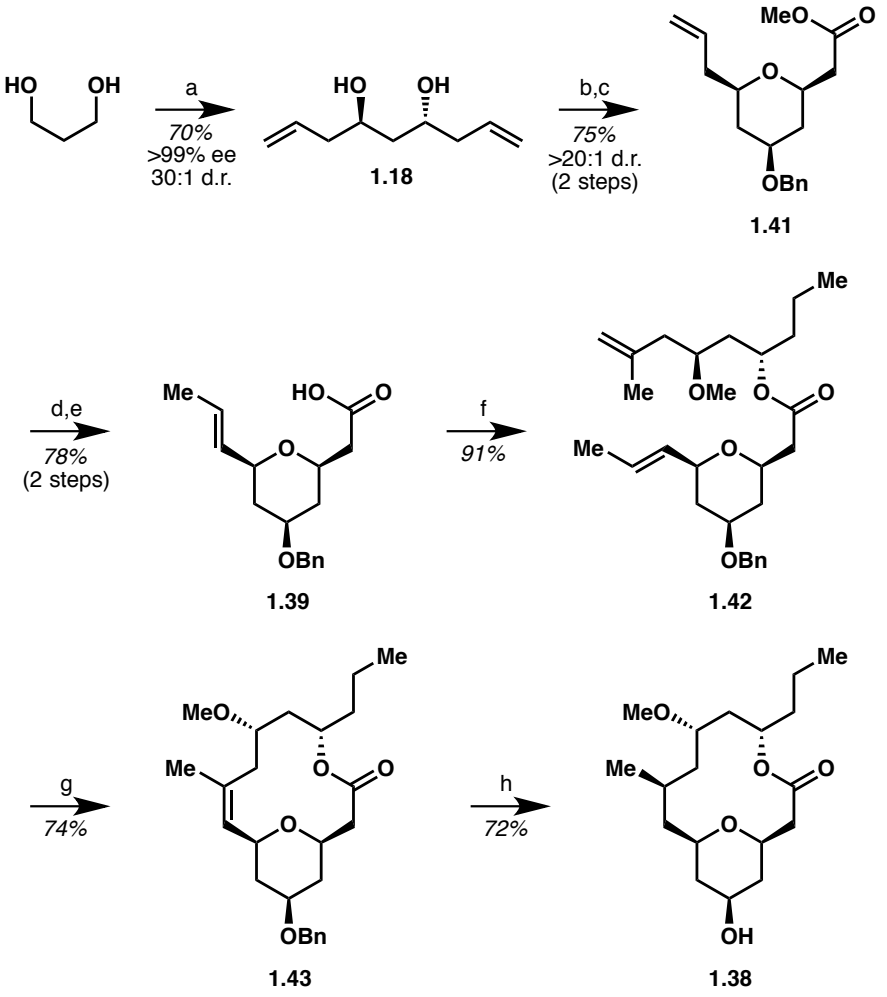

Key: (a) allyl acetate, $[Ir(cod)Cl]_2$, (*R*)-Cl,MeO-BIPHEP, Cs_2CO_3, 4-Cl-3-NO_2BzOH, dioxane, 110 °C, 3 d; (b) $PdCl_2$, $CuCl_2$, CO, CH_3CN, MeOH; (c)BnO(NH=C)CCl_3, CF_3SO_3H, CH_2Cl_2, 0 °C; (d) Grubbs' 2nd Generation, MeOH, 60 °C; (e) LiOH, THF, MeOH; (f) **1.40**, MNBA, DMAP, CH_2Cl_2; (g) Hoveryda-Grubbs 2nd Generation, toluene, 80 °C; (h) Pd/C, H_2, EtOH.

1.2.5 Mandelalide A

Mandelalide A **1.44** was isolated from a new species of *Lissoclinum* located in Algoa Bay, South Africa (Figure 1.11).[36] The compound exhibited significant cytotoxicity against mouse Neuro-2A neuroblastoma cells as well as human NCI-H460 lung cancer cells. Structurally, mandelalide A **1.44** is composed of a 20-membered macrolactone with an embedded tetrahydropyran ring, tetrahydofuran ring, and an *E*/*Z* diene. Its impressive biological

activity but scarce supply coupled with its interesting molecular architecture inspired Fürstner and coworkers to embark on a total synthesis of the natural product in 2014.[37] Further structural reassignment and total synthesis of the corrected structure was reported the following year.[38]

Figure 1.11 Molecular structure of mandelalide A **1.44** and proposed precursor **1.45**.

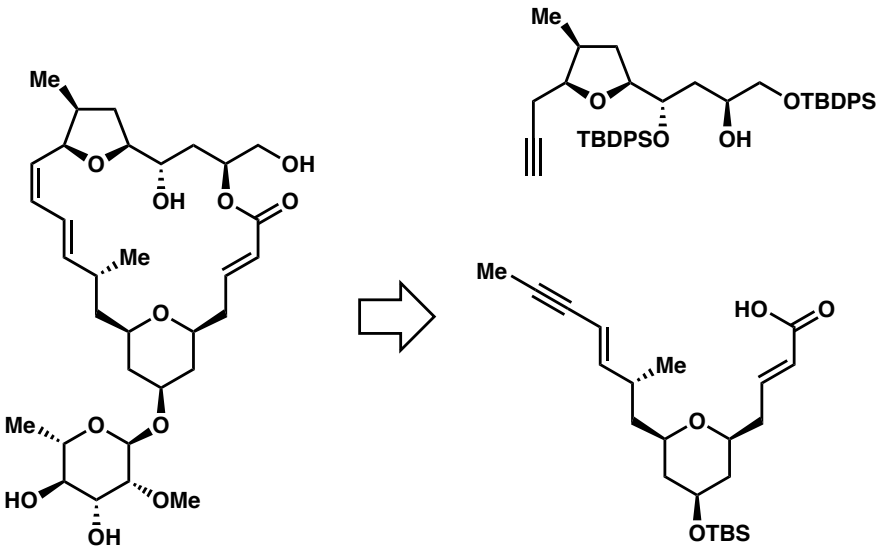

The synthesis of pyran fragment **1.45** began with Krische two-directional allylation of propanediol to provide known C_2-symmetric, chiral diol **1.15**. Iodoetherification and subsequent protection of the secondary hydroxyl group as the TBS ether provided pyran **1.46**. Reaction with the lithium enolate of chiral auxiliary **1.47** followed by reductive removal of the auxiliary gave primary alcohol **1.48**. Cross-metathesis with methyl acrylate followed by oxidation of the primary alcohol afforded aldehyde **1.49**. Aldehyde **1.49** was subjected to conditions for Takai olefination to furnish vinyl iodide **1.50**. Modified Suzuki propargylation followed by hydrolysis of the methyl ester completed the synthesis of fragment **1.45**. The synthesis of fragment **1.45** was achieved in just 10 steps from 1,3-propanediol and was further elaborated to complete the total synthesis of mandelalide A **1.44**.

Scheme 1.12 Synthesis of **1.45**, a precursor in the total synthesis of mandelalide A **1.44**.

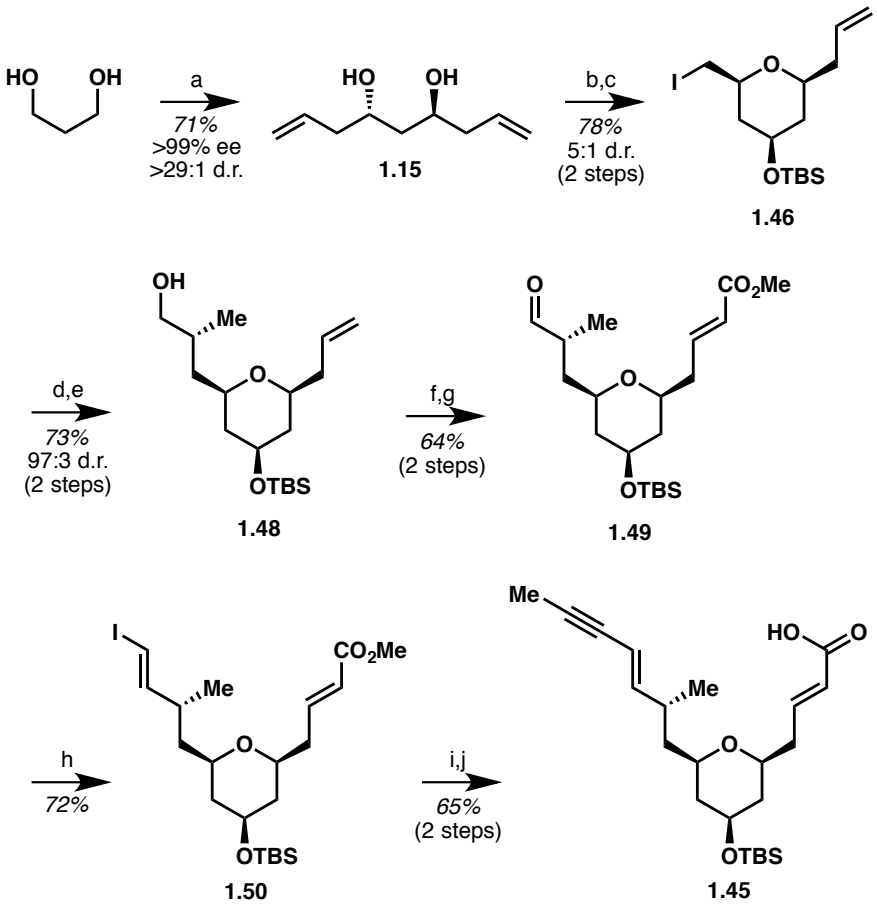

Key: (a) allyl acetate, $[Ir(cod)Cl]_2$, (*S*)-Cl,MeO-BIPHEP, Cs_2CO_3, 4-Cl-3-NO_2BzOH, dioxane, 90 °C; (b) I_2, $NaHCO_3$, MeCN, -40 °C; (c) TBSOTf, 2,6-lutidine, CH_2Cl_2, 0 °C; (d) **1.47**, LDA, LiCl, THF, 0 → 45 °C; (e) LDA, $BH_3{\cdot}NH_3$, THF, 0 → 25 °C; (f) methyl acrylate, Hoveyda-Grubbs' 2nd Generation, CH_2Cl_2; (g) DMP, CH_2Cl_2, 0 → 25 °C; (h) CHI_3, $CrCl_2{\cdot}$THF, THF, -8 °C; (i) propynyl sodium, $B(OMe)_3$, $[Pd(dppf)Cl_2{\cdot}(CH_2Cl_2)$, THF, 70 °C; (j) Me_3SiOK, Et_2O.

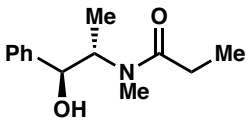

1.47

1.2.6 C8-epi-Cryptolatifolione

The dihydropyranone motif is structural element associated with many diverse families of natural products. Compounds containing a dihydropyranone ring display a broad range of biological properties, including antitumor,[39] antimicrobial[40] and antiparasite[41] activity, inhibition of HIV protease[42] and hepatitis C virus polymerase,[43] induction of apoptosis,[44] and molluscicidal activity.[45] Cryptolatifolione is one such compound and was isolated by Wijewardene and

coworkers in 1996 from the bark of *Cryptocaria latifolia* (Figure 1.12).[46] As the relative stereochemistry of the natural product was unknown, Pilli and coworkers completed the first total synthesis of cryptolatifolione as well as C8-*epi*-cryptolatifolione **1.51** in 2015.[47]

Figure 1.12 Molecular structure of cryptolatifolione and C8-*epi*-cryptolatifolione **1.51**.

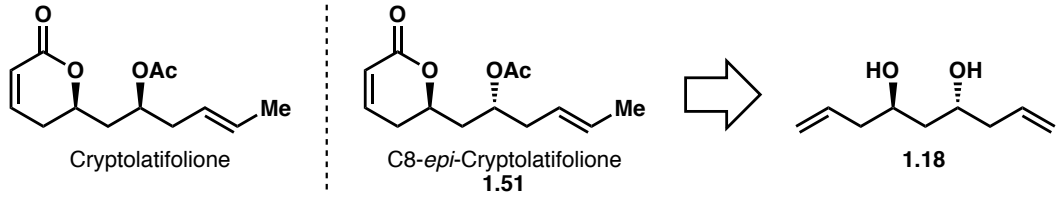

The synthesis of C8-*epi*-cryptolatifolione began with Krische two-directional allylation of 1,3-propanediol to furnish known C_2-symmetric, chiral diol **1.18**. Desymmetrization was achieved by selective *O*-allylation of just one of the two hydroxyl groups to provide allyl ether **1.52**. The acetate moiety was installed with acetic anhydride to give acetate **1.53**. Ring-closing metathesis with Grubbs' 2nd generation catalyst afforded dihydropyran **1.54**. Selective allylic radical-based C-H oxidation at the C2 position was achieved with PCC to give dihydropyranone **1.55**. Cross-metathesis with 3-hexene in the presence of Grubbs' 2nd generation catalyst furnished C8-*epi*-cryptolatifolione **1.51**. The total synthesis of **1.51** was completed in just eight steps from 1,3-propanediol.

Scheme 1.13 Synthesis of C8-*epi*-cryptolatifolione **1.51**.

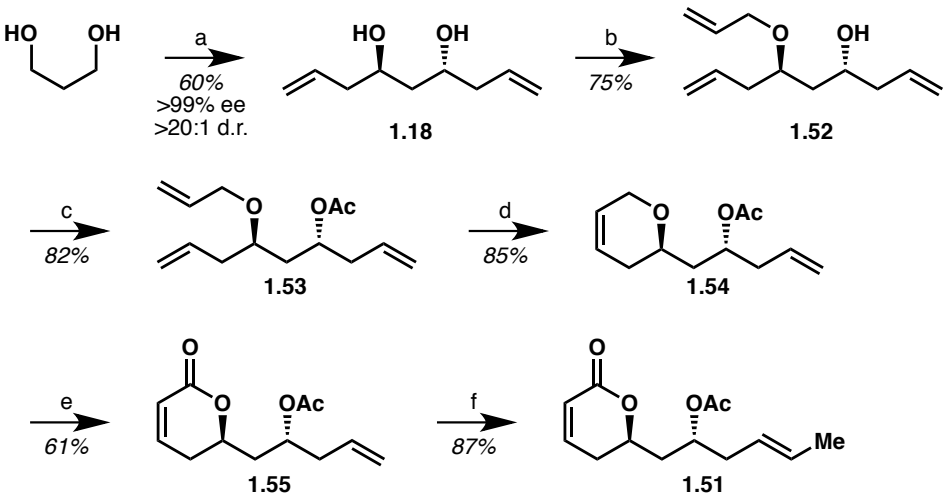

Key: (a) allyl acetate, $[Ir(cod)Cl]_2$, (*R*)-BINAP, Cs_2CO_3, 4-Cl-3-NO_2BzOH, dioxane, 90 °C, 3 d; (b) allyl bromide, NaH, DMF; (c) Ac_2O, Et_3N, DMAP, CH_2Cl_2, 0 °C; (d) Grubbs' 2nd Generation, CH_2Cl_2, 40 °C; (e) PCC, pyridine, CH_2Cl_3, 40 °C; (f) 3-hexene, Grubbs' 2nd Generation, CH_2Cl_2.

1.2.7 Cryptomoscatone E3

Pilli and coworkers also reported the stereochemical assignment and total synthesis of cryptomoscatone E3 **1.56**, another dihydropyranone-containing natural product (Figure 1.13).[48] The natural product was first isolated by Cavalheiro and Yoshida in 2000 from the bark of the Brazilian tree *Cryptocarya mandiocanna*.[49] Preliminary studies on the pharmacological properties of the cryptomoscatone family of natural products indicated that some of these types of structures possess G2 checkpoint inhibitory properties. However, a more thorough study of the biological activity of this family of natural products is necessary.

Figure 1.13 Molecular structure of cryptomoscatone E3 **1.56**.

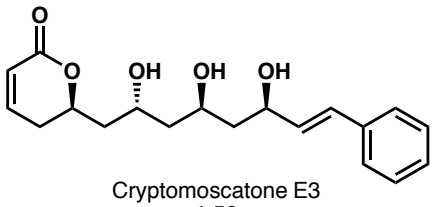

Cryptomoscatone E3
1.56

As before, the synthesis began with Krische two-directional allylation of 1,3-propanediol to furnish known C_2-symmetric, chiral diol **1.18**. Desymmetrization was achieved via selective

O-allylation of a single hydroxyl group to afford **1.52**. The remaining free hydroxyl group was protected as the corresponding PMB ether **1.57**. Upon exposure to Grubbs' 2nd generation catalyst, ring-closure occurred and furnished dihydropyran **1.58**. Selective oxidation at the C2 position proved quite difficult, presumably due to competitive deprotection of the PMB ether under the reaction conditions; however, sufficient quantities of dihydropyranone **1.59** were obtained. Wacker oxidation of the terminal olefin generated ketone **1.60**, which upon treatment with Cy_2BCl and exposure to cinnamaldehyde provided alcohol **1.61**. Selective 1,3-*syn* reduction of the ketone was achieved with $LiBH_4$ and Et_2BOMe at low temperature to afford diol **1.62**. Unfortunately, all attempts to remove the PMB ether under oxidative conditions were unsuccessful. The total synthesis of cryptomoscatone E3 **1.56** was completed from a separate and complementary route.

Scheme 1.14 Attempted synthesis of cryptomoscatone E3 **1.56**.

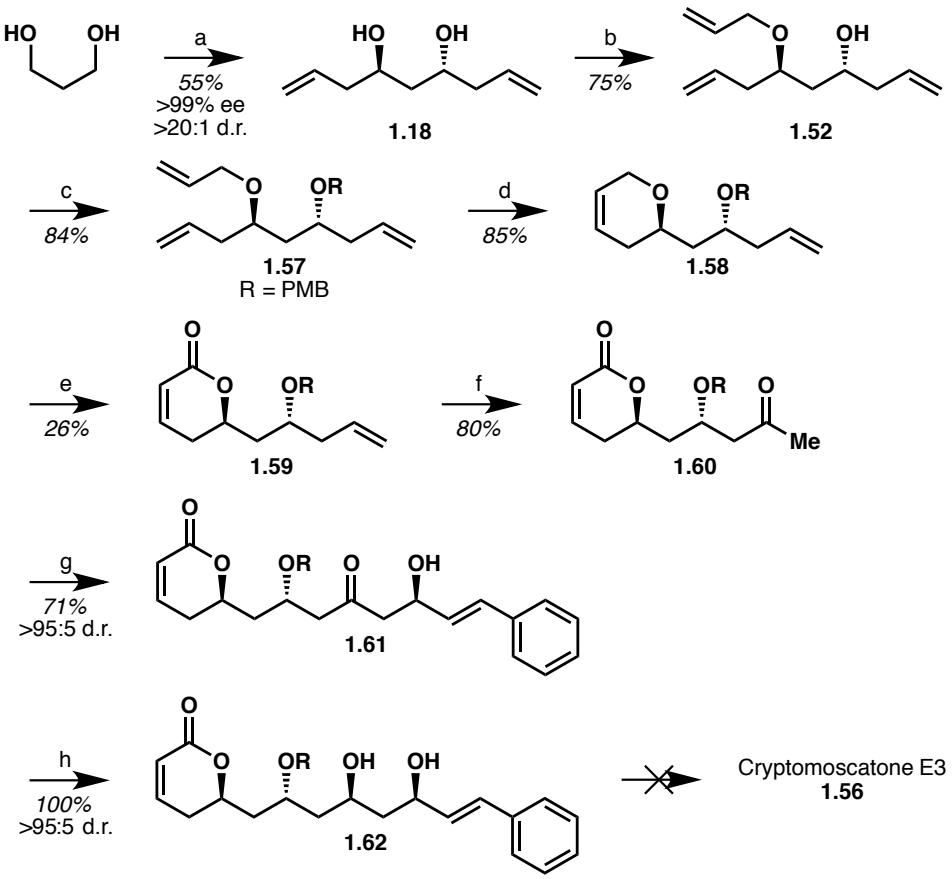

Key: (a) allyl acetate, $[Ir(cod)Cl]_2$, (*R*)-BINAP, Cs_2CO_3, 4-Cl-3-NO_2BzOH, dioxane, 90 °C, 3 d; (b) allyl bromide, NaH, DMF; (c) PMBCl, NaH, TBAI, DMF; (d) Grubbs' 2nd Generation, CH_2Cl_2, 40 °C; (e) PCC, CH_2Cl_2, 80 °C; (f) $PdCl_2$, CuCl, air, DMF, H_2O; (g) Cy_2BCl, Et_3N, -40 °C, then cinnamaldehyde at -78 °C; (h) $LiBH_4$, Et_2BOMe, THF, MeOH, -78 °C.

1.3 Brief Overview of Carbonyl Crotylation

1.3.1 Introduction

Asymmetric carbonyl crotylation is a powerful method for the construction of vicinal stereogenic centers and facilitates the construction of substructures commonly found in nature (Figure 1.14). The development of methods for enantioselective carbonyl crotylation has been of considerable interest to the synthetic community for over half of a century. The majority of these methods are analogous to methods for asymmetric carbonyl allylation in that they frequently require the use preformed crotyl metal species, which in some cases are used stoichiometrically.

A particular challenging aspect of asymmetric carbonyl crotylation is control of diastereoselectivity as both 1,2-*syn* and 1,2-*anti* products are possible. A number of reviews have been published on the myriad methods available for carbonyl crotylation.[13, 50] The methodology that will be the focus of this section will be catalytic redox-triggered transfer hydrogenative methods for chirality transfer as a means to access products of carbonyl crotylation with high levels of stereoselectivity.

Figure 1.14 The products of a generic carbonyl crotylation reaction and examples of two complex natural products that contain similar substructures.

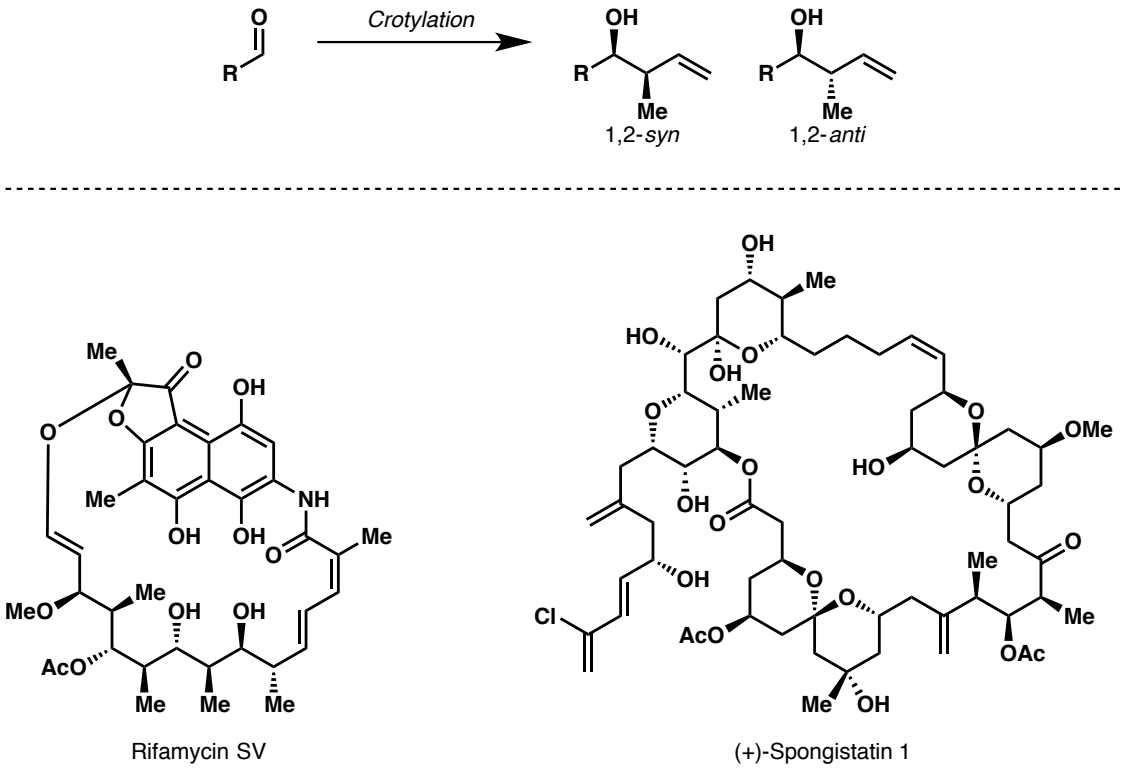

1.3.2 Redox-Triggered Transfer Hydrogenative Methods for Chirality Transfer

In 2009, Krische and coworkers published the first transfer hydrogenative method for enantioselective carbonyl crotylation.[51] Using conditions similar to those found to effective for carbonyl allylation via transfer hydrogenation, products of carbonyl crotylation were obtained when α-methyl allyl acetate was employed. Prior to the development of this technology, all methods for carbonyl crotylation require the use of premetallated allyl donors. Just as the

Krische allylation was capable of constructing products of carbonyl addition from the primary alcohol or aldehyde oxidation level, the crotylation reaction was also capable of using alcohols directly. The reaction was also tolerant of alkyl, aryl, and heteroaryl substrates (Scheme 1.15).

Scheme 1.15 Abbreviated scope of the asymmetric transfer hydrogenative crotylation reaction.

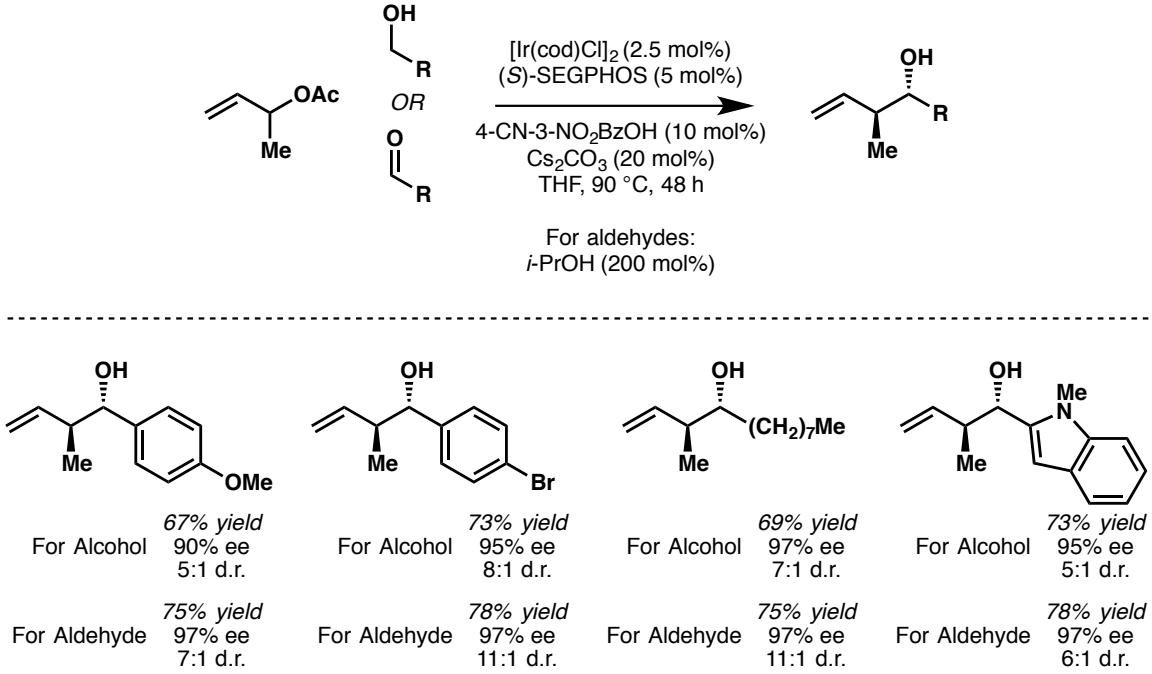

Mechanistically, the crotylation pathway is quite similar to that of the allylation reaction. An important difference is at the stage of ionization of α-methyl allyl acetate, in which isomerization between the *cis*-π-crotyl the *trans*-π-crotyl complex would lead to the erosion of diastereoselectivity. Since the *cis*-π-crotyl complex engages the carbonyl partner by way of an (*E*)-crotyl iridium intermediate, the product of crotylation becomes the 1,2-*anti* homoallylic alcohol. Conversely, the *trans*-π-crotyl complex engages the carbonyl partner by way of a (*Z*)-crotyl iridium intermediate and gives rise to 1,2-*syn* products (Figure 1.15). In all cases in which α-methyl allyl acetate is employed, a significant preference for products of 1,2-*anti* carbonyl crotylation are observed presumably due to the kinetic preference for formation of the *cis*-π-crotyl complex. In the stereochemical model proposed in the initial report, the preference of the methyl group to be in a pseudo-equitorial position leads to formation of 1,2-*anti* products.

Figure 1.15 Stereochemical features associated with formation and isomerization of the purported crotyl iridium intermediates and stereochemical model indicating the pseudo-equitorial positioning of the methyl group.

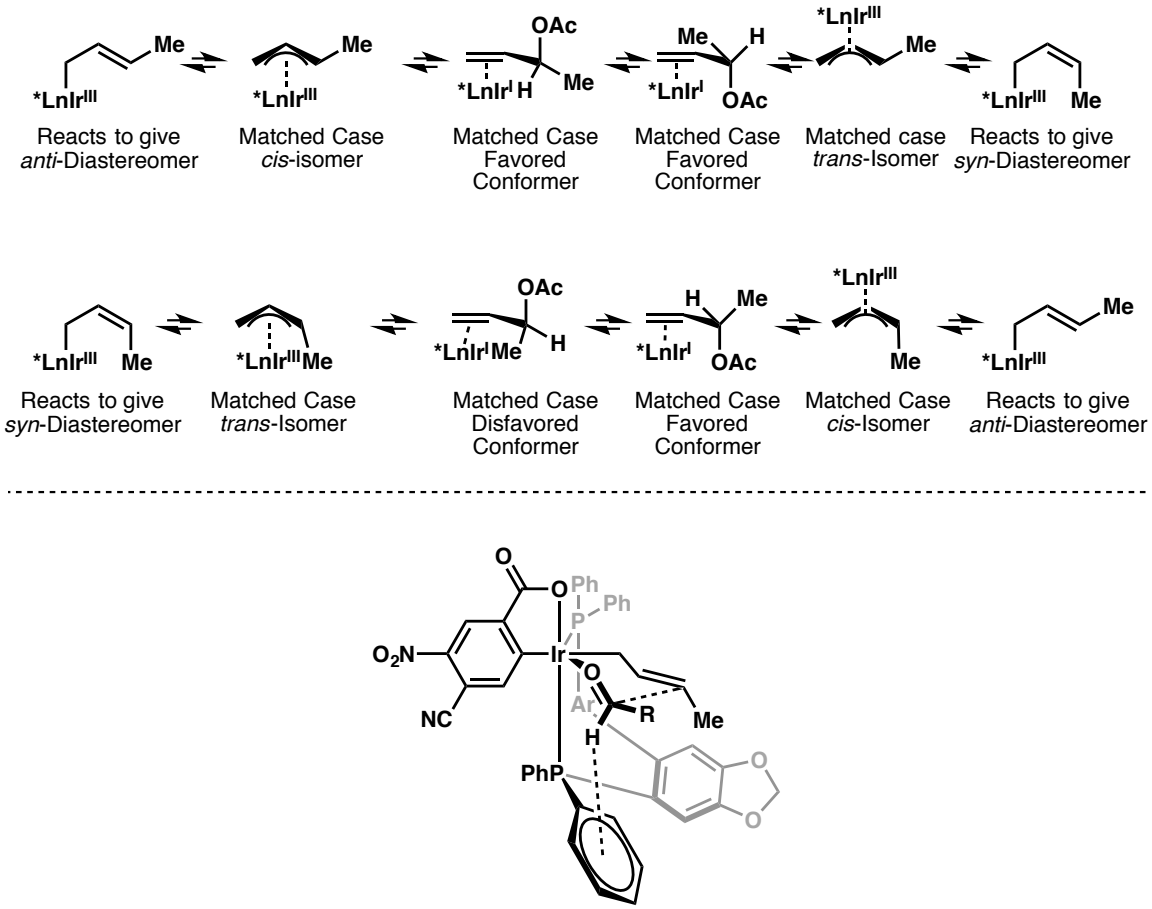

While the development of this technology was a step forward in the art of synthesizing molecules that possess the 1,2-*anti* structural motif, it was not suitable for construction of the 1,2-*syn* structural motif that is also quite prevalent in nature. This challenge was overcome through modification of the crotyl donor. In 2011, Krische and coworkers reported a ruthenium-catalyzed method for diastereo- and enantioselective hydrohydroxyalkylation of 2-silyl butadienes to give access to products of 1,2-*syn* crotylation from either the alcohol or aldehyde oxidation state. Unlike in the case of the 1,2-*anti* crotylation is which α-methyl allyl acetate acted as the allyl donor, 1,2-*syn* crotylation products were obtained from 2-silyl-butadienes (Figure 1.16). Steric clash between the bulky silyl group and the ligand, DM-SEGPHOS, leads to

the methyl group and silyl groups to adopt pseudo-axial conformation in the transition state. This pseudo-axial conformer, upon C-C bond formation affords the product of 1,2-*syn* crotylation.

Figure 1.16 Abbreviated scope of the asymmetric ruthenium-catalyzed hydrohydroxylalkylation of 2-silyl-butadienes and a stereochemical model for addition.

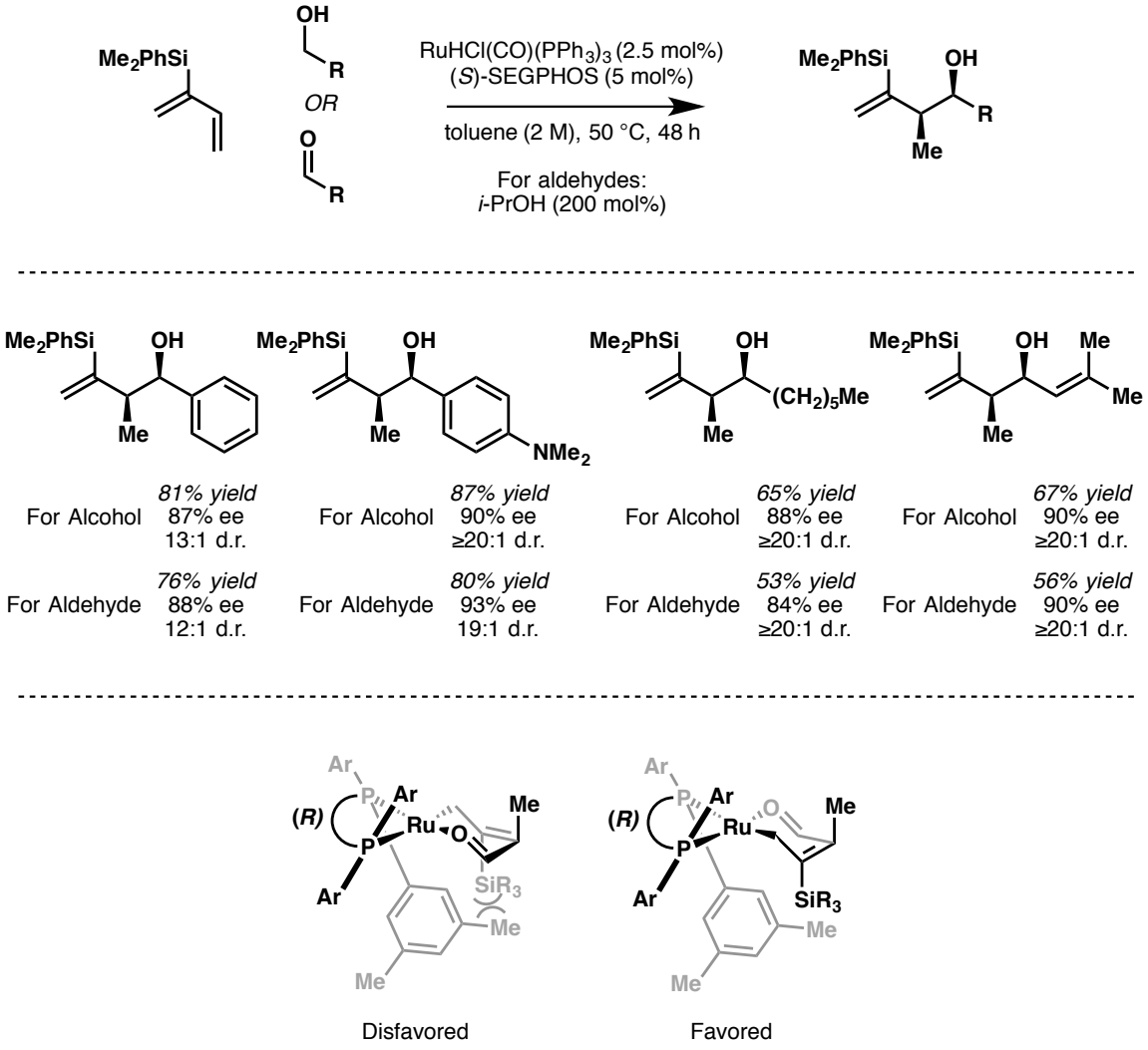

Having developed complementary methods for 1,2-*anti* and 1,2-*syn* crotylation reactions, Krische and coworkers turned their focus to further simplification of the crotyl donor. Butadiene represents the most ideal choice for a crotyl donor as all atoms are transferred to the product and there is no inherent waste or further manipulations necessary to reveal the product of carbonyl crotylation. Although catalytic systems that exhibit the essential reactivity with butadiene had

been developed, stereocontrolled hydrohydroxyalkylation of butadiene had proven elusive when either iridium[52] or ruthenium[53] catalysts were employed. While enantioselectivity was a challenging aspect of this type of coupling reaction, it was observed that addition of bulky sulfonic acid additives afforded products of 1,2-*anti* crotylation with moderate levels of diastereoselectivity.

Encouraged by this discovery, Krische and coworkers investigated the use of chiral phosphoric acid additives in the ruthenium-catalyzed crotylation of aldehydes and alcohols with butadiene.[54] Interestingly, it was observed that the chiral phosphoric acid constructed from the 3'-ethyl-H_8 derivative of BINOL enhanced the diastereo- and enantioselectivity of the reaction significantly (Figure 1.17). However, one limitation was found to be the intolerance of the reaction to any substrates other than aryl aldehydes or alcohols.

Figure 1.17 Abbreviated scope of the asymmetric ruthenium-catalyzed hydrohydroxylalkylation of butadiene.

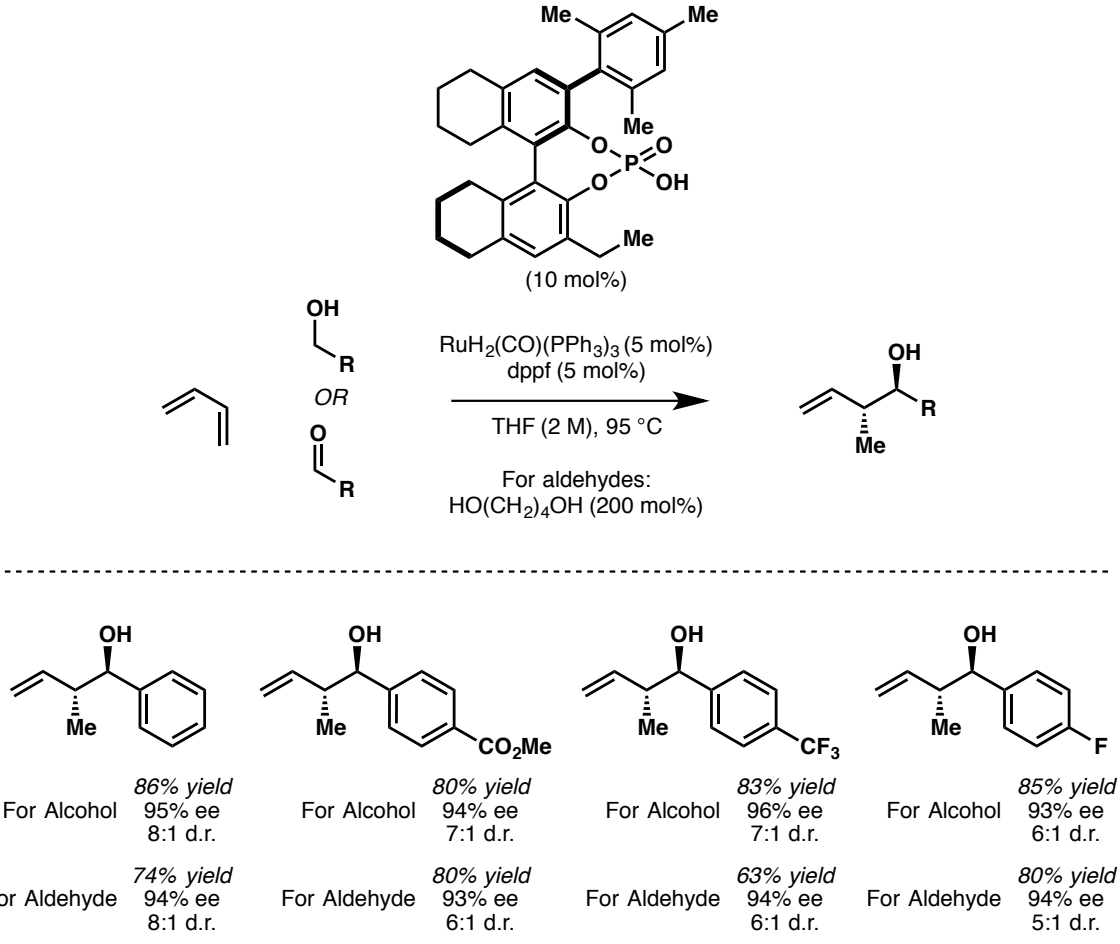

Mechanistically, it was proposed that hydrometallation of butadiene delivers two isomeric π-allyl complexes (Figure 1.18). The *syn*- and *anti*-π-allyl complexes exist in equilibrium with each other as well as with the corresponding (*E*)- and (*Z*)-σ-allyl haptomers. The considerable bulk of the chiral phosphoric acid ligand promotes partitioning of the (*E*)- and (*Z*)-isomers, which precedes stereospecific carbonyl addition by way of the σ-crotylruthenium haptomer through a closed transition state. Using this method, a number of electron-rich and electron-deficient aryl aldehydes and alcohols were successfully coupled with butadiene to give products of carbonyl crotylation with very high levels of enantioselectivity and good levels of diastereoselectivity.

Figure 1.18 Counterion-dependent partitioning of (*E*)- and (*Z*)-σ-crotylruthenium isomers (X = chiral phosphoric acid).

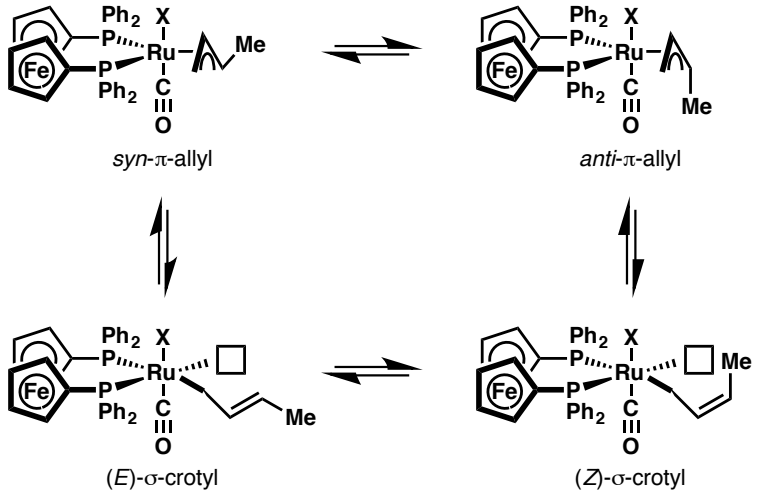

While this methodology was significant in that allowed for the direct coupling of feedstock chemicals butadiene and aryl alcohols and aldehydes with high 1,2-*anti* diastereoselectivity, further modification was necessary in order to access the more challenging 1,2-*syn* products as well as a method that could tolerate aliphatic substrates. In 2012, Krische and coworkers reported that use of a chiral ligand, such as (*S*)-SEGPHOS in addition to TADDOL-derived phosphoric acid additives led to selective formation of 1,2-*syn* products of carboyl crotylation from either the alcohol or aldehyde oxidation state (Figure 1.19).[55] Additionally, under these conditions aliphatic substrates were tolerated and were shown to engage in coupling with butadiene with high levels of enantioselectivity and good levels of diastereoselectivity. In this reaction, it is proposed that the (*Z*)-σ-crotylruthenium species is kinetically favored due to reduced steric interaction between the methyl group of the crotyl donor and the bulky TADDOL moiety.

Figure 1.19 Postulated mechanistic rationale illustrating partitioning of (*E*)- and (*Z*)-σ-crotylruthenium isomers as a consequence of the stericac demand of the TADDOL ligand.

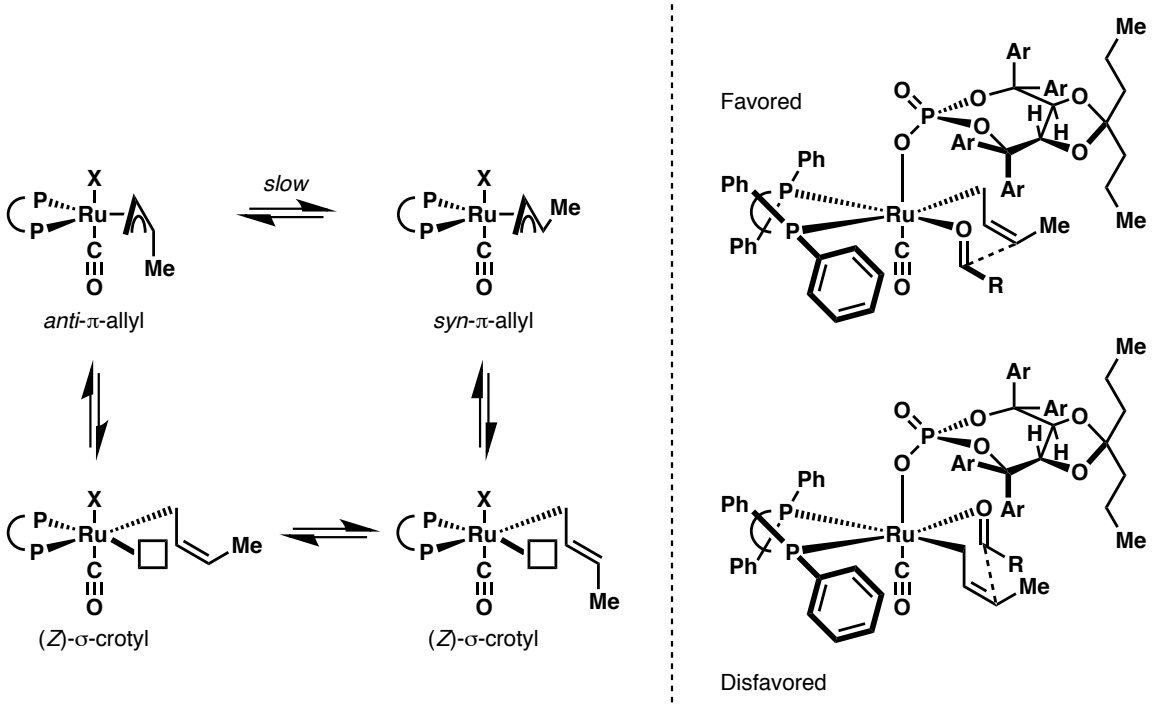

Having successfully developed methods for the construction asymmetric carbonyl crotylation products, it was once again envisioned that the newly discovered crotylation technology could be applied to 1,3-diol systems. In 2011, Krische and coworkers reported the first two-directional crotylation of 1,3-propanediol and related 2-substituted-1,3-propanediols (Figure 1.20).[56] Most interestingly, this methodology proved to be quite selective particularly in the case of 2-methyl-1,3-propanediol, which under the reaction conditions furnished the compound in 6:1 d.r, which refers to the proportion of the product relative to the combination of all of the stereoisomers. As this reaction sets potentially four stereocenters, there are a possible 16 stereoisomers that could be formed.

Figure 1.20 Calculated theoretical distribution of stereoisomers obtained in the double crotylation of 2-methyl-1,3-propanediol based on 98% ee for both *syn*- and *anti*-crotylation events and a 15:1 *anti*:*syn* d.r., as well as the observed results.

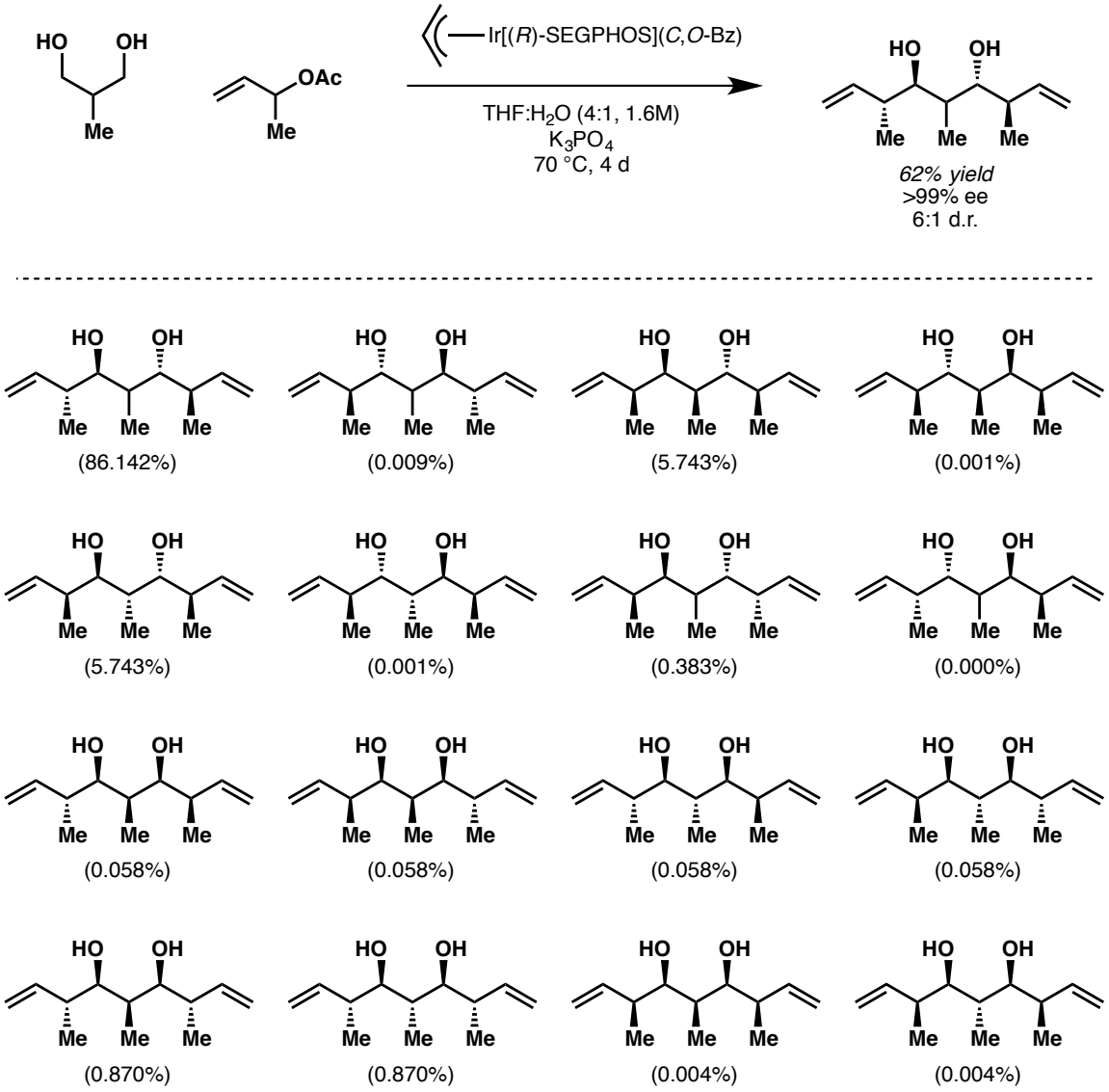

This double crotylation process has no counterpart in conventional crotylmetal chemistry and is unique in its ability to produce acyclic stereoquintets from achiral reactants with good levels of relative and absolute stereocontrol. In addition to the installation of four stereocenters, the reaction also constructs two C-C bonds and the product contains two terminal olefins that could be used as synthetic handles.

1.4 Iridium-Catalyzed Two-Directional Crotylation in Total Synthesis

Methods for the construction of stereoquintet substructures are important due to the prevalence of such motifs in polyketide natural products. Iridium-catalyzed two-directional crotylation affords chiral C_2-symmetric 1,3-diols in a single transformation from inexpensive, highly tractable glycols. As such, this methodology has been applied to the total synthesis of a number of complex natural products. As a consequence of the simplicity with which these complex substructures can be assembled, each total synthesis that has implemented the iridium-catalyzed two-directional allylation represents the most concise route to that natural product. The following is a brief summary of the natural products constructed through application of this technology and will aim to demonstrate how the implementation of this methodology facilitated such concise syntheses.

1.4.1 6-Deoxyerythronolide B

Erythromycin A was the first macrolide antibiotic, produced by Eli Lilly in 1952 (Figure 1.21). Beyond its pharmaceutical impact, the challenges associated with the synthesis of erythromycin A and related polyketides has inspired advances in acyclic stereocontrol via carbonyl addition, such as the construction of C-C bonds using the aldol reaction[57] as well as carbonyl crotylation.[13, 50a, 50c-h] However, despite these advances all reported total syntheses of erythromycin A and related natural products have required lengthy synthetic sequences employing over 20 linear steps. 6-Deoxyerythronolide B **1.63**, a biogentic precursor to many members of the erythromycin family of natural products, was chosen as a testing ground to evaluate the power and versatility of the Krische asymmetric two-directional crotylation in the construction of such a large number of stereogenic centers.

Figure 1.21 Erythromycin A, 6-deoxyerythronolide B **1.63**, and fragment **1.64** constructed via two-directional asymmetric crotylation.

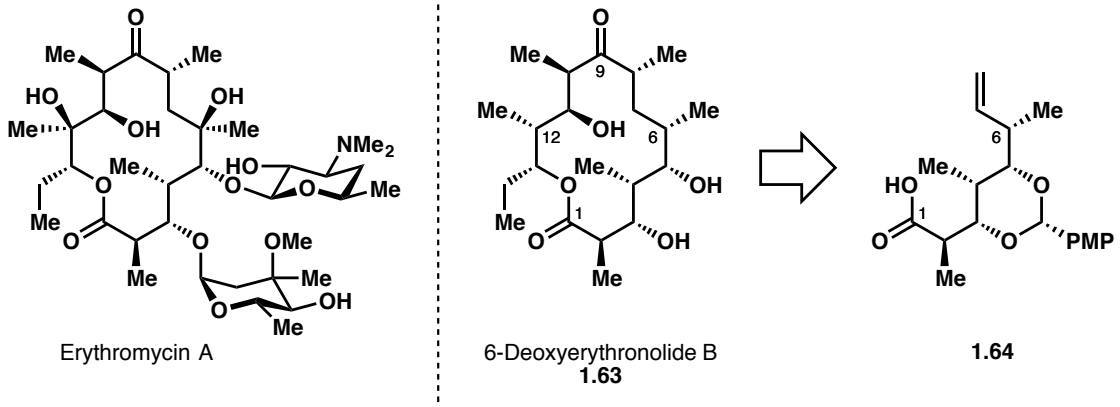

6-Deoxyerthronlide B **1.63** was synthesized from fragment **1.64** (Scheme 1.16).[58] The synthesis of this fragment began with two-directional asymmetric crotylation of 2-methyl-1,3-propanediol in the presence of catalyst **1.65** to afford C_2-symmetric, chiral diol **1.66**. Iodoetherification of **1.66** differentiates the olefin termini and diol moieties and defines the nonstereogenic chirotopic center at C4, which upon benzylation delivers pyran **1.67**. Oxidative cleavage of the terminal olefin with catalytic OsO_4 and oxone followed by Bernet-Vasella cleavage[59] of the iodoether affords β-hydroxy carboxylic acid **1.68**. To convert **1.68** into fragment **1.64**, epimerization of the C3 hydroxy group was necessary. This stereoinversion was accomplished via conversion of **1.68** to β-lactone **1.69** using choromethanesulfonyl chloride. Hydrolysis of the lactone with LiOH and protection of the secondary alcohol furnished fragment **1.64**.

Scheme 1.16 Synthesis of fragment **1.64** of 6-deoxyerythronolide B **1.63**.

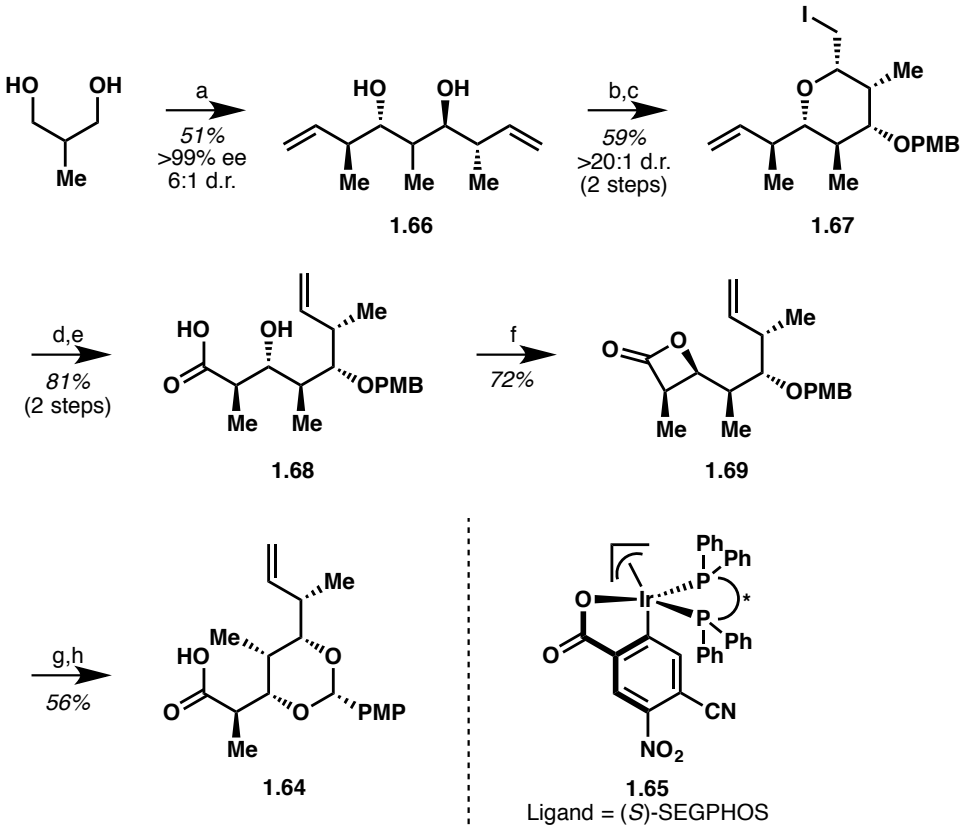

Key: (a) **1.65**, 2-methyl-1,3-propanediol, Na_2CO_3, H_2O, THF, 70 °C; (b) I_2, $NaHCO_3$, MeCN, -20 → 0 °C; (c) $Cl_3C(=NH)OPMB$, CSA, Et_2O, 30 °C; (d) OsO_4, oxone, $NaHCO_3$, DMF; (e) Zn, NH_4Cl, EtOH, reflux; (f) *s*-BuLi, $ClCH_2SO_2Cl$, THF:HMPA, -78 → 0 °C, then pyridine, H_2O, 35 °C; (g) LiOH, dioxane:H_2O; (h) DDQ, 4 Å MS, CH_2Cl_2, 0 °C.

The synthesis of fragment **1.64** was accomplished in just eight steps from 2-methyl-1,3-propanediol. Successful fragment union and further elaboration led to the completion of the total synthesis of 6-deoxyerythronolide B in just 14 linear steps. This represents the most concise total synthesis of any member of the erythromycin family of natural products to date.

1.4.2 Premisakinolide A and C(19)-C(32) of Swinholide A

The efficacy of anticancer agents that disrupt microtubule dynamics (e.g. paclitaxel, docetaxel, ixabepilone, eribulin mesylate)[60] suggests that agents that exhibit the ability to bind actin hold promise for cancer therapy.[61] One such actin-binding compound is swinholide A **1.70**, a marine polyketide isolated from the marine Okinawan sponge *Theonella swinholei* in 1985

(Figure 1.22).[62] Many marine natural products, such as premisakinolide A **1.71**, have structural features in common with swinholide A. The Krische group is currently investigating the application of the two-directional asymmetric crotylation to the total synthesis of swinholide A **1.70**. Recently, Krische and coworkers have reported the synthesis of the C(19)-C(32) domain of swinholide A **1.70**, fragment **1.72**, which also represents a formal synthesis of premisakinolide A **1.71**.[63]

Figure 1.22 Swinholide A **1.70**, premisakinolide A **1.71**, and fragment **1.72**.

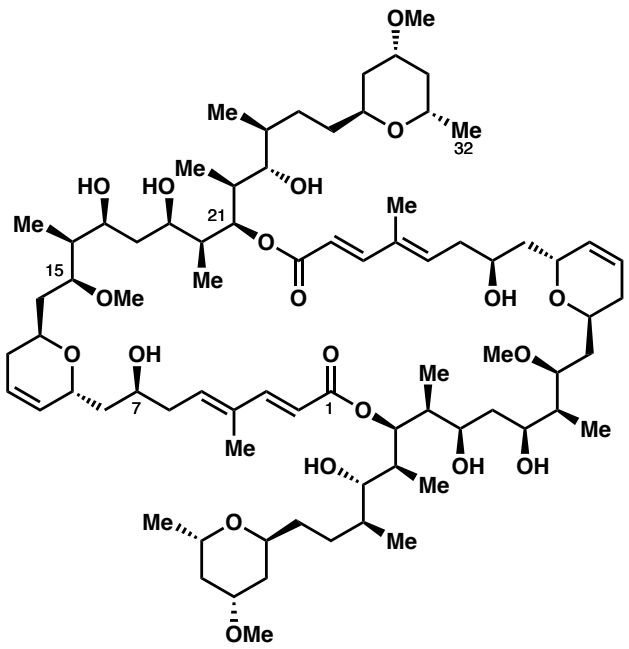

Swinholide A,
1.70

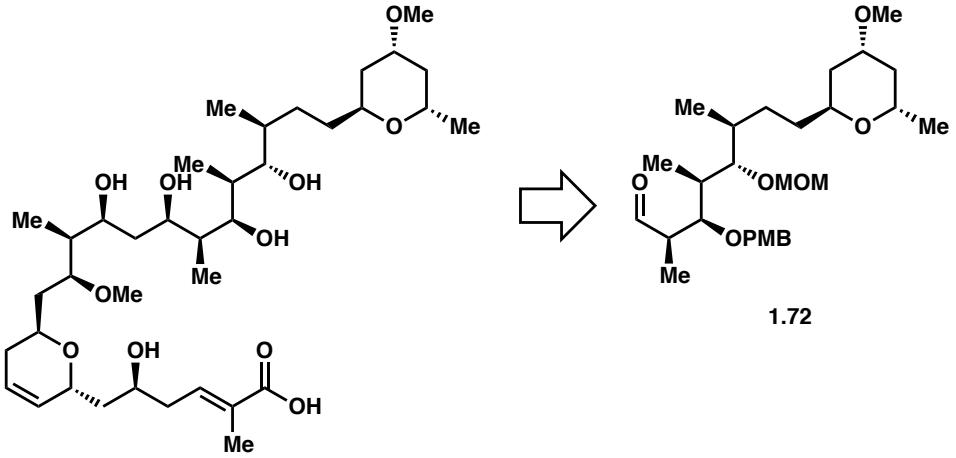

1.72

Premisakinolide A,
1.71

The synthesis of **1.72** began with the construction of the pyran moiety (Scheme 1.17). Iridium-catalyzed asymmetric allylation of commercially available (*S*)-1,3-butanediol affords homoallylic alcohol **1.73**. Cross-metathesis with *cis*-1,4-diacetoxy-2-butene delivers **1.74** (5:1 *E*:*Z*). Tsuji-Trost cyclization using the chiral palladium catalyst modified with ligand **1.75** afforded pyran **1.76** as a 4:1 mixture of diastereomers. Methylation of the secondary alcohol

generates **1.77**. Cross-metathesis between **1.77** with **1.67**, prepared previously in the synthesis of 6-deoxyerythronolide A (Scheme 1.16), furnished **1.78**. Unfortunately, this cross-metathesis proved quite difficult due to the competing isomerization of the terminal olefin of **1.67**. In order to overcome this challenge, five equivalents of **1.67** were used in the reaction. While these conditions were far from ideal, a significant portion of the excess **1.67** could be recovered and recycled. After extensive evaluation of methods for the reduction of the alkene present in **1.78**, it was found that diimide-mediated hydrogenation occurred without partial reduction of the C-I bond or epimerization at C27, which after Bernet-Vasella cleavage of the iodoether delived **1.79**. Protection of the secondary alcohol as the corresponding MOM ether and oxidative cleavage of the terminal olefin furnished **1.72** and completed the formal synthesis of premisakinolide A **1.71** as well as the C19-C32 domain of swinholide A **1.70**. The synthesis of fragment **1.72** was completed in nine steps from (*S*)-1,3-butanediol, which is five steps shorter than the previously reported synthesis.[64]

Scheme 1.17 Formal synthesis of premisakinolide A **1.71** and C(19)-C(32) of swinhoilde A **1.70** via fragment **1.72**.

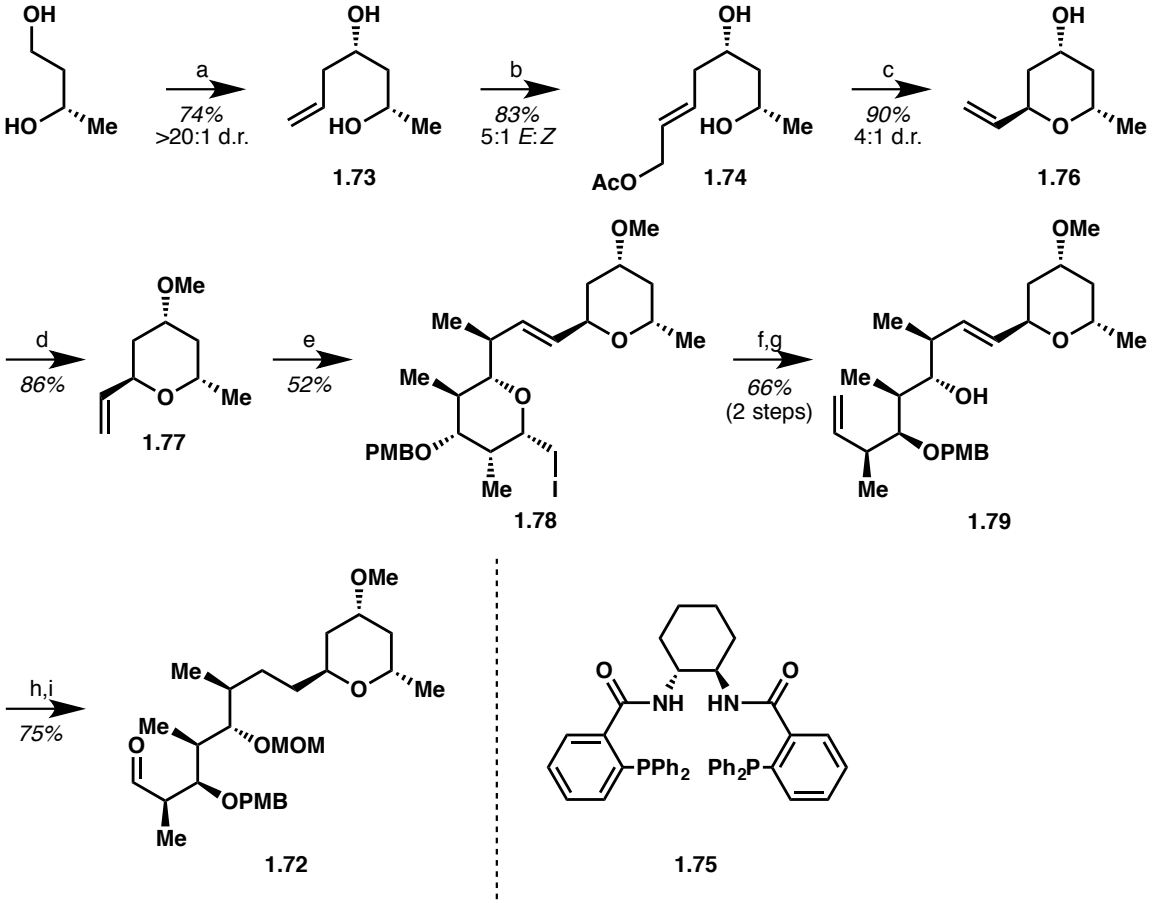

Key: (a) allyl acetate, $[Ir(cod)Cl]_2$, (*S*)-Cl,MeO-BIPHEP, 4-Cl-3-NO_2BzOH, Cs_2CO_3, THF, 100 °C; (b) *cis*-1,4-diacetoxy-2-butene, Grubbs' 2nd Generation, CH_2Cl_2, 50 °C; (c) $Pd_2(dba)_3{\cdot}CHCl_3$, **1.75**, Et_3N, CH_2Cl_2; (d) MeI, ^{t}BuOK, THF; (e) **1.67**, Hoveyda-Grubbs' 2nd Generation, benzoquinone, DCE, 80 °C; (f) $TsNHNH_2$, NaOAc, DME, 95 °C; (g) Zn, NH_4Cl, EtOH, 80 °C; (h) MOMCl, $^i Pr_2NEt$, DCE, 60 °C; (i) OsO_4, NMO, dioxane:H_2O, then $NaIO_4$.

1.4.3 Zincophorin Methyl Ester

Isolated from an asporogenus strain of *Streptomyces griseus* in 1984,[65] zincophorin **1.80** is a polyketide ionophore antibiotic that exhibits potent (<1 ppm) *in vivo* activity against Gram-positive bacteria (Figure 1.23).[66] While there have been many prior syntheses of zincophorin **1.80** and its methyl ester **1.81**, all have required at least 21 steps in the longest linear sequence.[67] Inspired by the previous impact of the two-directional asymmetric crotylation reaction in facilitating a more concise route to natural products, Krische and coworkers sought to demonstrate the power and versatility of this reaction once again in the context of the total

synthesis of zincophorin methyl ester **1.81**. It was anticipated that the molecule could be constructed from pyran fragment **1.82**.

Figure 1.23 Structures of zincophorin **1.80**, zincophorin methyl ester **1.81**, and fragment **1.82**.

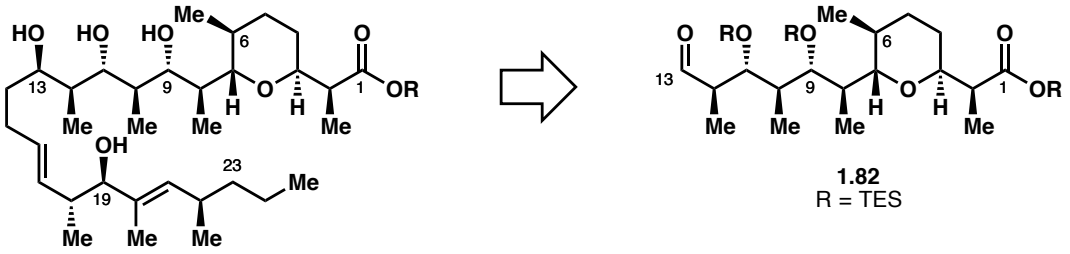

R = H, (+)-Zincophorin **1.80**
R = Me, (+)-Zincophorin methyl ester **1.81**

1.82
R = TES

The synthesis of fragment **1.82** began with two-directional asymmetric crotylation of 2-methyl-1,3-propanediol followed by iodoetherification to generate iodoether **1.83**.[68] Cross-metathesis with *cis*-butene diol diacetate, Bernet-Vasella cleavage of the iodoether, followed by protection of the 1,3-diol as the acetonide delivered allylic alcohol **1.84**. Diastereoselective epoxidation using the Sharpless protocol[69] and subsequent treatment with Gilman's reagent furnishes primary alcohol **1.85**.[70] Hydroformylation of the terminal alkene provides the linear aldehyde,[71] which upon exposure to methanol in the presence of substoichiometric *p*-toluenesulfonic acid delivers pyran **1.86** as a 3:1 mixture of diastereomers that is seperable. Protection of the three free hydroxyl groups as the corresponding TES ethers and subsequent Swern oxidation resulted in the cleavage of the primary TES ether and oxidation to afford fragment **1.82**.

Scheme 1.18 Synthesis of fragment **1.82** using Krische two-directional asymmetric crotylation reaction.

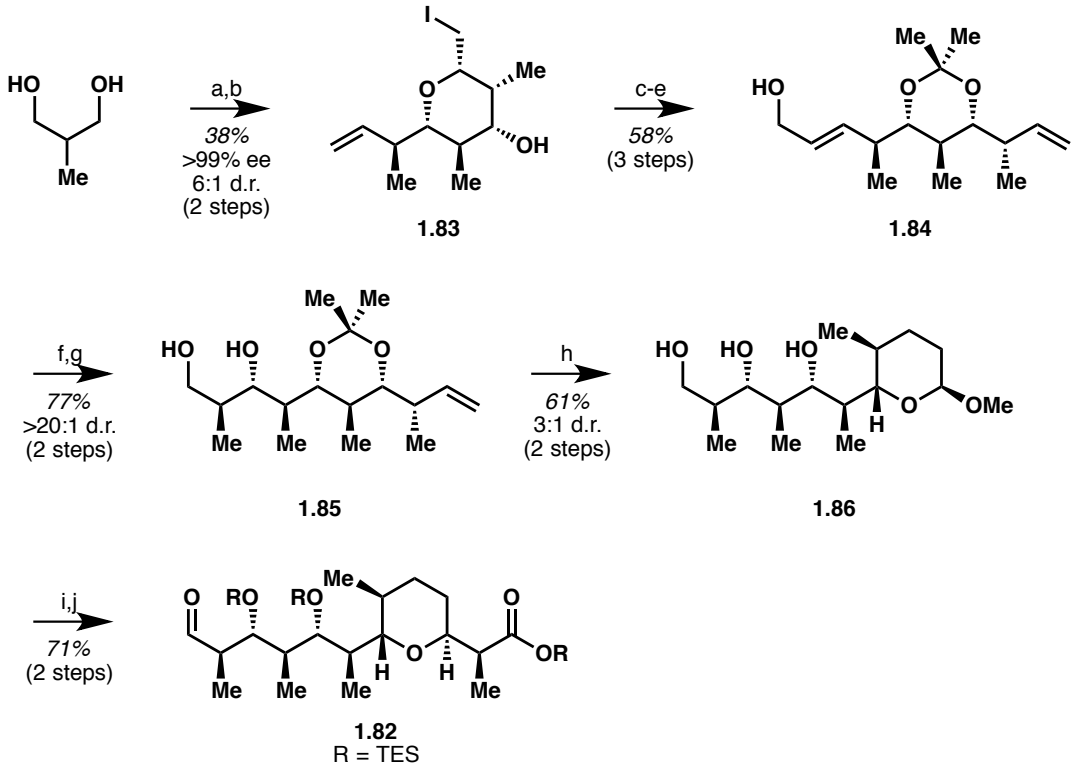

Key: (a) (*S*)-Ir-SEGPHOS, 3-butenyl-2-acetate, Na_2CO_3, H_2O, THF, 70 °C; (b) I_2, $NaHCO_3$, MeCN, -20 → 0 °C; (c) *cis*-butene diol diacetate, Stewart-Grubbs, CH_2Cl_2, 40 °C; (d) Zn, NH_4Cl, MeOH, 85 °C; (e) $Me_2C(OMe)_2$, *p*-TsOH, CH_2Cl_2; (f) (-)-DIPT, $Ti(O^iPr)_4$, *t*-BuOOH, CH_2Cl_2, -20 °C; (g) CuCN, MeLi, THF, -78 → 0 °C; (h) H_2/CO, Rh(CO)(acac), Xantphos, THF, 100 °C, then *p*-TsOH, MeOH, 25 °C; (i) Et_3SiCl, imidazole, DMF; (j) $(COCl)_2$, DMSO, CH_2Cl_2, -78 °C, then Et_3N.

Fragment union and further elaboration concluded with the completion of the total synthesis of (+)-zincophorin methyl ester **1.81** in 13 linear steps. This represents the most concise total synthesis of the natural product to date and is eight steps shorter than the next shortest total synthesis. It is anticipated that the concise nature of this synthetic route will allow for a more complete investigation into its biological properties, studies that are currently underway.

1.5 Conclusions and Outlook

Methods for enantioselective carbonyl allylation and crotylation are of great importance in the field of synthetic organic chemistry. Despite significant progress in achieving high levels

of stereoselectivity and in designing catalytic systems for the transfer of chirality, most methods for carbonyl allylation still rely on the use of preformed stoichiometric allyl metal species. Krische and coworkers developed a suite highly enantioselective methods for constructing products of carbonyl allylation from either the aldehyde or alcohol oxidation state. Most importantly, the ability to employ the corresponding primary alcohols has facilitated the construction of homoallylic alcohol products that would not be accessible via traditional methods for carbonyl allylation.

Diols are inexpensive chemical building blocks useful in the construction of polyol products. The two-directional asymmetric allylation and crotylation reactions with 1,*n*-glycols represent powerful methods for the construction of polyketide natural products as they allow for the construction of two C-C bonds and set mulitple stereocenters in a single transformation. This technology has been implemented in the total synthesis of a number of complex natural products and has resulted in the shortest routes reported to date in all cases in which it has been applied. Further demonstration of the utility of this methodology is ongoing as more biologically active and structurally interesting natural products are isolated and characterized.

Chapter 2: Background Cyanolide A

2.1 Introduction

Natural products are an important source of complex chemical structures that often exhibit biological activity.[72] The identification and development of compounds derived from natural products has yielded new small molecule medicines.[73] Hence, access to the compounds in quantities sufficient for biological evaluation is of critical importance. Methods for the acquisition of such compounds are typically limited to isolation from the natural source directly or through novel chemical synthesis.

Polyketides isolated from soil bacteria are an important class of natural products and represent roughly 20% of the top-selling small molecule drugs.[74] It is estimated that polyketides are five times more likely to possess drug activity compared with other natural product classes.[75] However, culture of soil bacteria is a long-standing problem and less than 5% of soil bacteria that produce polyketides are amenable to culture.[76] Therefore, synthetic methods that provide facile access to complex polyketides are highly desirable, and it is anticipated that polyketides will become even more important as these methods improve and diversify.

Polyketides exhibit biological activity in areas outside of human medicine as well, such as pesticides. Pesticides are of great importance in agriculture, environmental protection, and in preventing the spread of a number of diseases.[77] Schistosomiasis, also known as bilharzia, snail fever, and Katayama fever, is one of the most prevalent parasitic infections with an estimated 207 million people currently infected and 779 million people at risk of infection.[78] At least 200,000 deaths per year are related to the disease,[79] which is caused by parasitic flatworms of the *Schistosoma* genus. Symptoms of schistosomiasis include abdominal pain, diarrhea, popular rash, fatigue, and fever. In individuals who have been infected over a long period of time, liver damage, kidney failure, or bladder cancer may occur. The disease is triggered via a complex immune system response to the eggs laid by a parasitic worm in a human host. It is estimated that 50% are destroyed through inflammation, which can result in scarring and organ

dysfunction. 50% of the eggs laid in a human host ulcerate through the wall of the bowel into the stool. When the eggs reach freshwater, they hatch and release microscopic larvae called miracidium.[79] These tiny larvae next locate and penetrate an aquatic snail, typically of the genus *Biomphalaria*.[80] Inside the snail vector, the miracidium transforms into a sporocyst, which begins to multiply. The daughter sporocysts reproduce asexually and produce thousands of new parasitic larvae, known as cercariae, which leave the snail and enter the surrounding water where they seek a mammalian host to complete their life cycle.

The complexity of the life cycle of these parasitic worms makes prevention of worm transmission problematic.[81] Even if one can eradicate the disease in the host, there remains the possibility of reinfection from exposure to aquatic environments that are inhabited by the snail vector. For this reason, development and application of molluscidal compounds have been explored as a method of controlling the spread of the disease. The most widely available molluscicide is niclosamide **2.1** (Scheme 2.1). While effective, niclosamide is expensive, exhibits poor water solubility, and adversely affects native fish. Alternative methods that circumvent these issues could be of considerable importance in the control of schistosomiasis.

Figure 2.1. Structures of niclosamide **2.1**, (−)-cyanolide **2.2**, and clavosolides A-D **2.3a-d**.

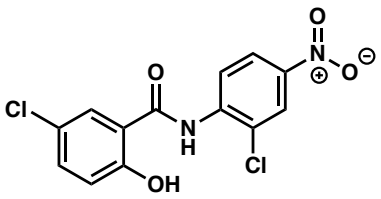

Niclosamide, **2.1**

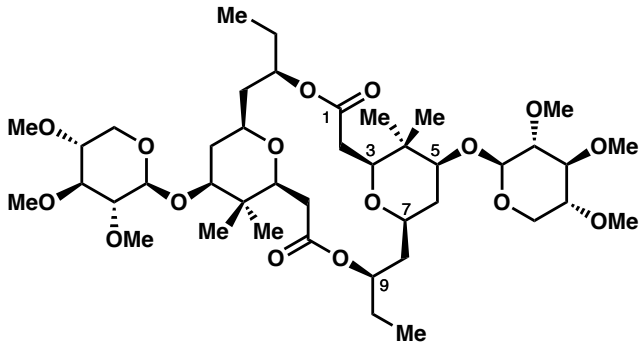

Cyanolide A, **2.2**

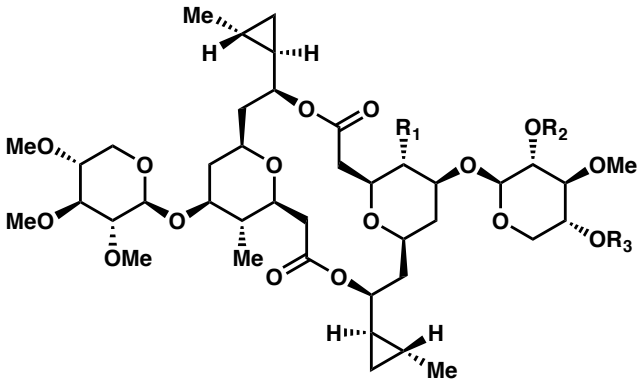

	R_1	R_2	R_3
Clavosolide A, **2.3a**	-Me	-Me	-Me
Clavosolide B, **2.3b**	-Me	-H	-Me
Clavosolide C, **2.3c**	-Me	-Me	-H
Clavosolide D, **2.3d**	-H	-Me	-Me

2.2 Isolation and Bioactivity

In 2010, Gerwick and coworkers isolated and identified cyanolide A **2.2**,[81] a dimeric, glycosidic diolide that exhibits potent molluscicidal activity (LC_{50} = 1.2 μM) against *Biomphalaria glabrata*, a species of snail known to be a host for *Schistosoma*. The compound was found in samples of cyanobacteria, which were identified as *Lyungbya bouillonii*. The biological material was obtained in the form of a dark-reddish mat and was collected by scuba from a shallow reef outside Pigeon Island, Papa New Guinea. The material was extracted multiple times with CH_2Cl_2/MeOH (2:1) and the extract was fractionated by silica gel vacuum

column chromatography. The highly bioactive and spectroscopically interesting fraction was further purified to afford 1.2 mg of cyanolide A.

The bioactivity was evaluated according to a previously developed procedure using the test organism *Biomphalaria glabrata*.[82] A stock solution of cyanolide A (20 mg/mL) in EtOH was prepared. 35 μL of the stock solution was diluted to 7 mL with distilled H_2O. Snails were placed in wells of varying concentrations and observed after 24 h. Snails were assessed to be dead if no heartbeat could be detected upon examination under a dissecting microscope (20x magnification).

2.3 Stuctural Elucidation

Gerwick and coworkers determined the relative structure of cyanolide A. Observation of a parent ion at m/z 855.4735 via HRESIMS was consistent with the molecular formula $C_{42}H_{72}O_{16}$ and 7 degrees of unsaturation. IR spectroscopy indicated the presence of ester and ether linkages and a lack of hydroxyl groups. The ^{1}H NMR spectrum in $CDCl_3$ displayed a methane doublet at δ 4.24, which suggested the presence of a sugar-like moiety. ^{13}C NMR analysis revealed only 21 peaks, which indicated that the molecule contained a plane of symmetry. Comprehensive analysis of cyanolide A using 2D NMR including HSQC, HMBC, COSY, and NOESY were consistent with a dimeric and symmetric structure.

Absolute stereochemistry was proposed assuming that the sugar moieties were derived from D-xylose. Structurally, cyanolide A is most closely related to the clavosolide family of natural products, isolated from the Philipine marine sponge *Myriastra clavosa*.[83] Cyanolide A and the clavosolide family of natural products (**2.3a-2.3d**, Figure 2.1) share a flat dimeric macrocyclic framework that contains xylose-derived moieties. Cyanolide A lacks the *trans*-2-methylcyclopropyl substructure and contains geminal dimethyl substitution at C4, whereas the clavosolides have a single methyl group. Absolute stereochemistry was assigned through total synthesis.

2.4 Prior Total and Formal Syntheses

The synthetic challenges involved with cyanolide A include the stereoselective synthesis of the pyran core of the natural product, installation of the trimethylated D-xylose moiety, and dimerization to afford the macrodiolide structure. There have been six previous syntheses published from the laboratories of Hong, Reddy, She, Pabbaraja, Rychnovsky, and Jennings. Each synthesis will be reviewed focusing primarily on how the above synthetic challenges were overcome.

2.4.1 Hong's Total Synthesis of (−)-Cyanolide A

Hong and coworkers completed the first total synthesis of cyanolide A and confirmed its absolute stereochemistry.[84] The successful synthetic strategy relied on a tandem oxidation/oxa-Michael cyclization of allylic alcohol **2.8** to generate pyran **2.7** (Scheme 2.1). Formation of the macrodiolide structure was proposed via diastereoselective ethylation to give monomer **2.6**, which was anticipated to undergo dimerization to provide **2.4**. Glycosylation of the dimeric macrodiolide was predicted to furnish the natural product. A second approach to the natural product was achieved by ethylation and glycosylation of **2.7** to give monomer **2.5**, which was anticipated to undergo dimerization to provide the natural product.

Scheme 2.1 Hong's retrosynthesis of (–)-cyanolide A.

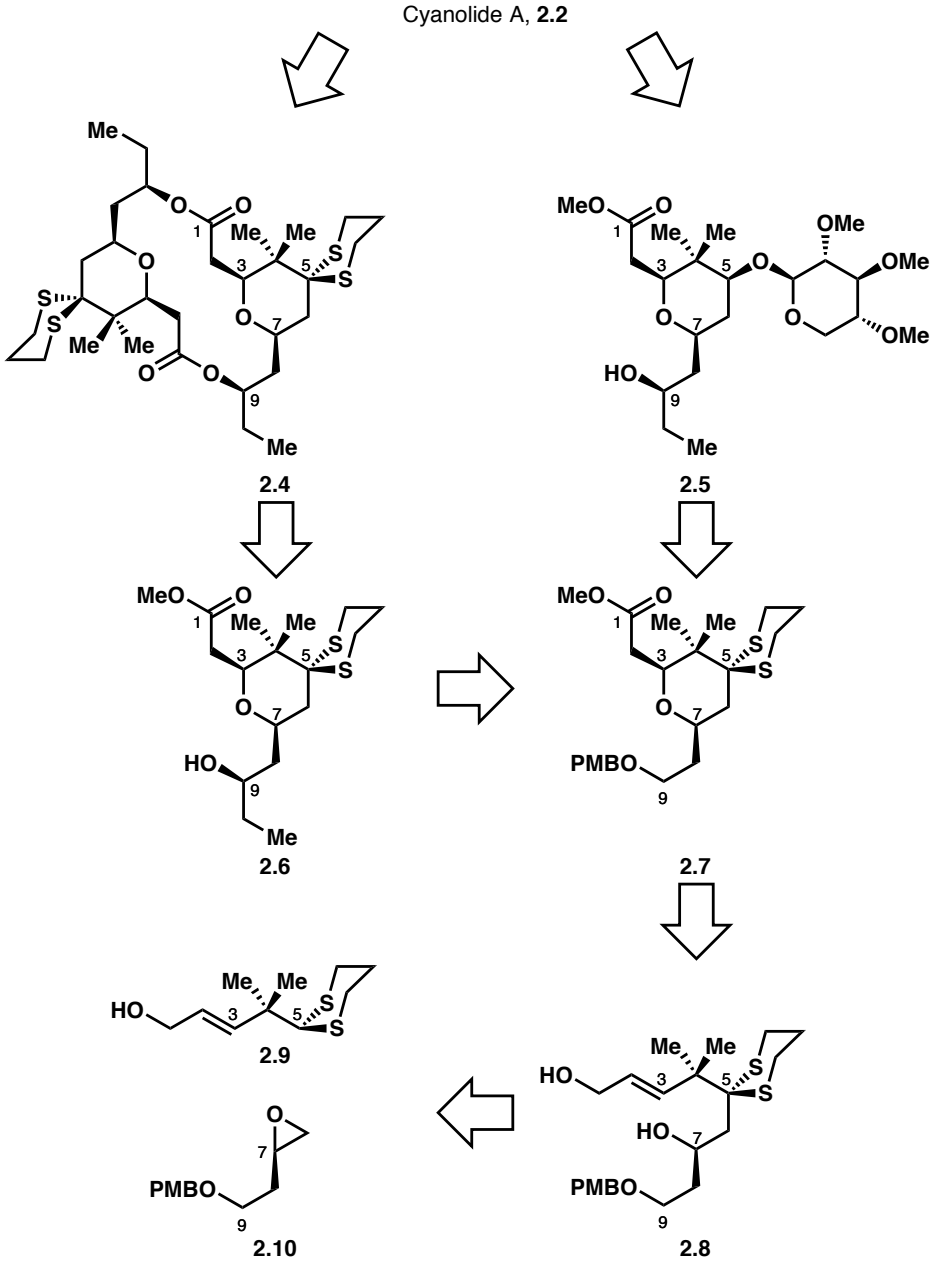

The forward synthesis of the natural product began with generation of the enamine **2.12**, which upon exposure to chloride **2.14** provided aldehyde **2.15** after workup (Scheme 2.2). Wittig homologation followed by DIBAL reduction afforded allylic alcohol **2.9**.[85] Dithiane coupling of **2.9** with known chiral epoxide **2.10** afforded the necessary allylic alcohol (**2.8**) for cyclization.

Treatment of **2.8** with MnO_2 and dimethyl triazolium iodide in the presence of DBU furnished pyran **2.7** in 6 steps from commercially available 1,3-dithiane **2.13**.

Scheme 2.2 Synthesis of common intermediate **2.7**.

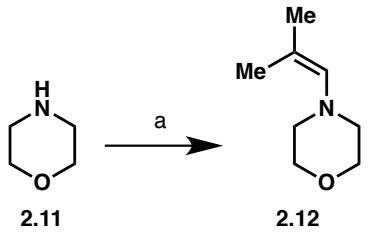

2.11 **2.12**

Key: (a) isobutyraldehyde, removal of H_2O.

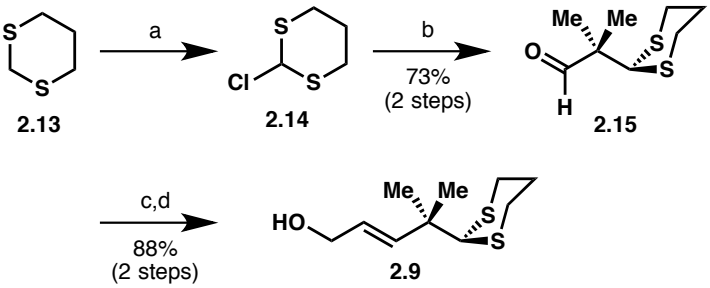

2.13 **2.14** **2.15** **2.9**

Key: (a) N-chlorosuccinamide, benzene; (b) **2.12**, THF:ether (1:1);
(c) trimethyl phosphonoacetate, KO*t*-Bu, THF 0 °C; (d) DIBAL-H, toluene, -78 °C.

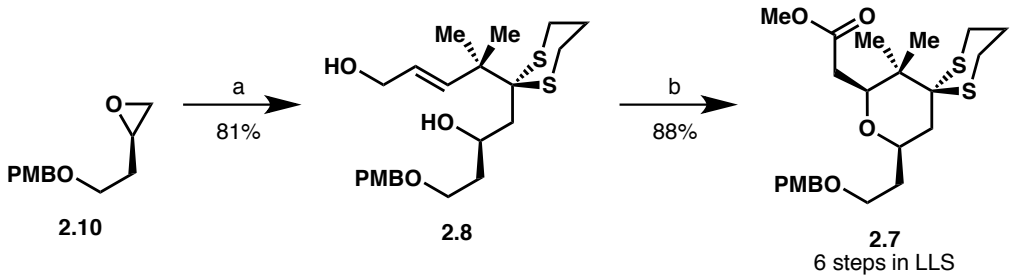

2.10 **2.8** **2.7**
6 steps in LLS

Key: (a) **2.9**, *t*-BuLi, HMPA/THF, -78 °C; (b) MnO_2, CH_2Cl_2, dimethyl triazolium iodide, DBU, MeOH, MnO_2, 4Å MS, 25 °C.

With key intermediate **2.7** in hand, Hong and coworkers first attempted to complete the total synthesis via a strategy consisting of dimerization and then late-stage glycosylation (Scheme 2.3). Deprotection of the PMB group was achieved using DDQ to afford primary alcohol **2.16**. Swern oxidation of **2.16** yielded aldehyde **2.17**, which was subjected to ethylation using Et_2Zn and (+)-MIB to give monomer **2.6**. The monomer **2.6** then underwent macrolactonization under Shiina's conditions to give macrodiolide **2.4**.[86]

Scheme 2.3 Synthesis of the macrodiolide framework.

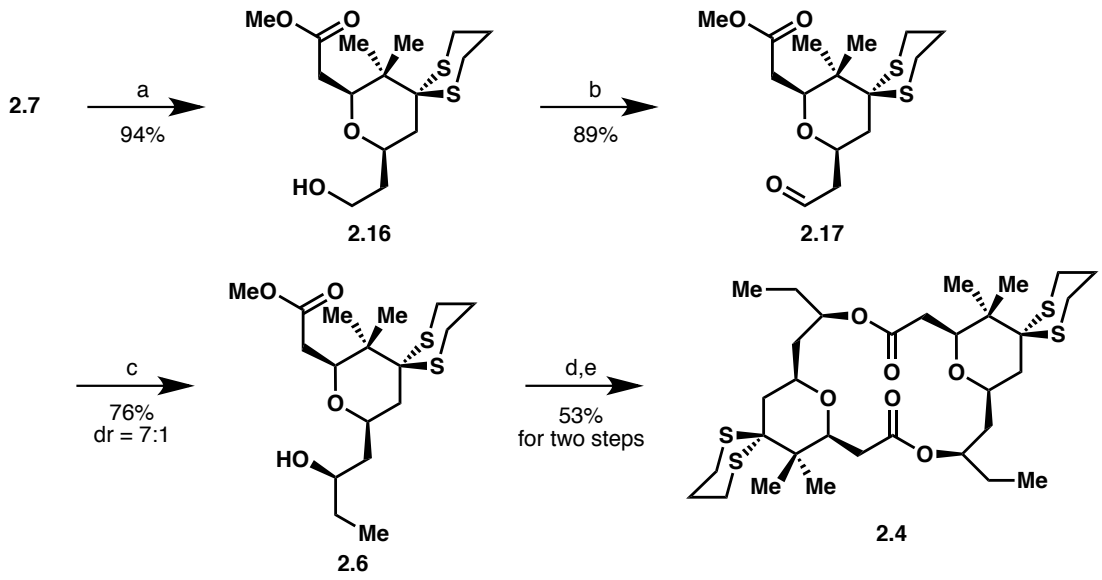

Key: (a) DDQ, H_2O:CH_2Cl_2 (1:10), 25 °C; (b) SO_3·pyr, Et_3N:DMSO:CH_2Cl_2 (1:1:10), 0 to 25 °C; (c) Et_2Zn, (+)-MIB, toluene:hexanes (1:2), 0 °C; (d) LiOH, THF:MeOH:H_2O (2:1:1), 25 °C; (e) MNBA, DMAP, toluene, 90 °C.

Thiophenyl glycoside **2.20** was prepared according to a procedure by Willis and coworkers (Scheme 2.4).[87] The synthesis began with the peracetylation of D-xylose to give **2.18**, which was treated with thiophenol in the presence of BF_3·OEt_2. Hydrolysis with sodium methoxide followed by an acidic workup provided triol **2.19**. Finally, methylation was achieved using NaH with MeI to afford thiophenyl glycoside **2.20**.

Scheme 2.4 Synthesis of thiophenyl glycoside **2.20**.

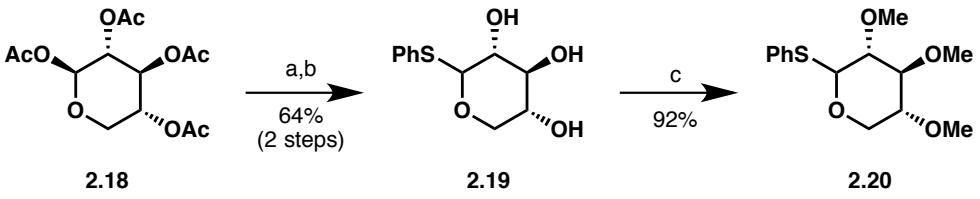

Key: (a) thiophenol, BF_3·OEt_2, CH_2Cl_2, 0 °C; (b) NaOMe, MeOH, 25 °C, then Amberlite IR-120(H^+) resin; (c) NaH, MeI, DMF.

Completion of the first-generation route to cyanolide A was accomplished by deprotection of the 1,3-dithiane protecting group to provide the corresponding ketone **2.21** (Scheme 2.5). Reduction of the ketone functionalities with $NaBH_4$ afforded cyanolide A aglycon **2.22**. The final glycosylation of the aglycon was achieved by treating **2.22** with thiophenyl

glycoside **2.20** in the presence of MeOTf; however, the diastereoselectivity was quite poor (21:33:13, **2.2**: β,α-anomer: α,α-anomer). This first-generation synthesis was completed with a longest linear sequence (LLS) of 14 steps.

Scheme 2.5 Completion of the first generation total synthesis of (–)-cyanolide A.

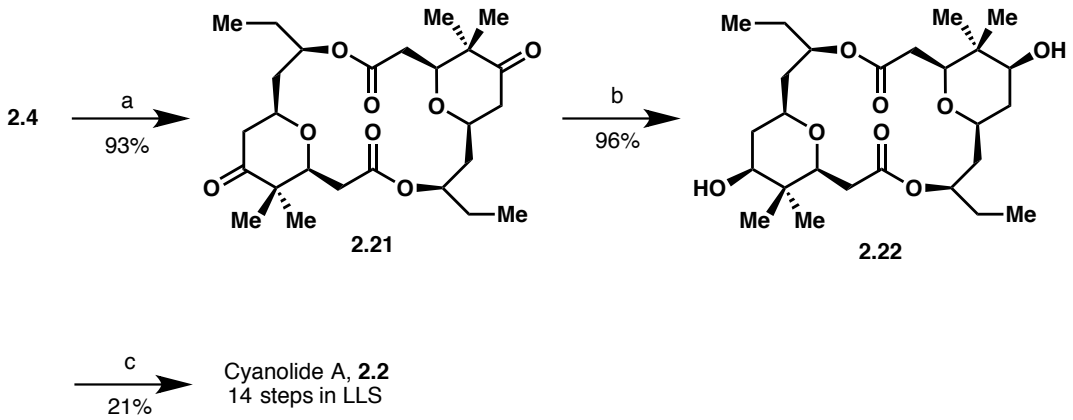

Key: (a) I_2, sat. aq. $NaHCO_3$:CH_3CN (1:1), 0 °C; (b) $NaBH_4$, MeOH, -40 to -20 °C; (c) **2.20**, MeOTf, ether, 4Å MS, 25 °C.

Hong and coworkers also explored a second route in which glycosylation would precede dimerization (Scheme 2.6). Compound **2.7** was first deprotected to afford secondary neopentyl alcohol **2.23**. Glycosylation at this stage with thiophenyl glycoside **2.20** in the presence of MeOTf provided **2.24** as a 3.7:1 mixture of anomers favoring the desired β-anomer. Deprotection of the PMB ether with DDQ, oxidation of the resulting primary alcohol to the aldehyde oxidation state, and diastereoselective ethylation provided methyl ester **2.5**. Ester hydrolysis followed by macrolactonization furnished the natural product in 14 steps (LLS).

Scheme 2.6 Second-generation total synthesis of (–)-cyanolide A.

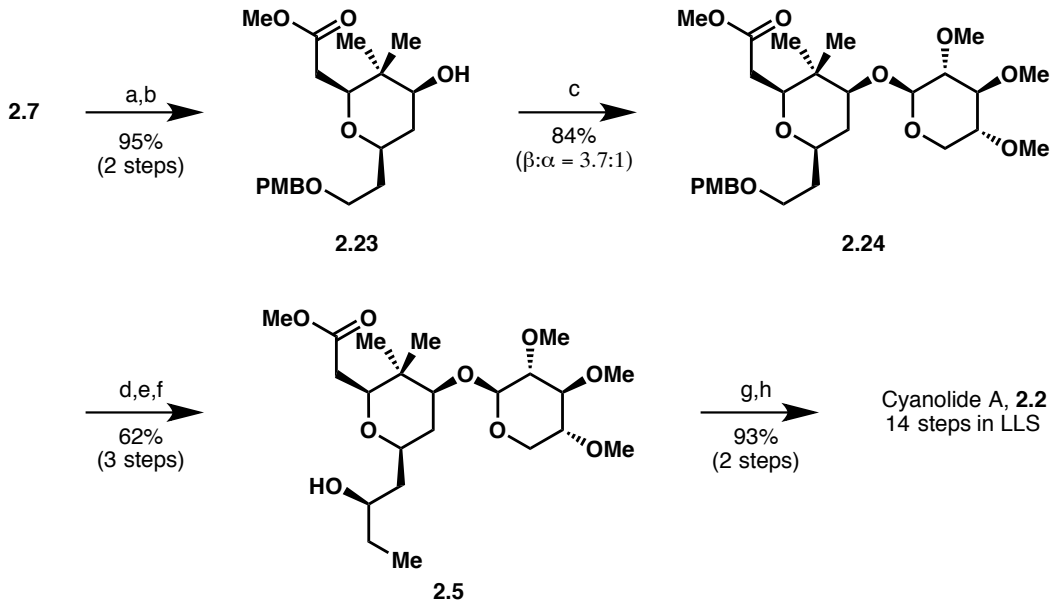

Reagents: (a) I_2, sat. aq. $NaHCO_3$:CH_3CN (1:1), 0 °C; (b) $NaBH_4$, MeOH, -40 to -20 °C; (c) **2.20**, MeOTf, ether, 4Å MS, 25 °C; (d) DDQ, H_2O:CH_2Cl_2 (1:10), 25 °C; (e) TPAP, NMO, 4Å MS, CH_2Cl_2, 25 °C; (f) Et_2Zn, (+)-MIB, toluene:hexanes (1:2), 0 °C; (g) LiOH, THF:MeOH:H_2O (2:1:1), 25 °C; (h) MNBA, DMAP, toluene, 90 °C.

The completion of the second-generation synthesis of (–)-cyanolide A provided the key insight that the installation of the xylose-derived moiety prior to dimerization resulted in higher levels of diastereoselectivity. Comparison of the $[\alpha]^{25}_D$ with that of natural **2.2** enabled the confirmation of the absolute stereochemistry of the natural product.

2.4.2 Reddy's Formal Synthesis of (–)-Cyanolide A

Reddy and coworkers accomplished the formal synthesis of (–)-cyanolide A aglycon starting from (–)-pantolactone (**2.29**, ~$25 / g, Scheme 2.7).[88] Their strategy relied on an oxa-Michael cyclization to construct pyran **2.25**. The requisite alcohol for cyclization, **2.26**, was constructed via Mukaiyama aldol addition to aldehyde **2.28**, which had been prepared previously in the literature.[89]

Scheme 2.7 Reddy's retrosynthesis of (–)-cyanolide A.

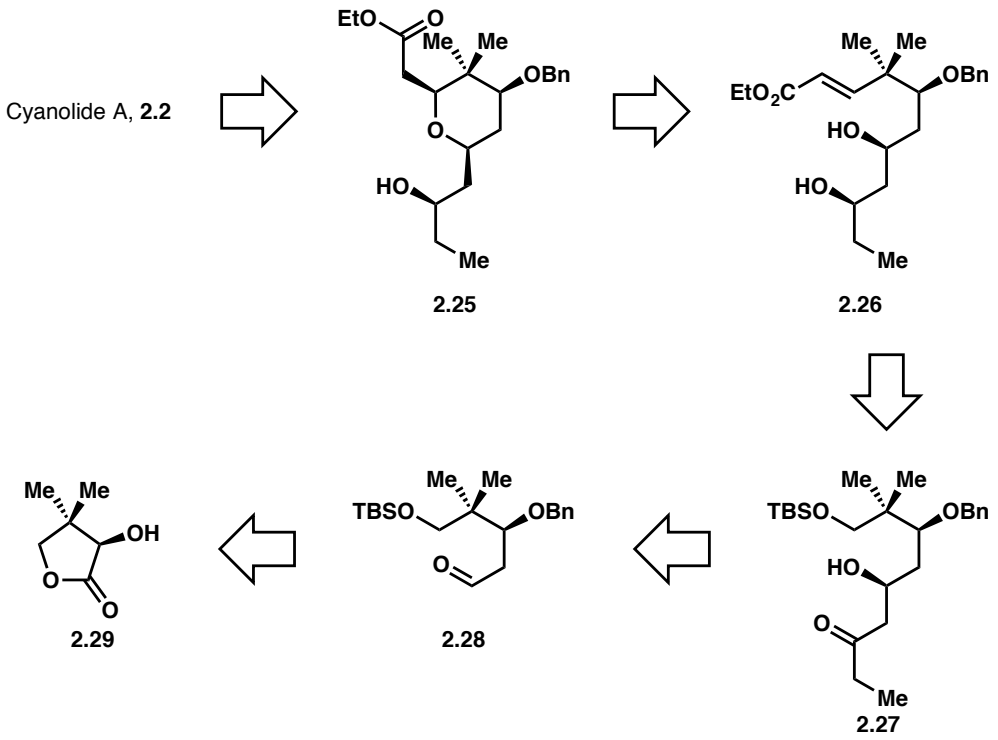

The synthesis began with protection of the secondary neopentyl alcohol of **2.29** as a benzyl ether followed by DIBAL reduction to provide lactol **2.31** (Scheme 2.8). Wittig olefination of the lactol afforded primary alcohol **2.32**, which was protected as TBS ether **2.33**. Hydroboration-oxidation of the terminal alkene produced primary alcohol **2.34**, which was further oxidized to aldehyde **2.28** under Swern conditions.

Scheme 2.8 Synthesis of known aldehyde **2.28**.

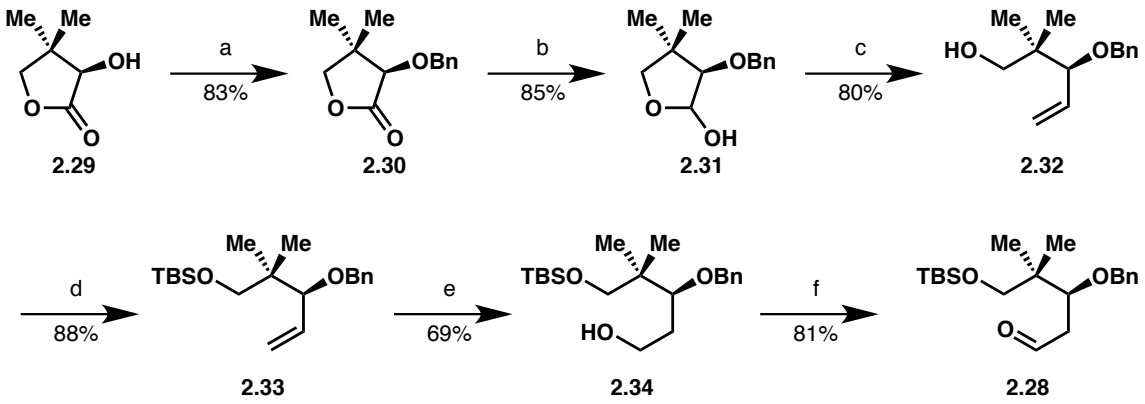

Key: (a) AgO, BnBr, DMF, 0 °C; (b) DIBAL-H, DCM, -78 °C; (c) methyl triphenylphosphonium bromide, THF, n-BuLi in hexanes, 0 °C; (d) TBDMSCl, DMAP, pyridine, 0 °C; (e) BH_3·THF, THF, -20 °C to rt, then NaOH, H_2O_2; (f) $(COCl)_2$, DCM, DMSO, Et_3N, -78 °C.

Mukaiyama aldol of silyl enol ether **2.35** and aldehyde **2.28** afforded the desired β-hydroxy ketone **2.27** with very good diastereoselectivity (>95%, Scheme 2.9). Reduction of the ketone was achieved using catecholborane and the resulting *syn*-1,3-diol was protected as acetonide **2.36**. Next, deprotection of the primary silyl ether and Swern oxidation provide the aldehyde necessary for Wittig olefination, which furnished enone **2.37**. Treatment with PTSA facilitated oxa-Michael cyclization delivering ester **2.25**, which was hydrolyzed and subjected to conditions for Yamaguchi macrolactonization.[90] Completion of the formal synthesis was achieved after hydrogenative deprotection of the benzyl ethers and provided (–)-cyanolide A aglycon **2.22** in 16 steps from (–)-pantolactone **2.29**.

Scheme 2.9 Completion of the formal synthesis of (–)-cyanolide A.

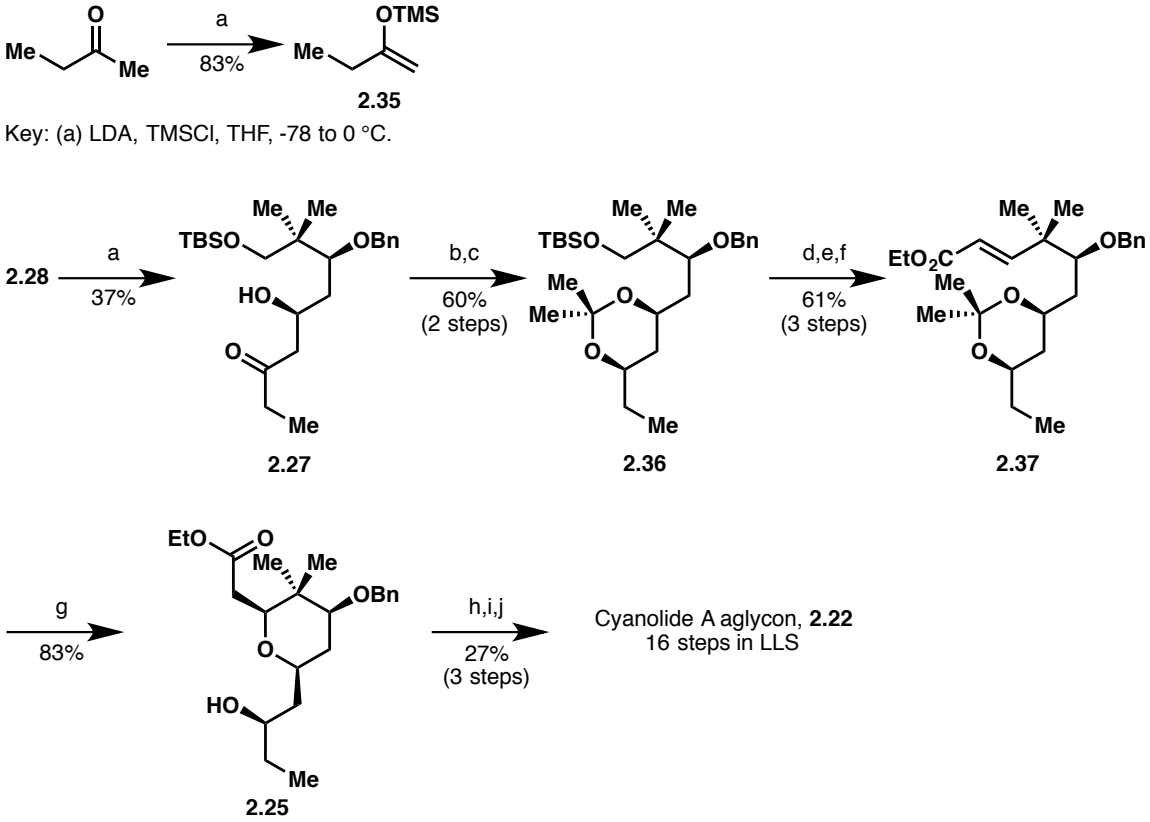

Key: (a) **2.35**, $BF_3{\cdot}Et_2O$, DCM, -78 °C; (b) catecholborane, THF, -10 °C; (c) 2,2-dimethoxypropane, PPTS, DCM, 25 °C; (d) TBAF, THF, 60 °C; (e) $(COCl)_2$, DMSO, Et_3N, DCM, -78 °C; (f) $Ph_3PCHCOOEt$, toluene, reflux. (g) PTSA, $CHCl_3$, reflux; (h) $LiOH{\cdot}H_2O$, H_2O:MeOH:THF (1:1:2), 25 °C; (i) 2,4,6-trichlorobenzoyl chloride, Et_3N, THF, DMAP, toluene, reflux; (j) $Pd(OH)_2$, MeOH, H_2, rt.

2.4.3 She's Formal Synthesis of (–)-Cyanolide A

She and coworkers' approach to (–)-cyanolide A required the synthesis of methyl ester **2.5** (Scheme 2.10),[91] which could undergo macrolactonization to access the natural product as previously described by the Hong group.[84] Synthesis of pyran **2.38** was anticipated to come from a Pd-catalyzed intramolecular alkoxycarbonylation reaction of terminal alkene **2.39**. Installation of the prenyl moiety was to be achieved from oxidative cleavage of alkene **2.40** and a subsequent Barbier-type reaction.

Scheme 2.10 She's retrosynthesis of (–)-cyanolide A.

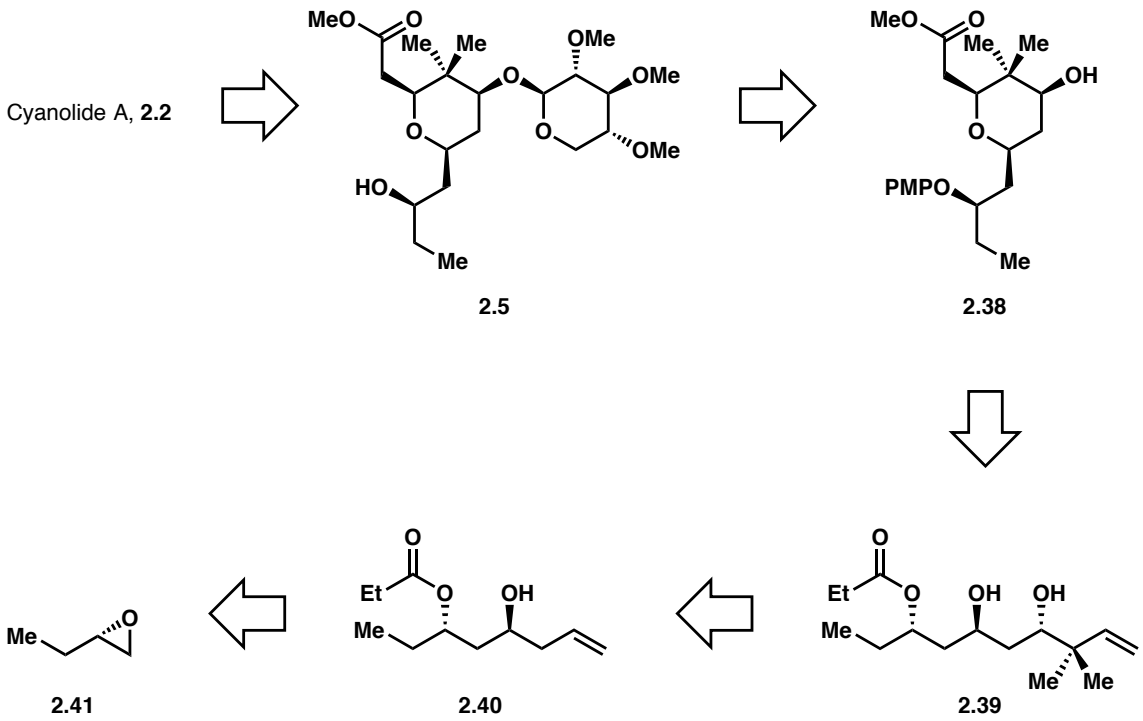

The synthesis began with the coupling of chiral epoxide **2.41** with 2-allyl-1,3-dithiane followed by deprotection to give ketone **2.43** (Scheme 2.11). Evans-Tishchenko reduction in the presence of ethyl formate provided terminal alkene **2.40**. Barbier-type coupling with prenyl bromide afforded alkene **2.39** as a 1:1 mixture of diastereomers (only one diastereomer is shown, however both were successfully converted to the natural product).

Scheme 2.11 Synthesis of pyran precursor **2.39**.

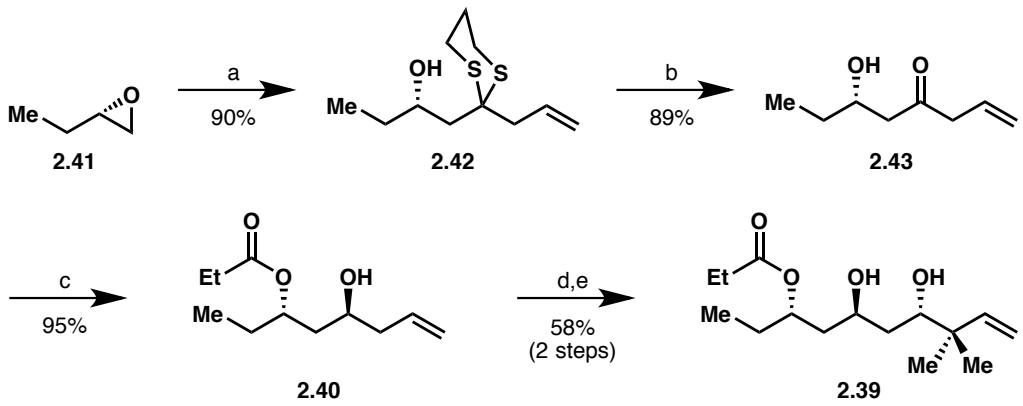

Key: (a) 2-allyl-1,3-dithiane, BuLi, THF, 0 °C; (b) I_2, $CaCO_3$, THF:H_2O (4:1), 0 °C; (c) SmI_2, EtCHO, THF, -10 °C; (d) O_3, DCM, -78 °C; (e) Zn, prenyl bromide, aq. NH_4Cl:THF (4:1), 0 °C.

Acetonide protection of the 1,3-diol substructure followed by reductive deprotection of the ethyl ester yielded terminal alkene **2.44** (Scheme 2.12). The stereochemistry of the free hydroxyl group was inverted under Mitsunobu conditions with 4-methoxyphenol, and acidic hydrolysis of the acetonide gave PMB ether **2.45**. Upon exposure to carbon monoxide in the presence of $CuCl_2$ and catalytic $PdCl_2$, compound **2.45** underwent intramolecular alkoxycarbonylation to afford pyran **2.38**. Glycosylation of the secondary neopentyl alcohol with **2.20** followed by oxidative removal of the PMP ether furnished known methyl ester **2.5** and thus completed the formal synthesis of (–)-cyanolide A in 13 steps from chiral epoxide **2.41**.

Scheme 2.12 Completion of the formal synthesis of (–)-cyanolide A.

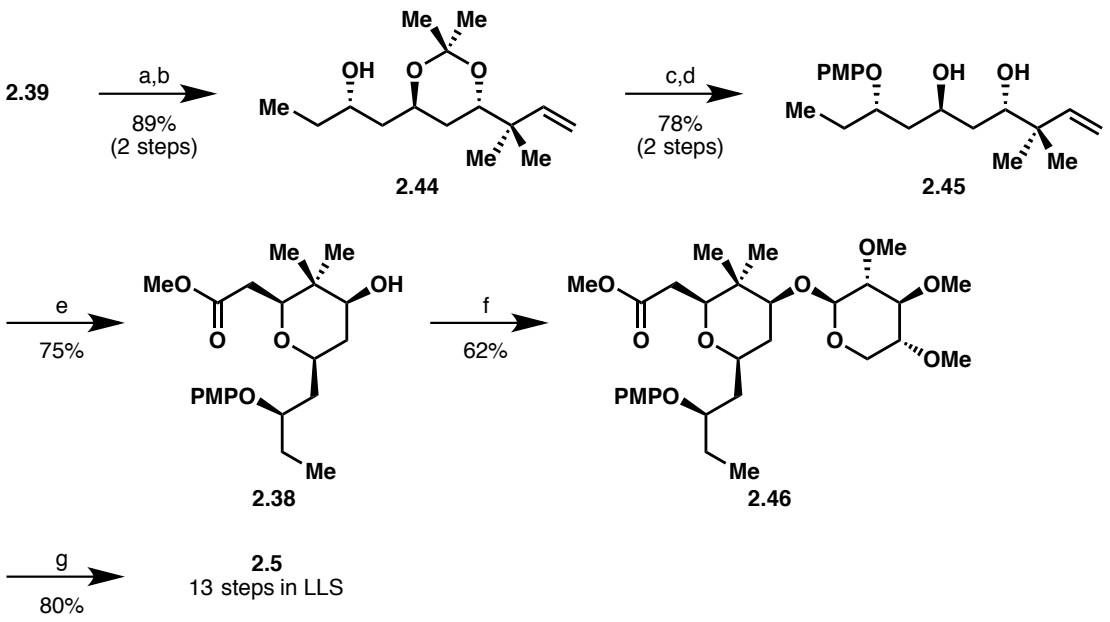

Key: (a) 2,2-dimethoxypropane, TsOH (cat.), DCM, 0 °C; (b) $LiAlH_4$, THF, 0 °C; (c) 4-methoxyphenol, DIAD, PPh_3, THF, 25 °C; (d) 1 N HCl, MeOH, 0 °C; (e) $PdCl_2$ (cat.), $CuCl_2$, CH_3CN, MeOH, CO, 30 °C; (f) **2.20**, MeOTf, 4Å MS, 25 °C; (g) CAN, CH_3CN:H_2O (4:1), 0 °C.

2.4.4 Pabbaraja's Formal Synthesis of (–)-Cyanolide A

The Pabbaraja group's formal synthesis of (–)-cyanolide A[92] was proposed beginning with **2.29** in a manner similar to that of Reddy (Scheme 2.13) with the goal of synthesizing cyanolide A algycon **2.22**. Their strategy to access the aglycon hinged on oxidation and dimerization of alcohol **2.47**. This alcohol was to be synthesized from lactone **2.48** via a tandem reaction involving Wittig olefination and oxa-Michael cyclization.

Scheme 2.13 Pabbaraja's retrosynthesis of (–)-cyanolide A.

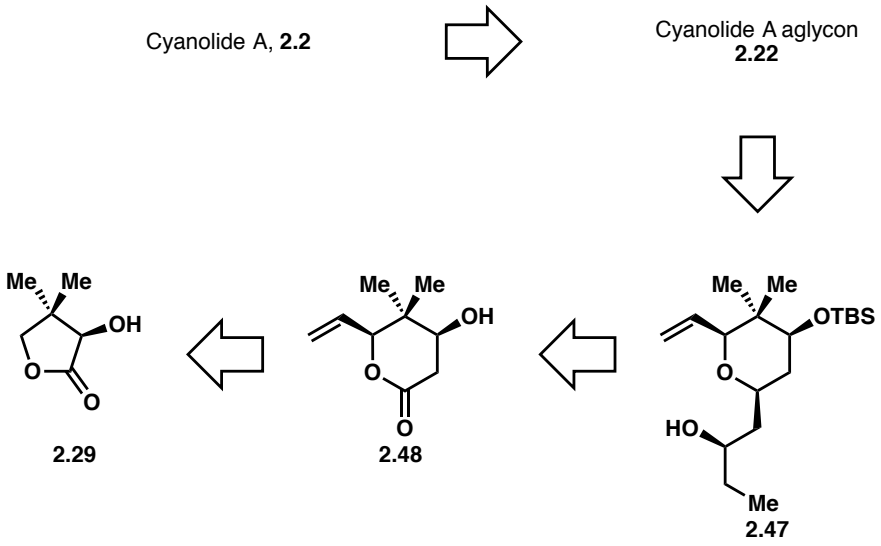

The synthesis began from known alcohol **2.32** that was synthesized in three steps from **2.29** (Scheme 2.14). Oxidation of the primary alcohol followed by a Crimmin's acetate aldol reaction produced alcohol **2.50** with good levels of stereoinduction, 9:1, favoring the desired diastereomer. Compound **2.50** was transformed into amide **2.51** upon exposure to Weinreb's salt and imidazole. Treatment of the amide with lithium naphthalenide resulted in debenzylation as well as cleavage of the *N-O* bond to afford diol **2.52**. Exposure of diol **2.52** to $Ba(OH)_2 \cdot 8H_2O$ led to the formation of lactone **2.48**.

Scheme 2.14 Synthesis of lactone **2.48**.

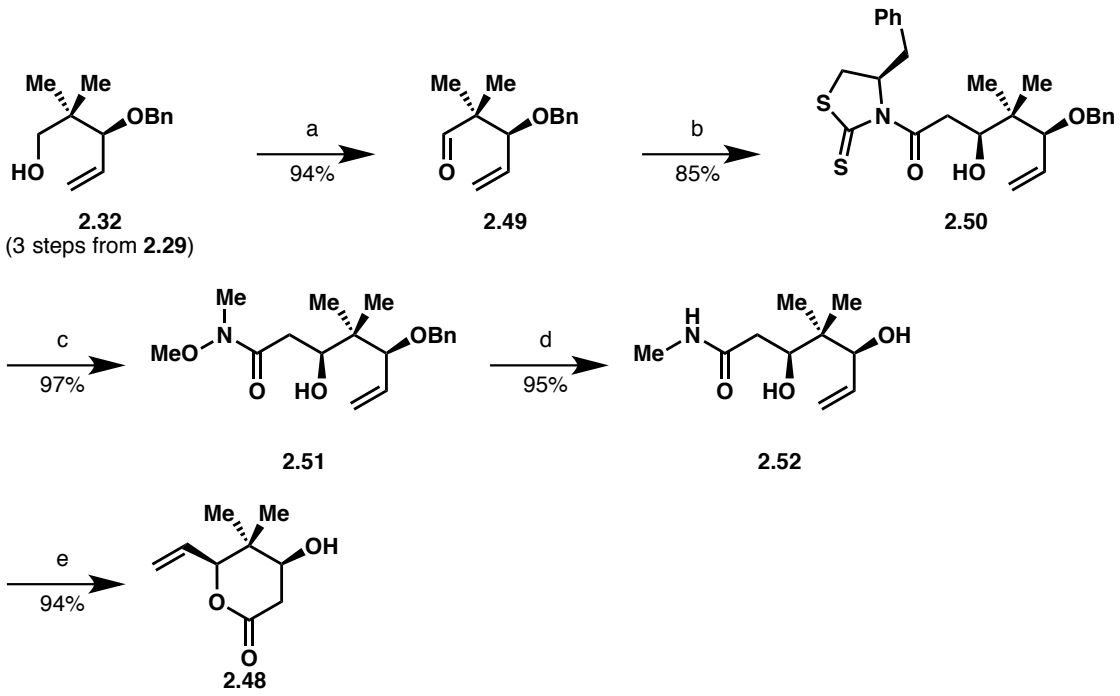

Key: (a) PCC, CH_2Cl_2, rt; (b) (*R*)-1-(4-benzyl-2-thioxothiazolidin-3-yl)ethanone, $TiCl_4$, DIPEA, CH_2Cl_2, 0 °C to -78 °C; (c) $CH_3NHOCH_3{\cdot}HCl$, imidazole, CH_2Cl_2, rt; (d) lithium naphthalenide, THF, -20 °C; (e) $Ba(OH)_2{\cdot}8H_2O$, THF:H_2O (1:1), rt.

Elaboration of **2.48** began with reduction of the lactone to the lactal and subsequent tandem Wittig olefination and oxa-Michael cyclization, which provided **2.53** as an inseperable mixture of diastereomers (7:2 in favor of the stereochemistry shown, Scheme 2.15). The secondary neopentyl alcohol was protected as a TBS ether and the ketone was reduced using the (*S*)-CBS catalyst to afford alcohol **2.47** as a seperable mixture of diasteromers (4:1 in favor of the stereochemistry shown). The terminal olefin underwent hydroboration-oxidation to provide primary alcohol **2.55**. Selective oxidation of the primary alcohol with TEMPO and BAIB yielded the requisite seco-acid for macrolactonization, which proceeded smoothly under Shiina's conditions to furnish macrodiolide **2.56**. Deprotection of the silyl protecting groups completed the formal synthesis of (–)-cyanolide A in 16 steps from **2.29**.

Scheme 2.15 Completion of the formal synthesis of (–)-cyanolide A.

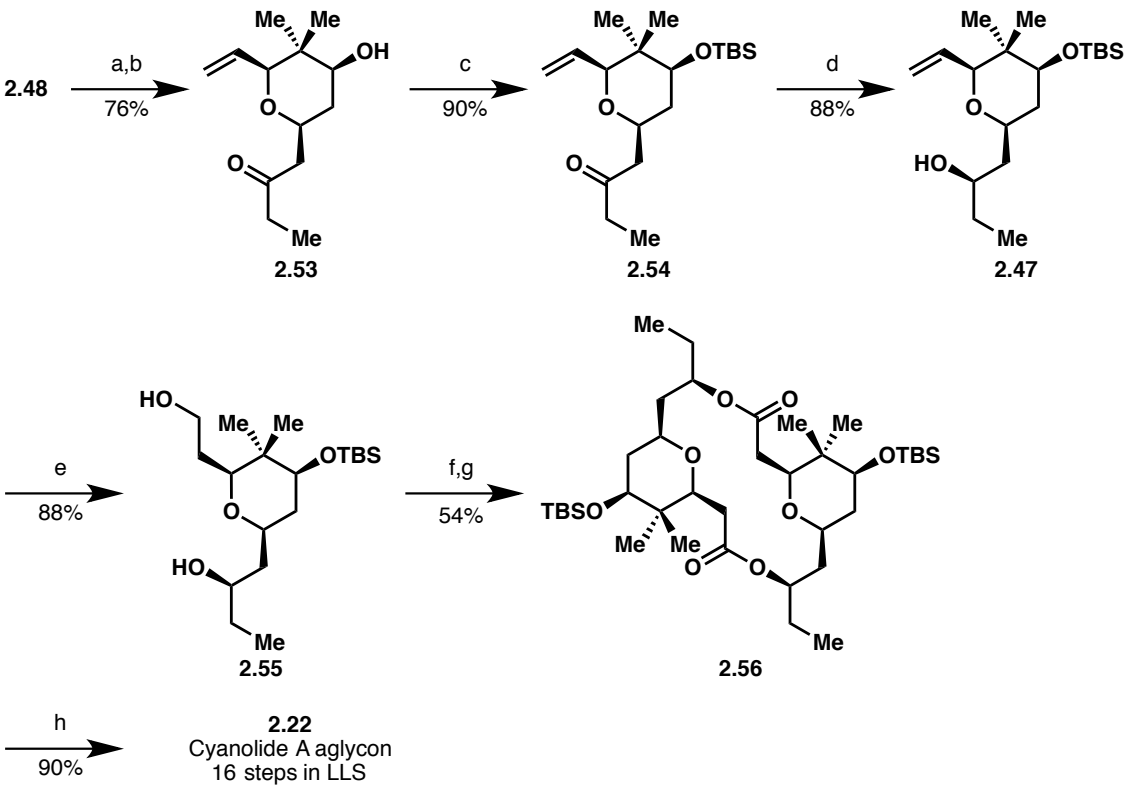

Key: (a) DIBAL-H, CH_2Cl_2, -78 °C; (b) 1-(triphenylphosphoranylidene)butan-2-one, benzene, reflux; (c) TBSCl, 2,6-lutidine, DMF, 0 °C to rt; (d) (*S*)-CBS, BH_3·DMS, THF, -30 °C; (e) BH_3·DMS, NaOH, H_2O_2, THF, 0 °C; (f) TEMPO, BAIB, CH_2Cl_2:H_2O (2:1) 0 °C to rt; (g) MNBA, DMAP, toluene, 90 °C; (h) 70% HF.pyr, THF, 0 °C to rt.

2.4.5 Rychnovsky's Formal Synthesis of (–)-Cyanolide A

The formal synthesis proposed by Rychnovsky and coworkers showcased a Sakurai dimerization of allylsilane **2.57**, which was to be converted to known ketone **2.21** (Scheme 2.16).[93] The allylsilane was believed to be accessible from α-bromo ester **2.59**.

Scheme 2.16 Rychnovsky's retrosynthesis of (–)-cyanolide A.

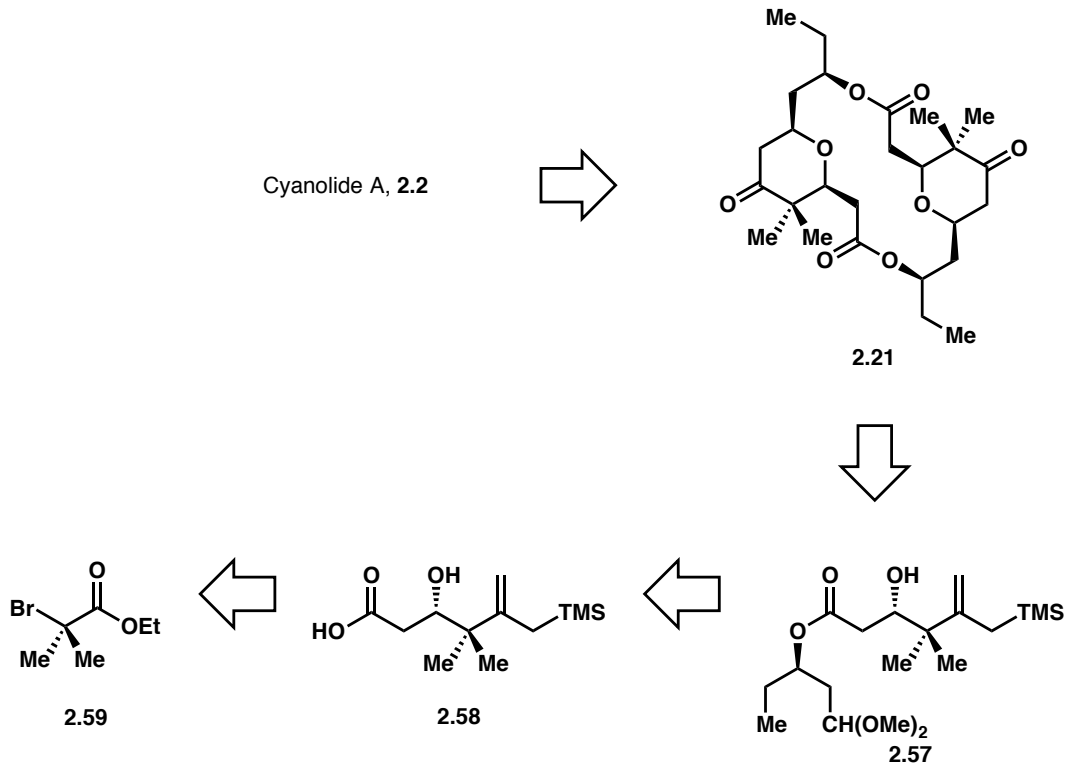

The synthesis of carboxylic fragment **2.58** began with Barbier-type coupling of α-bromo ester **2.59** and ethylorthoformate to generate acetal **2.60** (Scheme 2.17). Exposure of the acetal to $LiCH_2TMS$ followed by enol triflate formation using KHMDS and $PhNTf_2$ produced vinyl triflate **2.62**. Kumada coupling and deprotection of the acetal under mildly acidic conditions afforded aldehyde **2.64**. Aldol reaction with Nagao's auxiliary under Sammakia's conditions yielded alcohol **2.65**, which upon hydrolysis revealed carboxylic acid **2.58**.

Scheme 2.17 Synthesis of carboxylic acid **2.58**.

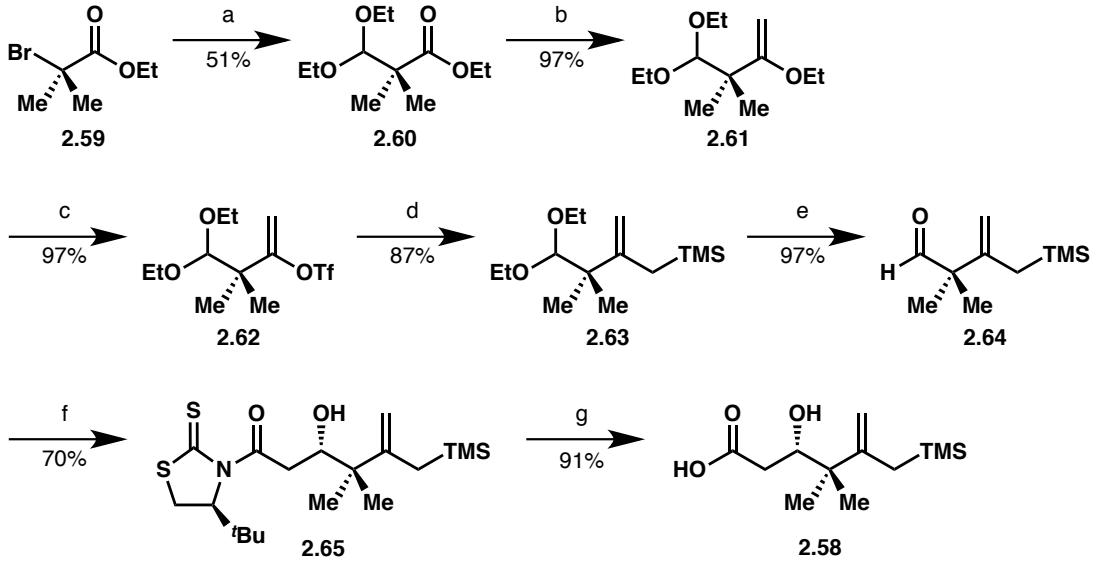

Key: (a) Zn, ethylorthoformate, benzene; (b) $LiCH_2TMS$, pentane, 0 °C; (c) KHMDS, $PHNTf_2$, THF, -78 °C; (d) $ClMgCH_2TMS$, $Pd(PPh_3)_4$, LiCl, Et_2O, 0 °C; (e) *p*TSA·H_2O, H_2O:acetone (1:1); (f) (*S*)-1-(4-(tert-butyl)-2-thioxothiazolidin-3-yl)ethanone, (-)-sparteine, $PhBCl_2$, CH_2Cl_2, 0 °C; (g) LiOH·H_2O, H_2O:THF (1:2.6), 0 °C.

Acetal fragment **2.68** was synthesized in two steps from chiral epoxide **2.66** (Scheme 2.18). Coupling of fragment **2.68** and **2.58** was achieved under Yamaguchi's conditions for esterification to produce β-hydroxy ester **2.57**. Sakurai dimerization was achieved through treatment of **2.57** with TMSOTf to give macrodiolide **2.69**, which was subsequently oxidized to furnish known ketone **2.21**. The formal synthesis was completed in 10 steps from **2.59**.

Scheme 2.18 Completion of the formal synthesis of (–)-cyanolide A.

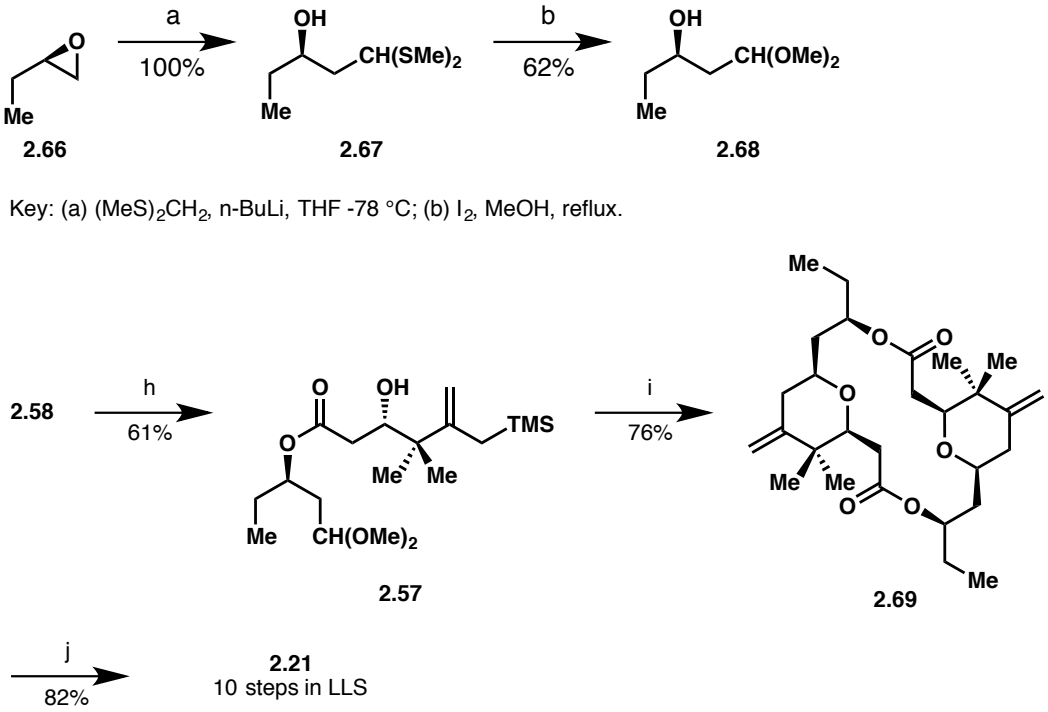

2.4.6 Jennings' Formal Synthesis of (–)-Cyanolide A

The formal synthesis of (–)-cyanolide A devised by Jennings and coworkers required seco-acid **2.70** for macrolactonization to provide access to aglycon **2.22**.[94] Jennings hypothesized that alkylation of lactone **2.**71 followed by a stereoselective oxocarbenium ion reduction would produce the desired monomer. Lactone **2.71** was anticipated to be accessible from aldehyde **2.72**, which could be synthesized from homoallylic alcohol **2.73**.

Scheme 2.19 Jenning's retrosynthesis of (–)-cyanolide A.

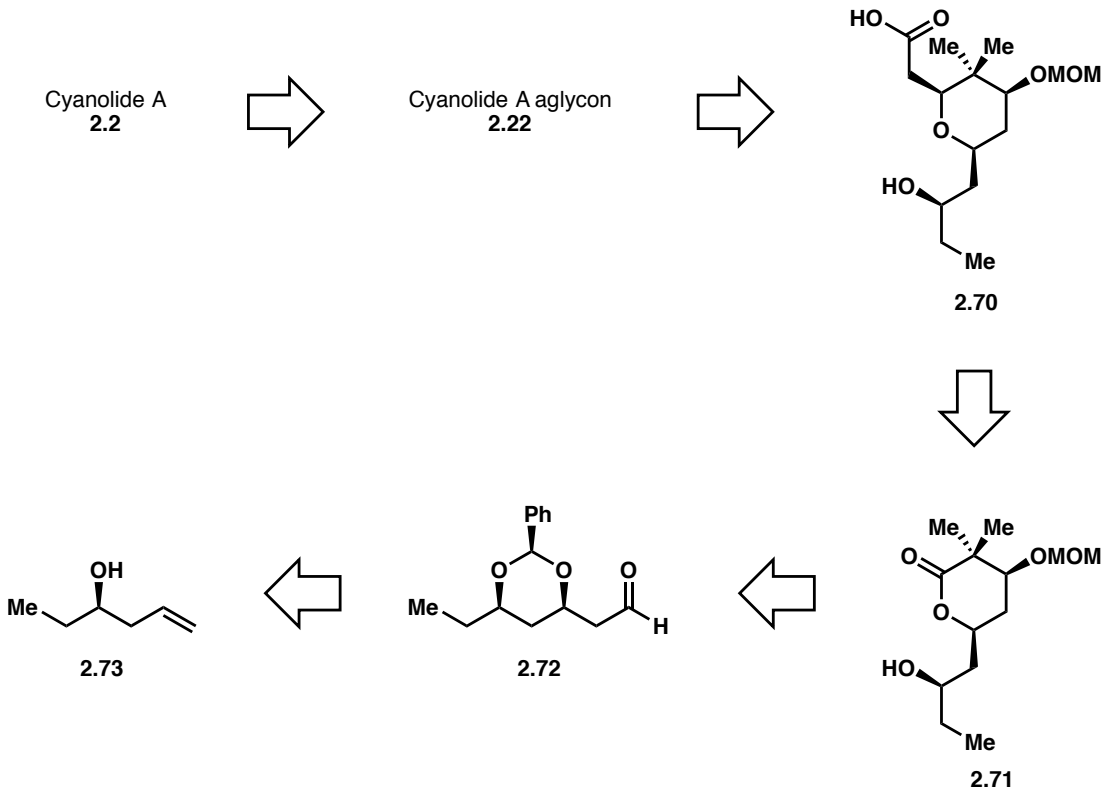

The forward synthesis began with homoallylic alcohol **2.73**, which had been prepared in three steps from (–)-α-pinene (Scheme 2.20). Cross-metathesis with 2-ethylhexyl acrylate provided enone **2.74**, which underwent tandem acetalization and oxa-Michael cyclization to afford acetal **2.75**. Reduction of the ester with DIBAL followed by diastereoselective Mukaiyama aldol gave β-hydroxy ester **2.76** and the hydroxyl group was protected as MOM ether **2.77**. Hydrogenation of **2.77** removed the acetal protecting group and subsequent treatment with TFA effected cyclization to yield lactone **2.71**.

Scheme 2.20 Synthesis of lactone **2.71**.

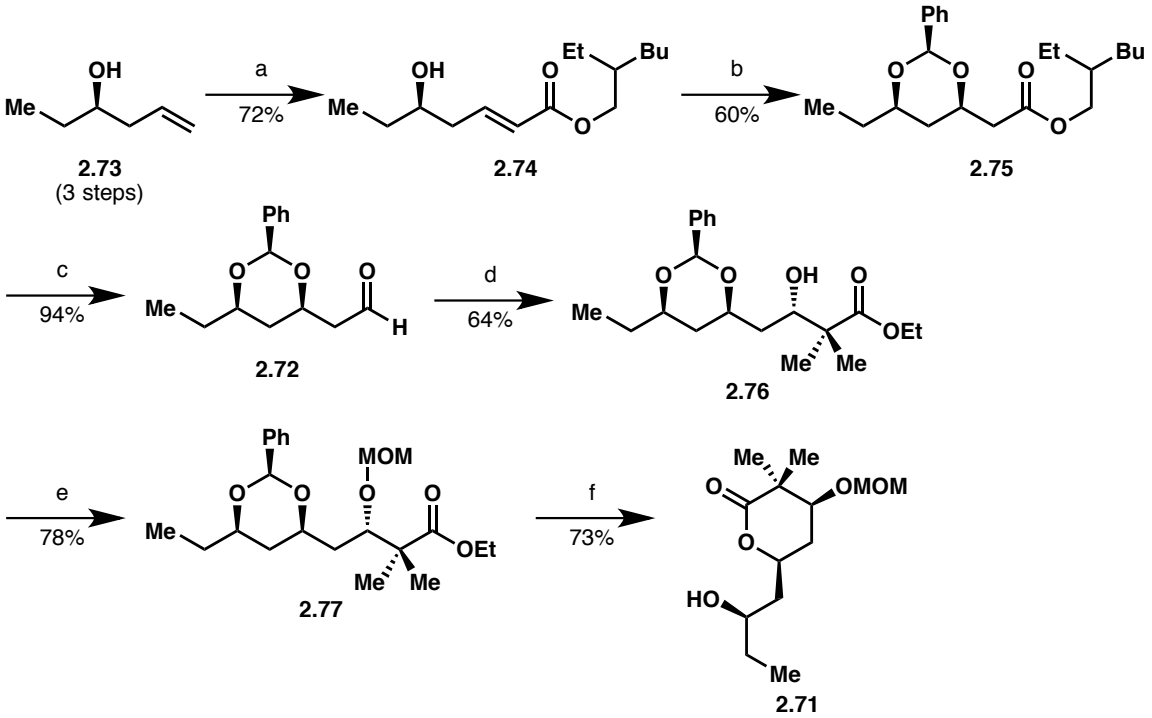

Key: (a) 2-ethylhexyl acrylate, Grubbs' 2nd Generation, benzene, rt; (b) PhCHO, tBuOK, THF, 0 °C; (c) DIBAL, CH_2Cl_2, -78 °C; (d) ((1-ethoxy-2-methylprop-1-en-1-yl)oxy)trimethylsilane, $BF_3{\cdot}Et_2O$, CH_2Cl_2, -78 °C; (e) MOMCl, DIPEA, CH_2Cl_2; (f) $Pd(OH)_2$, H_2, MeOH, rt, then TFA, THF, H_2O.

The key step in Jennings' synthesis was alkylation of lactone **2.71** and stereoselective reduction of the oxocarbenium ion generated under acidic conditions (Scheme 2.21). Coupling of allylmagnesium bromide to lactone **2.71** at low temperature followed by addition of TFA led to formation of an oxocarbenium ion, which was selectively reduced with Et_3SiH to afford pyran **2.78**. Ozonolysis of the terminal alkene followed by Pinnick oxidation provided seco-acid **2.70**, which underwent macrolactonization under Yamaguchi's conditions to furnish macrodiolide **2.80**. Deprotection of the MOM ether produced (–)-cyanolide A aglycon and completed the formal synthesis in 14 steps (LLS) from (–)-α-pinene.

Scheme 2.21 Completion of the formal synthesis of (–)-cyanolide A.

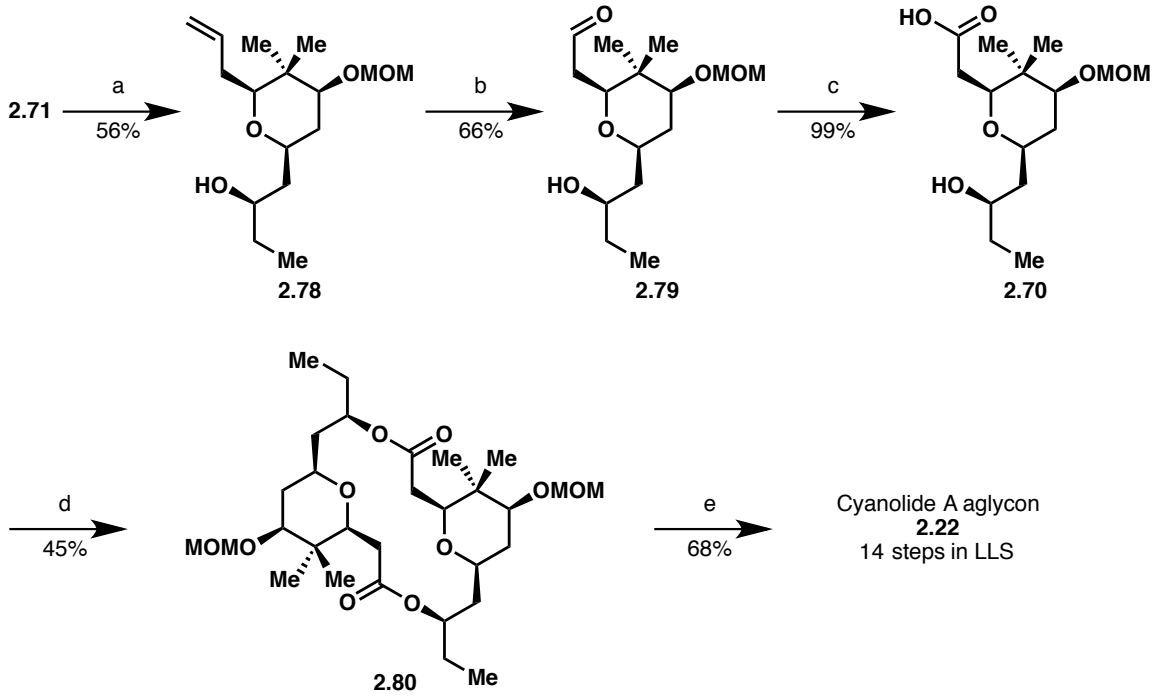

Key: (a) allylmagnesium bromide, THF, -78 °C, then TFA, CH_2Cl_2; (b) O_3, CH_2Cl_2, -78 °C; (c) $NaClO_2$, NaH_2PO_4, 2-methyl-2-butene, ^tBuOH, -10 °C; (d) 2,4,6-trichlorobenzoyl chloride, DMAP, toluene, 125 °C; (e) $LiBF_4$, CH_3CN:H_2O, 60 °C.

2.5 Conclusions

The potent molluscicidal activity and complex structure compelled researchers to synthesize cyanolide A. Each of these completed syntheses confirmed the proposed structure and illustrated the utility and limitations of methodologies used to construct polyketides. However, these routes typically required synthetic concessions such as multiple protecting group manipulations and repeated oxidation state adjustments. Our intention was to develop a more concise and versatile synthetic route that combines the information learned from these previous syntheses with our newly developed metal-catalyzed transformations. In doing so, this would lead to the development of a synthetic route to (–)-cyanolide A that requires roughly half of the steps as the shortest previous synthesis, thereby enabling rapid access to this important natural product.

Chapter 3: Total Synthesis of (−)-Cyanolide A

3.1 First-Generation Total Synthesis of (−)-Cyanolide A

Within the field of synthetic organic chemistry, total synthesis has often been the testing ground for new methodologies and strategies.[95] As chemical technology advances, the question of synthetic feasibility has diminished while concern for practicality and efficiency has been augmented. This balance between feasibility and efficiency is specifically exemplified in the synthesis of polyketide natural products. Progress made in the field of carbonyl addition chemistry has led to the development of a plethora of methods for the construction of polyketides; however, these methods typically require the use of stoichiometric chiral auxiliaries and pre-metallated reagents. While these transformations address the feasibility of complex chemical synthesis, they represent an interim solution to the challenge of *de novo* polyketide construction. As organic molecules are compounds composed of carbon and hydrogen, the terminal solutions to this challenge will encompass stereoselective and atom-efficient methods for skeletal assembly involving the addition, removal, or redistribution of hydrogen in the absence of protecting groups, discrete oxidation level adjustment, or non-constructive functional group interconversions.[96] Therefore, methods that allow for the direct transformation of feedstock chemicals into complex, value-added compounds are ideal. The concept of ideality in regards to chemical synthesis has garnered significant attention over the last half century.

In 1975, Hendrickson first defined parameters that he believed could be used to evaluate a synthetic sequence in an effort to establish the ideal chemical synthesis.[97] His definition of an ideal synthesis involves a synthetic sequence that begins with available small molecules and is comprised only of successive construction events that require no intermediary re-functionalization. Furthermore, functional groups should be correctly placed when installed within the carbon framework. Recently, Baran and coworkers have constructed a metric to evaluate and quantify the ideality of a synthesis. They define the percent ideality as the sum of construction reactions and strategic redox reactions divided by total number of steps (multiplied

by 100%). Non-strategic reactions included reduction and oxidation reactions that do not install functionality in the oxidation state present in the final compound as well as protecting group manipulations. Reducing the number of synthetic steps required to produce complex molecules is important as it reduces time, effort, and expenses associated with the development and implementation of a chemical synthesis.

In prior syntheses of (–)-cyanolide A **3.1**, multiple synthetic concessions were made in order to access the desired final compound. Due to the highly oxygenated nature of **3.1**, oxidation state adjustments and differential protection of hydroxyl functional groups represented a significant fraction of the total number of synthetic transformations. Most syntheses began with commercially available chiral starting materials and thus stereoinduction was performed stoichiometrically. Even with a chiral center installed, many of the prior syntheses required chiral auxiliaries to enforce high levels of stereoselectivity. While chiral auxiliaries can sometimes be inexpensive and recyclable, their use still requires additional synthetic manipulations beyond the construction event. Finally, C-C bonds formed through the use of premetallated *C*-nucleophiles are often employed with great success; however, they typically require multiple stages of pre-activation and generate stoichiometric waste products. These waste products are often of higher molecular weight than the nucleophile that was incorporated into the chemical structure of the product. These issues of atom,[98] step,[99] and redox-economy[100] are all concessions and illustrate the need for synthetic methodologies and strategies that can be used to synthesize complex molecules in a more direct manner. These concerns helped guide and shape our synthetic strategy as it applied to the total synthesis of (–)-cyanolide A.

3.1.1 Retrosynthetic Analysis

Our synthetic strategy for the total synthesis of (–)-cyanolide A **3.1** was derived from the idea that the macrodiolide natural product could be constructed through elaboration and dimerization of pyran **3.2**, in a manner similar to that of the prior syntheses (Scheme 3.1).[101] Construction of pyran **3.2** was envisaged to take place via a bidirectional cross-metathesis of

chiral C_2-symmetric, chiral diol **3.3** with ethyl vinyl ketone and subsequent acid-promoted oxa-Michael cyclization. Chiral diol **3.3** had been previously prepared as an example of asymmetric iridium-catalyzed two-directional allylation.[102] The total synthesis would thus begin from neopentyl glycol **3.4**, an inexpensive (~$30 / mol) chemical feedstock.

Scheme 3.1 Retrosynthetic analysis of (–)-cyanolide A.

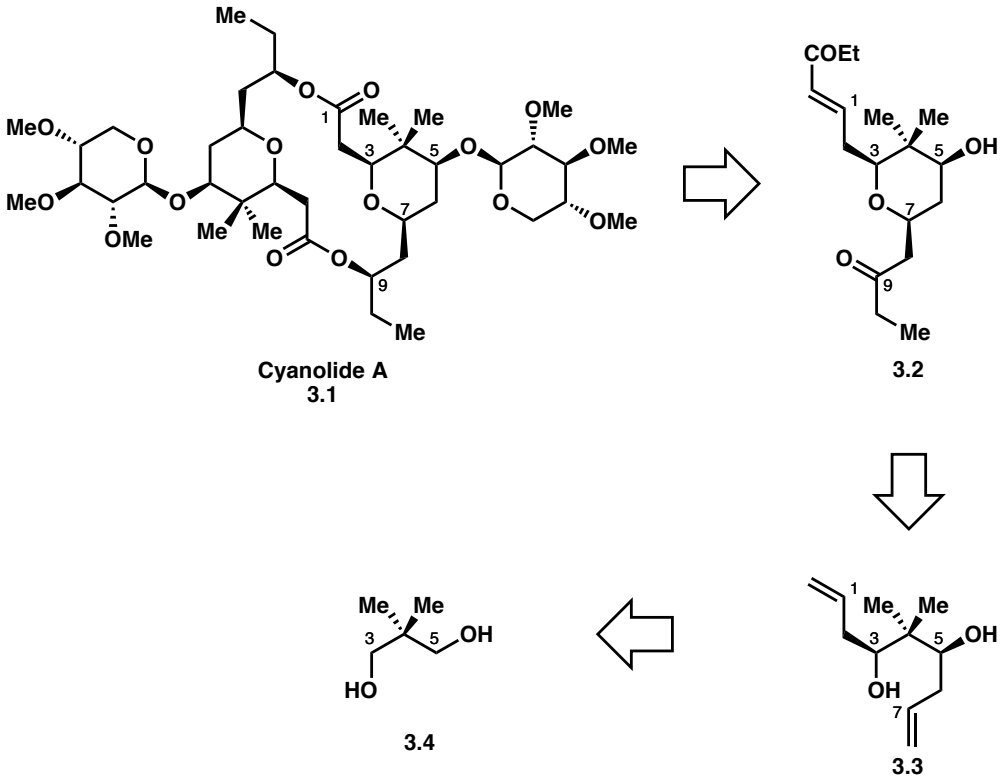

3.1.2 Synthesis of Pyran 3.2

Our synthesis began with the installation of the C3 and C5 stereocenters through asymmetric two-directional allylation (Scheme 3.2). It is worth emphasizing again that the construction of diol **3.3** via traditional methods for carbonyl addition would require 8 steps, more than half of which are non-strategic reactions. This lengthy preparation stems from the inherent instability of 1,3-dialdehydes, which can undergo enolization and self-condensation in cases when not fully substituted at the 2-position.[19] 1,3-dialdehydes that are fully substituted at the 2-position are susceptible to retro-aldol reaction and trimerization. However, when neopentyl

glycol **3.4** is exposed to allyl acetate in the presence of $[Ir(cod)Cl]_2$, (*S*)-Cl-MeO-BIPHEP, 4-Cl-3-NO_2-benzoic acid, and Cs_2CO_3 in 1,4-dioxane, C_2-symmetric, chiral diol **3.3** is obtained in 48% yield with very high levels of stereoselectivity (20:1 d.r., > 99% e.e.).[102]

While this transformation does generate a great deal of complexity in a single transformation directly from simple primary alcohols, it is not without its shortcomings. Extensive optimization was conducted during the initial development of the two-directional allylation and while yields were good for many substrates, the transformation of neopentyl glycol **3.4** into chiral diol **3.3** is less than 50% yield. This is most likely due to the steric hindrance of the methyl substitution at the 2-position of the 1,3-diol (C4 as depicted in the schemes). Alkylation of the transient aldehyde generated upon dehydrogenation of one of the alcohol functionalities could require significant energy to overcome the stereoelectronic effects of the gem-dimethyl moiety. The allylation reaction is performed in a sealed tube and heated to 100 °C, which can be a hazard if high enough pressures are generated within the vessel.

The major limitation is the cost of the chiral ligand. The results of the optimization screening of ligand indicated that (*S*)-Cl-MeO-BIPHEP provided the highest yield and stereoselectivity. While on small scale, use of this ligand was acceptable it was advantageous to identify a less expensive ligand for reactions on preparative scale for the total synthesis. It was found that (*S*)-binap could be used in gram-scale allylation reactions and provided similarly high levels of stereoselectivity, but the yield was limited to 40%. The development of conditions for catalyst recovery in these reactions has not been successful. Nevertheless, diol **3.3** was synthesized reproducibly on gram-scale directly from neopentyl glycol **3.4**.

Scheme 3.2 Synthesis of **3.3** via transfer hydrogenative C-C bond formation.

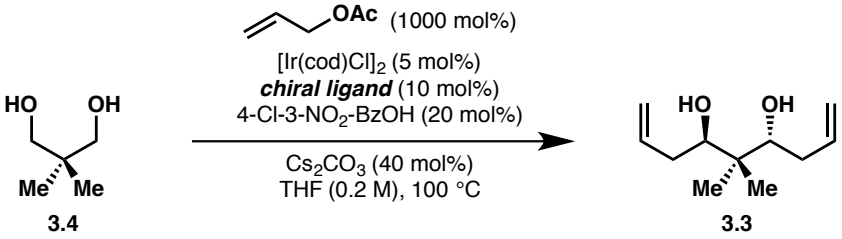

chiral ligand	d.r.	%ee	% yield
(*S*)-Cl-MeO-BIPHEP	20:1	>99	48
(*S*)-BINAP	20:1	>99	40

With **3.3** in hand it was anticipated that cross-metathesis with ethyl vinyl ketone (EVK) would install the desired C8-C11 fragment and furnish bis-enone **3.5** (Scheme 3.3). A number of parameters were screened including choice of metathesis catalyst, solvent, concentration and temperature. Exposure of **3.3** to ethyl vinyl ketone in the presence of Hoveyda-Grubbs 2nd Generation catalyst (HG-II) at room temperature in toluene afforded bis-enone **3.5** in high yield. Due to symmetry, both alkenes underwent metathesis with ethyl vinyl ketone; however, it was anticipated that desymmetrization would allow for the selective removal of the unwanted ethyl ketone moiety. Oxa-Michael cyclization was effected through treatment of **3.5** with PPTS in DCM and pyran **3.2** was obtained in 93% yield and ~6:1 d.r. in favor of the desired all *syn* pyran.

In the course of screening conditions for the cross-metathesis step, it was discovered that Fuwa and coworkers had developed conditions for tandem cross-metathesis and oxa-Michael cyclization to generate pyrans in a single transformation.[103] Application of the reported conditions furnished **3.2** in 76% yield and 10:1 d.r. directly from **3.3**. The improved diastereoselectivity can be attributed to thermodynamic control in the oxa-Michael cyclization. Through this synthetic sequence, three stereocenters and the entire non-sugar carbon framework of the natural product had been constructed in just two steps from neopentyl glycol **3.4**.

Scheme 3.3 Cross-metathesis and oxa-Michael cyclization.

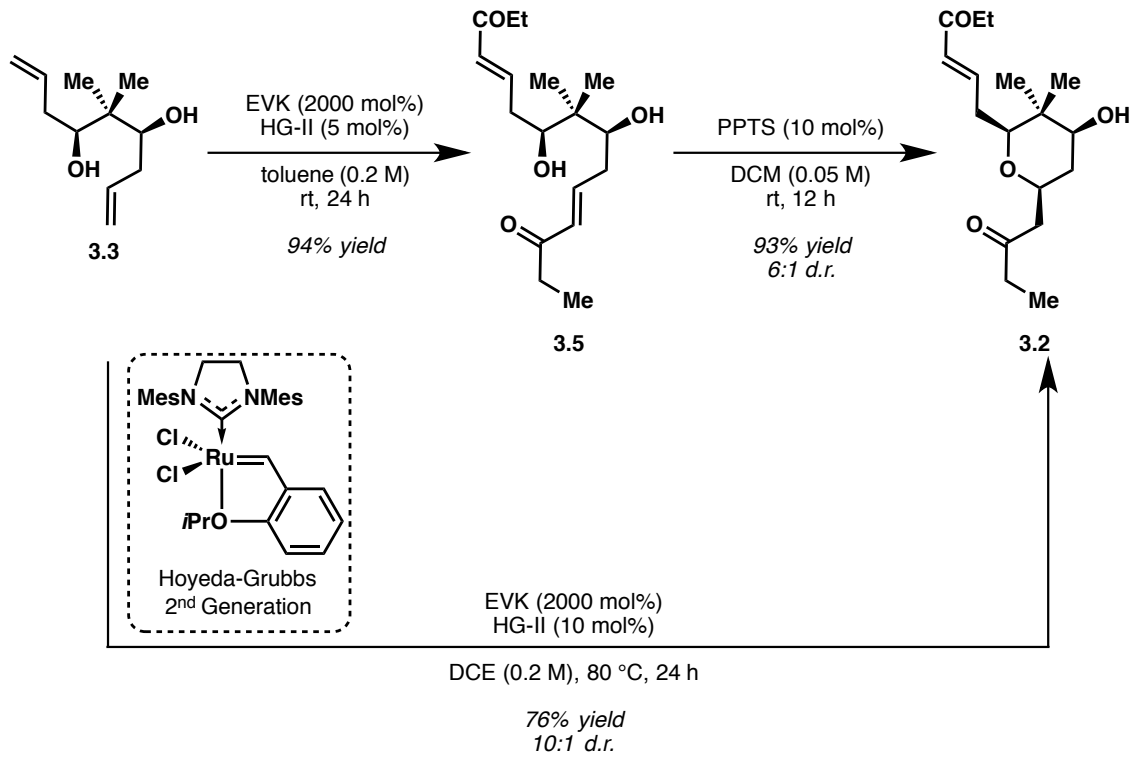

3.1.3 Completion of the First-Generation Total Synthesis

With the compound now desymmetrized pyran **3.2** in hand, we sought to remove the ethyl vinyl ketone fragment at C1 that is not present in the natural product (Scheme 3.4). It was found that exposure of **3.2** to HG-II under an atmosphere of ethylene gas resulted in the removal of the fragment and afforded alkene **3.6** in 70% yield. Attempts to perform the ethylene metathesis directly after cross-metathesis and oxa-Michael cyclization were unsuccessful presumably due to catalyst decomposition at the elevated reaction temperatures.[104] The secondary, neopentyl hydroxyl group was next glycosylated with thiophenyl glycoside **3.7**, which was prepared according to literature precedent in 3 steps from D-xylose,[87] to afford ketone **3.8** in 69% yield as a 2:1 separable mixture of anomers in favor of the desired β-anomer.

Scheme 3.4 Completion of the first-generation synthesis of (–)-cyanolide A **3.1**.

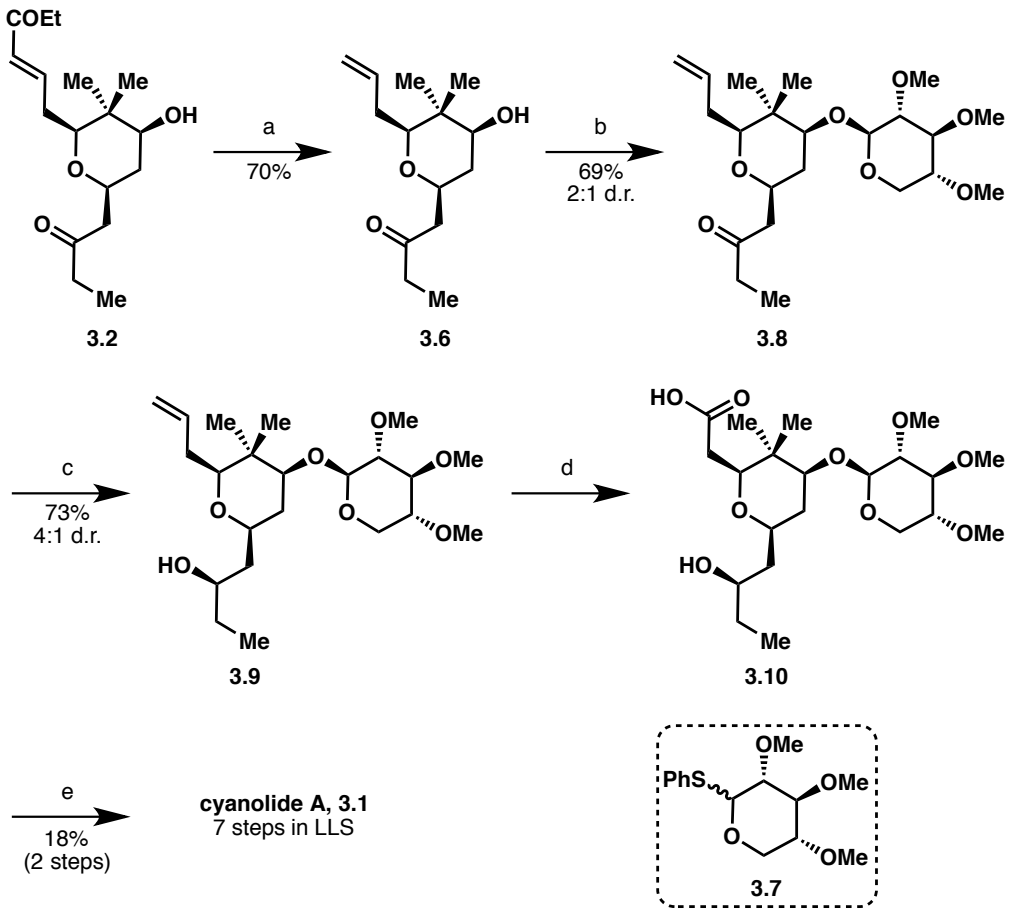

Key: (a) HG-II (10 mol%), ethylene, toluene (0.01 M), 60 °C; (b) **3.7** (150 mol%), MeOTf (200 mol%), 4 Å MS (200 wt%), Et_2O (0.07 M); (c) Li(*s*Bu)$_3$BH (100 mol%), THF (0.05 M), -78 °C; (d) OsO_4 (1 mol%), oxone (400 mol%), DMF (0.1 M); (e) 2-methyl-6-nitrobenzoic anhydride (300 mol%), DMAP (2000 mol%), toluene (0.004 M), 90 °C.

With the carbon framework successfully constructed, reduction of ketone **3.8** with L-Selectride provided alcohol **3.9** as a seperable 4:1 mixture of diastereomers in favor of the desired 1,3-*syn* relationship between C9 and C7. Less bulky hydride reagents such as LAH and $NaBH_4$ gave lower levels of diastereoselectivity even when applied in conjunction with chelating salts such as LiI and $ZnCl_2$, but ultimately L-Selectride was suitable for the reaction. The observed 1,3-*syn* diastereoselectivity using L-Selectride is in accordance with Evans' revision of Cram's polar model for the reduction of β-alkoxy ketones.[105] Modified conditions for Johnson-Lemieux oxidative cleavage of the terminal olefin in compound **3.9** was achieved using catalytic OsO_4 and superstoichiometric oxone as the terminal oxidant,[106] which afforded seco-acid **3.10**.

With the monomer in hand, macrolactonization was attempted. Upon treatment of seco-acid **3.10** with Shiina's reagent for esterification in the presence of DMAP,[86] (–)-cyanolide A **3.1** was synthesized in 18% yield (over 2 steps). The first-generation total synthesis of the natural product was completed in 7 steps (LLS) from neopentyl glycol **3.4**.

3.2 Second-Generation Total Synthesis of (–)-Cyanolide A

In evaluating the first-generation route to the natural product, it became clear that while the overall synthesis was quite concise there was still more opportunity for optimization of the sequence. In particular, it was recognized that the ruthenium-catalyzed ethenolysis of pyran **3.2** to afford terminal alkene **3.6** was a major concession, as it did not construct any missing functionality or structure to molecule, but rather was a means of correcting an undesired metathesis event. Additionally, ethenolysis of **3.2** was thought necessary as a means of eliminating the undesired ketone, which could complicate the reduction of the C9 carbonyl later in the synthetic sequence.

An ideal solution would have been to continue the synthesis and later attempt to oxidatively cleave the alkene directly to the desired carboxylic acid **3.10** (Scheme 3.5). This would no longer be a concession as it would correct for the erroneous installation of the ethyl ketone fragment while simultaneously installing the necessary functionality at C1. However, the viability of this proposed sequence would require that diastereoselective reduction of the C9 carbonyl be performed in the presence of the enone. As the product of this reduction directly from **3.2** was anticipated to be a triol, concerns arose with respect to the chemoselectivity of the glycosylation of the C5 hydroxyl group at a later stage. Therefore, to ensure chemoselectivity **3.2** was first glycosylated with **3.7** to provide enone **3.11**.

Scheme 3.5 Unsuccessful route to **3.10** without relying on ethenolysis.

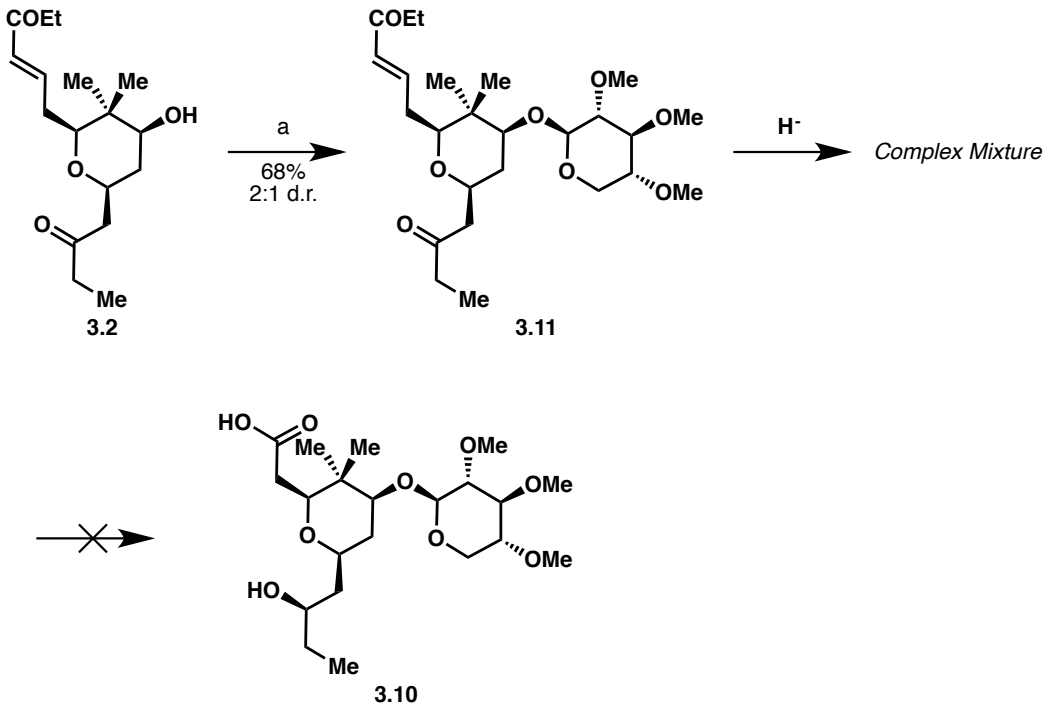

Reduction of **3.11** was attempted using a variety of hydride sources and conditions including $NaBH_4$, LAH, and L-Selectride. Due to the four possible sites for reduction, it was anticipated that four possible products could be produced. High diastereoselectivity at C9 was required but selectivity in the reduction of the carbonyl of the enone was inconsequential as that fragment was to later be cleaved. However, in the reduction the reaction mixture was further complicated due to competition between 1,2- and 1,4-reduction of the enone. To further complicate matters, if 1,4-reduction occurred, the resulting aliphatic ketone could be reduced in the presence of excess hydride to give an alcohol. The products of 1,4-reduction would no longer contain the alkene necassry for oxidative cleavage and thus this route to **3.10** would not be feasible. Various conditions were explored to enforce 1,2-reduction of the enone carbonyl including the conditions developed by Luche,[107] as well as $Zn(BH_4)_2$ in 1,2-dimethoxyethane.[108] However, no set of conditions was identified to provide simplified reaction mixtures.

Faced with this challenge of chemoselectivity, a new strategy for overcoming this obstacle was of significant importance. Since the proposed route of diastereoselective reduction

followed by oxidative cleavage had proven to be problematic, investigation into first performing oxidative cleavage followed by diastereoselective reduction was examined (Scheme 3.6). Typically, ozonides generated from the ozonolysis of alkenes are reduced using dimethyl sulfide or triphenylphosphine to give aldehydes. Reduction of the ozonide to primary alcohols is performed far less frequently, but a report by Srikrishna and coworkers demonstrated that ozonolysis and subsequent reduction with sodium borohydride afforded the corresponding primary alcohol directly from the alkene.[109] Motivated by this precedent, attempts were made to perform the tandem oxidative cleavage and diastereoselective reduction of ketone **3.11**.

Scheme 3.6 Completion of the second-generation synthesis of (–)-cyanolide A.

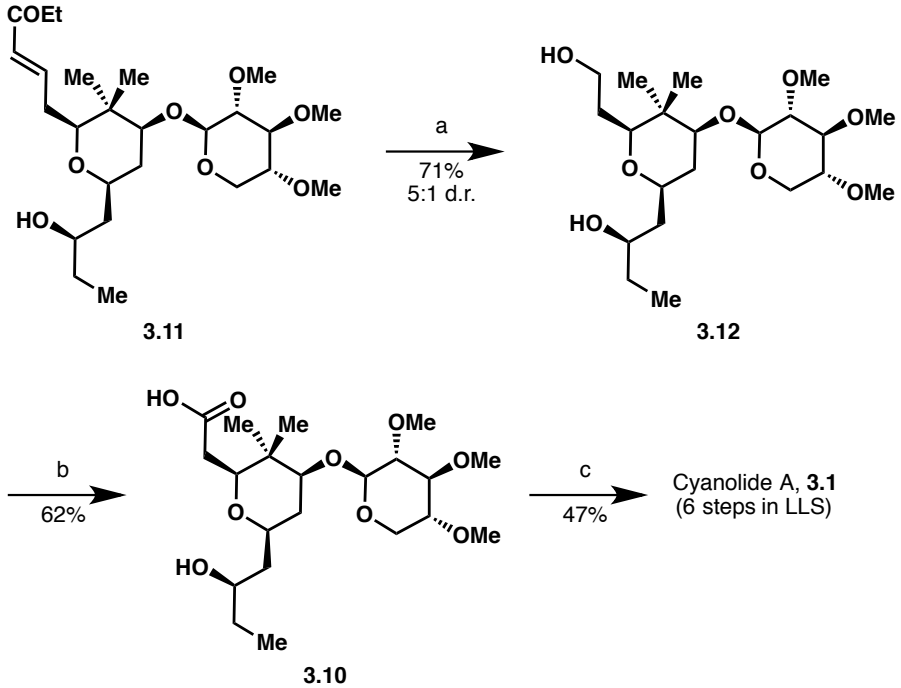

3.11 **3.12** **3.10**

Key: (a) ozone, THF (0.05 M), -78 °C then Li(*s*Bu)$_3$BH (1000 mol%), -78 to 25 °C; (b) TEMPO (30 mol%), NaClO (225 mol%), NaHCO$_3$ (aq.), CH$_2$Cl$_2$ (0.05 M), 0 °C then isobutylene (1400 mol%), NaClO$_2$ (225 mol%), Na$_2$HPO$_4$ (aq.), NaBr (aq.), *t*BuOH (0.06 M); (c) 1,3,5-Cl$_3$BzCl (120 mol%), Et$_3$N (140 mol%), DMAP (500 mol%), toluene, 120 °C.

Exposure of **3.11** to ozone under cryogenic conditions followed by addition of L-Selectride afforded diol **3.12** as a seperable 5:1 mixture of diastereomers in favor of the desired diastereomer. At this stage, chemoselective oxidation of the primary alcohol to a carboxylic acid in the presence of the secondary alcohol was necessary. TEMPO oxidation selectively oxidized

the primary alcohol to the corresponding aldehyde and Pinnick oxidation of the aldehyde provided seco-acid **3.10** in 62% yield, which was obtained as a crystalline solid. Confirmation of the relative and absolute stereochemistry was obtained through X-ray diffraction analysis of **3.10** (Figure 3.1). Macrolactonization using the recrystallized product under Yamaguchi's conditions for macrolactonization furnished (–)-cyanolide A **3.1** in 47%. The second-generation route to the natural product was completed in just 6 steps (LLS) from neopentyl glycol **3.4**. This represents the most concise total synthesis of (–)-cyanolide A to date and requires half the number of steps (LLS) as the next shortest synthesis. Both generations of the synthesis of (–)-cyanolide A were done without protecting groups, chiral auxiliaries, and premetallated *C*-nucleophies, which significantly reduced the overall step count. According to Baran's metric for synthetic ideality, both routes described above are ~80% ideal. Notably, this is the only synthesis in which chirality was introduced in a catalytic manner as opposed to using a chiral starting material.

Figure 3.1 View of molecule **3.10** of 1 showing the atom-labeling scheme. Displacement ellipsoids are scaled to the 50% probability level. The hydrogen atoms on the disordered methyl carbon atoms were omitted for clarity.

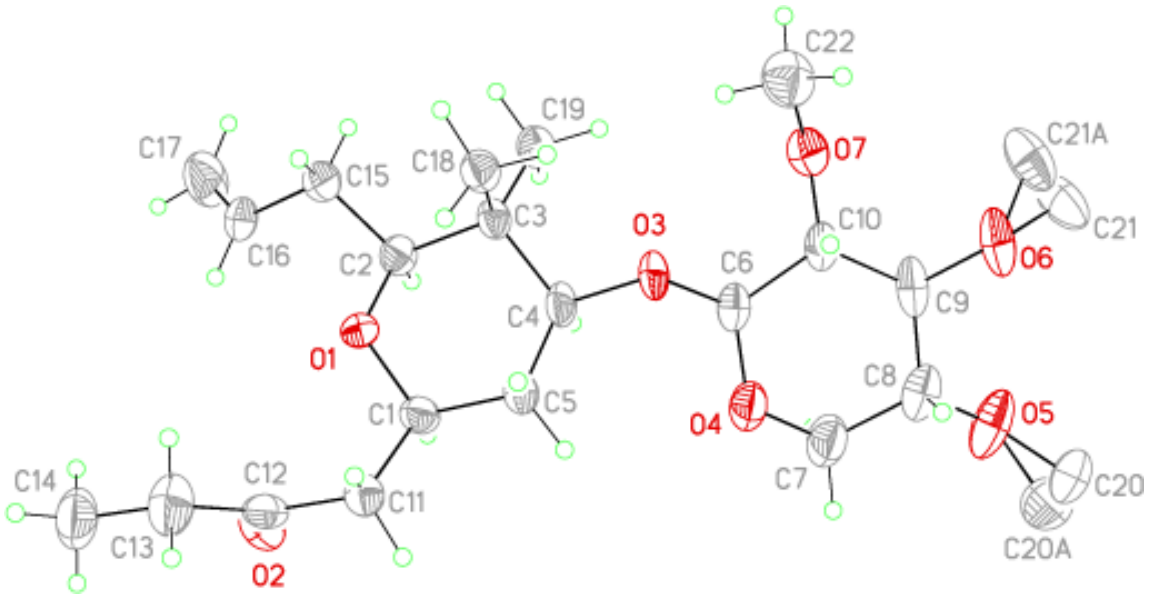

3.3 Conclusions

Diastereoselectivity and chemoselectivity proved to be significant challenges in successfully completing the total synthesis of (–)-cyanolide A **3.1**. Identification of conditions that facilitated multiple transformations in a single step was of critical importance with regard to overall step count, while some synthetic challenges required reorganization of the proposed synthetic sequence. Of critical importance was the rapid construction of the pyran core of the natural product, which was made possible through two metal-catalyzed reactions; asymmetric iridium-catalyzed two-directional allylation and ruthenium-catalyzed tandem cross-metathesis and oxa-Michael cyclization.

The asymmetric iridium-catalyzed transfer hydrogenative C-C bond forming methodology generated two stereocenters and installed a significant portion of the carbon framework of the natural product. It is important to note that concise methods to address the preparation of polyketides are of significant interest. Accordingly, the Krische laboratory has devised a suite of catalytic methods for construction of polyketide substructures in which hydrogen exchange is accompanied by C-C bond formation.[110] As illustrated by the present total syntheses of (–)-cyanolide A,[101] application of this methodology has availed the most concise route to any member of this polyketide natural product family.

3.4 Experimental Details

3.4.1 General Information

All reactions were run under an atmosphere of argon under anhydrous conditions unless otherwise indicated. Dichloroethane (DCE) and dichloromethane (CH_2Cl_2) were distilled over CaH_2. Diethyl ether (Et_2O), tetrahydrofuran (THF), and toluene (PhMe) were distilled over sodium and benzophenone. Pressure tubes (25x150 mm, PYREXPLUS, and 350 mL flask, purchased from Chem Glass) were dried in an oven overnight and cooled under a stream of nitrogen prior to use. Commercially available allyl acetate (Aldrich) was purified by distillation prior to use. Neopentyl glycol was purified by sublimation prior to use. Ethyl vinyl ketone was

purified by distillation prior to use. All other commercial reagents were used directly without further purification unless specified. All analytical thin-layer chromatography (TLC) was carried out using 0.2 mm commercial silica gel plates (DC-Fertigplatten Kieselgel 60 F254). Plates were visualized by treatment with UV, acidic p-anisaldehyde stain, ceric ammonium molybdate stain, or KMnO4 stain with gentle heating. Infrared spectra were recorded on a Nicolet 380 FTIR.

3.4.2 Spectrometry and Spectroscopy

Infrared spectra were recorded on a Thermo Nicolet 380 spectrometer. Low- and high-resolution mass spectra (LRMS or HRMS) were obtained on a Karatos MS9 and are reported as m/z (relative intensity). Accurate masses are reported for the molecular ion or a suitable fragment ion. Melting points were obtained on a Stuart SMP3 apparatus and are uncorrected. ^{1}H NMR spectra were recorded on a Varian Gemini (400 MHz) spectrometer at ambient temperature. Chemical shifts are reported in delta (d) units, parts per million (ppm), relative to the center of the singlet at 7.26 ppm for deuteriochloroform, or other reference solvents as indicated. Data are reported as chemical shift, multiplicity (s = singlet, d = doublet, t = triplet, q = quartet, m = multiplet), integration and coupling constant(s) in Hz. ^{13}C NMR spectra were recorded on a Varian Gemini (100 MHz) spectrometer and were routinely run with broadband decoupling. Chemical shifts are reported in ppm, with the center peak of the residual solvent resonance employed as an internal standard ($CDCl_3$ at 77.0 ppm).

3.4.3 Procedures and Spectra

(4S,6S)-5,5-dimethylnona-1,8-diene-4,6-diol (3.3)

To an oven-dried sealed tube under one atmosphere of argon gas charged with $[Ir(cod)Cl]_2$ (0.672 g, 1.00 mmol, 5 mol%), (*S*)-BINAP (1.25 g, 2.00 mmol, 10 mol%), Cs_2CO_3 (2.61 g, 8.00 mmol, 40 mol%) and 4-chloro-3-nitrobenzoic acid (0.806 g, 4.00 mmol, 20 mol%) was added THF (50 mL) followed by allyl acetate (20.0 g, 200 mmol, 1000 mol%). The reaction mixture was stirred at 90 ºC for 0.5 h before cooling to ambient temperature. Neopentyl glycol (2.08 g, 20.0 mmol, 100 mol%) in THF (50 mL) was added and the reaction mixture was stirred

at 100 ºC for 5 days. The reaction mixture was cooled to ambient temperature, filtered, and excess solvent was removed under reduced pressure. Purification of the product by column chromatography (SiO_2: ethyl acetate:hexanes, 1:6 to 1:4 with 0.1% TEA) provided **3.3** (1.48 g, 40% yield, dr > 20:1, ee > 99%) as a pale yellow oil.

TLC (SiO_2): R_f = 0.25 (ethyl acetate:hexanes, 1:4).

^{1}H NMR: (400 MHz, $CDCl_3$): δ 5.94-5.83 (m, 2H), 5.18-5.13 (m, 4H), 3.58-3.55 (m, 2H), 2.97 (s, 2H), 2.35-2.30 (m, 2H), 2.19-2.07 (m, 2H), 0.93 (s, 6H).

^{13}C NMR: (100 MHz, $CDCl_3$): δ 136.2, 117.8, 77.4, 40.0, 36.5, 20.9.

FTIR (neat): ν 3368, 3074, 2972, 2940, 2909, 2874, 1708, 1637, 1472, 1423, 1370, 1249, 1054 cm^{-1}.

HRMS: (ESI) Calcd. for $C_{11}H_{20}O_2Na$ $(M+Na)^+$: 207.1356, Found: 207.1355.

$[\alpha]^{20}_D$: -18.77 ° (c = 0.52, $CHCl_3$).

HPLC: The enantiomeric excess was determined by chiral HPLC as described by Krische and coworkers.[102]

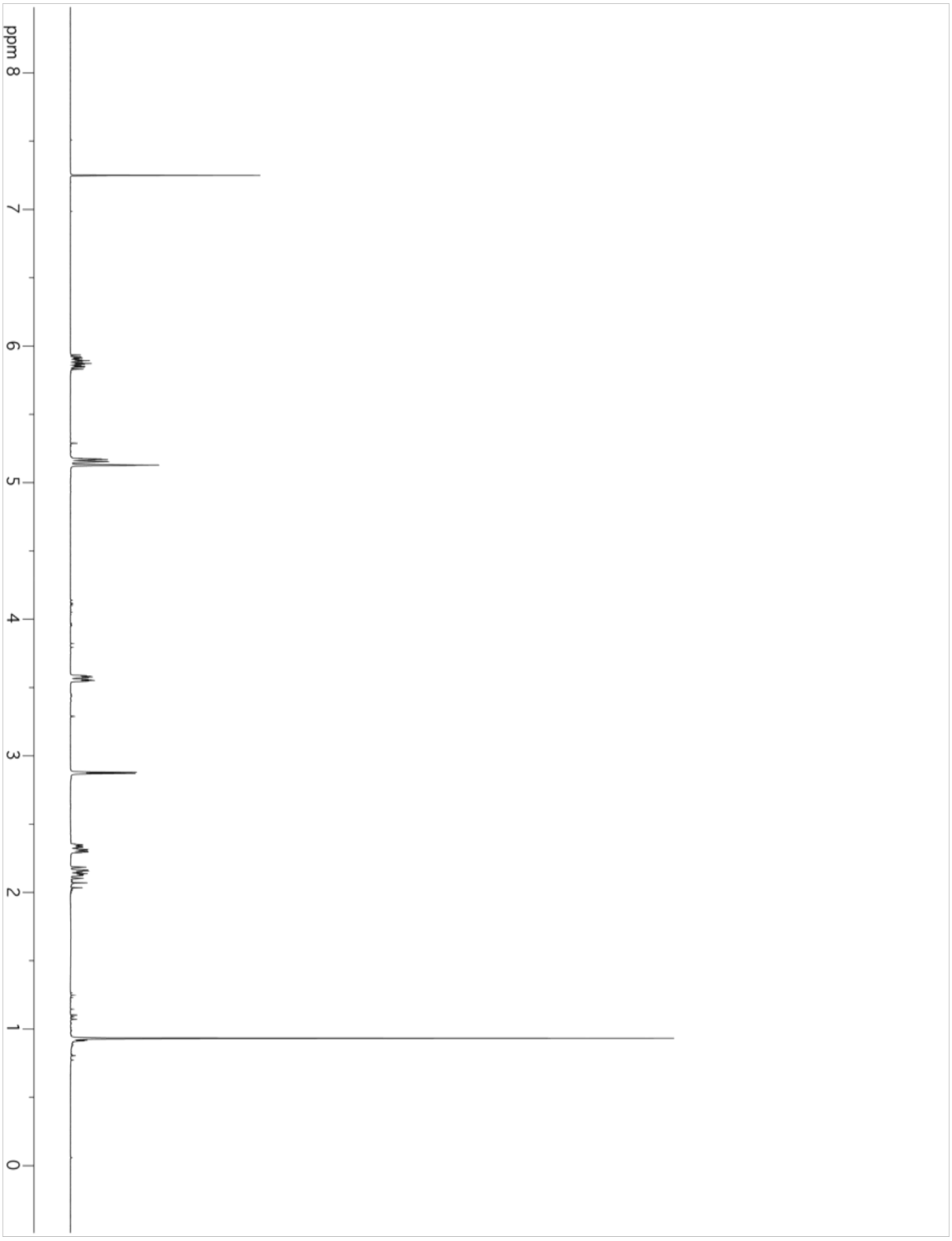
ppm
8
7
6
5
4
3
2
1
0

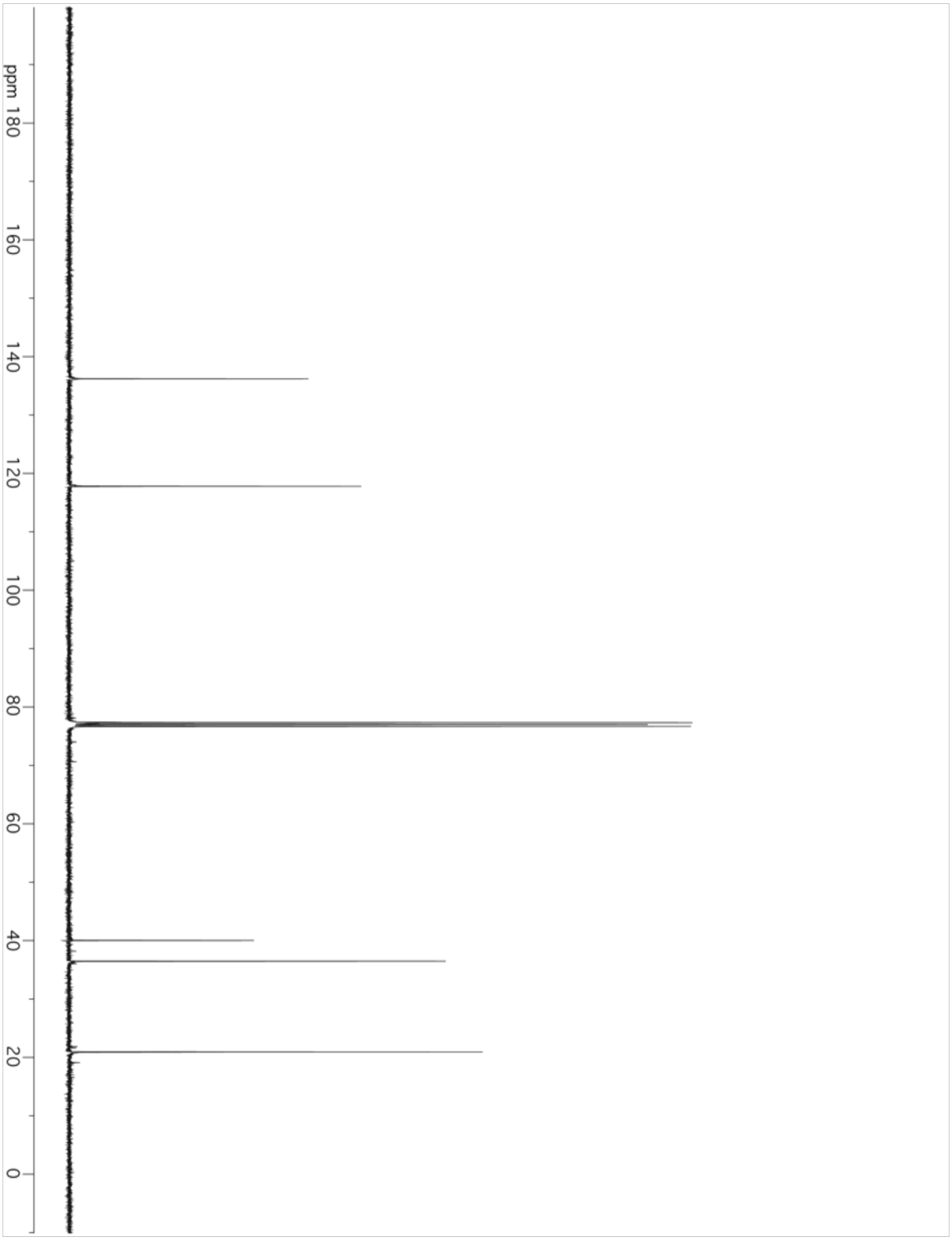
ppm
180
160
140
120
100
80
60
40
20
0

(*E*)-6-((2*S*,4*S*,6*S*)-4-hydroxy-3,3-dimethyl-6-(2-oxobutyl)tetrahydro-2*H*-pyran-2-yl)hex-4-en-3-one (3.2)

To a stirred solution of **3.3** (747 mg, 4.05 mmol, 100 mol%) in DCE (21 mL, 0.2 M) was added ethyl vinyl ketone (6.82 g, 81.1 mmol, 2000 mol%, 8.1 mL) followed by Hoveyda-Grubbs 2nd Generation catalyst (254 mg, 0.405 mmol, 10 mol%). The resulting mixture was stirred at 80 ºC for 24 h. The reaction mixture was cooled to ambient temperature. KO_2CCH_2NC (200 mg, 40 mol%) in MeOH (2 mL) was added[111] and the mixture was stirred for 0.5 h. The mixture was filtered through Celite and the excess solvent was removed under reduced pressure. The crude material was purified *via* column chromatography (SiO_2: ethyl acetate:hexane 3:7 to 2:3) to afford **3.2** (918 mg, 77% yield, dr =10:1) as a light brown oil.

TLC (SiO_2): R_f = 0.12 (ethyl acetate:hexanes, 2:5)

^{1}H NMR: (400 MHz; $CDCl_3$): δ 6.78 (dt, *J* = 16.0, 6.8 Hz, 1H), 6.08 (d, *J* = 16.0 Hz, 1H), 3.86-3.80 (m, 1H), 3.45 (dd, *J* = 11.5, 4.7 Hz, 1H), 3.07 (dd, *J* = 10.1, 2.6 Hz, 1H), 2.69 (dd, *J* = 15.4, 8.1 Hz, 1H), 2.56 (q, *J* = 7.3 Hz, 2H), 2.47-2.25 (m, 5H), 1.76 (ddd, *J* = 12.5, 4.7, 2.4 Hz, 1H), 1.42 (q, *J* = 12.0 Hz, 1H), 1.25 (t, *J* = 7.1 Hz, 1H), 1.08 (t, *J* = 7.3 Hz, 3H), 0.99 (t, *J* = 7.3 Hz, 3H), 0.94 (s, 3H), 0.84 (s, 3H).

^{13}C NMR: (100 MHz, $CDCl_3$): δ 209.5, 201.3, 144.8, 131.6, 82.8, 75.4, 72.8, 48.4, 39.0, 37.3, 36.8, 33.0, 32.3, 22.5, 12.6, 8.3, 7.6.

FTIR (neat): ν 3467, 2974, 2939, 2878, 1711, 1669, 1629, 1459, 1412, 1375, 1258, 1200, 1109, 1030 cm^{-1}.

HRMS: (ESI) Calcd. for $C_{17}H_{29}O_4$ $(M+H)^+$: 297.2066, Found: 297.2066.

$[\alpha]^{23}_D$: -40.72 ° (c = 0.88, CH_2Cl_2).

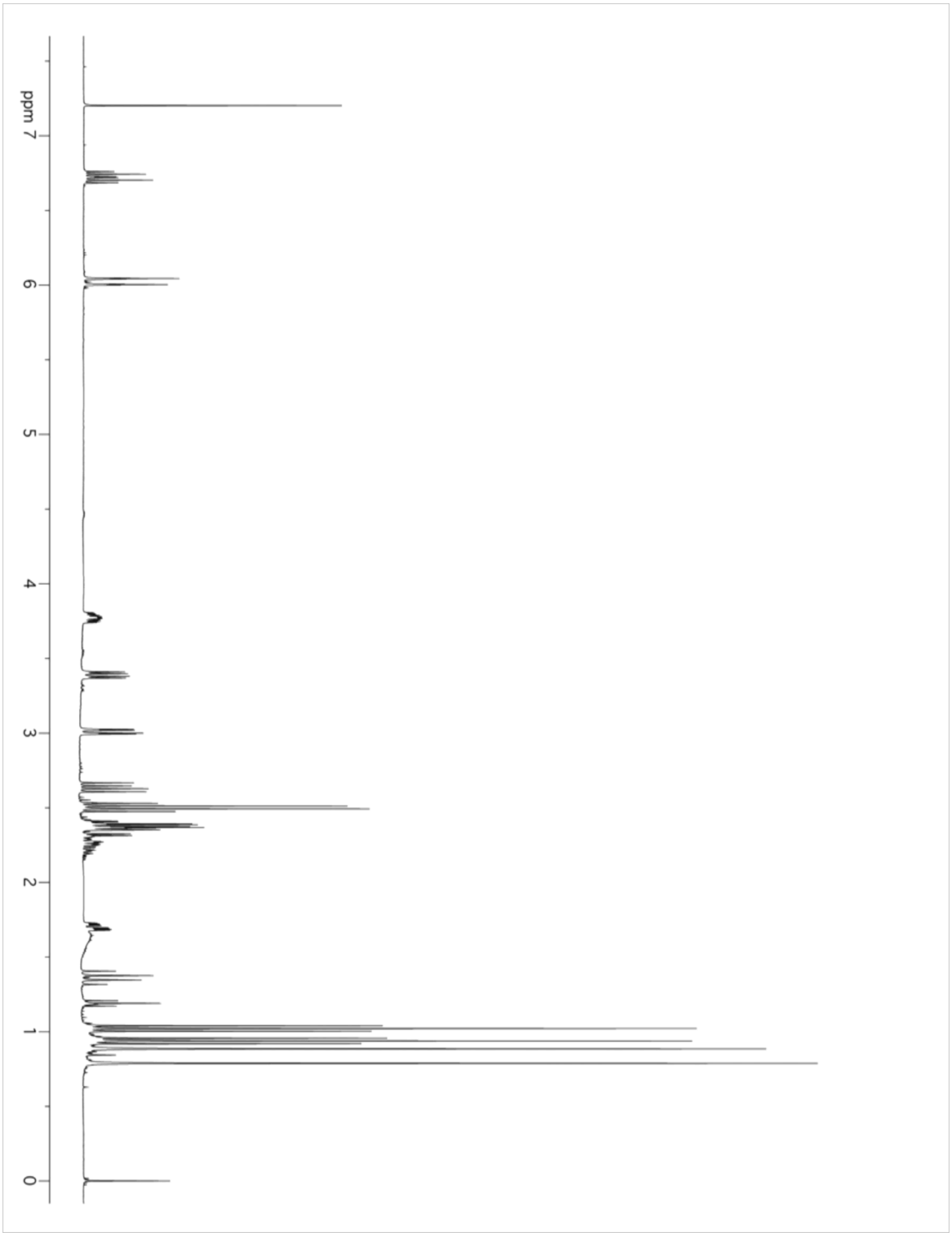
ppm
7
6
5
4
3
2
1
0

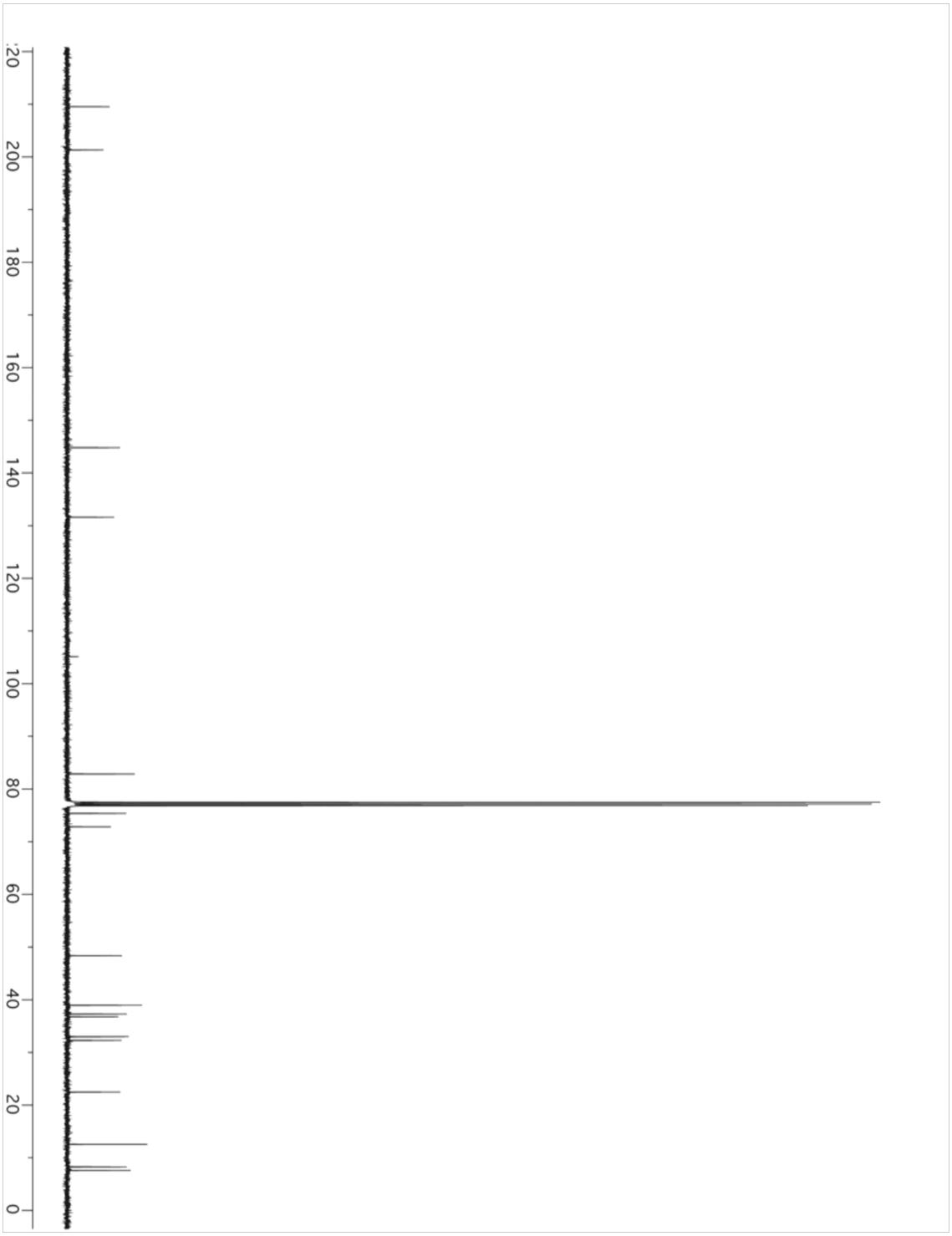
220
200
180
160
140
120
100
80
60
40
20
0

1-((2S,4S,6S)-6-allyl-4-hydroxy-5,5-dimethyltetrahydro-2H-pyran-2-yl)butan-2-one (3.6)

To a stirred solution of **3.2** (1.109 g, 3.740 mmol) in toluene (374 mL, 0.01M) at 60 ºC under an atmosphere of ethylene was added Hoveyda-Grubbs 2nd Generation catalyst (235 mg, 0.374 mmol, 10 mol%) and the solution was sparged with ethylene for 10 minutes. The solution continued to stir at 60 ºC under one atmosphere of ethylene gas for 24 h. The reaction mixture was cooled to ambient temperature. KO_2CCH_2NC (184 mg, 40 mol%) in MeOH (2 mL) was added[111] and the mixture was stirred for 0.5 h. The reaction mixture was filtered through Celite, and the solvent was removed under reduced pressure. The crude material was purified *via* column chromatography (SiO_2: ethyl acetate:hexanes, 2:5) to afford **3.6** (756 mg, 84% yield) as a light brown oil.

TLC (SiO_2): R_f = 0.23 (ethyl acetate:hexanes, 2:5)

^{1}H NMR (400 MHz; $CDCl_3$): δ 5.86-5.76 (m, 1H), 5.01 (t, *J* = 14.5 Hz, 2H), 3.85-3.78 (m, 1H), 3.45 (d, *J* = 11.8 Hz, 1H), 2.99 (dt, *J* = 10.1, 2.4 Hz, 1H), 2.72 (dd, *J* = 15.0, 8.1 Hz, 1H), 2.59-2.37 (m, 3H), 2.22 (dd, *J* = 14.7, 7.1 Hz, 1H), 2.11 (dt, *J* = 15.8, 7.8 Hz, 1H), 1.78 (ddt, *J* = 12.4, 4.7, 2.4 Hz, 1H), 1.47-1.38 (m, 2H), 1.04 (t, *J* = 8.7 Hz, 3H), 0.96 (s, 3H), 0.86 (s, 3H).

^{13}C NMR (100 MHz, $CDCl_3$): δ 210.1, 136.7, 115.9, 83.4, 75.6, 72.9, 48.6, 38.9, 37.3, 37.0, 33.6, 22.5, 12.6, 7.6.

FTIR (neat): υ 3459, 3074, 2970, 2940, 2874, 2361, 1737, 1710, 1641, 1412, 1366, 1228, 1217, 1092, 1076, 1025 cm^{-1}.

LRMS (ESI) Calcd. for $C_{14}H_{25}O_3$ $(M+H)^+$: 241.2, Found: 241.2.

$[\alpha]^{28}_D$: -7.75 ° (c = 0.29, CH_2Cl_2).

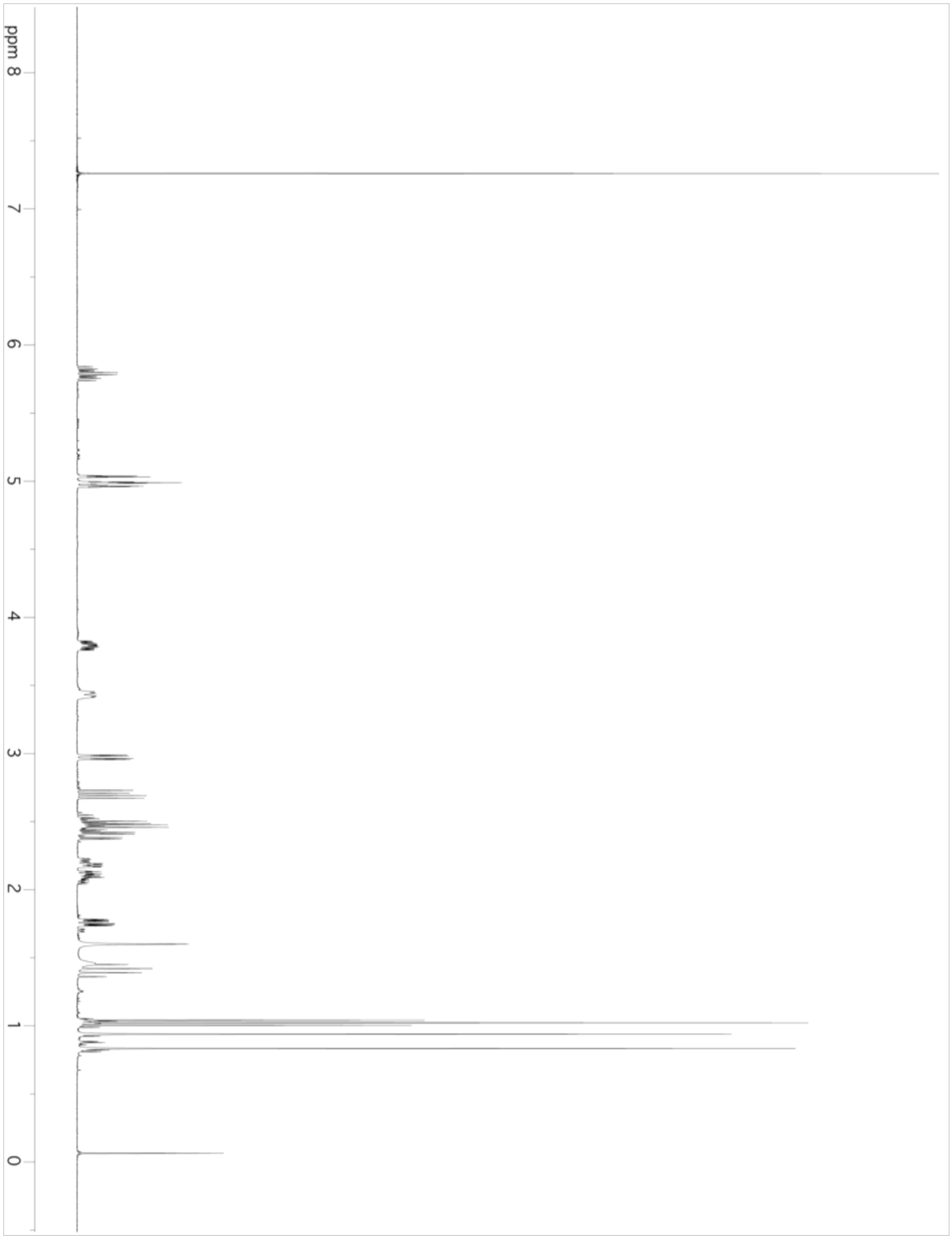
ppm
8
7
6
5
4
3
2
1
0

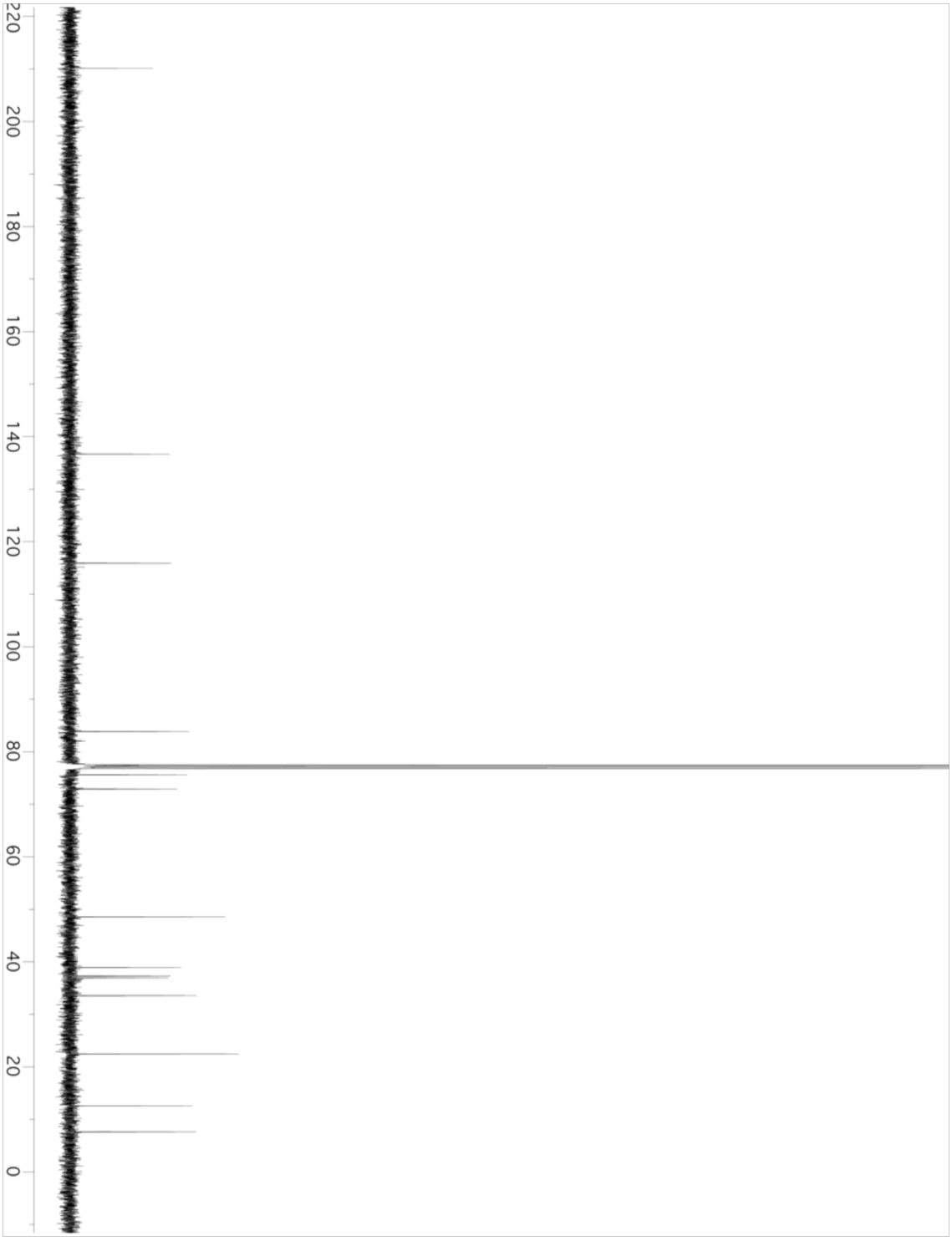
220
200
180
160
140
120
100
80
60
40
20
0

1-((2*S*,4*S*,6*S*)-6-allyl-5,5-dimethyl-4-(((2*S*,3*R*,4*S*,5*R*)-3,4,5-trimethoxytetrahydro-2*H*-pyran-2-yl)oxy)tetrahydro-2*H*-pyran-2-yl)butan-2-one (3.8)

To a stirred solution of **3.7** (189 mg, 0.786 mmol, 100 mol%) and **3.7** (336 mg, 1.18 mmol, 150 mol%) in Et_2O (11.3 mL, 0.07 M) was added 4 Å MS (380 mg, 200 wt. %) followed by MeOTf (0.017 mL, 1.572 mmol, 200 mol%). The resulting mixture was stirred at ambient temperature for 48 h. The reaction was quenched with $NaHCO_3$ and the mixture was extracted with Et_2O (3 x 10 mL). The ethereal extracts were washed with brine, dried over $MgSO_4$, and concentrated under reduced pressure. The crude material was purified *via* column chromatography (SiO_2: ethyl acetate:hexanes, 1:3.33) to afford **3.8** (223.7 mg, 69%, dr = 2:1, seperable) as a colorless oil.

TLC (SiO_2): R_f = 0.38 (ethyl acetate:hexanes, 2:5)

^{1}H NMR (β-anomer): (400 MHz; $CDCl_3$): δ 5.85-5.74 (m, 1H), 5.01 (t, *J* = 13.8 Hz, 2H), 4.24 (d, *J* = 7.6 Hz, 1H), 3.96 (dd, *J* = 11.7, 5.1 Hz, 1H), 3.82-3.75 (m, 1H), 3.63 (s, 3H), 3.62 (s, 3H), 3.54-3.49 (m, 1H), 3.47 (s, 3H), 3.31-3.21 (m, 2H), 3.12-3.05 (m, 2H), 3.01-2.95 (m, 2H), 2.70 (dd, *J* = 15.1, 8.3 Hz, 1H), 2.56-2.35 (m, 3H), 2.20 (dd, *J* = 14.0, 7.3 Hz, 1H), 2.14-2.06 (m, 1H), 1.93 (ddd, *J* = 12.7, 4.8, 2.2 Hz, 1H), 1.03 (t, *J* = 7.2 Hz, 3H), 0.99 (s, 3H), 0.91 (s, 3H).

^{13}C NMR (β-anomer): (100 MHz, $CDCl_3$): δ 210.0, 136.6, 115.9, 106.1, 85.7, 85.6, 84.2, 84.0, 79.5, 73.0, 63.4, 61.1, 61.0, 58.9, 48.6, 39.0, 37.3, 36.6, 33.5, 22.3, 13.6, 7.6.

FTIR (neat): υ 2969, 2935, 2904, 1715, 1460, 1408, 1368, 1343, 1248, 1162, 1092, 1037, 1014 cm^{-1}.

LRMS: (ESI) Calcd. for $C_{22}H_{38}O_7Na$ $(M+Na)^+$: 437.3, Found: 437.3.

$[\alpha]^{25}_D$: -72.73 ° (c = 0.33, CH_2Cl_2).

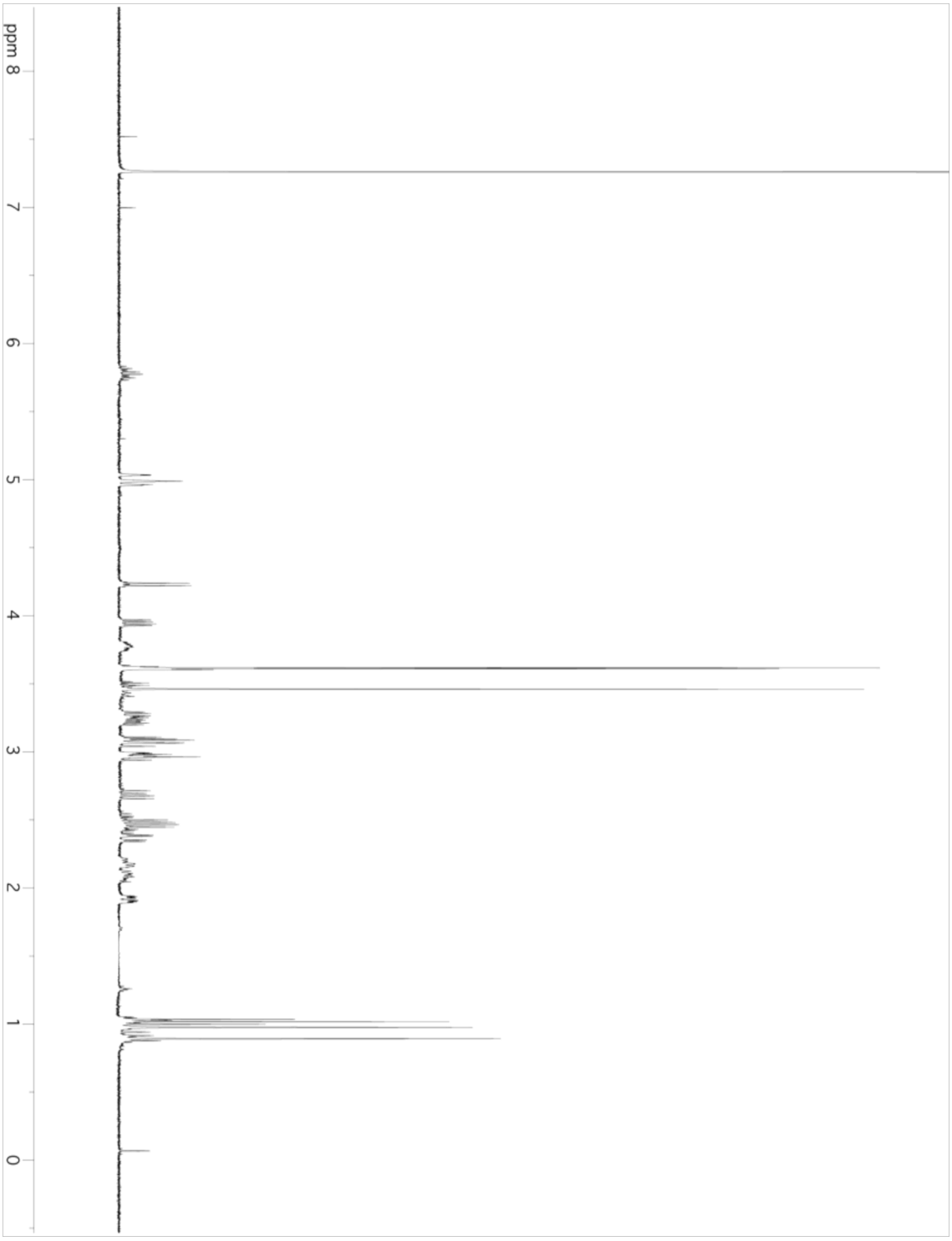
ppm
8
7
6
5
4
3
2
1
0

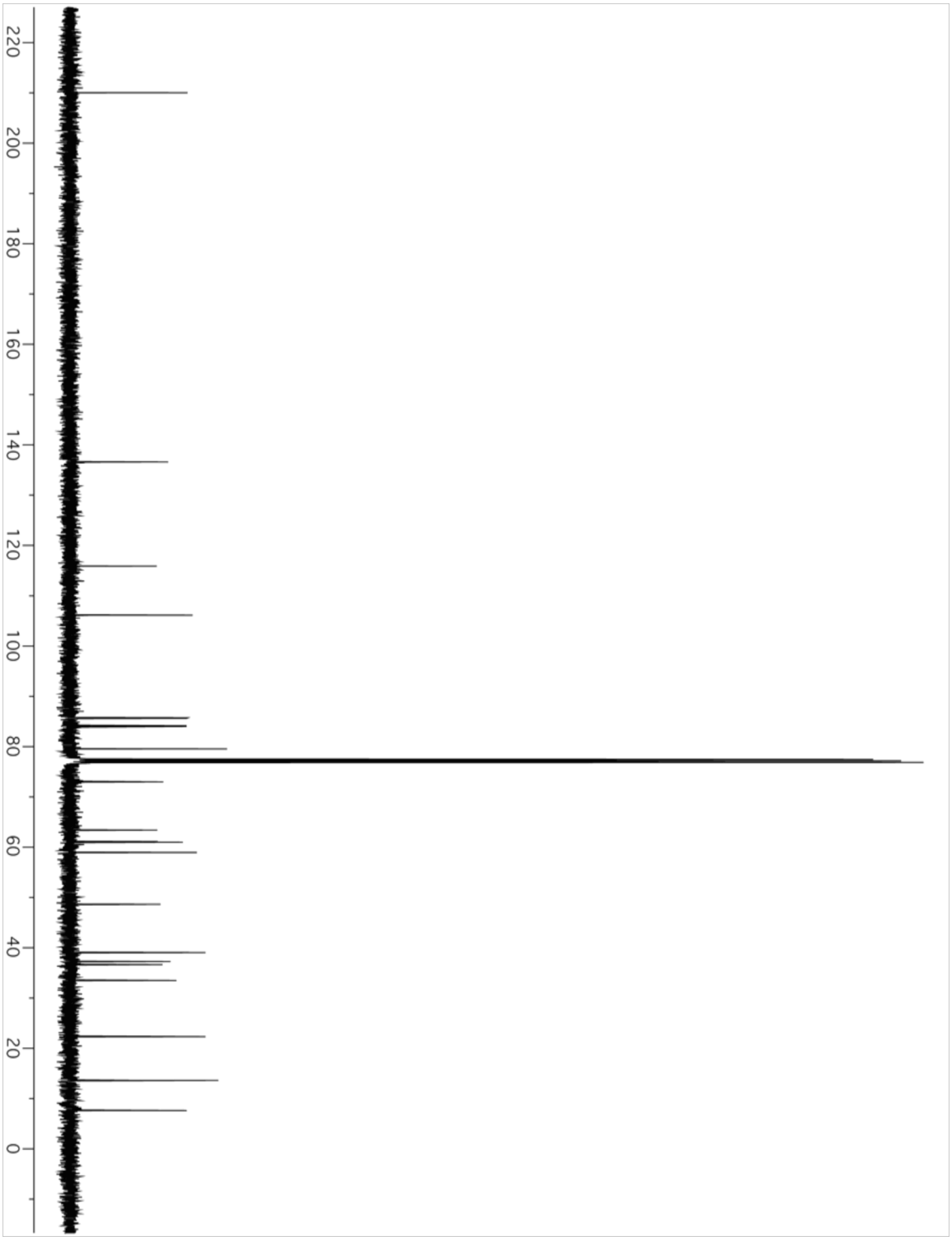
220
200
180
160
140
120
100
80
60
40
20
0

(*R*)-1-((2*R*,4*S*,6*S*)-6-allyl-5,5-dimethyl-4-(((2*S*,3*R*,4*S*,5*R*)-3,4,5-trimethoxytetrahydro-2*H*-pyran-2-yl)oxy)tetrahydro-2*H*-pyran-2-yl)butan-2-ol (3.9)

To a stirred solution of **3.8** (23.2 mg, 0.056 mmol, 100 mol%) in THF (1.12 mL, 0.05 M) was added a 1 M solution of L-selectride (0.056 mL, 0.056 mmol, 100 mol%) in THF. The resulting mixture was stirred for 1.5 h at ambient temperature. The reaction mixture was concentrated onto silica gel and purified *via* column chromatography (SiO_2: ethyl acetate:hexanes, 1:5 to 2:5) to afford **3.9** (17.1 mg, 73% yield, dr = 4:1, seperable) as a colorless oil.

TLC (SiO_2): R_f = 0.34 (ethyl acetate:hexanes, 2:5)

^{1}H NMR: (400 MHz; ($(CD_3)_2CO$): δ 5.83 (m, 1H), 5.04 (ddd, *J* = 17.1, 3.6, 1.5 Hz, 1H), 4.98 (ddt, *J* = 10.2, 2.2, 1.2 Hz, 1H), 4.29 (d, *J* = 7.6 Hz, 1H), 3.90 (dd, *J* = 11.0, 4.9 Hz, 1H), 3.67 – 3.56 (m, 1H), 3.55 (s, 3H), 3.53 (s, 3H), 3.41 (s, 3H), 3.40 – 3.30 (m, 1H), 3.18 – 2.97 (m, 3H), 2.82 (dt, *J* = 10.8, 5.4 Hz, 3H), 2.28 (ddd, *J* = 8.3, 6.6, 2.1 Hz, 1H), 1.91 (ddd, *J* = 12.9, 4.8, 2.3 Hz, 1H), 1.62 – 1.24 (m, 6H), 1.00 (s, 3H), 0.89 (app. t, *J* = 7.0 Hz, 6H).

^{13}C NMR: (100 MHz, $(CD_3)_2CO$): δ 137.6, 116.5, 106.7, 86.5, 85.4, 85.1, 84.4, 80.5, 76.9, 72.2, 72.1, 63.7, 60.9, 60.7, 58.7, 43.4, 39.7, 37.9, 34.3, 22.4, 13.8, 10.2.

FTIR (neat): υ 3519, 2934, 1738, 1643, 1463, 1369, 1259, 1161, 1094, 1016 cm^{-1}.

LRMS: (ESI) Calcd. for $C_{22}H_{40}O_7Na$ $(M+Na)^+$: 439.3, Found: 439.3.

$[\alpha]^{28}_D$:: -145.5 ° (c = 1.29, CH_2Cl_2).

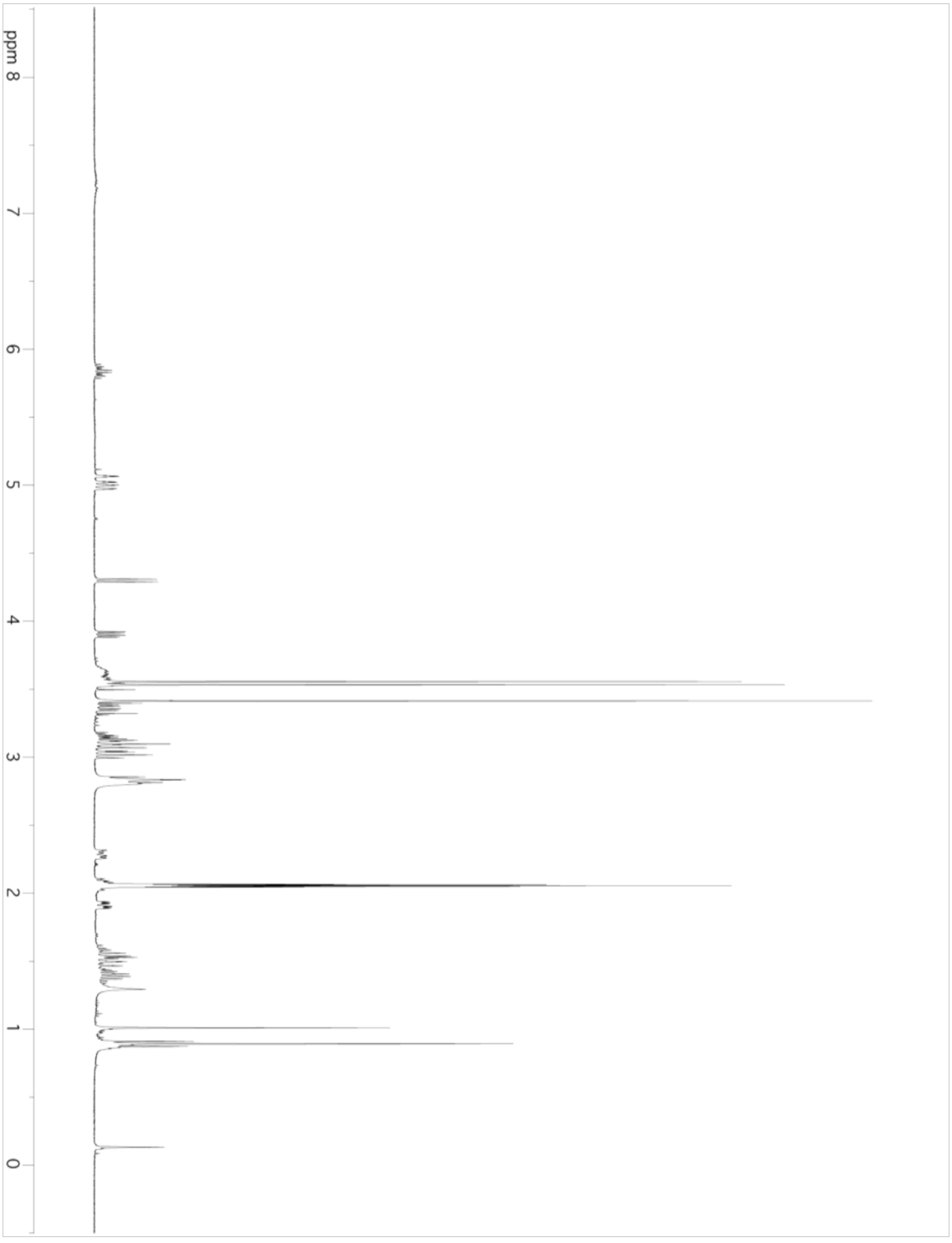
ppm
8
7
6
5
4
3
2
1
0

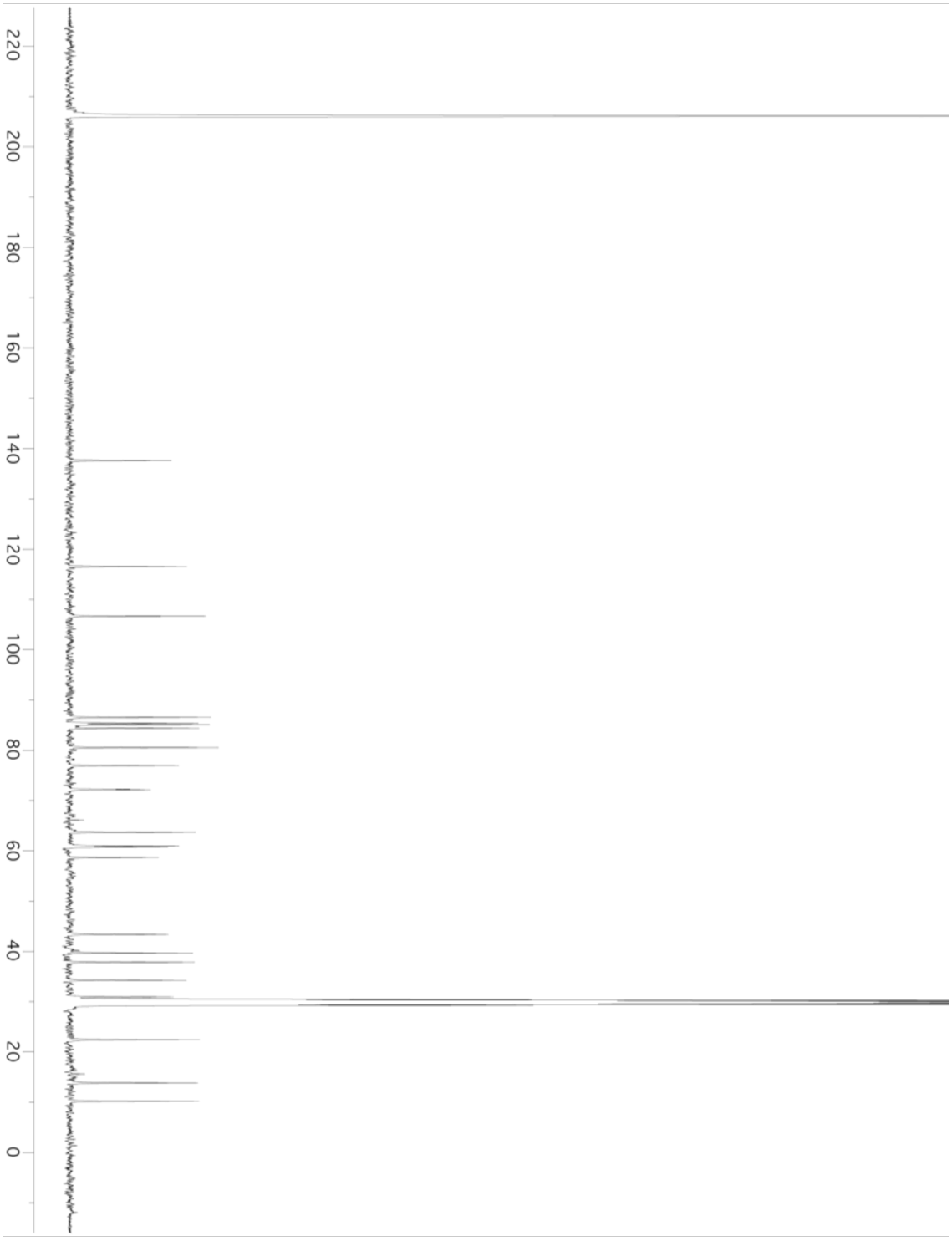
220
200
180
160
140
120
100
80
60
40
20
0

2-((2S,4S,6R)-6-((R)-2-hydroxybutyl)-3,3-dimethyl-4-(((2S,3R,4S,5R)-3,4,5-trimethoxytetrahydro-2H-pyran-2-yl)oxy)tetrahydro-2H-pyran-2-yl)acetic acid (3.10)

To a stirred solution of **3.12** (41.4 mg, 0.0984 mmol) in CH_2Cl_2 (2.2 mL, 0.045 M) and sat. aq. $NaHCO_3$ (0.27 mL) was added a 0.5 M aqueous solution of NaBr (5.67 mg, 0.055 mmol, 56 mol%, 0.11 mL) and a 0.5 M aqueous solution of tetrabutylammonium bromide (35.2 mg, 0.109 mmol, 111 mol%, 0.22 mL). TEMPO was added as a 0.5 M solution in CH_2Cl_2 (4.61 mg, 0.0295 mmol, 30 mol%, 0.059 mL) and the mixture was cooled to 0 ºC. A 5% w/w solution of NaOCl (16.5 mg, 0.222 mmol, 225 mol%, 0.33 mL) was added and the reaction was vigorously stirred for 1 h while warming to ambient temperature. The reaction mixture was acidified with 2N HCl, and ^{t}BuOH (1.64 mL) and 2-methyl-2-butene (0.72 mL) were added. $NaClO_2$ (107 mg, 1.18 mmol, 1200 mol%) and $NaHPO_4$ (87.4 mg, 0.728 mmol, 740 mol%) were dissolved in H_2O (0.43 mL) and slowly added to the reaction mixture over a period of 15 minutes. The resulting mixture stirred at ambient temperature for 2 h and was then diluted with sat. NaH_2PO_4 (5 mL) and extracted with EtOAc (3 x 10 mL). The organic layers were combined, dried over $MgSO_4$, and concentrated under reduced pressure. The crude seco-acid was purified *via* column chromatography (SiO_2: ethyl acetate:hexanes 7:3) to afford seco-acid **3.10** (26.4 mg, 62% yield) as a white crystalline solid.

TLC (SiO_2): R_f = 0.21 (ethyl acetate:hexanes, 7:3)

^{1}H NMR: (400 MHz; $CDCl_3$): δ 4.23 (d, *J* = 7.6 Hz, 1H), 3.94 (dd, *J* = 11.5, 5.2 Hz, 1H), 3.86 (dd, *J* = 8.7, 5.1 Hz, 1H), 3.72 – 3.64 (m, 1H), 3.62 (s, 3H), 3.60 (s, 3H), 3.55 (dd, *J* = 9.5, 3.2 Hz, 1H), 3.46 (s, 3H), 3.30 (dd, *J* = 11.5, 4.7 Hz, 1H), 3.23 (ddd, *J* = 10.1, 8.6, 5.2 Hz, 1H), 3.13 – 3.04 (m, 2H), 2.96 (dd, *J* = 9.1, 7.6 Hz, 1H), 2.48 – 2.36 (m, 2H), 1.92 – 1.82 (m, 1H), 1.69 – 1.37 (m, 6H), 0.99 (s, 3H), 0.90 (s, 3H), 0.87 (d, *J* = 7.5 Hz, 3H).

^{13}C NMR: (100 MHz, CD_3OH): δ 175.9, 106.9, 86.6, 85.9, 85.1, 82.0, 80.7, 76.2, 72.3, 63.9, 61.1, 60.9, 58.8, 43.4, 39.5, 37.8, 35.9, 30.5, 22.4, 13.8, 10.1.

FTIR (neat): ν 3475, 2935, 1727, 1445, 1370, 1252, 1162, 1089, 1016 cm^{-1}.

HRMS: (ESI) Calcd. for $C_{21}H_{38}O_9Na$ $(M+Na)^+$: 457.2408, Found: 457.2410.

$[\alpha]^{25}_D$: -50.34 ° (c = 0.99, CH_2Cl_2).

MP: 137 – 139 °C

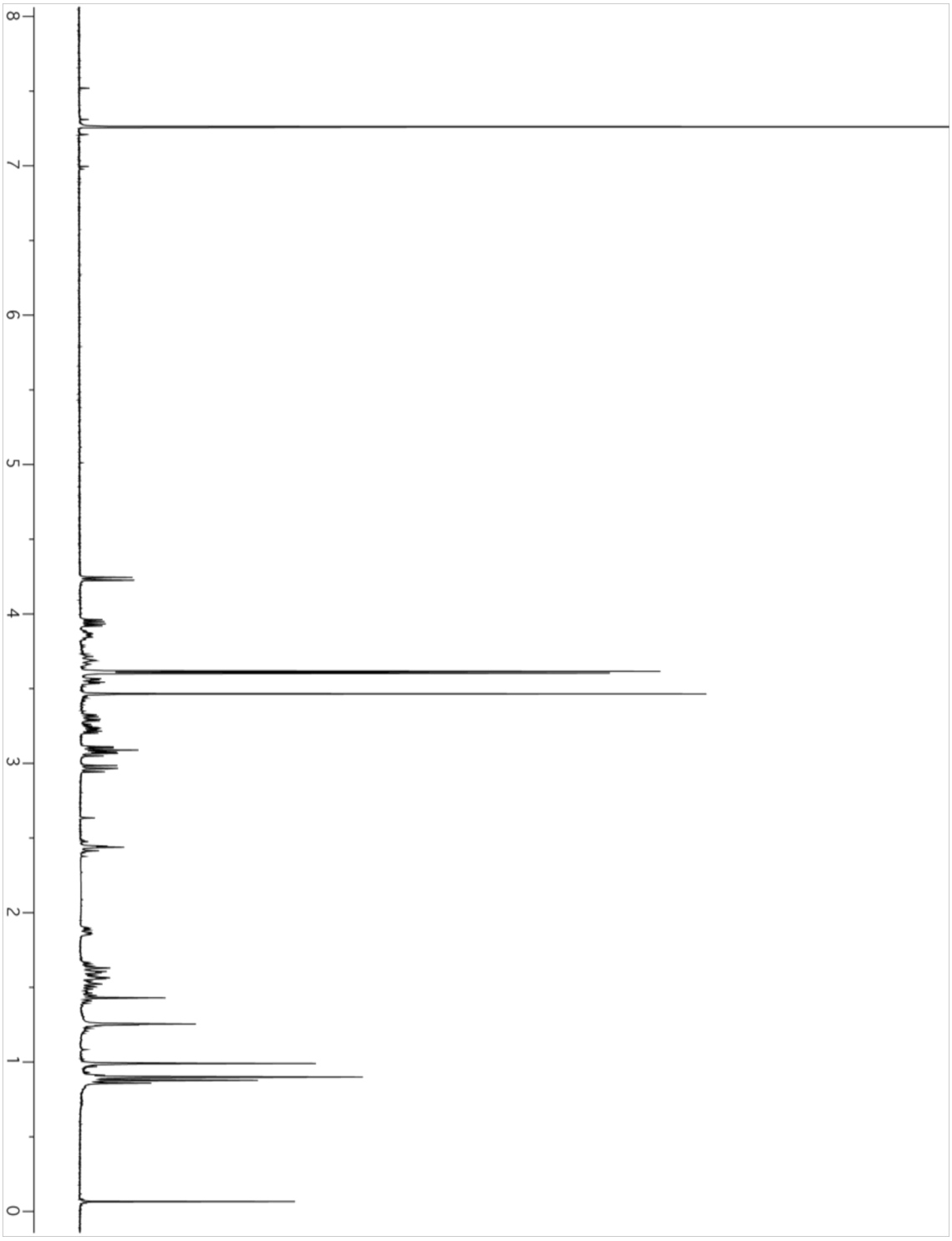
8
7
6
5
4
3
2
1
0

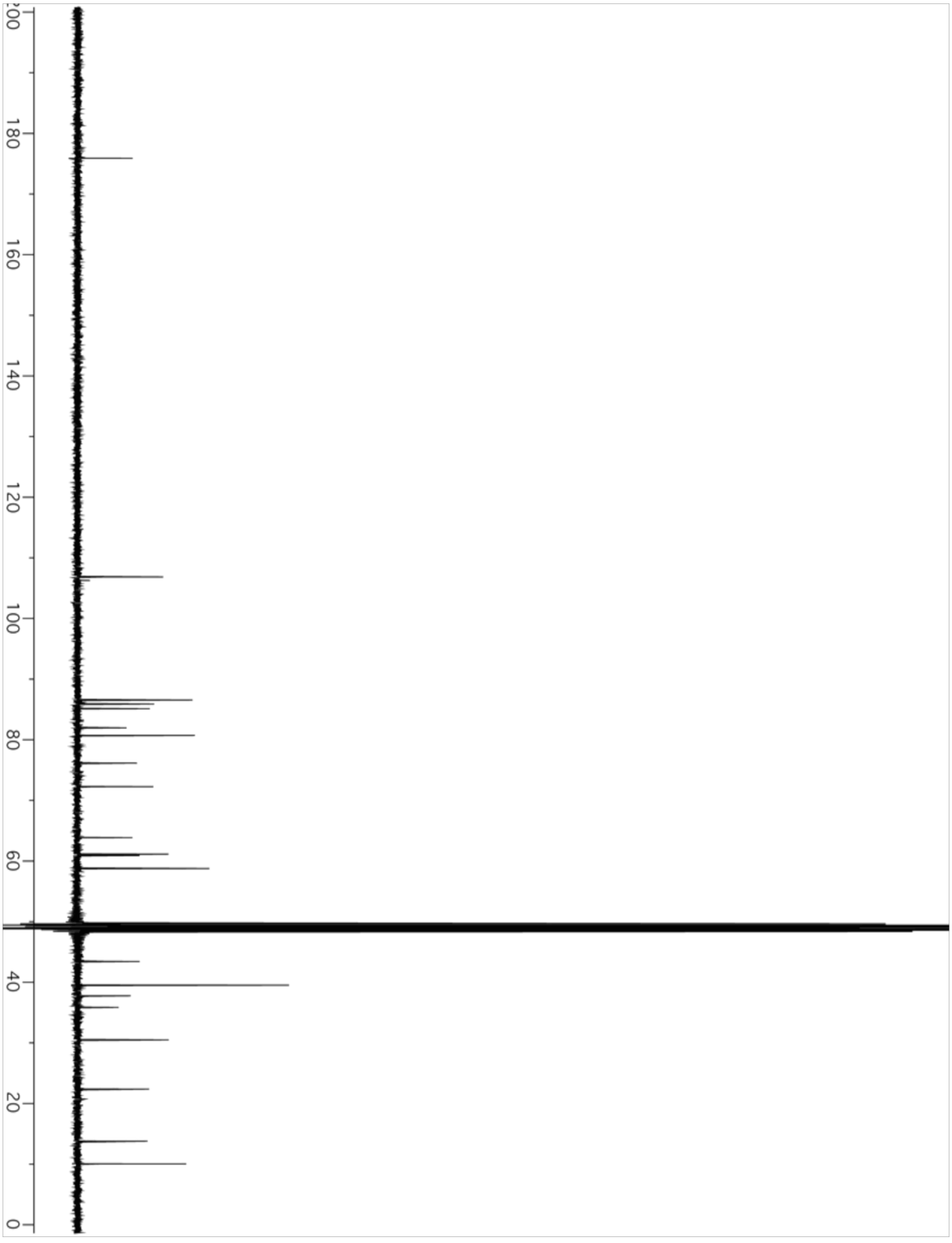
200
180
160
140
120
100
80
60
40
20
0

(*E*)-6-((2*S*,4*S*,6*S*)-3,3-dimethyl-6-(2-oxobutyl)-4-(((2*S*,3*R*,4*S*,5*R*)-3,4,5-trimethoxytetrahydro-2*H*-pyran-2-yl)oxy)tetrahydro-2*H*-pyran-2-yl)hex-4-en-3-one (3.11)

To a stirred solution of **3.2** (189 mg, 0.786 mmol, 100 mol%) and **3.7** (336 mg, 1.18 mmol, 150 mol%) in Et_2O (11.3 mL, 0.07 M) was added 4 Å MS (380 mg, 200 wt. %) followed by MeOTf (0.017 mL, 1.572 mmol, 200 mol%). The resulting mixture was stirred for 48 h at ambient temperature. $NaHCO_3$ was added and the mixture was extracted with Et_2O (3 x 10 mL). The ethereal extracts were washed with brine, dried over $MgSO_4$, and concentrated under reduced pressure. The crude material was purified *via* column chromatography (SiO_2: ethyl acetate: hexanes, 3:10) to afford **3.11** (189 mg, 68% yield, dr = 2:1, seperable) as a pale yellow oil.

TLC (SiO_2): R_f = 0.44 (Et_2O:DCM, 1:5)

^{1}H NMR (β-anomer): (400 MHz; $CDCl_3$): δ 6.77 (dt, *J* = 16.0, 6.8 Hz, 1H), 6.08 (d, *J* = 16.0 Hz, 1H), 4.23 (d, *J* = 7.6 Hz, 1H), 3.95 (dd, *J* = 11.5, 5.2 Hz, 1H), 3.87 – 3.76 (m, 1H), 3.61 (s, 3H), 3.61 (s, 3H), 3.46 (s, 3H), 3.28 (dd, *J* = 11.5, 4.7 Hz, 1H), 3.25 – 3.19 (m, 1H), 3.11 – 3.03 (m, 3H), 2.96 (dd, *J* = 9.1, 7.6 Hz, 1H), 2.68 (dd, *J* = 15.4, 8.4 Hz, 1H), 2.56 (q, *J* = 7.3 Hz, 2H), 2.47 – 2.19 (m, 5H), 1.92 (ddd, *J* = 12.7, 4.7, 2.3 Hz, 1H), 1.54 (q, *J* = 11.7 Hz, 1H), 1.08 (t, *J* = 7.3 Hz, 3H), 0.99 (t, *J* = 7.3 Hz, 3H), 0.98 (s, 3H), 0.90 (s, 3H).

^{13}C NMR (β-anomer): (100 MHz, $CDCl_3$): δ 209.5, 201.3, 144.7, 131.7, 106.1, 85.7, 85.3, 84.1, 83.0, 79.5, 72.9, 63.4, 61.1, 61.0, 59.0, 48.4, 39.0, 37.3, 36.4, 33.0, 32.2, 22.9, 13.6, 8.2, 7.6.

FTIR (neat): ν 3343, 1637, 1265, 1096, 733, 704 cm^{-1}.

HRMS: (ESI) Calcd. for $C_{25}H_{42}O_8Na$ $(M+Na)^+$: 493.2772, Found: 493.2775.

$[\alpha]^{23}_D$: -80.21 ° (c = 0.16, CH_2Cl_2).

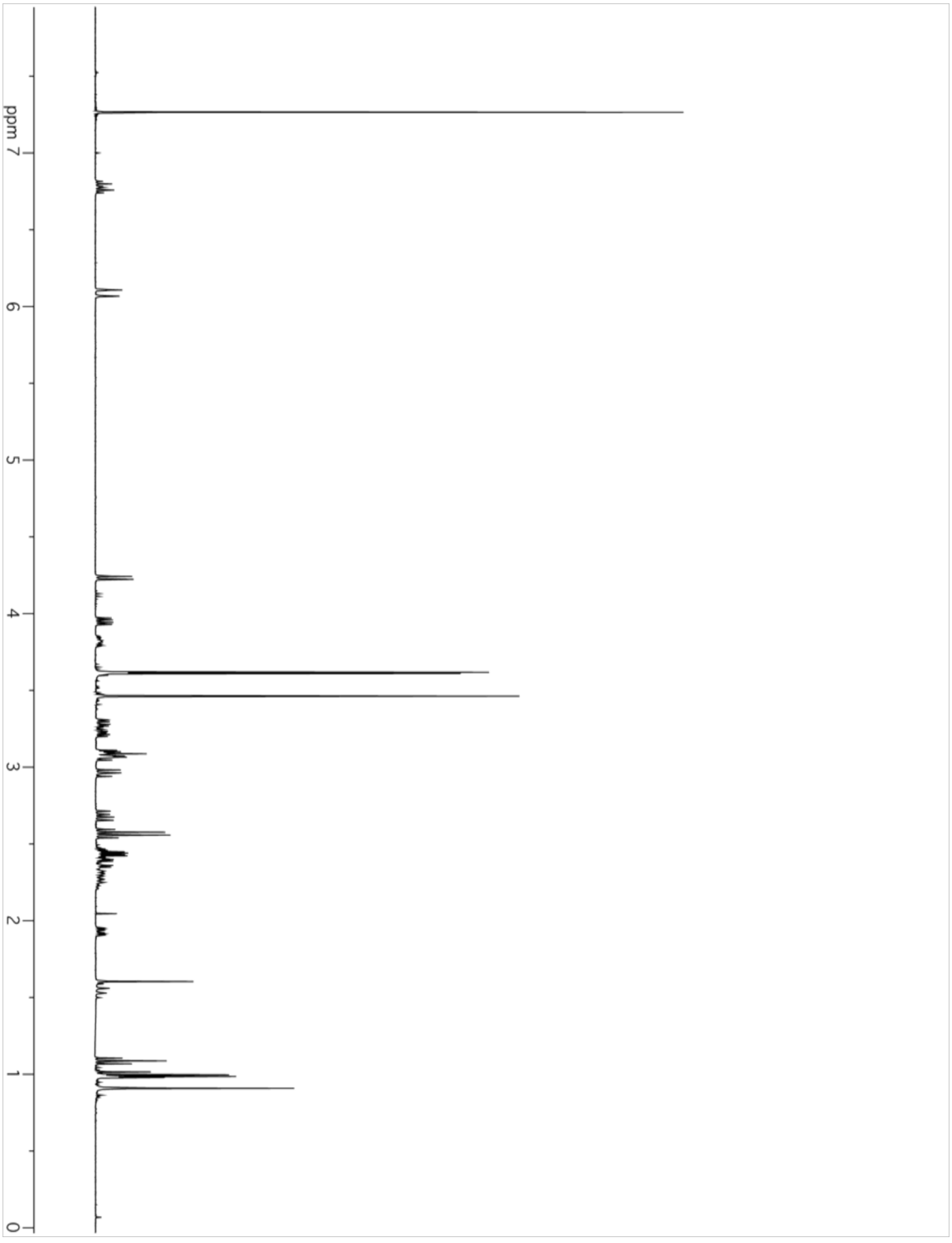
ppm
7
6
5
4
3
2
1
0

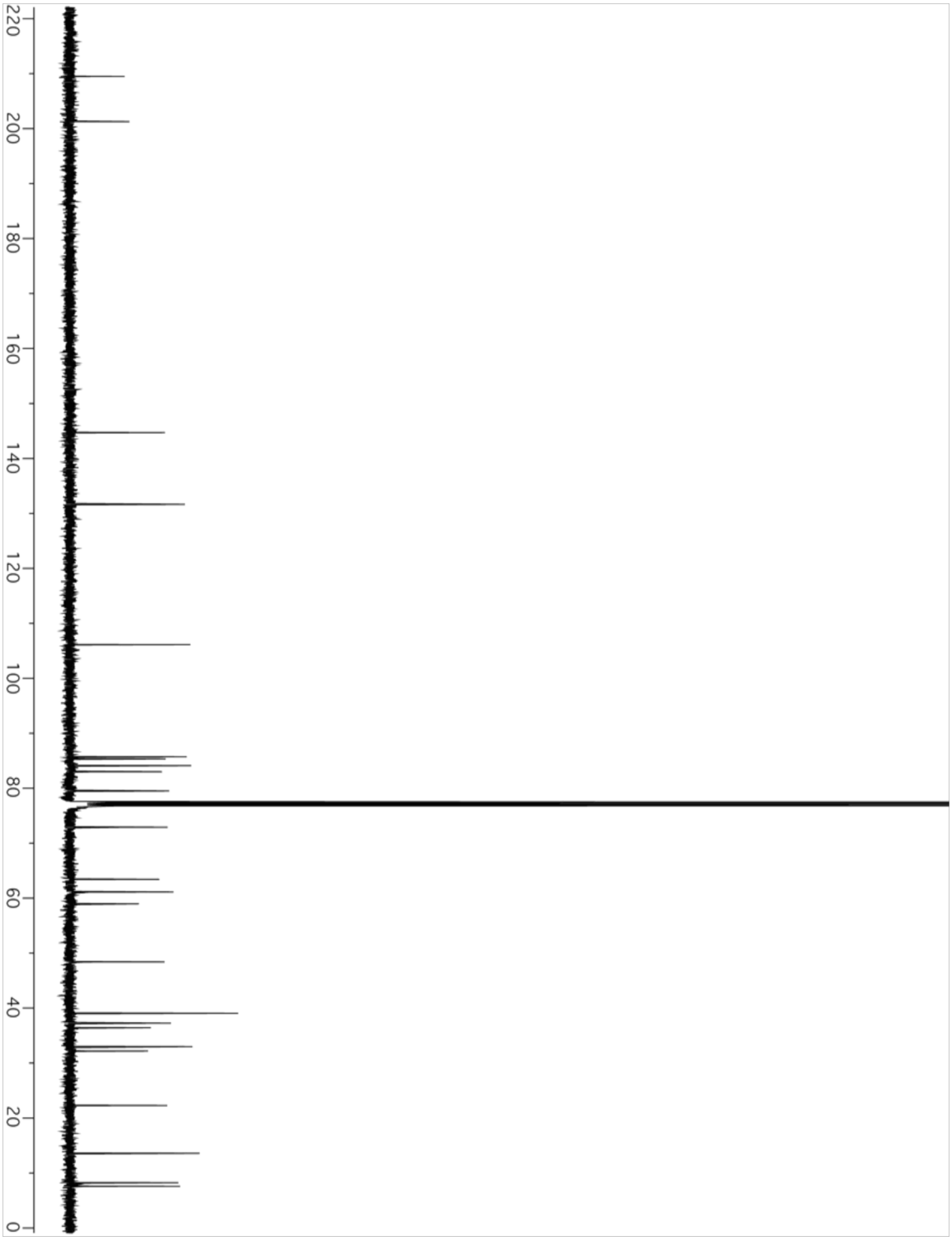
220
200
180
160
140
120
100
80
60
40
20
0

(R)-1-((2R,4S,6S)-6-(2-hydroxyethyl)-5,5-dimethyl-4-(((2S,3R,4S,5R)-3,4,5-trimethoxytetrahydro-2H-pyran-2-yl)oxy)tetrahydro-2H-pyran-2-yl)butan-2-ol (3.12)

A stirred solution of **3.11** (166 mg, 0.353 mmol, 100 mol%) in THF (7.06 mL, 0.05 M) was cooled to -78 ºC. Ozone was bubbled through the solution until a light blue color persisted (about 3 min.). The solution was then sparged with O_2 for 3 minutes followed by argon for 5 minutes. L-selectride (3.53 mL, 3.53 mmol, 1000 mol%, 1M in THF) was added dropwise and the solution was allowed to warm to ambient temperature over the course of 1 h. The reaction was concentrated onto silica gel and purified *via* column chromatography (SiO_2: ethyl acetate:hexanes, 1:1) to afford **3.12** (105.4 mg, 71% yield, dr = 5:1, seperable) as a white solid.

TLC (SiO_2): R_f = 0.10 (ethyl acetate:hexanes, 2:5)

^{1}H NMR: (400 MHz; $CDCl_3$): δ 4.23 (d, *J* = 7.6 Hz, 1H), 3.94 (dd, *J* = 11.5, 5.2 Hz, 1H), 3.79 – 3.67 (m, 3H), 3.61 (s, 3H), 3.61 (s, 3H), 3.46 (s, 3H), 3.30 – 3.18 (m, 3H), 3.12 – 3.03 (m, 2H), 2.96 (dd, *J* = 9.1, 7.6 Hz, 1H), 1.88 (ddd, *J* = 12.9, 4.8, 2.3 Hz, 1H), 1.77 – 1.51 (m, 6H), 1.51 – 1.40 (m, 2H), 0.97 (s, 3H), 0.91 (t, *J* = 7.5 Hz, 3H), 0.91 (s, 3H).

^{13}C NMR: (100 MHz, $CDCl_3$): δ 106.2, 105.2, 85.7, 85.4, 84.1, 83.2, 79.5, 76.6, 73.1, 63.4, 61.4, 61.2, 61.0, 59.0, 42.2, 39.1, 37.1, 31.3, 30.7, 22.3, 13.6.

FTIR (neat): ν 3427, 2933, 1464, 1370, 1162, 1091, 1017 cm^{-1}.

HRMS: (ESI) Calcd. for $C_{21}H_{40}O_8Na$ $(M+Na)^+$: 444.2650, Found: 444.2650.

$[\alpha]^{24}_D$: -38.16 ° (c = 0.76, CH_2Cl_2).

MP: 129 – 131 °C

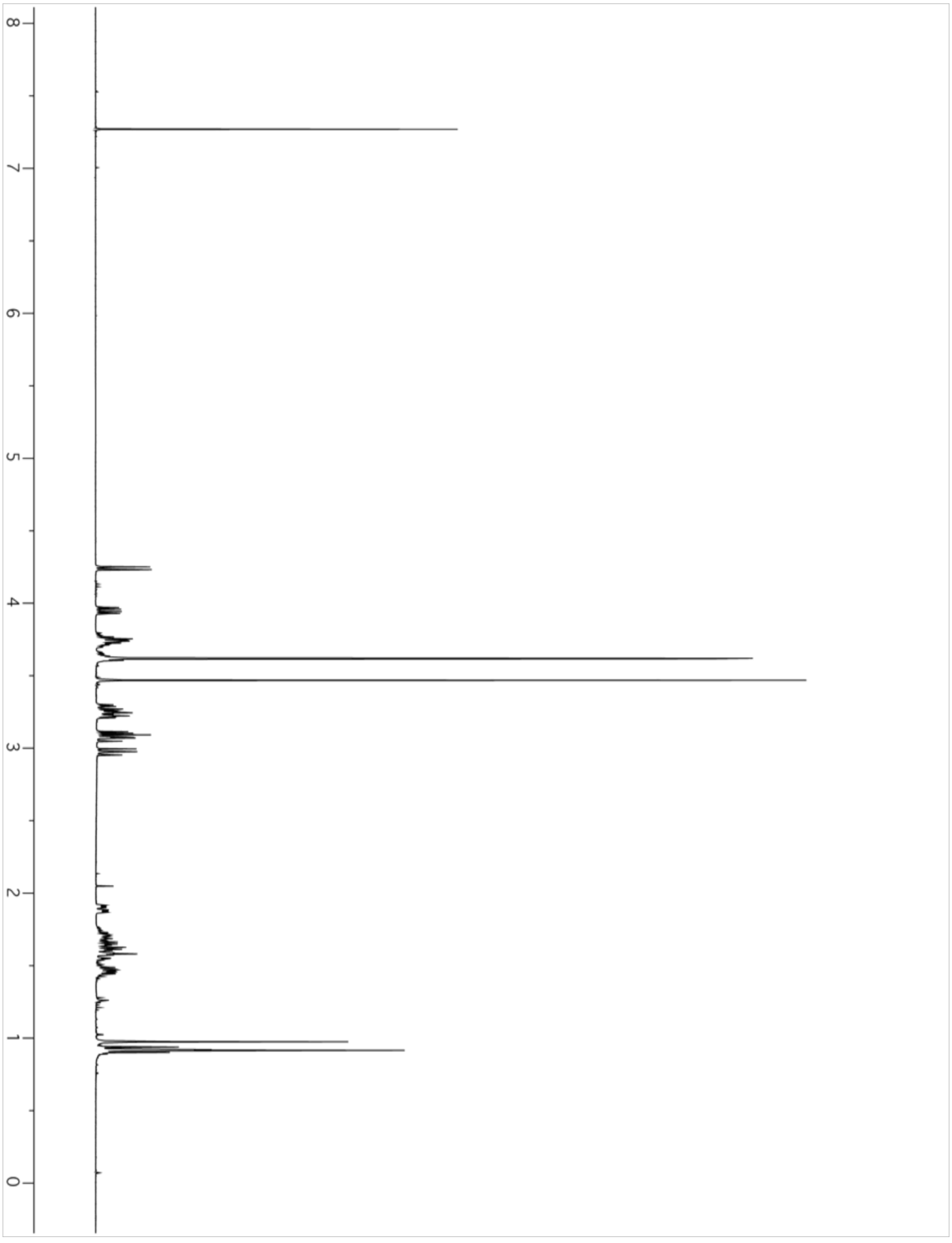
8
7
6
5
4
3
2
1
0

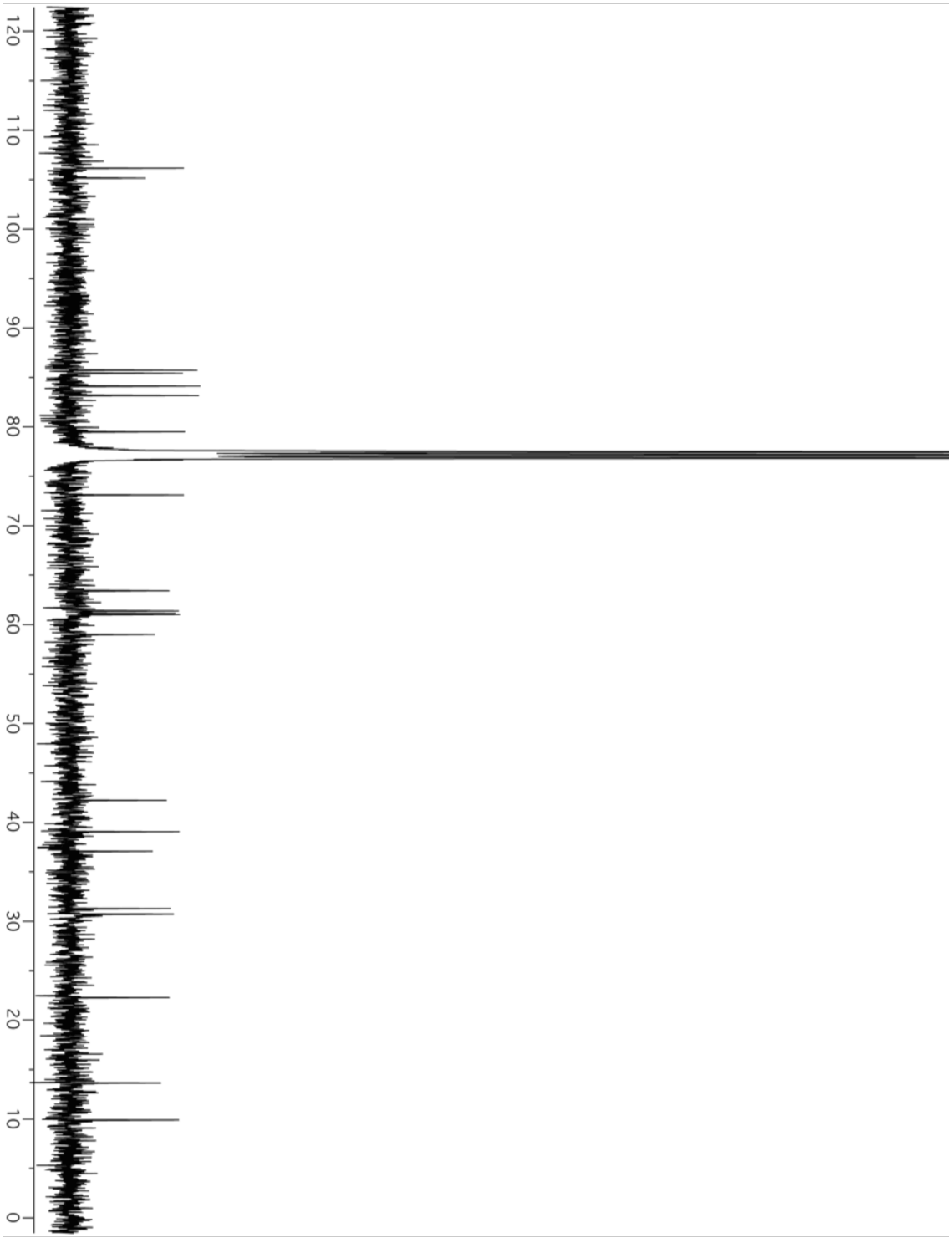
120
110
100
90
80
70
60
50
40
30
20
10
0

(−)-Cyanolide A (3.1)

To a stirred solution of **3.10** (45.1 mg, 0.104 mmol, 100 mol%) in THF (1 mL) was added Et_3N (0.02 mL, 0.145 mmol, 140 mol%) and 2,4,6-trichlorobenzoyl chloride (0.02 mL, 0.125 mmol, 120 mol%). The solution was stirred at ambient temperature for 2.5 h. The reaction mixture was diluted with toluene (7 mL) and added dropwise over 5 h to a solution of DMAP (63.5 mg, 0.520 mmol, 500 mol%) in toluene (27 mL) at 120 ºC. The syringe was rinsed with 2 mL of dry toluene and added dropwise to the refluxing solution over 0.5 h. The reaction mixture continued to stir at 120 ºC for an additional 15 h. The solution was then cooled to ambient temperature and the solvent removed under reduced pressure. The crude material was purified *via* column chromatography (ethyl acetate:hexanes, 3:7) to afford **3.1** (20.4 mg, 47%) as a pale yellow oil.

TLC (SiO_2): R_f = 0.5 (ethyl acetate:hexanes, 3:5)

^{1}H NMR: (400 MHz; $CDCl_3$): δ 4.91 (q, *J* = 6.9 Hz, 2H), 4.25 (d, *J* = 6.4 Hz, 2H), 3.97 (dd, *J* = 11.0, 4.5 Hz, 2H), 3.62 (s, 6H), 3.61 (s, 6H), 3.46 (s, 6H), 3.47-3.40 (m, 4H), 3.35-3.29 (m, 2H), 3.29-3.21 (m, 2H), 3.09 (t, *J* = 9.6 Hz, 4H), 2.96 (q, *J* = 7.1 Hz, 2H), 2.38 (d, *J* = 16.2 Hz, 2H), 2.27 (dd, *J* = 16.2, 9.2 Hz, 2H), 1.98 (d, *J* = 12.8 Hz, 2H), 1.82 (dt, *J* = 15.6, 8.1 Hz, 2H), 1.64 – 1.42 (m, 8H), 0.96 (s, 6H), 0.88 (s, 6H), 0.85 (d, *J* = 7.7 Hz, 6H).

^{13}C NMR: (100 MHz, $CDCl_3$): δ 172.0, 106.3, 85.9, 85.7, 84.3, 80.7, 79.7, 75.6, 74.2, 63.6, 61.3, 61.2, 59.1, 40.9, 39.0, 37.3, 35.4, 28.6, 22.4, 13.9, 9.8.

FTIR (neat): ν 2966, 2932, 2360, 2340, 1739, 1465, 1370, 1302, 1259, 1162, 1095, 1019 cm^{-1}.

HRMS: (ESI) Calcd. for $C_{42}H_{73}O_{16}$ $(M+H)^+$: 833.4893, Found: 833.4900.

$[\alpha]^{23}_D$: -41.92 ° (c = 0.33, $CHCl_3$).

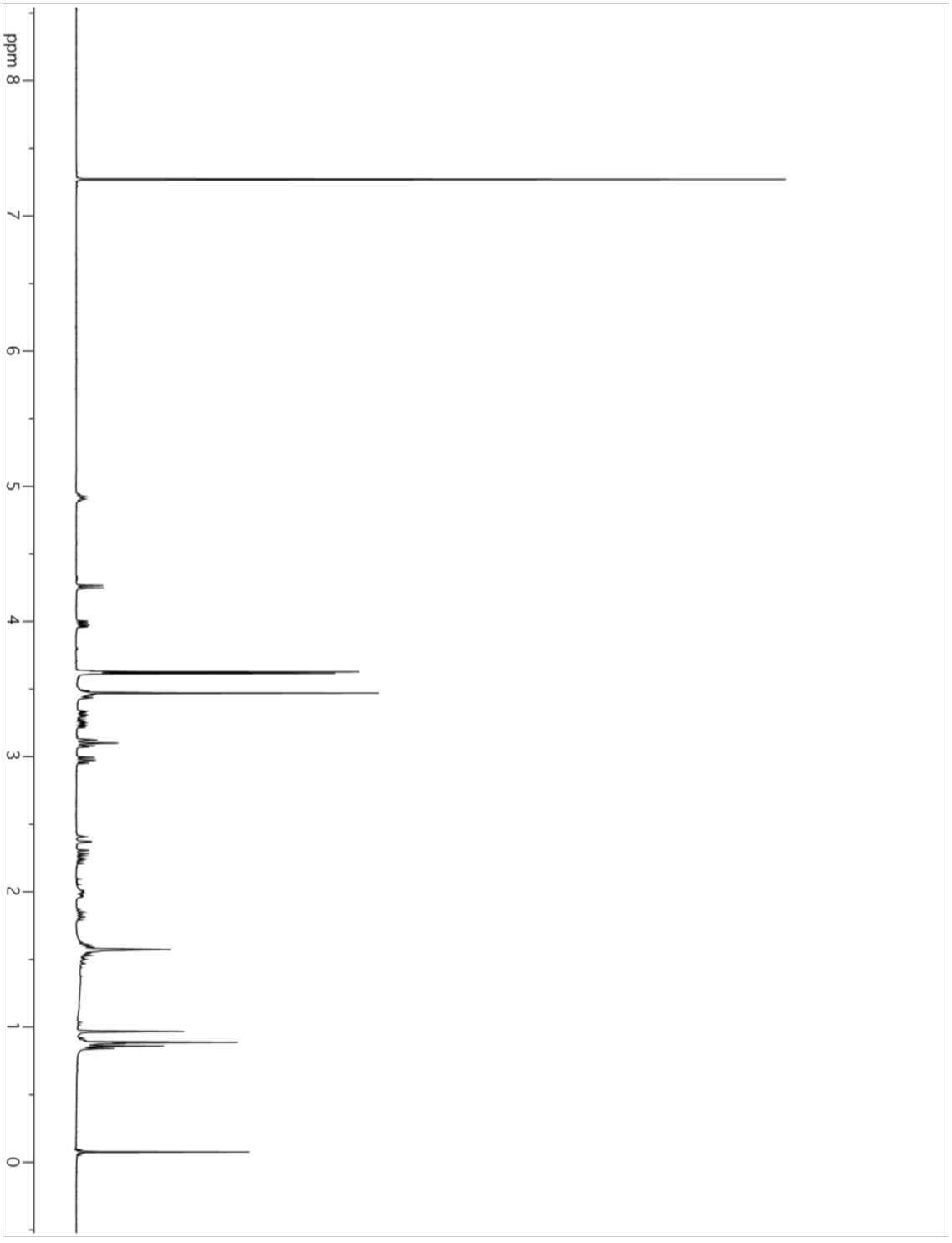
ppm
8
7
6
5
4
3
2
1
0

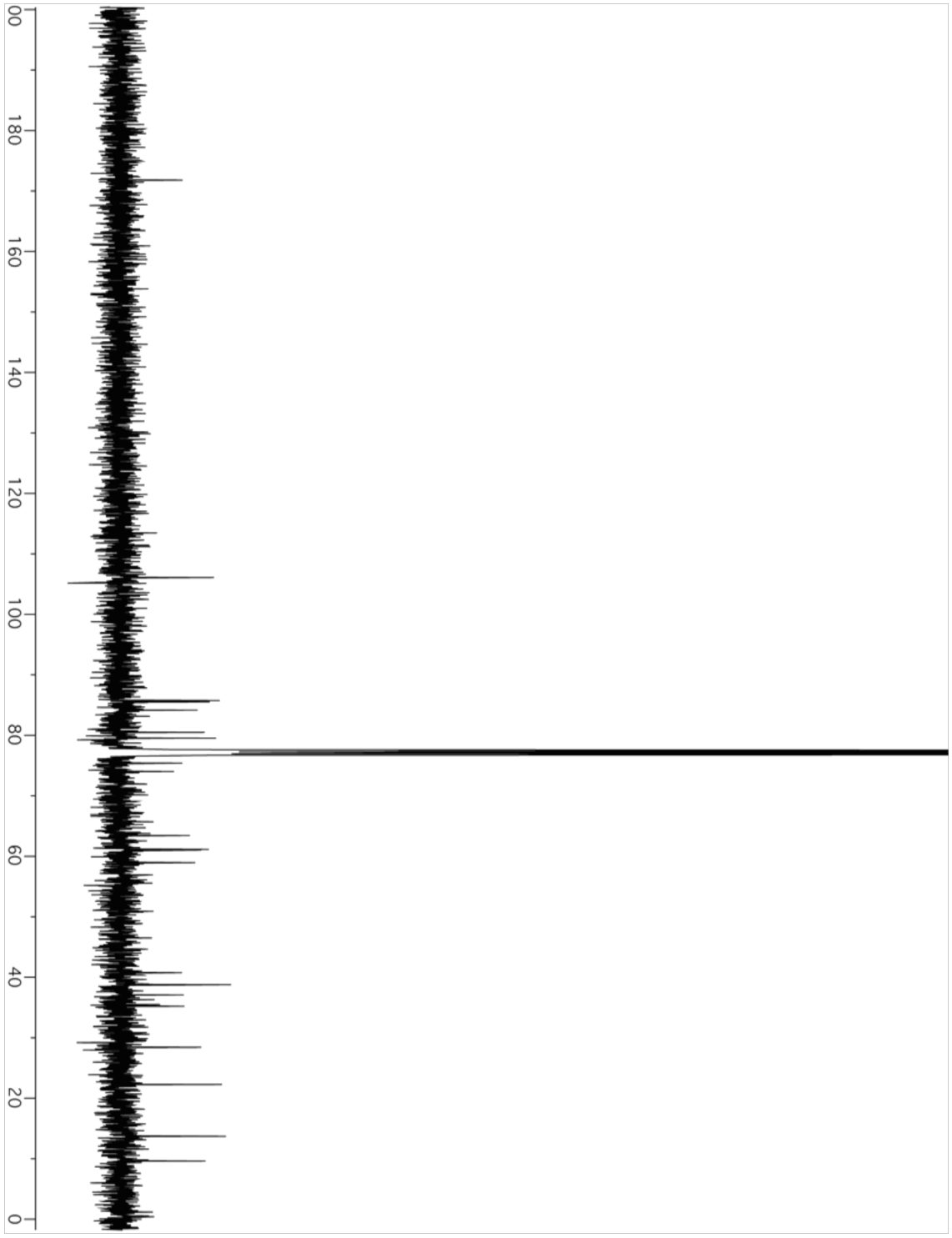
200
180
160
140
120
100
80
60
40
20
0

cyanolide A (natural)
cyanolide A (synthetic)
ppm
0.997
1.038
1.001
6.118
5.143
1.038
1.046
2.009
1.030
1.044
1.073
1.015
1.067
6.809
3.136
6.563

3.4.4 Crystal Data and Structure Refinement for 3.10

Empirical formula	C22 H38 O7	
Formula weight	414.52	
Temperature	153(2) K	
Wavelength	0.71075 Å	
Crystal system	Triclinic	
Space group	P1	
Unit cell dimensions	a = 8.377(4) Å	a= 81.422(11)°.
	b = 11.083(6) Å	b= 89.682(10)°.
	c = 12.860(6) Å	g = 88.711(11)°.
Volume	1180.3(10) $Å^3$	
Z	2	
Density (calculated)	1.166 Mg/m^3	
Absorption coefficient	0.085 mm^{-1}	
F(000)	452	
Crystal size	0.26 x 0.16 x 0.05 mm	
Theta range for data collection	3.03 to 27.48°.	
Index ranges	-10<=h<=10, -14<=k<=14, -16<=l<=16	
Reflections collected	12596	
Independent reflections	5388 [R(int) = 0.0940]	
Completeness to theta = 27.48°	99.6 %	
Absorption correction	Semi-empirical from equivalents	
Max. and min. transmission	1.00 and 0.443	
Refinement method	Full-matrix least-squares on F^2	
Data / restraints / parameters	5388 / 51 / 559	
Goodness-of-fit on F^2	1.004	
Final R indices [I>2sigma(I)]	R1 = 0.0719, wR2 = 0.1309	
R indices (all data)	R1 = 0.1567, wR2 = 0.1673	
Largest diff. peak and hole	0.202 and -0.255 $e.Å^{-3}$	

Table 3.1 Atomic coordinates (x 10^4) and equivalent isotropic displacement parameters ($Å^2$x10^3) for **3.10**. U(eq) is defined as one third of the trace of the orthogonalized U^{ij} tensor.

	x	y	z	U(eq)
O1	2368(4)	7582(4)	1590(3)	30(1)
O2	-1183(5)	7598(4)	546(4)	44(1)
O3	4172(5)	5233(3)	4145(3)	33(1)
O4	2381(5)	3907(4)	4963(3)	43(1)
O5	2908(7)	983(4)	6708(4)	65(2)
O6	5784(6)	2288(4)	7020(3)	56(1)
O7	6747(5)	3684(4)	5018(3)	41(1)
C1	1187(7)	6847(6)	2185(5)	33(1)
C2	3772(7)	6894(6)	1375(4)	31(1)
C3	4639(7)	6414(5)	2431(4)	29(1)
C4	3451(7)	5637(6)	3121(4)	33(2)
C5	1854(7)	6291(6)	3266(5)	33(2)
C6	3963(8)	4029(5)	4576(5)	35(2)
C7	2084(9)	2654(7)	5397(6)	53(2)
C8	3160(8)	2257(6)	6350(5)	44(2)
C9	4873(8)	2437(6)	6075(5)	45(2)
C10	5190(8)	3688(6)	5450(5)	37(2)
C11	-246(7)	7692(6)	2270(5)	39(2)
C12	-847(7)	8238(6)	1191(5)	35(2)
C13	-977(10)	9592(6)	930(6)	54(2)
C14	-1528(10)	10092(7)	-168(6)	63(2)
C15	4754(8)	7734(6)	593(5)	37(2)
C16	3916(8)	8037(6)	-451(5)	42(2)
C17	4560(10)	7967(7)	-1358(6)	61(2)
C18	5201(7)	7479(5)	2977(5)	34(1)
C19	6079(7)	5594(6)	2221(5)	36(2)
C22	7675(9)	4689(7)	5192(6)	56(2)
O8	7435(4)	3447(4)	10045(3)	32(1)

O9	3907(5)	3441(4)	11112(4)	44(1)
O10	9113(5)	5802(4)	7485(3)	35(1)
O11	7241(5)	7121(4)	6654(3)	45(1)
O12	7587(8)	10022(4)	4903(4)	75(2)
O13	10584(7)	8738(5)	4607(3)	57(1)
O14	11590(6)	7368(4)	6608(4)	46(1)
C23	6228(7)	4185(6)	9448(5)	34(1)
C24	8801(7)	4141(5)	10233(4)	30(1)
C25	9653(7)	4631(5)	9197(4)	28(1)
C26	8405(7)	5404(5)	8508(4)	31(1)
C27	6865(7)	4734(6)	8384(5)	32(1)
C28	8834(8)	7007(6)	7056(5)	37(2)
C29	6875(10)	8365(7)	6213(6)	57(2)
C30	7920(10)	8760(6)	5261(5)	49(2)
C31	9679(9)	8597(6)	5551(5)	47(2)
C32	10033(8)	7342(6)	6176(5)	38(2)
C33	4857(7)	3336(6)	9378(5)	39(2)
C34	4230(7)	2790(6)	10468(5)	34(2)
C35	4029(9)	1436(6)	10668(6)	53(2)
C36	3430(9)	959(7)	11775(5)	58(2)
C37	9801(8)	3280(6)	11039(5)	37(2)
C38	9003(8)	2989(6)	12082(5)	40(2)
C39	9619(10)	3081(7)	12986(6)	58(2)
C40	11036(7)	5447(6)	9407(5)	34(2)
C41	10293(7)	3576(5)	8642(5)	34(1)
C42	6834(13)	10325(8)	3988(7)	88(3)
C43	11749(14)	9589(9)	4492(8)	101(4)
C44	12605(9)	6386(8)	6421(6)	59(2)
C21	6750(20)	1258(14)	7251(15)	62(6)
C21A	7304(12)	1763(14)	6982(11)	60(5)
C20	2280(40)	682(16)	7708(14)	51(8)
C20A	1755(17)	711(11)	7481(10)	61(5)

Table 3.2 Bond lengths [Å] and angles [°] for **3.10**.

O1-C2	1.435(7)	C7-H7B	0.99
O1-C1	1.439(7)	C8-C9	1.487(10)
O2-C12	1.207(7)	C8-H8	1.00
O3-C6	1.381(7)	C9-C10	1.523(9)
O3-C4	1.457(6)	C9-H9	1.00
O4-C6	1.415(7)	C10-H10	1.00
O4-C7	1.444(8)	C11-C12	1.512(9)
O5-C20	1.385(10)	C11-H11A	0.99
O5-C20A	1.388(9)	C11-H11B	0.99
O5-C8	1.438(7)	C12-C13	1.490(9)
O6-C21	1.380(9)	C13-C14	1.508(9)
O6-C21A	1.391(9)	C13-H13A	0.99
O6-C9	1.425(7)	C13-H13B	0.99
O7-C10	1.415(8)	C14-H14A	0.98
O7-C22	1.418(8)	C14-H14B	0.98
C1-C11	1.519(8)	C14-H14C	0.98
C1-C5	1.536(8)	C15-C16	1.508(8)
C1-H1	1.00	C15-H15A	0.99
C2-C15	1.517(9)	C15-H15B	0.99
C2-C3	1.560(7)	C16-C17	1.294(9)
C2-H2	1.00	C16-H16	0.95
C3-C4	1.524(8)	C17-H17A	0.95
C3-C19	1.541(8)	C17-H17B	0.95
C3-C18	1.544(8)	C18-H18A	0.98
C4-C5	1.531(8)	C18-H18B	0.98
C4-H4	1.00	C18-H18C	0.98
C5-H5A	0.99	C19-H19A	0.98
C5-H5B	0.99	C19-H19B	0.98
C6-C10	1.526(8)	C19-H19C	0.98
C6-H6	1.00	C22-H22A	0.98
C7-C8	1.530(9)	C22-H22B	0.98
C7-H7A	0.99	C22-H22C	0.98

O8-C24	1.435(7)	C33-C34	1.537(9)
O8-C23	1.437(7)	C33-H33A	0.99
O9-C34	1.203(7)	C33-H33B	0.99
O10-C28	1.382(7)	C34-C35	1.497(9)
O10-C26	1.451(7)	C35-C36	1.529(9)
O11-C28	1.429(8)	C35-H35A	0.99
O11-C29	1.438(8)	C35-H35B	0.99
O12-C42	1.333(9)	C36-H36A	0.98
O12-C30	1.428(8)	C36-H36B	0.98
O13-C43	1.364(9)	C36-H36C	0.98
O13-C31	1.418(8)	C37-C38	1.490(9)
O14-C44	1.414(8)	C37-H37A	0.99
O14-C32	1.423(8)	C37-H37B	0.99
C23-C27	1.512(8)	C38-C39	1.293(9)
C23-C33	1.513(8)	C38-H38	0.95
C23-H23	1.00	C39-H39A	0.95
C24-C37	1.538(8)	C39-H39B	0.95
C24-C25	1.540(8)	C40-H40A	0.98
C24-H24	1.00	C40-H40B	0.98
C25-C26	1.535(8)	C40-H40C	0.98
C25-C40	1.535(8)	C41-H41A	0.98
C25-C41	1.544(8)	C41-H41B	0.98
C26-C27	1.524(8)	C41-H41C	0.98
C26-H26	1.00	C42-H42A	0.98
C27-H27A	0.99	C42-H42B	0.98
C27-H27B	0.99	C42-H42C	0.98
C28-C32	1.519(8)	C43-H43A	0.98
C28-H28	1.00	C43-H43B	0.98
C29-C30	1.517(10)	C43-H43C	0.98
C29-H29A	0.99	C44-H44A	0.98
C29-H29B	0.99	C44-H44B	0.98
C30-C31	1.522(10)	C44-H44C	0.98
C30-H30	1.00	C21-H21A	0.98
C31-C32	1.523(9)	C21-H21B	0.98
C31-H31	1.00	C21-H21C	0.98
C32-H32	1.00	C21A-H21D	0.98

C21A-H21E	0.98	C20-H20C	0.98
C21A-H21F	0.98	C20A-H20D	0.98
C20-H20A	0.98	C20A-H20E	0.98
C20-H20B	0.98	C20A-H20F	0.98

C2-O1-C1	112.9(4)	C5-C4-H4	108.2
C6-O3-C4	116.7(5)	C4-C5-C1	109.5(5)
C6-O4-C7	110.6(5)	C4-C5-H5A	109.8
C20-O5-C8	116.7(9)	C1-C5-H5A	109.8
C20A-O5-C8	116.4(7)	C4-C5-H5B	109.8
C21-O6-C9	118.4(8)	C1-C5-H5B	109.8
C21A-O6-C9	117.0(7)	H5A-C5-H5B	108.2
C10-O7-C22	114.3(5)	O3-C6-O4	108.3(5)
O1-C1-C11	105.9(5)	O3-C6-C10	108.4(5)
O1-C1-C5	110.5(5)	O4-C6-C10	111.7(5)
C11-C1-C5	112.5(5)	O3-C6-H6	109.4
O1-C1-H1	109.3	O4-C6-H6	109.4
C11-C1-H1	109.3	C10-C6-H6	109.4
C5-C1-H1	109.3	O4-C7-C8	110.0(6)
O1-C2-C15	106.4(5)	O4-C7-H7A	109.7
O1-C2-C3	109.1(4)	C8-C7-H7A	109.7
C15-C2-C3	114.6(5)	O4-C7-H7B	109.7
O1-C2-H2	108.9	C8-C7-H7B	109.7
C15-C2-H2	108.9	H7A-C7-H7B	108.2
C3-C2-H2	108.9	O5-C8-C9	109.2(6)
C4-C3-C19	108.3(5)	O5-C8-C7	108.1(6)
C4-C3-C18	110.8(5)	C9-C8-C7	111.4(5)
C19-C3-C18	109.9(5)	O5-C8-H8	109.4
C4-C3-C2	106.8(4)	C9-C8-H8	109.4
C19-C3-C2	109.6(5)	C7-C8-H8	109.4
C18-C3-C2	111.2(5)	O6-C9-C8	108.9(6)
O3-C4-C3	108.9(5)	O6-C9-C10	109.1(6)
O3-C4-C5	109.5(5)	C8-C9-C10	113.0(5)
C3-C4-C5	113.9(5)	O6-C9-H9	108.6
O3-C4-H4	108.2	C8-C9-H9	108.6
C3-C4-H4	108.2	C10-C9-H9	108.6

O7-C10-C9	109.1(5)	C16-C17-H17A	120.0
O7-C10-C6	110.1(5)	C16-C17-H17B	120.0
C9-C10-C6	111.5(5)	H17A-C17-H17B	120.0
O7-C10-H10	108.7	C3-C18-H18A	109.5
C9-C10-H10	108.7	C3-C18-H18B	109.5
C6-C10-H10	108.7	H18A-C18-H18B	109.5
C12-C11-C1	110.9(5)	C3-C18-H18C	109.5
C12-C11-H11A	109.5	H18A-C18-H18C	109.5
C1-C11-H11A	109.5	H18B-C18-H18C	109.5
C12-C11-H11B	109.5	C3-C19-H19A	109.5
C1-C11-H11B	109.5	C3-C19-H19B	109.5
H11A-C11-H11B	108.0	H19A-C19-H19B	109.5
O2-C12-C13	120.5(6)	C3-C19-H19C	109.5
O2-C12-C11	121.1(6)	H19A-C19-H19C	109.5
C13-C12-C11	118.4(6)	H19B-C19-H19C	109.5
C12-C13-C14	116.3(6)	O7-C22-H22A	109.5
C12-C13-H13A	108.2	O7-C22-H22B	109.5
C14-C13-H13A	108.2	H22A-C22-H22B	109.5
C12-C13-H13B	108.2	O7-C22-H22C	109.5
C14-C13-H13B	108.2	H22A-C22-H22C	109.5
H13A-C13-H13B	107.4	H22B-C22-H22C	109.5
C13-C14-H14A	109.5	C24-O8-C23	112.1(4)
C13-C14-H14B	109.5	C28-O10-C26	116.4(4)
H14A-C14-H14B	109.5	C28-O11-C29	110.6(5)
C13-C14-H14C	109.5	C42-O12-C30	118.2(6)
H14A-C14-H14C	109.5	C43-O13-C31	117.8(6)
H14B-C14-H14C	109.5	C44-O14-C32	114.1(5)
C16-C15-C2	111.5(5)	O8-C23-C27	110.9(5)
C16-C15-H15A	109.3	O8-C23-C33	105.0(5)
C2-C15-H15A	109.3	C27-C23-C33	113.1(5)
C16-C15-H15B	109.3	O8-C23-H23	109.3
C2-C15-H15B	109.3	C27-C23-H23	109.3
H15A-C15-H15B	108.0	C33-C23-H23	109.3
C17-C16-C15	125.1(7)	O8-C24-C37	104.7(5)
C17-C16-H16	117.4	O8-C24-C25	111.2(4)
C15-C16-H16	117.4	C37-C24-C25	115.9(5)

O8-C24-H24	108.3	O12-C30-H30	109.8
C37-C24-H24	108.3	C29-C30-H30	109.8
C25-C24-H24	108.3	C31-C30-H30	109.8
C26-C25-C40	109.0(5)	O13-C31-C32	109.4(6)
C26-C25-C24	106.3(4)	O13-C31-C30	108.1(5)
C40-C25-C24	110.3(5)	C32-C31-C30	111.5(6)
C26-C25-C41	110.4(5)	O13-C31-H31	109.3
C40-C25-C41	109.6(5)	C32-C31-H31	109.3
C24-C25-C41	111.1(5)	C30-C31-H31	109.3
O10-C26-C27	110.1(5)	O14-C32-C28	109.6(5)
O10-C26-C25	108.4(4)	O14-C32-C31	107.4(5)
C27-C26-C25	113.4(5)	C28-C32-C31	112.3(6)
O10-C26-H26	108.3	O14-C32-H32	109.2
C27-C26-H26	108.3	C28-C32-H32	109.2
C25-C26-H26	108.2	C31-C32-H32	109.2
C23-C27-C26	110.4(5)	C23-C33-C34	112.1(5)
C23-C27-H27A	109.6	C23-C33-H33A	109.2
C26-C27-H27A	109.6	C34-C33-H33A	109.2
C23-C27-H27B	109.6	C23-C33-H33B	109.2
C26-C27-H27B	109.6	C34-C33-H33B	109.2
H27A-C27-H27B	108.1	H33A-C33-H33B	107.9
O10-C28-O11	108.2(5)	O9-C34-C35	122.9(6)
O10-C28-C32	108.3(5)	O9-C34-C33	120.3(6)
O11-C28-C32	110.5(5)	C35-C34-C33	116.8(6)
O10-C28-H28	109.9	C34-C35-C36	113.7(6)
O11-C28-H28	109.9	C34-C35-H35A	108.8
C32-C28-H28	109.9	C36-C35-H35A	108.8
O11-C29-C30	110.5(6)	C34-C35-H35B	108.8
O11-C29-H29A	109.6	C36-C35-H35B	108.8
C30-C29-H29A	109.6	H35A-C35-H35B	107.7
O11-C29-H29B	109.6	C35-C36-H36A	109.5
C30-C29-H29B	109.6	C35-C36-H36B	109.5
H29A-C29-H29B	108.1	H36A-C36-H36B	109.5
O12-C30-C29	108.0(6)	C35-C36-H36C	109.5
O12-C30-C31	108.8(6)	H36A-C36-H36C	109.5
C29-C30-C31	110.7(6)	H36B-C36-H36C	109.5

C38-C37-C24	113.3(5)	O13-C43-H43A	109.5
C38-C37-H37A	108.9	O13-C43-H43B	109.5
C24-C37-H37A	108.9	H43A-C43-H43B	109.5
C38-C37-H37B	108.9	O13-C43-H43C	109.5
C24-C37-H37B	108.9	H43A-C43-H43C	109.5
H37A-C37-H37B	107.7	H43B-C43-H43C	109.5
C39-C38-C37	126.3(7)	O14-C44-H44A	109.5
C39-C38-H38	116.9	O14-C44-H44B	109.5
C37-C38-H38	116.9	H44A-C44-H44B	109.5
C38-C39-H39A	120.0	O14-C44-H44C	109.5
C38-C39-H39B	120.0	H44A-C44-H44C	109.5
H39A-C39-H39B	120.0	H44B-C44-H44C	109.5
C25-C40-H40A	109.5	O6-C21-H21A	109.5
C25-C40-H40B	109.5	O6-C21-H21B	109.5
H40A-C40-H40B	109.5	O6-C21-H21C	109.5
C25-C40-H40C	109.5	O6-C21A-H21D	109.5
H40A-C40-H40C	109.5	O6-C21A-H21E	109.5
H40B-C40-H40C	109.5	H21D-C21A-H21E	109.5
C25-C41-H41A	109.5	O6-C21A-H21F	109.5
C25-C41-H41B	109.5	H21D-C21A-H21F	109.5
H41A-C41-H41B	109.5	H21E-C21A-H21F	109.5
C25-C41-H41C	109.5	O5-C20-H20A	109.5
H41A-C41-H41C	109.5	O5-C20-H20B	109.5
H41B-C41-H41C	109.5	O5-C20-H20C	109.5
O12-C42-H42A	109.5	O5-C20A-H20D	109.5
O12-C42-H42B	109.5	O5-C20A-H20E	109.5
H42A-C42-H42B	109.5	H20D-C20A-H20E	109.5
O12-C42-H42C	109.5	O5-C20A-H20F	109.5
H42A-C42-H42C	109.5	H20D-C20A-H20F	109.5
H42B-C42-H42C	109.5	H20E-C20A-H20F	109.5

Table 3.3 Anisotropic displacement parameters (Å2x 103) for **3.10**. The anisotropic displacement factor exponent takes the form: -2p2[h2 a*2U11 + ... + 2 h k a* b* U12]

	U^{11}	U^{22}	U^{33}	U^{23}	U^{13}	U^{12}
O1	24(2)	34(2)	31(2)	1(2)	5(2)	0(2)
O2	43(3)	49(3)	41(3)	-10(2)	-9(2)	7(2)
O3	46(3)	31(3)	21(2)	2(2)	-9(2)	2(2)
O4	49(3)	38(3)	39(3)	8(2)	-3(2)	-4(2)
O5	110(5)	36(3)	46(3)	8(2)	16(3)	-11(3)
O6	85(4)	54(3)	27(3)	0(2)	-17(3)	17(3)
O7	46(3)	42(3)	35(3)	-5(2)	-4(2)	4(2)
C1	27(3)	41(4)	29(3)	-3(3)	1(3)	2(3)
C2	34(3)	37(4)	23(3)	-4(3)	1(3)	0(3)
C3	33(3)	29(3)	24(3)	-2(3)	-7(3)	0(3)
C4	40(4)	35(4)	20(3)	4(3)	-6(3)	1(3)
C5	33(3)	39(4)	25(3)	3(3)	-3(3)	1(3)
C6	48(4)	26(4)	30(4)	3(3)	-2(3)	3(3)
C7	60(5)	45(5)	48(4)	11(4)	-5(4)	-12(4)
C8	67(5)	32(4)	32(4)	-1(3)	5(4)	-3(3)
C9	72(5)	33(4)	26(4)	1(3)	-9(3)	13(4)
C10	47(4)	33(4)	29(3)	5(3)	-1(3)	5(3)
C11	35(4)	43(4)	35(4)	3(3)	1(3)	3(3)
C12	23(3)	45(4)	36(4)	-7(3)	2(3)	-2(3)
C13	72(5)	45(5)	44(4)	1(3)	-9(4)	-6(4)
C14	71(5)	53(5)	57(5)	17(4)	-13(4)	-4(4)
C15	35(4)	41(4)	33(4)	0(3)	-5(3)	-4(3)
C16	43(4)	45(4)	32(4)	13(3)	-2(3)	-3(3)
C17	64(5)	80(6)	35(4)	5(4)	-3(4)	15(4)
C18	35(3)	34(4)	32(3)	-2(3)	-5(3)	-2(3)
C19	37(4)	34(4)	36(4)	-3(3)	-1(3)	4(3)
C22	64(5)	54(5)	51(5)	-11(4)	-8(4)	-5(4)
O8	29(2)	37(2)	28(2)	2(2)	-3(2)	-6(2)
O9	40(3)	55(3)	39(3)	-12(2)	7(2)	-8(2)

O10	41(2)	34(3)	25(2)	3(2)	6(2)	-1(2)
O11	42(3)	46(3)	41(3)	13(2)	2(2)	2(2)
O12	141(6)	36(3)	42(3)	7(2)	-24(3)	9(3)
O13	89(4)	59(3)	25(3)	-4(2)	19(3)	-28(3)
O14	52(3)	45(3)	40(3)	-5(2)	5(2)	-11(2)
C23	30(3)	42(4)	27(3)	3(3)	-4(3)	1(3)
C24	33(3)	27(3)	27(3)	3(3)	0(3)	-3(3)
C25	27(3)	26(3)	30(3)	-1(3)	4(3)	1(3)
C26	37(4)	27(3)	26(3)	2(3)	0(3)	2(3)
C27	34(3)	33(4)	28(3)	2(3)	0(3)	1(3)
C28	49(4)	30(4)	29(4)	2(3)	5(3)	-2(3)
C29	68(5)	48(5)	49(5)	12(4)	-3(4)	10(4)
C30	94(6)	27(4)	23(3)	8(3)	1(4)	-6(4)
C31	83(6)	36(4)	23(3)	-4(3)	7(4)	-13(4)
C32	54(4)	37(4)	22(3)	-1(3)	1(3)	-8(3)
C33	34(3)	57(4)	24(3)	-1(3)	-2(3)	-4(3)
C34	22(3)	41(4)	38(4)	0(3)	-2(3)	-2(3)
C35	64(5)	43(4)	49(4)	5(4)	14(4)	4(4)
C36	62(5)	60(5)	45(4)	9(4)	7(4)	4(4)
C37	35(4)	40(4)	32(4)	5(3)	-5(3)	4(3)
C38	39(4)	50(4)	27(4)	10(3)	0(3)	-3(3)
C39	65(5)	67(5)	40(4)	4(4)	-9(4)	-3(4)
C40	37(4)	39(4)	27(3)	-5(3)	7(3)	-3(3)
C41	38(4)	32(3)	32(3)	-6(3)	3(3)	-2(3)
C42	123(9)	67(6)	71(6)	-2(5)	-44(6)	22(6)
C43	139(10)	96(8)	78(7)	-40(6)	47(7)	-70(7)
C44	57(5)	78(6)	45(5)	-17(4)	2(4)	3(5)
C21	51(10)	55(12)	78(11)	-6(10)	-25(9)	18(9)
C21A	68(10)	44(9)	69(9)	-12(7)	-30(8)	18(7)
C20	64(15)	41(11)	44(11)	9(9)	7(12)	-9(10)
C20A	57(9)	51(7)	70(9)	4(6)	-2(7)	-11(6)

Table 3.4 Hydrogen coordinates (x 10^4) and isotropic displacement parameters ($Å^2$x 10^3) for **3.10**.

	x	y	z	U(eq)
H1	876	6176	1792	39
H2	3445	6180	1039	37
H4	3235	4898	2787	39
H5A	2009	6943	3702	40
H5B	1088	5705	3632	40
H6	4134	3496	4021	42
H7A	2298	2122	4856	64
H7B	950	2570	5611	64
H8	2863	2739	6922	53
H9	5228	1798	5646	53
H10	5126	4310	5938	45
H11A	-1110	7229	2664	46
H11B	57	8354	2663	46
H13A	81	9932	1039	65
H13B	-1727	9894	1435	65
H14A	-783	9821	-680	94
H14B	-1564	10985	-255	94
H14C	-2596	9793	-281	94
H15A	4953	8497	880	44
H15B	5800	7335	489	44
H16	2830	8301	-443	50
H17A	5644	7708	-1399	74
H17B	3949	8175	-1981	74
H18A	4300	8042	3043	51
H18B	6048	7915	2557	51
H18C	5614	7157	3678	51
H19A	6554	5224	2892	54
H19B	6877	6086	1800	54
H19C	5723	4949	1837	54

H22A	7175	5448	4838	84
H22B	8752	4597	4910	84
H22C	7738	4718	5949	84
H23	5871	4855	9843	40
H24	8427	4853	10572	36
H26	8136	6144	8840	37
H27A	6059	5310	8018	39
H27B	7072	4079	7951	39
H28	8960	7545	7607	44
H29A	7050	8903	6749	68
H29B	5737	8444	6004	68
H30	7672	8269	4692	59
H31	9981	9239	5979	57
H32	10018	6717	5691	45
H33A	5217	2666	8996	46
H33B	3978	3790	8970	46
H35A	5068	1032	10555	64
H35B	3265	1208	10149	64
H36A	4221	1121	12293	87
H36B	3268	78	11839	87
H36C	2417	1373	11903	87
H37A	10027	2511	10756	44
H37B	10836	3663	11135	44
H38	7940	2709	12083	48
H39A	10679	3357	13026	70
H39B	9012	2872	13610	70
H40A	11509	5808	8737	51
H40B	11848	4956	9835	51
H40C	10633	6098	9784	51
H41A	9457	2973	8630	51
H41B	11223	3187	9023	51
H41C	10604	3897	7919	51
H42A	7476	10049	3425	132
H42B	6680	11213	3842	132
H42C	5793	9935	4023	132
H43A	11268	10399	4515	151

H43B	12290	9583	3816	151
H43C	12524	9397	5064	151
H44A	12139	5613	6738	89
H44B	13653	6469	6734	89
H44C	12726	6394	5662	89
H21A	7521	1224	6681	93
H21B	6089	530	7326	93
H21C	7318	1286	7910	93
H21D	7603	1353	7685	90
H21E	8072	2400	6744	90
H21F	7307	1166	6492	90
H20A	1484	1308	7839	77
H20B	3132	637	8229	77
H20C	1760	-110	7765	77
H20D	1804	-165	7748	91
H20E	696	932	7183	91
H20F	1951	1173	8060	91

Table 3.5 Torsion angles [°] for **3.10**.

C2-O1-C1-C11	-175.9(5)	O4-C7-C8-C9	-56.0(8)
C2-O1-C1-C5	62.0(6)	C21-O6-C9-C8	108.7(13)
C1-O1-C2-C15	170.3(4)	C21A-O6-C9-C8	145.5(9)
C1-O1-C2-C3	-65.5(6)	C21-O6-C9-C10	-127.6(13)
O1-C2-C3-C4	58.6(6)	C21A-O6-C9-C10	-90.8(10)
C15-C2-C3-C4	177.8(5)	O5-C8-C9-O6	-72.2(7)
O1-C2-C3-C19	175.8(5)	C7-C8-C9-O6	168.6(5)
C15-C2-C3-C19	-65.0(7)	O5-C8-C9-C10	166.4(5)
O1-C2-C3-C18	-62.4(6)	C7-C8-C9-C10	47.1(8)
C15-C2-C3-C18	56.8(7)	C22-O7-C10-C9	-131.0(6)
C6-O3-C4-C3	-136.6(5)	C22-O7-C10-C6	106.4(6)
C6-O3-C4-C5	98.3(6)	O6-C9-C10-O7	72.1(7)
C19-C3-C4-O3	65.7(6)	C8-C9-C10-O7	-166.6(5)
C18-C3-C4-O3	-55.0(6)	O6-C9-C10-C6	-166.1(5)
C2-C3-C4-O3	-176.3(5)	C8-C9-C10-C6	-44.8(8)
C19-C3-C4-C5	-171.9(5)	O3-C6-C10-O7	-67.4(7)
C18-C3-C4-C5	67.5(6)	O4-C6-C10-O7	173.2(5)
C2-C3-C4-C5	-53.8(6)	O3-C6-C10-C9	171.3(5)
O3-C4-C5-C1	173.4(5)	O4-C6-C10-C9	52.0(7)
C3-C4-C5-C1	51.3(7)	O1-C1-C11-C12	58.2(6)
O1-C1-C5-C4	-52.2(7)	C5-C1-C11-C12	178.9(5)
C11-C1-C5-C4	-170.2(5)	C1-C11-C12-O2	54.0(8)
C4-O3-C6-O4	-75.6(6)	C1-C11-C12-C13	-124.5(6)
C4-O3-C6-C10	162.9(5)	O2-C12-C13-C14	-0.5(10)
C7-O4-C6-O3	178.3(5)	C11-C12-C13-C14	178.0(6)
C7-O4-C6-C10	-62.3(7)	O1-C2-C15-C16	-66.1(7)
C6-O4-C7-C8	63.9(7)	C3-C2-C15-C16	173.2(5)
C20-O5-C8-C9	122.1(18)	C2-C15-C16-C17	-131.1(7)
C20A-O5-C8-C9	146.5(9)	C24-O8-C23-C27	60.7(6)
C20-O5-C8-C7	-116.6(18)	C24-O8-C23-C33	-176.9(5)
C20A-O5-C8-C7	-92.2(10)	C23-O8-C24-C37	169.8(5)
O4-C7-C8-O5	-175.9(6)	C23-O8-C24-C25	-64.4(6)

O8-C24-C25-C26	57.8(6)	C43-O13-C31-C32	-113.6(8)
C37-C24-C25-C26	177.2(5)	C43-O13-C31-C30	124.8(8)
O8-C24-C25-C40	175.9(5)	O12-C30-C31-O13	-73.2(7)
C37-C24-C25-C40	-64.8(7)	C29-C30-C31-O13	168.3(6)
O8-C24-C25-C41	-62.3(6)	O12-C30-C31-C32	166.5(5)
C37-C24-C25-C41	57.0(7)	C29-C30-C31-C32	48.0(7)
C28-O10-C26-C27	99.1(6)	C44-O14-C32-C28	108.0(6)
C28-O10-C26-C25	-136.2(5)	C44-O14-C32-C31	-129.7(6)
C40-C25-C26-O10	65.9(6)	O10-C28-C32-O14	-68.7(6)
C24-C25-C26-O10	-175.1(4)	O11-C28-C32-O14	172.9(5)
C41-C25-C26-O10	-54.6(6)	O10-C28-C32-C31	172.0(5)
C40-C25-C26-C27	-171.4(5)	O11-C28-C32-C31	53.6(7)
C24-C25-C26-C27	-52.5(6)	O13-C31-C32-O14	73.1(7)
C41-C25-C26-C27	68.1(6)	C30-C31-C32-O14	-167.3(5)
O8-C23-C27-C26	-53.0(7)	O13-C31-C32-C28	-166.3(6)
C33-C23-C27-C26	-170.6(5)	C30-C31-C32-C28	-46.8(7)
O10-C26-C27-C23	173.1(5)	O8-C23-C33-C34	59.0(6)
C25-C26-C27-C23	51.5(6)	C27-C23-C33-C34	-180.0(5)
C26-O10-C28-O11	-76.7(6)	C23-C33-C34-O9	50.1(8)
C26-O10-C28-C32	163.5(5)	C23-C33-C34-C35	-130.8(6)
C29-O11-C28-O10	179.0(5)	O9-C34-C35-C36	-1.9(10)
C29-O11-C28-C32	-62.7(7)	C33-C34-C35-C36	179.0(6)
C28-O11-C29-C30	64.9(7)	O8-C24-C37-C38	-66.0(7)
C42-O12-C30-C29	-110.8(9)	C25-C24-C37-C38	171.2(5)
C42-O12-C30-C31	129.1(8)	C24-C37-C38-C39	-128.8(8)
O11-C29-C30-O12	-175.9(6)		
O11-C29-C30-C31	-56.8(8)		

Chapter 4: Background Cryptocaryol A

4.1 Introduction

Protein kinase C (PKC) has been of significant interest to drug developers since it was first identified as the receptor for tumor promoter phorbol ester.[112] While PKC has been shown to play a role in numerous diseases, such as Parkinson's disease,[113] Alzheimer's disease,[114] ischemic heart disease,[115] and cancer,[116] no drugs have been approved that specifically target PKC. The challenges associated with selective modulation and regulation of PKC has led to the search for alternative downstream kinase targets such as mTOR and Akt. It is anticipated that regulation of these alternative targets will produce desirable results, such as tumor suppression without exhibiting cytotoxicity to non-cancer cells.[117]

Programmed cell death 4 (PDCD4), a downstream target of Akt, is a novel tumor suppressor protein.[118] Downregulation of PDCD4 has been linked to diverse human cancers, including liver,[119] colorectal,[120] brain,[121] and breast.[122] Conversely, murine epidermal cells that possess elevated levels of PDCD4 are resistant to tumor promotion. Phosphorylation of PDCD4 by PI3K/Akt leads to ubiquitination and proteasomal degradation.[123] Knowledge of this degradation pathway coupled with the associated benefits of increased expression levels has made novel agents capable of stabilizing PDCD4 attractive targets.

4.2 Isolation and Bioactivity

In 2011, using a high-throughput cell-based reporter assay[124] to screen extracts of a collection of the plant *Cryptocarya* sp. (Lauraceae, NSC number N098347), Gustafson and coworkers identified a new class of small-molecule PDCD4-stabilizers, the amphiphilic type I polyketides cryptocaryols A-H (purported structure **4.1a-h**, Figure 4.1).[125] These compounds were found in samples of a shrub, identified as *Cryptocarya*, which were collected in the East Sepik Province, Papua New Guinea in 1995. The sample material was extracted multiple times with CH_2Cl_2/MeOH (1:1) and 100% MeOH. The extract was fractionated using diol flash chromatography eluting sequentially with hexanes, EtOAc, and MeOH. PDCD4-stabilizing

activity was observed in the EtOAc extract, which was subjected to flash chromatography, size exclusion chromatography, and finally semipreparative reversed-phase HPLC separation to afford **4.1a** (0.5 mg), **4.1b** (1.1 mg), **4.1c** (1.5 mg), **4.1d** (0.9 mg), **4.1e** (0.3 mg), **4.1f** (1.0 mg), **4.1g** (2.0 mg), and **4.1h** (1.8 mg).

Figure 4.1 Purported structures of cryptocaryols A-H, **4.1a-h** and revised structures of cryptocaryol A and B, **4.2a** and **4.2b**.

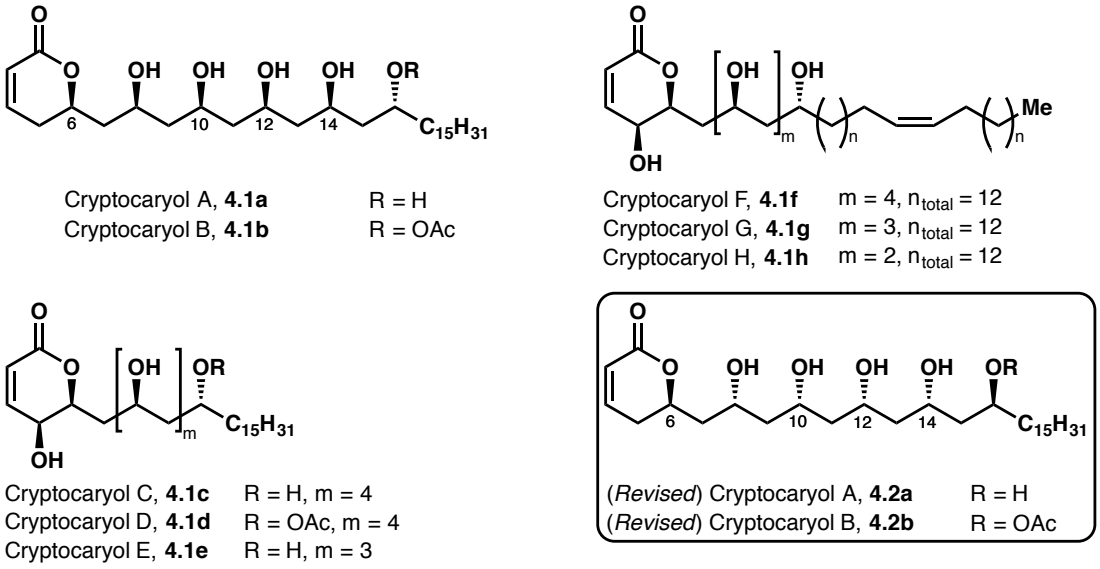

Stabilization of PDCD4 was evaluated according to a previously developed procedure.[124] HEK-39 cells expressing a fusion protein comprised of a fragment of PDCD4 containing the regulatory region (amino acids 39-91) and luciferase were plated and allowed to attach overnight. TPA (final concentration 10 nM) was added followed by test samples or controls. After 8 h incubation, luciferase activity was measured. Cryptocaryols A-H **4.1a-h** were found to exhibit EC_{50} values in the low μM range, and the EC_{50} of cryptocaryol A **4.1a** was found to be 4.9 μM.

4.3 Structural Elucidation

Gustafson and coworkers reported the relative structure of cryptocaryol A **4.1a**. Observation of the $[M + H]^+$ ion at m/z 529.4105 via HRESIMS was consistent with the molecular formula $C_{30}H_{56}O_7$ and 3 degrees of unsaturation. Comprehensive analysis of

cryptocaryol A using ^{1}H NMR, ^{13}C NMR, HMBC, COSY, and ECD were used to elucidate the structure. The absolute configuration of the pyranone at C6 was assigned as *R* from its Cotton effect.[126] The relative configuration of the all *syn*-tetraol moiety was assigned according to Kishi's ^{13}C NMR database.[127] The database indicates the expected ^{13}C NMR chemical shifts for the C3 in a 1,3,5-polyol are 66.3 ± 0.5 for an *anti*/*anti* orientation, 68.6 ± 0.5 for *syn*/*anti* or *anti*/*syn*, and 70.7 ± 0.5 for *syn*/*syn* arrangements. The measured ^{13}C NMR shifts for C10, C12, and C14 were 69.9, 70.2, and 68.3, respectively. This revealed that C10 and C12 had *syn*/*syn* configurations relative to their neighboring hydroxyl groups, and C14 was either *syn*/*anti* or *anti*/*syn* relative to C16. As C12 could be assigned as *syn*/*syn*, C14 could be assigned to *syn*/*anti*, thus the relative stereochemistry of the polyol portion of the molecule was reported as 8*S**, 10*S**, 12*S**, 14*S**, 16*R**. However, it was not possible to relate the absolute configuration of C6 with C8 or any other chiral carbons in **4.1a** due to extensive overlap of NMR signals even in a variety of solvents.

Due to the convolution of the NMR spectra, the structures of cryptocaryol A and B, **4.1a** and **4.1b**, were initially incorrectly reported as (6*R*, 8*S**, 10*S**, 12*S**, 14*S**, 16*R**). The erroneous assignment of these structures was later discovered and corrected by O'Doherty and coworkers during the course of their total synthesis of these natural products. They found that the correct structure for cryptocaryols A and B, **4.1a** and **4.1b** was (6*R*, 8*R**, 10*R**, 12*R**, 14*R**, 16R*).[128]

4.4 Prior Total Syntheses

The synthetic challenges involved with cryptocaryol A include the construction of the polyol fragment and the stereoselective installation of the rather sensitive pyrone moiety, along with the determination and validation of the absolute stereochemistry of the natural product. There have been four previous syntheses published from the laboratories of Mohapatra, O'Doherty, Dias, and Cossy.[128-129] Each synthesis will be reviewed focusing primarily on how the above synthetic challenges were overcome.

4.4.1 Mohapatra's Total Synthesis of Purported Cryptocaryol A (4.1a)

Mohapatra and coworkers completed the first total synthesis of the purported structure of cryptocaryol A, **4.1a**.[129a] The successful synthetic strategy relied on ring-closing metathesis (RCM) of acrylate **4.3** to install the pyrone moiety (Scheme 4.1). The polyol substructure was accessed in a linear manner through iterative epoxidation and ring-opening with vinylmagnesium bromide beginning from iodide **4.4**, which was anticipated to be accessible via Bartlett-Smith iodocarbonate cyclization. The first stereocenter was to be installed via the Maruoka-modifed Keck allylation of cetyl alcohol **4.5**.

Scheme 4.1 Mohapatra's retrosynthesis of purported cryptocaryol A **4.1a**.

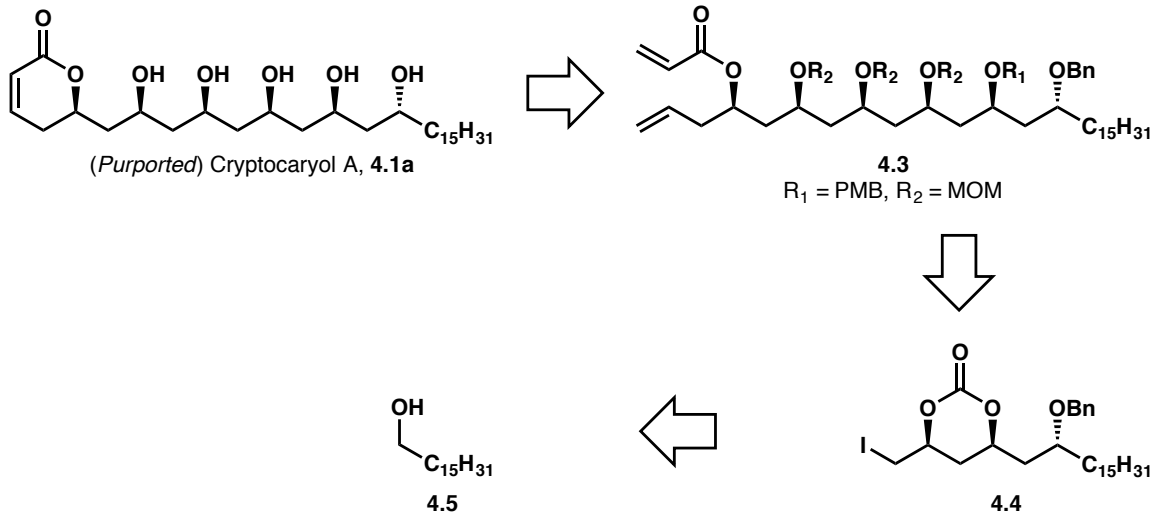

The forward synthesis began with oxidation of cetyl alcohol to an aldehyde followed by asymmetric Keck allylation using Maruoka's bis-titanium catalyst, which provided homoallylic alcohol **4.6** (Scheme 4.2).[130] Benzylation of the hydroxyl group afforded benzyl ether **4.7**. Oxidative cleavage of the terminal olefin followed by Sakurai allylation gave homoallylic alcohol **4.8**.

Scheme 4.2 Synthesis of homoallylic alcohol **4.8**.

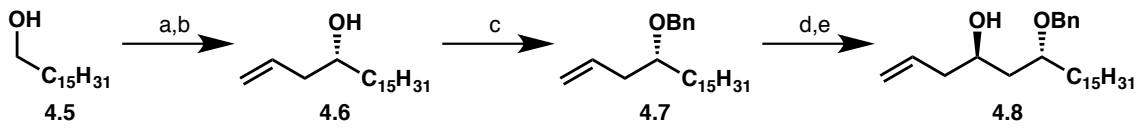

Key: (a) PCC, CH_2Cl_2, rt; (b) $TiCl_4$, $Ti(OiPr)_4$, (*S*)-BINOL, Ag_2O, allyltributylstannane, -20 °C; (c) NaH, BnBr, THF, 0 °C; (d) OsO_4, $NaIO_4$, 2,6-lutidine, dioxane, rt; (e) allylTMS, $TiCl_4$, -78 °C.

Next, homoallylic alcohol **4.8** was protected as carbonate ester **4.9** (Scheme 4.3). Exposure to *N*-iodosuccinimide effected Bartlett-Smith iodocyclization to afford cyclic carbonate **4.4**. Upon treatment with K_2CO_3, iodocarbonate **4.4** underwent hydrolysis and intramolecular S_N2 reaction to give epoxy alcohol **4.10**. Protection of the hydroxyl group as PMB ether **4.11** followed by epoxide opening with vinylmagnesium bromide furnished homoallylic alcohol **4.12**.

Scheme 4.3 Synthesis of homoallylic alcohol **4.12**.

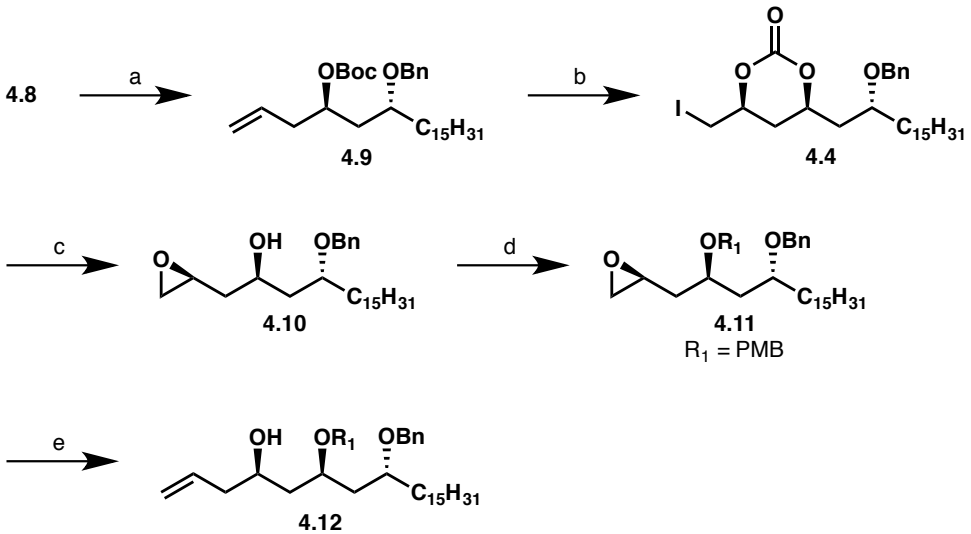

Key: (a) Boc_2O, Et_3N, CH_2Cl_2, rt; (b) NIS, CH_3CN, -40 to 0 °C; (c) K_2CO_3, MeOH, rt; (d) NaH, PMBCl, THF, DMF, 0 °C; (e) vinylmagnesium bromide, CuI, THF, -20 °C.

Homoallylic alcohol **4.12** was subjected to almost exactly the same sequence of steps shown in Scheme 4.3 to afford homoallylic alcohol **4.13**, which again underwent another iteration of the five-step procedure to give homoallylic alcohol **4.14** (Scheme 4.4). Homoallylic alcohol **4.14** was subjected to one final cycle of this procedure to provide homoallylic alcohol

4.15, which was acylated with acryloyl chloride to give acrylate **4.3**. Ring-closing metathesis proceeded smoothly with Grubbs I to furnish pyrone **4.16**, which upon deprotection afforded the purported structure of cryptocaryol A **4.1a**. This highly linear synthesis required 28 steps (LLS) from cetyl alcohol.

Scheme 4.4 Completion of the total synthesis of purported cryptocaryol A **4.1a**.

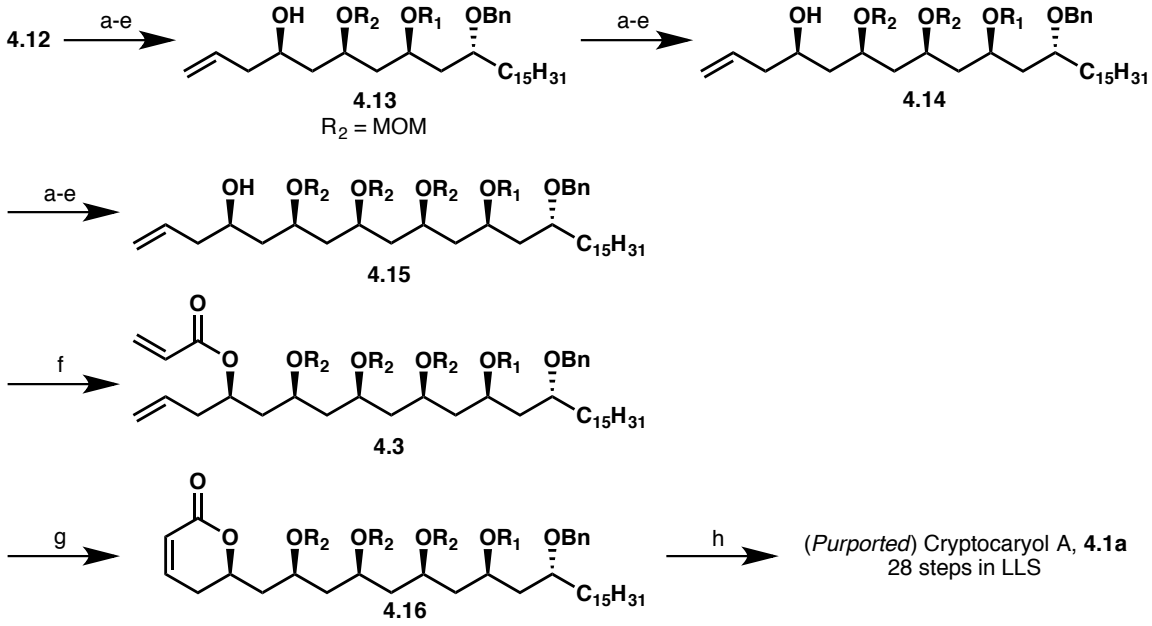

Key: (a) Boc_2O, Et_3N, CH_2Cl_2, rt; (b) NIS, CH_3CN, -40 to 0 °C; (c) K_2CO_3, MeOH, rt; (d) NaH, MOMCl, THF, DMF, 0 °C; (e) vinylmagnesium bromide, CuI, THF, -20 °C; (f) acryloyl chloride, DIPEA, CH_2Cl_2, 0 °C; (g) Grubbs I, CH_2Cl_2, reflux; (h) $TiCl_4$, CH_2Cl_2, rt.

4.4.2 O'Doherty's Total Synthesis of (+)-Cryptocaryol A

In 2013, O'Doherty and coworkers elucidated the correct structure of cryptocaryol A **4.2a** and completed the first total synthesis.[128] Ring-closing metathesis of acrylate **4.17** was anticipated to give the desired pyrone, which would be deprotected to furnish the natural product **4.2a** (Scheme 4.5). Acrylate **4.17** was anticipated to be accessible after Noyori reduction of ynone **4.18**. The ynone was to be constructed from enoate **4.19**, which was synthesized from 5-hexyn-1-ol **4.20**.

Scheme 4.5 O'Doherty's retrosynthesis of (+)-cryptocaryol A **4.2a**.

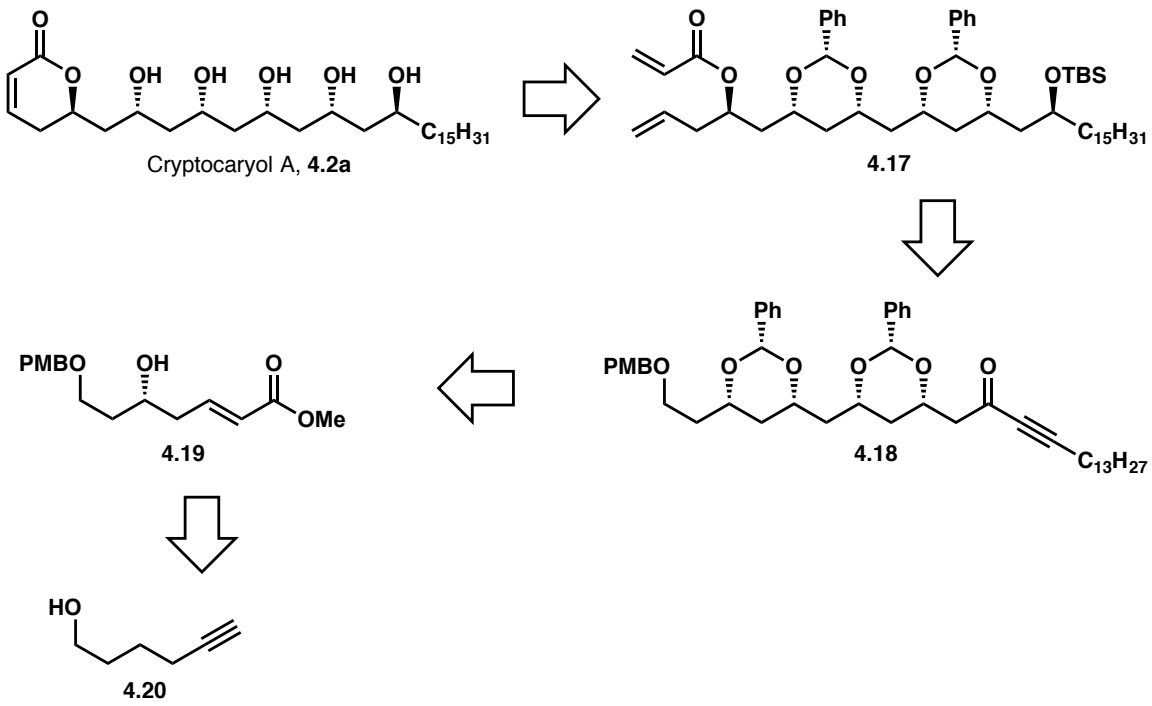

The synthesis began with PMB protection of alkyne **4.20** followed by homologation of the terminal alkyne with methyl chloroformate, which provided ynoate **4.21** (Scheme 4.6). Upon treatment with PPh_3 and phenol, ynoate **4.21** underwent isomerization to afford dienoate **4.22**. Asymmetric Sharpless epoxidation of the alkene distal to the ester followed by protection of the 1,2-diol gave carbonate **4.23**. Regioselective reduction of **4.23** with catalytic $PdPPh_3$, HCO_2H, and Et_3N furnished δ-hydroxy enoate **4.19**.

Scheme 4.6 Synthesis of enoate **4.19**.

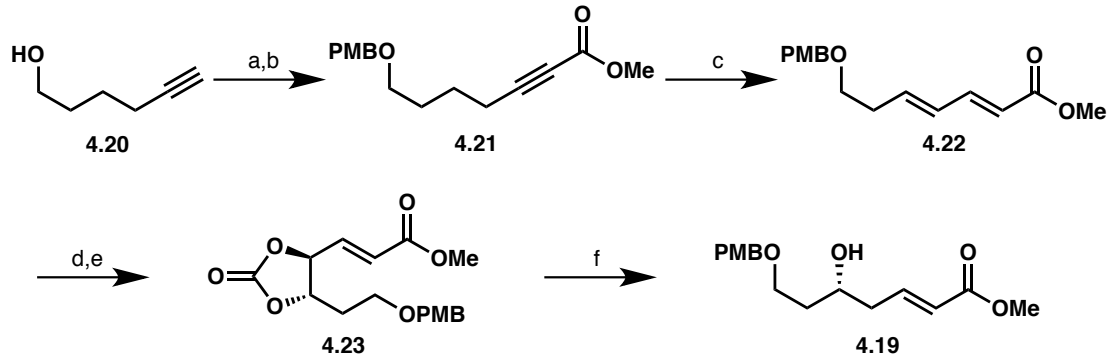

Key: (a) PMBCl, NaH, TFAB, 0 °C; (b) $ClCO_2Me$, *n*-BuLi, THF, -78 to 0 °C; (c) PPh_3, PhOH, benzene, 50 °C; (d) AD-mix-b, *t*-BuOH/H_2O, 0 °C; (e) triphosgene, pyridine, DMAP, CH_2Cl_2, -78 °C; (f) $PdPPh_3$, Et_3N, HCO_2H, THF, reflux.

Evans' conditions for diastereoselective acetalization transformed **4.19** into benzylidene **4.24** (Scheme 4.7).[131] Ester-to-aldehyde reduction with DIBAL followed by Leighton allylation afforded homoallylic alcohol **4.25**.[132] Cross-metathesis of homoallylic alcohol **4.25** with ethyl acrylate using Grubbs II followed by another diastereoselective acetalization furnished benzylidene **4.26**. Ester-to-aldehyde reduction was accomplished with DIBAL and nucleophilc alkyne addition to the aldehyde followed by oxidation of the resulting alcohol afforded ynone **4.18**.

Scheme 4.7 Synthesis of ynone **4.18**.

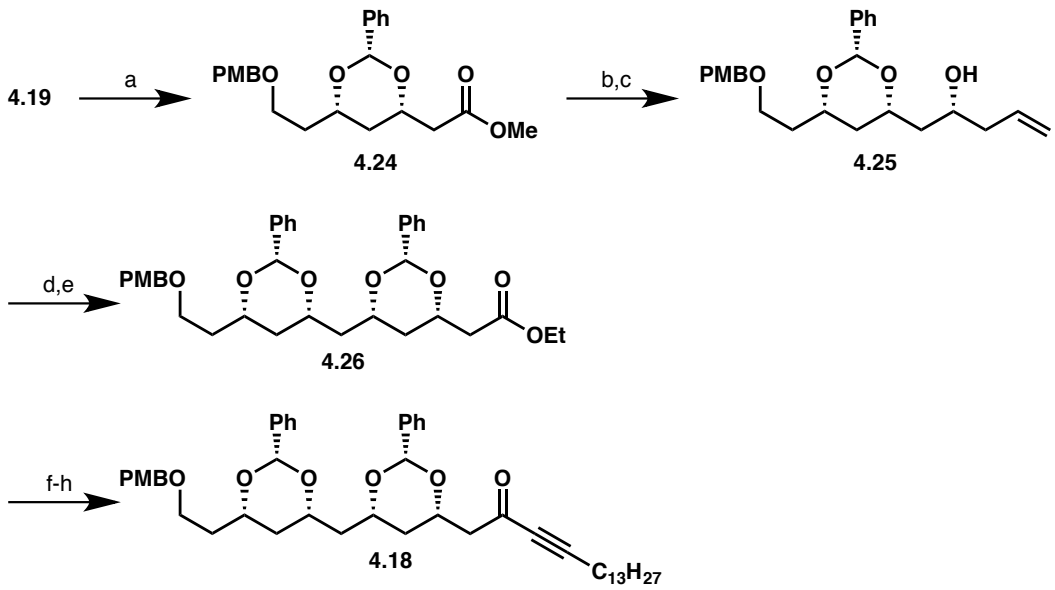

Key: (a) PhCHO, KO*t*Bu, THF, 0 °C; (b) DIBALH, CH_2Cl_2, -78 °C; (c) (*R,R*)-Leighton, $Sc(OTf)_3$, CH_2Cl_2, -10 °C, (d) ethyl acrylate, Grubbs II, CH_2Cl_2; (e) PhCHO, KO*t*Bu, THF, 0 °C; (f) DIBALH, CH_2Cl_2, -78 °C; (g) 1-pentadecyne, *n*-BuLi, THF, -78 °C; (h) DMP, CH_2Cl_2, 0 °C.

Asymmetric Noyori reduction of ynone **4.18** followed by diimide reduction of the alkyne gave secondary alcohol **4.27** (Scheme 4.8). Protection of the secondary alcohol as a TBS ether and deprotection of the PMB provided primary alcohol **4.28**. Alcohol-to-aldehyde oxidation was followed by Leighton allylation and acylation of the resulting homoallylic alcohol afforded acrylate **4.17**. Ring-closing metathesis was achieved using Grubbs I, and subsequent global deprotection furnished (+)-cryptocaryol A **4.2a**. O'Doherty and coworkers completed the total synthesis in 23 steps (LLS) and established the absolute stereochemistry of the natural product.

Scheme 4.8 Completion of the total synthesis of (+)-cryptocaryol A **4.2a**.

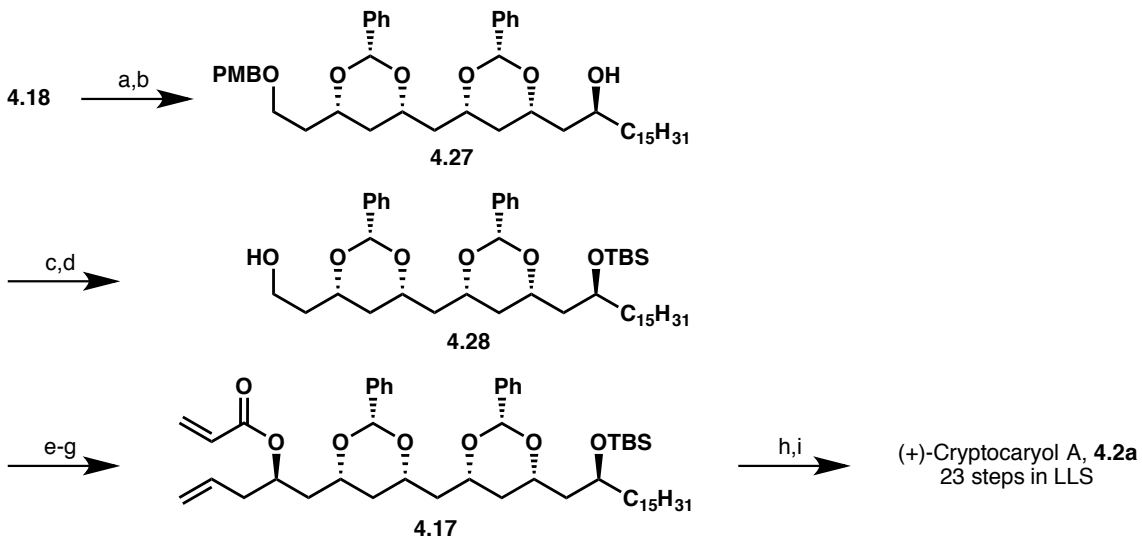

Key: (a) (*R,R*)-Noyori, Et_3N, HCO_2H; (b) NBSH, Et_3N, CH_2Cl_2; (c) TBSCl, imidazole, DMF; (d) DDQ, CH_2Cl_2, H_2O, 0 °C; (e) DMP, CH_2Cl_2, 0 °C; (f) (*S,S*)-Leighton, $Sc(OTf)_3$, CH_2Cl_2, -10 °C; (g) acrylic acid, DCC, DMAP, CH_2Cl_2; (h) Grubbs I, CH_2Cl_2, reflux; (i) $AcOH/H_2O$ = 4:1, 80 °C.

4.4.3 Dias' Total Synthesis of (−)-Cryptocaryol A ent-4.2a

In 2015, Dias and coworkers completed the total synthesis of (−)-cryptocaryol A ***ent*-4.2a**,[129b] and they are the only group to not utilize ring-closing metathesis to install the pyrone substructure opting instead for a lactonization strategy (Scheme 4.9). The synthesis hinged on diastereoselective 1,5-*anti* aldol reaction between ketone **4.29** and hexadecanal to install the long aliphatic moiety. The ketone was to be synthesized from terminal alkene **4.30**, which was anticipated to be accessible from ketone **4.31** via diastereoselective 1,5-*anti* aldol coupling. The synthesis began from commercially available homoallylic alcohol **4.**

Scheme 4.9 Dias' retrosynthesis of (–)-cryptocaryol A ***ent*-4.2a**.

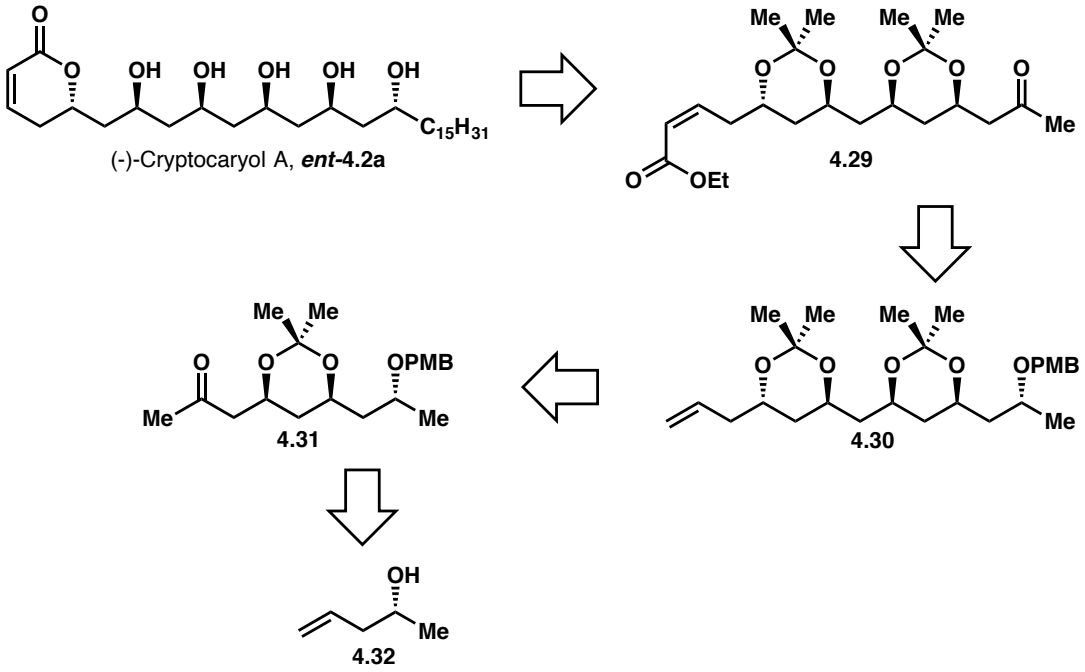

The synthesis began from homoallylic alcohol **4.32**, which was protected as PMB ether **4.33** (Scheme 4.10). Wacker oxidation of the terminal alkene provided ketone **4.34**, which underwent diastereoselective boron-mediated 1,5-*anti* aldol reaction with 3-butenal to afford β-hydroxy ketone **4.35**. Diastereoselective 1,3-*syn* reduction of **4.35** was achieved using $LiBH_4$ in the presence of Et_2BOMe to give diol **4.36**. The diol was protected as acetonide **4.37** and subsequent Wacker oxidation furnished ketone **4.31**.

Scheme 4.10 Synthesis of ketone **4.31**.

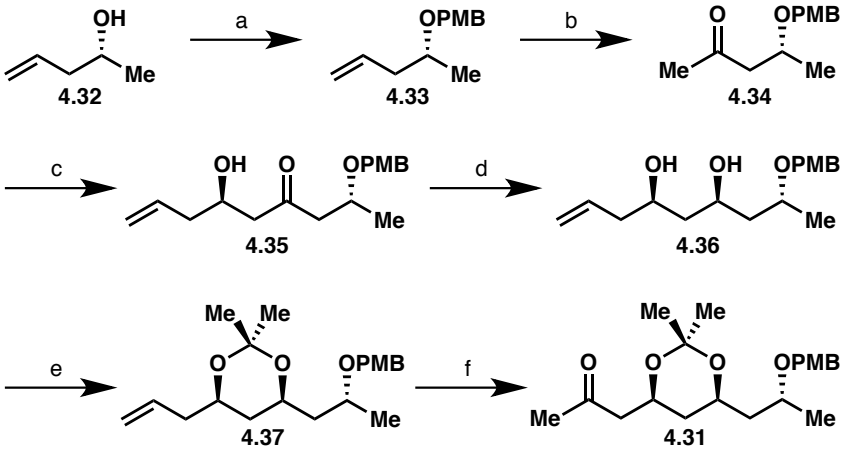

Key: (a) PMB trichloroacetimidate, CSA, CH_2Cl_2, rt; (b) $PdCl_2$, CuCl, O_2, DMF, H_2O, rt; (c) (1) Cy_2BCl, Et_3N, Et_2O, -30 °C (2) 3-butenal, -78 °C; (d) $LiBH_4$, Et_2BOMe, THF, MeOH, -78 °C; (e) 2,2-DMP, CSA, rt; (f) $PdCl_2$, CuCl, O_2, DMF, H_2O, rt.

Diastereoselective 1,5-*anti* aldol reaction between ketone **4.31** and 3-butenal provided homoallylic alcohol **3.38** (Scheme 4.11). 1,3-*anti* reduction was achieved using $Me_4NB(OAc)_3$ and gave diol **4.39**, which was protected as an acetonide to afford terminal alkene **4.30**.

Scheme 4.11 Synthesis of terminal alkene **4.30**.

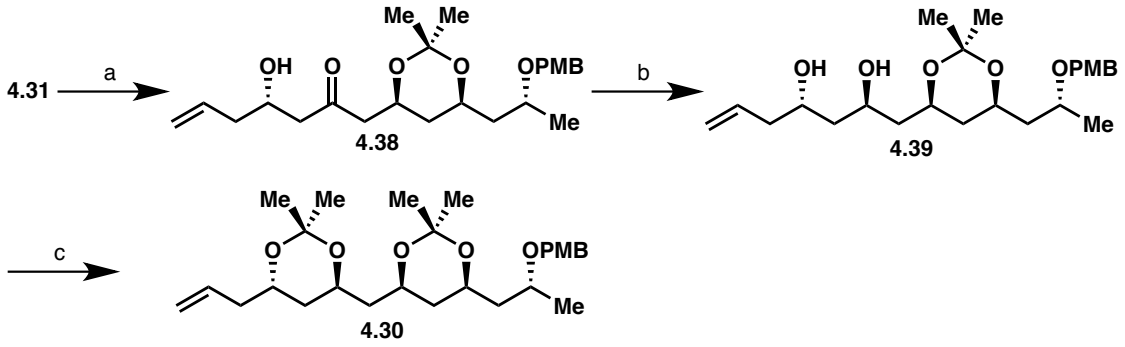

Key: (a) (1) Cy_2BCl, Et_3N, Et_2O, -30 °C (2) 3-butenal, -78 °C; (b) $Me_4NHB(OAc)_3$, MeCN, AcOH, -30 to -20 °C; (c) 2,2-DMP, PPTS, rt.

Deprotection of the PMB ether of **4.30** gave secondary alcohol **4.40**, which was oxidized to ketone **4.41** via Swern oxidation (Scheme 4.12). Oxidative cleavage of the terminal olefin provided aldehyde **4.42**. Horner-Wadsworth-Emmons olefination of aldehyde **4.42** with ethyl-2-(bis(*o*-tolyloxy)phosphoryl)acetate afforded enoate **4.29**. Diastereoselective 1,5-*anti* aldol reaction between ketone **4.29** and 1-hexadecanal followed by 1,3-*anti* reduction gave diol **4.43**. Treatment with CSA led to tandem global deprotection and lactonization to furnish (–)-

cryptocaryol A ***ent*-4.2a**. The synthesis accomplished by Dias and coworkers required 17 steps (LLS).

Scheme 4.12 Completion of the synthesis of (–)-cryptocaryol A ***ent*-4.2a**.

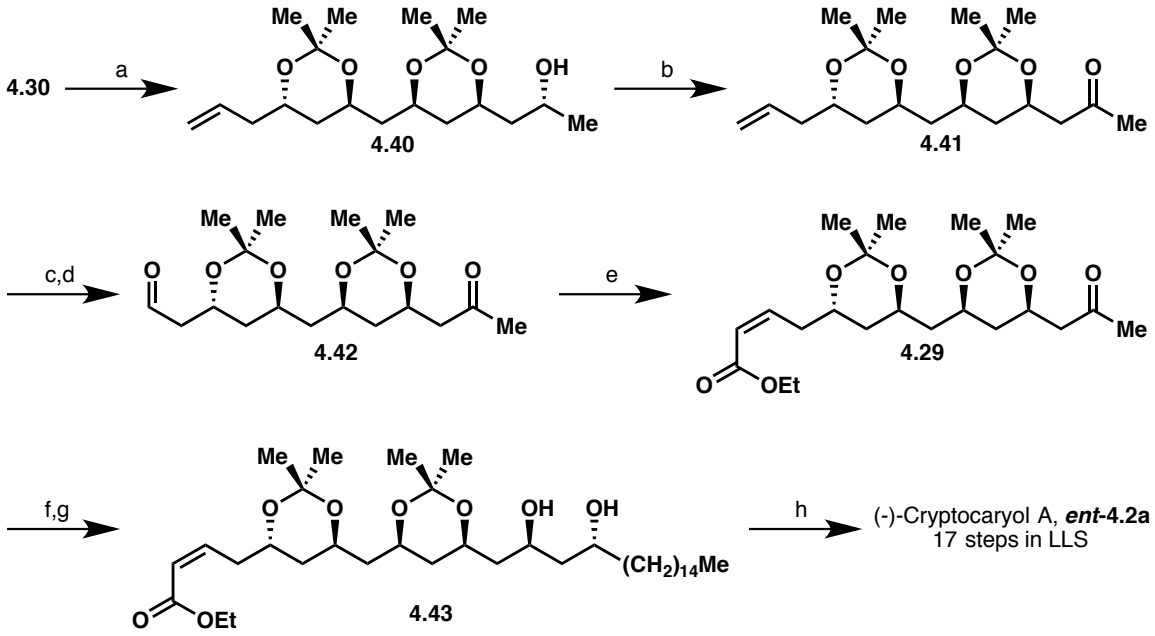

Key: (a) DDQ, CH_2Cl, buffer, 0 °C; (b) $(COCl)_2$, DMSO, Et_3N, CH_2Cl_2, -78 °C; (c) OsO_4, NMO, *t*-BuOH, THF, H_2O, rt; (d) $NaIO_4$, THF, H_2O; (e) ethyl 2-(bis(*o*-tolyloxy)phosphoryl)acetate, NaH, THF, -78 °C; (f) (1) Cy_2BCl, Et_3N, Et_2O, -30 °C (2) palmitaldehyde, CH_2Cl_2, -78 °C; (g) $Me_4NHB(OAc)_3$, MeCN, AcOH, -30 to -20 °C; (h) CSA, MeOH.

4.4.4 Cossy's Total Synthesis of (+)-Cryptocaryol A

In 2015, Cossy and coworkers published their total synthesis of cryptocaryol A **4.2a**.[129c] The synthesis was envisaged from aldehyde **4.47** and heptadecan-2-one by using a diastereoselective boron-mediated aldol coupling (Scheme 4.13). It was anticipated that aldehyde **4.47** could be accessed from bis-pyran **4.45** by reductive cleavage and ring-closing metathesis. Bis-pyran **4.45** was to be synthesized from pyran **4.46** via Prins cyclization. Pyran **4.46** would be obtained by a Prins cyclization between aldehyde **4.47** and homoallylic alcohol **4.48**.

Scheme 4.13 Cossy's retrosynthesis of (+)-cryptocaryol A **4.2a**.

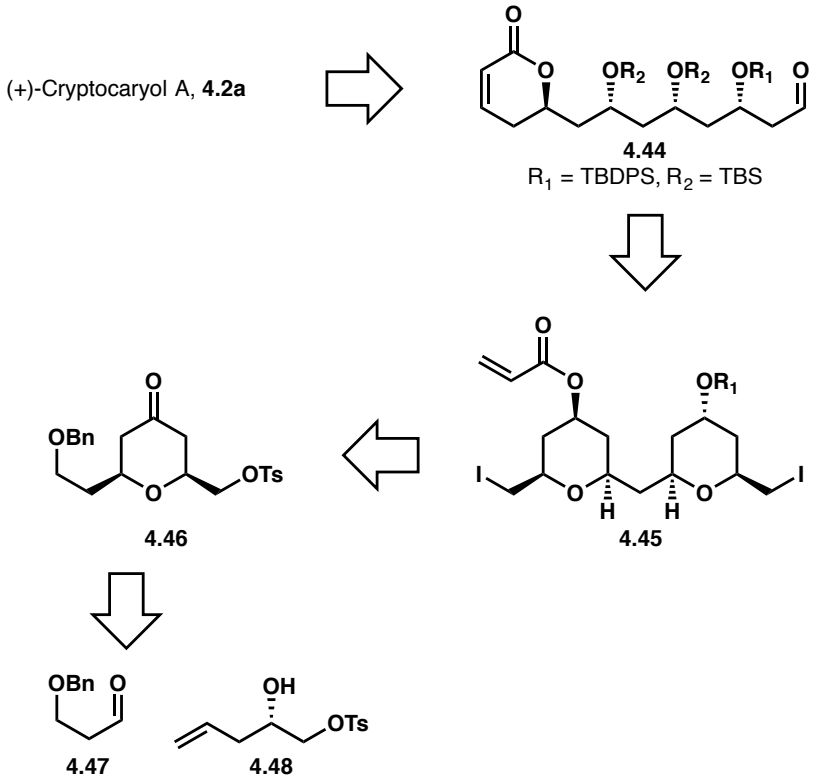

The synthesis began with preparation of aldehyde **4.47** and homoallylic alcohol **4.48** (Scheme 4.14). Monoprotection of 1,3-propanediol followed by oxidation using PCC provided aldehyde **4.47**. Tosylation of (*R*)-glycidol followed by epoxide-opening with vinylmagnesium bromide in the presence of a catalytic amount of Li_2CuCl_4 produced the desired homoallylic alcohol **4.48**. Prins cyclization between **4.47** and **4.48** was achieved using TFA to produce **4.51** as a mixture of diastereomers (25:75 in favor of the undesired diastereomer). The mixture was next exposed to Dess-Martin periodinane, which oxidized the secondary alcohol to afford ketone **4.46**.

Scheme 4.14 Synthesis of pyran **4.46**.

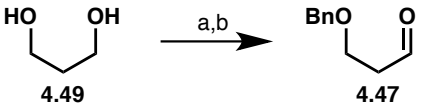

Key: (a) NaH, BnBr, *n*-Bu_4NI, THF, rt, 7h; (b) PCC, NaOAc, 4 Å MS, CH_2Cl_2, rt, 3h.

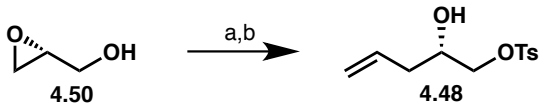

Key: (a) TsCl, Et_3N, DMAP, CH_2Cl_2, 0 °C to rt, 3 h; (b) Li_2CuCl_4, vinylmagnesium bromide, THF, -40 °C, 3h.

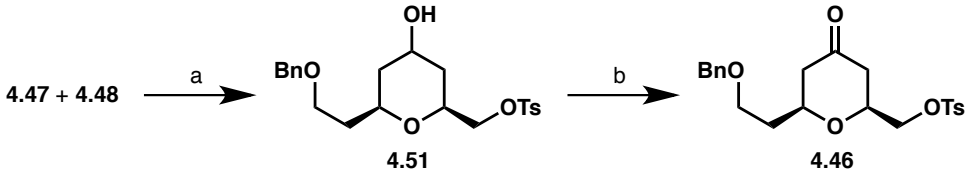

Key: (a) TFA, CH_2Cl_2, rt, 3 h then $NaHCO_3$, Et_3N; (b) DMP, CH_2Cl_2, rt 2.5 h.

Next, diastereoselective reduction of ketone **4.46** was performed with L-selectride to afford **4.51** again, but now as an 80:20 mixture of diastereomers in favor of the desired diastereomer (as depicted, Scheme 4.15). Protection of the secondary alcohol as the TBDPS ether and deprotection of the benzyl ether was followed by oxidation of the primary alcohol to generate aldehyde **4.52**. Exposure of aldehyde **4.52** to **4.48** in the presence of TFA resulted in Prins cyclization, and oxidation of the resulting secondary alcohol with Dess-Martin periodinane afforded ketone **4.53**. Reduction of ketone **4.53** with $NaBH_4$ led to formation of secondary alcohol **4.54** with high diastereoselectivity (95:5, seperable). Double S_N2 displacement of the tosylates was achieved with NaI under microwave irradiation to provide bis-iodide **4.55**. Esterification with acryolyl chloride furnished bis-pyran **4.45**.

Scheme 4.15 Synthesis of bis-pyran **4.45**.

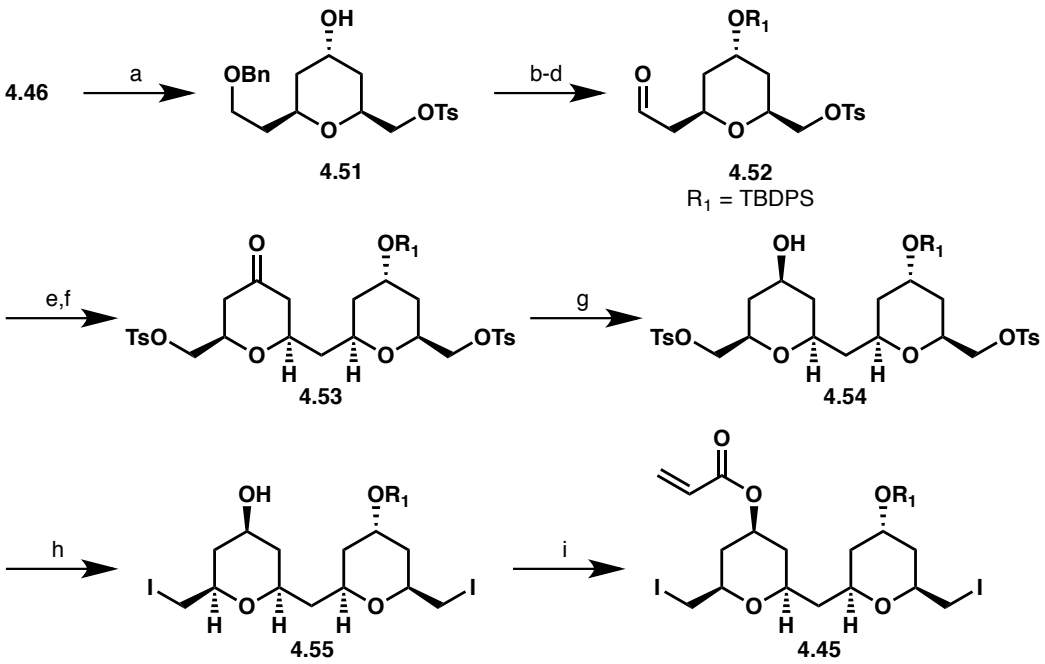

Key: (a) L-Selectride, THF, -78 °C, 1 h; (b) TBDPSCl, imidazole, CH_2Cl_2, rt, 14 h; (c) H_2, Pd/C, MeOH, EtOAc, rt, 16 h; (d) TPAP, NMO, CH_2Cl_2, rt, 2 h; (e) **4.48**, TFA, CH_2Cl_2, rt, 3 h then Et_3N, $NaHCO_3$ (aq); (f) DMP, CH_2Cl_2, rt, 2 h; (g) $NaBH_4$, MeOH, -40 °C, 1 h; (h) NaI, acetone, μw, 120 ºC, 2 h; (i) acryloyl chloride, iPr_2NEt, CH_2Cl_2, 0 °C to rt, 3.5 h;

Bernet-Vasella ring-opening of bis-pyran **4.45** gave diol **4.56** (Scheme 16). Protection of the hydroxyl groups as TBS ethers and ring-closing metathesis to install the pyrone was followed by oxidative cleavage of the terminal olefin to afford aldehyde **4.44**. 1,3-*syn*-Aldol reaction between heptadecan-2-one and aldehyde **4.44** successfully installed the aliphatic moiety and subsequent diastereoselective reduction followed by global deprotection furnished the natural product **4.2a**. The total synthesis was completed in 20 steps (LLS).

Scheme 4.16 Completion of the total synthesis of (+)-cryptocaryol A **4.2a**.

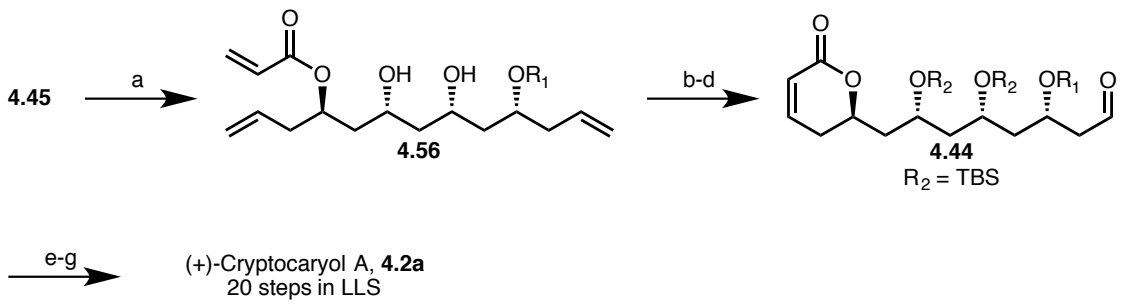

Key: (a) Zn, THF/H_2O = 5:1, 70 °C, 1 h; (b) TBSOTf, 2,6-lutidine, CH_2Cl_2, -78 °C, 1 h; (c) Grubbs I (10 mol%), CH_2Cl_2, 45 °C, 2.5 h; (d) O_3, CH_2Cl_2, -78 °C then PPh_3; (e) (1) heptadecan-2-one, Cy_2BCl, Et_3N, pentane, 0 °C, 2 h (2) **4.44**, pentane, -78 °C to 40 °C, 4 h (3) MeOH/pH7 buffer/H_2O_2, -40 °C to rt, 16 h; (f) $Me_4NBH(OAc)_3$, CH_3CN/MeOH = 1:1, -20 °C, 7 h; (g) HF•CH_3CN, rt, 2.5 h.

4.5 Conclusions

Cryptocaryol A possesses impressive PDCD4 stabilization ability and interesting structure combining both a pyrone moiety and a long polyoxygenated substructure. These interesting structural and biological features inspired researchers to synthesize the natural product. While the initial total synthesis was later found to have been the incorrect structure, work by O'Doherty and coworkers revealed the absolute structure of the natural product. The prior syntheses illustrate the utility and limitations of methodologies used to construct polyketides. However, these routes typically required many synthetic concessions such as repeated protecting group manipulations and oxidation state adjustments. Additionally, all of the prior syntheses are quite linear and therefore generally lack synthetic efficiency.[95, 97, 100, 133]

Our intention was to develop a more concise, convergent, and versatile synthetic route that combines the information learned from these previous syntheses with our newly developed metal-catalyzed transformations. In doing so, development of a synthetic route to (+)-cryptocaryol A that requires fewer than half the number of steps as the shortest previous synthesis was accomplished, thereby enabling rapid access to this important polyketide natural product.

Chapter 5: Total Synthesis of (+)-Cryptocaryol A

5.1 Initial Efforts Toward (+)-Cryptocaryol A

In prior syntheses of cryptocaryol A **5.1**, relatively lengthy syntheses were required in order to construct the natural product (Scheme 5.1). Due to the highly oxygenated nature of **5.1**, oxidation state adjustments and differential protection of hydroxyl functional groups represented a significant fraction of the total number of synthetic transformations. While the majority of syntheses used catalytic, enantioselective methods in order to introduce chirality, many of the syntheses required the use of premetallated *C*-nucleophiles. While premetallated carbanions are often employed with great success, their synthesis typically requires multiple stages of pre-activation and generates stoichiometric waste products. These waste products are often of higher molecular weight than the nucleophile that was incorporated into the chemical structure of the product. Finally, every prior synthesis of the natural product was based on a linear strategy for construction of the molecule.

While these strategies ultimately led to the successful total synthesis of the natural product, the overall yield of each synthesis was quite poor due to the shear number of synthetic transformations performed. These issues of atom,[98] step,[99] and redox-economy[100] are all concessions and illustrate the need for synthetic methodologies and strategies that can be used to synthesize complex molecules in a more direct manner. These concerns helped to guide and shape our synthetic strategy as it applied to the total synthesis of (+)-cryptocaryol A and it was anticipated that the use of the iridium-catalyzed two-directional allylation could dramatically reduce the number of steps require to synthesize the natural product.

5.1.1 Retrosynthetic Analysis

Recognizing the significant number of steps required in prior linear syntheses of cryptocaryol A **5.1**, we sought to develop a more convergent approach. As a consequence of the polyol structure of the natural product, it was believed that a convergent approach would be possible and would not only reduce the steps required to construct the carbon framework of the

molecule but also significantly simplify the protecting group strategy. We envisaged that (+)-cryptocaryol A **5.1** could be constructed from aldehyde **5.2** and ketone **5.3** via a boron-mediated 1,5-*anti* aldol reaction (Scheme 5.1). Aldehyde **5.2**, containing the 1,3-*anti* diol moiety, was anticipated to be synthesized from chiral C_2-symmetric diol **5.4**, which could be prepared directly from 1,3-propanediol **5.5** (~$11 / mol) via asymmetric iridium-catalyzed two-directional allylation. The pyrone substructure was to be constructed via ring-closing metathesis. Ketone fragment **5.3** was proposed to come from cetyl alcohol **5.6**, a commercially available and inexpensive (~$8 / mol) chemical feedstock.

Scheme 5.1 Retrosynthetic analysis of (+)-cryptocaryol A.

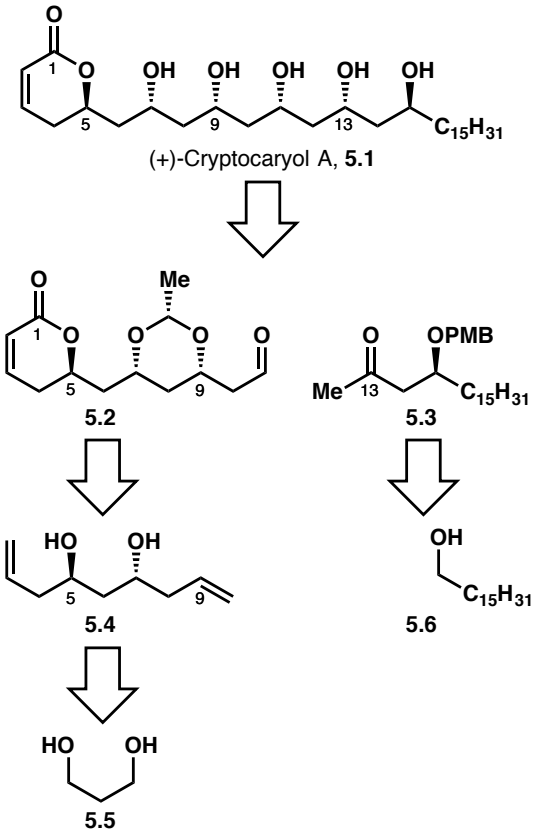

5.1.2 Initial Synthesis of Aldehyde 5.2 and Ketone 5.3

Our synthesis began with the installation of the C5 and C7 stereocenters through asymmetric two-directional allylation of 1,3-propanediol **5.5** to afford chiral, C_2-symmetric diol

5.4 (Scheme 5.2). Upon exposure of **5.5** to allyl acetate in the presence of $[Ir(cod)Cl]_2$, (*R*)-Cl-MeO-BIPHEP, 4-Cl-3-NO_2-benzoic acid, and Cs_2CO_3 in 1,4-dioxane, C_2-symmetric, chiral diol **5.4** is obtained in 70% yield with very high levels of stereoselectivity (30:1 d.r., > 99% e.e.). As with the total synthesis of (−)-cyanolide A, (*R*)-BINAP was substituted for the (*R*)-Cl-MeO-BIPHEP on large-scale reactions in order to reduce costs; however, the yield of the two-directional allylation was reduced to 54%. Nevertheless, diol **5.4** was synthesized reproducibly on gram-scale directly from 1,3-propanediol **5.6**.

Scheme 5.2 Synthesis of diol **5.4**.

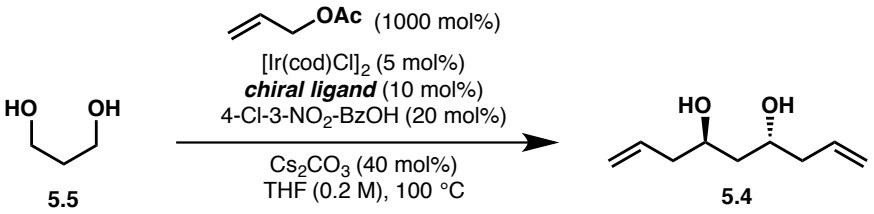

chiral ligand	d.r.	%e.e.	%yield
(*R*)-Cl-MeO-biphep	30:1	>99	70
(*R*)-binap	20:1	>99	54

With chiral, C_2-symmetric diol **5.4** in hand, desymmetrization was achieved via a borinic-acid catalyzed monoacylation developed by Taylor and coworkers to provide acrylate **5.7** in 97% yield (Scheme 5.3, top).[134] At this stage, it was anticipated that tandem ring-closing-metathesis-cross-metathesis (RCM/CM) with acrolein would install the pyrone moiety as well as establish the aldehyde functionality necessary for aldol coupling in a later step. Significant screening of temperature, catalyst, solvent, and mode of addition was performed; however, the highest yield of the desired pyrone **5.8** was only 14%, which was not sufficient to carry forward in the synthesis. The reaction produced a complex mixture hypothesized to come from side reactions involving carbonyl or conjugate addition of the C7 hydroxyl group onto the aldehyde or enoate

moieties as well as the possibility of intramolecular ring-closing metathesis (Scheme 5.3, bottom).

Scheme 5.3 Synthesis of pyrone **5.8** and potential side products.

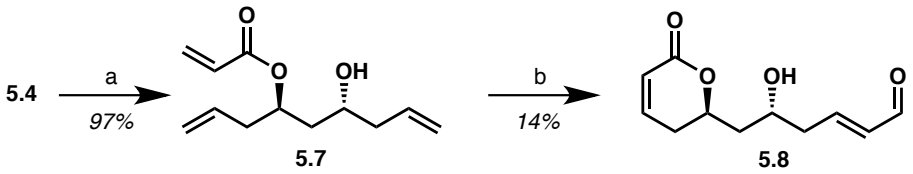

Key: (a) acryloyl chloride (150 mol%), *i*-Pr_2NEt (200 mol%), 2-aminoethyl diphenylborinate (10 mol%), MeCN (0.2 M); (b) acrolein (2000 mol%), HG-II (10 mol%), toluene (0.05 M), rt to 120 °C.

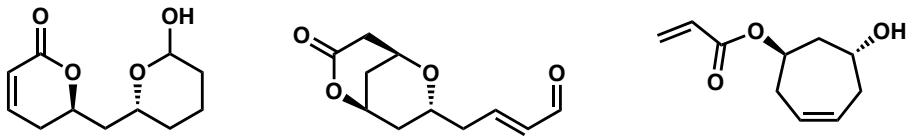

Carbonyl addition **Conjugate Addition** **Intramolecular RCM**

5.1.3 Revised Strategy and Attempted Synthesis of the Ketone Fragment

Undeterred by our initial failure, we hypothesized that carbonyl addition that led to an undesired side product could be suppressed if acrolein was exchanged for methyl vinyl ketone. Importantly, this would require that the aldehyde and ketone partners for the key fragment union would need to be swapped and the substrate-directed aldol would be a 1,5-*syn* aldol, in which the β-alkoxy stereocenter of the ketone fragment would influence the stereochemistry of the newly formed stereocenter to give a 1,5-*syn* relationship between the two. While boron-mediated 1,5-*anti* aldol reactions are well known in the literature, 1,5-*syn* aldol reactions are much less common and frequently suffer from poor diastereoselectivity unless chiral boron reagents are employed. It was anticipated that the requisite 1,5-*syn* aldol reaction could be overcome and thus we turned our attention to the synthesis of ketone **5.9** (Scheme 5.4, top). Unfortunately, treatment of acrylate **5.7** with methyl vinyl ketone in the presence of HG-II was unsuccessful and polymerization hindered identification of the side products. This was presumably due to side reactions involving conjugate addition of the C7 hydroxyl group onto the enoate moiety as well as the possibility of intramolecular ring-closing metathesis (Scheme 5.4, bottom).

Scheme 5.4 Attempt to synthesis of pyrone **5.9** and potential side products.

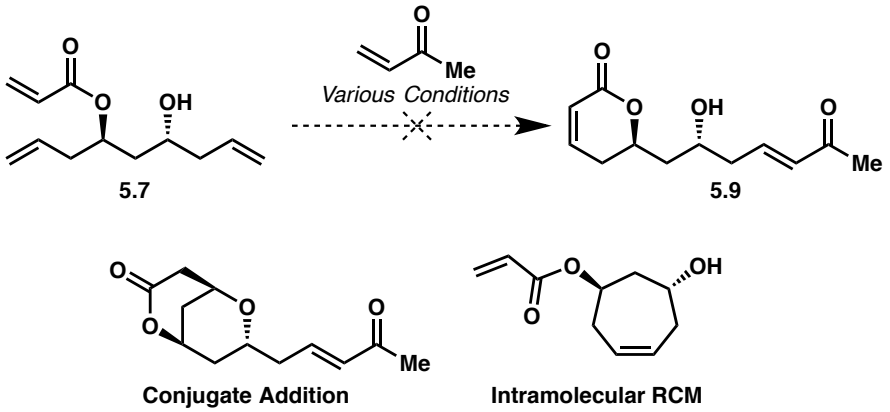

In order to test the plausibility of the tandem RCM/CM, removal of the acrylate moiety was desired as a means to eliminate the conjugate addition pathway. *O*-allylation of diol **5.4** with allyl bromide afforded allylic alcohol **5.10** (Scheme 5.5). Exposure of **5.10** to methyl vinyl ketone in the presence of HG-II went smoothly to produce pyran **5.11** in excellent yield. This made it clear that not only was the tandem reaction possible but that the problem with earlier attempts had been due to the presence of the C7 hydroxyl group and the acrylic ester. With pyran **5.11** in hand, we sought to install the C9 hydroxyl group in a stereoselective manner. Under Evans' conditions for oxa-conjugate and acetal formation, pyran **5.11** was transformed into ketone **5.12**. It was anticipated that installation of the C1 carbonyl would be possible through allylic oxidation; however, two locations for allylic oxidation were possible. All attempts to selectively oxidize C1 were unsuccessfully and reactions typically produced mixtures of C1 and C4 oxidatized material. The low selectivity of the oxidation coupled with a yield that was typically quite low (<40% combined yield for both isomers) forced us to go back and redesign our synthetic route.

Scheme 5.5 Synthesis of pyrone **5.12**.

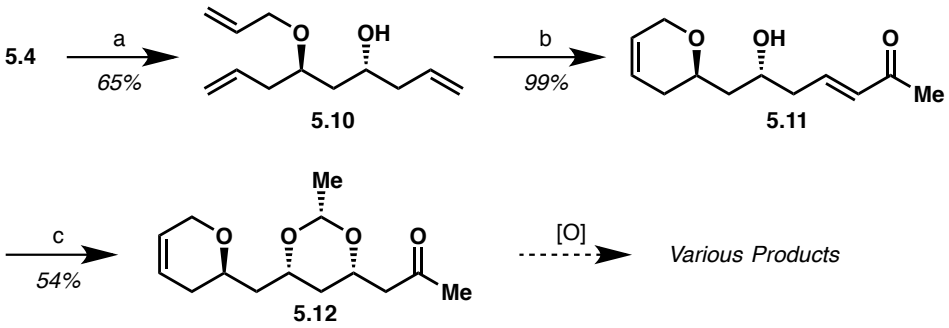

Key: (a) allyl bromide, KI (100 mol%), K_2CO_3 (110 mol%), 2-aminoethyl diphenylborinate (10 mol%), MeCN (0.2 M), 60 °C; (b) methyl vinyl ketone (500 mol%), G-II (5 mol%), CH_2Cl_2 (0.01 M), 50 °C; (c) acetaldehyde (2000 mol%), $Bi(NO_3)_3 \cdot 5H_2O$ (10 mol%), CH_2Cl_2 (0.1 M).

5.1.4 Revised Strategy and Attempted Coupling

The difficulty associated with selective allylic oxidation of pyran **5.12** posed a significant challenge, as the development of conditions for tandem RCM/CM had met with great success without oxygenation at C1. It was hypothesized that the tandem reaction using acrylate **5.7** could be made possible through protection of the C7 hydroxyl group prior to metathesis. While we initially viewed this step as a concession, it was believed that careful choice of the protecting group could still allow for a single step global deprotection at the conclusion of the synthesis.

Protection of acrylate **5.7** was accomplished with TESOTf and 2,6-lutidine to give silyl ether **5.13** (Scheme 5.6). Gratifyingly, exposure of **5.13** to methyl vinyl ketone in the presence of the Hoveyda-Grubbs II catalyst in refluxing toluene afforded pyrone **5.14** in 71% yield. Acetalization and intermolecular oxa-conjugate cyclization of **5.14** with acetaldehyde under Taylor's conditions delivered ketone **5.15**.[134] The versatility of this method is of significance as it promoted acetalization directly from the silyl ether without necessitating deprotection prior to the reaction and allowed another synthetic concession to be circumvented.

Scheme 5.6 Synthesis of ketone **5.12**.

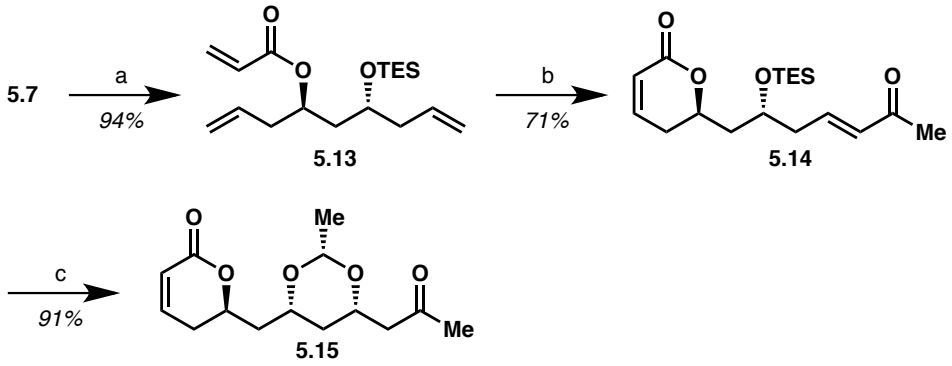

Key: (a) TESOTf (150 mol%), 2,6-lutidine (200 mol%), CH_2Cl_2 (0.05 M), -78°C; (b) methyl vinyl ketone (300 mol%), HG-II (10 mol%), toluene (0.01 M), rt to 120 °C; (c) acetaldehyde (2000 mol%), $Bi(NO_3)_3 \cdot 5H_2O$ (10 mol%), CH_2Cl_2 (0.1 M).

With the ketone fragment in hand, our focus shifted towards the synthesis of the requisite aldehyde for aldol coupling. Commerically available cetyl alcohol **5.6** underwent asymmetric iridium-catalyzed allylation to afford chiral homoallylic alcohol **5.16** (Scheme 5.7). Protection of the secondary hydroxyl group was achieved with *p*-methoxybenzyl trichloroacetimidate with catalytic $La(OTf)_3$ to provide alkene **5.17**. Oxidative cleavage using OsO_4 and $NaIO_4$ furnished aldehyde **5.18** in an efficient three-step sequence from cetyl alcohol with an overall yield of 47%.

Scheme 5.7 Synthesis of aldehyde **5.18**.

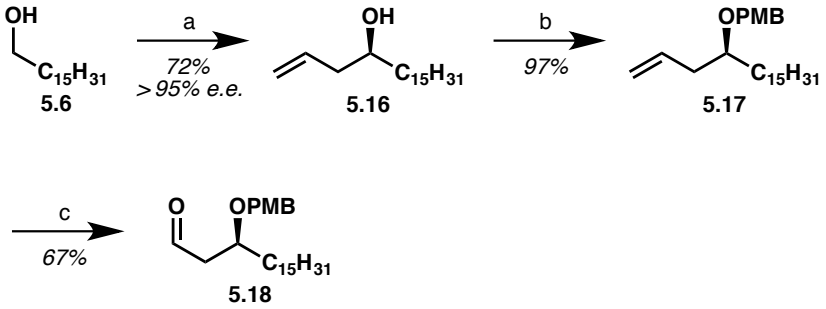

Key: (a) allyl acetate (200 mol%), $[Ir(cod)Cl]_2$ (2.5 mol%), (*R*)-binap (5 mol%), 4-Cl-3-NO_2-BzOH (10 mol%), Cs_2CO_3 (20 mol%), THF (0.2 M), 100 °C; (b) *p*-methoxybenzyl trichloroacetimidate (150 mol%), $La(OTf)_3$ (5 mol%), toluene (0.15 M); (c) OsO_4 (2 mol%), $NaIO_4$ (400 mol%), 2,6-lutidine (200 mol%), 1,4-dioxane:H_2O 3:1 (0.09 M).

With ketone **5.15** and aldehyde **5.18** in hand, the stage was set for the key aldol coupling reaction (Scheme 5.8). With the aldehyde and ketone functionalities reversed compared with

respect to the original fragments proposed in the retrosynthesis, the current aldol would require construction of a 1,5-*syn* relationship between C9 and C13 in the aldol product. Highly diastereoselective methods for such boron-mediated aldol reactions are quite challenging[135] and Mukaiyama 1,5-*syn* aldol reactions are also difficult.[136] Various conditions for generation of the enolborinate of ketone **5.15** were tested. The boron sources screened included Bu_2BOTf, Cy_2BCl, and (–)-diisopinocampheylborane chloride. Amine bases assessed were Et_3N, iPr_2NEt, and 2,6-lutidine. In all cases, the aldol reaction with aldehyde **5.18** produced a complex inseparable mixture that proved difficult to characterize. It was hypothesized that not only did the coupling suffer from poor diastereoselectivity but also retro aldol could be a competing side reaction. In order to circumvent the inherent challenges associated with overcoming the substrate's proclivity to 1,5-*anti* addition, and having discovered that the tandem RCM/CM was successful upon protection of the C7 hydroxyl group, it was decided to attempt the original synthetic plan once more.

Scheme 5.8 Attempted boron-mediated aldol coupling.

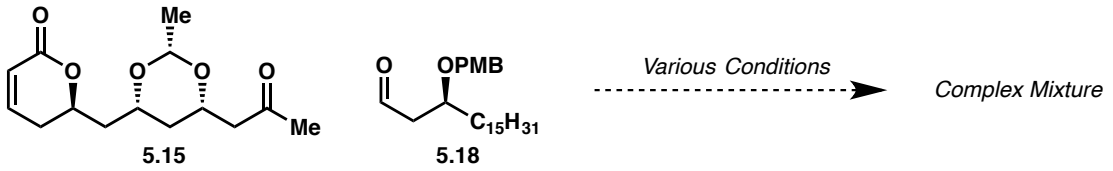

5.2 Final Strategy for (+)-Cryptocaryol A

The important lessons learned in the first approach to the total synthesis of (+)-cryptocaryol A **5.1** were used to help guide the second attempt of the synthesis of aldehyde **5.2**. As protection of the C7 hydroxyl group had proven to be essential in the successful tandem metathesis reactions, it was hypothesized that coupling of silyl ether **5.13** with acrolein would provide the desired α,β-unsaturated aldehyde. Gratifyingly, exposure of **5.13** to acrolein and a catalytic amount of Hoveyda-Grubbs II in refluxing toluene afforded enal **5.19** in 58% yield (Scheme 5.9). The reaction was further optimized and the yield increased to 82% by switching

the solvent to F_8-toluene, which had previously been shown to enhance efficiency in metathesis reactions.[137]

Scheme 5.9 Synthesis of aldehyde **5.2**.

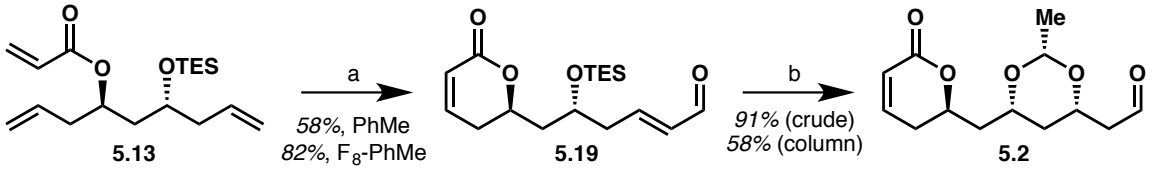

Key: (a) acrolein (180 mol%), HG-II (10 mol%), *solvent* (0.05 M), rt to 120 °C; (b) acetaldehyde (2000 mol%), $Bi(NO_3)_3 \cdot 5H_2O$ (10 mol%), CH_2Cl_2 (0.1 M).

With aldehyde **5.2** in hand, our focus shifted to the synthesis of the ketone fragment **5.3** (Scheme 5.10). Fortunately, access to the ketone was achieved through Wacker oxidation of homoallylic alcohol **5.16** using Sigman's modified conditions.[138]

Scheme 5.10 Sigman's modified conditions for Wacker oxidation to provide ketone **5.3**.

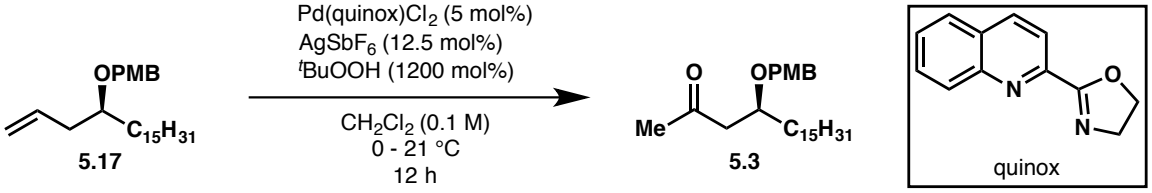

Having successfully synthesized aldehyde **5.2** and ketone **5.3**, we next attempted the crucial aldol coupling (Scheme 5.11). While the 1,5-*syn* aldol reaction had proven to be quite challenging, there existed many examples of high diastereoselectivity in boron-mediated 1,5-*anti* aldol couplings.[139] Exposure of ketone **5.3** to Cy_2BCl and Et_3N in Et_2O at -30 °C resulted in a white suspension, which was further cooled to -78 °C. Addition of a solution of aldehyde **5.2** in Et_2O resulted in the formation of β-hydroxy ketone **5.20** as a single diastereomer in 64% yield. Hydroxy-directed reduction of the aldol product delivered diol **5.21** in 94% yield with good levels of 1,3-diastereoselectivity (15:1). Finally, global deprotection of the acetal and PMB ether using triflic acid and 1,3-dimethoxybenzene[140] furnished (+)-cryptocaryol A **5.1**. The total synthesis was accomplished in 8 steps (LLS) from 1,3-propanediol, fewer than half the number of steps as the next shortest synthesis.

Scheme 5.11 Completion of the total synthesis of (+)-cryptocaryol A **5.1**.

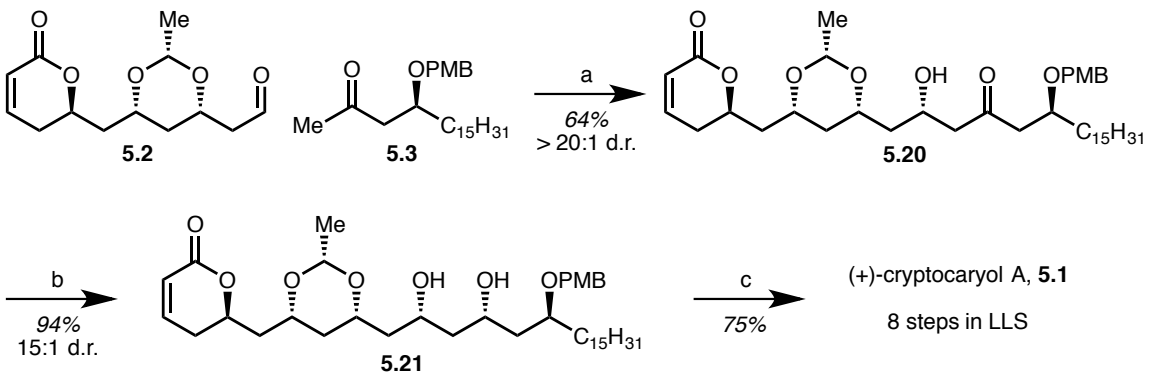

Key: (a) Cy_2BCl (250 mol%), Et_3N (270 mol%), Et_2O (0.05 M), -30 °C to -78 °C; (b) Et_2BOMe (200 mol%), $NaBH_4$ (110 mol%), THF:MeOH (4:1, 0.1 M), -78 °C; (c) TfOH (300 mol%), 1,3-$(MeO)_2Ph$ (900 mol%), CH_2Cl_2 (0.02 M).

5.3 Conclusions

Application of C-C bond forming hydrogenation methods facilitated a remarkably concise synthesis of (+)-cryptocaryol A. Over the course of our synthetic efforts, many challenges had to be overcome. First, the inability to directly perform the tandem RCM/CM reaction on the desired acrylate forced us to reconsider our forward synthetic strategy. Secondly, once the fragments had been synthesized, the boron-mediated 1,5-*syn* aldol reaction was unsuccessful and necessitated redesign of our synthetic strategy. Finally, protection of the C7 hydroxyl group was determined to be essential for the success of the RCM/CM reaction and changing the solvent from toluene to F_8-toluene improved the yield significantly. According to the metric for synthetic efficiency developed by Baran,[95] the current synthesis of (+)-cryptocaryol A is ~64% ideal. The major synthetic concessions were the need to protect the C7 and C15 hydroxyl groups, the latter of which required deprotection at the conclusions of the synthesis. Despite these concessions, the strategy employed in the total synthesis of (+)-cryptocaryol A has produced the most concise synthesis of the natural product to date.

In summary, with the exception of eribulin,[141] all FDA approved polyketides are accessed through fermentation or semi-synthesis, as current synthetic methodology cannot address the preparation of these complex structures in a concise manner. Accordingly, the Krische laboratory

has developed a suite of catalytic methods for the construction of polyketides which addition or exchange of hydrogen is accompanied by C-C bond formation.[110] As illustrated by the present total synthesis of (+)-cryptocaryol A, application of this technology has availed the most concise route to any member of this family of polyketide natural products.

5.4 Experimental Details

5.4.1 General Information

All reactions were run under an atmosphere of argon under anhydrous conditions unless otherwise indicated. Dichloroethane (DCE), triethylamine (Et_3N), Hünig's Base (iPr$_2$EtN), acetonitrile (MeCN), and dichloromethane (CH_2Cl_2) were distilled over CaH_2. Diethyl ether (Et_2O), tetrahydrofuran (THF), and toluene (PhMe) were distilled over sodium. Pressure tubes (25x150 mm, PYREXPLUS, and 350 mL flask, purchased from Chem Glass) were dried in an oven overnight and cooled under a stream of nitrogen prior to use. Commercially available allyl acetate (Aldrich) was purified by distillation prior to use. Acrolein was purified by distillation prior to use. All other commercial reagents were used directly without further purification unless specified. All analytical thin-layer chromatography (TLC) was carried out using 0.2 mm commercial silica gel plates (DC-Fertigplatten Kieselgel 60 F_{254}). Plates were visualized by treatment with UV, acidic *p*-anisaldehyde stain, ceric ammonium molybdate stain, or $KMnO_4$ stain with gentle heating.

5.4.2 Spectrometry and Spectroscopy

Infrared spectra were recorded on a Nicolet 380 FTIR. High-resolution mass spectra (HRMS) were obtained on a Karatos MS9 and are reported as m/z (relative intensity). Accurate masses are reported for the molecular ion ($[M+H]^+$, $[M-H]^+$, or $[M+Na]^+$). Nuclear magnetic resonance spectra (^{1}H NMR and ^{13}C NMR) were recorded with a Varian Gemini (400 MHz or 600 MHz) spectrometer for $CDCl_3$ and $(CD_3)_2O$ solutions and chemical shifts are reported as parts per million (ppm) relative to residual $CHCl_3$ δ_H (7.26 ppm), $CDCl_3$ δ_C (77.0 ppm), CD_3OD δ_H (4.87 ppm), CD_3OD δ_C (49.0 ppm) respectively, as internal standards. Coupling constants are

reported in hertz (Hz). Optical rotations were measured on an ATAGO AP-300 automatic polarimeter at a path length of 100 mm.

5.4.3 Procedures and Spectra

(4*R*,6*R*)-nona-1,8-diene-4,6-diol (5.4)

To an oven-dried sealed tube under one atmosphere of argon gas charged with $[Ir(cod)Cl]_2$ (0.672 g, 1.00 mmol, 5 mol%), (*R*)-BINAP (1.25 g, 2.00 mmol, 10 mol%), Cs_2CO_3 (2.61 g, 8.00 mmol, 40 mol%) and 4-chloro-3-nitrobenzoic acid (0.806 g, 4.00 mmol, 20 mol%) was added THF (50 mL) followed by allyl acetate (20.0 g, 200 mmol, 1000 mol%). The reaction mixture was stirred at 90 ºC for 0.5 h before cooling to ambient temperature. 1,3-propanediol **5.5** (1.52 g, 20.0 mmol, 100 mol%) in THF (50 mL, 0.2 M overall) was added and the reaction mixture was stirred at 100 ºC for 5 days. The reaction mixture was cooled to ambient temperature, filtered through Celite, and excess solvent was removed under reduced pressure. The crude material was dissolved in EtOAc (50 mL) and vigorously stirred. Et_2O (100 mL) was added slowly followed by hexanes (100 mL). The precipitate was filtered through Celite and the solution was then concentrated onto silca gel. Purification of the product by column chromatography (SiO_2, EtOAc:hexanes, 1:6 to 1:4 with 0.1% TEA) provided **5.4** (1.68 g, 54% yield, dr = 20:1, ee > 99%) as a pale yellow oil.

TLC (SiO_2): R_f = 0.25 (EtOAc:hexanes, 1:4).

^{1}H NMR: (400 MHz, $CDCl_3$): δ 5.87-5.77 (m, 2H), 5.17-5.15 (m, 2H), 5.13-5.12 (m, 2H), 4.04-3.97 (m, 2H), 2.39 (d, *J* = 3.5 Hz, 2H), 2.30-2.24 (m, 4H), 1.66-1.63 (m, 2H).

^{13}C NMR: (100 MHz, $CDCl_3$): δ 134.8, 118.4, 68.2, 42.2, 41.6.

FTIR (neat): ν 3333, 2936, 2359, 2342, 1214, 1434, 1325, 1133, 1047.cm^{-1}.

HRMS: (ESI) Calcd. for $C_9H_{16}O_2Na$ $(M+Na)^+$: 179.1048, Found: 179.1042.

HPLC: The enantiomeric excess was determined by chiral HPLC as described by Krische and coworkers.[102]

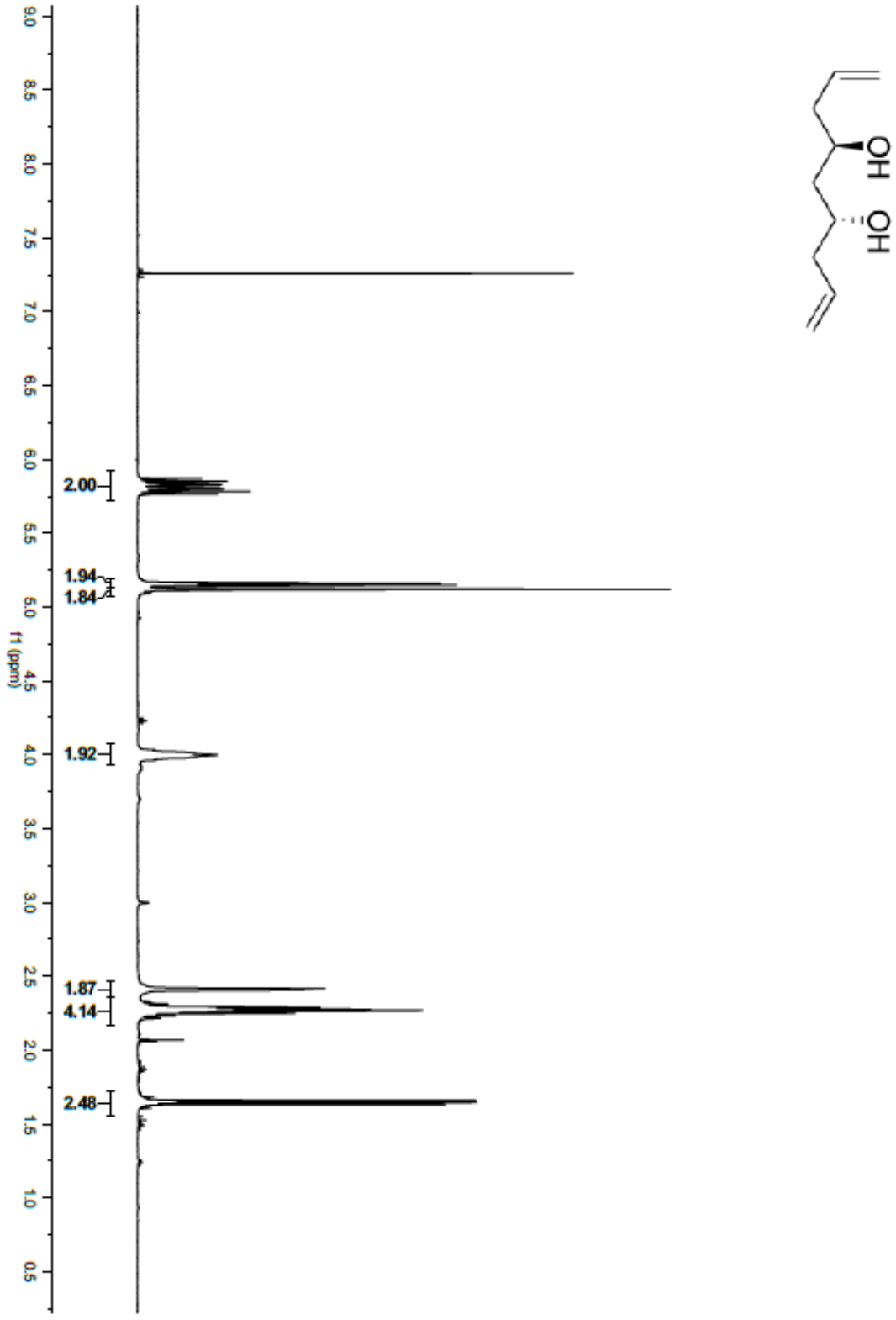
OH
OH
2.00
1.94
1.84
1.92
1.87
4.14
2.48
f1 (ppm)

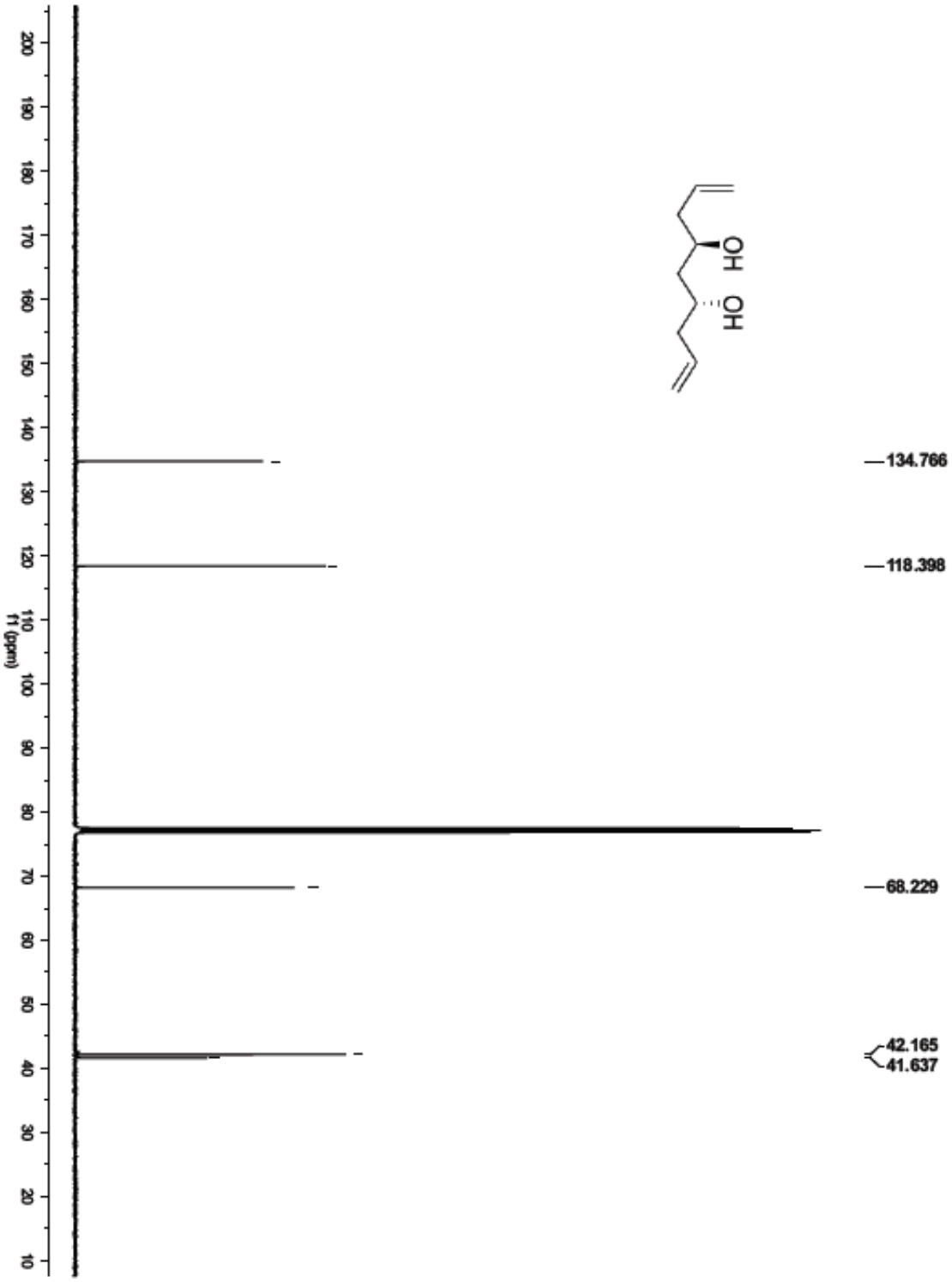
f1 (ppm)
134.766
118.398
68.229
42.165
41.637
HO
HO

(4*R*,6*R*)-6-hydroxynona-1,8-dien-4-yl acrylate (5.7)

To a stirred solution of diol **5.4** (104.1 mg, 0.666 mmol, 100 mol%) in dry MeCN (3.30 mL, 0.2 M) was added $^{i}Pr_2NEt$ (230 μL, 1.33 mmol, 200 mol%) followed by 2-aminoethyl diphenylborinate (14.9 mg, 0.07 mmol, 10 mol%). Acryloyl chloride (90.5 mg, 1.00 mmol, 150 mol%) was added dropwise and the solution was stirred at ambient temperature for 3 h. The reaction mixture was poured into H_2O and EtOAc and extracted with EtOAc (3 x 10 mL). The combined organic extracts were washed with brine, dried over anhydrous $MgSO_4$, filtered through Celite, and concentrated by rotary evaporation. The crude material was purified via flash column chromatography (SiO_2, EtOAc:hexanes 1:9) to afford **5.7** (136.4 mg, 97% yield) as a colorless oil.

TLC (SiO_2): R_f = 0.21 (1:9 EtOAc:hexanes)

^{1}H NMR: (400 MHz, $CDCl_3$): δ = 6.43 (dd, *J* = 17.3, 1.4 Hz, 1H), 6.13 (dd, *J* = 17.3, 10.4 Hz, 1H), 5.87 (dd, *J* = 10.4, 1.4 Hz, 1H), 5.84-5.71 (m, 2H), 5.27-5.21 (m, 1H), 5.13-5.06 (m, 4H), 3.61-3.54 (m, 1H), 2.83 (d, *J* = 3.8 Hz, 1H), 2.41-2.37 (m, 2H), 2.25-2.21 (m, 2H), 1.74-1.60 (m, 2H).

^{13}C NMR: (100 MHz, $CDCl_3$): δ = 166.9, 134.7, 133.3, 131.4, 128.2, 118.0, 117.6, 70.9, 66.5, 41.6, 41.6, 39.2.

FTIR (neat): ν 3464, 3016, 2970, 1739, 1407, 1366, 1297, 1228, 1217, 1206, 1049 cm^{-1}.

HRMS: (ESI) Calcd. for $C_{12}H_{18}O_3Na$ $(M+Na)^+$: 233.1154, Found: 233.1147

$[\alpha]^{23}_D$: - 28.94° (c = 0.36, $CHCl_3$).

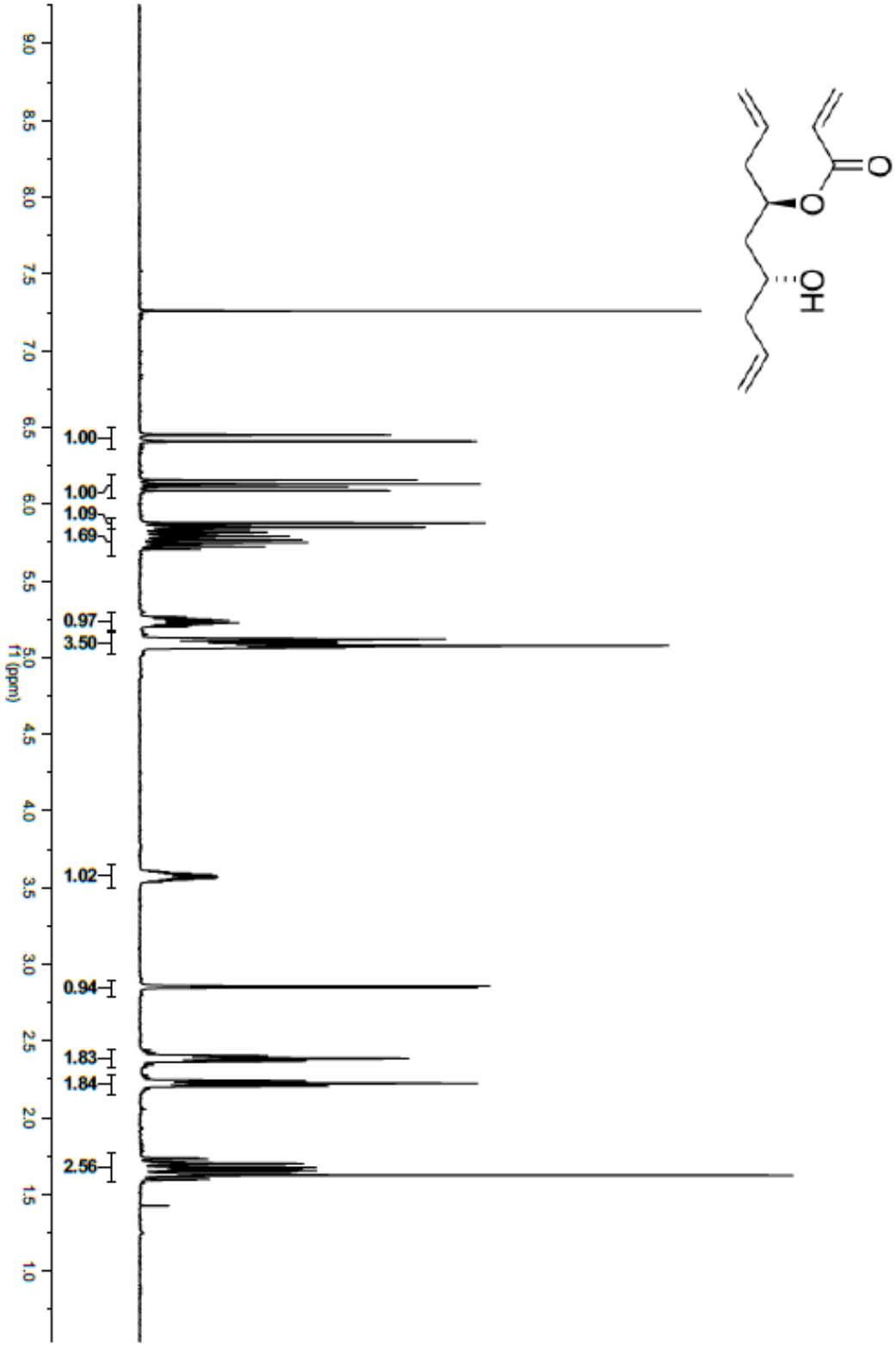
9.0
8.5
8.0
7.5
7.0
6.5
6.0
5.5
5.0
4.5
4.0
3.5
3.0
2.5
2.0
1.5
1.0
f1 (ppm)
1.00
1.00
1.09
1.69
0.97
3.50
1.02
0.94
1.83
1.84
2.56
O
O
HO

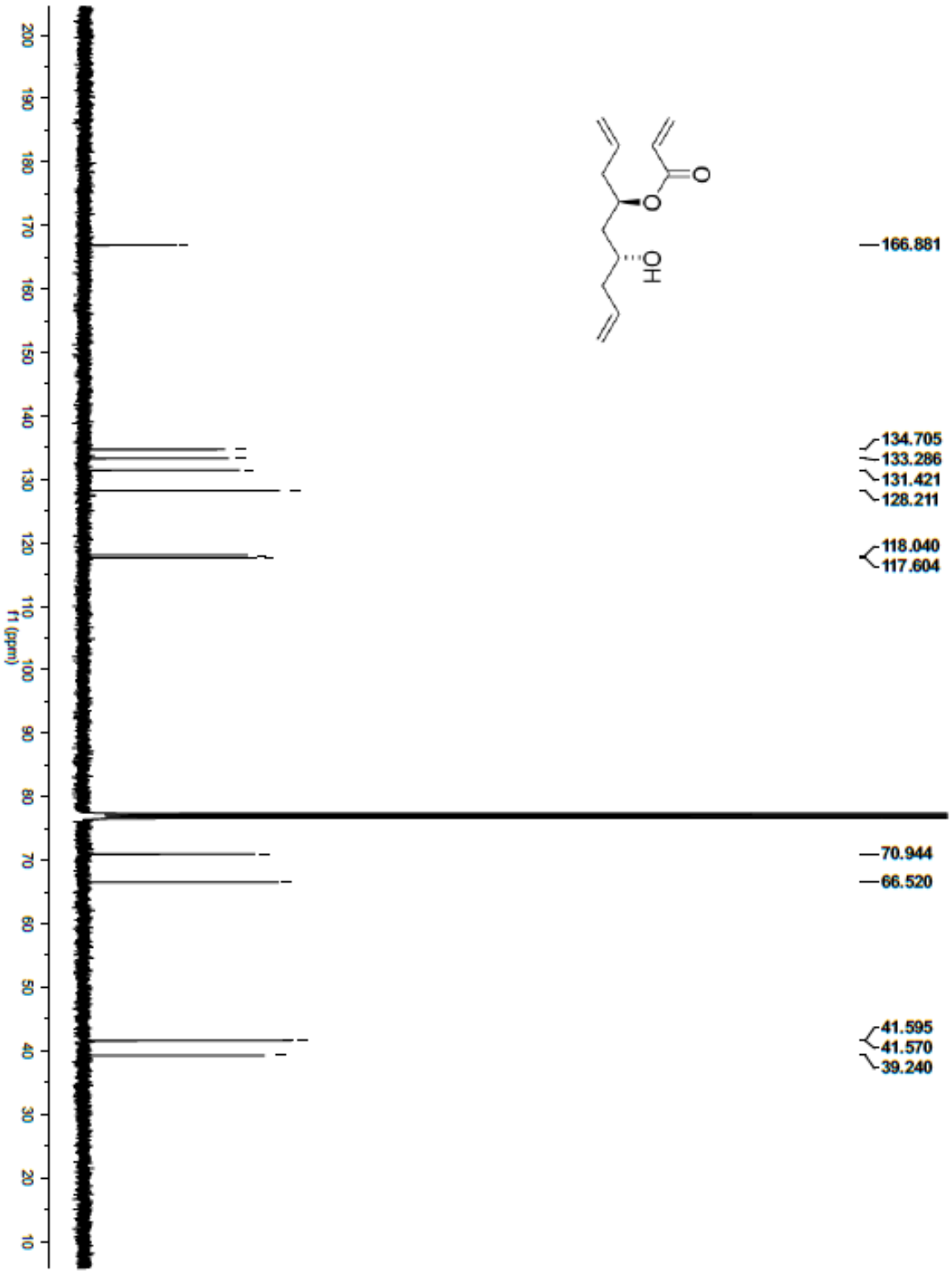
166.881
134.705
133.286
131.421
128.211
118.040
117.604
70.944
66.520
41.595
41.570
39.240
f1 (ppm)

(*R*,*E*)-5-hydroxy-6-((*R*)-6-oxo-3,6-dihydro-2*H*-pyran-2-yl)hex-2-enal (5.8)

To a solution of **5.7** (48.6 mg, 0.231 mmol, 100 mol%) in dry toluene (23.1 mL, 0.01 M) was added acrolein (0.046 mL, 0.693 mmol, 300 mol%). Hoveyda-Grubbs II (14.5 mg, 0.023 mmol, 10 mol%) was added and the reaction was heated to reflux for 3 h. The crude reaction mixture was concentrated under vacuum and purified via flash column chromatography (SiO_2, acetone:$CHCl_3$ 1:9 to 3:7) to afford **5.8** (6.8 mg, 14% yield) as a brown oil.

TLC (SiO_2): R_f = 0.35 (3:7 acetone:$CHCl_3$)

^{1}H NMR: (400 MHz, $CDCl_3$): δ = 9.54 (d, *J* = 7.8 Hz, 1H), 6.94-6.85 (m, 2H), 6.24-6.17 (m, 1H), 6.04 (dt, *J* = 9.8, 1.9 Hz, 1H), 4.76 (dtd, *J* = 10.2, 7.9, 2.3 Hz, 1H), 4.31-4.28 (m, 1H), 2.61-2.49 (m, 2H), 2.39-2.36 (m, 2H), 2.12-2.11 (m, 1H), 1.93 (ddd, *J* = 14.5, 10.0, 2.4 Hz, 1H), 1.74 (ddd, *J* = 14.5, 10.2, 2.6 Hz, 1H).

^{13}C NMR: (100 MHz, $CDCl_3$): δ = 193.8, 164.2, 153.5, 145.4, 135.6, 121.5, 74.6, 65.9, 42.0, 41.1, 29.9

FTIR (neat): ν 3423, 2923, 1683, 1393, 1254, 1138, 1045 cm^{-1}.

HRMS: (ESI) Calcd. for $C_{11}H_{14}O_4Na$ $(M+Na)^+$: 233.07840, Found: 233.07900

$[\alpha]^{23}_D$: + 8.82° (c = 0.68, $CHCl_3$).

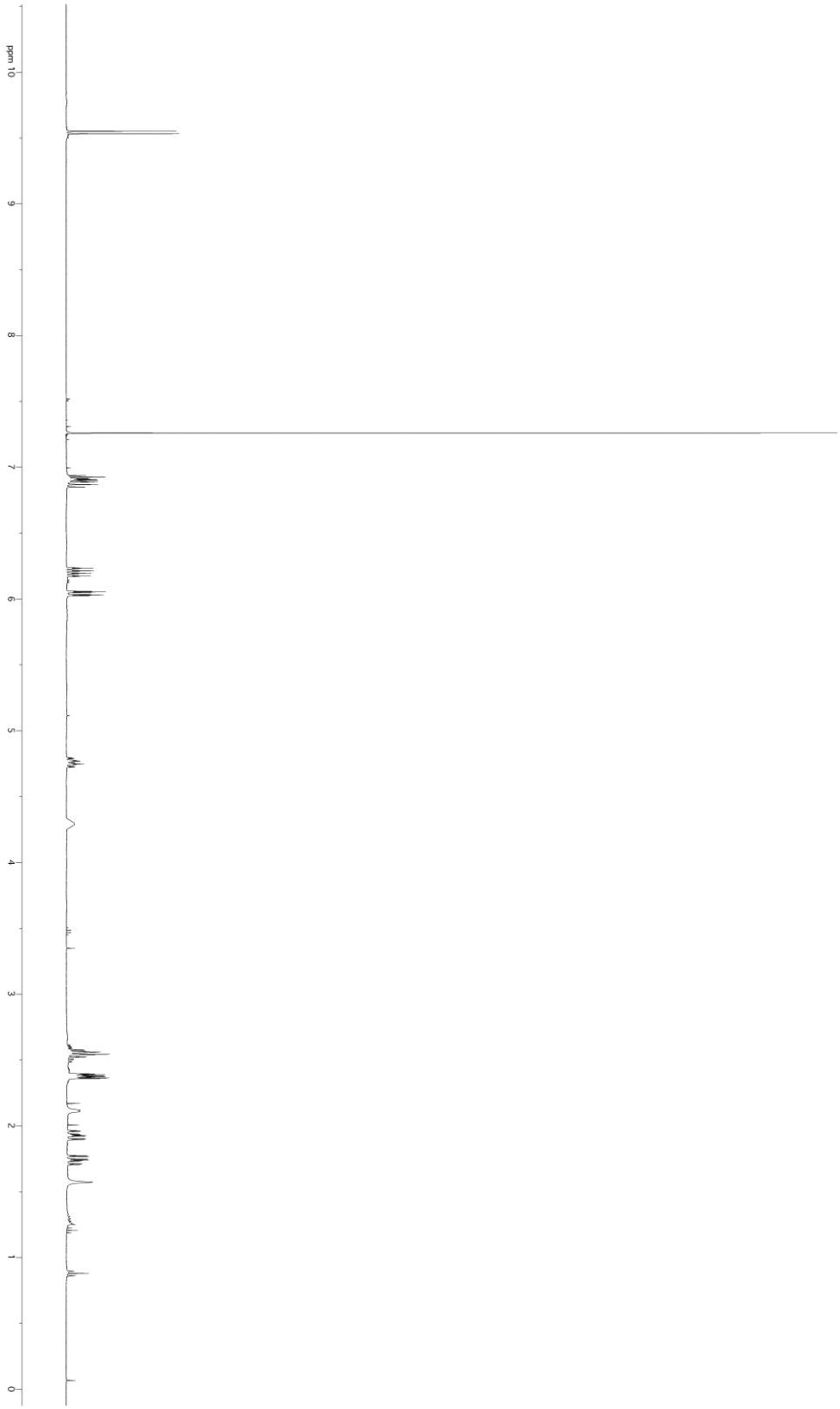
ppm 10
9
8
7
6
5
4
3
2
1
0

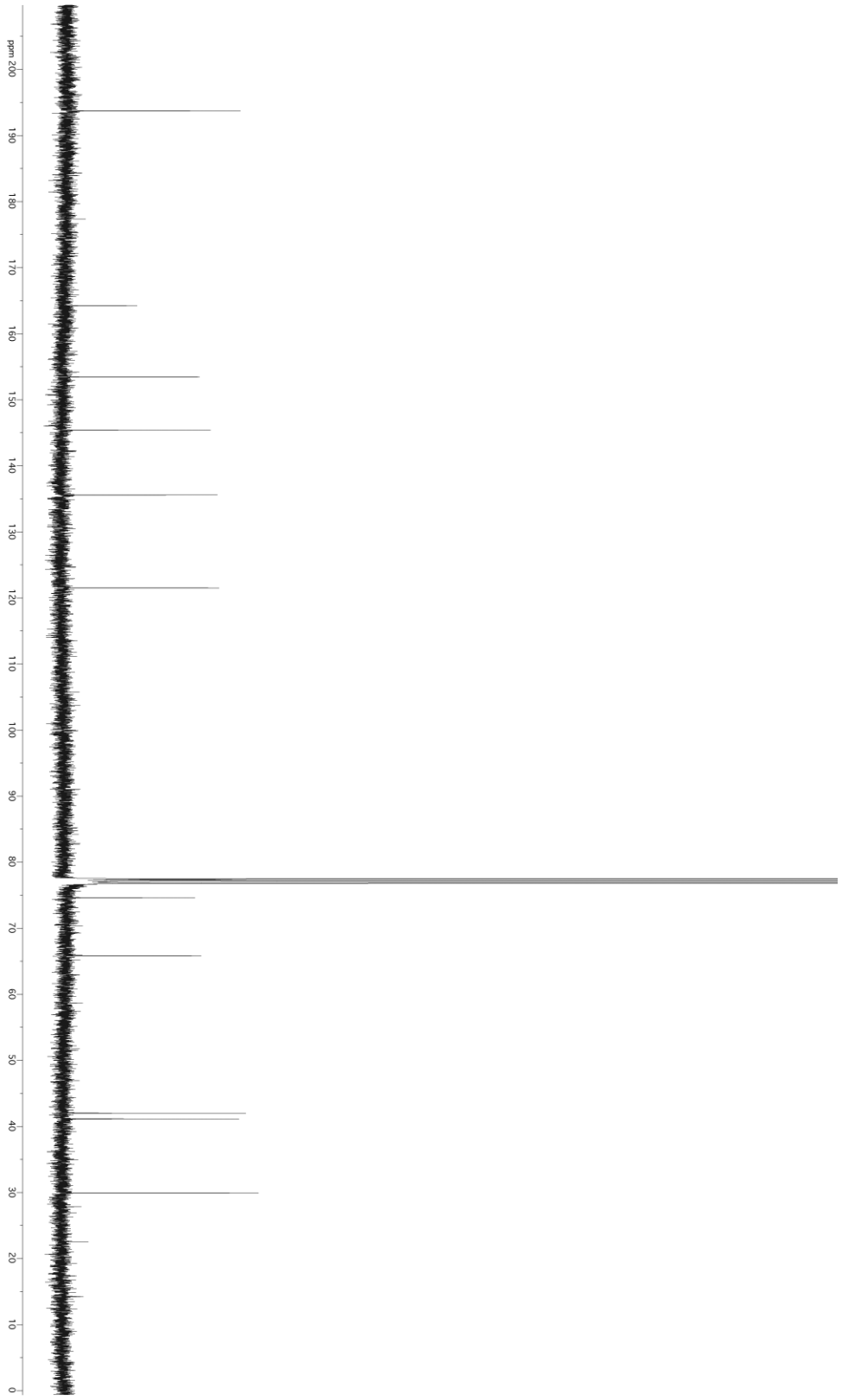
ppm 200
190
180
170
160
150
140
130
120
110
100
90
80
70
60
50
40
30
20
10
0

(4*R*,6*R*)-6-(allyloxy)nona-1,8-dien-4-ol (5.10)

To a stirred solution of diol **5.4** (501.5 mg, 3.21 mmol, 100 mol%) in dry MeCN (16.0 mL, 0.2 M) was added 2-aminoethyl diphenylborinate (72.3 mg, 0.321 mmol, 10 mol%) followed by KI (532.9 mg, 3.21 mmol, 100 mol%) and K_2CO_3 (487.9 mg, 3.53 mmol, 110 mol%) and the solution was heated to 60 °C. Freshly distilled allyl bromide (0.83 mL, 9.63 mmol, 300 mol%) was added dropwise and the solution was stirred at 60 °C for 24 h. The reaction mixture was poured into H_2O (15 mL) and extracted with EtOAc (3 x 15 mL). The combined organic extracts were washed with brine, dried over anhydrous $MgSO_4$, filtered through Celite, and concentrated by rotary evaporation. The crude material was purified via flash column chromatography (SiO_2, EtOAc:hexanes 1:9) to afford **5.10** (407.5 mg, 65% yield) as a colorless oil.

TLC (SiO_2): R_f = 0.19 (1:9 EtOAc:hexanes)

^{1}H NMR: (400 MHz, $CDCl_3$): δ = 5.97-5.73 (m, 3H), 5.27 (dq, *J* = 17.2, 1.6 Hz, 1H), 5.19-5.05 (m, 5H), 4.11 (ddt, *J* = 12.6, 5.5, 1.4 Hz, 1H), 4.03-3.94 (m, 2H), 3.73-3.68 (m, 1H), 2.65 (d, *J* = 3.7 Hz, 1H), 2.43-2.37 (m, 1H), 2.32-2.21 (m, 3H), 1.64 (t, *J* = 5.7 Hz, 2H).

^{13}C NMR: (100 MHz, $CDCl_3$): δ = 135.05, 134.95, 134.55, 117.83, 117.58, 117.18, 76.44, 70.45, 67.72, 42.38, 39.70, 38.27

HRMS: (ESI) Calcd. for $C_{12}H_{20}O_2Na$ $(M+Na)^+$: 219.1356, Found: 219.1355

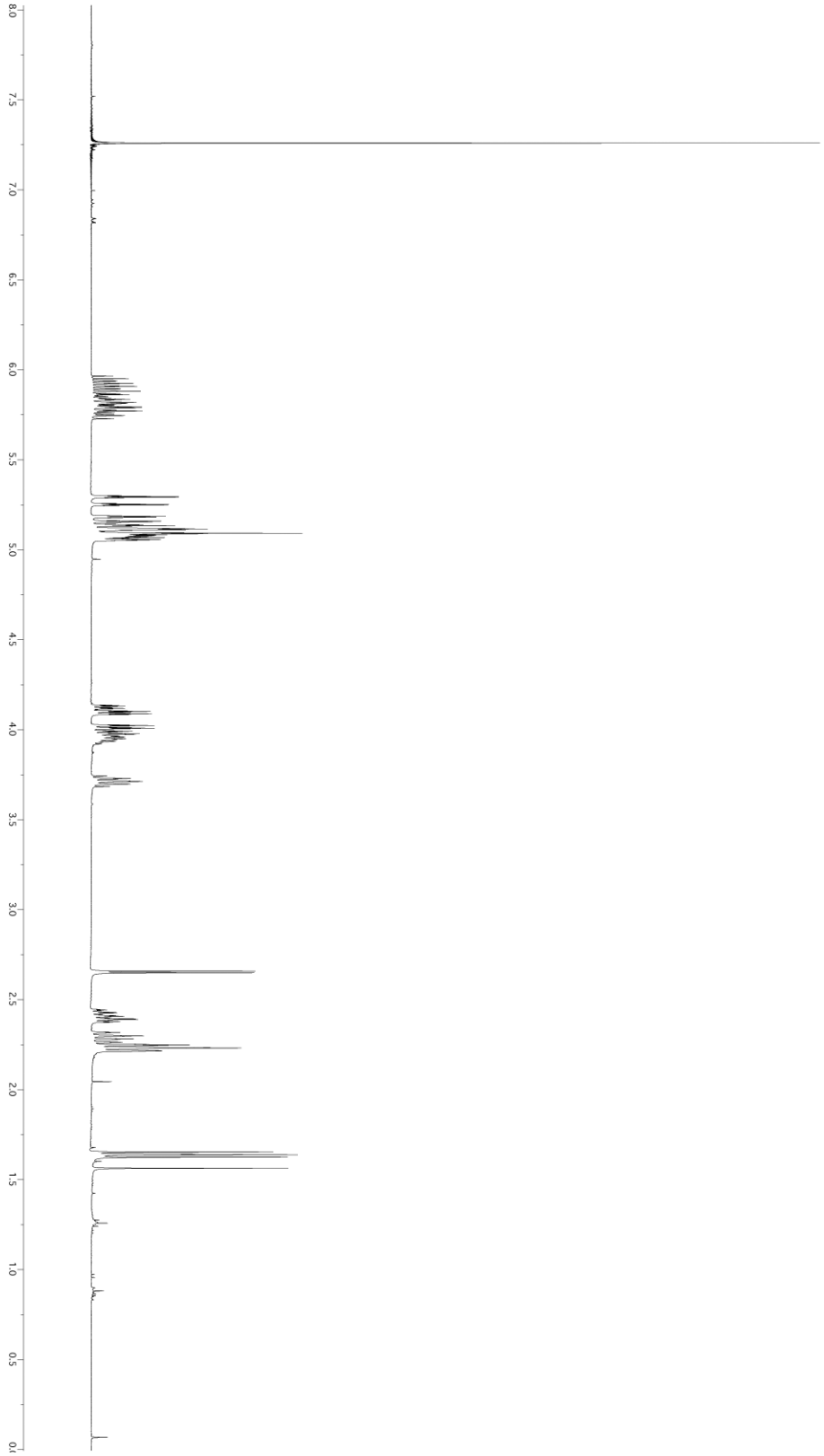
8.0
7.5
7.0
6.5
6.0
5.5
5.0
4.5
4.0
3.5
3.0
2.5
2.0
1.5
1.0
0.5

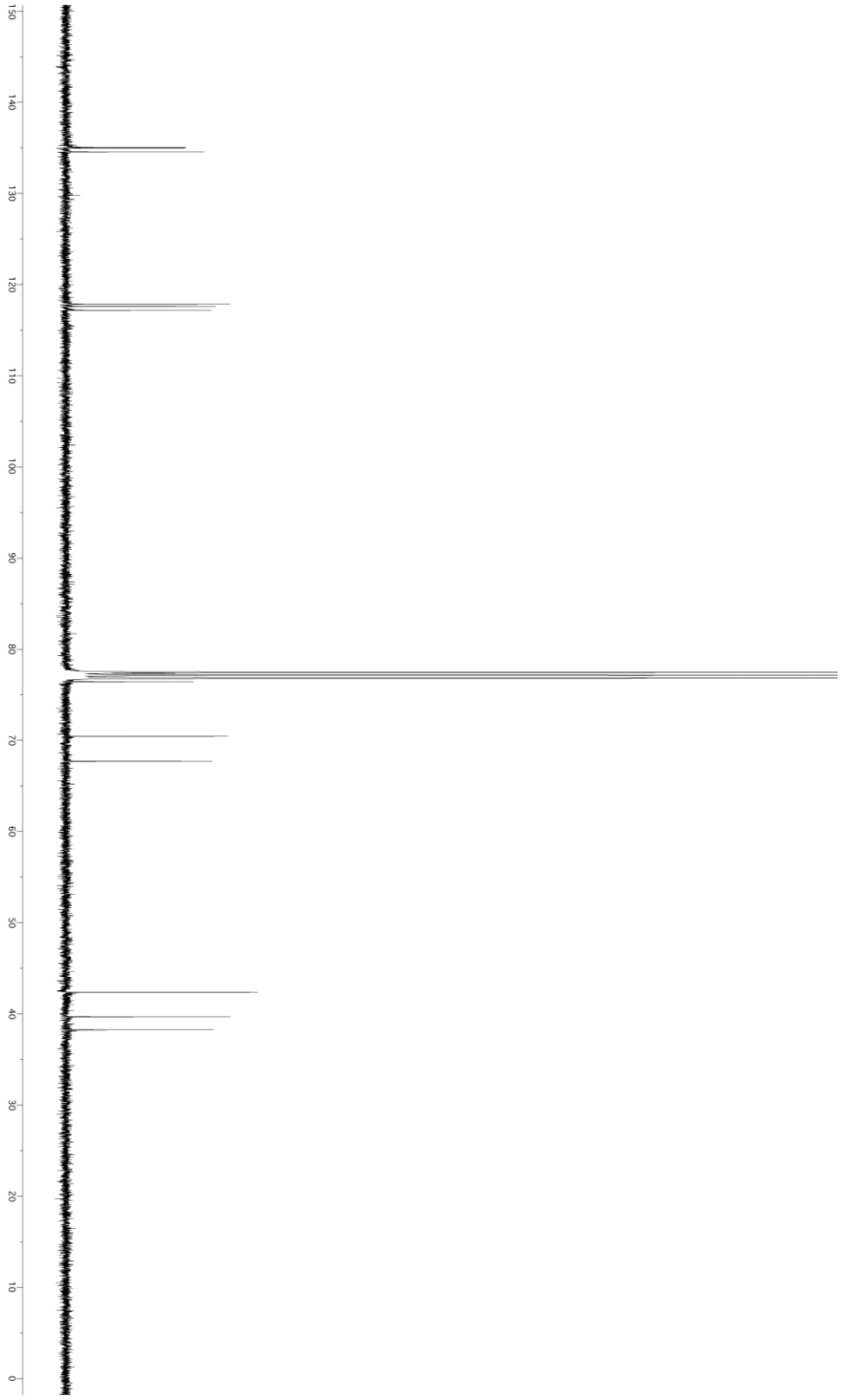
150
140
130
120
110
100
90
80
70
60
50
40
30
20
10
0

(*R*,*E*)-7-((*R*)-3,6-dihydro-2*H*-pyran-2-yl)-6-hydroxyhept-3-en-2-one (5.11)

To a stirred solution of **5.10** (167.7 mg, 0.854 mmol, 100 mol%) in dry CH_2Cl_2 (62 mL) was added freshly distilled methyl vinyl ketone (0.37 mL, 4.27 mmol, 500 mol%) and the solution was heated to 50 °C. A solution of Grubbs II (36.3 mg, 0.043 mmol, 5 mol%) in dry CH_2Cl_2 (12 mL, 0.01M final concentration) was added via syringe pump addition over 5 h and the solution was left to stir at 50 °C overnight. The reaction was cooled to room temperature and concentrated by rotary evaporation. The crude material was purified via flash column chromatography (SiO_2, EtOAc:hexanes 2:3 to 1:1) to afford **5.11** (178.4 mg, 99% yield) as a light brown oil.

TLC (SiO_2): R_f = 0.17 (1:1 EtOAc:hexanes)

^{1}H NMR: (400 MHz, $CDCl_3$): δ = 6.86 (dt, *J* = 16.0, 7.2 Hz, 1H), 6.14 (dt, *J* = 16.0, 1.4 Hz, 1H), 5.83-5.80 (m, 1H), 5.73-5.70 (m, 1H), 4.21-4.18 (m, 2H), 4.11-4.08 (m, 1H), 3.87-3.83 (m, 1H), 2.95 (d, *J* = 4.7 Hz, 1H), 2.45-2.40 (m, 2H), 2.26 (s, 3H), 2.17-2.13 (m, 1H), 1.95-1.89 (m, 1H), 1.74-1.70 (m, 2H).

^{13}C NMR: (100 MHz, $CDCl_3$): δ = 198.7, 144.7, 133.5, 126.0, 124.2, 71.3, 67.8, 66.1, 41.5, 40.6, 30.7, 27.0

HRMS: (ESI) Calcd. for $C_{12}H_{18}O_3Na$ $(M+Na)^+$: 233.1148, Found: 233.1149

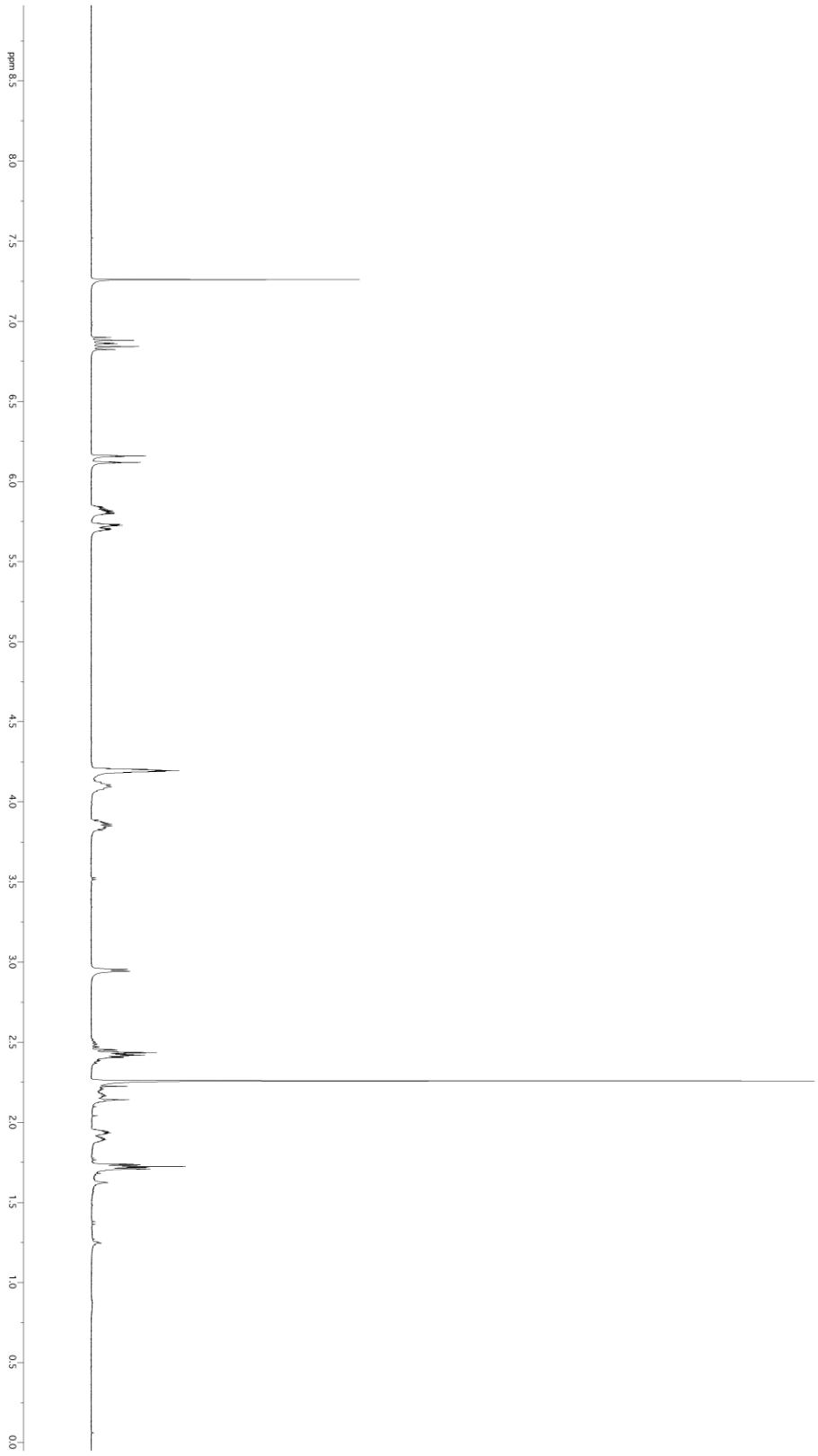
ppm
8.5
8.0
7.5
7.0
6.5
6.0
5.5
5.0
4.5
4.0
3.5
3.0
2.5
2.0
1.5
1.0
0.5
0.0

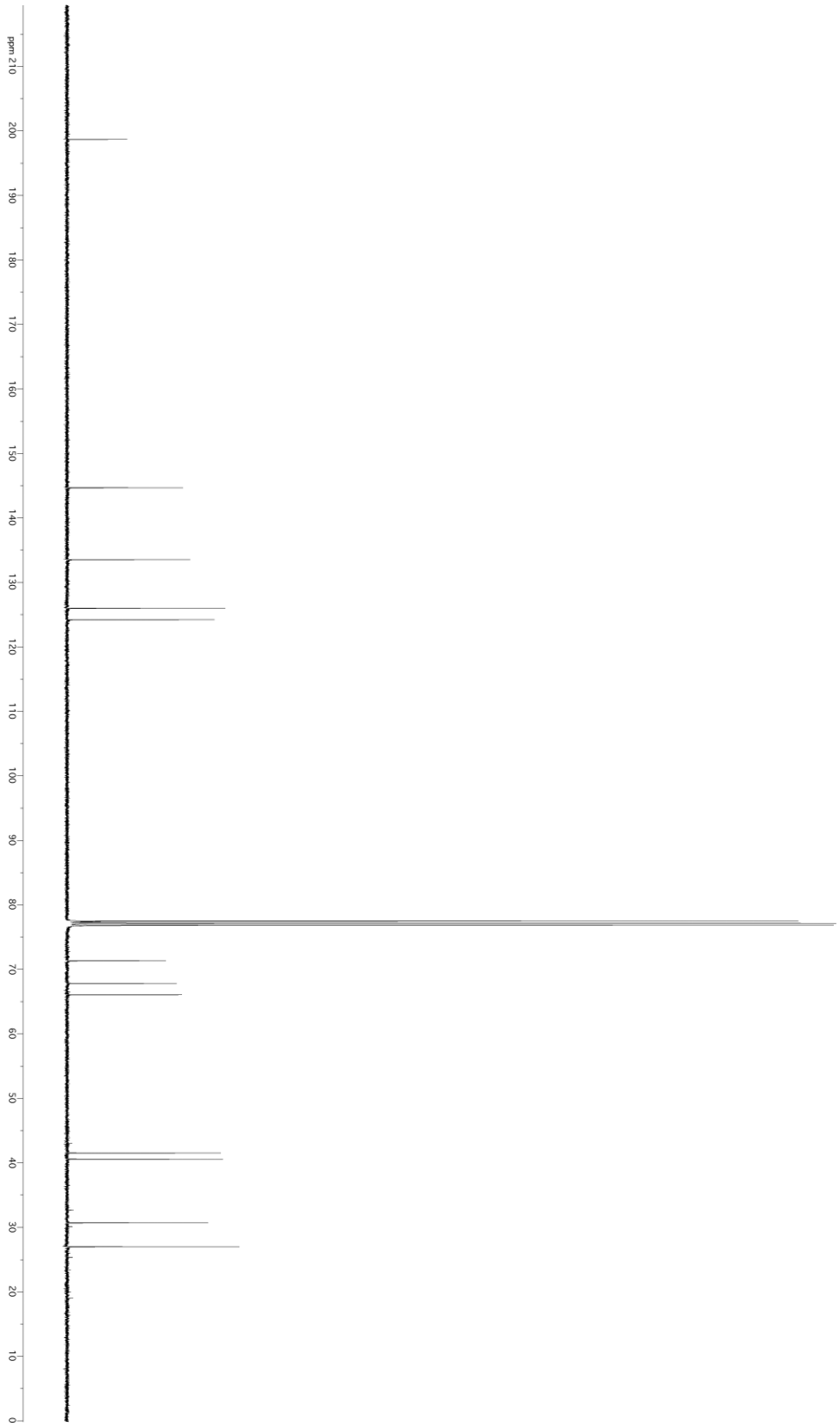
ppm
210
200
190
180
170
160
150
140
130
120
110
100
90
80
70
60
50
40
30
20
10
0

1-((2*S*,4*S*,6*S*)-6-(((*R*)-3,6-dihydro-2*H*-pyran-2-yl)methyl)-2-methyl-1,3-dioxan-4-yl)propan-2-one (5.12)

To a solution of **5.11** (129.0 mg, 0.613 mmol, 100 mol%) in dry CH_2Cl_2 (6.1 mL, 0.1 M) was added acetaldehyde (0.70 mL, 12.27 mmol, 2000 mol%). $Bi(NO_3)_3 \cdot 5H_2O$ (29.7 mg, 0.061 mmol, 10 mol%) was added and the solution was allowed to stir at room temperature for 24 h. The solution was then poured into sat. aq. $NaHCO_3$ (10 mL) and extracted with CH_2Cl_2 (3 x 10 mL). The combined organic extracts were dried over $MgSO_4$, filtered through Celite, and concentrated via rotary evaporation. The crude material was purified via flash column chromatography (SiO_2, EtOAc:hexanes 1:9 to 2:3) to afford **5.12** (83.8 mg, 54% yield) as a colorless oil.

TLC (SiO_2): R_f = 0.21 (1:1 EtOAc:hexanes)

^{1}H NMR: (400 MHz, $CDCl_3$): δ = 5.82-5.77 (m, 1H), 5.71 (ddq, *J* = 10.3, 3.3, 1.7 Hz, 1H), 4.74 (q, *J* = 5.1 Hz, 1H), 4.22-4.15 (m, 2H), 4.11 (dddd, *J* = 11.2, 7.4, 5.1, 2.4 Hz, 1H), 3.93-3.86 (m, 1H), 3.77-3.71 (m, 1H), 2.75 (dd, *J* = 16.1, 7.4 Hz, 1H), 2.46 (dd, *J* = 16.1, 5.2 Hz, 1H), 2.18 (s, 3H), 2.00-1.96 (m, 2H), 1.69-1.55 (m, 4H), 1.29 (d, *J* = 5.1 Hz, 3H).

^{13}C NMR: (100 MHz, $CDCl_3$): δ = 206.8, 126.4, 124.4, 98.7, 72.8, 72.4, 69.8, 66.0, 49.7, 42.6, 37.3, 31.6, 31.3, 21.2

HRMS: (ESI) Calcd. for $C_{14}H_{22}O_4Na$ $(M+Na)^+$: 277.1410, Found: 277.1408

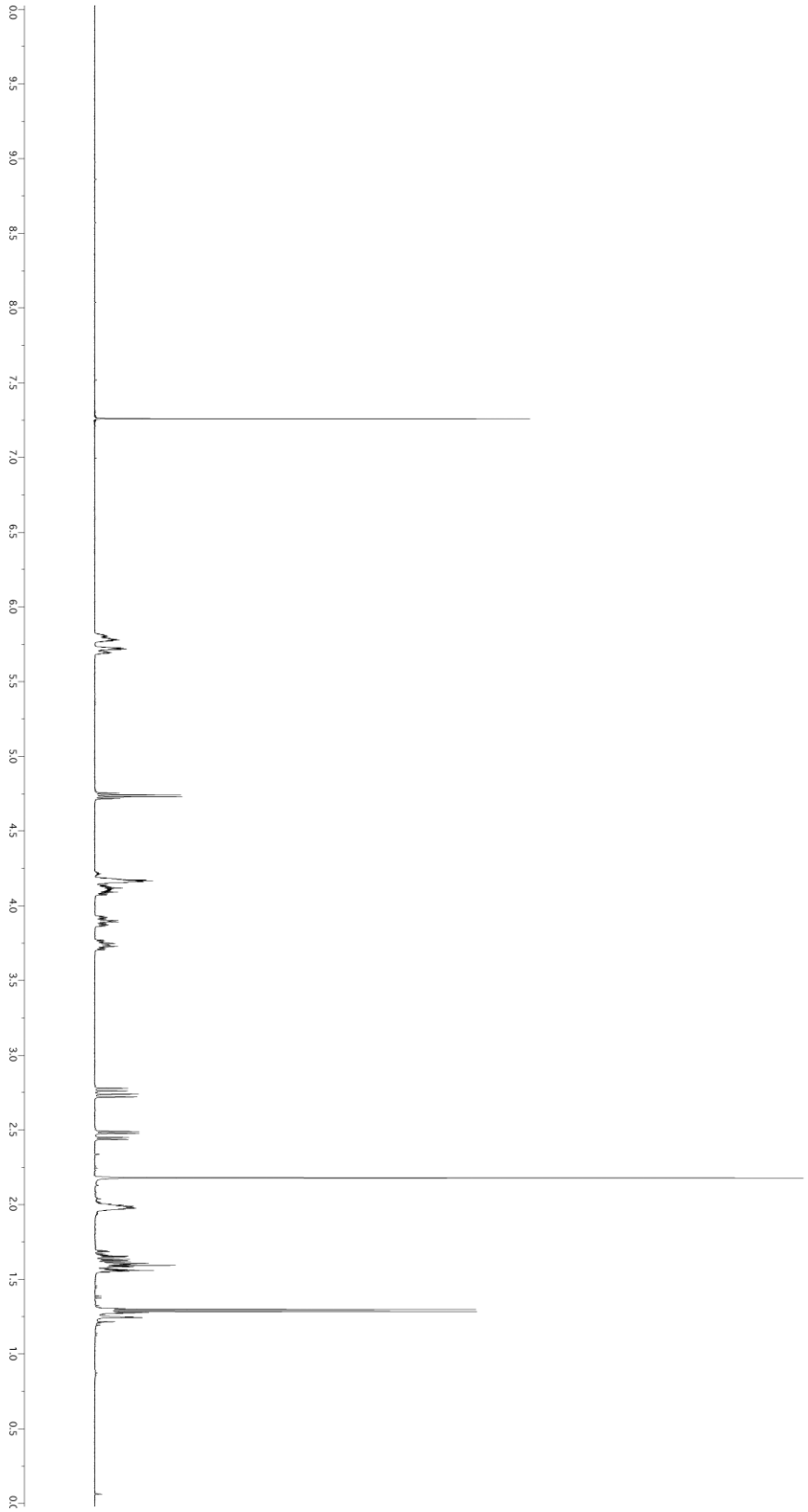
0.0
9.5
9.0
8.5
8.0
7.5
7.0
6.5
6.0
5.5
5.0
4.5
4.0
3.5
3.0
2.5
2.0
1.5
1.0
0.5

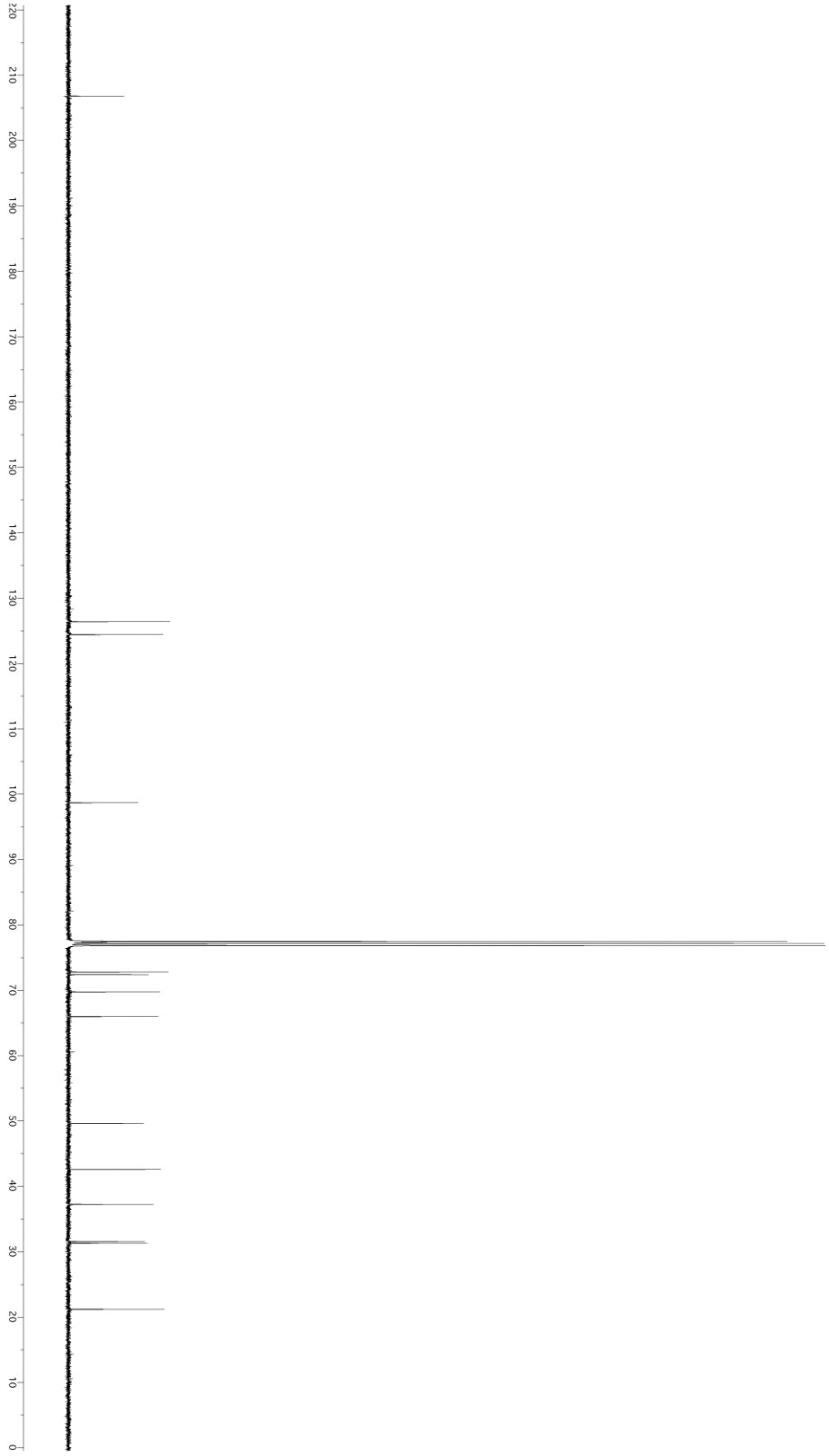
220
210
200
190
180
170
160
150
140
130
120
110
100
90
80
70
60
50
40
30
20
10
0

(4*R*,6*R*)-6-((triethylsilyl)oxy)nona-1,8-dien-4-yl acrylate (5.13)

To a stirred solution of acrylate **5.7** (136.4 mg, 0.65 mmol, 100 mol%) in dry CH_2Cl_2 (13.0 mL, 0.05 M) was added 2,6-lutidine (150 μL, 1.30 mmol, 200 mol%) and the reaction cooled to -78 °C. TESOTf (220 μL, 0.97 mmol, 150 mol%) was added dropwise and the solution was stirred at -78 °C for 1.5 h. The reaction was quenched with sat. aq. NH_4Cl and warmed to ambient temperature. The reaction mixture was poured into H_2O and extracted with CH_2Cl_2 (3 x 15 mL). The combined organic extracts were washed with brine, dried over anhydrous $MgSO_4$, filtered through Celite, and concentrated by rotary evaporation. The crude material was purified via flash column chromatography (SiO_2, EtOAc:hexanes 1:32) to afford **5.13** (198.4 mg, 94% yield) as a colorless oil.

TLC (SiO_2): R_f = 0.42 (1:19 ethyl acetate:hexanes)

^{1}H NMR: (400 MHz, $CDCl_3$): δ = 6.38 (dd, *J* = 17.3, 1.5 Hz, 1H), 6.10 (dd, *J* = 17.3, 10.4 Hz, 1H), 5.84-5.70 (m 2H), 5.80 (dd, *J* = 10.4, 1.5 Hz, 1H), 5.09-5.03 (m, 5H), 3.84-3.78 (m, 1H), 2.40-2.36 (m, 2H), 2.26-2.22 (m, 2H), 1.76 (ddd, *J* = 14.5, 9.5, 3.2 Hz, 1H), 1.62 (ddd, *J* = 14.5, 9.0, 3.2 Hz, 1H), 0.94 (t, *J* = 7.9 Hz, 9H), 0.57 (q, *J* = 8.0 Hz, 6H).

^{13}C NMR: (100 MHz, $CDCl_3$): δ = 165.8, 134.6, 133.5, 130.5, 129.0, 118.0, 117.5, 71.3, 68.7, 42.9, 40.7, 39.3, 7.1, 5.2.

FTIR (neat): ν 3016, 2970, 1739, 1405, 1366, 1229, 1217, 1205, 1092 cm^{-1}.

HRMS: (ESI) Calcd. for $C_{18}H_{32}O_3SiNa$ $(M+Na)^+$: 347.2018, Found: 347.2015

$[\alpha]^{23}_D$: -30.87 ° (c = 0.65, $CHCl_3$).

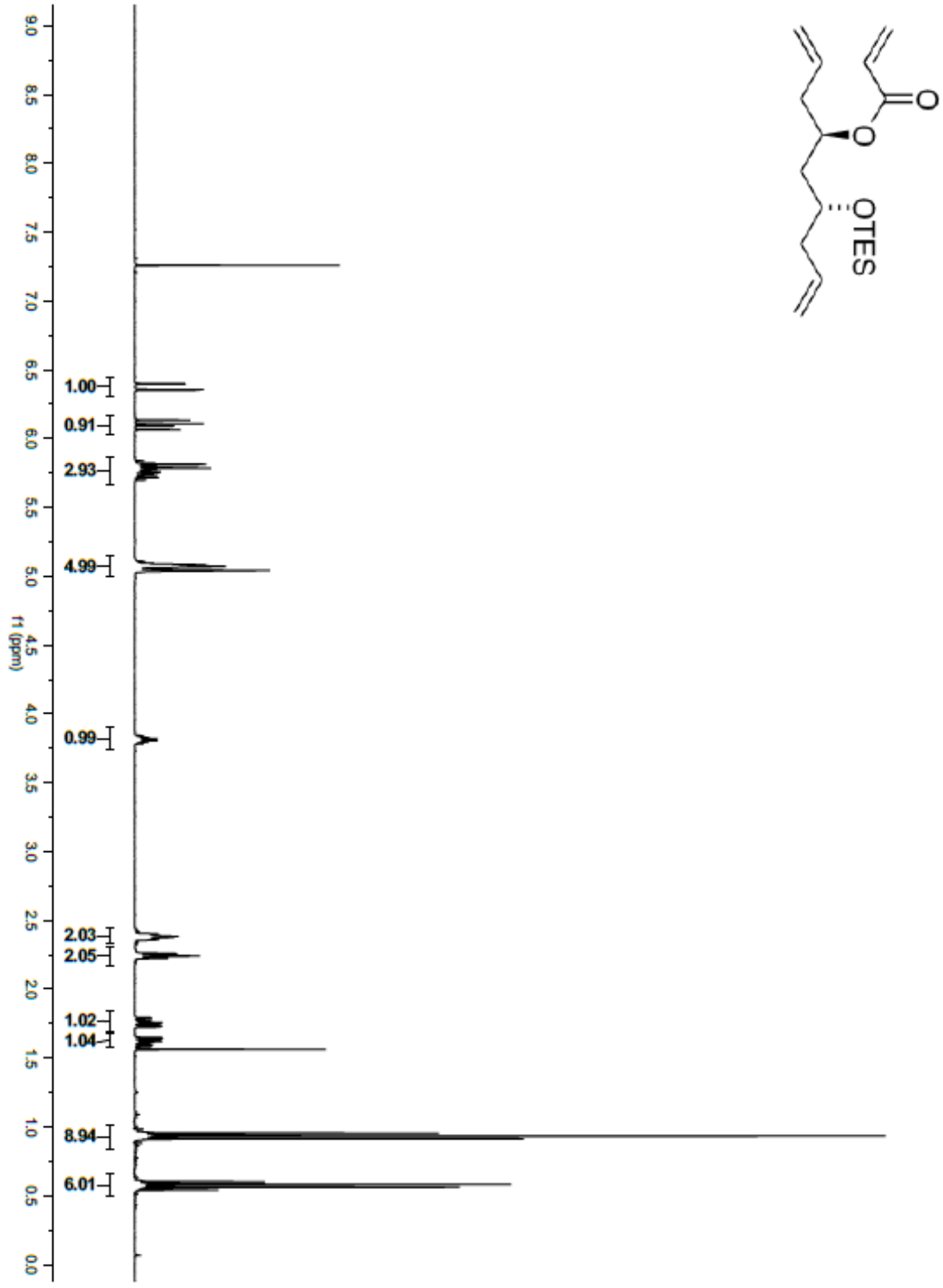
OTES
O
O
f1 (ppm)
9.0
8.5
8.0
7.5
7.0
6.5
6.0
5.5
5.0
4.5
4.0
3.5
3.0
2.5
2.0
1.5
1.0
0.5
0.0
1.00
0.91
2.93
4.99
0.99
2.03
2.05
1.02
1.04
8.94
6.01

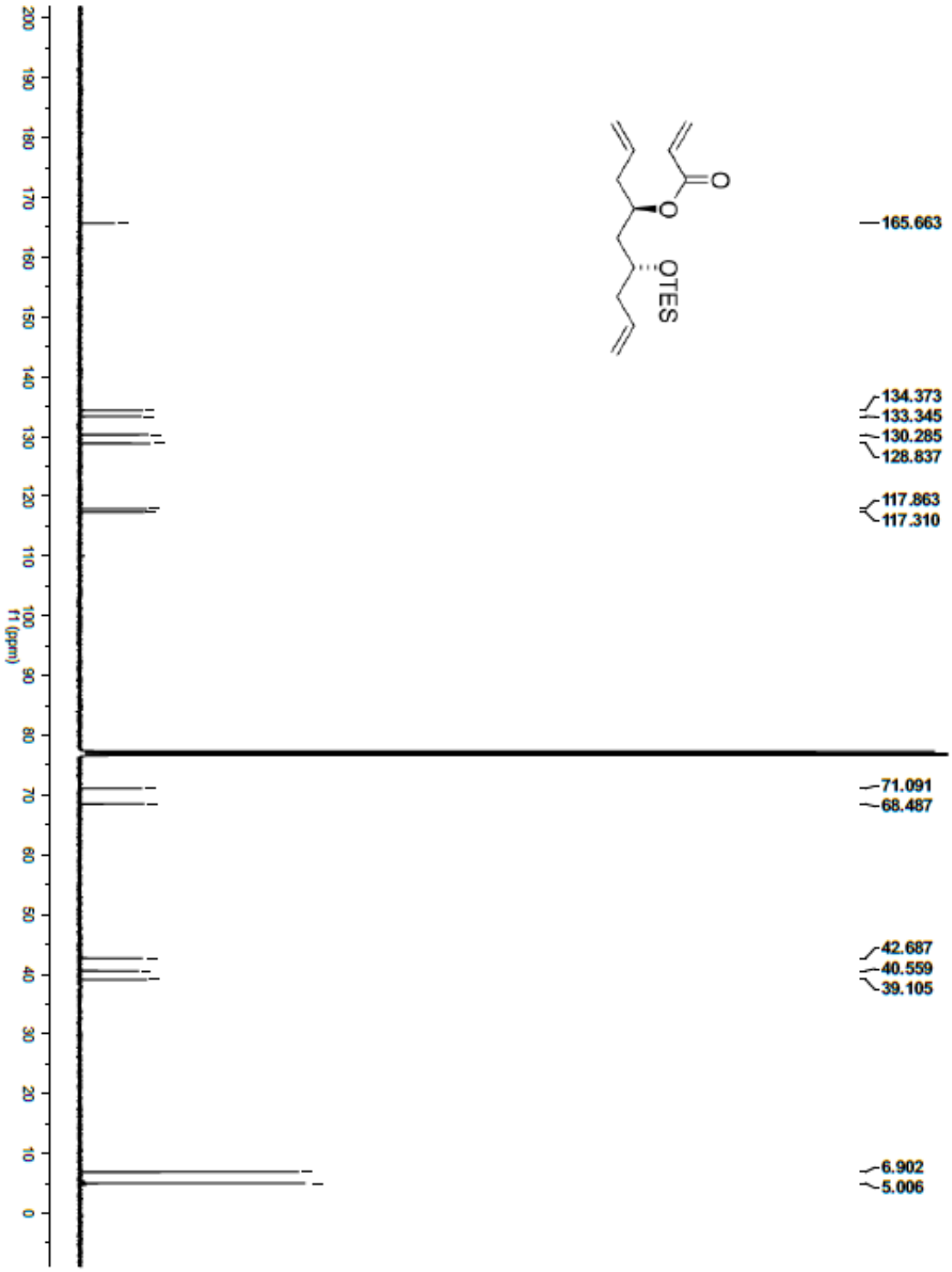
OTES
O
O
165.663
134.373
133.345
130.285
128.837
117.863
117.310
71.091
68.487
42.687
40.559
39.105
6.902
5.006
f1 (ppm)

(*R*)-6-((*R*,*E*)-6-oxo-2-((triethylsilyl)oxy)hept-4-en-1-yl)-5,6-dihydro-2*H*-pyran-2-one (5.14)

To a solution of **5.13** (503.9 mg, 1.55 mmol, 100 mol%) in dry toluene (155 mL, 0.01 M) was added freshly distilled methyl vinyl ketone (326.5 mg, 0.43 mL, 4.66 mmol, 300 mol%) followed by Hoveyda-Grubbs 2nd Generation catalyst (97.1 mg, 0.155 mmol, 10 mol%) and the solution stirred at rt for 1.5 h. The reaction mixture was then heated to 120 °C for 3 h. The solvent was then removed in vacuo and the crude material purified by flash column chromatography (SiO_2, EtOAc:hexanes 1:4 to 1:2) to afford **5.14** (371.8 mg, 71% yield) as a tan oil.

TLC (SiO_2): R_f = 0.18 (1:2 ethyl acetate:hexanes)

^{1}H NMR: (400 MHz, $CDCl_3$): δ 6.89 (ddd, *J* = 9.8, 4.8, 3.7 Hz, 1H), 6.78 (dt, *J* = 16.0, 7.4 Hz, 1H), 6.11 (dt, *J* = 16.0, 1.4 Hz, 1H), 6.03 (dt, *J* = 9.8, 1.8 Hz, 1H), 4.63-4.56 (m, 1H), 4.30-4.24 (m, 1H), 2.48-2.39 (m, 2H), 2.34-2.30 (m, 2H), 2.26 (s, 3H), 1.83 (ddd, *J* = 14.3, 10.3, 2.4 Hz, 1H), 1.65-1.59 (m, 1H), 0.95 (t, *J* = 7.9 Hz, 9H), 0.63 (q, *J* = 8.0 Hz, 6H).

^{13}C NMR: (100 MHz, $CDCl_3$): δ 198.4, 164.1, 145.4, 143.3, 134.1, 121.6, 74.4, 66.5, 42.5, 41.4, 30.1, 27.0, 7.0, 5.0.

FTIR (neat): ν 2955, 2913, 2877, 1720, 1674, 1628, 1423, 1381, 1362, 1250, 1179, 1150, 1086, 1061, 1005 cm^{-1}.

HRMS: (ESI) Calcd. for $C_{18}H_{30}O_4SiNa$ $(M+Na)^+$: 361.1811, Found: 361.1809

$[\alpha]^{23}_D$: -18.63 ° (c = 0.31, $CHCl_3$).

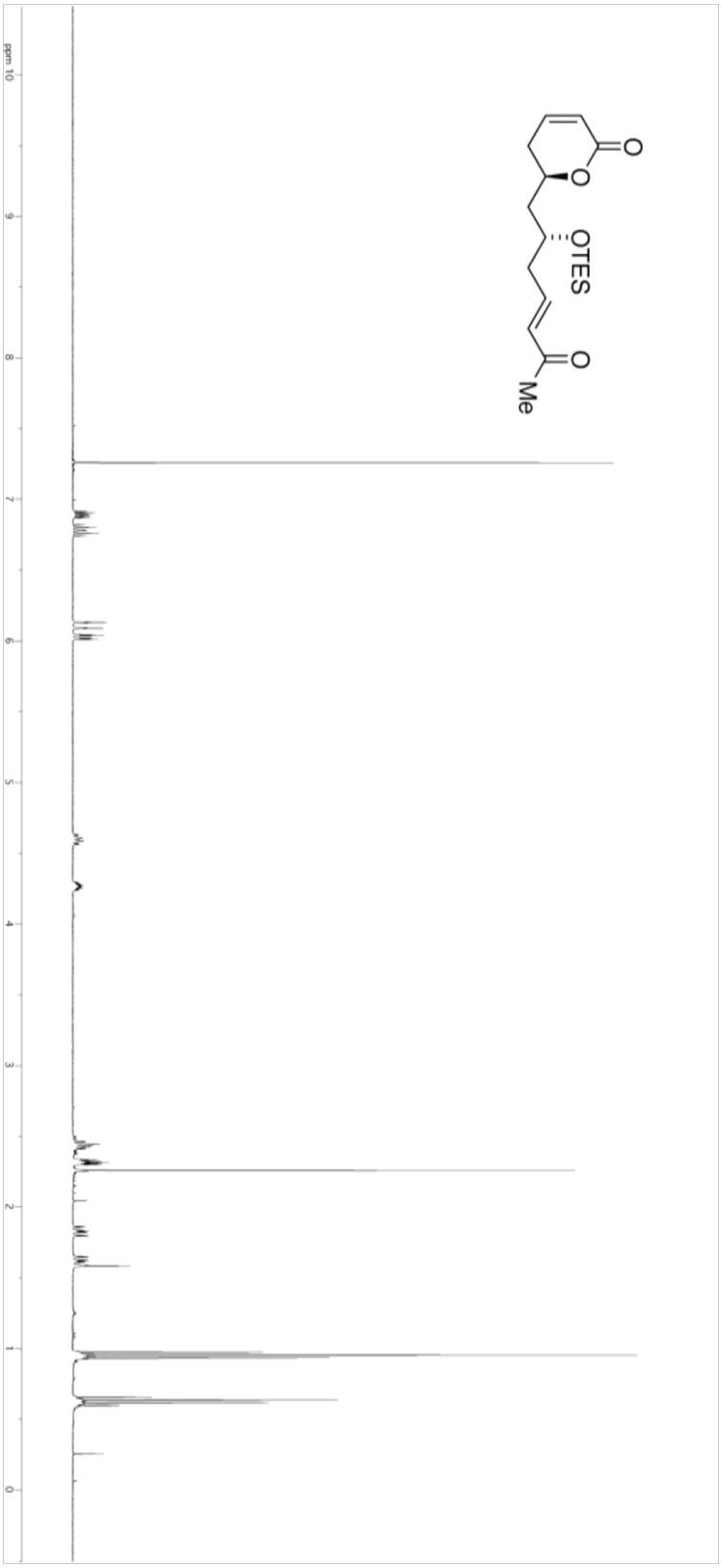
O
O
OTES
O
Me
ppm 10
9
8
7
6
5
4
3
2
1
0

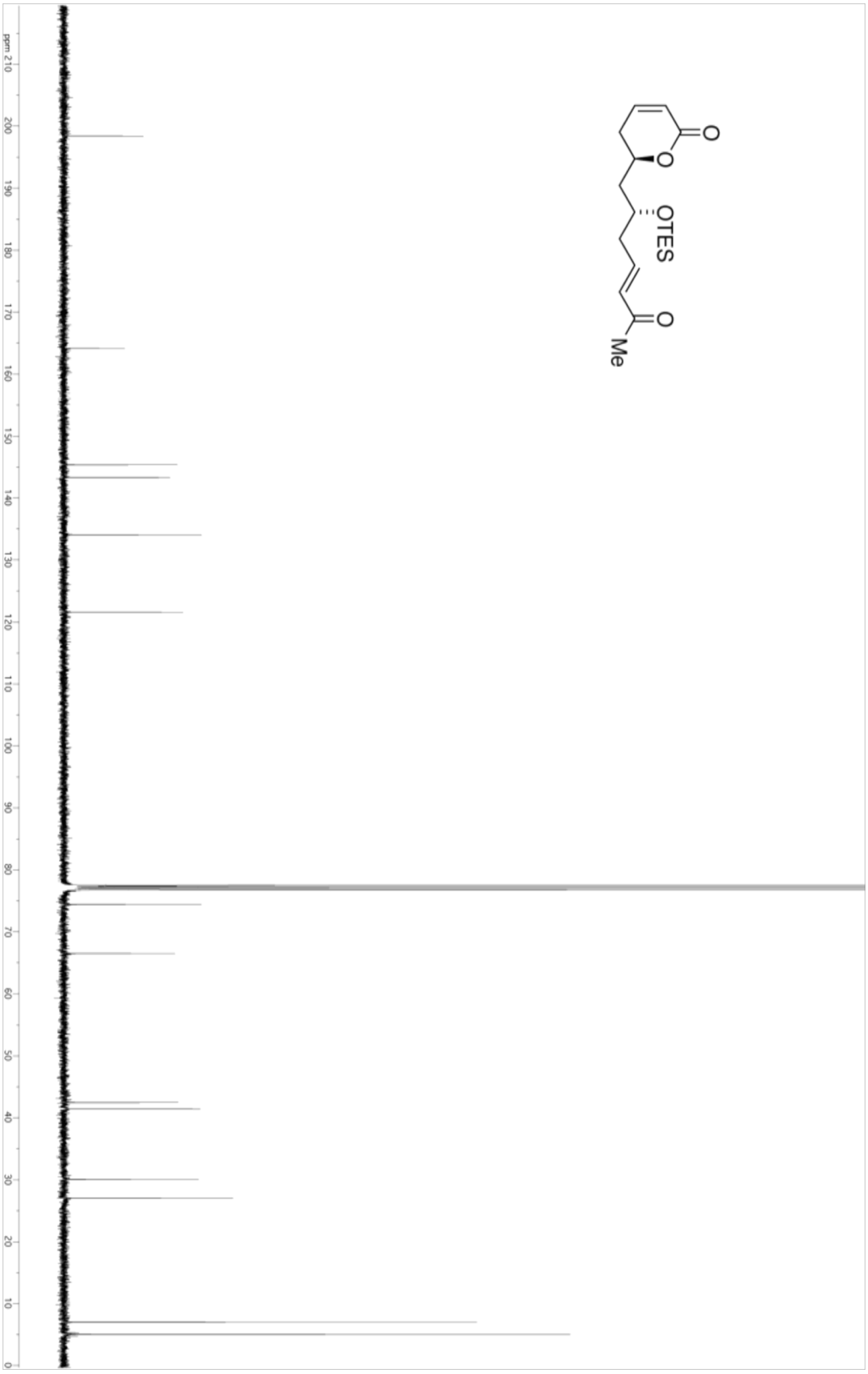
O
O
OTES
O
Me
ppm 210
200
190
180
170
160
150
140
130
120
110
100
90
80
70
60
50
40
30
20
10
0

(*R*)-6-(((2*S*,4*R*,6*S*)-2-methyl-6-(2-oxopropyl)-1,3-dioxan-4-yl)methyl)-5,6-dihydro-2*H*-pyran-2-one (5.15)

To a solution of enone **5.14** (371.8 mg, 1.10 mmol, 100 mol%) in CH_2Cl_2 (11 mL, 0.1 M) at rt was added acetaldehyde (967.6 mg, 1.25 mL, 22.0 mmol, 2000 mol%) followed by $Bi(NO_3)_3 \cdot 5H_2O$ (53.4 mg, 0.11 mmol, 10 mol%) and was stirred at rt for 5 days. The reaction mixture was poured into sat. $NaHCO_3$ and extracted with CH_2Cl_2 (3 x 25 mL) then the organic extracts were combined and dried over anhydrous Na_2SO_4. The solution was decanted and the solvent removed in vacuo. The crude material was purified via flash column chromatography (SiO_2, EtOAc:hexanes 1:1 to 2:1) to afford **5.15** (268.8 mg, 91% yield) as a tan oil.

TLC (SiO_2): R_f = 0.29 (7:3 ethyl acetate:hexanes)

^{1}H NMR: (400 MHz, $CDCl_3$): δ 6.90-6.86 (m, 1H), 6.03 (ddd, *J* = 9.8, 2.5, 1.2 Hz, 1H), 4.76-4.68 (m, 2H), 4.11 (dddd, *J* = 11.1, 7.4, 5.2, 2.3 Hz, 1H), 4.06-3.99 (m, 1H), 2.75 (dd, *J* = 16.1, 7.2 Hz, 1H), 2.48 (dd, *J* = 16.1, 5.3 Hz, 1H), 2.37-2.31 (m, 2H), 2.20 (s, 3H), 1.88 (ddd, *J* = 14.6, 9.6, 2.4 Hz, 1H), 1.75 (ddd, *J* = 14.6, 10.0, 2.9 Hz, 1H), 1.61-1.57 (m, 2H), 1.28 (d, *J* = 5.11 Hz, 3H).

^{13}C NMR: (100 MHz, $CDCl_3$): δ 206.5, 164.4, 145.3, 121.6, 98.7, 74.0, 72.3, 71.4, 49.5, 41.5, 36.8, 31.2, 30.0, 21.1.

FTIR (neat): ν 3016, 2943, 2364, 1714, 1653, 1379, 1251, 1215, 1191, 1093, 1040 cm^{-1}.

HRMS: (ESI) Calcd. for $C_{14}H_{20}O_5Na$ $(M+Na)^+$: 291.1208, Found: 298.1205

$[\alpha]^{24}_D$: -263.6 ° (c = 0.38, $CHCl_3$).

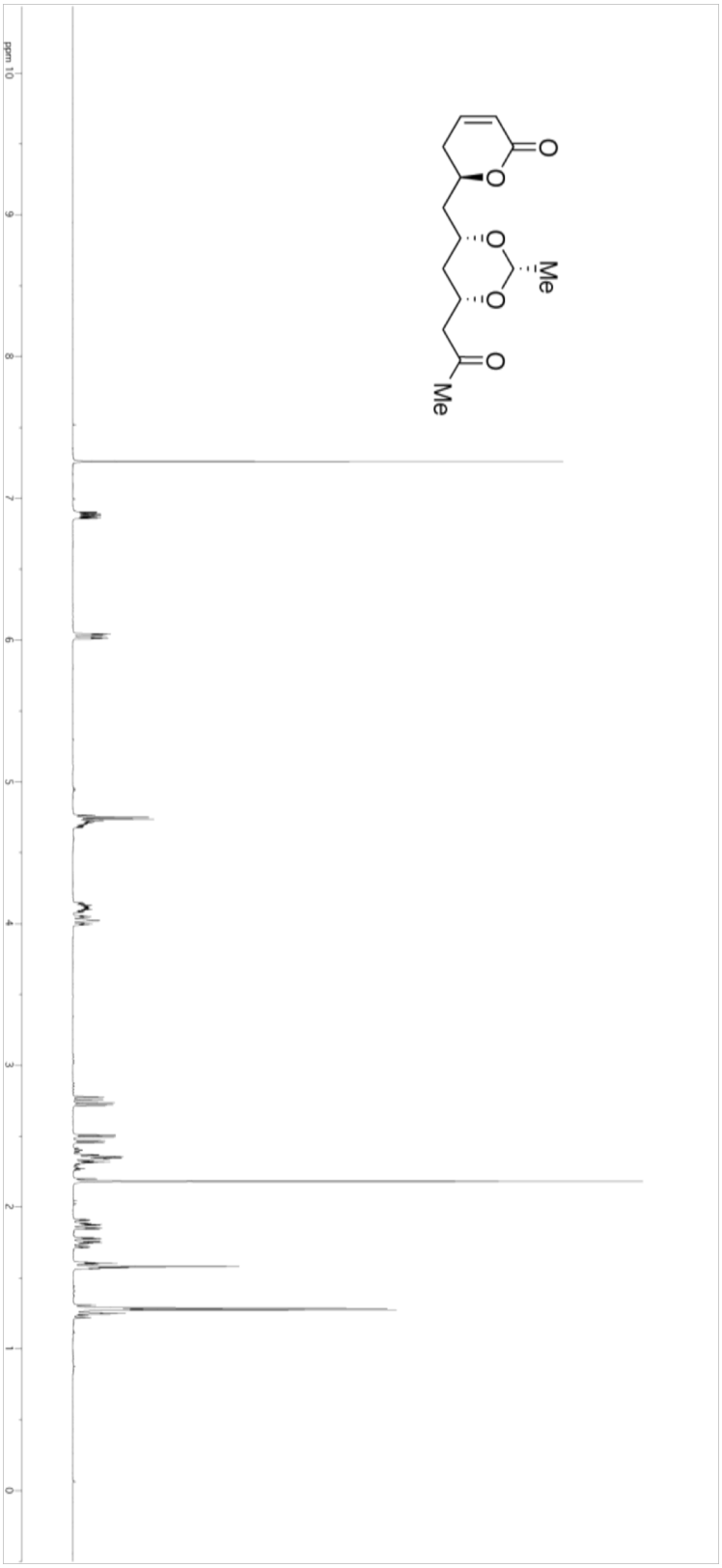
ppm 10
9
8
7
6
5
4
3
2
1
0
O
O
O
O
Me
O
Me

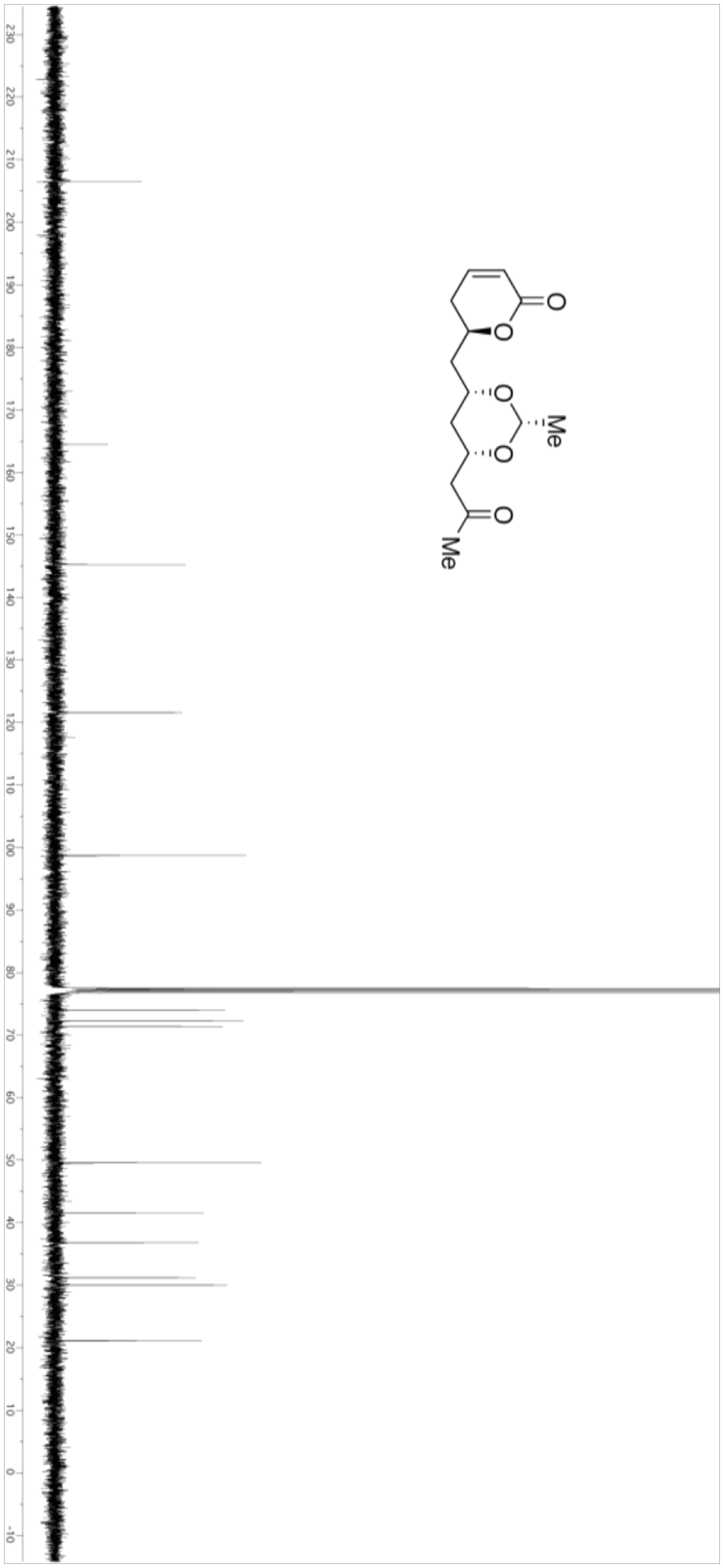
O
O
Me
O
O
O
Me
230
220
210
200
190
180
170
160
150
140
130
120
110
100
90
80
70
60
50
40
30
20
10
0
-10

(*S*)-nonadec-1-en-4-ol (5.16)

Cetyl alcohol **5.6** (4.849 g, 20.0 mmol, 100 mol%), $[Ir(cod)Cl]_2$ (336.0 mg, 0.50 mmol, 2.5 mol%), (*R*)-BINAP (622.7 mg, 1.00 mmol, 5 mol%), 4-chloro-3-nitrobenzoic acid (403.1 mg, 2.00 mmol, 10 mol%), and Cs_2CO_3 (1.303 g, 4.00 mmol, 20 mol%) were added to a flame-dried pressure tube equipped with a magnetic stir bar and purged with Ar for 5 minutes. Dry THF (100 mL, 0.2 M) was added followed by freshly distilled allyl acetate (4.4 mL, 40.0 mmol, 200 mol%) and the vessel sealed. The reaction mixture was heated to 100 °C for 24 h. The reaction mixure was then cooled to room temperature and poured through a plug of Celite, which was washed with fresh THF. The solvent was then removed by rotary evaporation and the crude material purified via column chromatography (SiO_2, Et_2O:hexanes 1:19) to afford **5.16** (4.091 g, 72% yield) as a waxy white solid.

TLC (SiO_2): R_f = 0.20 (1:19 ethyl acetate:hexanes)

^{1}H NMR: (400 MHz, $CDCl_3$): δ 5.85-5.78 (m, 1H), 5.16-5.14 (m, 1H), 5.13-5.11 (m, 1H), 3.65-3.63 (m, 1H), 2.30-2.27 (m, 1H), 2.17-2.12 (m, 1H), 1.56-1.54 (m, 1H), 1.47-1.43 (m, 3H), 1.34-1.23 (m, 25H), 0.89-0.86 (m, 3H).

^{13}C NMR: (100 MHz, $CDCl_3$): δ 135.1, 118.2, 70.8, 42.1, 37.0, 32.1, 29.8, 29.8, 29.5, 25.8, 22.9, 14.3.

FTIR (neat): ν 3319, 2915, 2849, 2360, 1636, 1470 cm^{-1}.

HRMS: (CI) Calcd. for $C_{19}H_{39}O$ $(M+H)^+$: 283.3001, Found: 283.3000

MP: 47 - 48 °C

$[\alpha]^{23}_D$: -18.33 ° (c = 0.36, $CHCl_3$).

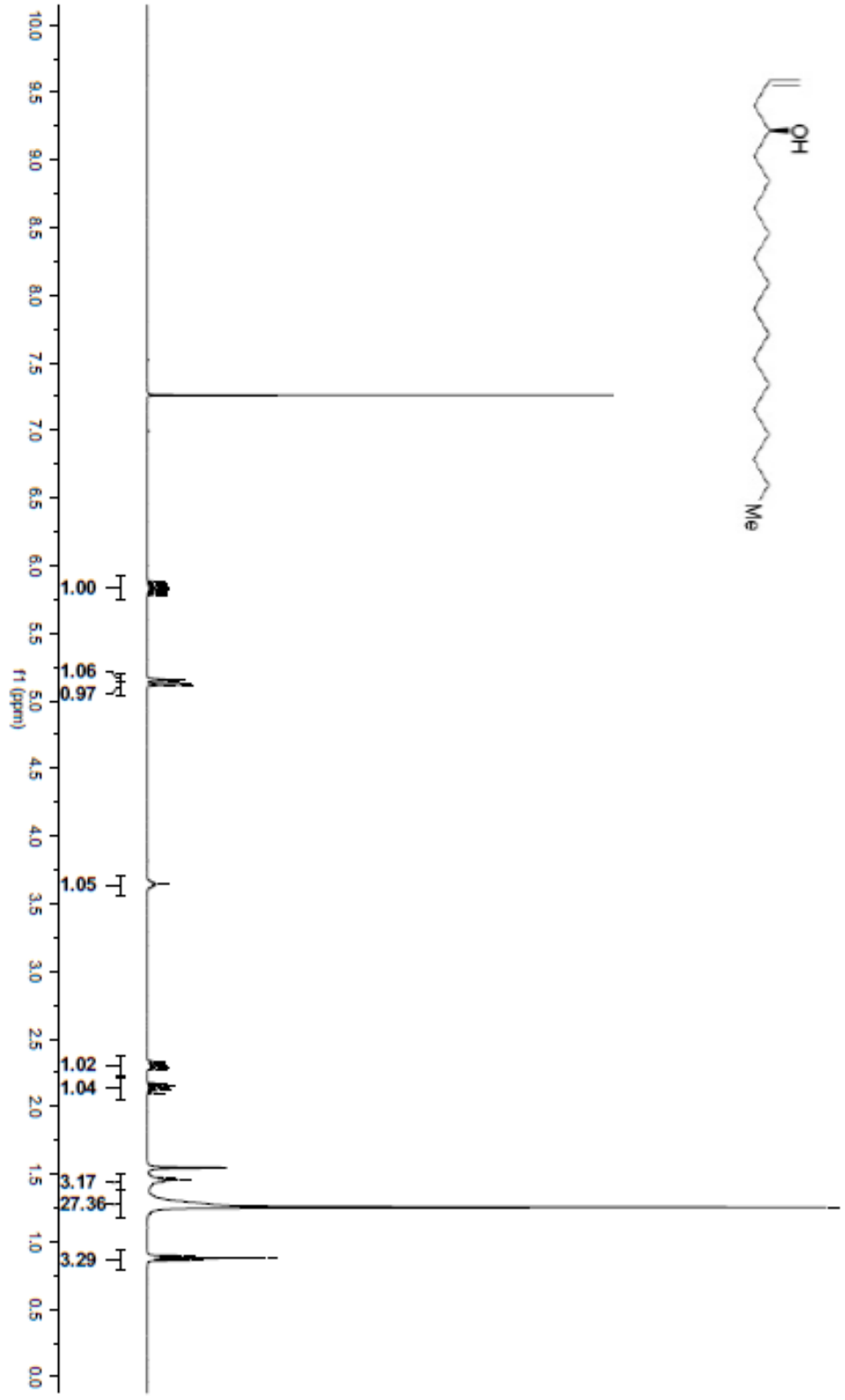
OH
Me
1.00
1.06
0.97
1.05
1.02
1.04
3.17
27.36
3.29
f1 (ppm)

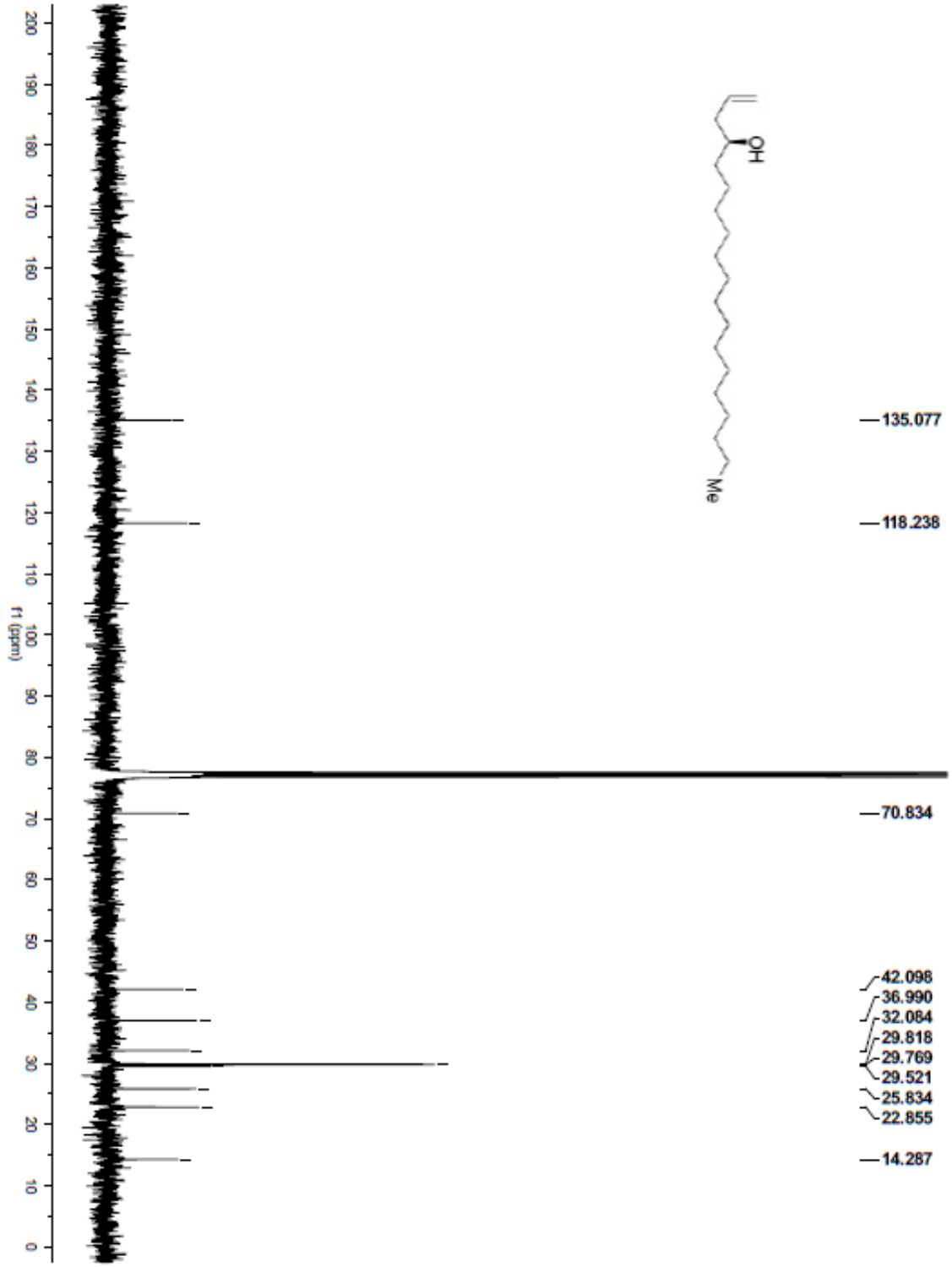
OH
Me
135.077
118.238
70.834
42.098
36.990
32.084
29.818
29.769
29.521
25.834
22.855
14.287
f1 (ppm)

(*S*)-1-methoxy-4-((nonadec-1-en-4-yloxy)methyl)benzene (5.17)

To a solution of alcohol **5.16** (1.009 g, 3.57 mmol, 100 mol%) in dry toluene (24 mL, 0.15 M) was added 4-methoxybenzyl-2,2,2-trichloroacetimidate (1.514 g, 5.36 mmol, 150 mol%) followed by $La(OTf)_3$ (0.1046 g, 0.179 mmol, 5 mol%). The solution was stirred at rt overnight. The reaction mixture was poured into H_2O and hexanes, extracted with hexanes (5 x 35 mL), dried over Na_2SO_4, filtered, and concentrated in vacuo onto silica gel. The crude material was purified via column chromatography (SiO_2, Et_2O:hexanes 1:19) to afford **5.17** (1.333 g, 93% yield) as a colorless oil.

TLC (SiO_2): R_f = 0.36 (1:19 Et_2O:hexanes)

^{1}H NMR: (400 MHz, $CDCl_3$): δ 7.29-7.25 (m, 2H), 6.89-6.85 (m, 2H), 5.85 (ddt, *J* = 17.2, 10.1, 7.1 Hz, 1H), 5.11-5.03 (m, 2H), 4.46 (q, *J* = 15.2 Hz, 2H), 3.80 (s, 3H), 3.41 (qd, *J* = 6.0, 5.5 Hz, 1H), 2.34-2.28 (m, 2H), 1.54-1.46 (m, 2H), 1.34-1.21 (m, 26H), 0.88 (t, *J* = 6.9 Hz, 3H).

^{13}C NMR: (100 MHz, $CDCl_3$): δ 159.0, 135.2, 131.0, 129.3, 116.7, 113.7, 78.2, 70.5, 55.3, 38.3, 33.8, 31.9, 29.7, 29.7, 29.7, 29.7, 29.6, 29.4, 25.4, 22.7, 14.1.

FTIR (neat): ν 2924, 2853, 1513, 1247, 1215, 1037 cm^{-1}.

HRMS: (ESI) Calcd. for $C_{27}H_{46}O_2Na$ $(M+Na)^+$: 425.3396, Found: 425.3372

$[\alpha]^{24}_D$: -3.62 ° (c = 0.57, $CHCl_3$).

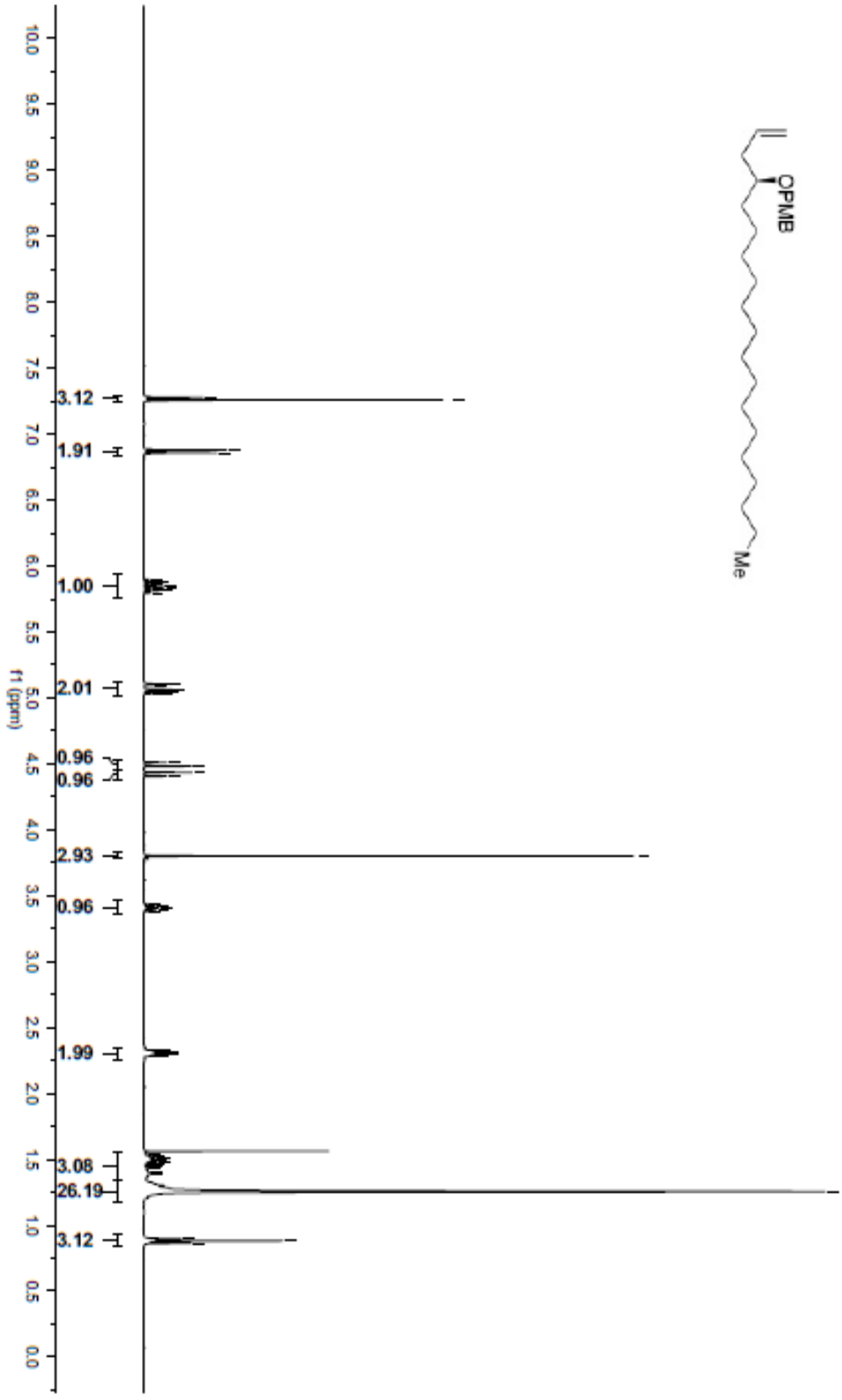
OPMB
Me
3.12
1.91
1.00
2.01
0.96
0.96
2.93
0.96
1.99
3.08
26.19
3.12
f1 (ppm)

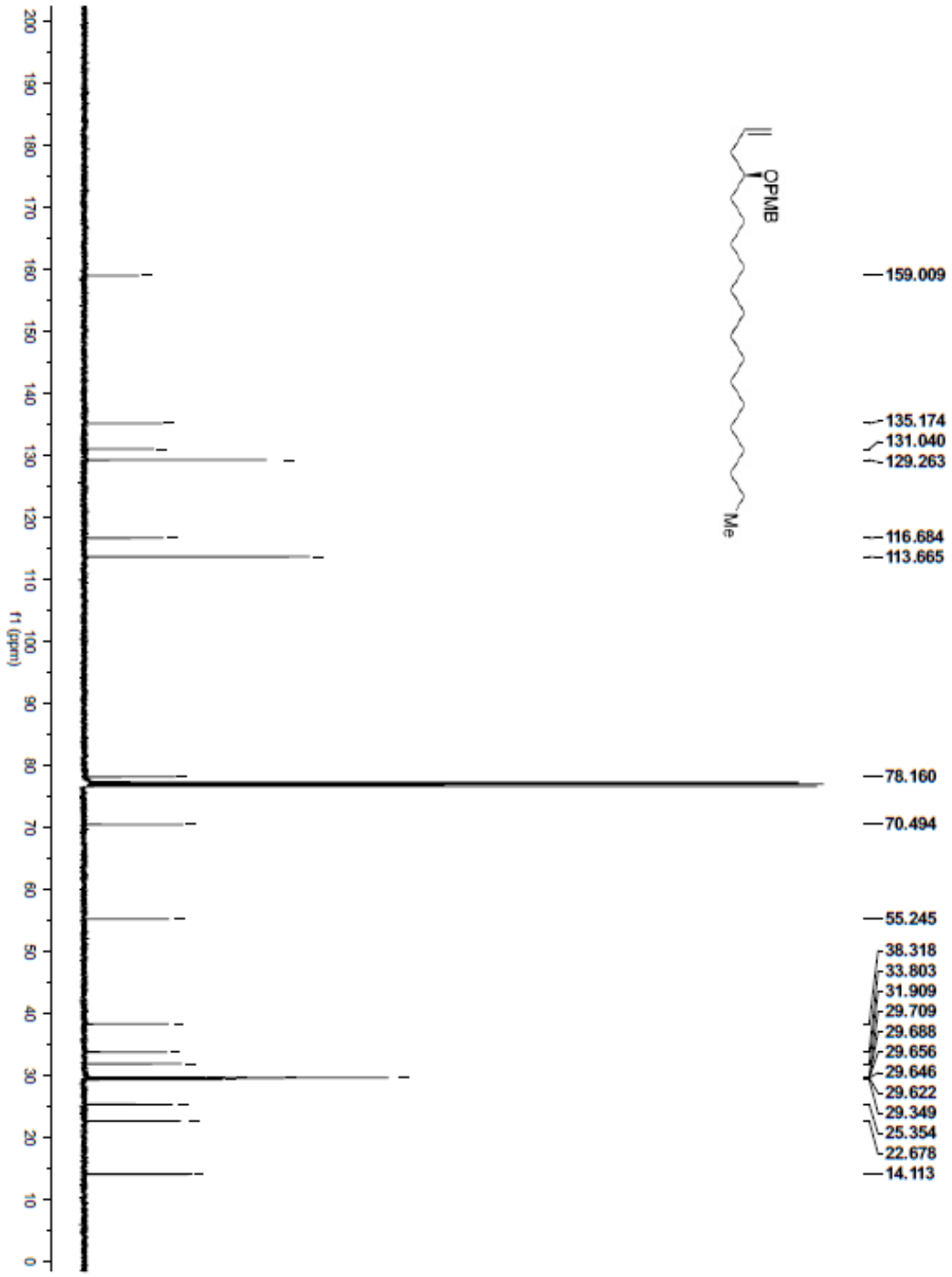
OPMB
Me
159.009
135.174
131.040
129.263
116.684
113.665
78.160
70.494
55.245
38.318
33.803
31.909
29.709
29.688
29.656
29.646
29.622
29.349
25.354
22.678
14.113
f1 (ppm)

(*S*)-3-((4-methoxybenzyl)oxy)octadecanal (5.18)

To a solution of alkene **5.17** (1.333 g, 3.31 mmol, 100 mol%) in 1,4-dioxane (27.6 mL) and H_2O (9.2 mL) was added 2,6-lutidine (0.77 mL, 6.62 mmol, 200 mol%) followed by OsO_4 in 1,4-dioxane (16.8 mg, 0.066 mg, 2 mol%). $NaIO_4$ (2.832 g, 13.24 mmol, 400 mol%) and the solution stirred at rt overnight. The reaction mixture was poured into H_2O and CH_2Cl_2, extracted with CH_2Cl_2 (5 x 35 mL), dried over $NaSO_4$, filtered, and concentrated in vacuo. The crude material was purified via column chromatography (SiO_2, ethyl acetate:hexanes 1:19 to 1:9) to afford **5.18** (896.1 mg, 67%) as a colorless oil.

TLC (SiO_2): R_f = 0.28 (1:4 Et_2O:hexanes)

^{1}H NMR: (400 MHz, $CDCl_3$): δ 9.78 (dd, *J* = 2.5, 2.0 Hz, 1H), 7.25-7.22 (m, 2H), 6.89-6.85 (m, 2H), 4.47 (q, *J* = 9.8 Hz, 2H), 3.95-3.89 (m, 1H), 3.80 (s, 3H), 2.65 (ddd, *J* = 16.3, 7.3, 2.6 Hz, 1H), 2.54 (ddd, *J* = 16.3, 4.7, 1.9 Hz, 1H), 1.67-1.62 (m, 1H), 1.52 (dd, *J* = 9.5, 4.4 Hz, 1H), 1.35-1.26 (m, 26H), 0.88 (t, *J* = 6.9 Hz, 3H).

^{13}C NMR: (100 MHz, $CDCl_3$): δ 202.1, 159.4, 130.5, 129.5, 114.0, 74.1, 71.0, 55.4, 48.5, 34.4, 32.1, 29.85, 29.83, 29.82, 29.80, 29.77, 29.74, 29.72, 29.52, 25.3, 22.8, 14.3.

FTIR (neat): ν 2922, 2852, 1724, 1613, 1513, 1465, 1302, 1173, 1063, 1036 cm^{-1}.

HRMS: (ESI) Calcd. for $C_{26}H_{44}O_3Na$: 427.3188, Found: 427.3182

$[\alpha]^{26}_D$: -2.50 ° (c = 0.4, $CHCl_3$).

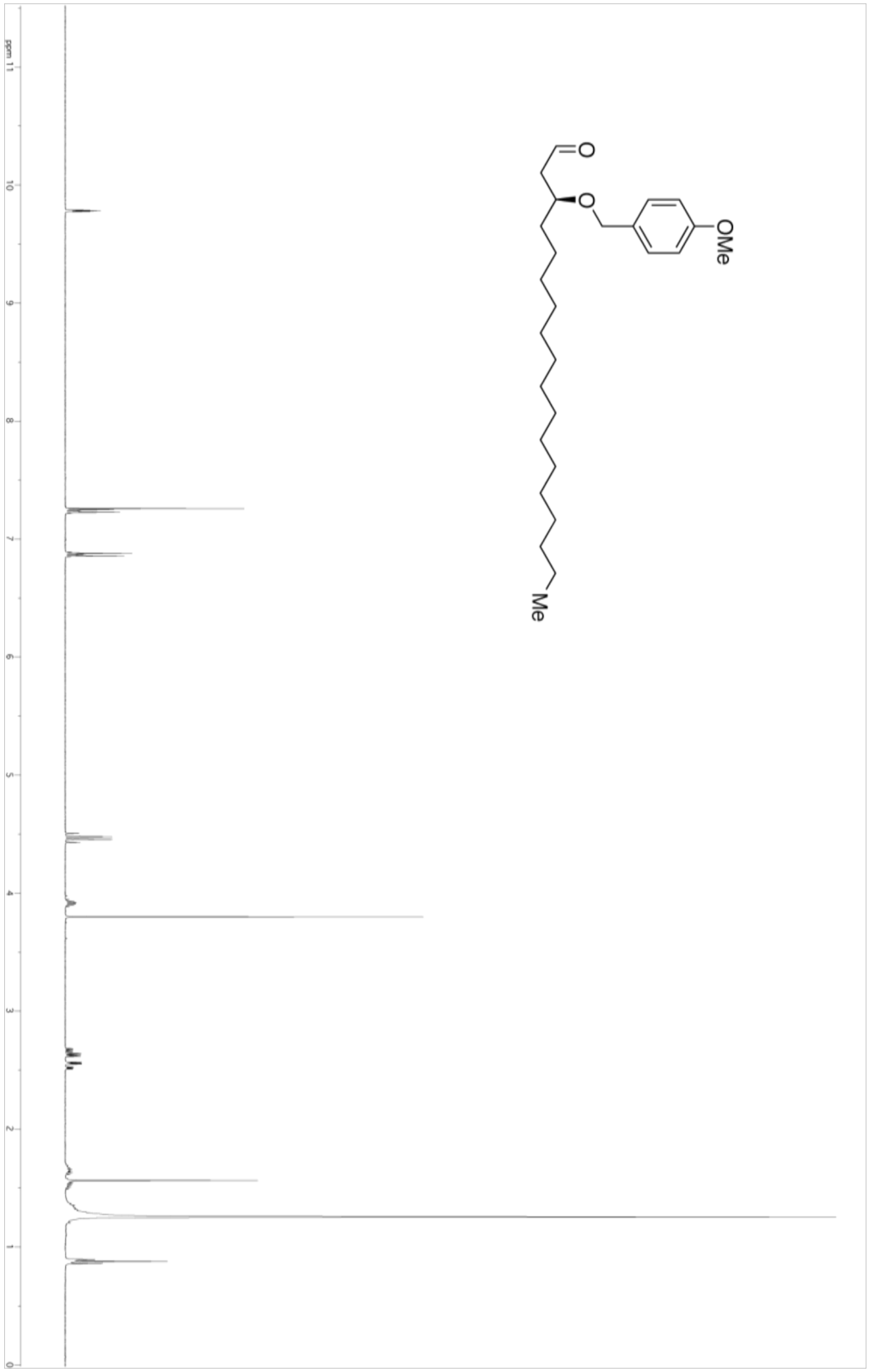
ppm
11
10
9
8
7
6
5
4
3
2
1
0
O
O
OMe
Me

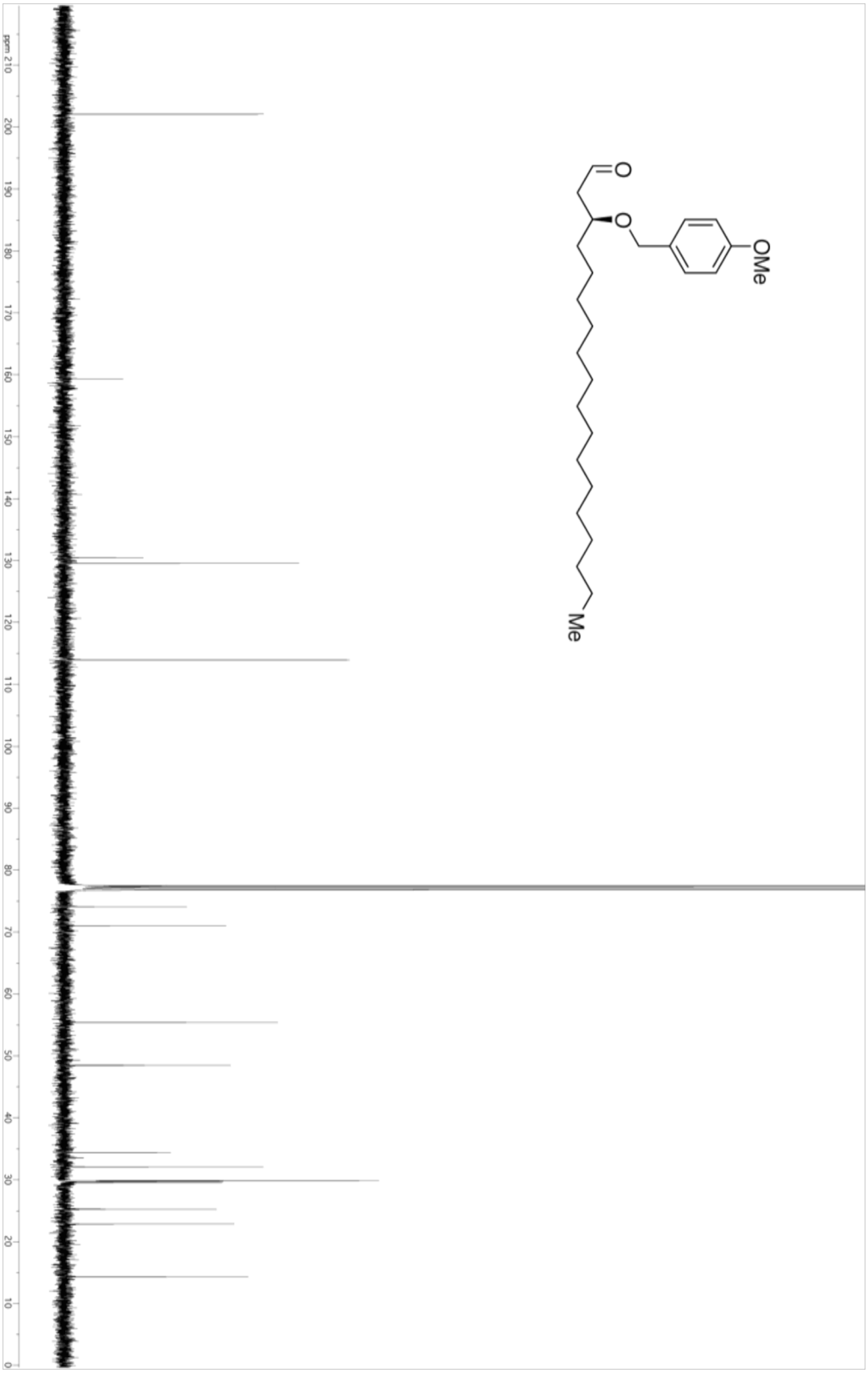
OMe
O
O
Me
ppm 210
200
190
180
170
160
150
140
130
120
110
100
90
80
70
60
50
40
30
20
10
0

(R,E)-6-((R)-6-oxo-3,6-dihydro-2H-pyran-2-yl)-5-((triethylsilyl)oxy)hex-2-enal (5.19)

A 100 mL round bottom flask was charged with Hoveyda-Grubbs II catalyst (62.7 mg, 0.10 mmol, 10 mol%), stir bar, and fitted with a reflux condenser. The flask was purged with argon, sealed with a septum and octafluorotoluene (10 mL) was injected and degassed by bubbling argon. A solution of the **5.13** (325.5 mg, 1.0 mmol, 100 mol%), freshly distilled acrolein (100 mg, 1.8 mmol, 180 mol%) in octafluorotoluene (10 mL, 0.05 M overall) was injected and degassed with bubbling argon for another 5 minutes. The solution was stirred at room temperature for 10 minutes and gradually heated to 120 °C over 30 minutes. Stirring at 120 °C was continued for 2 h and the mixture was cooled to room temperature. The mixture was concentrated in vacuo to a dark oil. Purification by flash column chromatography (SiO_2, EtOAc:hexanes 1:4 to 3:7) gave **5.19** as an orange oil (269.1 mg, 82% yield).

TLC (SiO_2): 0.29 (3:7 EtOAc:hexanes).

^{1}H NMR: (400 MHz, $CDCl_3$): δ = 9.52 (d, *J*=7.9, 1H), 6.94 – 6.79 (m, 2H), 6.16 (ddt, *J*=15.7, 7.9, 1.3, 1H), 6.03 (dt, *J*=9.8, 1.8, 1H), 4.66 – 4.52 (m, 1H), 4.37 – 4.25 (m, 1H), 2.60 (ddd, *J*=14.4, 6.7, 1.4, 1H), 2.56 – 2.46 (m, 1H), 2.35 – 2.27 (m, 2H), 1.82 (ddd, *J*=14.3, 10.3, 2.4, 1H), 1.63 (ddd, *J*=14.3, 10.1, 2.2, 1H), 0.95 (t, *J*=7.9, 9H), 0.63 (q, *J*=7.8, 6H).

^{13}C NMR: (100 MHz, $CDCl_3$): δ = 193.8, 164.1, 153.5, 145.3, 135.6, 121.5, 74.3, 66.3, 42.4, 41.5, 30.0, 7.0, 5.0.

FTIR (neat): 2954, 2876, 1720, 1689, 1381, 1246 cm^{-1}

HRMS: (ESI) Calcd. for $C_{17}H_{28}O_4SiNa$ $(M+Na)^+$: 347.16490, Found: 347.16530.

$[\alpha]^{22}_D$: -11.42 ° (c = 1.08, $CHCl_3$).

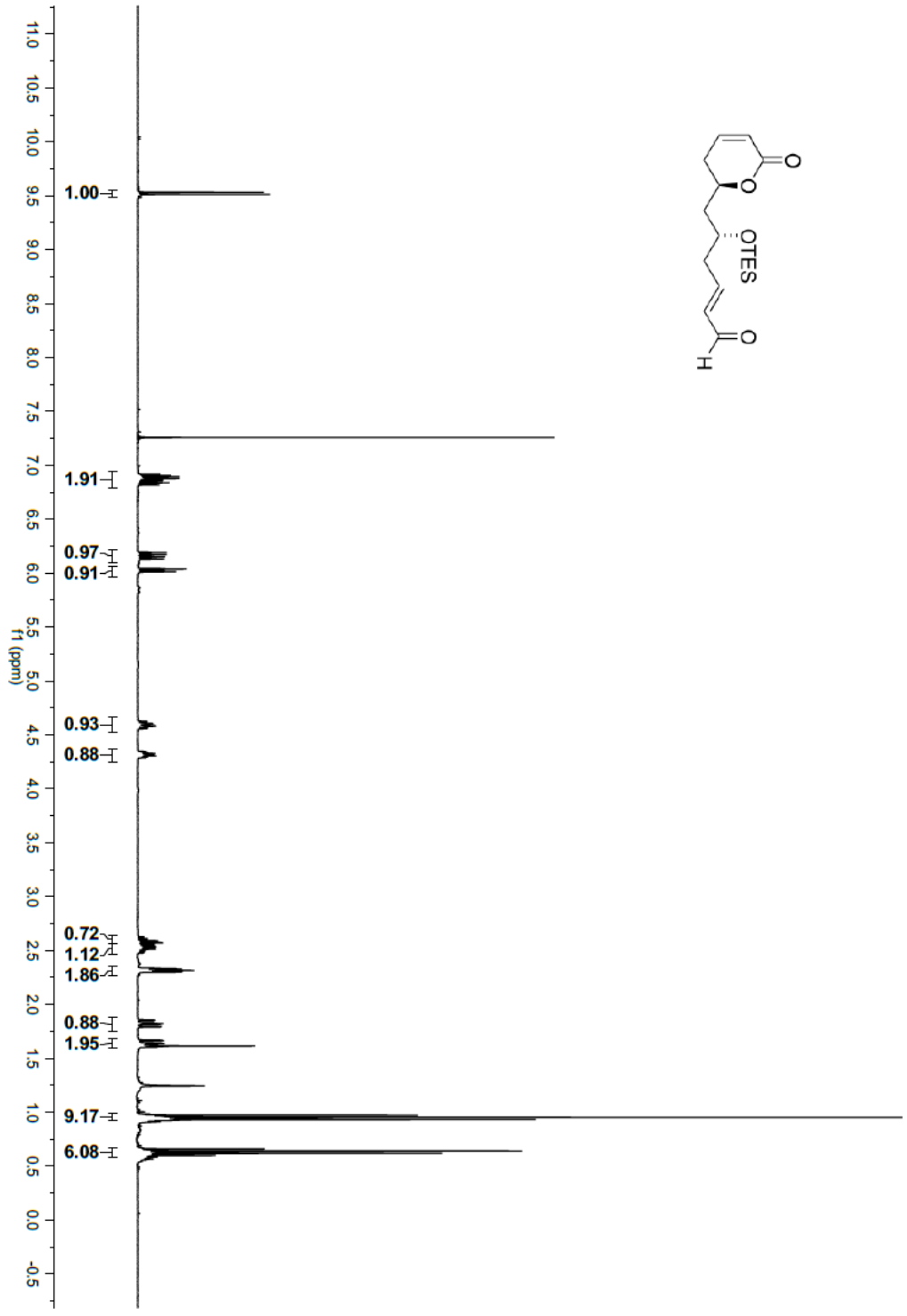
1.00
1.91
0.97
0.91
0.93
0.88
0.72
1.12
1.86
0.88
1.95
9.17
6.08
f1 (ppm)
OTES
O
H

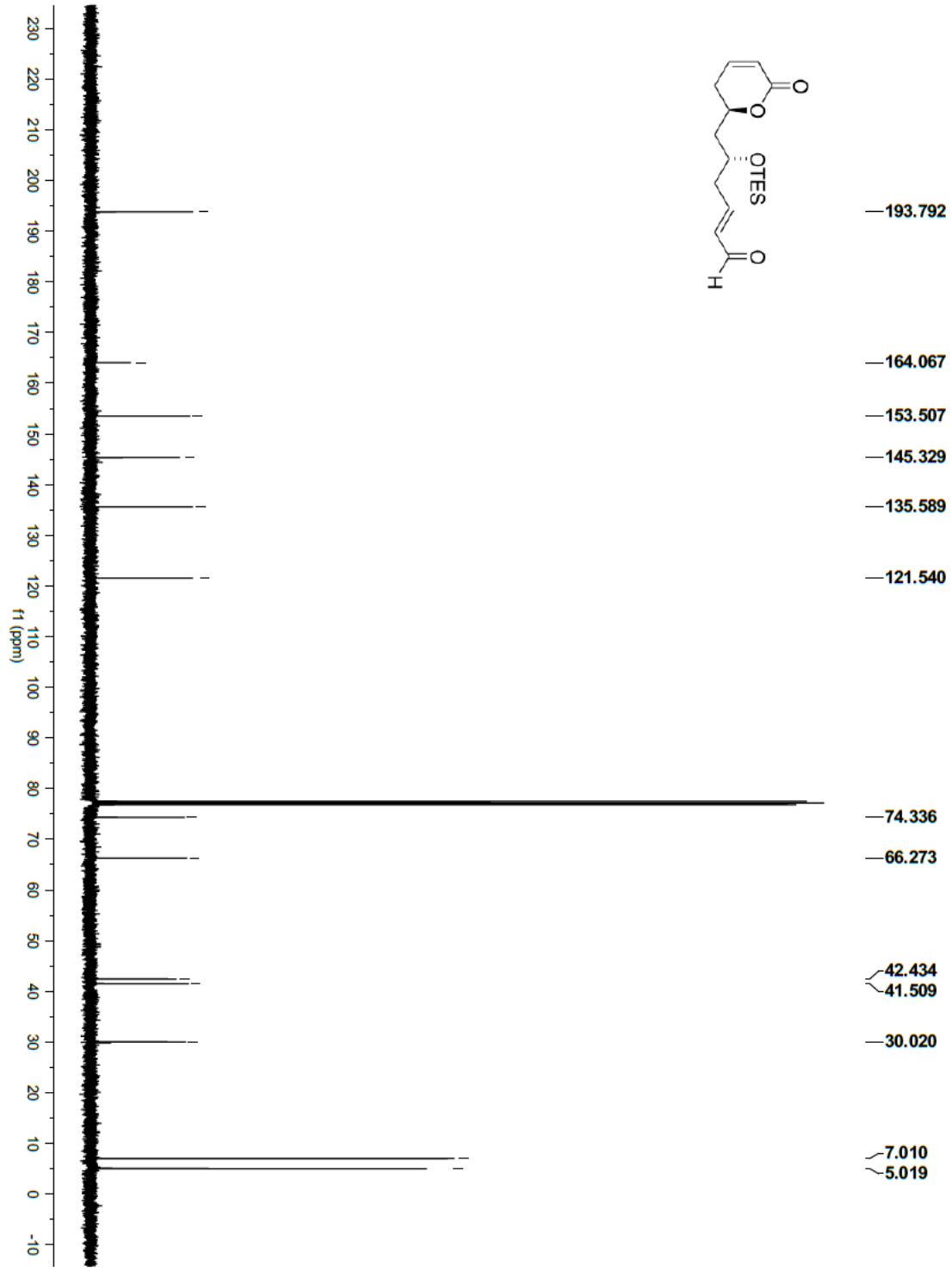
193.792
164.067
153.507
145.329
135.589
121.540
74.336
66.273
42.434
41.509
30.020
7.010
5.019
OTES
f1 (ppm)

2-((4S,6R)-2-methyl-6-(((R)-6-oxo-3,6-dihydro-2H-pyran-2-yl)methyl)-1,3-dioxan-4-yl)acetaldehyde (5.2)

A 10 mL screw cap tube was charged with $Bi(NO_3)_3 \square 5H_2O$ (14.9 mg, 0.031 mmol, 10 mol%) and a solution of **5.19** (100 mg, 0.308 mmol, 100 mol%) and acetaldehyde (271.3 mg, 6.16 mmol, 2000 mol%) in dichloromethane (3.1 mL, 0.1 M) was added. A stir bar was added and the mixture was stirred for three days at room temperature. The cloudy mixture was filtered through Celite, washing with chloroform (10 mL). The filtrate was washed with saturated $NaHCO_3$ (3 x 5 mL), water (5 x 5 mL), brine (1 x 5 mL) and dried over anhydrous Na_2SO_4. The organic extract was filtered and concentrated to a yellow oil, which was dissolved in acetonitrile (5 mL) and washed with pentane (4 x 5 mL) to remove residual triethylsilanol. The acetonitrile layer was concentrated to a viscous yellow oil, providing the aldehyde (71.5 mg, 91% yield) in good purity. The aldehyde could be further purified by flash chromatography (florisil, EtOAc:$CHCl_3$, 1:19 to 2:3) to provide the aldehyde **5.2** as a clear viscous oil (45.4 mg, 58% yield).

TLC (SiO_2): 0.26 (1:4 EtOAc:$CHCl_3$).

^{1}H NMR: (400 MHz, $CDCl_3$): δ = 9.81 – 9.74 (m, 1H), 6.87 (ddd, *J*=9.7, 5.6, 2.9, 1H), 6.01 (ddd, *J*=9.7, 2.4, 1.2, 1H), 4.75 (q, *J*=5.1, 1H), 4.72 – 4.63 (m, 1H), 4.18 (dddd, *J*=11.2, 7.5, 4.9, 2.5, 1H), 4.07 – 3.97 (m, 1H), 2.66 (ddd, *J*=16.7, 7.5, 2.4, 1H), 2.51 (ddd, *J*=16.7, 4.9, 1.6, 1H), 2.41 – 2.23 (m, 2H), 1.86 (ddd, *J*=14.6, 9.8, 2.4, 1H), 1.74 (ddd, *J*=14.6, 10.1, 2.7, 1H), 1.57 (dt, *J*=12.9, 2.5, 1H), 1.29-1.38 (m, 1H), 1.27 (d, *J*=5.1, 3H).

^{13}C NMR: (100 MHz, $CDCl_3$): δ 200.5, 164.4, 145.3, 121.5, 98.8, 73.9, 71.3, 71.2, 49.4, 41.5, 36.7, 30.0, 21.1.

FTIR (neat): 2918, 1716, 1380, 1342, 1248, 1133, 1096 cm^{-1}

HRMS: (ESI) Calcd. for $C_{13}H_{18}O_5Na$ $(M+Na)^+$: 277.1046, Found: 277.1044.

$[\alpha]^{22}_D$: +16.49 ° (c = 0.93, $CHCl_3$).

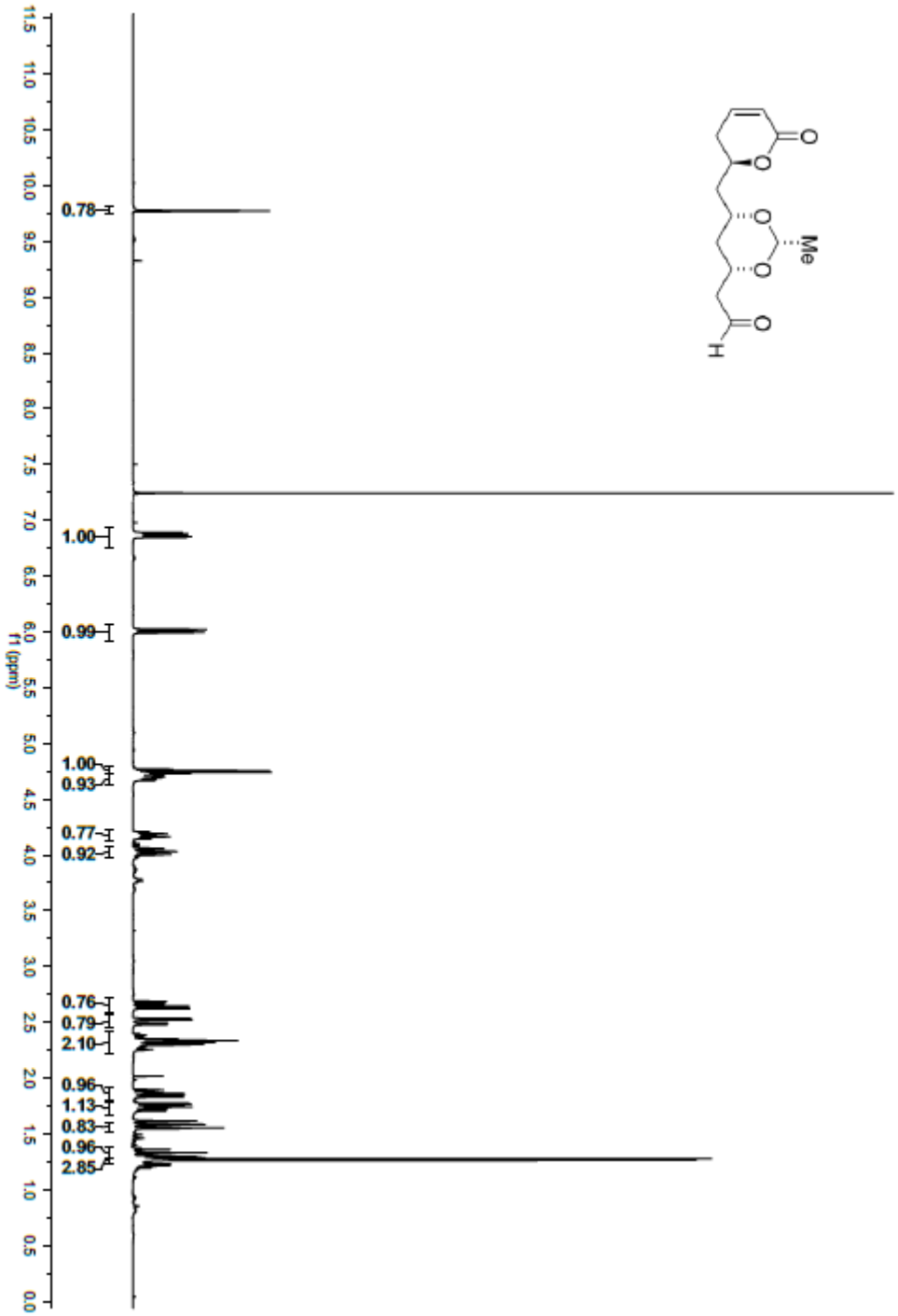
0.78
1.00
0.99
1.00
0.93
0.77
0.92
0.76
0.79
2.10
0.96
1.13
0.83
0.96
2.85
f1 (ppm)
Me

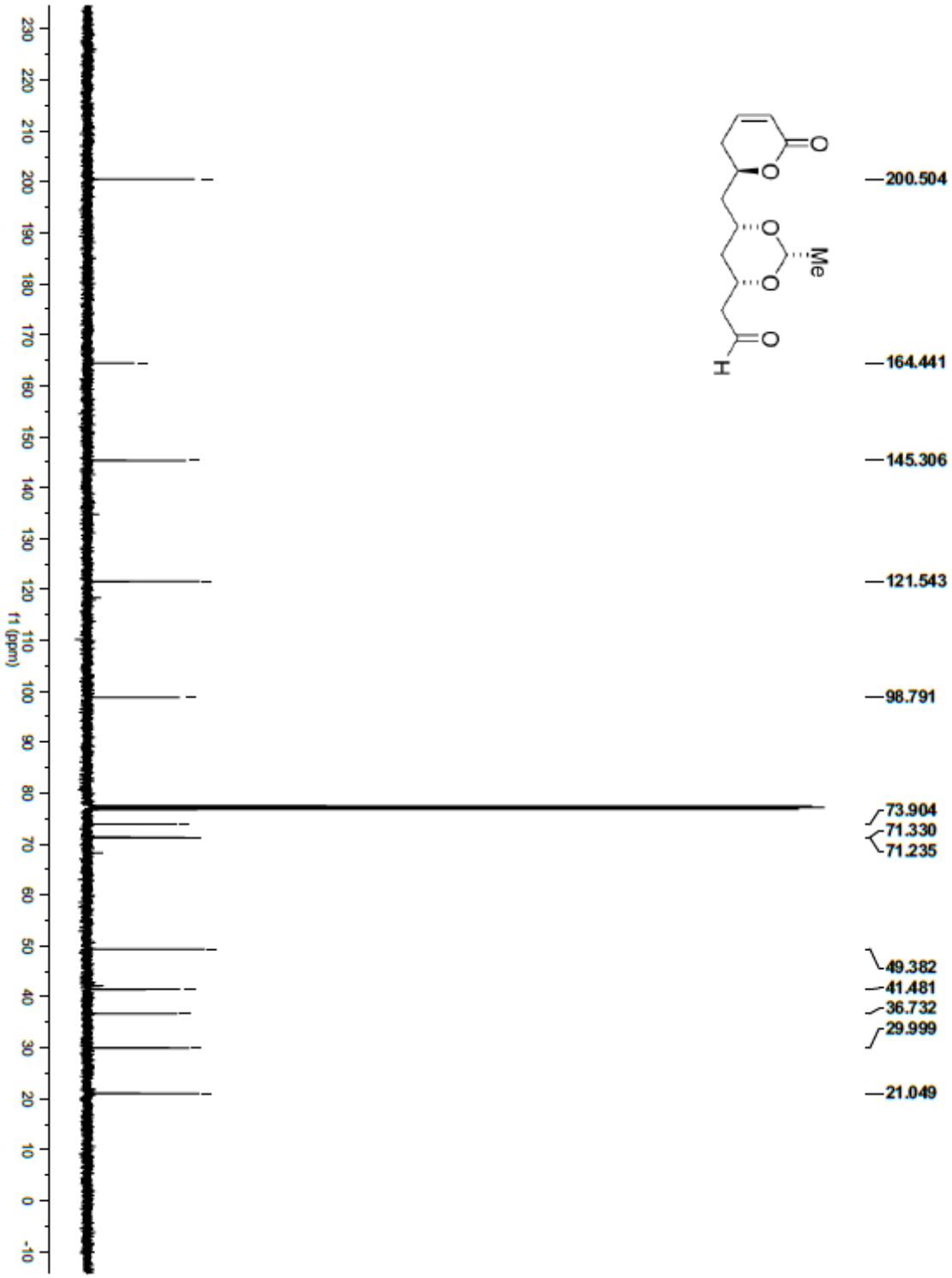
f1 (ppm)
200.504
164.441
145.306
121.543
98.791
73.904
71.330
71.235
49.382
41.481
36.732
29.999
21.049
Me

(S)-4-((4-methoxybenzyl)oxy)nonadecan-2-one (5.3)

The following procedure was performed in the dark. To a sealed tube was added Pd(Quinox)Cl_2 (7.1 mg, 0.0159 mmol, 5 mol%) and $AgSbF_6$ (16.2 mg, 0.0472 mmol, 12.5 mol%) followed by CH_2Cl_2 (2.8 mL). The solution was stirred at rt for 10 minutes before ^{t}BuOOH (70% w/w, 0.64 mL, 4.54 mmol, 1200 mol%) was added and the reaction cooled to 0 °C. After 10 minutes, PMB ether **5.17** (152.2 mg, 0.378 mmol, 100 mol%) in CH_2Cl_2 (1.0 mL, 0.1 M overall) was added dropwise. The reaction was warmed to rt and let stir for 16 h. The reaction mixture was diluted with hexanes and washed with sat. aq. $Na_2S_2O_3$ (2 x 10 mL). The aqueous portion was then extracted with hexanes (2 x 15 mL) and the combined organic extracts were dried over Na_2SO_4, filtered, and concentrated under vacuum. The crude reaction mixture was purified via column chromatography (SiO_2, Et_2O:$CHCl_3$ 1:99) to afford ketone **5.3** (112.3 mg, 71% yield) as a colorless oil.

TLC (SiO_2): R_f = 0.45 (1:4 EtOAc:hexanes)

^{1}H NMR (400 MHz, $CDCl_3$) δ = 7.23 (d, *J*=8.7, 2H), 6.86 (d, *J*=8.7, 2H), 4.46 (d, *J*=10.9, 1H), 4.41 (d, *J*=10.9, 1H), 3.94 – 3.84 (m, 1H), 3.79 (s, 3H), 2.73 (dd, *J*=15.7, 7.6, 1H), 2.49 (dd, *J*=15.8, 4.8, 1H), 2.15 (s, 3H), 1.25 (s, 28H), 0.88 (t, *J*=6.9, 3H).

^{13}C NMR (100 MHz, $CDCl_3$) δ = 207.9, 159.1, 130.6, 129.4, 113.7, 75.4, 71.2, 55.3, 55.2, 48.6, 34.3, 31.9, 31.2, 31.2, 29.7, 29.6, 29.4, 25.2, 22.7, 14.1.

FTIR (neat): 2922, 2852, 1717, 1613, 1513, 1465, 1356, 1249 cm^{-1}

HRMS: (ESI) Calcd. for $C_{27}H_{46}O_2Na$ $(M+Na)^+$: 425.3396, Found: 425.3372

$[\alpha]^{24}_D$: +6.03 ° (c = 0.94, $CHCl_3$).

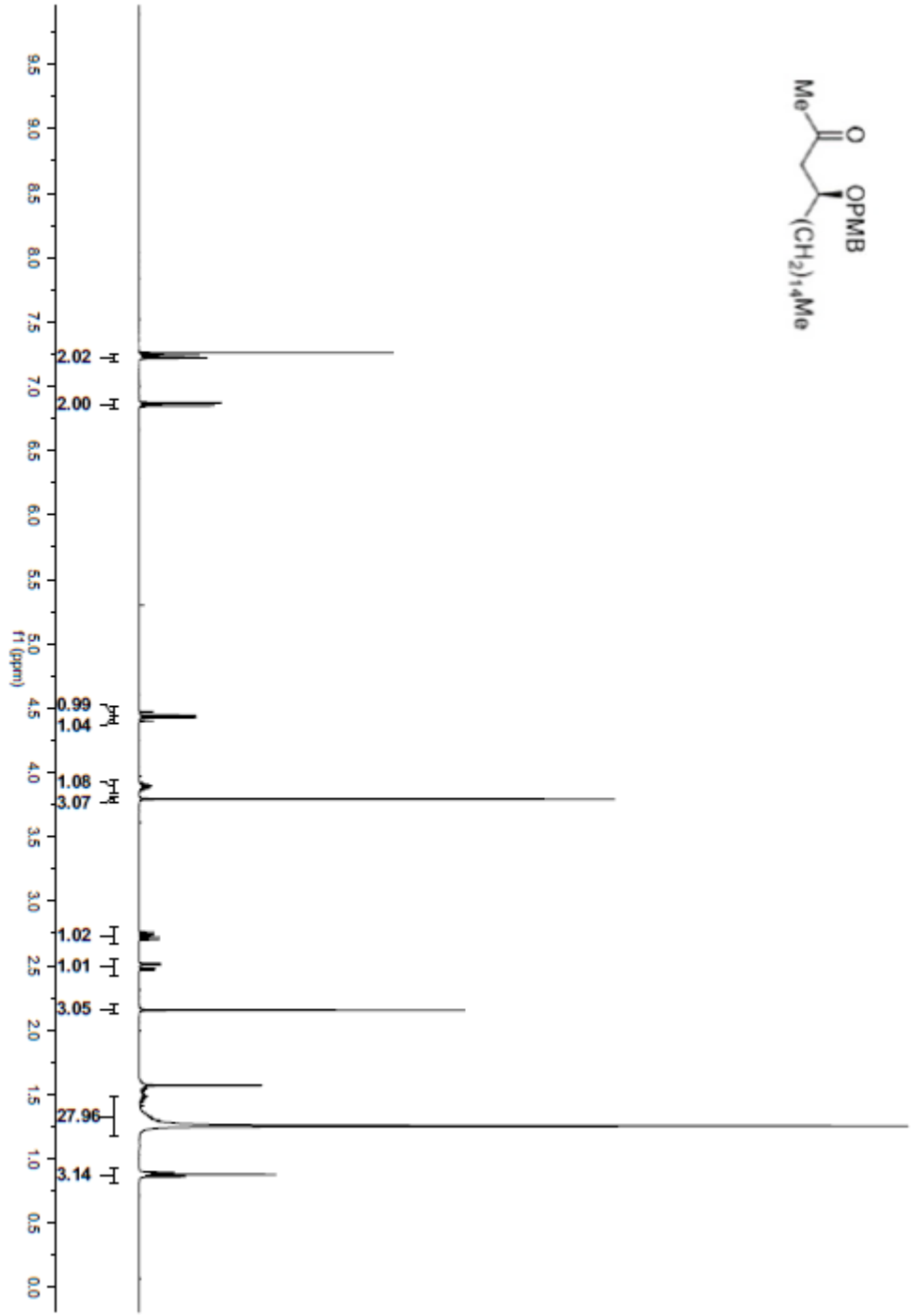
Me
O
OPMB
(CH2)14Me
f1 (ppm)
2.02
2.00
0.99
1.04
1.08
3.07
1.02
1.01
3.05
27.96
3.14

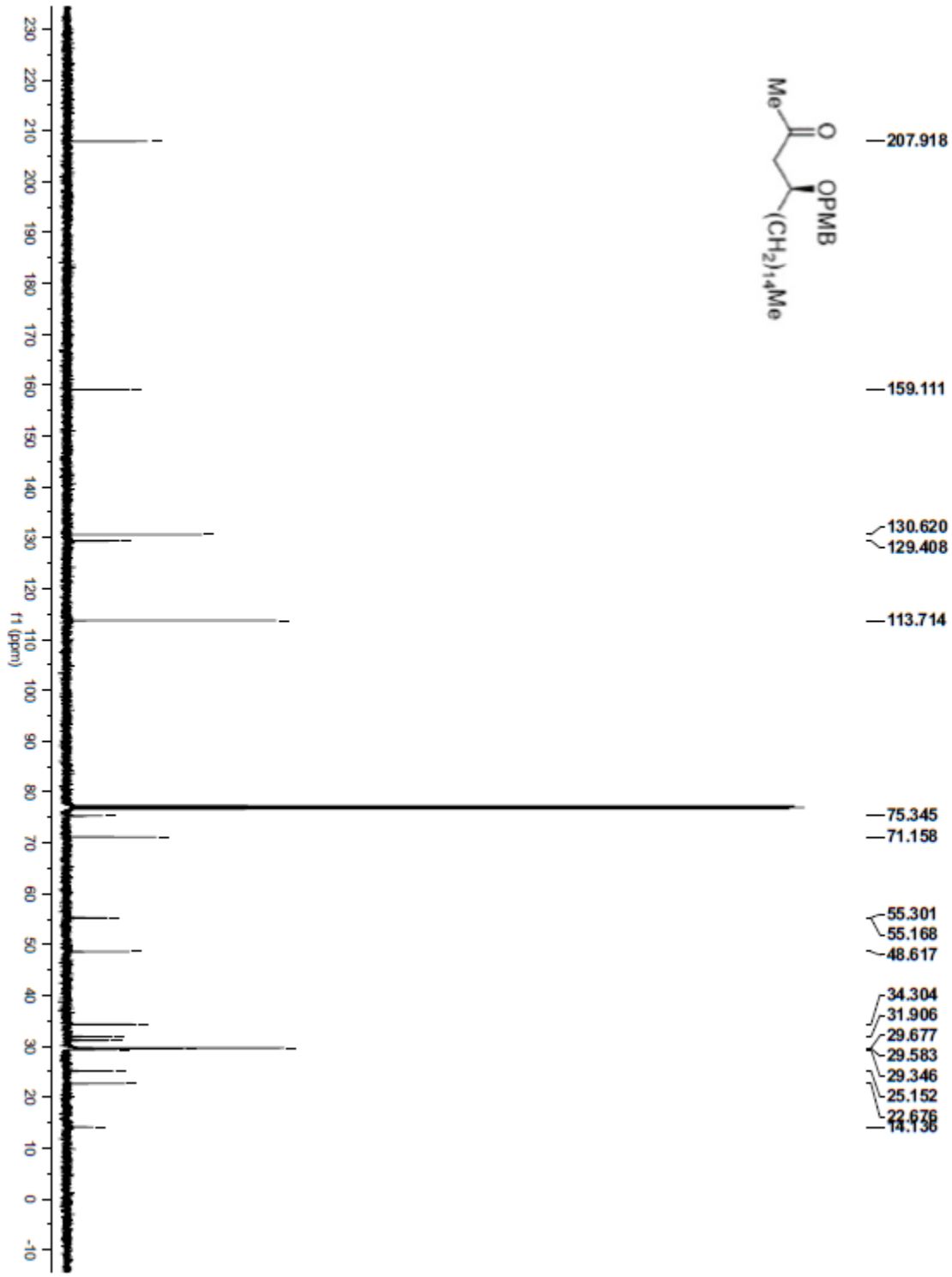
f1 (ppm)
230
220
210
200
190
180
170
160
150
140
130
120
110
100
90
80
70
60
50
40
30
20
10
0
-10
Me
O
OPMB
(CH2)14Me
207.918
159.111
130.620
129.408
113.714
75.345
71.158
55.301
55.168
48.617
34.304
31.906
29.677
29.583
29.346
25.152
22.676
14.136

(6R)-6-(((4R,6R)-6-((2S,6S)-2-hydroxy-6-((4-methoxybenzyl)oxy)-4-oxohenicosyl)-2-methyl-1,3-dioxan-4-yl)methyl)-5,6-dihydro-2H-pyran-2-one (5.20)

A 50 mL round bottom flask was charged with ketone **5.3** (205.7 mg, 0.491 mmol, 125 mol%), stir bar and diethyl ether (9.0 mL, 0.05 M). The solution was degassed with bubbling argon and cooled to -30 °C. Dicyclohexylchloroborane (208.9, 0.983 mmol, 250 mol%) was injected neat and the mixture stirred vigorously for 15 minutes. Triethylamine (107.9 mg, 1.06 mmol, 270 mol%) was injected and the cloudy mixture stirred for 30 minutes. The mixture was cooled to -78 °C and aldehyde **5.2** (100 mg, 0.393 mmol, 100 mol%) in a solution of diethyl ether (800 μL) was added drop wise with stirring. The mixture was allowed to stir for 1.5 h, then warmed to 0 °C. A solution of methanol, pH 7 buffer and 30% hydrogen peroxide (1:1:1, 6 mL) was added. The biphasic mixture was allowed to stir overnight, washed with saturated $NaHCO_3$ (3 x 10 mL), brine (1 x 10 mL) and dried over anhydrous Na_2SO_4. The organic extract was filtered and concentrated in vacuo to a clear oil and purified by flash column chromatography (SiO_2, acetone:hexanes 1:9 to 1:4) to provide **5.20** as a clear, colorless oil (168.5 mg, 64% yield).

TLC (SiO_2): R_f = 0.31 (1:2 acetone:hexanes)

^{1}H NMR: (400 MHz, $CDCl_3$): δ = 7.24 – 7.18 (m, 2H), 6.92 – 6.81 (m, 3H), 6.03 (ddd, *J*=9.7, 2.4, 1.1, 1H), 4.78 – 4.66 (m, 2H), 4.46 (d, *J*=10.9, 1H), 4.39 (d, *J*=10.9, 1H), 4.27 (dq, *J*=12.0, 3.9, 1H), 4.00 (ddd, *J*=13.5, 3.9, 1.6, 1H), 3.95 – 3.84 (m, 2H), 3.79 (s, 3H), 3.44 (s, 1H), 2.75 (dd, *J*=15.8, 7.9, 1H), 2.63 (dd, *J*=16.9, 7.8, 1H), 2.52 (ddd, *J*=18.4, 16.4, 4.5, 2H), 2.42 – 2.25 (m, 2H), 1.87 (ddd, *J*=14.6, 9.7, 2.3, 1H), 1.80 – 1.65 (m, 2H), 1.60 – 1.42 (m, 3H), 1.36 – 1.18 (m, 31H), 0.87 (t, *J*=6.9, 3H).

^{13}C NMR: (100 MHz, $CDCl_3$): δ 209.8, 164.5, 159.3, 145.3, 130.7, 129.5, 121.6, 113.9, 98.5, 75.6, 75.5, 74.0, 71.5, 71.4, 66.5, 55.4, 50.9, 48.8, 41.5, 37.0, 34.4, 32.1, 30.0, 29.9, 29.8, 29.8, 29.5, 25.3, 22.8, 21.2, 14.3.

FTIR (neat): 3529, 3432, 2923, 2853, 1810, 1713, 1613, 1587, 1514, 1487, 1465, 1380, 1342, 1248, 1171, 1138, 1094, 1058, 1035 cm^{-1}.

HRMS: (ESI) Calcd. for $C_{40}H_{64}O_8Na$ $(M+Na)^+$: 695.4499, Found: 695.4495.

$[\alpha]^{22}_D$: -11.81° (c = 0.57, $CHCl_3$).

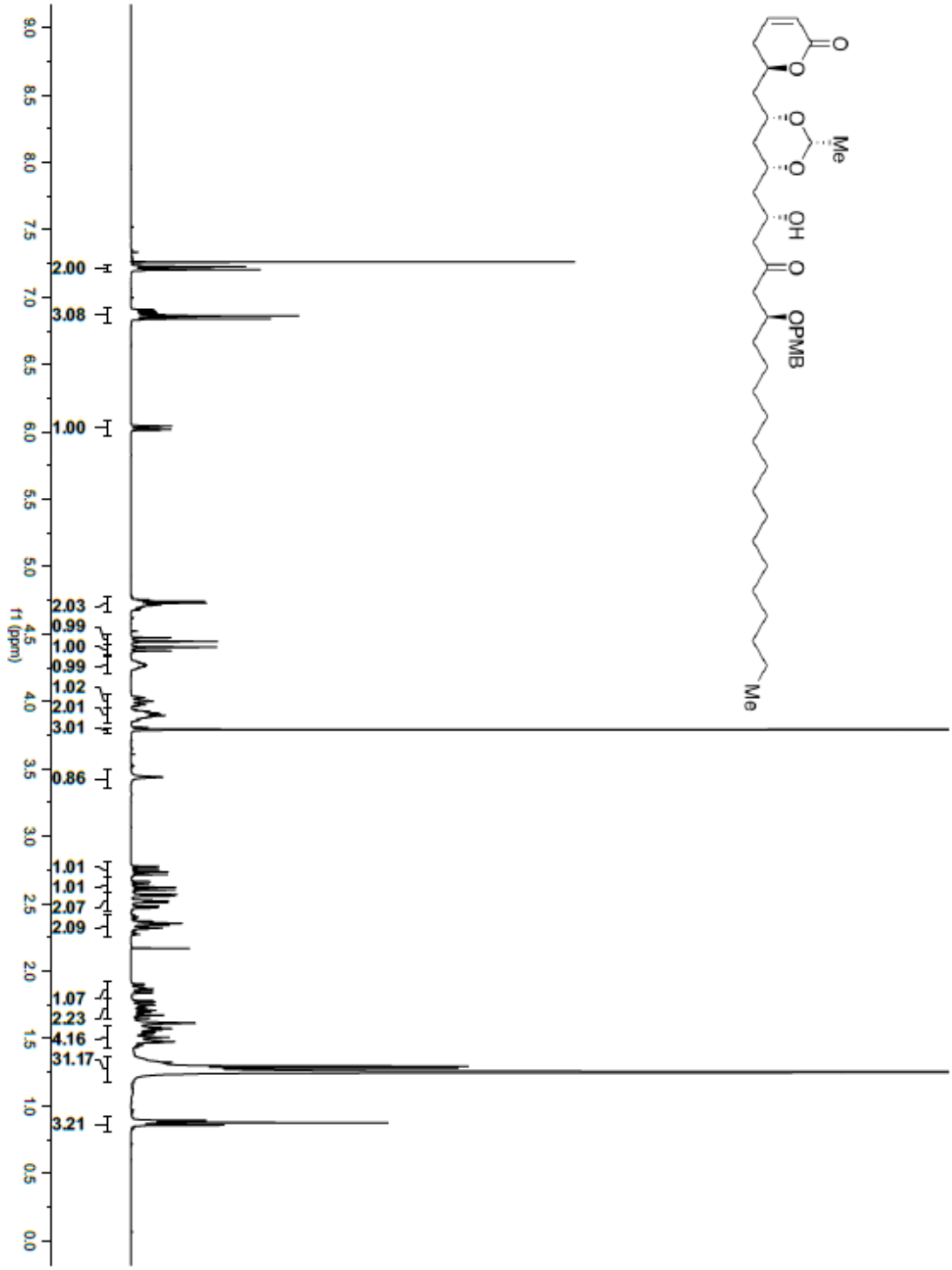
f1 (ppm)
2.00
3.08
1.00
2.03
0.99
1.00
0.99
1.02
2.01
3.01
0.86
1.01
1.01
2.07
2.09
1.07
2.23
4.16
31.17
3.21
Me
OH
O
OPMB
Me

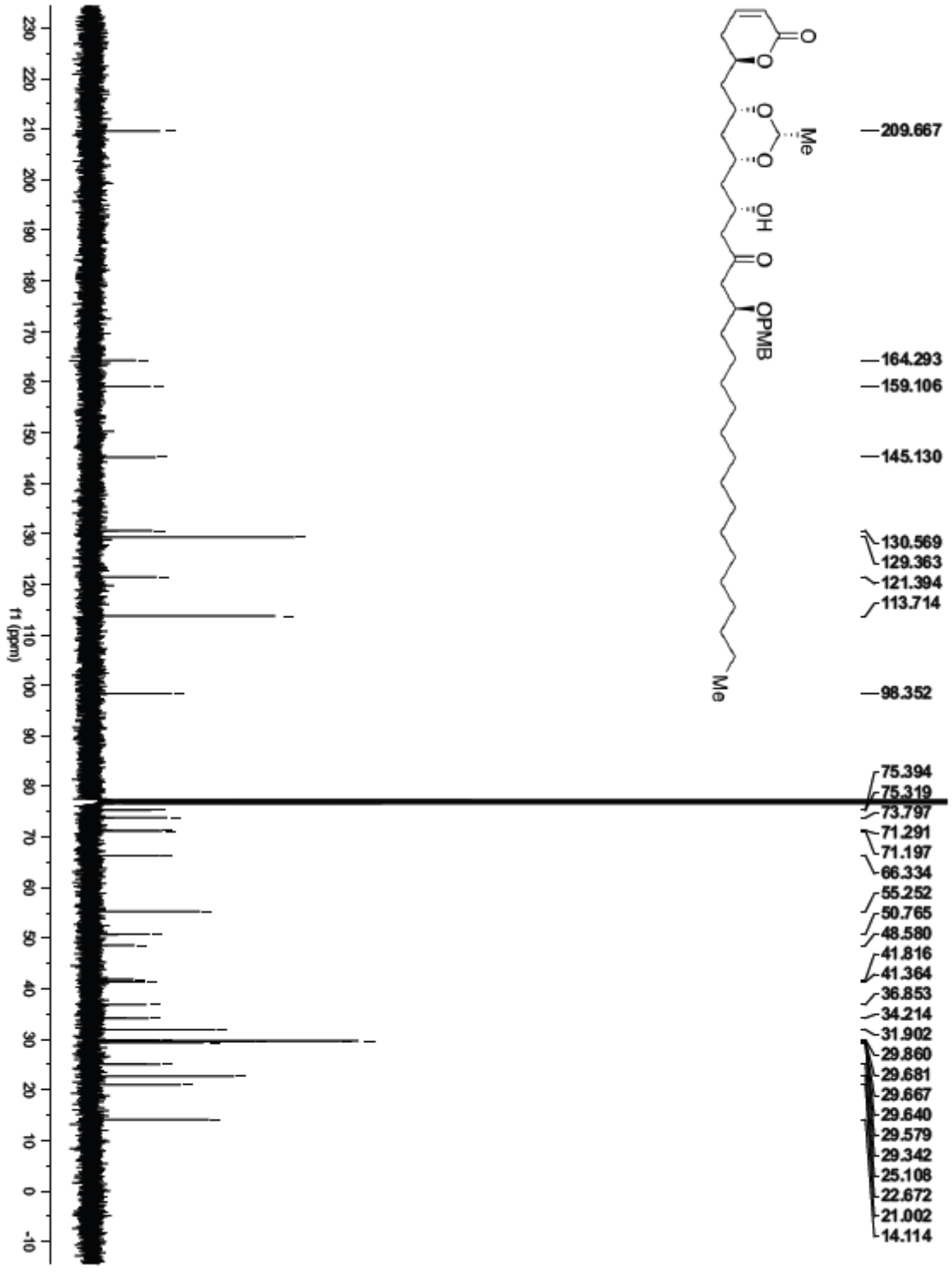
f1 (ppm)
209.667
164.293
159.106
145.130
130.569
129.363
121.394
113.714
98.352
75.394
75.319
73.797
71.291
71.197
66.334
55.252
50.765
48.580
41.816
41.364
36.853
34.214
31.902
29.860
29.681
29.667
29.640
29.579
29.342
25.108
22.672
21.002
14.114
Me
OH
OPMB
Me

(6R)-6-(((4R,6R)-6-((2R,4S,6S)-2,4-dihydroxy-6-((4-methoxybenzyl)oxy)henicosyl)-2-methyl-1,3-dioxan-4-yl)methyl)-5,6-dihydro-2H-pyran-2-one (5.21)

A solution of ketone **5.20** (67.2 mg, 0.100 mmol, 100 mol%) in THF:MeOH (4:1, 0.1 M, 1 mL) was cooled to –78 °C under argon. To this solution was added diethylmethoxy borane (200 μL, 1.0 M in THF, 0.2 mmol, 200 mol%) and the mixture was allowed to stir for 0.5 h before adding $NaBH_4$ (220 μL, 0.5 M in diglyme, 0.110 mmol, 110 mol%). After stirring for 3 h at -78 °C, the mixture was warmed to 0 °C, diluted with Et_2O (10 mL), and stirred vigorously with a mixture of methanol, pH 7 buffer, and 30% hydrogen peroxide (1.5 mL, 1:1:1), then the solution was warmed to room temperature. After 1 h at room temperature, the organic phase was washed with saturated $NaHCO_3$ (3 x 5 mL), brine (1 x 5 mL), dried over anhydrous Na_2SO_4, filtered, and concentrated in vacuo to provide diol **5.21** as a yellow oil (63.2 mg, 94% yield).

TLC (SiO_2): R_f = 0.24 (3:7 acetone:hexanes)

^{1}H NMR: (400 MHz, $CDCl_3$): δ = 7.29 – 7.23 (m, 2H), 6.94 – 6.80 (m, 3H), 6.03 (ddd, *J*=9.7, 2.4, 1.1, 1H), 4.76 (q, *J*=5.2, 1H), 4.74 – 4.66 (m, 1H), 4.51 (d, *J*=11.0, 1H), 4.46 (d, *J*=11.0, 1H), 4.19 – 3.96 (m, 3H), 3.90 (ddd, *J*=21.3, 8.6, 6.4, 3H), 3.80 (s, 3H), 3.74 – 3.63 (m, 1H), 2.43 – 2.25 (m, 2H), 1.88 (ddd, *J*=14.6, 9.7, 2.4, 1H), 1.80 – 1.71 (m, 2H), 1.71 – 1.37 (m, 8H), 1.36 – 1.20 (m, 30H), 0.88 (t, *J*=6.9, 3H).

^{13}C NMR: (100 MHz, $CDCl_3$): δ 164.4, 159.4, 145.3, 130.8, 129.7, 121.6, 114.0, 98.5, 76.6, 76.0, 74.0, 71.6, 71.2, 69.2, 55.4, 44.0, 43.2, 41.6, 41.3, 37.2, 34.0, 32.1, 30.1, 30.0, 29.9, 29.8, 29.8, 29.8, 29.5, 25.5, 22.8, 21.2, 14.3.

FTIR (neat): 3488, 2924, 2853, 1716, 1248 cm^{-1}.

HRMS: (ESI) Calcd. for $C_{40}H_{66}O_8Na$ $(M+Na)^+$: 697.4650, Found:.697.4650

$[\alpha]^{22}_D$: +19.87 ° (c = 0.52, $CHCl_3$).

Synthesis of 5.21 starting from crude 5.2:

Due to the instability of **5.2** during storage and the instability of the aldol product **5.20** during chromatography, procedures were developed to carry out the aldol and reduction with crude reaction products. A 10 mL screw cap vial was charged with stir bar and solution of ketone **5.3** (41.9 mg, 0.1 mmol, 100 mol%) in diethyl ether (1 mL). The vial was sealed and the solution sparged with argon, then cooled to -30 °C. Chlorodicyclohexylborane (31.9 mg, 1.5 mmol, 150 mol%) was injected neat, resulting in a yellow solution. After 5 min, triethylamine (20.3 mg, 0.200 mmol, 200 mol%) was injected and a cloudy mixture formed immediately. The mixture was allowed to stir for 30 minutes, then cooled to -78 °C. Crude aldehyde **5.2** (31.8mg, 0.125 mmol, 125 mol%) in diethyl ether (1 mL) was added dropwise. After 4 hours, the mixture was warmed 0 °C and a solution of methanol, pH 7 buffer and 30% hydrogen peroxide (1:1:1, 6 mL) was added. The biphasic mixture was allowed to stir overnight at room temperature, extracted with diethyl ether (3 x 5 mL), washed with saturated $NaHCO_3$ (3 x 10 mL), brine (1 x 10 mL) and dried over anhydrous Na_2SO_4. The organic extract was filtered and concentrated in vacuo to a clear oil. The oil was dissolved in acetonitrile (5 mL), washed with pentane (4 x 5 mL) to remove methyl ketone **5.3**, then concentrated in vacuo to a clear oil, providing crude aldol (64.8 mg) in good purity. The methyl ketone **5.3** could be recovered from the pentane extract (6.2 mg, 15%).

A 10 mL screw cap vial was charged with crude aldol **5.20** (64.8 mg, 0.0964 mmol) and dissolved in THF/MeOH (4:1, 1 mL). The solution was cooled to -78 °C and diethylmethoxyborane (1.0 M in THF, 0.2 mL, 200 mol%) was added dropwise. The cloudy solution was stirred for 30 minutes then $NaBH_4$ (0.5 M in diglyme, 0.22 mL, 110 mol%) was added dropwise. The mixture was allowed to stir for 3 h, then warmed to 0 °C, diluted with diethyl ether (10 mL), and stirred vigorously with a mixture of methanol, pH 7 buffer, and 30% hydrogen peroxide (1.5 mL, 1:1:1) allowing the solution to warm to room temperature. After 1 h at room temperature, the organic phase was washed with saturated $NaHCO_3$ (3 x 5 mL), brine (1

x 5 mL), dried over anhydrous Na_2SO_4, filtered and concentrated to a yellow oil. Purification by flash column chromatography (SiO_2, 1:4 to 3:7 acetone:hexanes) provided **5.21** as a colorless oil (49.3 mg, 73% over two steps).

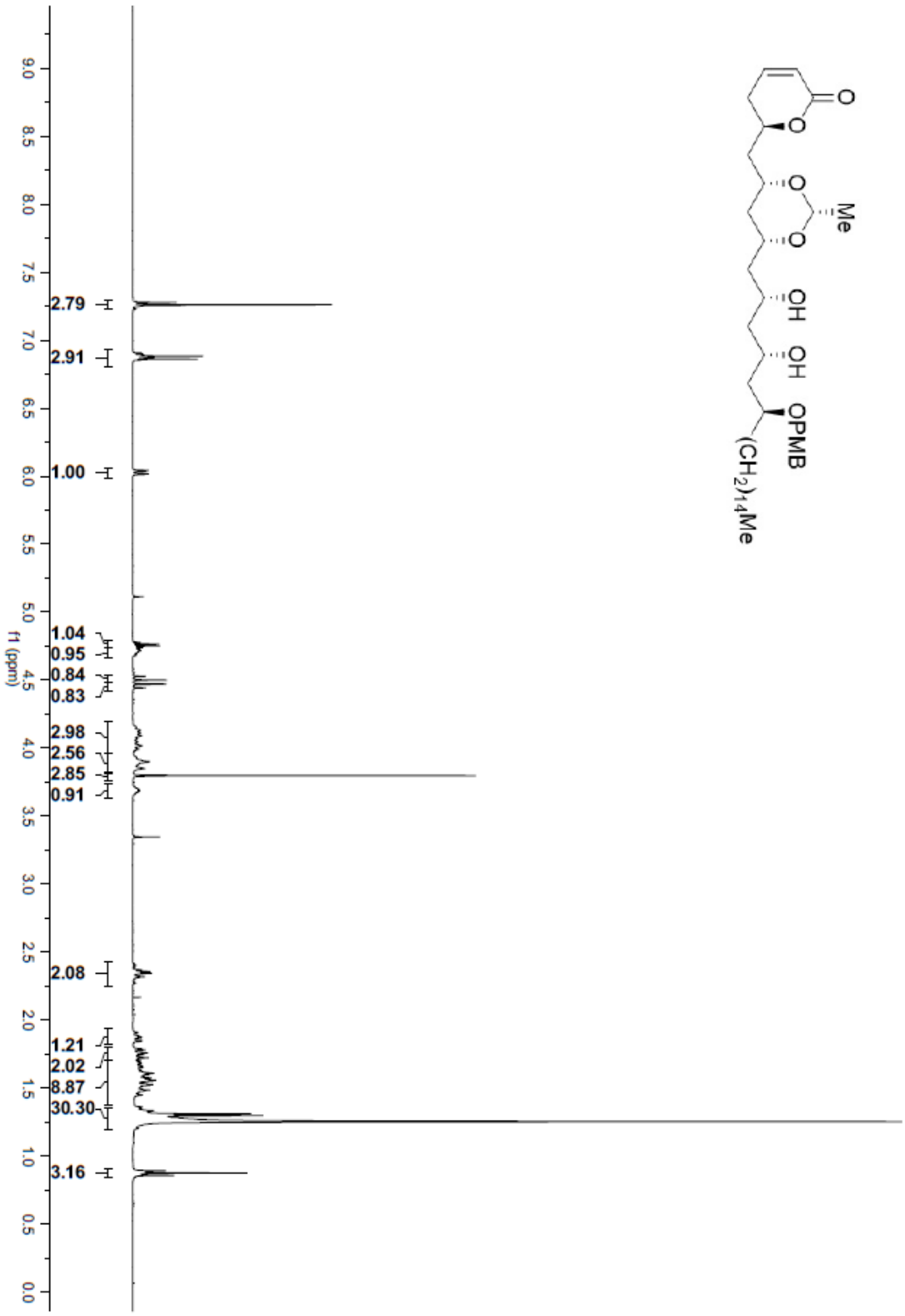
O
O
Me
O
O
OH
OH
OPMB
(CH2)14Me
f1 (ppm)
2.79
2.91
1.00
1.04
0.95
0.84
0.83
2.98
2.56
2.85
0.91
2.08
1.21
2.02
8.87
30.30
3.16

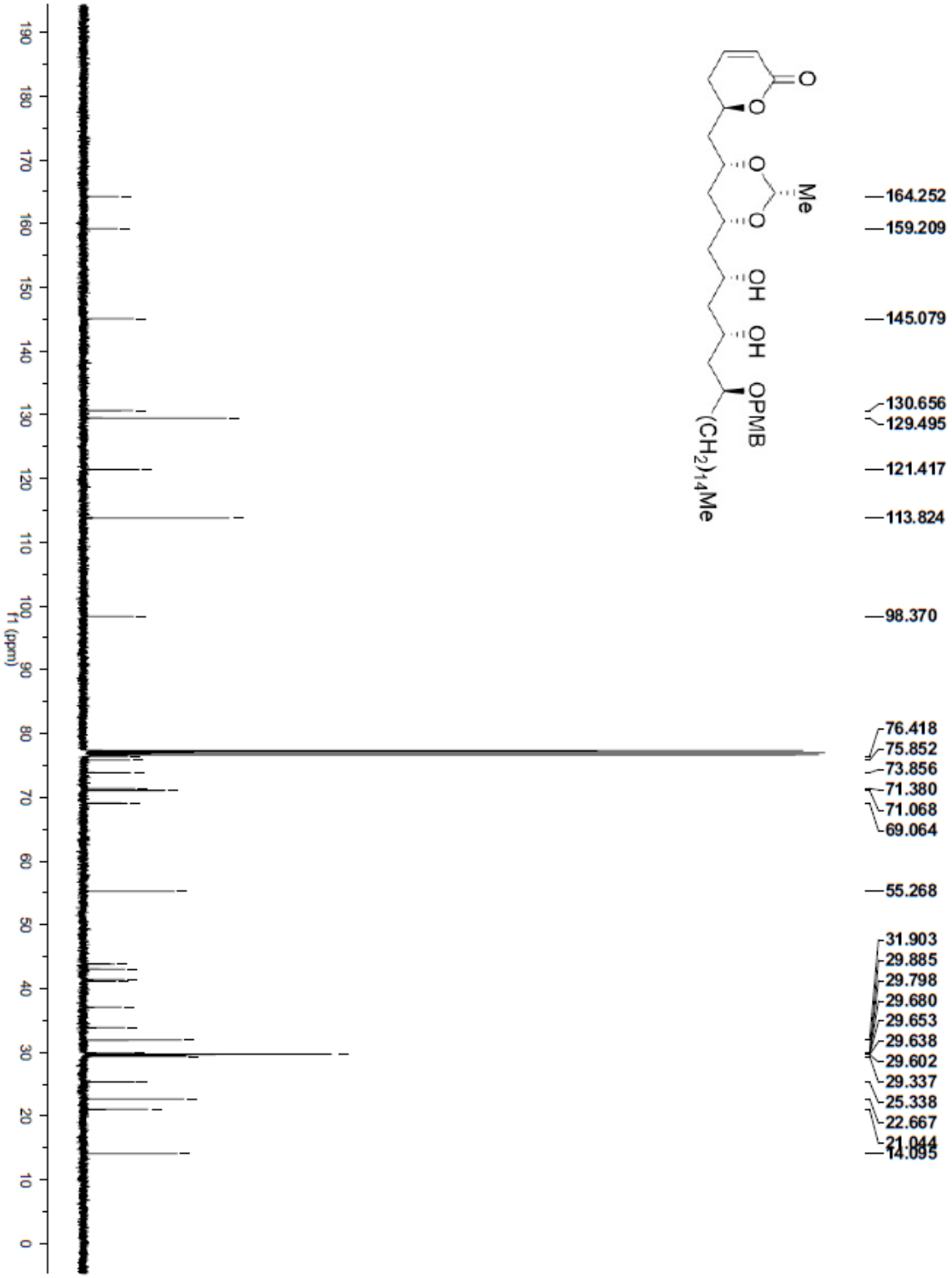
f1 (ppm)
0
10
20
30
40
50
60
70
80
90
100
110
120
130
140
150
160
170
180
190
O
O
O
Me
OH
OH
OPMB
(CH2)14Me
164.252
159.209
145.079
130.656
129.495
121.417
113.824
98.370
76.418
75.852
73.856
71.380
71.068
69.064
55.268
31.903
29.885
29.798
29.680
29.653
29.638
29.602
29.337
25.338
22.667
21.044
14.095

(+)-Cryptocaryol A (5.1)

A 10 mL screw cap vial was charged with **5.21** (32.4 mg, 0.0480 mmol, 100 mol%), 1,3-dimethoxybenzene (59.7 mg, 0.200 mmol, 900 mol%), stir bar, and dichloromethane (2.4 mL, 0.02 M). Triflic acid (21.6 mg, 0.144 mmol, 300 mol%) was added and a dark red solution developed immediately. The solution was stirred for 30 min at room temperature then quenched with saturated $NaHCO_3$ (5 mL) with vigorous stirring. The cloudy mixture was extracted with chloroform (5 x 5 mL), dried over anhydrous Na_2SO_4, and concentrated in vacuo to a white semi-solid. The semi-solid was absorbed onto silica gel and purified by flash column chromatography (SiO_2, MeOH:$CHCl_3$ 1:99 to 1:19) providing (+)-cryptocaryol A **5.1** as a white solid (19.1 mg, 75% yield).

TLC (SiO_2): 0.32 (1:9 MeOH:$CHCl_3$)

^{1}H NMR: (400 MHz, CD_3OD): δ = 7.05 (ddd, *J*=9.7, 5.9, 2.6, 1H), 5.98 (ddd, *J*=9.7, 2.6, 1.1, 1H), 4.82 – 4.61 (m, 1H), 4.22 – 3.92 (m, 4H), 3.90 – 3.69 (m, 1H), 2.46 (dddd, *J*=18.6, 5.8, 4.4, 1.1 Hz, 1H), 2.37 (ddt, *J*=18.7, 11.4, 2.6, 1H), 1.95 (ddd, *J*=14.5, 9.8, 2.6, 1H), 1.74 – 1.54 (m, 7H), 1.52 (dd, *J*=6.7, 5.5 Hz, 2H), 1.48 – 1.40 (m, 3H), 1.38 – 1.21 (m, 27H), 0.90 (t, *J*=6.9, 3H).

^{13}C NMR: (126 MHz, CD_3OD) δ = 166.9, 148.5, 121.4, 76.6, 70.1, 69.9, 69.1, 68.2, 66.6, 46.0, 45.9, 45.7, 45.2, 43.9, 39.2, 33.1, 30.9, 30.8-30.8 (9C), 30.5, 26.8, 23.7, 14.4.

FTIR (neat): 3365, 2916, 2849, 1718, 1470, 1389, 1268, 1139 cm^{-1}.

HRMS: (ESI) Calcd. for $C_{30}H_{56}O_7$ $(M+Na)^+$: 551.3918, Found: 551.3920.

$[\alpha]^{22}_D$: +27.45 ° (c = 0.51, MeOH).

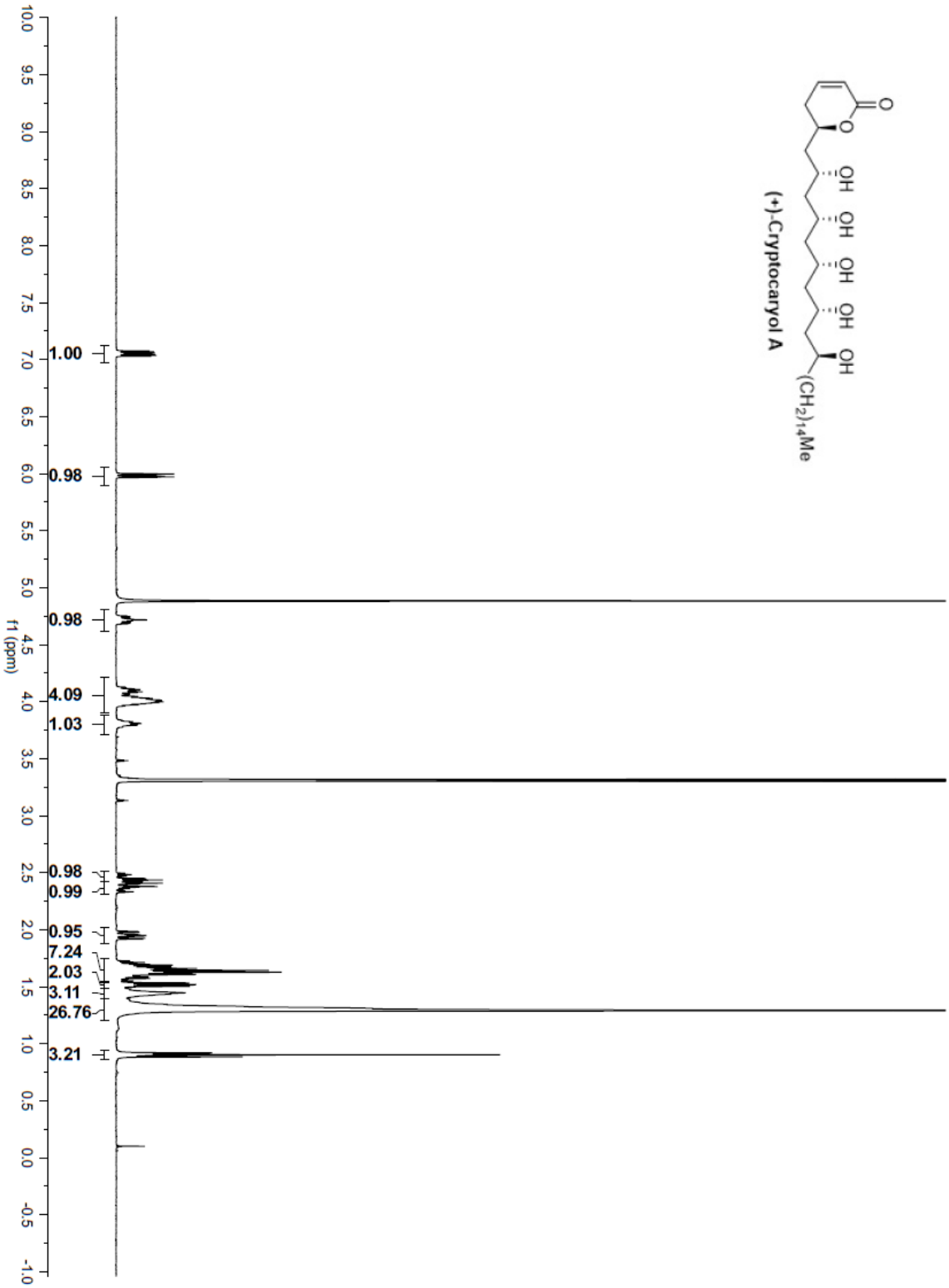
(+)-Cryptocaryol A
f1 (ppm)
1.00
0.98
0.98
4.09
1.03
0.98
0.99
0.95
7.24
2.03
3.11
26.76
3.21

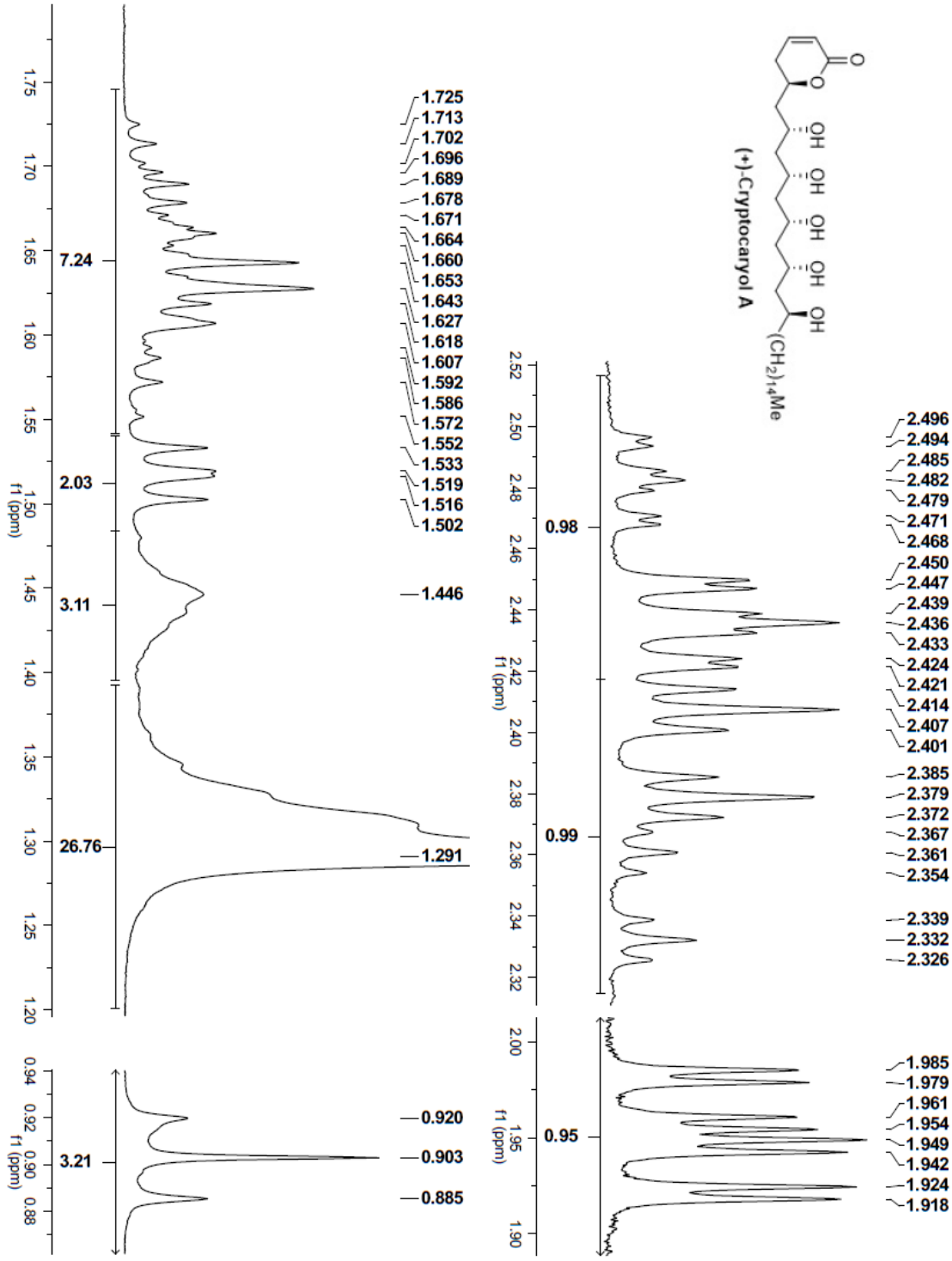
(+)-Cryptocaryol A
OH OH OH OH OH
(CH2)14Me
2.496
2.494
2.485
2.482
2.479
2.471
2.468
2.450
2.447
2.439
2.436
2.433
2.424
2.421
2.414
2.407
2.401
2.385
2.379
2.372
2.367
2.361
2.354
2.339
2.332
2.326
1.985
1.979
1.961
1.954
1.949
1.942
1.924
1.918
0.98
0.99
0.95
1.725
1.713
1.702
1.696
1.689
1.678
1.671
1.664
1.660
1.653
1.643
1.627
1.618
1.607
1.592
1.586
1.572
1.552
1.533
1.519
1.516
1.502
1.446
1.291
7.24
2.03
3.11
26.76
0.920
0.903
0.885
3.21
f1 (ppm)

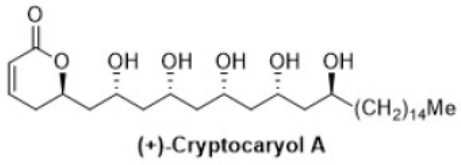

(+)-Cryptocaryol A

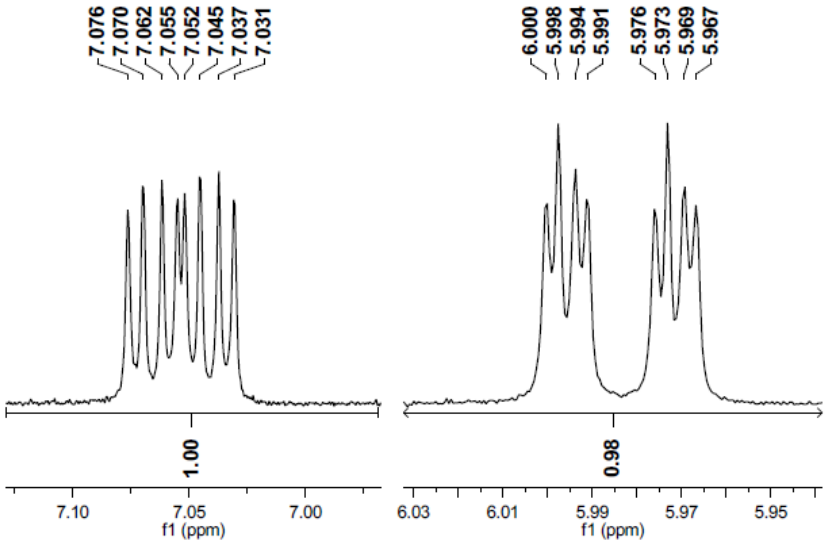

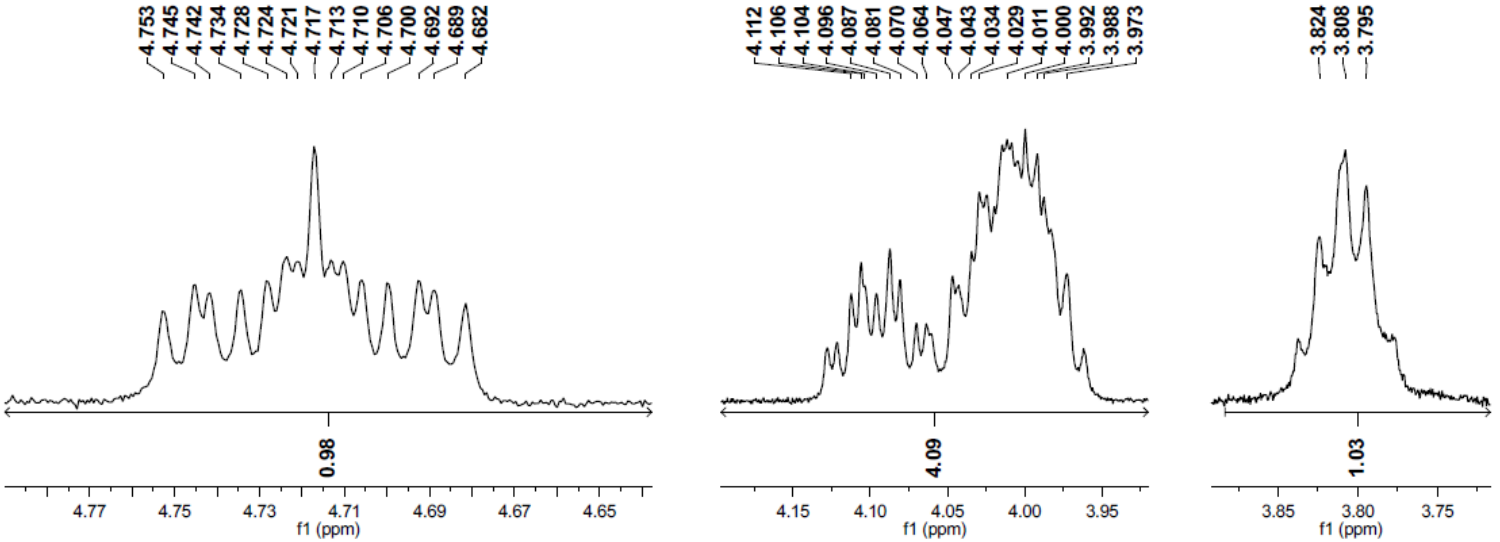

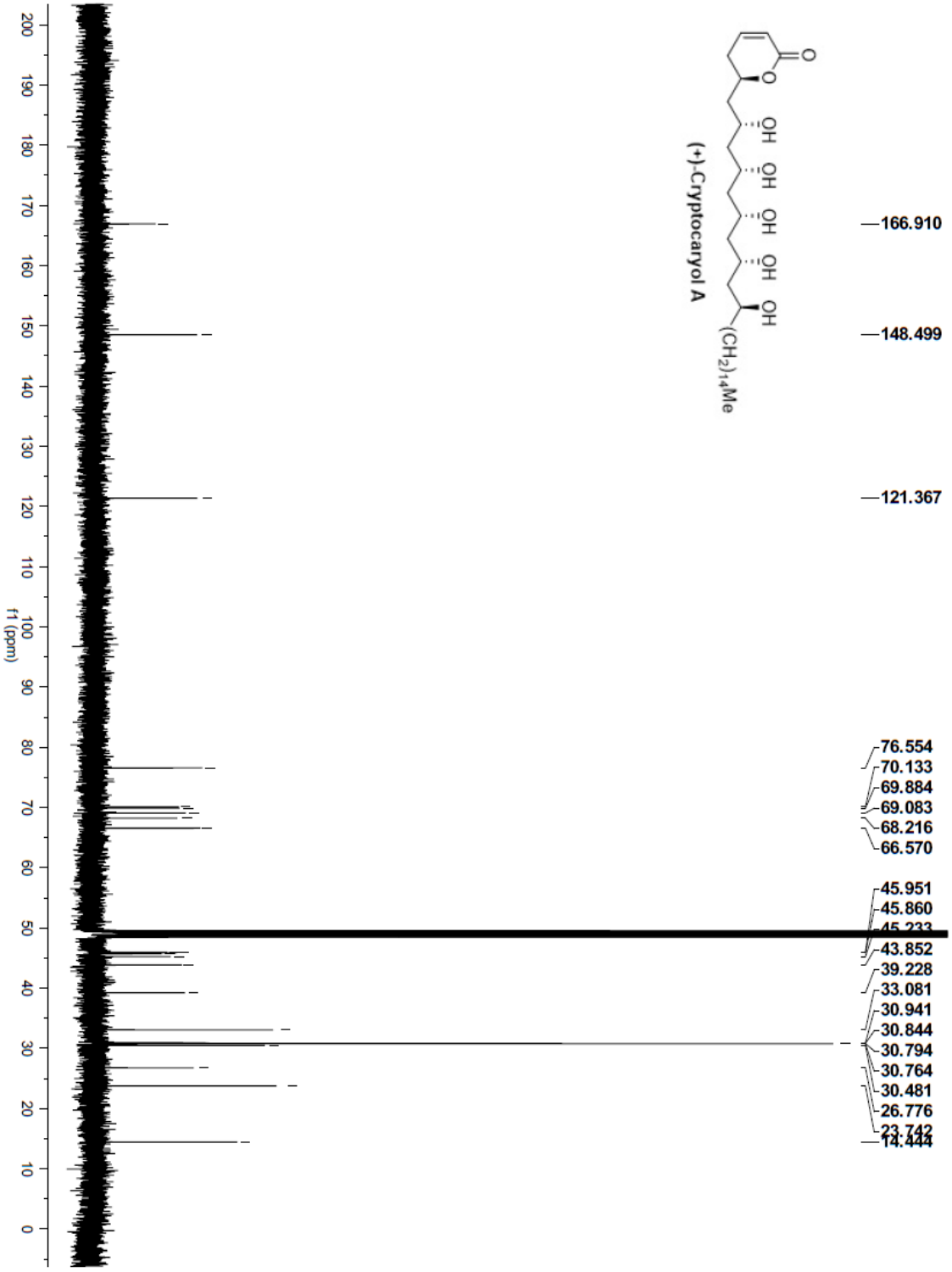
(+)-Cryptocaryol A
OH OH OH OH OH
(CH2)14Me
166.910
148.499
121.367
76.554
70.133
69.884
69.083
68.216
66.570
45.951
45.860
43.852
39.228
33.081
30.941
30.844
30.794
30.764
30.481
26.776
23.742
14.444
f1 (ppm)

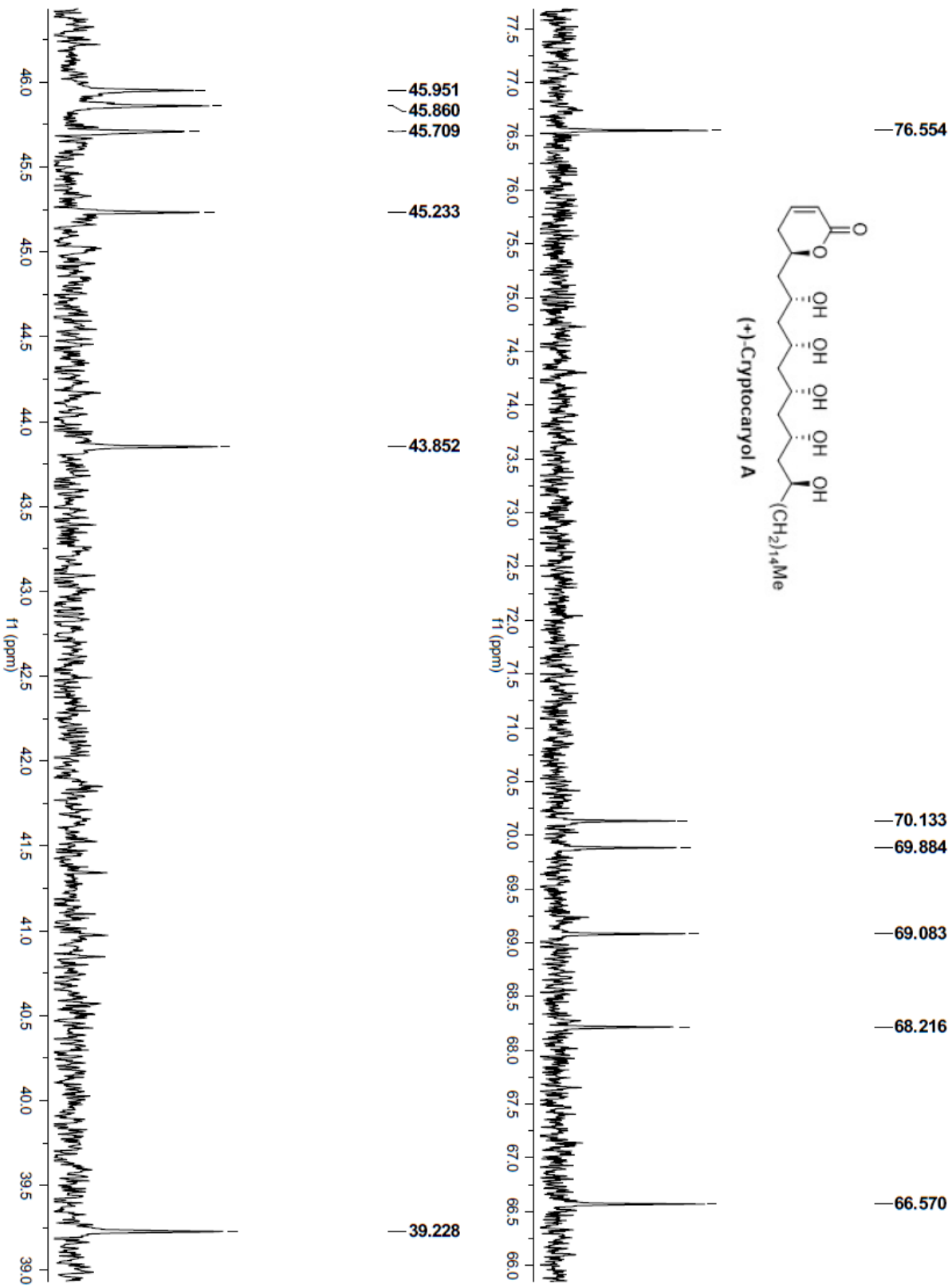
45.951
45.860
45.709
45.233
43.852
39.228
f1 (ppm)
76.554
70.133
69.884
69.083
68.216
66.570
f1 (ppm)
(+)-Cryptocaryol A

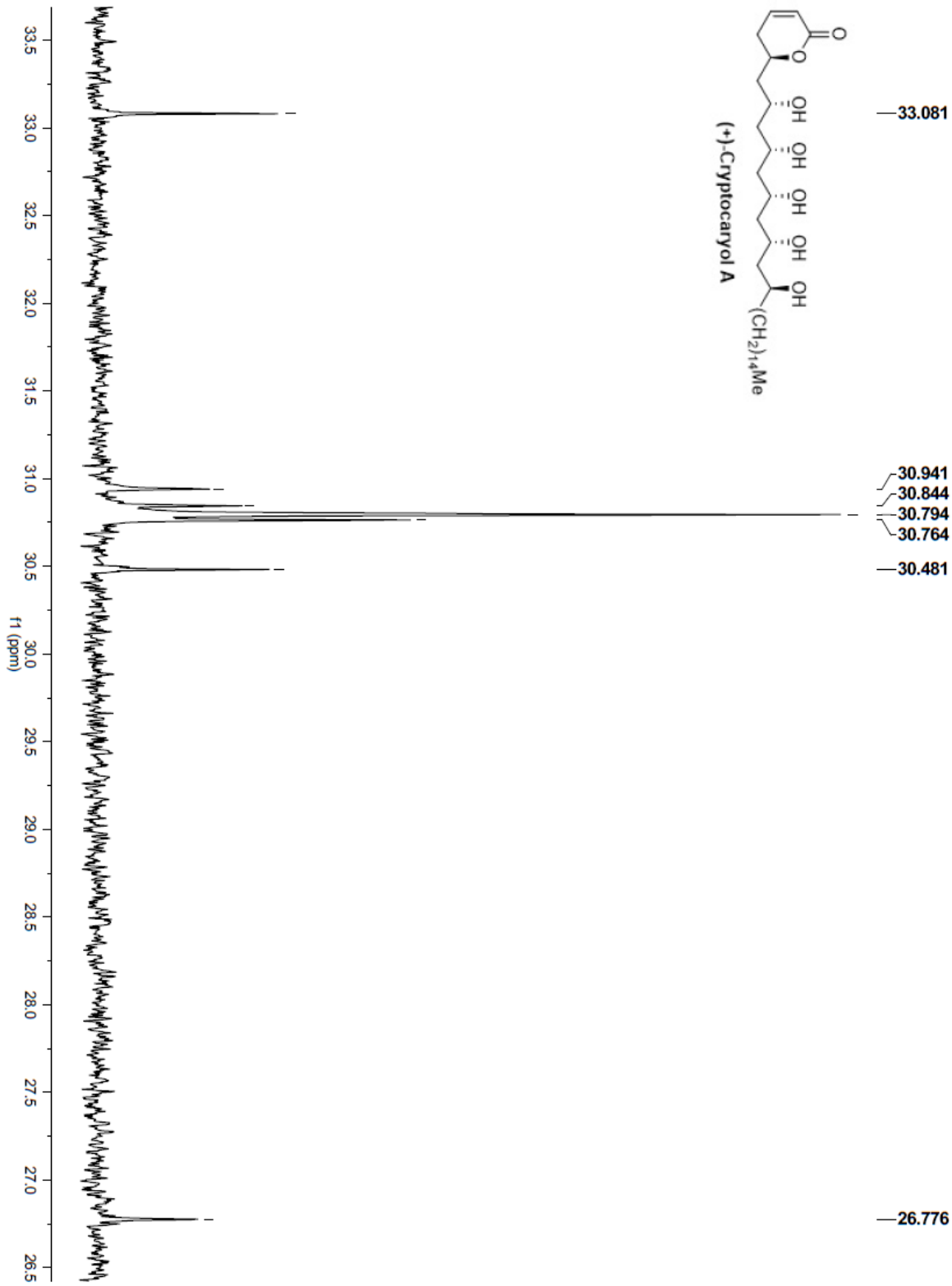
(+)-Cryptocaryol A
33.081
30.941
30.844
30.794
30.764
30.481
26.776
f1 (ppm)

Chapter 6: Ruthenium-Catalyzed Oxidative Spirolactonization

6.1 Background of Ruthenium-Catalyzed Reductive Couplings

The Krische research group had developed a suite of ruthenium-catalyzed hydrogenative methods for C-C bond formation. Specifically, methods had been established for crotylation,[53b, 54-55, 142] vinylation,[143] and propargylation[144] of aldehydes by reductive coupling of aldehydes and π-unsaturates, or by redox neutral coupling of primary alcohols and π-unsaturates. However, despite a growing understanding of the reactivity and selectivity in these transformations, coupling of π-unsaturates with ketones or secondary alcohols had not been achieved. There has been one exception, the cyclic keto-amide of isatin, which has been shown to undergo ruthenium- and iridium-catalyzed coupling via transfer hydrogenation.[145]

Recognizing this limitation, a literature survey was performed to identify ruthenium catalysts that act on secondary alcohols. A promising complex, $Ru_3(CO)_{12}$, was found to exhibit two characteristics crucial for transfer hydrogenative reductive coupling.[146] First, $Ru_3(CO)_{12}$ was shown to participate in the amination of α-hydroxy amides via transfer hydrogenation (Scheme 6.1).[147] This transformation occurs via a reductive amination pathway in which ruthenium-catalyzed dehydrogenation generates a keto-amide and ruthenium hydride. The newly formed carbonyl next undergoes condensation with a primary amine to produce an imine, which is hydrogenated by the ruthenium hydride to afford an α-amino amide as well as ruthenium(0).

Scheme 6.1 Ruthenium-catalyzed transfer hydrogenation of an α-hydroxy amide.

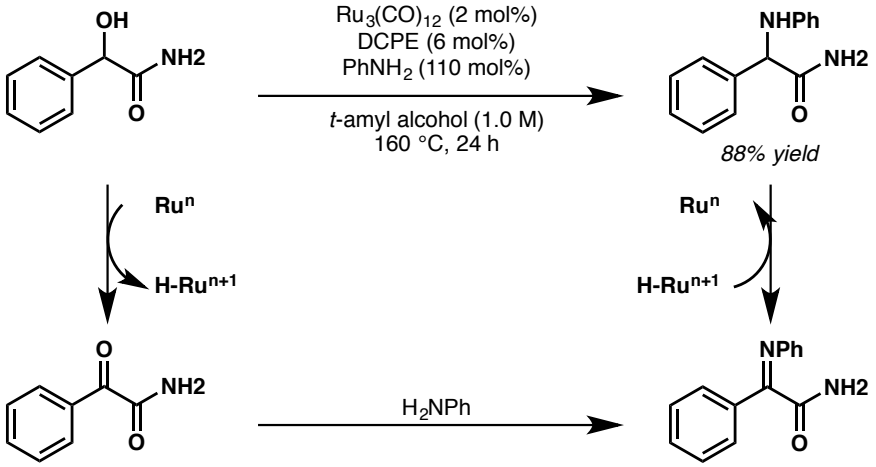

Second, $Ru_3(CO)_{12}$ was shown to catalyze a [2+2+1] oxidative coupling reaction between 1,2-dicarbonyl compounds, ethylene, and carbon monoxide to construct products of spirolactonization. (Scheme 6.2).[148] These characteristics indicate that a Ru^0 complex is capable of hydrogenation and oxidative coupling. It was anticipated that similar conditions could facilitate transfer hydrogenative coupling of π-unsaturates and α-hydroxy carbonyl compounds.

Scheme 6.2 Oxidative coupling of an α-keto ester with ethylene and CO using catalytic $Ru_3(CO)_{12}$.

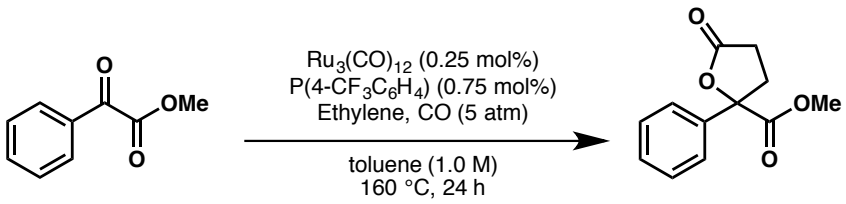

Inspired by these reports, application of similar reaction conditions was attempted in order to couple ethyl mandelate and isoprene. Fortunatly, after extensive optimization of the reaction conditions, it was found that coupling could be achieved (Scheme 6.3).[149] This oxidative coupling was unique in that, unlike other reductive couplings of dienes and carbonyl compounds, coupling took place at the C4 position of isoprene.

Scheme 6.3 Oxidative coupling of ethyl mandelate and isoprene via transfer hydrogenation.

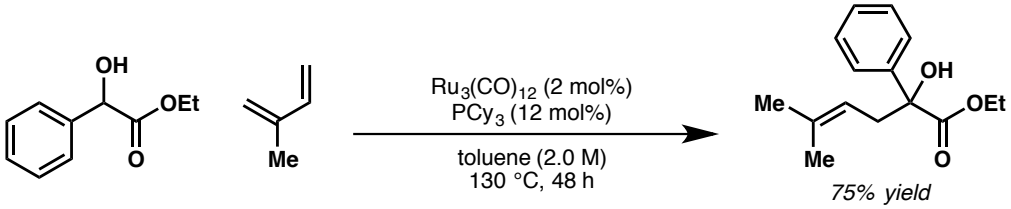

Modification of the reaction conditions led to successful couplings of isoprene to *N*-benzyl-3-hydroxyoxindole (Scheme 6.4, top), as well as to 1,2-diols. In the case of the 1,2-diols, dehydrogenation affords a 1,2-diketone. Upon coupling of the isoprene to one of the ketones, intramolecular addition to the adjacent ketone took place delivering the product of formal [4+2] cycloaddition (Scheme 6.4, bottom).[150]

Scheme 6.4 Oxidative coupling of isoprene to 3-hydroxyoxindole and 1,2-cyclohexane diol via transfer hydrogenation.

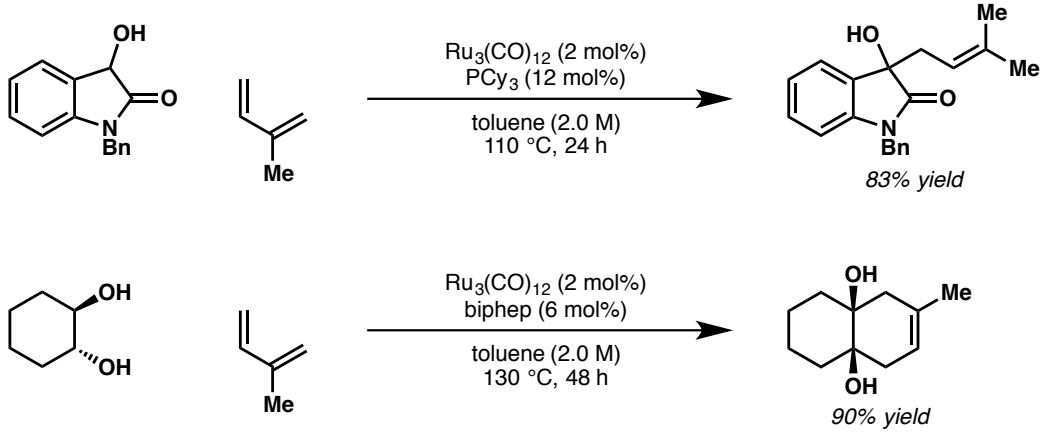

Encouraged by the successful ruthenium-catalyzed oxidative coupling with ketones, further applications of this reaction class were explored. The unique regioselectivity observed in the ruthenium-catalyzed oxidative couplings was of particular interest and further investigation revealed that α-olefins, a feedstock chemical, could be directly coupled with *N*-benzyl-3-hydroxyoxindole to afford products of carbonyl addition. Importantly, it was found that addition of 1-adamantanecarboxylic acid as an additive promoted efficient couplings of *N*-benzyl-3-hydroxyoxindole with a variety of α-olefins (Scheme 6.5).[151]

Scheme 6.5 Oxidative coupling of propene to 3-hydroxyoxindole via transfer hydrogenation.

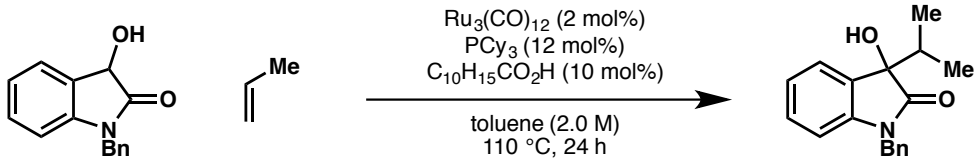

90% yield

6.2 Oxidative Coupling and Spirolactonization Using Acrylates

6.2.1 Introduction

In the course of evaluating suitable π-unsaturates that would couple under conditions of Ru^0 catalysis, methyl acrylate and other acrylic esters were investigated. Interestingly, it was found that oxidative coupling of *in* situ generated carbonyl compounds with acrylic esters furnished spirocyclic γ-butryolactones. These structurally intriguing functional groups are ubiquitous in natural products that exhibit a wide range of biological activity, including spironolactone and abyssomycin C (Figure 6.1).

Figure 6.1 Pharmaceutically active natural products containing spirolactones.

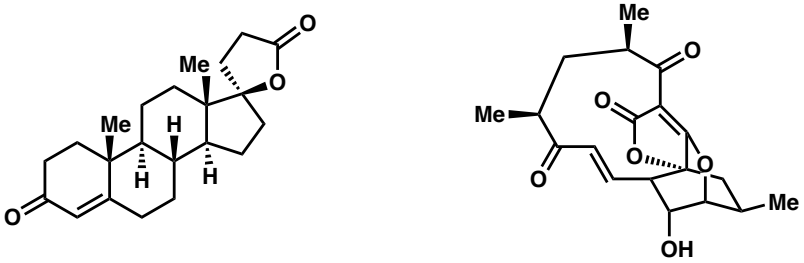

Spirocycles found in nature all contain a sterically congested quaternary center. Due to their interesting structure and prevalence in biologically active natural products, many methods have been developed for the construction of spirocyclic γ-butyrolactones. Examples of which include oxidative dearomatizations using iodine or cerium ammonium nitrate,[152] Michael additions using α,β-unsaturated esters,[153] cationic rearrangements of epoxides and bromonium ions,[154] *N*-heterocyclic carbene catalyzed Stetter reactions,[155] C-H hydroxylation of carboxylic

acids,[156] Reformatsky type reactions,[157] and Pauson-Khand and other types of carbonyl insertion reactions. [148, 158] However, it was expected that a method to construct spirolactones via transfer hydrogenative C-C bond formation would complement these methods and would represent a new functional group interconversion using methyl acrylate, an inexpensive feedstock chemical. Additionally, few examples exist for asymmetric spirolactonization and thus a metal-catalyzed methodology could potentially address this shortcoming.[159]

6.2.2 Reaction Development, Optimization, and Scope

To probe the reactivity of α,β-unsaturated esters with diols to access spirolactones, *trans*-1,2-hexanediol **6.1a** and methyl acrylate **6.2a** were exposed to $Ru_3(CO)_{12}$ and various ligands (Table 6.1). Contrary to previous reported work that illustrated PCy_3 to be an effective ligand, no product was obtained when it was used in the reaction (entry 1). Bidentate nitrogen-based ligands BIPY or Phen were similarly ineffective (entries 2-3). Conversely, the bidentate electron-rich phosphine ligand DPPP produced the desired spirolactone in 76% yield (entry 4). Increased loadings of methyl acrylate did enhance conversion (entries 5-7), however, efforts were focused on improving the reaction efficiency. Variation of the reaction temperature did not lead to improved conversion (entries 8-9). In previous work, it was found that carboxylic acid additives often have a significant effect on reaction yield.[151] This increase in yield was hypothesized to be a result of accelerated hydrogenolysis of the oxo-metallacycle formed upon oxidative coupling.[160] In the reaction of 1,2-*trans*-cyclohexanediol with methyl acrylate, addition of catalytic amounts of benzoic acid or 1-adamantanecarboxylic acid proved to be highly effective, with 1-adamantanecarboxylic acid performing best for a number of substrates (entries 10-11).

Table 6.1 Optimization of the spirolactonization reaction with **6.1a**.

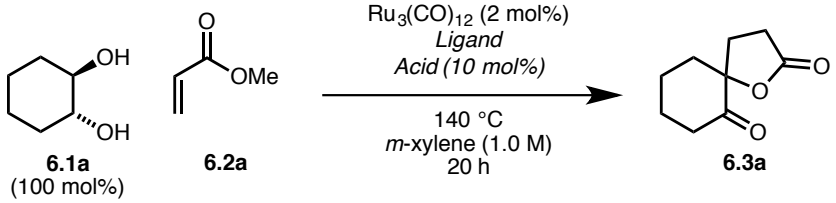

Entry	Ligand (mol%)	Acid	**6.2a** (mol%)	T (°C)	Yield (%)
1	PCy_3 (12)	--	300	140	trace
2	BIPY (6)	--	300	140	trace
3	Phen (6)	--	300	140	trace
4	DPPP (6)	--	300	140	76
5	DPPP (6)	--	200	140	56
6	DPPP (6)	--	400	140	88
7	DPPP (6)	--	500	140	79
8	DPPP (6)	--	300	130	33
9	DPPP (6)	--	300	150	69
10	DPPP (6)	benzoic acid	300	140	93
11	DPPP (6)	$C_{10}H_{15}CO_2H$	300	140	96

Having identified conditions for efficient conversion of diol **6.1a** to spirolactone **6.3a**, the scope of the reaction was assessed. A variety of cylic, acyclic, and polycyclic diols were found to undergo spirolactonization in high yield to afford spirolactones **6.3a-l** (Figure 6.2). In the case of nonsymmetric diols, regioselectivity was variable. Acyclic diols **6.1g-h** exhibited incomplete regioselectivity illustrated by the 4:1 r.r. for spirolactone **6.3g** and 1:1 r.r. for **6.3h**. However, cyclic nonsymmetric 1,2-diols exhibited complete regioselectivity. Importantly, both *cis*- and *trans*-1,2-diols were suitable substrates under the reaction conditions.

Figure 6.2 Spirolactones **6.3a-l** synthesized from coupling of diols **6.1a-l** with methyl acrylate **6.2a**.

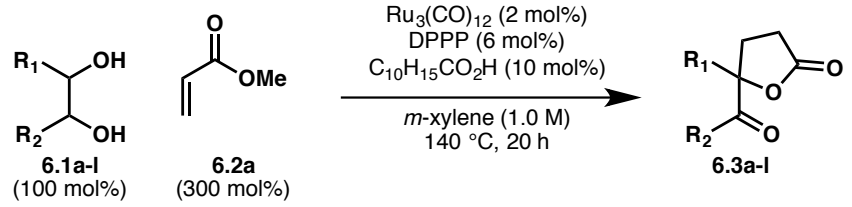

6.1a-l (100 mol%) **6.2a** (300 mol%) **6.3a-l**

6.1a $R_1,R_2=(CH_2)_4$	**6.1b** $R_1,R_2=(CH_2)_3$	**6.1c** $R_1,R_2=(CH_2)_5$	**6.1d** $R_1,R_2=(CH_2)_6$
6.1e R_1,R_2=Me	**6.1f** R_1,R_2=Ph	**6.1g** R_1=Ph, R_2=Me	**6.1h** R_1=*t*Bu, R_2=Me
6.1i Indanyl	**6.1j** H_4Naphthyl	**6.1k** Acenaphthyl	**6.1l** Me_2Chromanyl

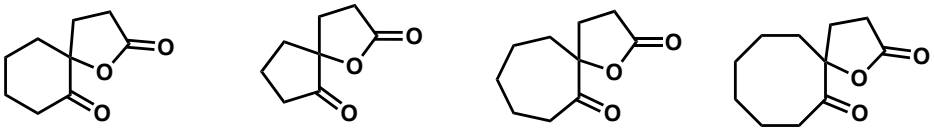

6.3a, 96% yield[a] **6.3b**, 85% yield[b,c] **6.3c**, 64% yield[d] **6.3d**, 79% yield[b]

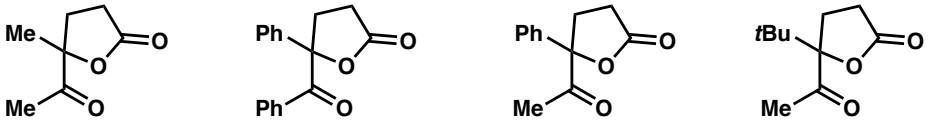

6.3e, 93% yield[d] **6.3f**, 90% yield[d] **6.3g**, 71% yield[a] 4:1 rr **6.3h**, 75% yield[a] 1.3:1 rr

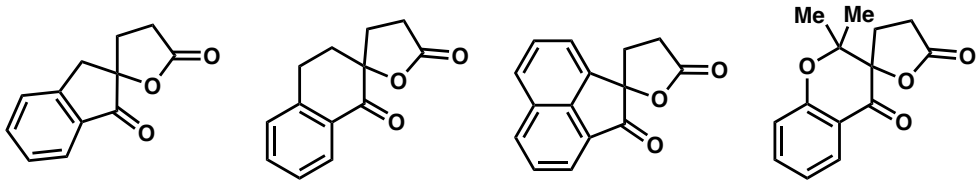

6.3i, 79% yield[a] >20:1 rr **6.3j**, 88% yield[d] >20:1 rr **6.3k**, 59% yield[d] **6.3l**, 74% yield[b] 20:1 rr

[a]*trans*-1,2-diol was employed, [b]*cis*-1,2-diol was employed, [c]400 mol% of **6.2a** was employed, [d]A mixture of *cis*- and *trans*-1,2-diol was employed

It was hypothesized that oxidative coupling occurs from the 1,2-diketone oxidation state. To evaluate this hypothesis, the reaction was performed from the 1,2-diol, α-hydroxy ketone, and 1,2-diketone oxidation levels (Scheme 6.6). It was anticipated that the 1,2-diol would participate via an oxidative pathway, the α-hydroxy ketone via a redox neutral pathway, and the 1,2-diketone via a reductive pathway. Indeed, all three pathways led to formation of **6.3f**, however, while diol **6.1f** and α-hydroxy ketone **6.4f** both afforded **6.3f** in excellent yield, significant attenuation of reactivity was observed with 1,2-diketone **6.5f**. The reason for this

reduction in yield could be due to competitive reduction of acrylate **6.2a** instead of oxidative coupling upon generation of a ruthenium hydride formed from the Ru^0 catalyst and reductant.

Scheme 6.6 Oxidative coupling of isoprene to 3-hydroxyoxindole and 1,2-cyclohexane diol via transfer hydrogenation.

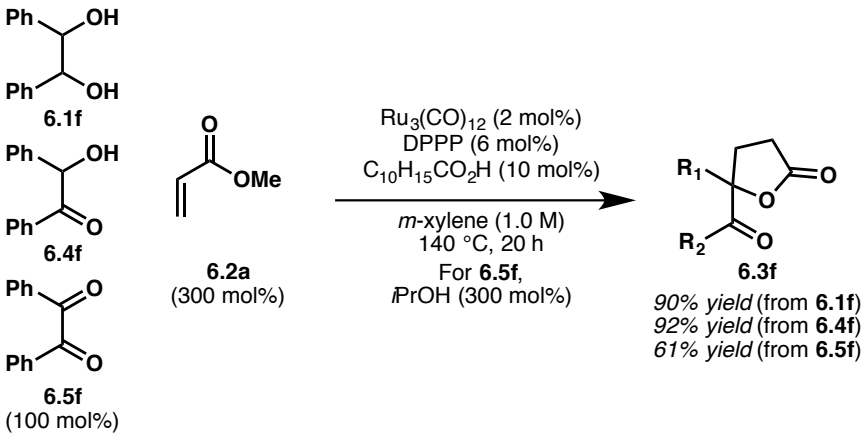

Regrettably, substituted α,β-unsaturated esters did not couple under these conditions. It was observed that substitution at the α or β position resulted in no product formation. However, 2-hydroxymethyl substituted methyl acrylate **6.2b** did engage in oxidative coupling, after which elimination of the hydroxyl group afforded α-methylene-γ-butyrolactone **6.6b** (Scheme 6.7). The ineffective coupling of substituted acrylates could be a result of poor coordination between the acrylate and the ruthenium due to the steric environment at the metal center. Alternatively, 2-hydroxymethyl substituted acrylate **6.2b** may chelate ruthenium and act as a directing group for olefin coordination and subsequent oxidative coupling.

Scheme 6.7 Generation of α-methylene-γ-butyrolactone **6.6b** via coupling of **6.1a** and 2-hydroxymethyl acrylate **6.2b**.

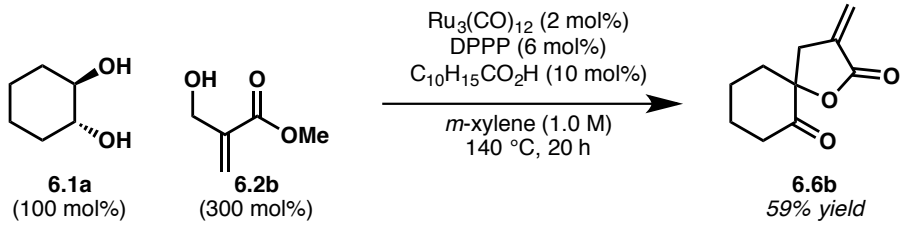

Prior work had illustrated that other α-hydroxyl carbonyl compounds, such as mandelic esters and 3-hydroxyoxindoles, could engage in oxidative coupling with dienes in the presence of $Ru_3(CO)_{12}$. Application of the reaction conditions for oxidative spirolactonization to mandelic ester **6.7a** and **6.7b** resulted in the successful formation of **6.8a** and **6.8b** (Scheme 6.8).

Scheme 6.8 Spirolactonization of mandelic esters **6.7a** and **6.7b** to afford **6.8a** and **6.8b**.

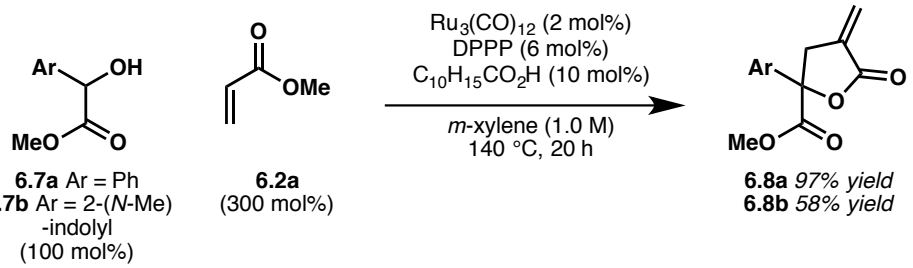

6.7a Ar = Ph
6.7b Ar = 2-(*N*-Me)-indolyl
(100 mol%)

6.2a
(300 mol%)

6.8a *97% yield*
6.8b *58% yield*

Unlike with 1,2-diols, 3-hydroxyoindole **6.9** was found to couple with various substituted acrylic esters (**6.2c-I**, Figure 6.3). It is hypothesized that the observed variation in reactivity between **6.9** and various 1,2-diols or α-hydroxy esters may be a result of strain energy in the 5-membered ring of the isatin that is formed upon dehydrogenation of 3-hydroxyoxindole. This increased energy may compensate for the inefficient ligation of substituted acrylic esters. Application of the established conditions for oxidative spirolactonization to 3-hydroxyoxindole **6.9** with methyl crotonate **6.2c** afforded the corresponding spirolactone quantitatively, but as a 1:1 mixture of diastereomers. Further reaction optimization was performed, which revealed that use of TERPY as a ligand and addition of KO*t*Bu (10 mol%) resulted in formation of **6.10c** as a single diastereomer in high yield. Expansion of the scope of this reaction with various substituted acrylates was successful and led to the generation of spirooxindole products **6.10a**, **c-i** (Figure 6.3). Use of β-substituted acrylic esters **6.2c-d**, **g-i** led to the formation of **6.10c-d**, **g-i** as a single diastereomer, while use of α-substituted methyl methacrylate **6.2e** resulted in formation of spirolactone **6.10e** as a mixture of diastereomers. The lack of diastereoselectivity in this example

may be due to epimerization of one of the chiral centers under the reaction conditions. β,β-disubstituted ester **6.2f** engaged in oxidative spirolactonization to furnish spirooxindole **6.10f**, which contained two adjacent quaternary centers, albeit in diminished yield.

Figure 6.3 Oxidative spirolactonization of 3-hydroxyoxindole **6.9** with substituted acrylic esters **6.2a**, **c-i** to generate spirooxindole products **6.10a**, **c-i**.

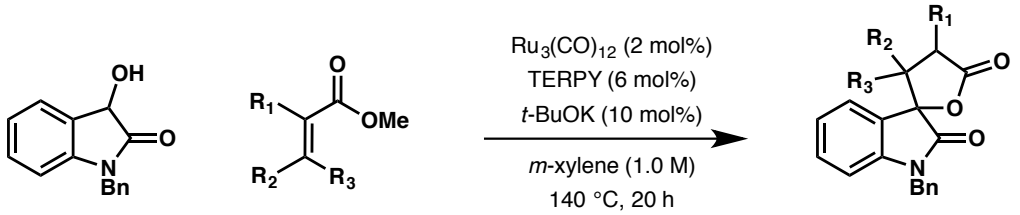

6.9 (100 mol%)

6.2a, **c-i** (300 mol%)

6.10a, **c-i**

6.2a R_1=R_2=R_3=H	**6.2c** R_1=R_2=H, R_3=H	**6.2d** R_1=R_2=H, R_3=Ph	**6.2e** R_1=Me, R_2=R_3=H
6.2f R_1=H, R_2=R_3=Me	**6.2g** R_1=R_2=H, R_3=Cy	**6.2h** R_1=R_2=H, R_3=2-piperonyl	**6.2i** R_1=R_2=H, R_3=2-thienyl

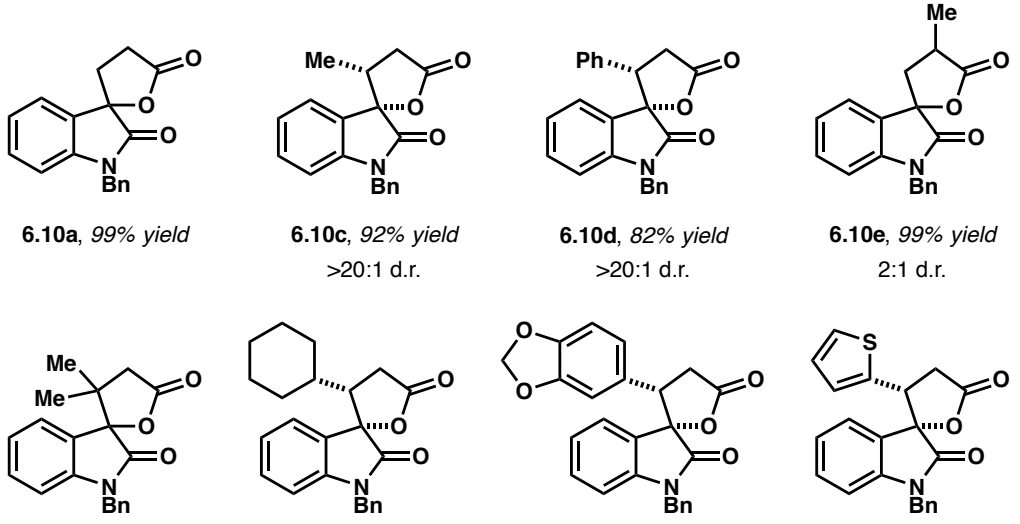

6.10a, *99% yield*

6.10c, *92% yield* >20:1 d.r.

6.10d, *82% yield* >20:1 d.r.

6.10e, *99% yield* 2:1 d.r.

6.10f, *52% yield*

6.10g, *77% yield* >20:1 d.r.

6.10h, *90% yield* >20:1 d.r.

6.10i, *87% yield* >20:1 d.r.

6.2.3 Mechanistic Considerations and Discussion

A plausible mechanism for the oxidative coupling of dione **6.5a**, formed upon dehydrogenation of **6.1a**, and methyl acrylate **6.2a** is shown in Figure 6.4. It is hypothesized that oxidative coupling of **6.5a** and **6.2a** by Ru^0 generates oxaruthenacycle **I**, which can interconvert

between the *C*-bound enolate **I** and the *O*-bound enolate **II** via isomerization. Protonolysis of the oxaruthenacycle generates ruthenium alkoxide **III** and it is hypothesized that this step is accelerated through use of the carboxylic acid additive, which results in a significant improvement in yield. Alkoxide **III** then undergoes lactonization, which upon release of the product **6.3a** regenerates Ru^{II} species **IV**. Ligand exchange of methoxide with the alkoxide of diol **6.1a** or α-hydroxy ketone **6.4a** expels methanol. The resulting ruthenium alkoxide undergoes β-hydride elimination to give **6.4a** or **6.5a**, and reductive elimination to regenerate the acid, HA, as well as the Ru^0 complex to close the catalytic cycle.

Figure 6.4 Proposed mechanism for oxidative spirolactonization of dione **6.5a** with methyl acrylate **6.2a**.

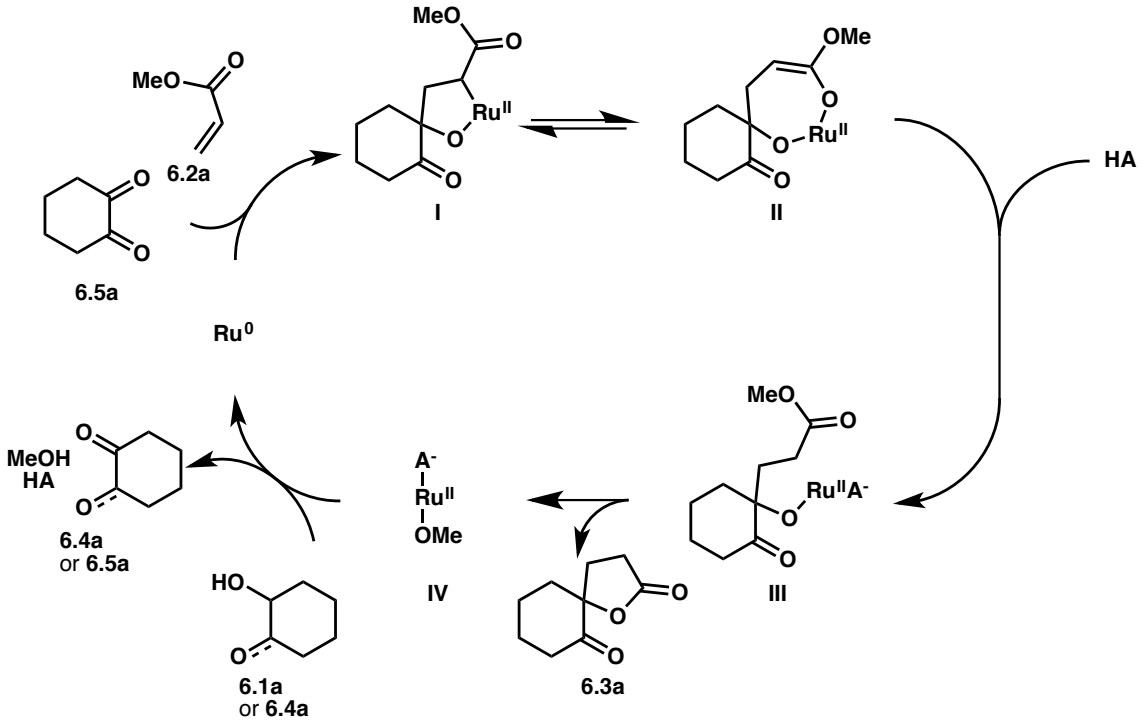

A monomeric ruthenium species is proposed for this mechanism, as previous work has suggested that the trimeric $Ru_3(CO)_{12}$ can be broken into monomeric form in the presence of phosphine ligands.[161] This hypothesis was confirmed through isolation of ruthenium complex **6.11**, which was obtained upon exposure of $Ru_3(CO)_{12}$ to DPPP and 1-adamantane carboxylic acid at 140 °C (Figure 6.5).

Figure 6.5 ORTEP representation of the structure of Ru(CO)(DPPP)[($H_{15}C_{10}O_2^-$)$_2$] **6.11**.

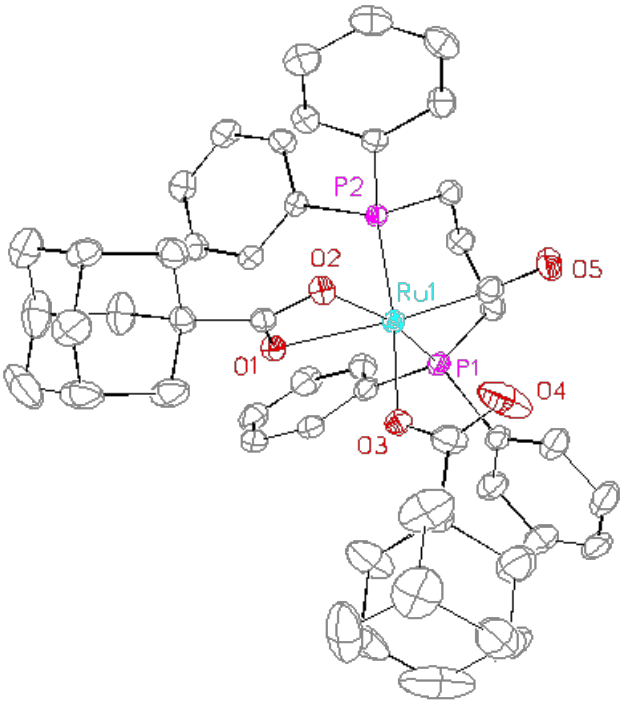

The isolated ruthenium complex proved to be catalytically competent, which suggests that protonation by the diol followed by β-hydride elimination and reductive elimination can reform the requisite Ru^0 for oxidative coupling (Scheme 6.9).

Scheme 6.9 Regeneration of Ru^0 catalyst from **6.11**.

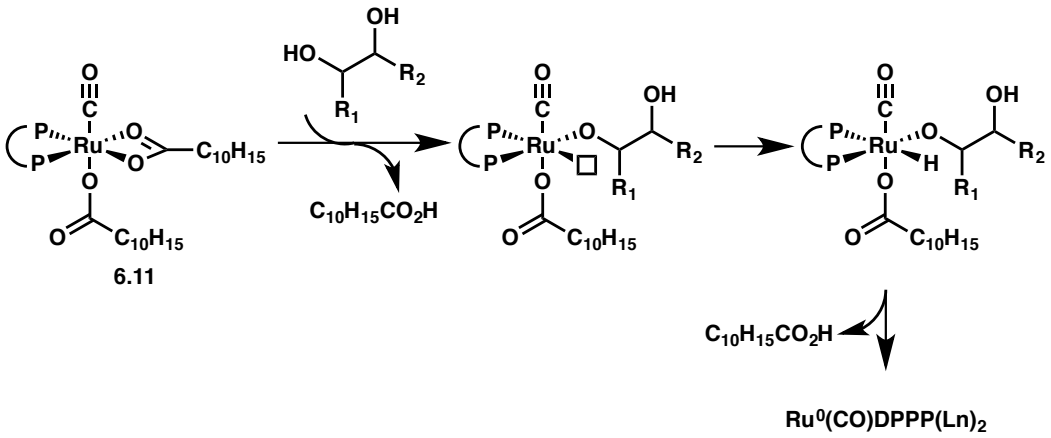

One can imagine other modes of coupling, including Lewis acid catalyzed Michael addition, in which the acrylate could undergo conjugate addition by the dienolate of the α-

hydroxy ketone that forms upon β-hydride elimination of the 1,2-diol. Control experiments were performed in order to investigate the plausibility of this type of reactivity mode. Exposure of α-hydroxy ketone **6.4j** to methyl acrylate in the presence of a variety of Lewis acids, including $Ru_3(CO)_{12}$, $RuCl_3$, $B(OMe)_3$, $MgCl_2$, $InCl_3$, and ZnI_2, led to only small quanitites (<16% yield) of the corresponding spirolactone product (Scheme 6.10). This indicates that while spirolactone products are capable of being synthesized through Michael addition, the reported catalytic system is significantly more effective.

Scheme 6.10 Control experiment to test plausibility of Lewis acid catalyzed Michael addition.

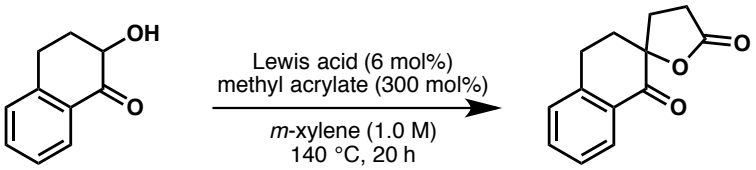

6.4j
(100 mol%)

6.3j
0-16% yield

Another control reaction was performed to evaluate the plausibility of an anionic addition pathway. α-hydroxy ketone **6.4j** was methylated to afford **6.4j-OMe**, which was subjected to the established reaction conditions (Scheme 6.11). Methylation of the hydroxyl group allowed for enolization and Michael addition but eliminated the possibility of an oxidative coupling pathway. The results of the reaction were that no product had formed and only the starting material was recovered, which could indicate that the diketone is necessary for C-C bond formation.

Scheme 6.11 Control experiment to test the exclusion of an oxidative coupling pathway.

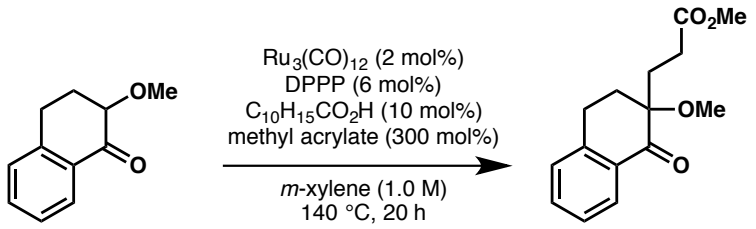

6.4j-OMe
(100 mol%)

6.3j
0-16% yield

Further investigation of the incongruent regioselectivities of products **6.3i**, **6.3j**, and **6.3l** compared to that of **6.3g** was warranted. Specifically, 1,2-diol **6.1g** underwent spirolactonization to provide spirolactone **6.3g** as a 4:1 mixture of regioisomers in favor of the product coupled at the benzylic postion, whereas 1,2-diol **6.1i** gave **6.3i** as a single diastereomer favoring coupling at the carbonyl distal to the aromatic ring when subjected to the reaction conditions. This regioselectivity is consistent with other reports of oxidative couplings to 1-phenyl-2,3-dione[162] as well as with reports of nucleophilic addition to, or hydrogenation of, 1,2-indanone.[163] Studies by Hoffman suggest that, in the conversion of bis-olefin complexes to metallocyclopentanes, regioselectivity is dictated by the interactions of frontier molecular orbitals, indicating that coupling should be preferred at the position which bears the largest LUMO coefficient.[164]

To understand the character of the frontier molecular orbitals involved in the spirolactonization reaction, density functional theory calculations were performed. 1,2-indanedione **6.5i** (synthesized from **6.1i**), 1-phenylpropan-1,2-dione **6.5g** (synthesized from **6.1g**), two para-substituted 1-phenylpropan-1,2-dione derivatives, 1-(4-methoxyphenyl)propane-1,2-dione **6.5m** and methyl 4-(2-oxopropanoyl)benzoate **6.5n** with varying electronic character in the aromatic ring were evaluated to deduce the role of the electronics in each system as it applied to regioselectivity. The experimentally observed regioselectivities when 1,2-diols **6.1g**, **i**, **m**, **n** are subjected to the reaction conditions as well as the calculated LUMO coefficients are presented in Table 6.2.

Table 6.2 LUMO coefficients and experimentally observed regioselectivities for diketones **6.5i**, **g**, **m**, and **n**.

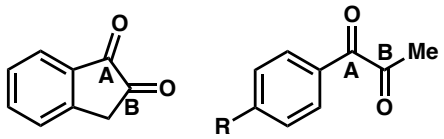

Dione	LUMO Coefficient A	B	Δ(A-B)	Experimental Ratio (A:B)
6.5i	-0.12189	-0.10896	0.013	1:>20
6.5m, R=OMe	-0.13750	-0.11802	0.019	1.3:1
6.5g, R=H	-0.13943	-0.11213	0.027	4:1
6.5n, R=CO_2Me	-0.13353	-0.09587	0.038	10:1

The carbonyl at the benzylic position (**A**) bore a larger LUMO coefficient than the carbonyl distal to the aromatic ring (**B**) for each diketone examined. While this is consistent with the observed regioselectivities for acyclic diketones **6.5g**, **m-n**, it did not explain the regioselectivity observed for 1,2-indanedione **6.5i**. However, it was found that as the difference between the LUMO coefficients at each carbonyl increased, so did the regioselectivity in favor of coupling at the benzylic carbonyl. The smallest difference in LUMO coefficients was found to be for 1,2-indanedione **6.5i** (0.013), which coupled at carbonyl **B** with complete regioselectivity. However, in the acyclic systems the smallest difference in LUMO coefficients was calculated for **6.5m** (0.019), but the spirolactone product was generated as a 1.3:1 mixture of regioisomers. Increasing the electron-deficient character of the aromatic ring, such as in the case of diketone **6.5n**, led to a larger gap in LUMO coefficients (0.038) and corresponded to a product that was a 10:1 mixture of regioisomers. While this trend is consistent with the observed regioselectivity, one must also consider other factors that could rationalize such a drastic change in regioselectivity. One such factor to be considered is that the DFT calculations were performed on the ground state diketones, which coordinate to ruthenium prior to oxidative coupling. DFT calculations of the ruthenium-bound diketones could reveal useful information about the reactivity, however the complexity of such calculations deterred further investigation.

Another consideration is that of the steric environment around either of the carbonyls. In the case of 1,2-indanedione **6.5i**, the majority of the atoms are sp^2 hybridized, resulting in a mostly planar molecular structure. As a result of this geometry, ketone **A** (Figure 6.6) would be coplanar with both an aryl hydrogen as well as ketone **B**, whereas ketone **B** is flanked by carbonyl **A** as well as a non-eclipsed methylene. This environment may favor coupling at ketone **B** further removed from the aromatic ring. In the acyclic system, for example **6.5g**, C-C bond rotation can minimize steric interactions permitting oxidative coupling to be achieved at the site bearing the larger LUMO coefficient.

Figure 6.6 Comparison of conformational flexibility of diketones **6.5i** and **6.5g**.

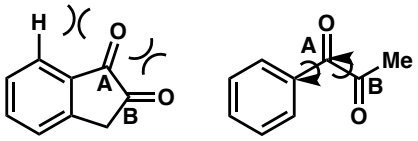

The reaction of α-hydroxy esters **6.7a-b** and 3-hydroxyoxindole **6.9** likely proceed through a similar mechanism to that shown in Figure 6.4. The stereochemical model shown in Figure 6.7 may explain the high levels of diastereoselectivity attained upon spirolactonization. One can envision that in the favored transition state, the metallacycle orients the ester substituent away from the ruthenium, and the ester and methyl substituents are positioned on opposite sides of the ring to avoid eclipsing interactions.

Figure 6.7 Stereochemical model for the diastereoselectivity observed in the oxidative coupling involved in spirooxindole formation.

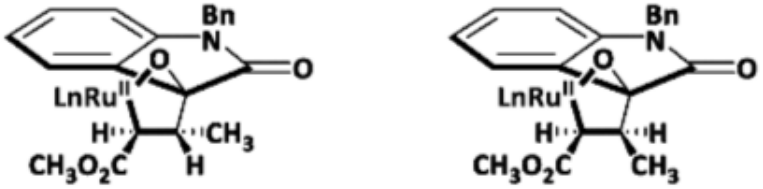

This model accurately describes the stereochemistry observed in spirooxindole formation, but further investigation of the role that the basic additives play in the diastereoselectivity was

also warranted. If the oxidative coupling were a concerted event, it would be anticipated that the favored transition state in Figure 6.7 would lead to formation of a single diastereomer. However, if protonolysis of the metallacycle occurs and generates the *C*-bound enolate, β-hydride elimination followed by another hydrometallation could scramble the stereocenter and lead to erosion of diastereoselectivity. Alternatively, upon protonolysis of the metallacycle, retro-Michael addition could expel 3-hydroxyoxindole **6.9** and could potentially scramble the olefin geometry of the crotonic ester **6.2c**. In other ruthenium catalyzed reactions, acceleration of ligand exchange is proposed when alkoxide additives are employed.[165] In the spirolactonization reaction, it is proposed that high levels of diastereoselectivity are the result of increased turnover and the prevention of other modes of reactivity that could erode the selectivity (Scheme 6.12).

Scheme 6.12 Proposed role of basic additives in the diastereoselectivity of spirooxindole formation.

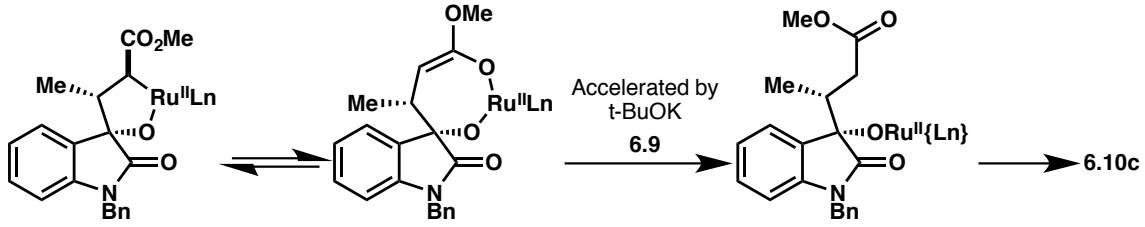

6.3 Conclusion

In summary, this work illustrates the conversion of 1,2-diols **6.1a-l**, α-hydroxy esters **6.7a-b**, and 3-hydroxyoxindole **6.9** to spirolactone products **6.3a-l**, **6.6b**, **6.8a-b**, and **6.10a**, **c-i** via coupling with acrylic esters **6.2a-i**. Direct transformation of inexpensive chemical feedstocks into complex molecules is of great importance in industrial synthesis. In that spirit, this reaction employs readily available, highly tractable diols and furnishes structurally complex and highly functionalized products. One limitation of this methodology is that use of substituted acrylic esters was not tolerated except when coupling to 3-hydroxyoxindole, which afforded spirooxindole products with complete levels of diastereoselectivity. Additionally, attempts at developing an asymmetric variant under the ruthenium catalysis conditions described were

unsuccessful. Furthermore, application of this methodology to simple, unactivated ketones is an unmet challenge. Expansion of the substrate scope and conditions for asymmetric induction will make this a more valuable and useful method.

6.4 Experimental Details

6.4.1 General Information

All reactions were run under an atmosphere of argon in sealed tubes (13x100 mm^2), dried overnight in an oven and cooled under a stream of argon prior to use. Anhydrous solvents were distilled using solvent stills and solvent was transferred by oven-dried syringe. Catalyst $Ru_3(CO)_{12,}$ all ligands and acid additives were used without purification. Diols **6.1c**, **6.1g**, **6.1h** and **6.1i** were prepared from the corresponding alkene using the protocol described by Hayashi et al.[166] Diol **6.1j** was prepared according to the method described by Rodrigues et al.[167] Diols **6.1k** and **6.1m** were prepared according to the method described by Dakdouki et al.[168] Diol **6.1l** was prepared from the corresponding chromene[169] by osmium catalyzed dihydroxylation. Hydroxyester **6.7b** was prepared by reduction of the corresponding oxoester[170] by the method described by Hui et al.[171] 3-Hydroxyoxindole **6.9** was prepared by the method described by Autrey and Tahk.[172] Alkynes were prepared by Sonagashira coupling, in a method analogous to that described by Krische et al.[143b] Thin-layer chromatography (TLC) was carried out using 0.25 mm commercial silica gel plates (Silicycle Siliaplate F-254). Visualization was accomplished with UV light followed by staining. Purification of product was carried out by flash column chromatography using Silicycle silica gel (40-63 um), according to the method described by Still.[173]

6.4.2 Spectrometry and Spectroscopy

Infrared spectra were recorded on a Thermo Nicolet 380 spectrometer. Low- and high-resolution mass spectra (LRMS or HRMS) were obtained on a Karatos MS9 and are reported as m/z (relative intensity). Accurate masses are reported for the molecular ion or a suitable fragment ion. Melting points were obtained on a Stuart SMP3 apparatus and are uncorrected. ^1H

NMR spectra were recorded on a Varian Gemini (400 MHz) spectrometer at ambient temperature. Chemical shifts are reported in delta (d) units, parts per million (ppm), relative to the center of the singlet at 7.26 ppm for deuteriochloroform, or other reference solvents as indicated. Data are reported as chemical shift, multiplicity (s=singlet, d=doublet, t=triplet, q=quartet, m=multiplet), integration and coupling constant(s) in Hz. ^{13}C NMR spectra were recorded on a Varian Gemini (100 MHz) spectrometer and were routinely run with broadband decoupling. Chemical shifts are reported in ppm, with the residual solvent resonance employed as the internal standard ($CDCl_3$ at 77.0 ppm). Regiochemical assignments were made by HMBC or NOESY NMR experiments.

6.4.3 Computational Analysis

All structures were optimized and characterized to determine each atom's contribution to the LUMO orbital. Density functional theory (DFT) calculations were carried out with QChem 4.0 using B3LYP hybrid functional and G-311G(d,p) basis set.

6.4.4 General Procedures for Spirolactonization

General Procedure A: To a re-sealable pressure tube (13 x 100 mm) equipped with magnetic stir bar, diol (or hydroxy ester) (0.3 mmol, 100 mol%), $Ru_3(CO)_{12}$ (3.8 mg, 0.006 mmol, 2 mol%), 1,3-bis(diphenylphosphino)propane (7.4 mg, 0.018 mmol, 6 mol%), and 1-adamantanecarboxylic acid (5.4 mg, 0.03 mmol, 10 mol%). The tube was sealed with a rubber septum and purged with argon. Methyl acrylate (**2a**) (81 μL, 0.90 mmol, 300 mol%) and *m*-xylene (0.22 mL, 1.0 M overall) were added. The rubber septum was quickly replaced with a screw cap. The mixture was heated at 140 °C (oil bath temperature) for 20 h, at which point the reaction mixture was allowed to cool to ambient temperature. The reaction mixture was concentrated and subjected to flash column chromatography to furnish the corresponding product of spirolactonization.

General Procedure B: To a re-sealable pressure tube (13 x 100 mm) equipped with magnetic stir bar, 1-benzyl-3-hydroxyoxindole (**6.9**) (72 mg, 0.30 mmol, 100 mol%), $Ru_3(CO)_{12}$

(3.8 mg, 0.006 mmol, 2 mol%), 2,2';6,2"-terpyridine (4.2 mg, 0.018 mmol, 6 mol%) and KO*t*Bu (3.3 mg, 0.03 mmol, 10 mol%) was added. The tube was sealed with a rubber septum and purged with argon. Acrylic ester (0.90 mmol, 300 mol%) and *m*-xylene (1.0 M overall) were added. The rubber septum was quickly replaced with a screw cap. The mixture was heated at 140 °C (oil bath temperature) for 20 h, at which point the reaction mixture was allowed to cool to ambient temperature. The reaction mixture was concentrated and subjected to flash column chromatography to furnish the corresponding product of spirolactonization.

6.4.5 Characterization of 6.3a-l, 6.6b, 6.8a-b, 6.10a, c-i

1-oxaspiro[4.5]decane-2,6-dione (6.3a)

In accordance with general procedure A using *trans*-**6.1a**, upon stirring at 140 °C for 20 h, the reaction mixture was concentrated and subjected to flash column chromatography (SiO_2: 50% EtOAc/hexanes) to furnish **6.3a** (48 mg, 0.29 mmol, 96% yield) as a clear, yellow oil. *The spectroscopic properties of this compound were consistent with the data available in the literature.*[156b]

TLC (SiO_2): R_f = 0.23 (hexanes:EtOAc = 1:1).

^{1}H NMR: (400 MHz, $CDCl_3$): δ 2.77-2.67 (m, 2H) 2.53 (dd, *J* = 9.5, 2.1 Hz, 1H), 2.52-2.50 (m, 1H), 2.47-2.41 (m, 1H), 2.20 (dddd, *J* = 13.2, 6.6, 3.5, 1.8 Hz, 1H), 2.04-1.67 ppm (m, 6H).

^{13}C NMR: (100 MHz, $CDCl_3$): δ 206.0, 175.5, 88.3, 39.2, 38.8, 28.7, 28.2, 26.8, 21.5 ppm.

HRMS (ESI): Calculated for $C_9H_{12}O_3$ $[M+Na]^+$: 191.06790, Found: 191.06790.

FTIR (neat): 3538, 2943, 2868, 1776, 1718, 1451, 1421, 1339, 1316, 1253, 1201, 1171, 1145, 1131, 1112, 1094, 1057, 1024 cm^{-1}.

^{1}H NMR of **6.3a**

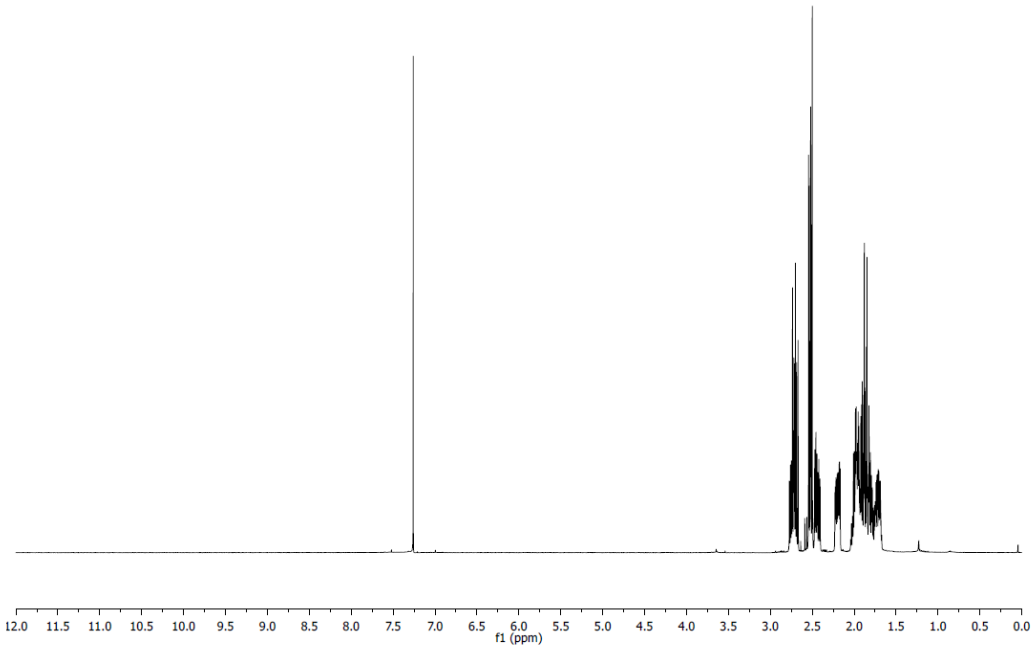

^{13}C NMR of **6.3a**

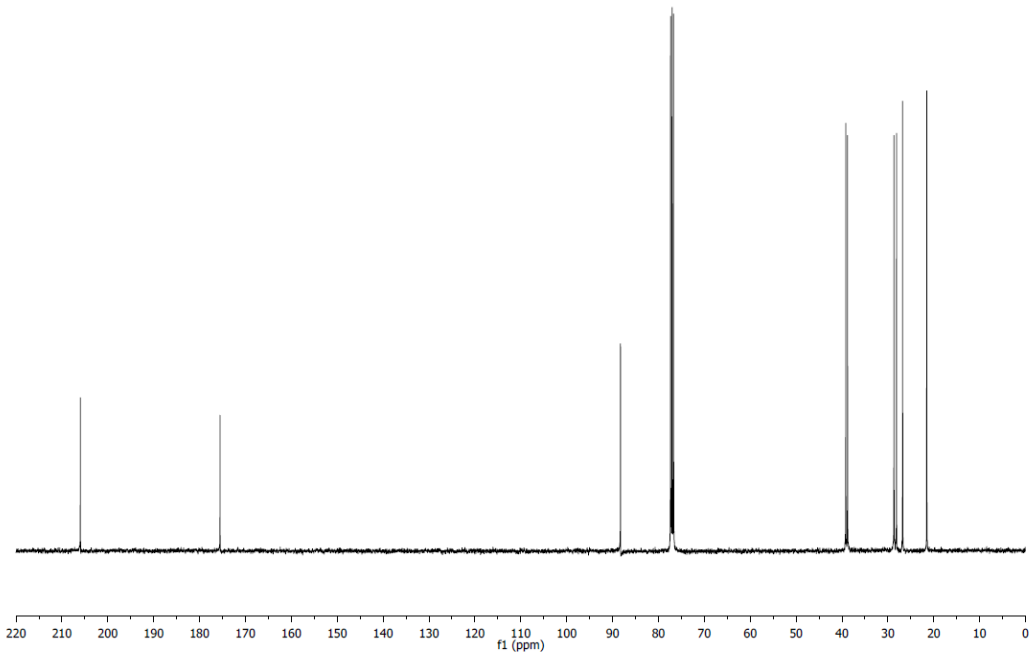

1-oxaspiro[4.4]nonane-2,6-dione (6.3b)

In modification of general procedure A using *cis*-**6.1b**, upon addition of $Ru_3(CO)_{12}$ (3.8 mg, 0.006 mmol, 2 mol%), 1,3-bis(diphenylphosphino)propane (7.4 mg, 0.018 mmol, 6 mol%), and 1-adamantanecarboxylic acid (5.4 mg, 0.03 mmol, 10 mol%), the reaction tube was sealed with a rubber septum and purged with argon. Methyl acrylate (**2a**) (109 μL, 1.20 mmol, 400 mol%) and *m*-xylene (0.19 mL, 1.0 M overall) were added upon stirring at 140 °C for 20 h, the reaction mixture was concentrated and subjected to flash column chromatography (SiO_2: 30% EtOAc/hexanes) to furnish **6.3b** (39 mg, 0.25 mmol, 85% yield) as a colorless solid. *The spectroscopic properties of this compound were consistent with the data available in the literature*.[156a]

TLC (SiO_2): R_f = 0.17 (hexanes: EtOAc = 3:1).

^{1}H NMR: (400 MHz, $CDCl_3$): δ 2.81 (dt, *J* = 9.7, 9.6 Hz, 1H), 2.57 (ddd, J = 17.8, 9.8, 4.0 Hz, 1H), 2.48-2.31 (m, 4H), 2.19-2.01 (m, 3H), 1.98-1.88 ppm (m, 1H).

^{13}C NMR: (100 MHz, $CDCl_3$): δ 213.6, 175.8, 86.6, 35.2, 35.0, 28.7, 28.1, 17.8 ppm.

MP: 103 – 104 °C.

HRMS (ESI): Calculated for $C_8H_{10}O_3$ $[M+Na]^+$:177.05220, Found: 177.05180.

FTIR (neat): 1981, 1772, 1745, 1454, 1398, 1246, 1222, 1156, 1037 cm^{-1}.

^{1}H NMR of **6.3b**

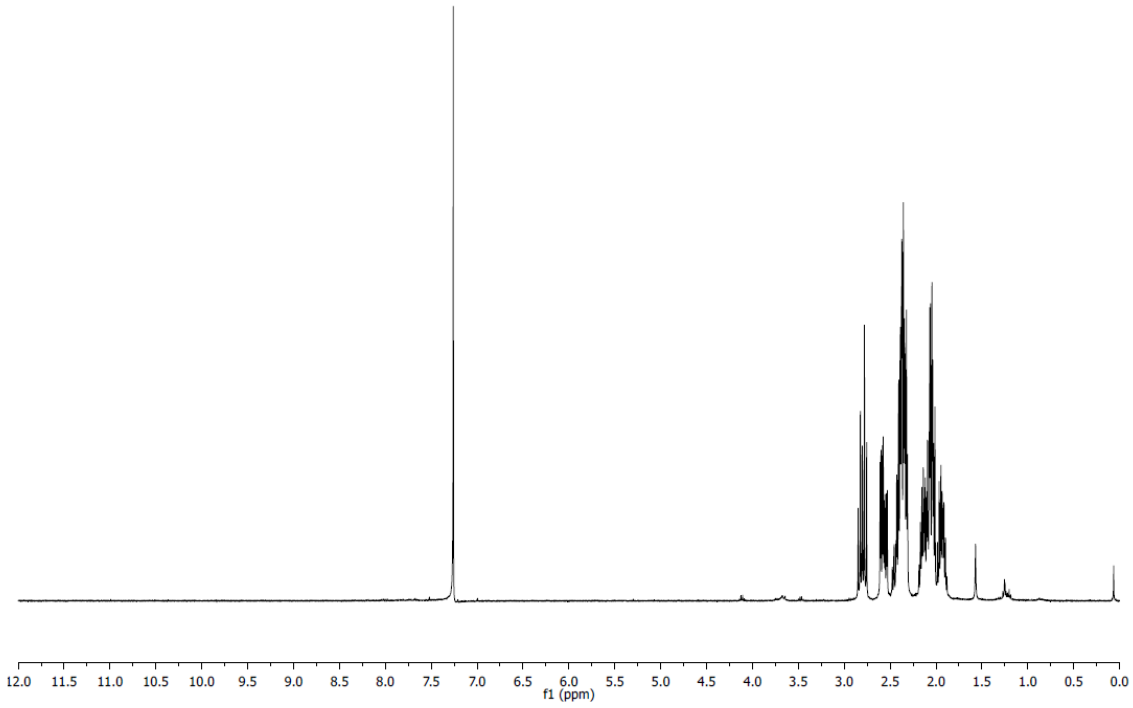

^{13}C NMR of **6.3b**

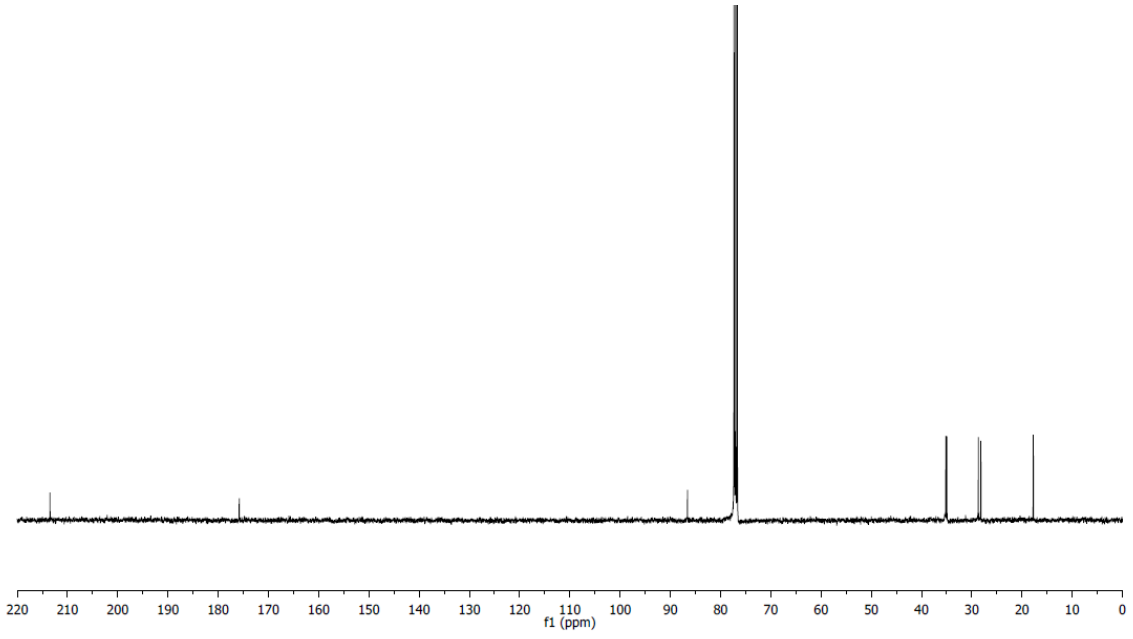

1-oxaspiro[4.6]undecane-2,6-dione (6.3c)

In accordance with general procedure A using a mixture of *cis*- and *trans*-**6.1c**, upon stirring at 140 °C for 20 h, the reaction mixture was concentrated and subjected to flash column chromatography (SiO_2: 40% EtOAc/hexanes) to furnish **6.3c** (35 mg, 0.19 mmol, 64% yield) as a colorless solid. *The spectroscopic properties of this compound were consistent with the data available in the literature*.[154a]

TLC (SiO_2): R_f = 0.3 (hexanes:EtOAc = 1:1).

^{1}H NMR: (400 MHz, $CDCl_3$): δ 2.68 (m, 1H), 2.63 – 2.49 (m, 3H), 2.42 (ddd, *J* = 13.0, 8.8, 4.1 Hz, 1H), 2.13 (ddd, *J* = 15.0, 7.1, 1.8 Hz, 1H), 1.99 (m, 1H), 1.94 – 1.56 (m, 6H), 1.41 ppm (m, 1H).

^{13}C NMR: (100 MHz, $CDCl_3$): δ 209.2, 176.0, 90.7, 40.1, 37.1, 31.3, 29.0, 27.9, 25.2, 24.7 ppm.

MP: 64 **-** 65 °C.

HRMS (ESI): Calculated for $C_{10}H_{14}O_3$ $[M+Na]^+$: 205.08350, Found: 205.08390.

FTIR (neat): 2930, 2860, 1773, 1713, 1455, 1227, 1150, 943, 694 cm^{-1}.

^{1}H NMR of **6.3c**

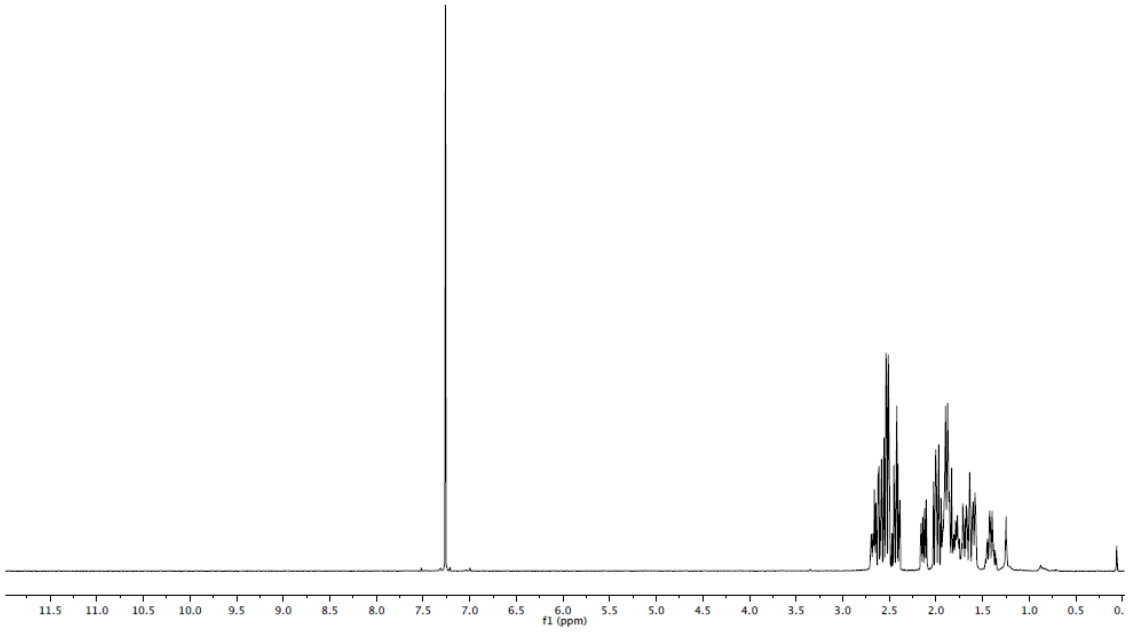

^{13}C NMR of **6.3c**

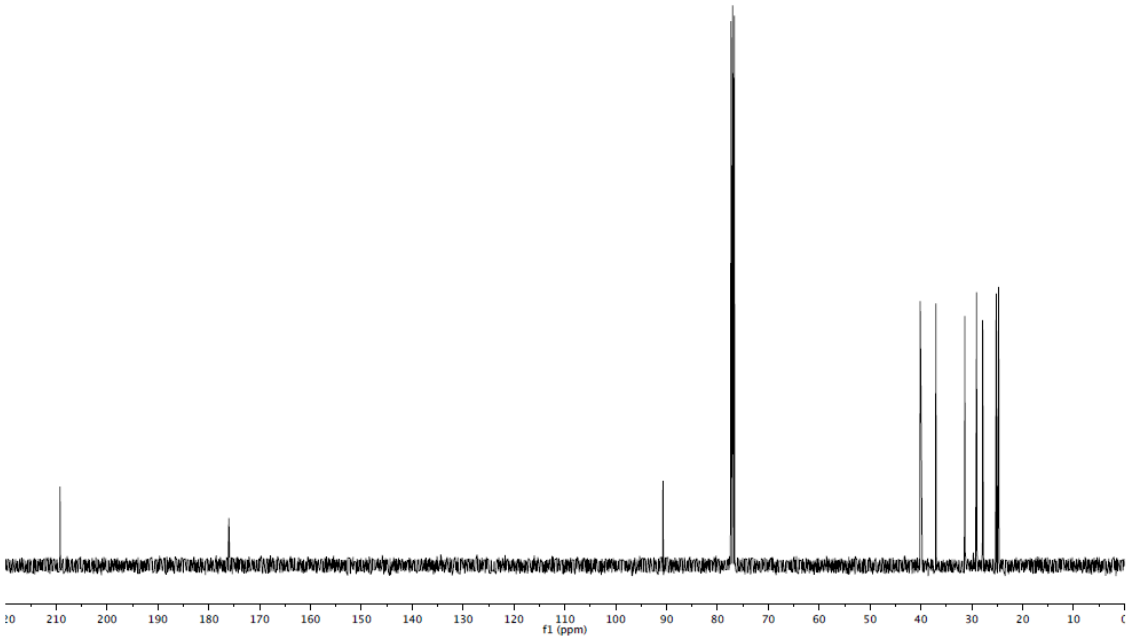

1-oxaspiro[4.7]dodecane-2,6-dione (6.3d)

In accordance with general procedure A using *cis*-**6.1d**, upon stirring at 140 °C for 20 h, the reaction mixture was concentrated and subjected to flash column chromatography (SiO_2: 40% EtOAc/hexanes) to furnish **6.3d** (46 mg, 0.24 mmol, 79% yield) as a clear yellow oil.

TLC (SiO_2): R_f = 0.27 (hexanes:EtOAc = 3:2).

^{1}H NMR: (400 MHz, $CDCl_3$): δ 2.60 (ddd, *J* = 12.2, 7.1, 4.0 Hz, 1H), 2.54-2.37 (m, 4H), 2.27 (ddd, *J* = 14.9, 11.7, 4.0 Hz, 1H), 2.10-1.92 (m, 3H), 1.90-1.62 (m, 3H), 1.60-1.34 ppm (m, 4H).

^{13}C NMR: (100 MHz, $CDCl_3$): δ 212.6, 176.0, 90.3, 38.1, 36.4, 31.0, 28.1, 27.7, 26.3, 24.4, 22.8 ppm.

HRMS (ESI): Calculated for $C_{11}H_{16}O_3$ $[M+Na]^+$: 219.09920, Found 219.09890.

FTIR (neat): 2923, 2854, 1708, 1438, 1408, 1205, 1170, 1032 cm^{-1}.

^{1}H NMR of **6.3d**

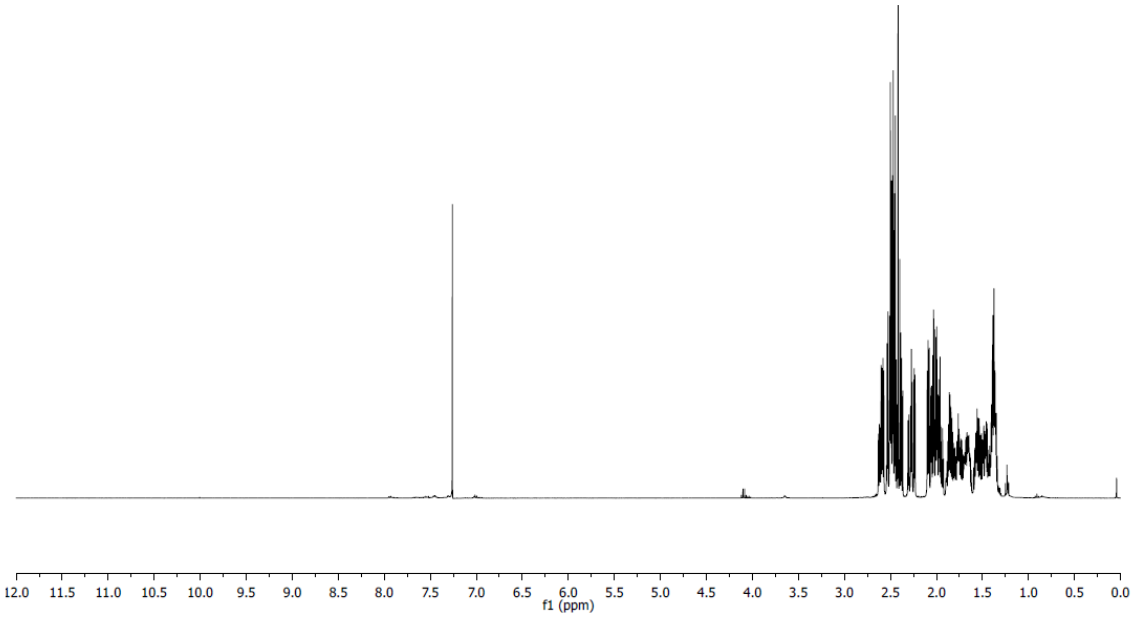

^{13}C NMR of **6.3d**

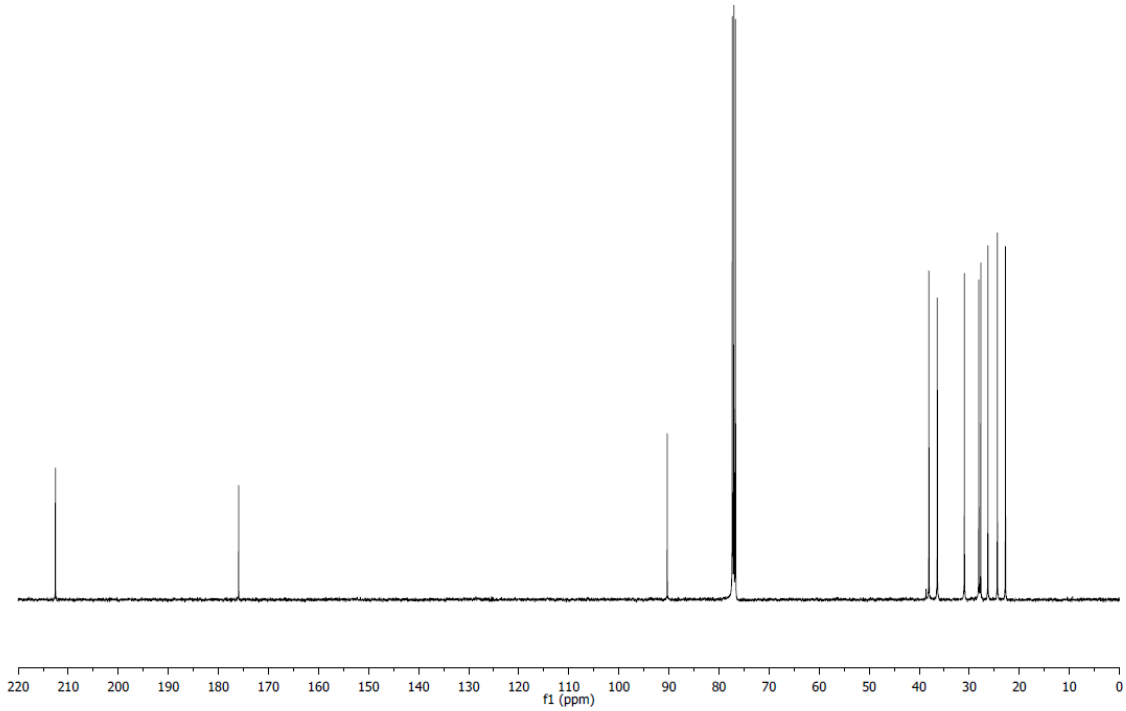

5-acetyl-5-methyldihydrofuran-2(3H)-one (6.3e)

In accordance with general procedure A using a mixture of *cis*- and *trans*-**6.1e**, upon stirring at 140 °C for 20 h, the reaction mixture was concentrated and subjected to flash column chromatography (SiO_2: 40% EtOAc/hexanes) to furnish **6.3e** (40 mg, 0.28 mmol, 93% yield) as a colorless solid. *The spectroscopic properties of this compound were consistent with the data available in the literature*.[148b]

TLC (SiO_2): R_f = 0.3 (hexanes:EtOAc = 2:1).

^{1}H NMR: (400 MHz, $CDCl_3$): δ 2.63-2.46 (m, 3H), 2.27 (s, 3H), 2.08-2.02 (m, 1H), 1.51 ppm (s, 3H).

^{13}C NMR: (100 MHz, $CDCl_3$): δ 207.1, 174.6, 88.2, 39.8, 27.3, 24.3, 22.4 ppm.

HRMS (ESI): Calculated for $C_7H_{10}O_3$ $[M+Na]^+$:165.05220, Found: 165.05200.

FTIR: (neat): 1774, 1718, 1361, 1234, 1209, 1166, 1139, 1092, 10003, 947, 903, 667 cm^{-1}.

^{1}H NMR of **6.3e**

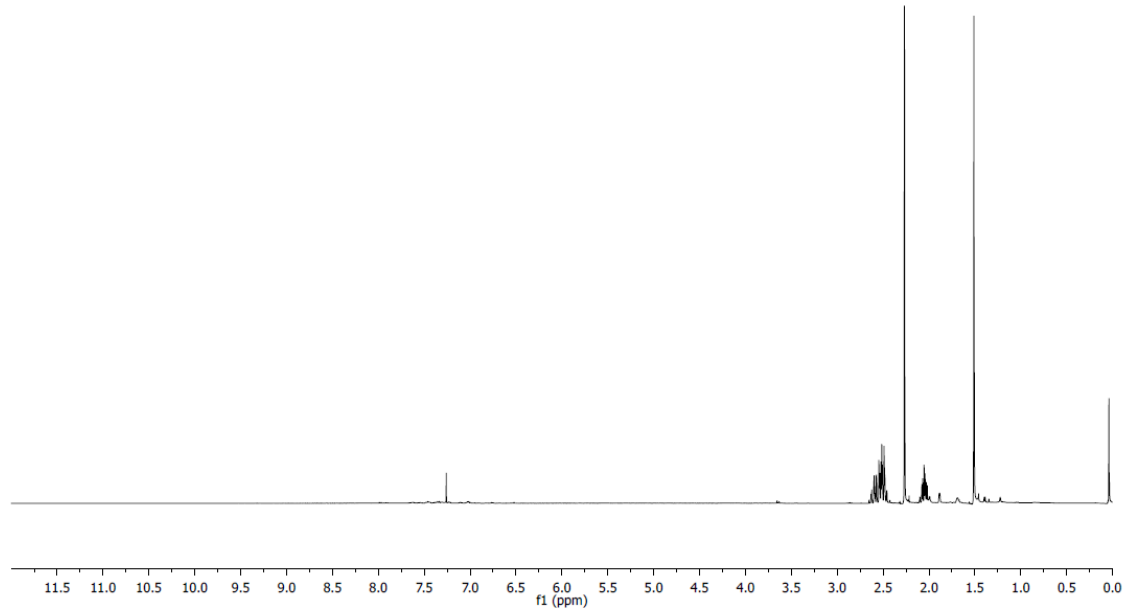

^{13}C NMR of **6.3e**

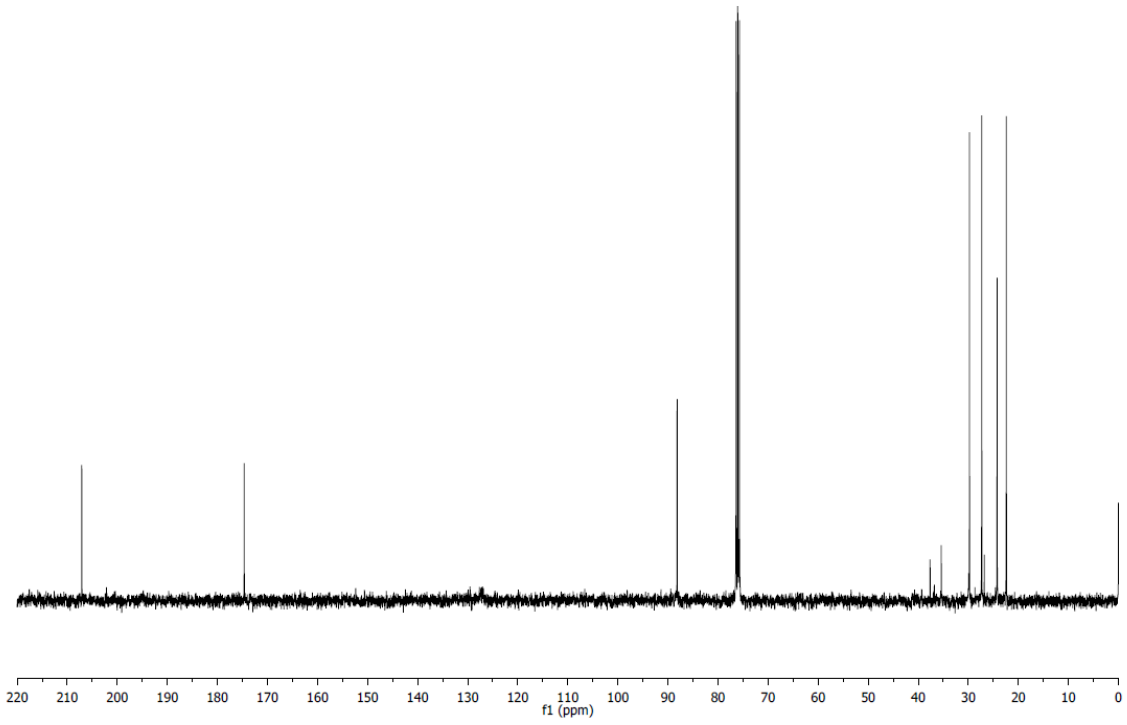

5-benzoyl-5-phenyldihydrofuran-2(3H)-one (6.3f)

In accordance with general procedure A using a mixture of *cis*- and *trans*-**6.1f**, upon stirring at 140 °C for 20 h, the reaction mixture was concentrated and subjected to flash column chromatography (SiO_2: 40% EtOAc/hexanes) to furnish **6.3f** (72 mg, 0.27 mmol, 90% yield) as a colorless oil. *The spectroscopic properties of this compound were consistent with the data available in the literature*.[148b]

TLC (SiO_2): R_f = 0.14 (hexanes:EtOAc = 9:1).

^{1}H NMR: (400 MHz, $CDCl_3$): δ 7.96-7.94 (m, 2H), 7.49-7.44 (m, 3H), 7.42-7.37 (m, 2H), 7.36-7.30 (m, 3H), 3.43 (ddd, *J* = 13.0, 8.3, 7.1 Hz, 1H), 2.60-2.55 (m, 2H), 2.34 ppm (dt, *J* = 13.0, 8.3 Hz, 1H).

^{13}C NMR: (100 MHz, $CDCl_3$): δ 195.2, 175.6, 139.3, 133.5, 133.4, 13.7, 129.3, 128.5, 128.3, 123.7, 92.1, 34.3, 28.0 ppm.

HRMS (ESI): Calculated for $C_{17}H_{14}O_3$ $[M+Na]^+$: 289.08350, Found: 289.08430.

FTIR (neat): 3062, 1784, 1580, 1597, 1448, 1268, 1159, 1086, 1056, 899, 758, 701, 687 cm^{-1}.

^{1}H NMR of **6.3f**

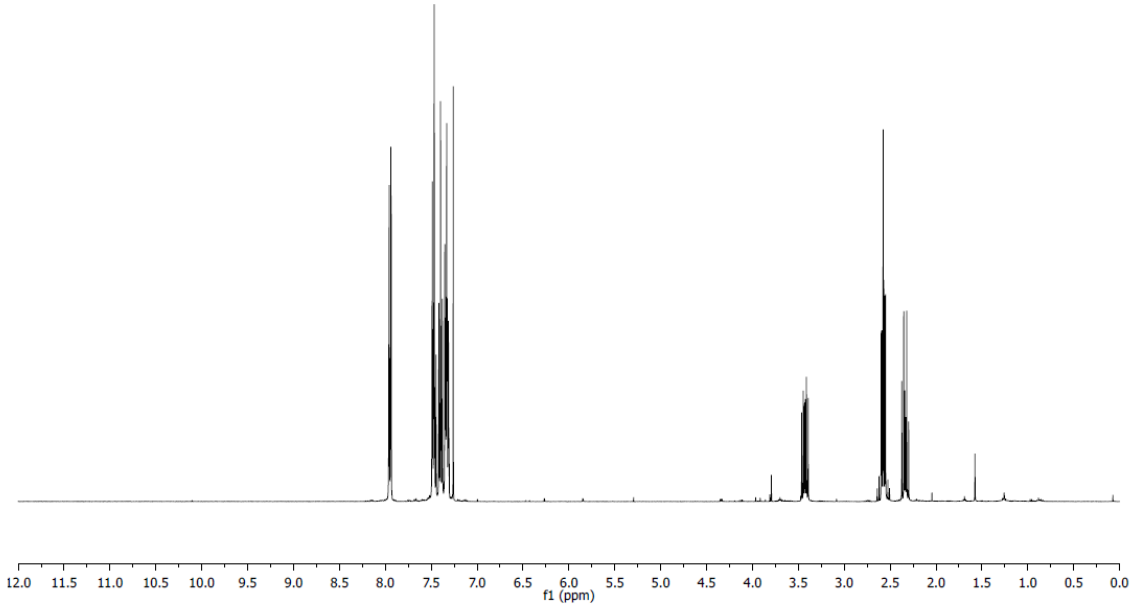

^{13}C NMR of **6.3f**

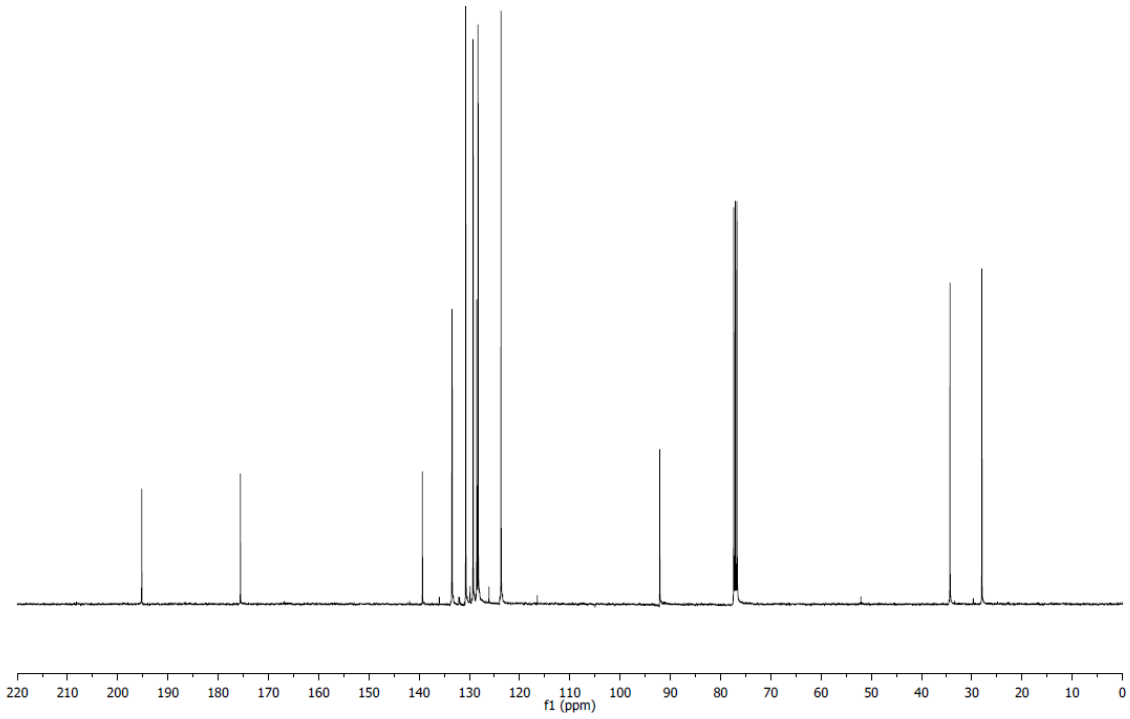

5-acetyl-5-phenyldihydrofuran-2(3H)-one (6.3g)

In accordance with general procedure A using *trans*-**6.1g**, upon stirring at 140 °C for 20 h, the reaction mixture was concentrated to afford the crude spirolactones (rr = 4:1, as determined by ^{1}H NMR spectroscopy). The crude reaction mixture was subjected to flash column chromatography (SiO_2: 30% EtOAc/hexanes) to furnish **6.3g** (36 mg, 0.18 mmol, 74% yield) as a colorless oil. *The spectroscopic properties of this compound were consistent with the data available in the literature*.[148b]

TLC (SiO_2): R_f = 0.57 (hexanes:EtOAc = 1:1).

^{1}H NMR: (400 MHz, $CDCl_3$): δ 7.46 – 7.33 (m, 5H), 3.12 (ddd, *J* = 12.9, 8.7, 7.0 Hz, 1H), 2.64 – 2.45 (m, 2H), 2.35 (m, 1H), 2.19 ppm (s, 3H).

^{13}C NMR: (100 MHz, $CDCl_3$): δ 204.7, 175.2, 137.7, 129.0, 128.8, 124.4, 92.1, 31.6, 28.2, 25.1 ppm.

HRMS (ESI): Calculated for $C_{12}H_{12}O_3$ $[M+Na]^+$: 227.06790, Found: 227.06790.

FTIR (neat): 3062, 2922, 2852, 1783, 1719, 1682, 1449, 1235, 1153, 1091, 700 cm^{-1}.

^{1}H NMR of **6.3g**

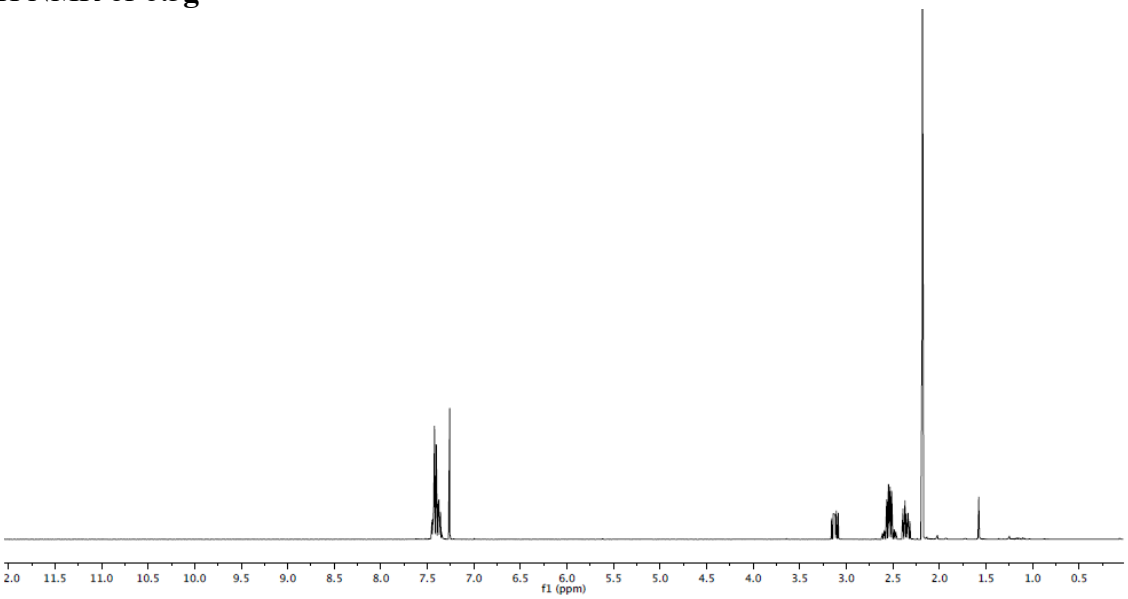

^{13}C NMR of **6.3g**

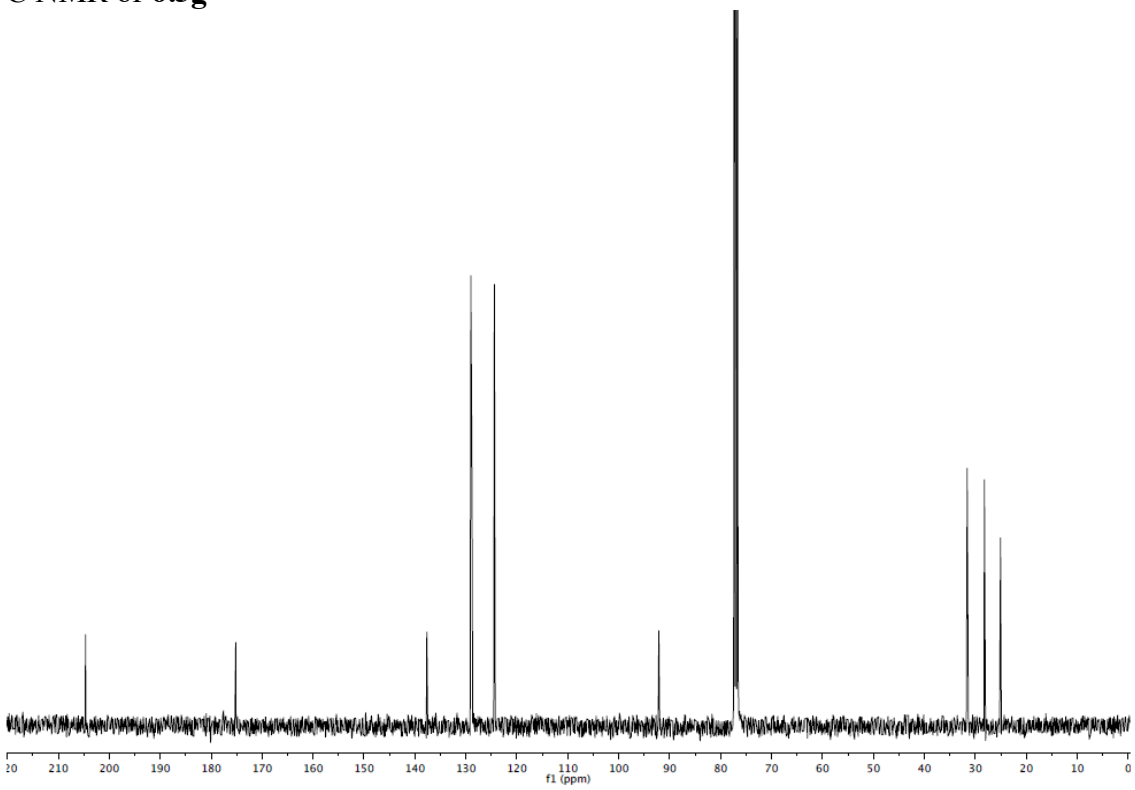

5-acetyl-5-(*tert*-butyl)dihydrofuran-2(3H)-one (6.3h)

In accordance with general procedure A using *trans*-**6.1h**, upon stirring at 140 °C for 20 h, the reaction mixture was concentrated to afford the crude spirolactones (rr = 1.3:1, as determined by ^{1}H NMR spectroscopy). The crude reaction mixture was subjected to flash column chromatography (SiO_2: 20% EtOAc/hexanes) to furnish **6.3h** (42 mg, 0.25 mmol, 75% yield) as a colorless oil.

TLC (SiO_2): R_f = 0.50 (hexanes:EtOAc = 2:1).

^{1}H NMR: (400 MHz, $CDCl_3$): δ 2.59-2.10 (m, 7.4H), 2.26 (s, 3H, *major*), 1.54 (s, 2.3H, *minor*), 1.24 (s, 7.4H, *minor*), 0.99 ppm (s, 9H, *major*).

^{13}C NMR: (100 MHz, $CDCl_3$): δ 214.9, 211.1, 175.9, 175.9, 96.8, 90.8, 44.9, 37.1, 33.4, 29.6, 28.8, 27.8, 26.9, 26.3, 26.3, 24.8 ppm.

HRMS (ESI): Calculated for $C_{10}H_{16}O_3$ $[M+Na]^+$: 207.09920, Found: 207.09910.

FTIR (neat): 2971, 1778, 1714, 1699, 1370, 1251, 1153, 1128, 1053, 1008, 904, 675 cm^{-1}.

^{1}H NMR of **6.3h**

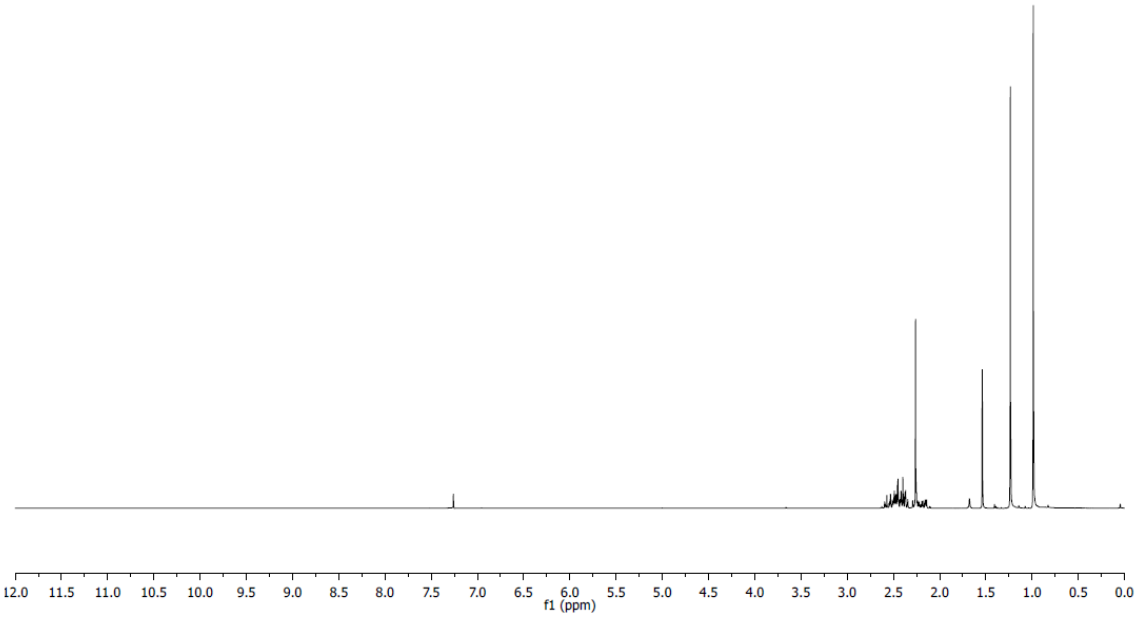

^{13}C NMR of **6.3h**

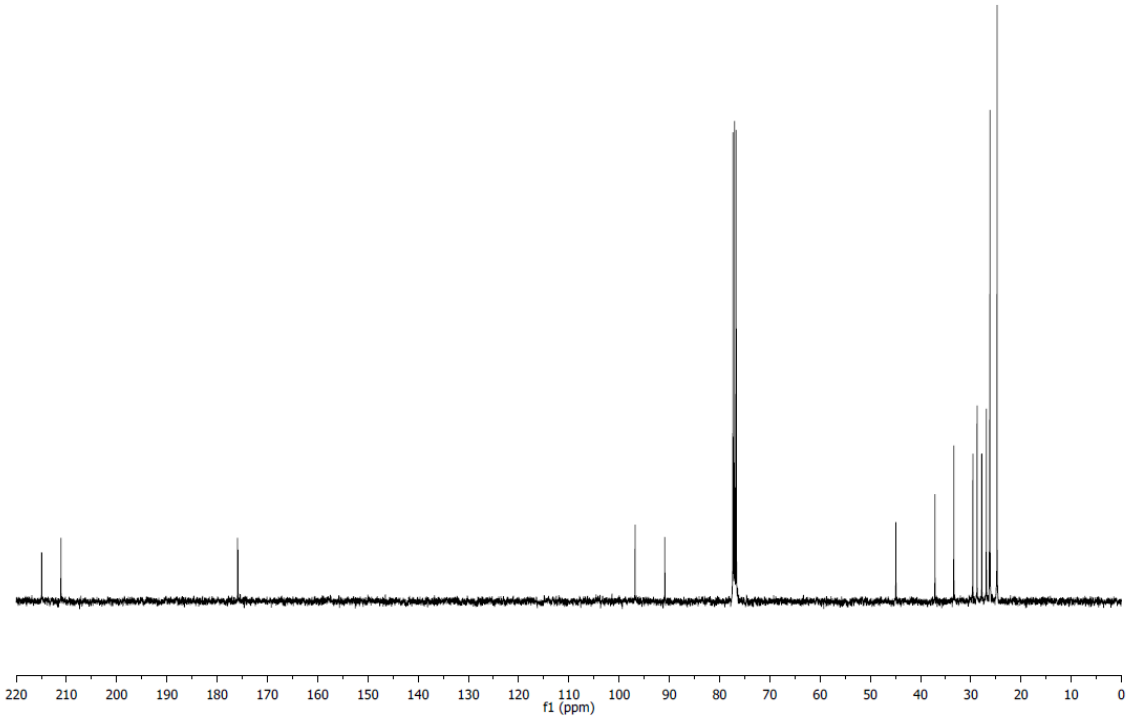

1,3-dihydrospiro[indene-2,2'-oxolane]-1,5'-dione (6.3i)

In accordance with general procedure A using *trans*-**6.1i**, upon stirring at 140 °C for 20 h, the reaction mixture was concentrated to afford the crude spirolactones (rr = >20:1, as determined by ^{1}H NMR spectroscopy). The crude reaction mixture was subjected to flash column chromatography (SiO_2: 50% EtOAc/hexanes) to furnish **6.3i** (54 mg, 0.27 mmol, 89% yield) as a colorless solid.

TLC (SiO_2): R_f = 0.35 (hexanes:EtOAc = 1:1).

^{1}H NMR: (400 MHz, $CDCl_3$): δ 7.80 (d, *J* = 7.7 Hz, 1H), 7.68 (td, *J* = 7.6, 1.2 Hz, 1H), 7.46 (m, 2H), 3.61 (d, *J* = 17.4 Hz, 1H), 3.33 (d, *J* = 17.4 Hz, 1H), 3.02 (dt, *J* = 17.7, 9.6 Hz, 1H), 2.67 (ddd, *J* = 17.7, 9.5, 4.0 Hz, 1H), 2.51 (ddd, *J* = 13.6, 9.7, 4.0 Hz, 1H), 2.27 ppm (dt, *J* = 13.1, 9.6 Hz, 1H).

^{13}C NMR: (100 MHz, $CDCl_3$): δ 201.5, 176.2, 150.1, 136.5, 133.1, 128.5, 126.6, 125.2, 86.4, 39.7, 31.2, 28.6 ppm.

MP: 68 - 70 °C.

HRMS (ESI): Calculated for $C_{12}H_{10}O_3$ $[M+Na]^+$:225.05220, Found: 225.05190.

FTIR (neat): 2942, 1776, 1713, 1603, 1462, 1227, 1167, 1061, 940, 759 cm^{-1}.

^{1}H NMR of **6.3i**

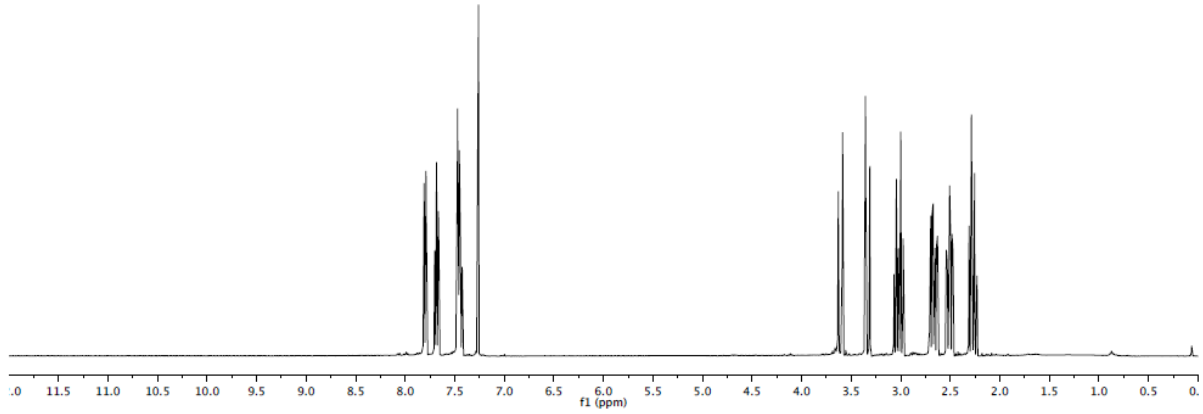

^{13}C NMR of **6.3i**

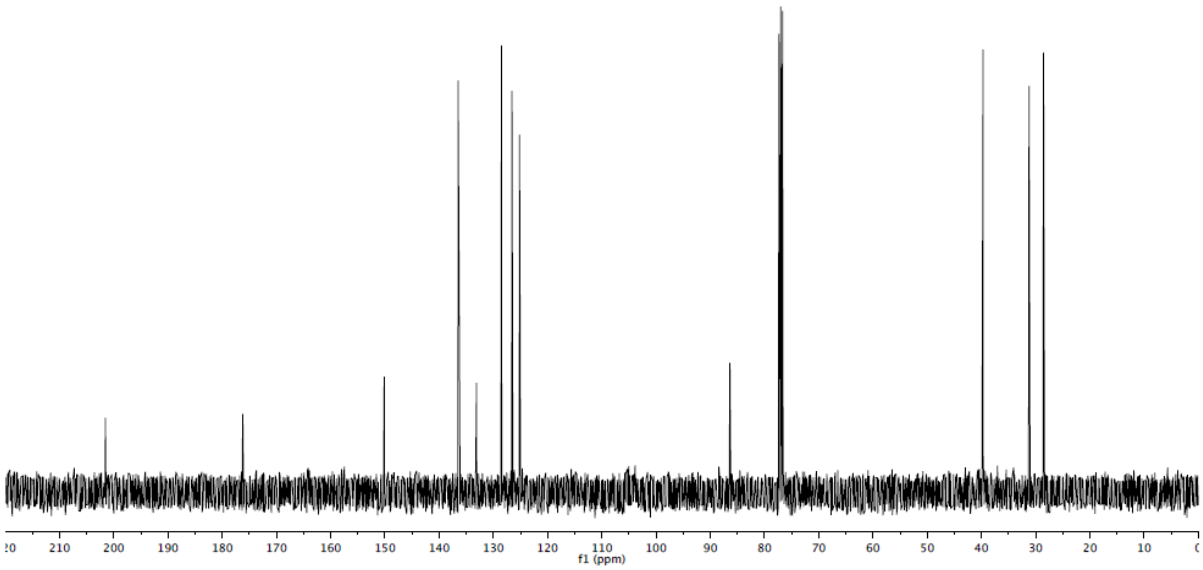

3,4-dihydro-1H-spiro[naphthalene-2,2'-oxolane]-1,5'-dione (6.3j)

In accordance with general procedure A using a mixture of *cis*- and *trans*-**6.1j**, upon stirring at 140 °C for 20 h, the reaction mixture was concentrated to afford the crude spirolactones (rr = >20:1, as determined by ^{1}H NMR spectroscopy). The crude reaction mixture was subjected to flash column chromatography (SiO_2: 30% EtOAc/hexanes) to furnish **6.3j** (57 mg, 0.26 mmol, 88% yield) as a colorless solid. *The spectroscopic properties of this compound were consistent with the data available in the literature*.[156b]

TLC (SiO_2): R_f = 0.38 (hexanes:EtOAc = 1:1).

^{1}H NMR: (400 MHz, $CDCl_3$): δ 8.07 (dd, *J* = 7.9, 1.3 Hz, 1H), 7.54 (td, *J* = 7.5, 1.4 Hz, 1H), 7.37 (dd, *J* = 7.8, 7.4 Hz, 1H), 7.28 (d, *J* = 7.8 Hz, 1H), 3.20 (dt, *J* = 17.2, 5.3 Hz, 1H), 3.09 (ddd, *J* = 17.2, 9.9, 4.7 Hz, 1H), 2.80 (ddd, *J* = 17.9, 10.8, 9.8 Hz, 1H), 2.59 (m, 3H), 2.31 (ddd, *J* = 13.5, 5.5, 5.0 Hz, 1H), 2.15 ppm (ddd, *J* = 13.0, 10.8, 9.7 Hz, 1H).

^{13}C NMR: (100 MHz, $CDCl_3$): δ193.5, 176.1, 143.0, 134.4, 130.0, 128.7, 128.5, 127.3, 85.0, 34.5, 29.6, 27.9, 25.7 ppm.

MP: 94 - 95 °C.

HRMS (ESI). Calculated for $C_{13}H_{12}O_3$ $[M+Na]^+$:239.06790, Found: 239.08610.

FTIR (neat): 2951, 2937, 1772, 1687, 1602, 1454, 1217, 1067, 949, 743 cm^{-1}.

^{1}H NMR of **6.3j**

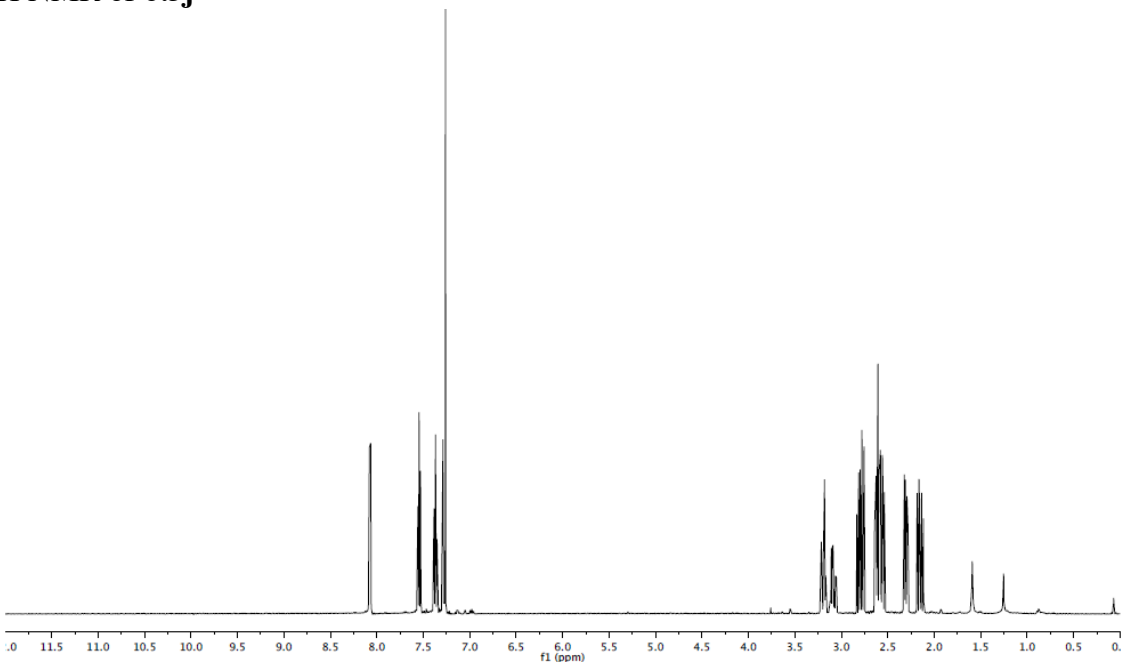

^{13}C NMR of **6.3j**

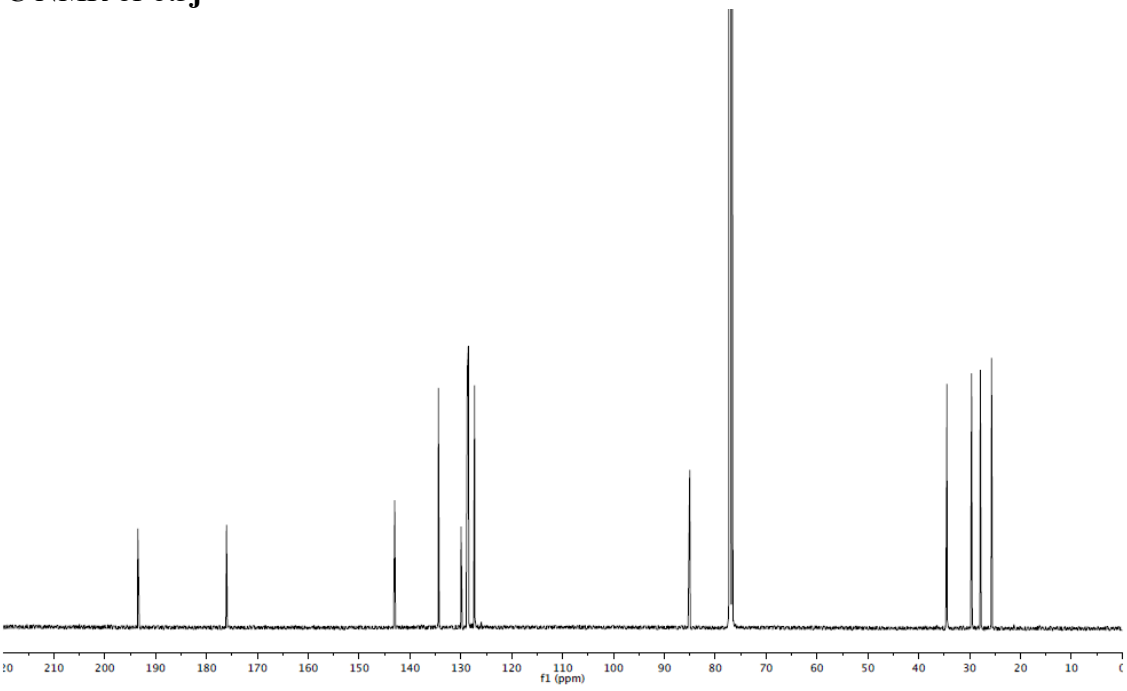

2H,3'H-spiro[acenaphthylene-1,2'-furan]-2,5'(4'H)-dione (6.3k)

In accordance with general procedure A using a mixture of *cis*- and *trans*-**6.1k**, upon stirring at 140 °C for 20 h, the reaction mixture was concentrated and subjected to flash column chromatography (SiO_2: 20% EtOAc/hexanes) to furnish **6.3k** (42 mg, 0.18 mmol, 59% yield) as a tan solid.

TLC (SiO_2): R_f = 0.28 (hexanes:EtOAc = 3:1).

^{1}H NMR: (400 MHz, $CDCl_3$): δ 8.19 (dd, *J* = 8.3, 0.6 Hz, 1H), 8.03 (dd, *J* = 7.1, 0.7 Hz, 1H), 7.98 (dd, *J* = 8.3, 0.7 Hz, 1H), 7.80 (dd, *J* = 8.3, 7.1 Hz, 1H), 7.74 (dd, *J* = 8.3, 7.1 Hz, 1H), 7.66 (dd, *J* = 7.1, 0.7 Hz, 1H), 3.25 (ddd, *J* = 17.7, 9.7, 10.4 Hz, 1H), 2.87 (ddd, *J* = 17.7, 9.0, 3.9 Hz, 1H), 2.68-2.55 ppm (m, 2H).

^{13}C NMR: (100 MHz, $CDCl_3$): δ 200.2, 176.3, 142.1, 136.1, 132.4, 130.6, 129.6, 128.9, 128.8, 126.6, 123.0, 120.8, 86.0, 31.3, 28.6 ppm.

MP: 131 - 132 °C.

HRMS (ESI): Calculated for $C_{15}H_{10}O_3$ $[M+Na]^+$:261.05220, Found: 261.05230.

FTIR (neat): 1778, 1719, 1493, 1452, 1203, 1179, 1160, 1135, 1029, 919, 876, 782 cm^{-1}.

^{1}H NMR of **6.3k**

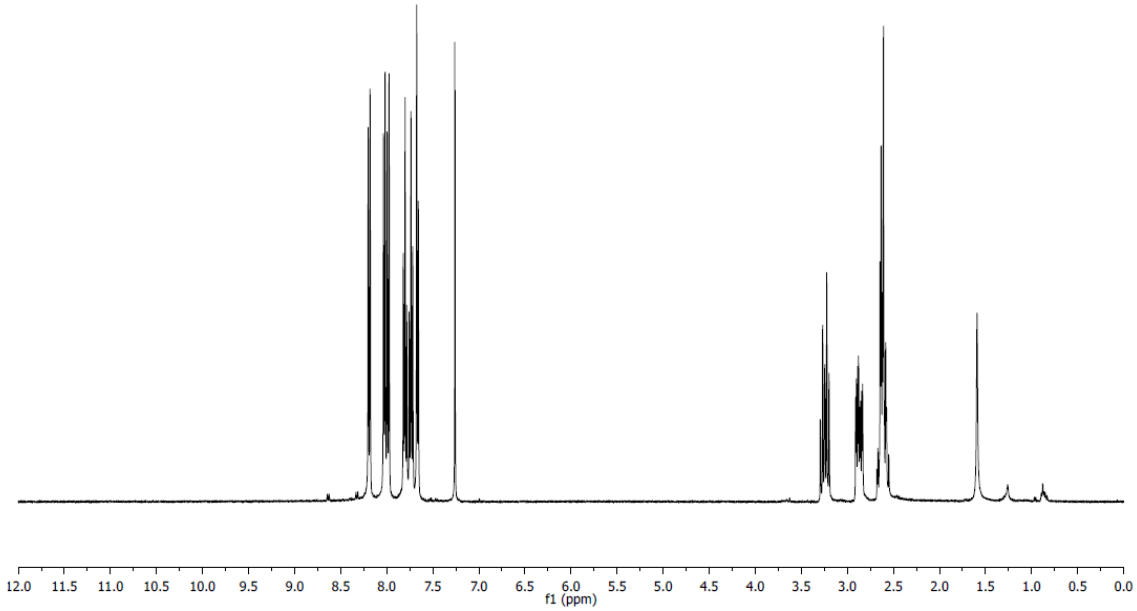

^{13}C NMR of **6.3k**

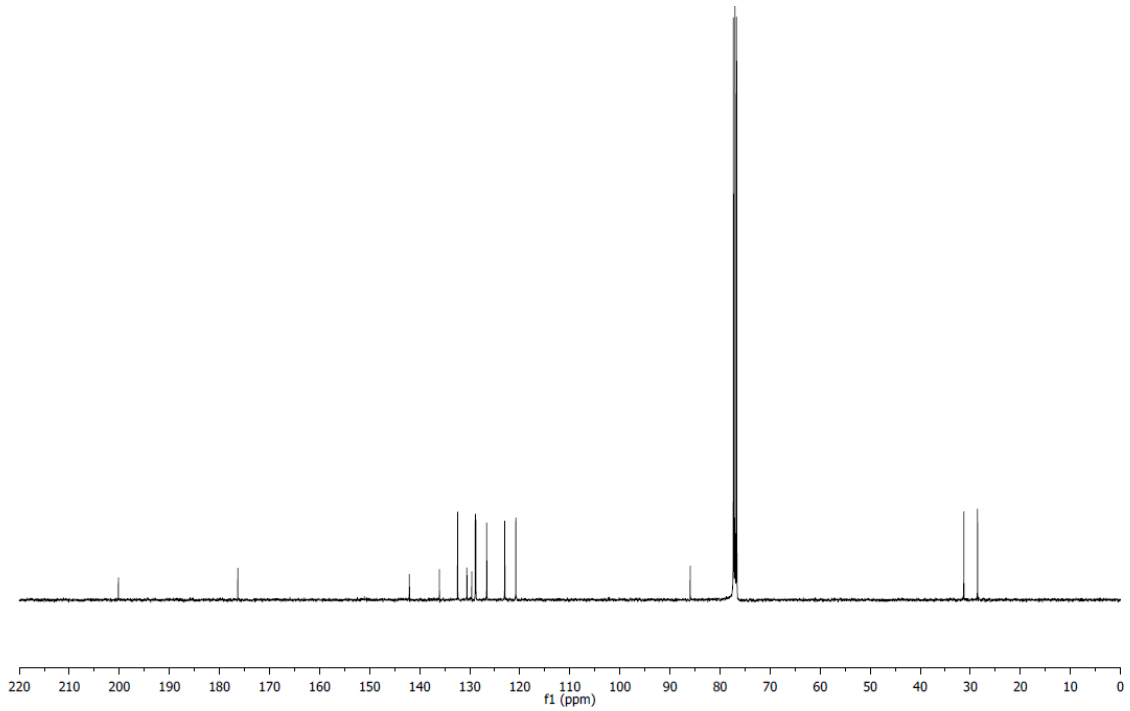

3,4-dihydro-1H-spiro[naphthalene-2,2'-oxolane]-1,5'-dione (6.3l)

In accordance with general procedure A using *cis*-**6.1l**, upon stirring at 140 °C for 20 h, the reaction mixture was concentrated to afford the crude spirolactones (rr = >20:1, as determined by ^{1}H NMR spectroscopy). The crude reaction mixture was subjected to flash column chromatography (SiO_2: 20% EtOAc/hexanes) to furnish **6.3l** (55 mg, 0.22 mmol, 74% yield) as a colorless solid.

TLC (SiO_2): R_f = 0.54 (hexanes:EtOAc = 1:1)

^{1}H NMR: (400 MHz, $CDCl_3$): δ 7.88 (dd, *J* = 7.9, 1.6 Hz, 1H), 7.53 (td, *J* = 8.5, 1.8 Hz, 1H), 7.05 (dt, *J* = 7.9, 0.9 Hz, 1H), 6.94 (dd, *J* = 8.4, 0.5 Hz, 1H), 2.74 (dt, *J* = 18.1, 10.0 Hz, 1H), 2.61 (ddd, *J* = 18.0, 9.4, 4.2 Hz, 1H), 2.36 (m, 2H), 1.49 (s, 3H), 1.46 ppm (s, 3H).

^{13}C NMR: (100 MHz, $CDCl_3$): δ 189.6, 175.4, 158.6, 137.0, 127.6, 121.7, 118.4, 118.2, 86.5, 81.8, 28.0, 24.6, 21.3, 21.2 ppm.

MP: 145 - 147 °C.

HRMS (ESI): Calculated for $C_{14}H_{14}O_4$ $[M+Na]^+$: 269.07840, Found: 269.07820.

FTIR (neat): 2982, 2921, 1776, 1703, 1610, 1462, 1424, 1327, 1307, 1165, 1138, 1065, 922, 749. cm^{-1}.

^{1}H NMR of **6.3l**

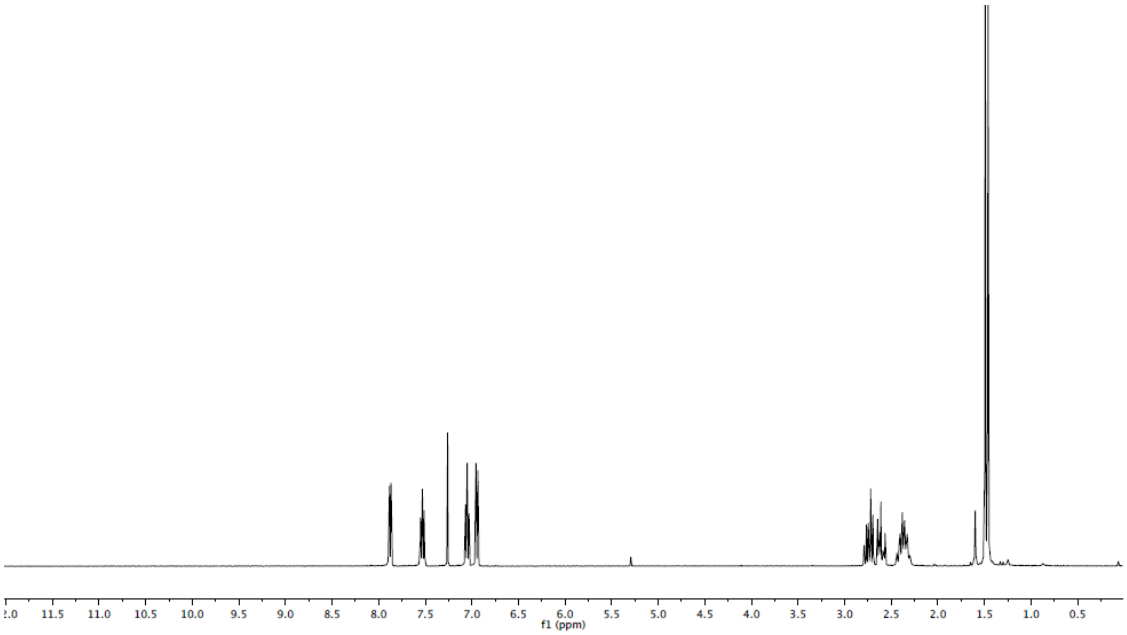

^{13}C NMR of **6.3l**

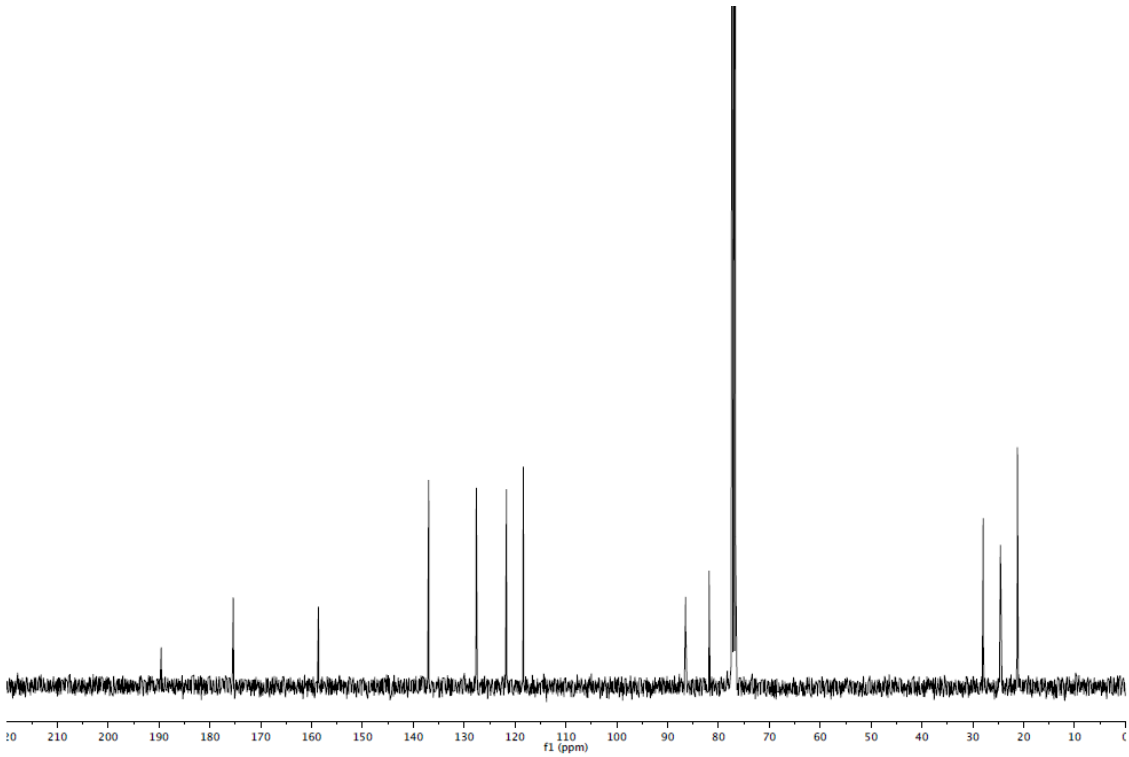

3-methylene-1-oxaspiro[4.5]decane-2,6-dione (6.6b)

In modification of general procedure A, upon addition *trans*-**6.1a** (0.3 mmol, 100 mol%), $Ru_3(CO)_{12}$ (3.8 mg, 0.006 mmol, 2 mol%), 1,3-bis(diphenylphosphino)propane (7.4 mg, 0.018 mmol, 6 mol%), and 1-adamantanecarboxylic acid (5.4 mg, 0.03 mmol, 10 mol%)., the tube was sealed with a rubber septum and purged with argon. Acrylate **6.2b** (104 mg, 0.90 mmol, 300 mol%) and m-xylenes (0.22 mL, 1.0 M overall) The reaction mixture was concentrated and subjected to flash column chromatography (SiO_2: 30% EtOAc/hexanes) to furnish **6.6b** (32 mg, 0.18 mmol, 59% yield) as a clear, colorless oil.

TLC (SiO_2): R_f = 0.23 (hexanes:EtOAc = 2:1).

^{1}H NMR: (400 MHz, $CDCl_3$): δ 6.24 (t, *J* = 2.9 Hz, 1H), 5.67 (t, *J* = 2.5 Hz, 1H), 3.53 (dt, *J* = 17.3, 2.6 Hz, 1H), 2.83 (ddd, *J* = 13.9, 10.9, 6.0 Hz, 1H), 2.51 (d, *J* = 17.3, 2.9Hz, 1H), 2.45 (m, 1H), 2.22 (m, 1H), 2.09 – 2.00 (m, 2H), 1.92 – 1.67 ppm (m, 3H).

^{13}C NMR: (100 MHz, $CDCl_3$): δ 205.1, 168.5, 133.4, 123.5, 85.3, 39.9, 38.8, 33.6, 27.1, 21.3 ppm.

HRMS (ESI): Calculated for $C_{10}H_{12}O_3$ $[M+Na]^+$: 203.06790, Found: 203.06750.

FTIR (neat): 2941, 2868, 1767, 1724, 1665, 1452, 1265, 1083, 957 cm^{-1}.

^{1}H NMR of **6.6b**

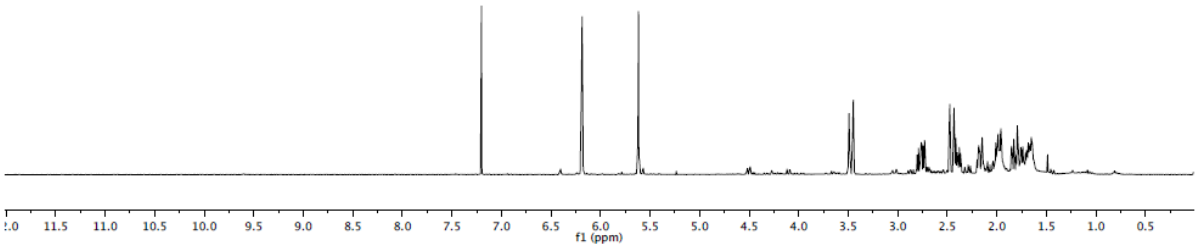

^{13}C NMR of **6.6b**

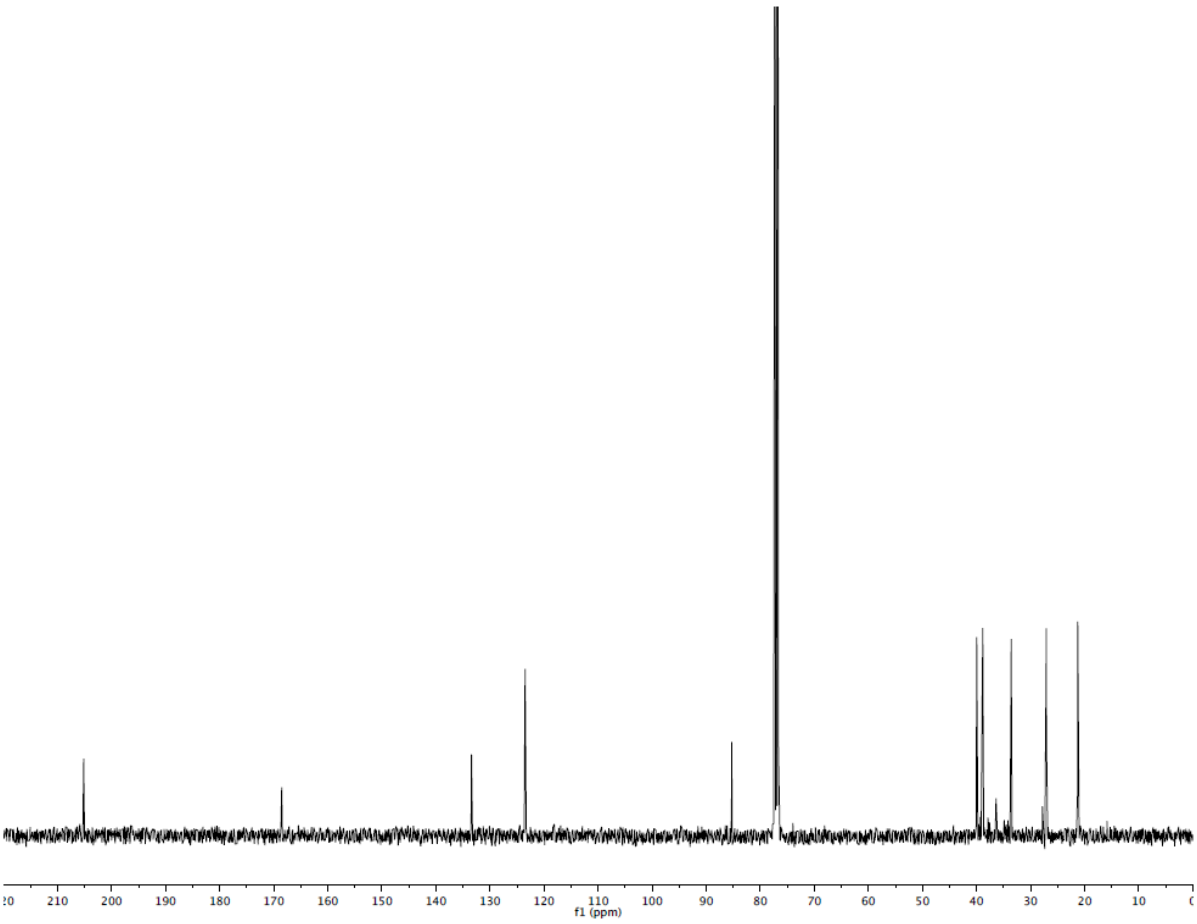

2H,3'H-spiro[acenaphthylene-1,2'-furan]-2,5'(4'H)-dione (6.8a)

In accordance with general procedure A using α-hydroxy ester **6.7a**, upon stirring at 140 °C for 20 h, the reaction mixture was concentrated and subjected to flash column chromatography (SiO_2: 30% EtOAc/hexanes) to furnish **6.8a** (64 mg, 0.29 mmol, 97% yield) as a colorless solid. *The spectroscopic properties of this compound were consistent with the data available in the literature*.[148a]

TLC (SiO_2): R_f = 0.31 (hexanes:EtOAc = 3:1).

^{1}H NMR: (400 MHz, $CDCl_3$): δ 7.52-7.50 (m, 2H), 7.42-7.34 (m, 3H), 3.75 (s, 3H), 3.10 (ddd, *J* = 10.5, 8.6, 3.1 Hz), 2.72-2.51 ppm (m, 3H).

^{13}C NMR: (100 MHz, $CDCl_3$): δ 174.9, 170.8, 138.0, 128.8, 128.7, 125.0, 53.4, 33.4, 28.1 ppm.

MP: 48 °C.

HRMS (ESI): Calculated for $C_{12}H_{12}O_4$ $[M+Na]^+$: 243.06280, Found: 243.06260.

FTIR (neat): 2957, 1783, 1737, 1450, 1262, 1228, 1190, 1156, 1091, 1058, 1005, 905, 742, 700 cm^{-1}.

^{1}H NMR of **6.8a**

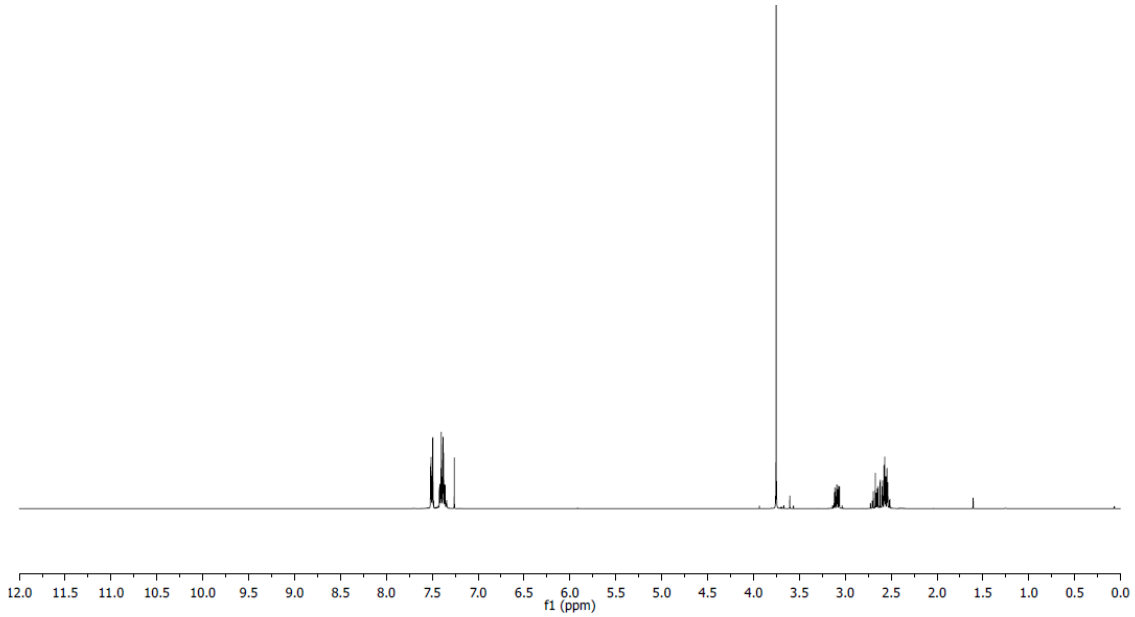

^{13}C NMR of **6.8a**

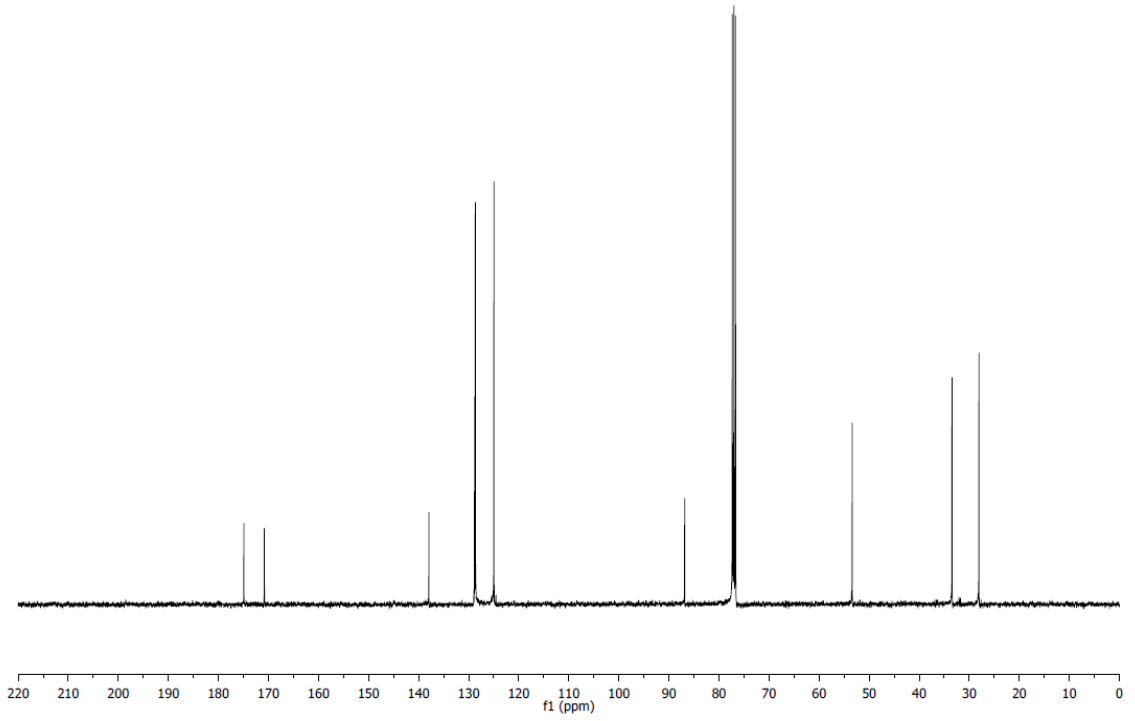

Methyl 2-(1-methyl-1*H*-indol-2-yl)-5-oxotetrahydrofuran-2-carboxylate (6.8b)

In accordance with general procedure A using α-hydroxy ester **6.7b**, upon stirring at 140 °C for 20 h, the reaction mixture was concentrated and subjected to flash column chromatography (SiO_2: 30% EtOAc/hexanes) to furnish **6.8b** (48 mg, 0.18 mmol, 58% yield) as a yellow solid.

TLC (SiO_2): R_f = 0.29 (hexanes:EtOAc = 2:1).

^{1}H NMR: (400 MHz, $CDCl_3$): δ 7.63 (dt, *J* = 8.0, 0.9 Hz, 1H), 7.36 – 7.27 (m, 2H), 7.14 (ddd, *J* = 8.0, 6.7, 1.2 Hz, 1H), 6.66 (d, *J* = 0.5 Hz, 1H), 3.79 (s, 3H), 3.75 (s, 3H), 3.06 (ddd, *J* = 12.1, 9.5, 8.2 Hz, 1H), 2.89 – 2.79 (m, 1H), 2.78 – 2.65 ppm (m, 2H).

^{13}C NMR: (100 MHz, $CDCl_3$): δ 174.9, 170.6, 138.8, 134.4, 126.3, 123.1, 121.2, 120.1, 109.5, 102.2, 82.5, 53.6, 31.5, 31.1, 27.8 ppm.

MP: 109 - 110 °C.

HRMS (ESI): Calculated for $C_{15}H_{15}NO_4$ $[M+Na]^+$: 296.08930, Found: 296.08980.

FTIR (neat): 2958, 2920, 1771, 1745, 1614, 1460, 1262, 1199, 1170, 1047, 800 cm^{-1}.

^{1}H NMR of **6.8b**

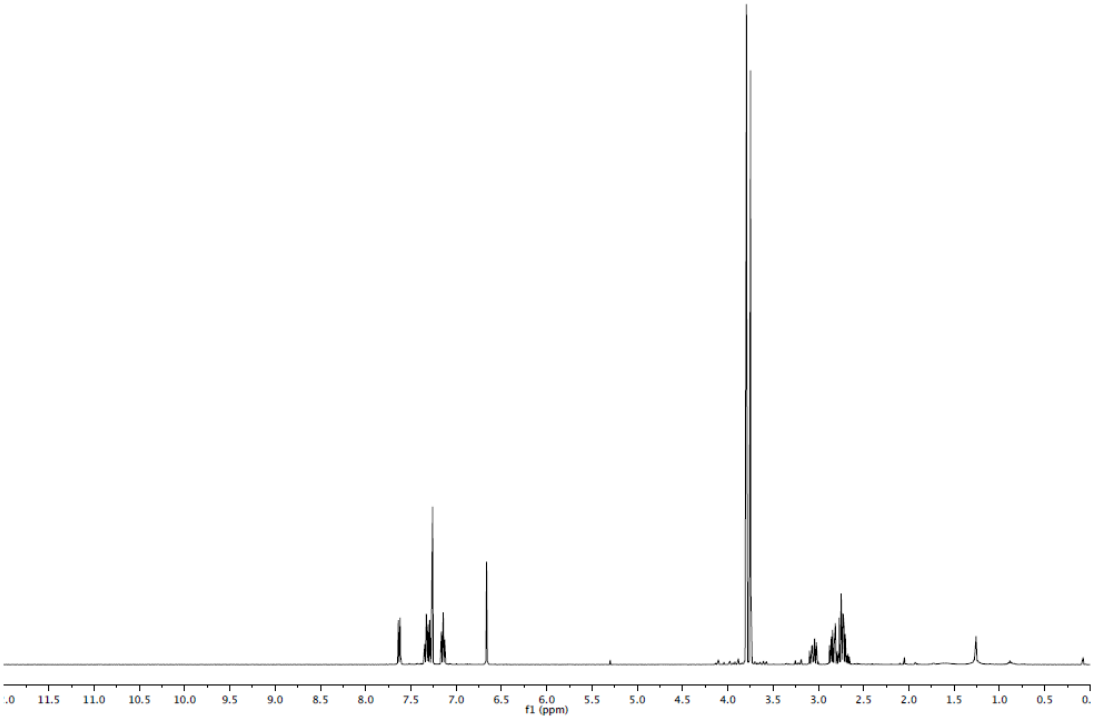

^{13}C NMR of **6.8b**

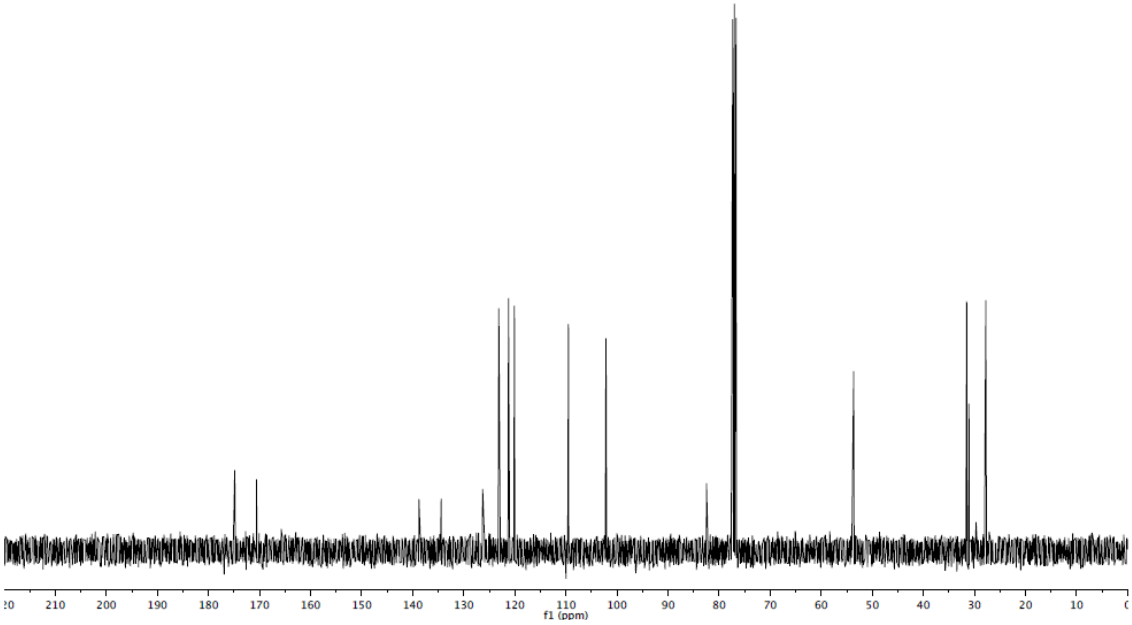

1'-benzyl-3H-spiro[furan-2,3'-indoline]-2',5(4H)-dione (6.10a)

In accordance with general procedure B using acrylic ester **6.2a**, upon stirring at 140 °C for 20 h, the reaction mixture was concentrated and subjected to flash column chromatography (SiO_2: 25% EtOAc/hexanes) to furnish **6.10a** (88 mg, 0.30 mmol, 99% yield) as a colorless solid.

TLC (SiO_2): R_f = 0.44 (hexanes:EtOAc = 5:2).

^{1}H NMR: (400 MHz, $CDCl_3$): δ 7.76-7.37 (m, 7H), 7.10 (td, J = 7.7, 0.9 Hz, 1H), 6.75 (d, *J* = 7.7 Hz, 1H), 4.88 (s, 2H), 3.26 (ddd, *J* = 17.6, 10.8, 9.7 Hz, 1H), 2.80 (ddd, *J* = 17.6, 9.6, 3.0 Hz, 1H), 2.64 (ddd, *J* = 13.4, 9.7, 3.0 Hz, 1H), 2.50 ppm (ddd, *J* = 13.4, 10.8, 9.6 Hz, 1H).

^{13}C NMR: (100 MHz, $CDCl_3$): δ 176.0, 174.4, 143.0, 134.9, 131.1, 128.9, 127.9, 127.2, 126.3, 124.3, 123.6, 109.9, 82.3, 43.9, 31.4, 28.3 ppm.

MP: 118 – 119 °C.

HRMS (ESI): Calculated for $C_{18}H_{15}NO_3$ $[M+Na]^+$: 316.09440, Found: 316.09430.

FTIR (neat): 1782, 1720, 1615, 1468, 1367, 1175, 1054, 983, 753, 723, 697, 680 cm^{-1}.

^{1}H NMR of **6.10a**

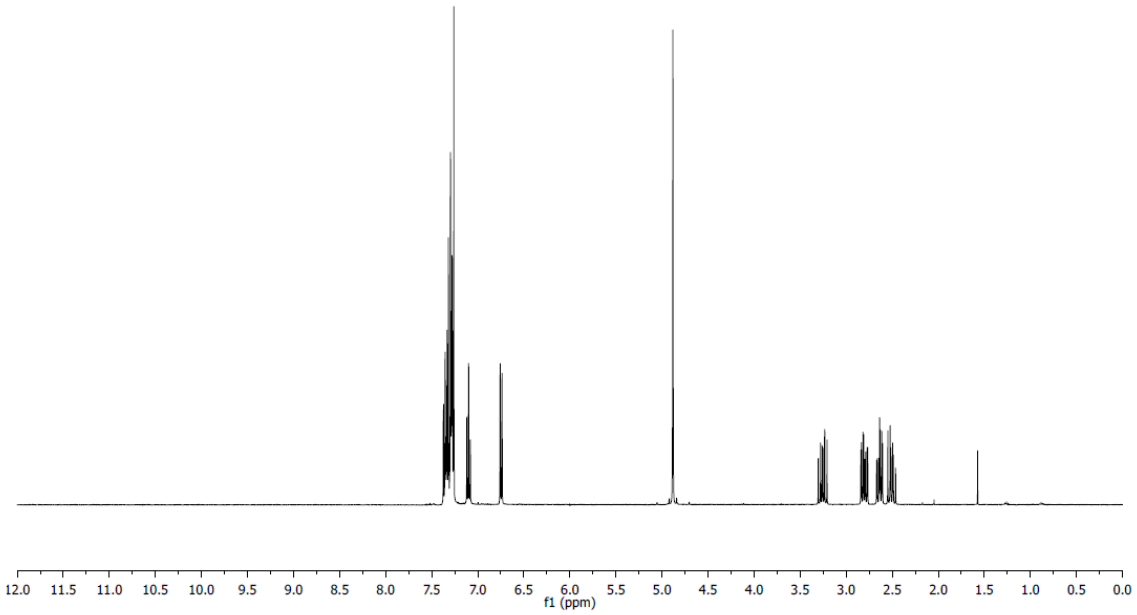

^{13}C NMR of **6.10a**

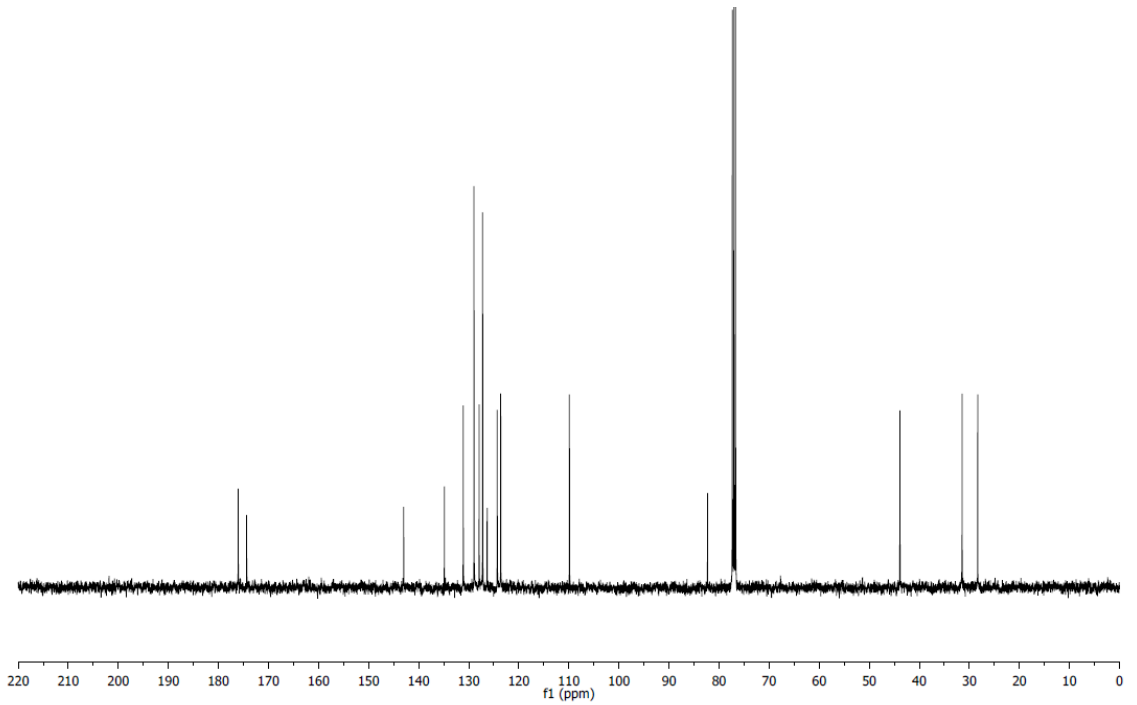

1'-benzyl-3-methyl-3H-spiro[furan-2,3'-indoline]-2',5(4H)-dione (6.10c)

In accordance with general procedure B using acrylic ester **6.2c**, upon stirring at 140 °C for 20 h, the reaction mixture was concentrated to afford the crude spirolactone (dr = >20:1, as determined by ^{1}H NMR spectroscopy). The crude reaction mixture was subjected to flash column chromatography (SiO_2: 25% EtOAc/hexanes) to furnish **6.10c** (85 mg, 0.28 mmol, 92% yield) as a colorless solid.

TLC (SiO_2): R_f = 0.50 (hexanes:EtOAc = 5:2).

^{1}H NMR: (400 MHz, $CDCl_3$): δ 7.35-7.26 (m, 7H), 7.07 (td, J = 7.7, 1.0 Hz, 1H), 6.77 (d, *J* = 7.8 Hz, 1H), 4.90 (dd, J = 62.3, 15.7 Hz, 2H), 3.28 (dd, *J* = 17.4, 8.4, 1H), 3.08-2.99 (m, 1H), 2.53 (dd, *J* = 17.4, 7.5 Hz, 1H), 1.04 ppm (d, *J* = 7.0 Hz, 1H).

^{13}C NMR: (100 MHz, $CDCl_3$): δ 175.4, 174.2, 143.0, 135.0, 130.9, 129.0, 127.9, 127.2, 137.2, 124.0, 123.0, 110.1, 85.8, 44.1, 37.3, 35.9, 16.2 ppm.

MP: 146 – 147 °C.

HRMS (ESI): Calculated for $C_{19}H_{17}NO_3$ $[M+H]^+$: 308.12810, Found: 308.12830.

FTIR (neat): 1783, 1727, 1612, 1490, 1471, 1373, 1212, 1164, 1004, 969, 767, 757, 734, 693, 673 cm^{-1}.

^{1}H NMR of **6.10c**

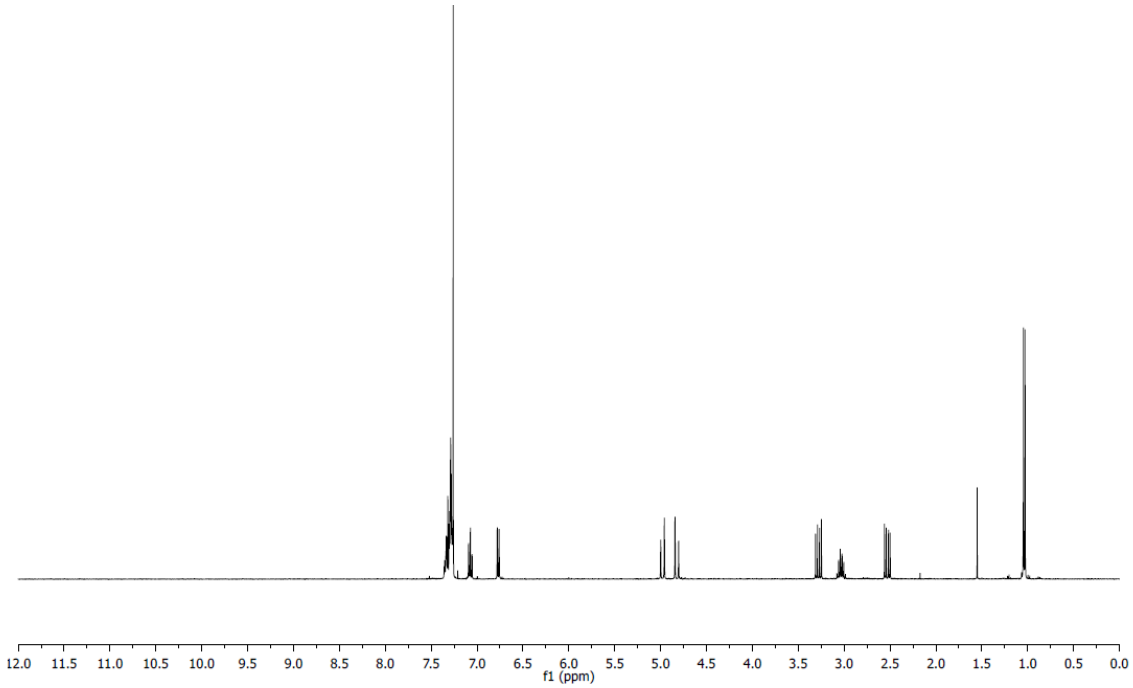

^{13}C NMR of **6.10c**

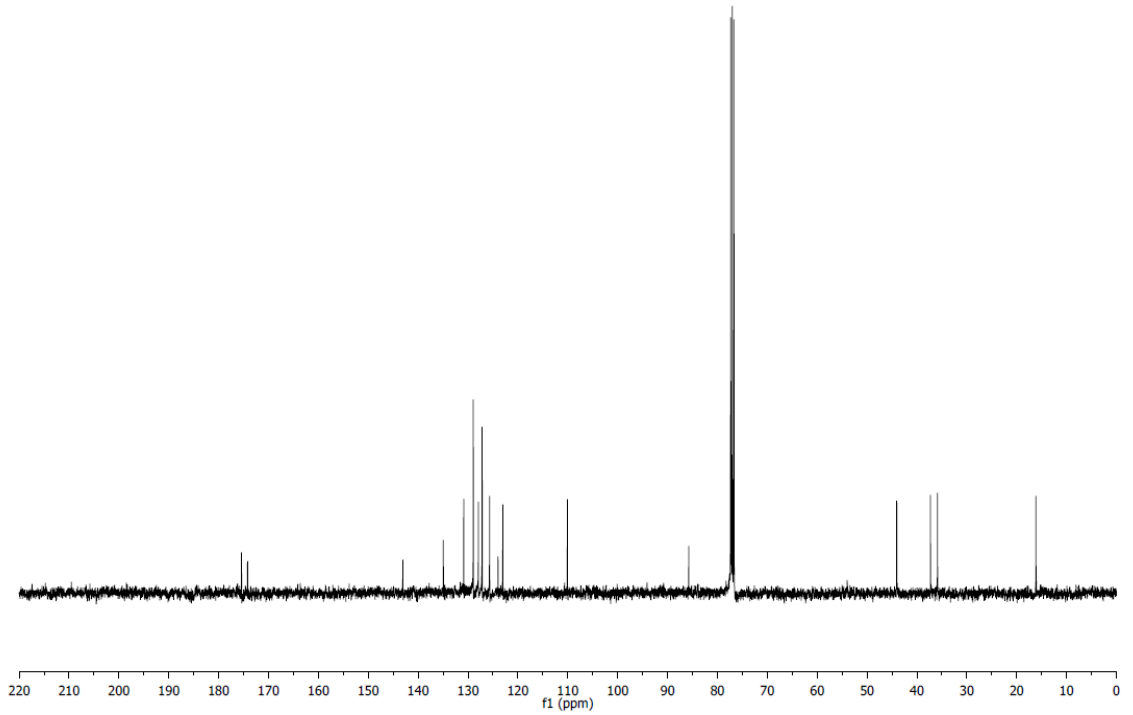

1'-benzyl-3-phenyl-3H-spiro[furan-2,3'-indoline]-2',5(4H)-dione (6.10d)

In accordance with general procedure B using acrylic ester **6.2d**, upon stirring at 140 °C for 20 h, the reaction mixture was concentrated to afford the crude spirolactone (dr = >20:1, as determined by ^{1}H NMR spectroscopy). The crude reaction mixture was subjected to flash column chromatography (SiO_2: 25% EtOAc/hexanes) to furnish **6.10d** (91 mg, 0.25 mmol, 82% yield) as a colorless solid. *The spectroscopic properties of this compound were consistent with the data available in the literature*.[172]

TLC (SiO_2): R_f = 0.62 (hexanes:EtOAc = 5:2).

^{1}H NMR: (400 MHz, $CDCl_3$): δ 7.35-7.19 (m, 7H), 7.10 (td, *J* = 7.8, 1.2 Hz, 1H), 7.02-6.99 (m, 2H), 6.73 (td, *J* = 7.6, 1.0 Hz, 1H), 6.62 (d, *J* = 7.8, 1H), 6.42 (dq, *J* = 7.6, 0.6 Hz, 1H), 4.98 (d, *J* = 15.8 Hz, 1H), 4.81 (d, *J* = 15.8 Hz, 1H), 4.08 (dd, *J* = 8.6, 5.8 Hz, 1H), 3.67 (dd, *J* = 17.4, 8.6 Hz, 1H) 3.15 ppm (3d, *J* = 17.4, 5.8 Hz, 1H).

^{13}C NMR: (100 MHz, $CDCl_3$): δ 175.7, 174.2, 142.9, 136.3, 134.8, 130.7, 128.9, 128.7, 128.2, 128.0, 127.9, 127.2, 126.0, 123.4, 122.7, 109.6, 86.0, 48.3, 44.0, 34.0 ppm.

MP: 176 – 177 °C.

HRMS (ESI): Calculated for $C_{24}H_{10}NO_3$ $[M+Na]^+$: 392.12570, Found: 392.12580.

FTIR (neat): 1793, 1723, 1614, 1468, 1365, 1182, 1153, 1029, 1001, 752, 699 cm^{-1}.

^{1}H NMR of **6.10d**

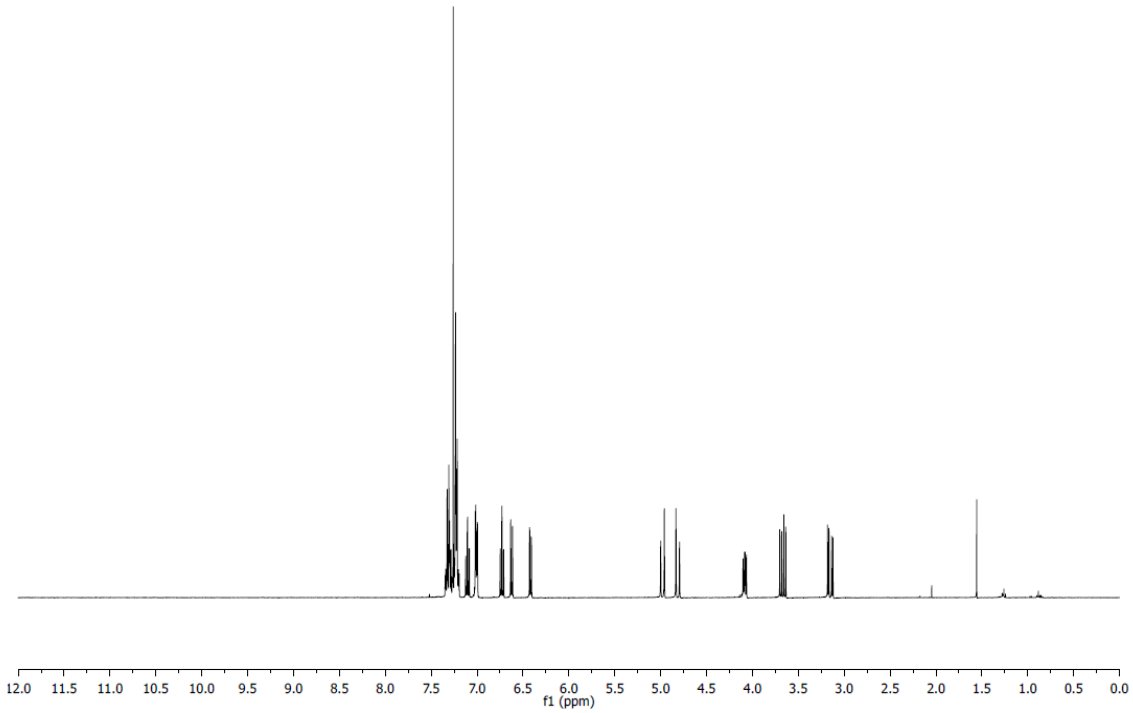

^{13}C NMR of **6.10d**

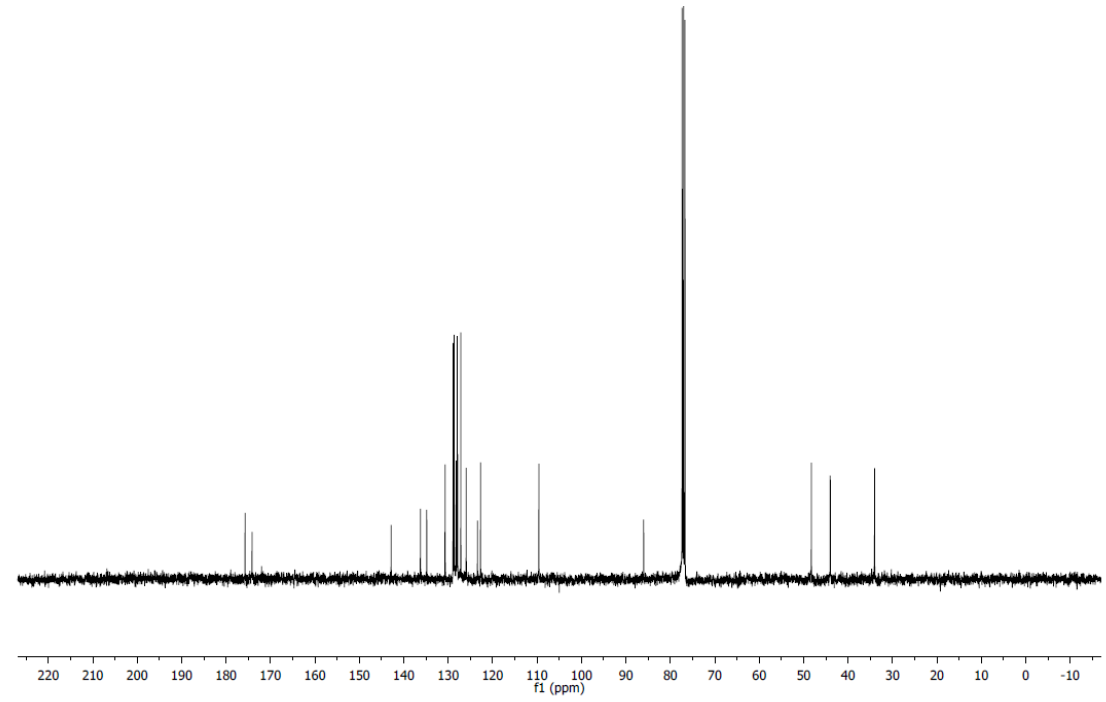

1'-benzyl-4-methyl-3H-spiro[furan-2,3'-indoline]-2',5(4H)-dione (6.10e)

In accordance with general procedure B using acrylic ester **6.2e**, upon stirring at 140 °C for 20 h, the reaction mixture was concentrated to afford the crude spirolactone (dr = 2:1, as determined by ^{1}H NMR spectroscopy). The crude reaction mixture was subjected to flash column chromatography (SiO_2: 25% EtOAc/hexanes) to furnish **6.10e** (92 mg, 0.30 mmol, 99% yield) as a colorless solid.

TLC (SiO_2): $R_{f\ (minor)}$= 0.62, $R_{f\ (major)}$= 0.47 (hexanes:EtOAc = 5:2).

Spectral Data for Major Isomer:

^{1}H NMR (400 MHz, $CDCl_3$): δ 7.35-7.23 (m, 7H), 7.06 (t, *J* = 7.6 Hz, 1H), 6.74 (d, *J* = 7.9 Hz, 1H), 4.94 (d, *J* = 15.6 Hz, 1H), 4.87 (d, *J* = 15.6 Hz, 1H), 3.20-3.10 (m, 1H), 2.62 (dd, *J* = 13.1, 9.5 Hz, 1H), 2.46 (dd, *J* = 13.1, 9.5 Hz, 1H), 1.54 ppm (d, *J* = 7.2 Hz, 3H).

^{13}C NMR (100 MHz, $CDCl_3$): δ 178.5, 173.8, 142.6, 134.9, 130.9, 128.9, 127.9, 127.8, 127.2, 123.7, 123.5, 110.0, 80.6, 44.1, 38.4, 34.7, 16.5 ppm.

MP: 122 – 123 °C.

HRMS (ESI): Calculated for $C_{19}H_{17}NO_3$ $[M+Na]^+$: 330.11010, Found: 330.11050.

FTIR (neat): 1783, 1727, 1615, 1489, 1469, 1369, 1178, 1024, 984, 752, 697 cm^{-1}.

^{1}H NMR of **6.10e**

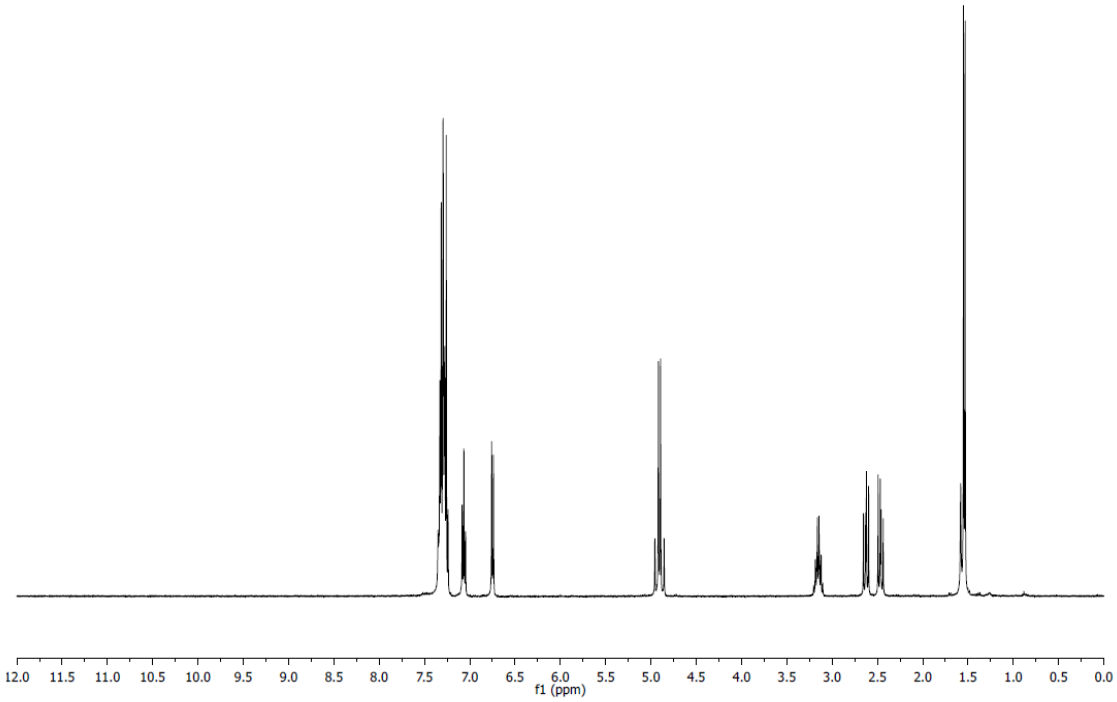

^{13}C NMR of **6.10e**

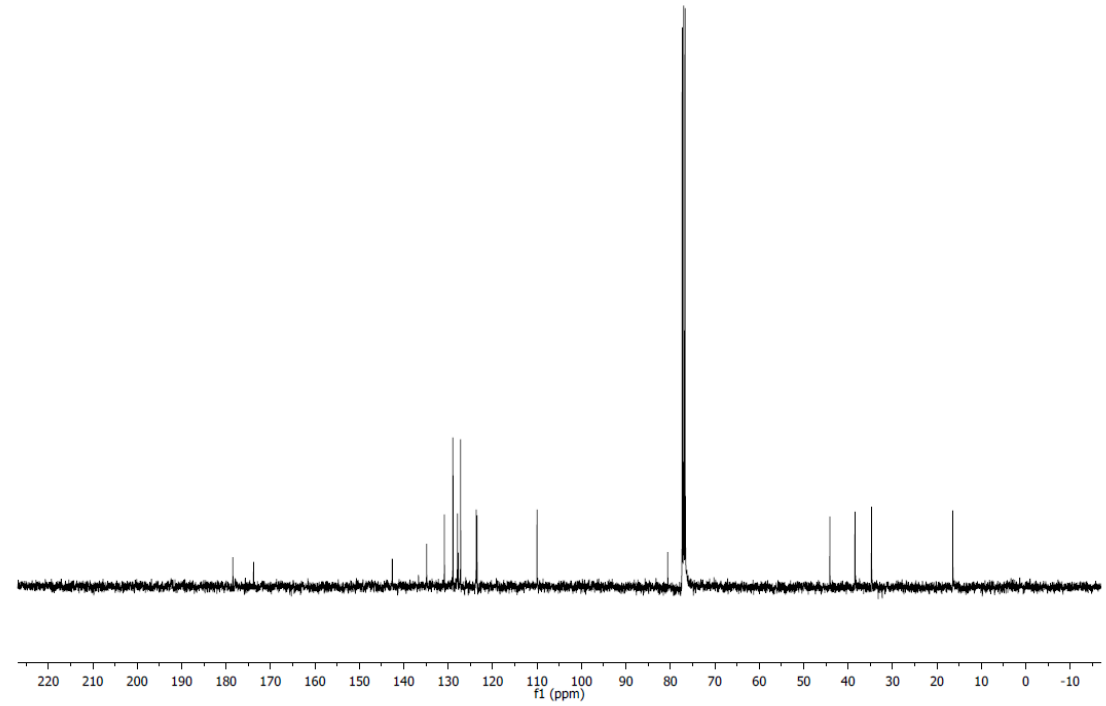

1'-benzyl-3,3-dimethyl-3H-spiro[furan-2,3'-indoline]-2',5(4H)-dione (6.10f)

In accordance with general procedure B using acrylic ester **6.2f**, upon stirring at 140 °C for 20 h, the reaction mixture was concentrated and subjected to flash column chromatography (SiO_2: 25% EtOAc/hexanes) to furnish **6.10f** (50 mg, 0.16 mmol, 52% yield) as a colorless solid.

TLC (SiO_2): R_f = 0.59 (hexanes:EtOAc = 5:2).

^{1}H NMR (400 MHz, $CDCl_3$): δ 7.30-7.27 (m, 7H), 7.07 (td, *J* = 7.6, 0.8 Hz, 1H), 6.76 (d, *J* = 7.6 Hz, 1H), 5.08 (d, *J* = 15.6 Hz, 1H), 4.66 (d, *J* = 15.6 Hz, 1H), 3.46 (d, *J* = 16.6 Hz, 1H), 2.41 (d, *J* = 16.6 Hz, 1H), 1.32 (s, 3H), 1.10 ppm (2, 3H).

^{13}C NMR (100 MHz, $CDCl_3$): δ 175.7, 174.9, 144.1, 135.1, 130.9, 128.9, 127.9, 127.3, 127.1, 122.7, 122.2, 109.8, 88.4, 44.0, 43.4, 41.7, 26.0, 21.7 ppm.

MP: 142 – 143 °C.

HRMS (ESI): Calculated for $C_{20}H_{19}NO_3$ $[M+Na]^+$: 344.12570, Found: 344.12580.

FTIR (neat): 1793, 1723, 1614, 1467, 1368, 1224, 1185, 1017, 755 cm^{-1}.

^{1}H NMR of **6.10f**

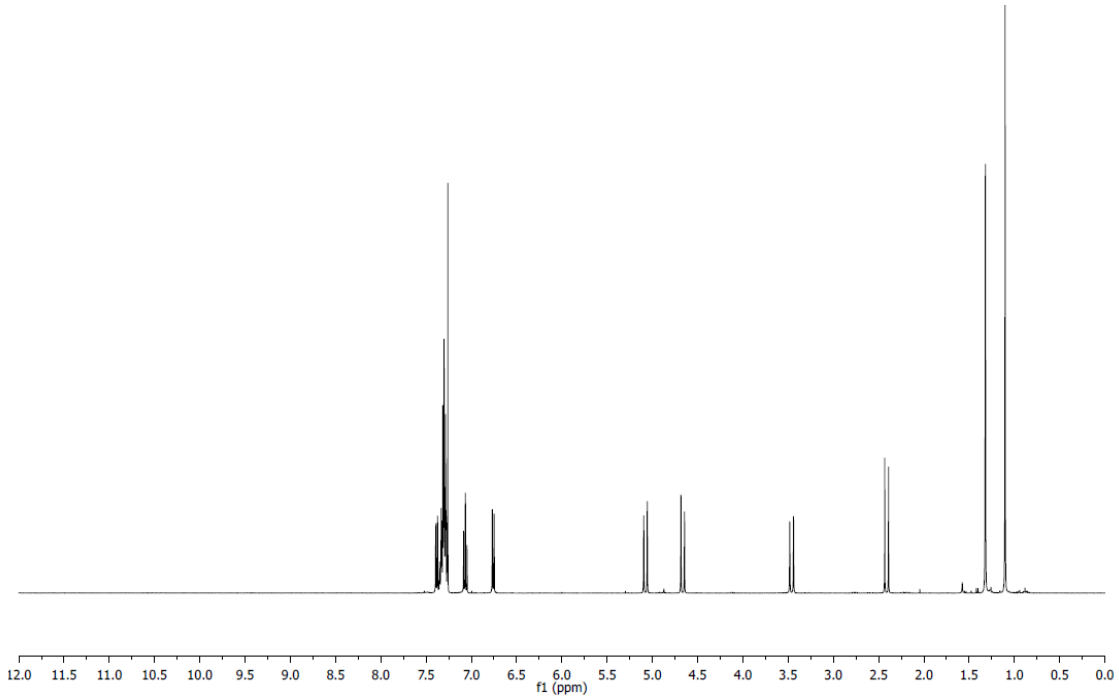

^{13}C NMR of **6.10f**

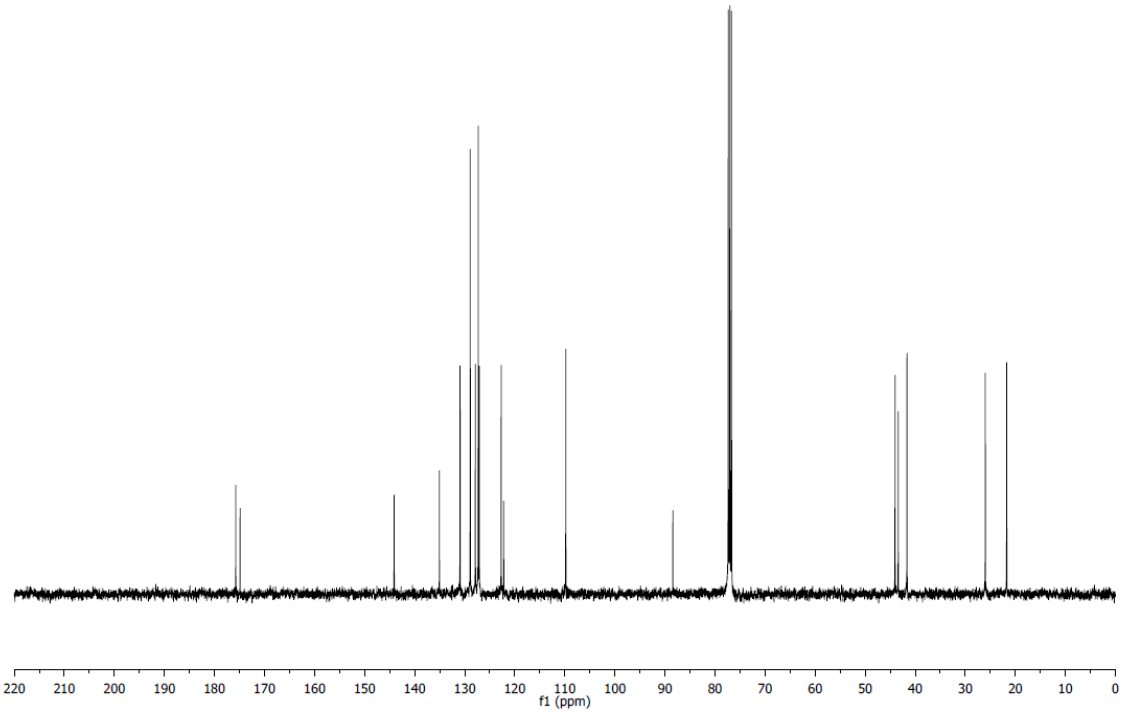

1'-benzyl-3- cyclohexyl-3H-spiro[furan-2,3'-indoline]-2',5(4H)-dione (6.10g)

In accordance with general procedure B using acrylic ester **6.2g**, upon stirring at 140 °C for 20 h, the reaction mixture was concentrated to afford the crude spirolactone (dr = >20:1, as determined by ^{1}H NMR spectroscopy). The crude reaction mixture was subjected to flash column chromatography (SiO_2: 25% EtOAc/hexanes) to furnish **6.10g** (86 mg, 0.23 mmol, 77% yield) as a tan solid.

TLC (SiO_2): R_f = 0.34 (hexanes:EtOAc = 7:3).

^{1}H NMR: (400 MHz, $CDCl_3$): δ 7.34-7.23 (m, 7H), 7.07 (td, *J* = 7.6, 0.9 Hz, 1H), 6.82 (d, *J* = 7.8 Hz, 1H), 4.98 (d, *J* = 15.4 Hz, 1H), 4.83 (d, *J* = 15.5 Hz, 1H), 3.00-2.86 (m, 2H), 2.74-2.60 (m, 1H), 1.73-1.62 (m, 2H), 1.53-1.46 (m, 1H), 1.36-1.21 (m, 2H), 1.17-0.98 (m, 3H), 0.93-0.84 (m, 1H), 0.77-0.67 ppm (m, 2H).

^{13}C NMR: (100 MHz, $CDCl_3$): δ 174.8, 173.2, 143.3, 134.9, 131.1, 128.9, 128.1, 127.8, 125.2, 124.7, 123.3, 110.3, 85.2, 47.9, 44.5, 38.8, 33.8, 31.8, 30.5, 25.8, 25.6, 25.2 ppm.

MP: 161 – 163 °C.

HRMS (ESI): Calculated for $C_{24}H_{25}NO_3$ $[M+Na]^+$: 398.17270, Found: 398.17290.

FTIR (neat): 2934, 1788, 1731, 1614, 1487, 1350, 1206, 1184, 1159, 976, 770, 753, 708 cm^{-1}.

^{1}H NMR of **6.10g**

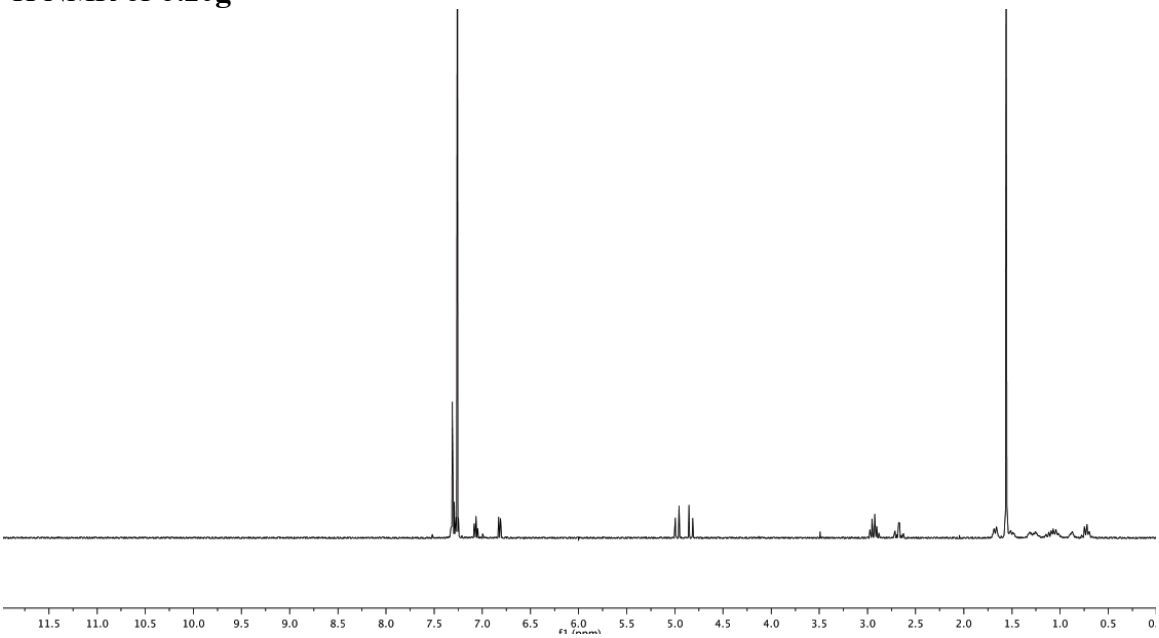

^{13}C NMR of **6.10g**

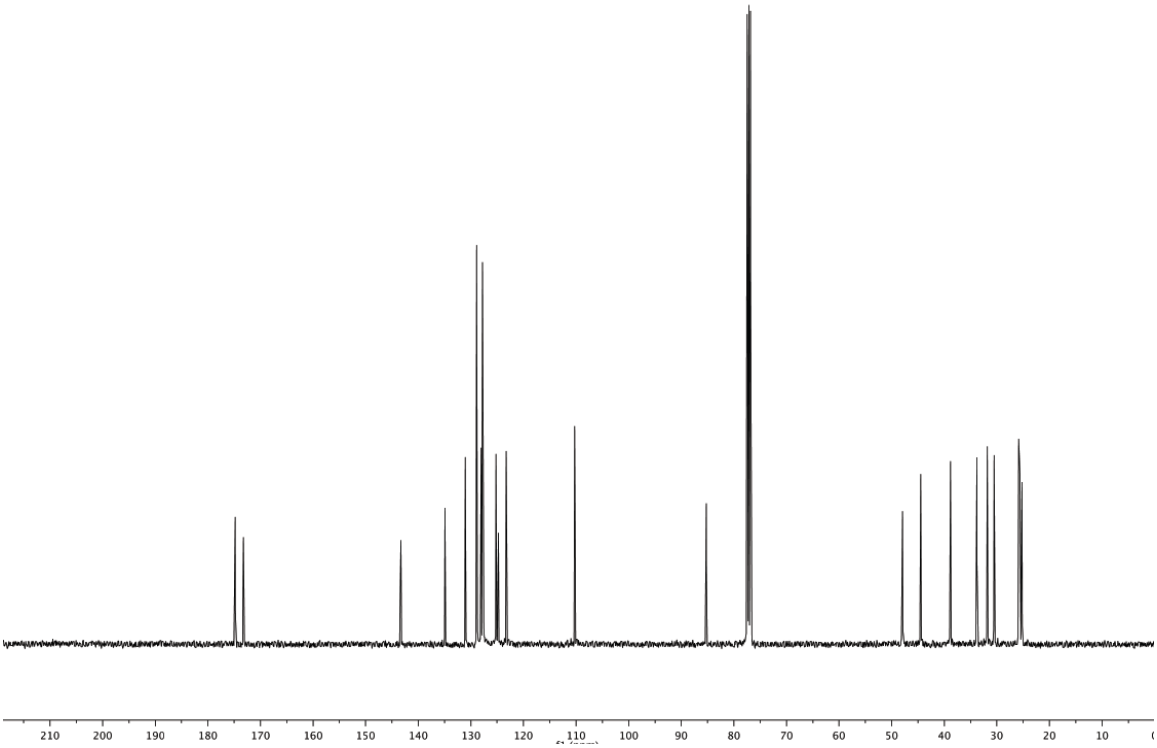

(3-(benzo[d][1,3]dioxol-5-yl)-1'-benzyl-3H-spiro[furan-2,3'-indoline]-2',5(4H)-dione (6.10h)

In accordance with general procedure B using acrylic ester **6.2h**, upon stirring at 140 °C for 20 h, the reaction mixture was concentrated to afford the crude spirolactone (dr = >20:1, as determined by ^{1}H NMR spectroscopy). The crude reaction mixture was subjected to flash column chromatography (SiO_2: 25% EtOAc/hexanes) to furnish **6.10h** (112 mg, 0.27 mmol, 90% yield) as a pale pink solid.

TLC (SiO_2): R_f = 0.28 (hexanes:EtOAc = 7:3).

^{1}H NMR: (400 MHz, $CDCl_3$): δ 7.34-7.22 (m, 5H), 7.14 (td, *J* = 7.8, 1.2 Hz, 1H), 6.82 (td, *J* = 7.6, 0.9 Hz, 1H), 6.66-6.61 (m, 3H), 6.50-6.48 (m, 2H), 5.92 (d, *J* = 1.4 Hz, 1H), 5.91 (d, *J* = 1.4 Hz, 1H), 4.99 (d, *J* = 15.8 Hz, 1H), 4.80 (d, *J* = 15.8, 1H), 4.03 (dd, *J* = 8.6, 6.4 Hz, 1H), 3.60 (dd, *J* = 17.5, 8.6 Hz, 1H), 3.08 ppm (dd, *J* = 17.5, 6.4 Hz, 1H).

^{13}C NMR: (100 MHz, $CDCl_3$): δ 175.5, 174.0, 147.9, 147.4, 142.9, 134.8, 130.8, 129.8, 128.9, 127.9, 127.1, 125.9, 123.5, 122.9, 121.3, 109.7, 108.3, 101.3, 86.1, 48.1, 44.0, 34.3, 14.2 ppm.

MP: 177 – 178 °C.

HRMS (ESI): Calculated for $C_{25}H_{19}NO_5$ $[M+Na]^+$: 436.11550, Found: 436.11510.

FTIR (neat): 1791, 1730, 1489, 1468, 1368, 1234, 1184, 1155, 1035, 1000, 760, cm^{-1}

^{1}H NMR of **6.10h**

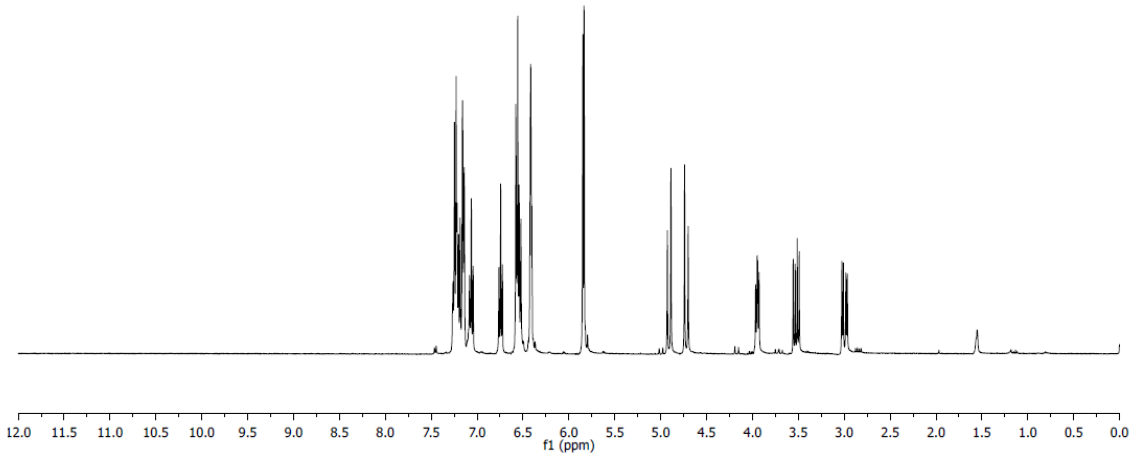

^{13}C NMR of **6.10h**

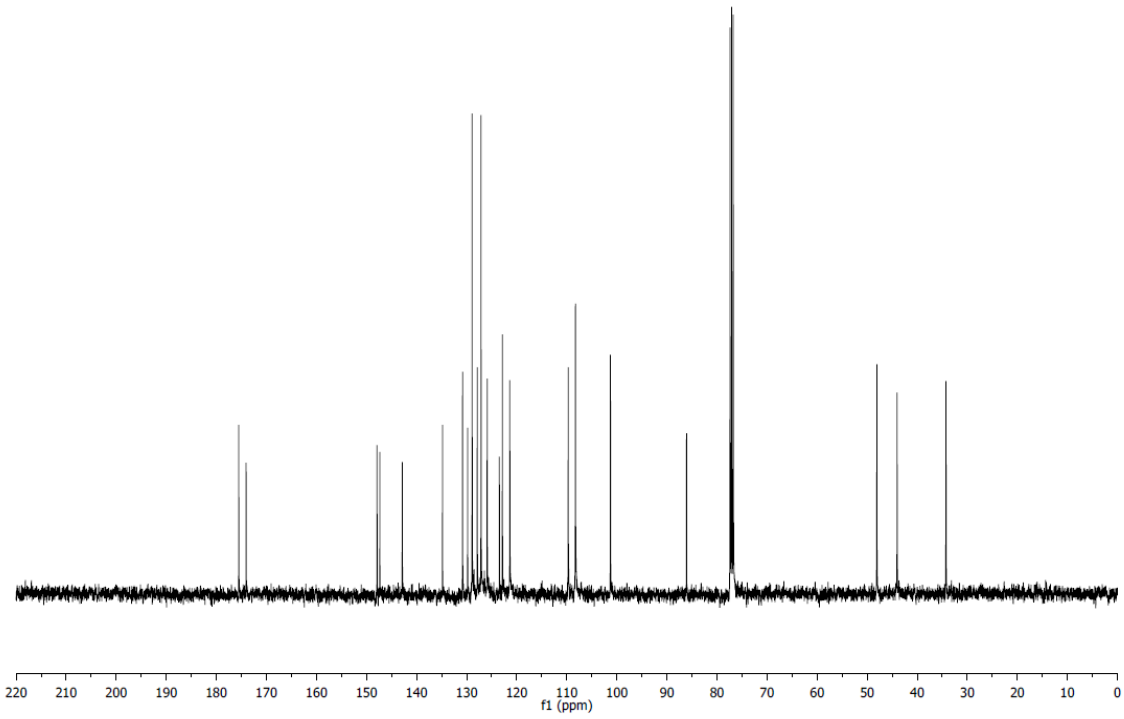

1'-benzyl-3-(thiophen-2-yl)-3H-spiro[furan-2,3'-indoline]-2',5(4H)-dione (6.10i)

In accordance with general procedure B using acrylic ester **6.2i**, upon stirring at 140 °C for 20 h, the reaction mixture was concentrated to afford the crude spirolactone (dr = >20:1, as determined by ^{1}H NMR spectroscopy). The crude reaction mixture was subjected to flash column chromatography (SiO_2: 25% EtOAc/hexanes) to furnish **6.10i** (98 mg, 0.26 mmol, 87% yield) as a white solid.

TLC (SiO_2): R_f = 0.49 (hexanes:EtOAc = 2:1).

^{1}H NMR: (400 MHz, $CDCl_3$): δ 7.33-7.26 (m, 3H), 7.22-7.19 (m, 2H), 7.16 (dd, *J* = 7.8, 1.2 Hz, 2H), 7.13 (dd, *J* = 5.1, 1.2 Hz, 1H), 6.89 (dd, *J* = 5.1, 3.6 Hz 1H), 6.85 (dd, *J* = 7.6, 0.9 Hz, 1H), 6.79 (ddd, *J* = 3.6, 1.1, 0.6 Hz, 1H), 6.72 (ddd, *J* = 7.6, 1.2, 0.6 Hz, 1H), 6.66 (d, *J* = 7.8 Hz, 1H), 4.96 (d, *J* = 15.8 Hz, 1H), 4.85 (d, *J* = 15.8 Hz, 1H), 4.38 (m, 1H), 3.65 (dd, *J* = 17.5, 8.7 Hz, 1H), 3.15 ppm (dd, *J* = 17.5, 7.2 Hz, 1H).

^{13}C NMR: (100 MHz, C_6D_6): δ 173.5, 173.3, 143.0, 138.7, 135.1, 130.5, 128.6, 126.9, 126.6, 126.2, 125.4, 124.7, 123.8, 122.5, 109.5, 85.2, 44.1, 43.4, 35.4 ppm.

MP: 158 – 159 °C.

HRMS (ESI): Calculated for $C_{22}H_{17}NO_3S$ $[M+Na]^+$:398.08210, Found: 398.08200.

FTIR (neat): 1790, 1722, 1614, 1467, 1379, 1368, 1194, 1183, 1155, 999, 768, 757, 732, 709, 694, 676 cm^{-1}.

^{1}H NMR of **6.10i**

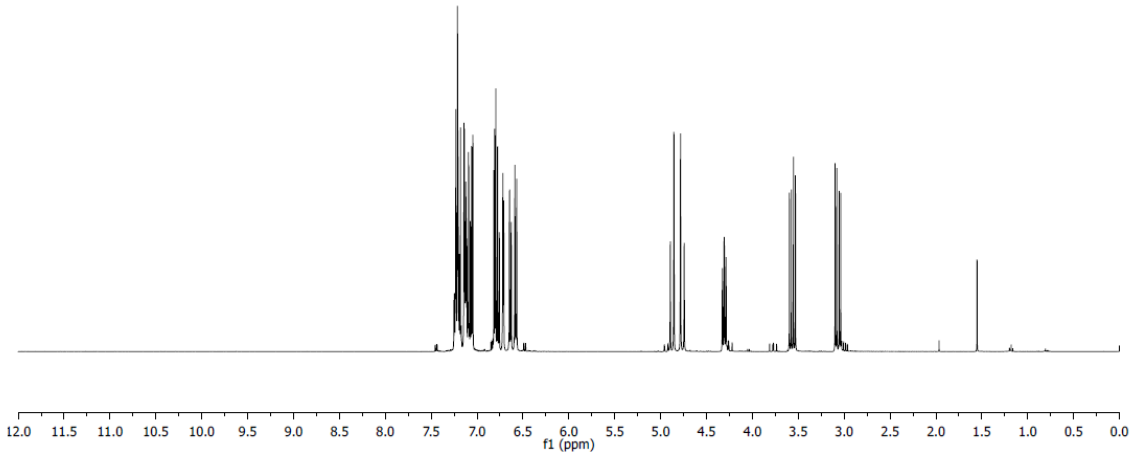

^{13}C NMR of **6.10i**

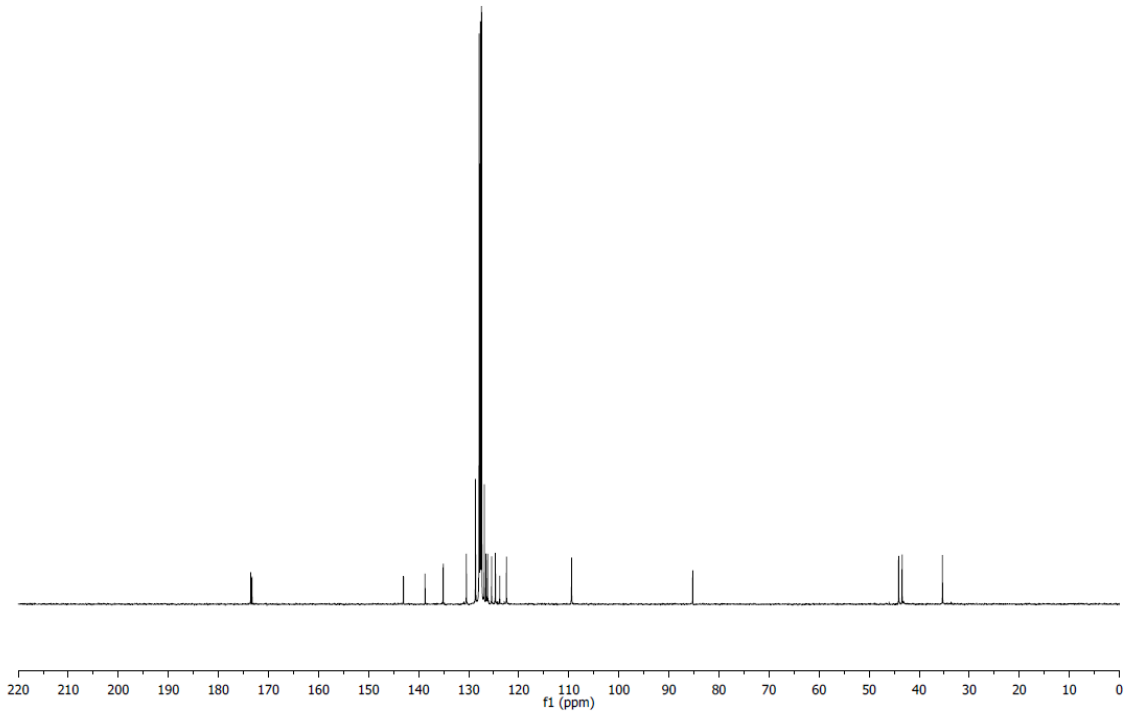

6.4.6 Crystal Data and Structure Refinement for 6.11

Empirical formula	C52 H60 Cl4 O5 P2 Ru	
Formula weight	1069.81	
Temperature	153(2) K	
Wavelength	0.71073 Å	
Crystal system	Triclinic	
Space group	P-1	
Unit cell dimensions	a = 11.3017(3) Å	α= 71.0490(10)°.
	b = 14.8706(4) Å	β= 86.7940(10)°.
	c = 15.7363(4) Å	γ = 81.2220(10)°.
Volume	2471.99(11) $Å^3$	
Z	2	
Density (calculated)	1.437 Mg/m^3	
Absorption coefficient	0.645 mm^{-1}	
F(000)	1108	
Crystal size	0.30 x 0.20 x 0.08 mm	
Theta range for data collection	1.46 to 27.50°.	
Index ranges	-14<=h<=14, -19<=k<=19, -20<=l<=20	
Reflections collected	57107	
Independent reflections	11369 [R(int) = 0.0478]	
Completeness to theta = 27.50°	99.9 %	
Absorption correction	Semi-empirical from equivalents	
Max. and min. transmission	1.00 and 0.855	
Refinement method	Full-matrix least-squares on F^2	
Data / restraints / parameters	11369 / 0 / 577	
Goodness-of-fit on F^2	1.206	
Final R indices [I>2sigma(I)]	R1 = 0.0419, wR2 = 0.0977	
R indices (all data)	R1 = 0.0529, wR2 = 0.1036	
Largest diff. peak and hole	2.563 and -1.677 e.$Å^{-3}$	

Table 6.3 Atomic coordinates (x 10^4) and equivalent isotropic displacement parameters ($Å^2$x10^3) for **6.11**. U(eq) is defined as one third of the trace of the orthogonalized U^{ij} tensor.

	x	y	z	U(eq)
C(1)	6057(3)	8955(2)	2956(2)	25(1)
C(2)	5030(3)	9625(2)	2787(2)	35(1)
C(3)	4799(3)	10278(2)	3262(3)	43(1)
C(4)	5581(4)	10260(2)	3902(2)	45(1)
C(5)	6596(4)	9595(3)	4081(3)	51(1)
C(6)	6844(3)	8935(2)	3607(2)	41(1)
C(7)	7551(2)	7226(2)	2889(2)	24(1)
C(8)	7186(3)	6477(2)	3600(2)	27(1)
C(9)	8022(3)	5702(2)	4046(2)	34(1)
C(10)	9208(3)	5670(2)	3780(2)	37(1)
C(11)	9576(3)	6403(2)	3083(2)	36(1)
C(12)	8759(3)	7192(2)	2640(2)	30(1)
C(13)	7172(2)	8926(2)	1318(2)	24(1)
C(14)	7647(2)	8488(2)	583(2)	27(1)
C(15)	6684(2)	8292(2)	55(2)	24(1)
C(16)	7020(2)	6250(2)	836(2)	19(1)
C(17)	7548(2)	6056(2)	80(2)	25(1)
C(18)	8431(2)	5271(2)	175(2)	29(1)
C(19)	8805(2)	4680(2)	1026(2)	29(1)
C(20)	8299(2)	4874(2)	1775(2)	26(1)
C(21)	7401(2)	5654(2)	1685(2)	22(1)
C(22)	4884(2)	7246(2)	-157(2)	20(1)
C(23)	4527(2)	6376(2)	-109(2)	24(1)
C(24)	3727(3)	6328(2)	-722(2)	32(1)
C(25)	3268(3)	7152(2)	-1392(2)	35(1)
C(26)	3616(3)	8023(2)	-1455(2)	34(1)
C(27)	4416(3)	8069(2)	-839(2)	29(1)
C(28)	4162(2)	5878(2)	2422(2)	20(1)

C(29)	3726(2)	4909(2)	2720(2)	21(1)
C(30)	4796(3)	4106(2)	2894(3)	38(1)
C(31)	4341(3)	3118(2)	3208(3)	49(1)
C(32)	3567(3)	3056(2)	2475(3)	41(1)
C(33)	2485(3)	3830(2)	2318(2)	29(1)
C(34)	2923(3)	4821(2)	1998(2)	31(1)
C(35)	1767(3)	3743(2)	3169(2)	39(1)
C(36)	2542(4)	3804(3)	3900(2)	47(1)
C(37)	3624(4)	3031(3)	4062(3)	63(1)
C(38)	2989(3)	4799(2)	3585(2)	39(1)
C(39)	2985(3)	8161(2)	3106(2)	32(1)
C(40)	2335(2)	8028(2)	4011(2)	25(1)
C(41)	2205(4)	8953(3)	4260(3)	54(1)
C(42)	1462(4)	8838(3)	5135(3)	62(1)
C(43)	2119(4)	8017(5)	5881(3)	87(2)
C(44)	2236(4)	7106(4)	5652(3)	82(2)
C(45)	2970(3)	7213(3)	4776(2)	58(1)
C(46)	1083(3)	7822(3)	3908(3)	55(1)
C(47)	364(3)	7704(3)	4791(3)	59(1)
C(48)	1006(4)	6894(3)	5515(4)	85(2)
C(49)	246(3)	8611(3)	5009(3)	58(1)
C(50)	4255(2)	8706(2)	1188(2)	23(1)
C(51)	1597(3)	7832(3)	619(4)	82(2)
O(1)	5128(2)	5994(1)	2722(1)	21(1)
O(2)	3571(2)	6602(1)	1858(1)	23(1)
O(3)	3932(2)	7568(1)	3112(1)	24(1)
O(4)	2574(2)	8809(2)	2436(2)	69(1)
O(5)	3896(2)	9425(1)	668(1)	34(1)
P(1)	6400(1)	8163(1)	2270(1)	20(1)
P(2)	5880(1)	7302(1)	693(1)	17(1)
Ru(1)	4859(1)	7516(1)	1934(1)	17(1)
Cl(1)	896(1)	8981(1)	379(2)	114(1)
Cl(2)	643(1)	7042(1)	500(1)	88(1)
C(52)	641(3)	10702(3)	1848(3)	51(1)
Cl(3)	-719(1)	10414(1)	2407(1)	77(1)
Cl(4)	1166(1)	11612(1)	2139(1)	92(1)

Table 6.4 Bond lengths [Å] and angles [°] for **6.11**.

C(1)-C(6)	1.383(4)	C(15)-H(15B)	0.99
C(1)-C(2)	1.386(4)	C(16)-C(21)	1.391(4)
C(1)-P(1)	1.828(3)	C(16)-C(17)	1.396(4)
C(2)-C(3)	1.393(4)	C(16)-P(2)	1.829(2)
C(2)-H(2)	0.95	C(17)-C(18)	1.389(4)
C(3)-C(4)	1.368(5)	C(17)-H(17)	0.95
C(3)-H(3)	0.95	C(18)-C(19)	1.389(4)
C(4)-C(5)	1.372(5)	C(18)-H(18)	0.95
C(4)-H(4)	0.95	C(19)-C(20)	1.376(4)
C(5)-C(6)	1.403(4)	C(19)-H(19)	0.95
C(5)-H(5)	0.95	C(20)-C(21)	1.395(4)
C(6)-H(6)	0.95	C(20)-H(20)	0.95
C(7)-C(8)	1.394(4)	C(21)-H(21)	0.95
C(7)-C(12)	1.397(4)	C(22)-C(23)	1.392(4)
C(7)-P(1)	1.814(3)	C(22)-C(27)	1.393(4)
C(8)-C(9)	1.389(4)	C(22)-P(2)	1.826(3)
C(8)-H(8)	0.95	C(23)-C(24)	1.383(4)
C(9)-C(10)	1.381(5)	C(23)-H(23)	0.95
C(9)-H(9)	0.95	C(24)-C(25)	1.383(4)
C(10)-C(11)	1.369(5)	C(24)-H(24)	0.95
C(10)-H(10)	0.95	C(25)-C(26)	1.381(4)
C(11)-C(12)	1.387(4)	C(25)-H(25)	0.95
C(11)-H(11)	0.95	C(26)-C(27)	1.387(4)
C(12)-H(12)	0.95	C(26)-H(26)	0.95
C(13)-C(14)	1.538(4)	C(27)-H(27)	0.95
C(13)-P(1)	1.828(3)	C(28)-O(1)	1.270(3)
C(13)-H(13A)	0.99	C(28)-O(2)	1.272(3)
C(13)-H(13B)	0.99	C(28)-C(29)	1.514(3)
C(14)-C(15)	1.522(4)	C(28)-Ru(1)	2.538(2)
C(14)-H(14A)	0.99	C(29)-C(38)	1.530(4)
C(14)-H(14B)	0.99	C(29)-C(30)	1.532(4)
C(15)-P(2)	1.829(3)	C(29)-C(34)	1.543(4)
C(15)-H(15A)	0.99	C(30)-C(31)	1.548(4)

C(30)-H(30A)	0.99	C(42)-H(42)	1.00
C(30)-H(30B)	0.99	C(43)-C(44)	1.497(8)
C(31)-C(37)	1.510(6)	C(43)-H(43A)	0.99
C(31)-C(32)	1.520(5)	C(43)-H(43B)	0.99
C(31)-H(31)	1.00	C(44)-C(48)	1.513(8)
C(32)-C(33)	1.516(4)	C(44)-C(45)	1.544(5)
C(32)-H(32A)	0.99	C(44)-H(44)	1.00
C(32)-H(32B)	0.99	C(45)-H(45A)	0.99
C(33)-C(35)	1.506(4)	C(45)-H(45B)	0.99
C(33)-C(34)	1.545(4)	C(46)-C(47)	1.543(6)
C(33)-H(33)	1.00	C(46)-H(46A)	0.99
C(34)-H(34A)	0.99	C(46)-H(46B)	0.99
C(34)-H(34B)	0.99	C(47)-C(49)	1.482(6)
C(35)-C(36)	1.516(5)	C(47)-C(48)	1.487(6)
C(35)-H(35A)	0.99	C(47)-H(47)	1.00
C(35)-H(35B)	0.99	C(48)-H(48A)	0.99
C(36)-C(37)	1.515(6)	C(48)-H(48B)	0.99
C(36)-C(38)	1.554(4)	C(49)-H(49A)	0.99
C(36)-H(36)	1.00	C(49)-H(49B)	0.99
C(37)-H(37A)	0.99	C(50)-O(5)	1.146(3)
C(37)-H(37B)	0.99	C(50)-Ru(1)	1.829(3)
C(38)-H(38A)	0.99	C(51)-Cl(1)	1.700(5)
C(38)-H(38B)	0.99	C(51)-Cl(2)	1.769(5)
C(39)-O(4)	1.231(4)	C(51)-H(51A)	0.99
C(39)-O(3)	1.277(3)	C(51)-H(51B)	0.99
C(39)-C(40)	1.534(4)	O(1)-Ru(1)	2.1816(17)
C(40)-C(46)	1.521(4)	O(2)-Ru(1)	2.1708(18)
C(40)-C(45)	1.522(4)	O(3)-Ru(1)	2.0964(18)
C(40)-C(41)	1.532(4)	P(1)-Ru(1)	2.2776(7)
C(41)-C(42)	1.546(5)	P(2)-Ru(1)	2.2985(7)
C(41)-H(41A)	0.99	C(52)-Cl(4)	1.752(4)
C(41)-H(41B)	0.99	C(52)-Cl(3)	1.768(4)
C(42)-C(49)	1.503(6)	C(52)-H(52A)	0.99
C(42)-C(43)	1.520(7)	C(52)-H(52B)	0.99

C(6)-C(1)-C(2)	119.3(3)	C(7)-C(12)-H(12)	120.1
C(6)-C(1)-P(1)	120.9(2)	C(14)-C(13)-P(1)	116.54(18)
C(2)-C(1)-P(1)	119.6(2)	C(14)-C(13)-H(13A)	108.2
C(1)-C(2)-C(3)	120.3(3)	P(1)-C(13)-H(13A)	108.2
C(1)-C(2)-H(2)	119.9	C(14)-C(13)-H(13B)	108.2
C(3)-C(2)-H(2)	119.9	P(1)-C(13)-H(13B)	108.2
C(4)-C(3)-C(2)	120.3(3)	H(13A)-C(13)-H(13B)	107.3
C(4)-C(3)-H(3)	119.8	C(15)-C(14)-C(13)	114.8(2)
C(2)-C(3)-H(3)	119.8	C(15)-C(14)-H(14A)	108.6
C(3)-C(4)-C(5)	120.0(3)	C(13)-C(14)-H(14A)	108.6
C(3)-C(4)-H(4)	120.0	C(15)-C(14)-H(14B)	108.6
C(5)-C(4)-H(4)	120.0	C(13)-C(14)-H(14B)	108.6
C(4)-C(5)-C(6)	120.4(3)	H(14A)-C(14)-H(14B)	107.6
C(4)-C(5)-H(5)	119.8	C(14)-C(15)-P(2)	114.45(19)
C(6)-C(5)-H(5)	119.8	C(14)-C(15)-H(15A)	108.6
C(1)-C(6)-C(5)	119.7(3)	P(2)-C(15)-H(15A)	108.6
C(1)-C(6)-H(6)	120.2	C(14)-C(15)-H(15B)	108.6
C(5)-C(6)-H(6)	120.2	P(2)-C(15)-H(15B)	108.6
C(8)-C(7)-C(12)	119.4(3)	H(15A)-C(15)-H(15B)	107.6
C(8)-C(7)-P(1)	117.7(2)	C(21)-C(16)-C(17)	119.1(2)
C(12)-C(7)-P(1)	122.7(2)	C(21)-C(16)-P(2)	121.37(19)
C(9)-C(8)-C(7)	119.8(3)	C(17)-C(16)-P(2)	119.5(2)
C(9)-C(8)-H(8)	120.1	C(18)-C(17)-C(16)	120.4(3)
C(7)-C(8)-H(8)	120.1	C(18)-C(17)-H(17)	119.8
C(10)-C(9)-C(8)	120.1(3)	C(16)-C(17)-H(17)	119.8
C(10)-C(9)-H(9)	120.0	C(19)-C(18)-C(17)	120.1(3)
C(8)-C(9)-H(9)	120.0	C(19)-C(18)-H(18)	120.0
C(11)-C(10)-C(9)	120.6(3)	C(17)-C(18)-H(18)	120.0
C(11)-C(10)-H(10)	119.7	C(20)-C(19)-C(18)	119.9(2)
C(9)-C(10)-H(10)	119.7	C(20)-C(19)-H(19)	120.0
C(10)-C(11)-C(12)	120.2(3)	C(18)-C(19)-H(19)	120.0
C(10)-C(11)-H(11)	119.9	C(19)-C(20)-C(21)	120.3(3)
C(12)-C(11)-H(11)	119.9	C(19)-C(20)-H(20)	119.8
C(11)-C(12)-C(7)	119.9(3)	C(21)-C(20)-H(20)	119.8
C(11)-C(12)-H(12)	120.1	C(16)-C(21)-C(20)	120.2(2)
		C(16)-C(21)-H(21)	119.9

C(20)-C(21)-H(21)	119.9	H(30A)-C(30)-H(30B)	108.2
C(23)-C(22)-C(27)	118.3(2)	C(37)-C(31)-C(32)	110.6(3)
C(23)-C(22)-P(2)	120.1(2)	C(37)-C(31)-C(30)	108.4(3)
C(27)-C(22)-P(2)	121.5(2)	C(32)-C(31)-C(30)	108.9(3)
C(24)-C(23)-C(22)	120.9(3)	C(37)-C(31)-H(31)	109.7
C(24)-C(23)-H(23)	119.6	C(32)-C(31)-H(31)	109.7
C(22)-C(23)-H(23)	119.6	C(30)-C(31)-H(31)	109.7
C(25)-C(24)-C(23)	120.0(3)	C(33)-C(32)-C(31)	109.9(3)
C(25)-C(24)-H(24)	120.0	C(33)-C(32)-H(32A)	109.7
C(23)-C(24)-H(24)	120.0	C(31)-C(32)-H(32A)	109.7
C(26)-C(25)-C(24)	120.1(3)	C(33)-C(32)-H(32B)	109.7
C(26)-C(25)-H(25)	120.0	C(31)-C(32)-H(32B)	109.7
C(24)-C(25)-H(25)	120.0	H(32A)-C(32)-H(32B)	108.2
C(25)-C(26)-C(27)	119.8(3)	C(35)-C(33)-C(32)	111.1(3)
C(25)-C(26)-H(26)	120.1	C(35)-C(33)-C(34)	108.4(2)
C(27)-C(26)-H(26)	120.1	C(32)-C(33)-C(34)	108.6(2)
C(26)-C(27)-C(22)	120.9(3)	C(35)-C(33)-H(33)	109.6
C(26)-C(27)-H(27)	119.5	C(32)-C(33)-H(33)	109.6
C(22)-C(27)-H(27)	119.5	C(34)-C(33)-H(33)	109.6
O(1)-C(28)-O(2)	118.0(2)	C(29)-C(34)-C(33)	109.9(2)
O(1)-C(28)-C(29)	121.3(2)	C(29)-C(34)-H(34A)	109.7
O(2)-C(28)-C(29)	120.7(2)	C(33)-C(34)-H(34A)	109.7
O(1)-C(28)-Ru(1)	59.25(12)	C(29)-C(34)-H(34B)	109.7
O(2)-C(28)-Ru(1)	58.77(12)	C(33)-C(34)-H(34B)	109.7
C(29)-C(28)-Ru(1)	178.97(18)	H(34A)-C(34)-H(34B)	108.2
C(28)-C(29)-C(38)	109.1(2)	C(33)-C(35)-C(36)	110.4(3)
C(28)-C(29)-C(30)	110.0(2)	C(33)-C(35)-H(35A)	109.6
C(38)-C(29)-C(30)	109.4(3)	C(36)-C(35)-H(35A)	109.6
C(28)-C(29)-C(34)	110.9(2)	C(33)-C(35)-H(35B)	109.6
C(38)-C(29)-C(34)	108.4(2)	C(36)-C(35)-H(35B)	109.6
C(30)-C(29)-C(34)	109.1(2)	H(35A)-C(35)-H(35B)	108.1
C(29)-C(30)-C(31)	109.6(2)	C(37)-C(36)-C(35)	110.2(3)
C(29)-C(30)-H(30A)	109.8	C(37)-C(36)-C(38)	108.3(3)
C(31)-C(30)-H(30A)	109.8	C(35)-C(36)-C(38)	108.7(3)
C(29)-C(30)-H(30B)	109.8	C(37)-C(36)-H(36)	109.9
C(31)-C(30)-H(30B)	109.8	C(35)-C(36)-H(36)	109.9

C(38)-C(36)-H(36)	109.9	C(42)-C(43)-H(43A)	109.7
C(31)-C(37)-C(36)	110.8(3)	C(44)-C(43)-H(43B)	109.7
C(31)-C(37)-H(37A)	109.5	C(42)-C(43)-H(43B)	109.7
C(36)-C(37)-H(37A)	109.5	H(43A)-C(43)-H(43B)	108.2
C(31)-C(37)-H(37B)	109.5	C(43)-C(44)-C(48)	109.6(3)
C(36)-C(37)-H(37B)	109.5	C(43)-C(44)-C(45)	109.9(4)
H(37A)-C(37)-H(37B)	108.1	C(48)-C(44)-C(45)	108.8(4)
C(29)-C(38)-C(36)	109.6(2)	C(43)-C(44)-H(44)	109.5
C(29)-C(38)-H(38A)	109.8	C(48)-C(44)-H(44)	109.5
C(36)-C(38)-H(38A)	109.8	C(45)-C(44)-H(44)	109.5
C(29)-C(38)-H(38B)	109.8	C(40)-C(45)-C(44)	109.6(3)
C(36)-C(38)-H(38B)	109.8	C(40)-C(45)-H(45A)	109.8
H(38A)-C(38)-H(38B)	108.2	C(44)-C(45)-H(45A)	109.8
O(4)-C(39)-O(3)	124.7(3)	C(40)-C(45)-H(45B)	109.8
O(4)-C(39)-C(40)	119.4(3)	C(44)-C(45)-H(45B)	109.8
O(3)-C(39)-C(40)	115.9(2)	H(45A)-C(45)-H(45B)	108.2
C(46)-C(40)-C(45)	109.3(3)	C(40)-C(46)-C(47)	110.5(3)
C(46)-C(40)-C(41)	107.7(3)	C(40)-C(46)-H(46A)	109.5
C(45)-C(40)-C(41)	108.4(3)	C(47)-C(46)-H(46A)	109.5
C(46)-C(40)-C(39)	107.6(3)	C(40)-C(46)-H(46B)	109.5
C(45)-C(40)-C(39)	112.9(2)	C(47)-C(46)-H(46B)	109.5
C(41)-C(40)-C(39)	110.6(2)	H(46A)-C(46)-H(46B)	108.1
C(40)-C(41)-C(42)	110.2(3)	C(49)-C(47)-C(48)	110.9(4)
C(40)-C(41)-H(41A)	109.6	C(49)-C(47)-C(46)	109.1(3)
C(42)-C(41)-H(41A)	109.6	C(48)-C(47)-C(46)	108.6(3)
C(40)-C(41)-H(41B)	109.6	C(49)-C(47)-H(47)	109.4
C(42)-C(41)-H(41B)	109.6	C(48)-C(47)-H(47)	109.4
H(41A)-C(41)-H(41B)	108.1	C(46)-C(47)-H(47)	109.4
C(49)-C(42)-C(43)	109.7(4)	C(47)-C(48)-C(44)	110.4(3)
C(49)-C(42)-C(41)	109.7(4)	C(47)-C(48)-H(48A)	109.6
C(43)-C(42)-C(41)	108.1(4)	C(44)-C(48)-H(48A)	109.6
C(49)-C(42)-H(42)	109.8	C(47)-C(48)-H(48B)	109.6
C(43)-C(42)-H(42)	109.8	C(44)-C(48)-H(48B)	109.6
C(41)-C(42)-H(42)	109.8	H(48A)-C(48)-H(48B)	108.1
C(44)-C(43)-C(42)	109.8(4)	C(47)-C(49)-C(42)	110.1(3)
C(44)-C(43)-H(43A)	109.7	C(47)-C(49)-H(49A)	109.6

C(42)-C(49)-H(49A)	109.6	C(50)-Ru(1)-O(2)	104.20(10)
C(47)-C(49)-H(49B)	109.6	O(3)-Ru(1)-O(2)	84.58(7)
C(42)-C(49)-H(49B)	109.6	C(50)-Ru(1)-O(1)	164.26(9)
H(49A)-C(49)-H(49B)	108.1	O(3)-Ru(1)-O(1)	79.94(7)
O(5)-C(50)-Ru(1)	174.9(2)	O(2)-Ru(1)-O(1)	60.08(6)
Cl(1)-C(51)-Cl(2)	112.5(2)	C(50)-Ru(1)-P(1)	89.08(8)
Cl(1)-C(51)-H(51A)	109.1	O(3)-Ru(1)-P(1)	91.91(5)
Cl(2)-C(51)-H(51A)	109.1	O(2)-Ru(1)-P(1)	166.62(5)
Cl(1)-C(51)-H(51B)	109.1	O(1)-Ru(1)-P(1)	106.61(5)
Cl(2)-C(51)-H(51B)	109.1	C(50)-Ru(1)-P(2)	86.14(8)
H(51A)-C(51)-H(51B)	107.8	O(3)-Ru(1)-P(2)	174.55(5)
C(28)-O(1)-Ru(1)	90.74(14)	O(2)-Ru(1)-P(2)	91.83(5)
C(28)-O(2)-Ru(1)	91.15(15)	O(1)-Ru(1)-P(2)	94.72(5)
C(39)-O(3)-Ru(1)	122.49(18)	P(1)-Ru(1)-P(2)	90.67(2)
C(7)-P(1)-C(13)	105.61(13)	C(50)-Ru(1)-C(28)	134.26(10)
C(7)-P(1)-C(1)	104.60(13)	O(3)-Ru(1)-C(28)	80.64(7)
C(13)-P(1)-C(1)	100.67(12)	O(2)-Ru(1)-C(28)	30.08(7)
C(7)-P(1)-Ru(1)	110.66(9)	O(1)-Ru(1)-C(28)	30.01(7)
C(13)-P(1)-Ru(1)	116.50(9)	P(1)-Ru(1)-C(28)	136.58(6)
C(1)-P(1)-Ru(1)	117.41(9)	P(2)-Ru(1)-C(28)	94.20(6)
C(22)-P(2)-C(15)	101.82(12)	Cl(4)-C(52)-Cl(3)	111.4(2)
C(22)-P(2)-C(16)	103.93(11)	Cl(4)-C(52)-H(52A)	109.3
C(15)-P(2)-C(16)	102.62(12)	Cl(3)-C(52)-H(52A)	109.3
C(22)-P(2)-Ru(1)	112.48(8)	Cl(4)-C(52)-H(52B)	109.3
C(15)-P(2)-Ru(1)	114.78(9)	Cl(3)-C(52)-H(52B)	109.3
C(16)-P(2)-Ru(1)	119.17(9)	H(52A)-C(52)-H(52B)	108.0
C(50)-Ru(1)-O(3)	98.70(9)		

Table 6.5 Anisotropic displacement parameters ($Å^2 x\ 10^3$) for **6.11**. The anisotropic displacement factor exponent takes the form: $-2\pi^2[\ h^2\ a^{*2}U^{11} + ... + 2\ h\ k\ a^*\ b^*\ U^{12}\ ]$

	U^{11}	U^{22}	U^{33}	U^{23}	U^{13}	U^{12}
C(1)	34(2)	20(1)	25(1)	-10(1)	6(1)	-8(1)
C(2)	36(2)	28(1)	43(2)	-17(1)	5(1)	-3(1)
C(3)	51(2)	27(2)	55(2)	-20(2)	18(2)	-6(1)
C(4)	76(3)	30(2)	39(2)	-21(1)	19(2)	-16(2)
C(5)	80(3)	42(2)	40(2)	-24(2)	-6(2)	-12(2)
C(6)	55(2)	33(2)	38(2)	-19(1)	-10(2)	0(1)
C(7)	28(1)	20(1)	25(1)	-11(1)	-4(1)	-2(1)
C(8)	35(2)	27(1)	23(1)	-12(1)	-3(1)	-2(1)
C(9)	54(2)	26(1)	22(1)	-8(1)	-5(1)	-2(1)
C(10)	41(2)	34(2)	38(2)	-18(1)	-14(1)	9(1)
C(11)	28(2)	40(2)	41(2)	-18(1)	-9(1)	2(1)
C(12)	30(2)	28(1)	32(2)	-9(1)	-6(1)	-3(1)
C(13)	25(1)	21(1)	28(1)	-8(1)	2(1)	-8(1)
C(14)	24(1)	28(1)	29(2)	-10(1)	7(1)	-10(1)
C(15)	28(1)	20(1)	23(1)	-6(1)	6(1)	-8(1)
C(16)	16(1)	18(1)	25(1)	-8(1)	3(1)	-4(1)
C(17)	22(1)	27(1)	23(1)	-7(1)	4(1)	-2(1)
C(18)	22(1)	33(1)	35(2)	-16(1)	8(1)	-2(1)
C(19)	18(1)	27(1)	41(2)	-12(1)	2(1)	1(1)
C(20)	22(1)	25(1)	30(2)	-7(1)	-3(1)	0(1)
C(21)	22(1)	22(1)	24(1)	-10(1)	1(1)	-3(1)
C(22)	17(1)	24(1)	20(1)	-8(1)	2(1)	-1(1)
C(23)	21(1)	25(1)	25(1)	-6(1)	0(1)	-4(1)
C(24)	25(1)	39(2)	37(2)	-15(1)	0(1)	-11(1)
C(25)	24(1)	52(2)	32(2)	-15(1)	-5(1)	-6(1)
C(26)	28(2)	38(2)	30(2)	-3(1)	-9(1)	2(1)
C(27)	28(1)	25(1)	32(2)	-7(1)	-2(1)	0(1)
C(28)	19(1)	20(1)	21(1)	-7(1)	4(1)	-2(1)

C(29)	20(1)	20(1)	22(1)	-4(1)	4(1)	-4(1)
C(30)	27(2)	25(1)	60(2)	-10(1)	-4(1)	-3(1)
C(31)	40(2)	25(2)	76(3)	-9(2)	-19(2)	1(1)
C(32)	38(2)	32(2)	57(2)	-20(2)	10(2)	-8(1)
C(33)	29(1)	34(2)	30(2)	-16(1)	2(1)	-9(1)
C(34)	33(2)	30(1)	28(2)	-7(1)	0(1)	-10(1)
C(35)	35(2)	44(2)	43(2)	-19(2)	15(1)	-18(1)
C(36)	64(2)	60(2)	28(2)	-18(2)	18(2)	-36(2)
C(37)	91(3)	49(2)	40(2)	15(2)	-26(2)	-38(2)
C(38)	48(2)	48(2)	32(2)	-21(1)	17(1)	-25(2)
C(39)	24(1)	40(2)	28(2)	-11(1)	2(1)	4(1)
C(40)	20(1)	25(1)	28(1)	-8(1)	4(1)	0(1)
C(41)	72(3)	42(2)	54(2)	-22(2)	26(2)	-22(2)
C(42)	88(3)	51(2)	59(3)	-37(2)	33(2)	-22(2)
C(43)	54(3)	170(6)	42(3)	-44(3)	6(2)	-9(3)
C(44)	58(3)	92(3)	42(2)	25(2)	22(2)	43(2)
C(45)	38(2)	69(3)	39(2)	6(2)	14(2)	23(2)
C(46)	30(2)	80(3)	72(3)	-46(2)	10(2)	-16(2)
C(47)	28(2)	68(3)	85(3)	-28(2)	19(2)	-17(2)
C(48)	76(3)	36(2)	117(4)	0(2)	62(3)	0(2)
C(49)	49(2)	53(2)	49(2)	-4(2)	17(2)	24(2)
C(50)	22(1)	22(1)	26(1)	-10(1)	4(1)	-3(1)
C(51)	30(2)	74(3)	99(4)	24(3)	9(2)	7(2)
O(1)	18(1)	20(1)	23(1)	-6(1)	1(1)	-3(1)
O(2)	21(1)	20(1)	26(1)	-5(1)	-1(1)	-3(1)
O(3)	24(1)	23(1)	23(1)	-9(1)	4(1)	0(1)
O(4)	49(2)	94(2)	30(1)	2(1)	6(1)	41(2)
O(5)	40(1)	21(1)	33(1)	-2(1)	-1(1)	4(1)
P(1)	22(1)	17(1)	22(1)	-8(1)	1(1)	-2(1)
P(2)	18(1)	16(1)	18(1)	-5(1)	2(1)	-2(1)
Ru(1)	17(1)	15(1)	19(1)	-5(1)	2(1)	-1(1)
Cl(1)	68(1)	102(1)	201(2)	-83(1)	-55(1)	3(1)
Cl(2)	65(1)	54(1)	127(1)	-21(1)	31(1)	15(1)
C(52)	42(2)	59(2)	48(2)	-14(2)	-4(2)	-1(2)
Cl(3)	36(1)	83(1)	98(1)	-13(1)	1(1)	0(1)
Cl(4)	104(1)	95(1)	90(1)	-38(1)	6(1)	-44(1)

Table 6.7 Hydrogen coordinates (x 10^4) and isotropic displacement parameters (Å^{2}x 10^3) for **6.11**.

	x	y	z	U(eq)
H(2)	4481	9640	2345	42
H(3)	4095	10737	3141	52
H(4)	5420	10708	4222	54
H(5)	7135	9582	4529	61
H(6)	7548	8476	3732	49
H(8)	6368	6496	3779	33
H(9)	7777	5193	4534	41
H(10)	9775	5136	4084	44
H(11)	10393	6370	2901	43
H(12)	9021	7708	2169	36
H(13A)	6614	9520	1036	29
H(13B)	7855	9116	1554	29
H(14A)	8144	8930	157	32
H(14B)	8174	7877	866	32
H(15A)	7060	8147	-477	29
H(15B)	6098	8883	-163	29
H(17)	7302	6463	-504	30
H(18)	8780	5138	-343	35
H(19)	9408	4143	1090	34
H(20)	8564	4474	2356	31
H(21)	7049	5778	2205	27
H(23)	4837	5807	351	29
H(24)	3494	5728	-682	39
H(25)	2713	7120	-1809	42
H(26)	3308	8589	-1920	41
H(27)	4649	8670	-882	35
H(30A)	5314	4151	3361	46
H(30B)	5277	4175	2337	46
H(31)	5039	2593	3325	58

H(32A)	4039	3140	1912	49
H(32B)	3301	2416	2656	49
H(33)	1968	3776	1846	35
H(34A)	3380	4899	1429	37
H(34B)	2226	5335	1883	37
H(35A)	1450	3122	3371	47
H(35B)	1080	4265	3053	47
H(36)	2065	3726	4468	57
H(37A)	4135	3091	4526	76
H(37B)	3357	2391	4288	76
H(38A)	2296	5316	3476	47
H(38B)	3488	4853	4059	47
H(41A)	1804	9495	3766	65
H(41B)	3007	9100	4345	65
H(42)	1377	9446	5291	74
H(43A)	2923	8164	5959	105
H(43B)	1671	7940	6454	105
H(44)	2649	6565	6152	99
H(45A)	3779	7350	4855	70
H(45B)	3058	6606	4631	70
H(46A)	1139	7227	3746	66
H(46B)	663	8356	3418	66
H(47)	-450	7556	4715	71
H(48A)	1085	6298	5353	102
H(48B)	540	6793	6082	102
H(49A)	-234	8548	5566	69
H(49B)	-176	9142	4516	69
H(51A)	1895	7605	1244	99
H(51B)	2297	7818	214	99
H(52A)	1250	10121	2006	61
H(52B)	517	10915	1190	61

Table 6.8 Torsion angles [°] for **6.11**.

C(6)-C(1)-C(2)-C(3)	0.6(5)
P(1)-C(1)-C(2)-C(3)	-175.5(2)
C(1)-C(2)-C(3)-C(4)	-0.3(5)
C(2)-C(3)-C(4)-C(5)	-0.2(5)
C(3)-C(4)-C(5)-C(6)	0.4(6)
C(2)-C(1)-C(6)-C(5)	-0.4(5)
P(1)-C(1)-C(6)-C(5)	175.7(3)
C(4)-C(5)-C(6)-C(1)	-0.1(6)
C(12)-C(7)-C(8)-C(9)	-0.7(4)
P(1)-C(7)-C(8)-C(9)	174.6(2)
C(7)-C(8)-C(9)-C(10)	-0.5(4)
C(8)-C(9)-C(10)-C(11)	0.6(5)
C(9)-C(10)-C(11)-C(12)	0.7(5)
C(10)-C(11)-C(12)-C(7)	-2.0(4)
C(8)-C(7)-C(12)-C(11)	2.0(4)
P(1)-C(7)-C(12)-C(11)	-173.1(2)
P(1)-C(13)-C(14)-C(15)	66.6(3)
C(13)-C(14)-C(15)-P(2)	-70.4(3)
C(21)-C(16)-C(17)-C(18)	0.8(4)
P(2)-C(16)-C(17)-C(18)	178.8(2)
C(16)-C(17)-C(18)-C(19)	-0.8(4)
C(17)-C(18)-C(19)-C(20)	0.0(4)
C(18)-C(19)-C(20)-C(21)	0.9(4)
C(17)-C(16)-C(21)-C(20)	0.0(4)
P(2)-C(16)-C(21)-C(20)	-177.9(2)
C(19)-C(20)-C(21)-C(16)	-0.8(4)
C(27)-C(22)-C(23)-C(24)	-0.1(4)
P(2)-C(22)-C(23)-C(24)	176.9(2)
C(22)-C(23)-C(24)-C(25)	-0.2(4)
C(23)-C(24)-C(25)-C(26)	0.6(5)
C(24)-C(25)-C(26)-C(27)	-0.8(5)
C(25)-C(26)-C(27)-C(22)	0.5(5)
C(23)-C(22)-C(27)-C(26)	-0.1(4)
P(2)-C(22)-C(27)-C(26)	-177.0(2)
O(1)-C(28)-C(29)-C(38)	86.4(3)
O(2)-C(28)-C(29)-C(38)	-94.0(3)
O(1)-C(28)-C(29)-C(30)	-33.7(3)
O(2)-C(28)-C(29)-C(30)	146.0(3)
O(1)-C(28)-C(29)-C(34)	-154.4(2)
O(2)-C(28)-C(29)-C(34)	25.3(3)
C(28)-C(29)-C(30)-C(31)	179.4(3)
C(38)-C(29)-C(30)-C(31)	59.5(3)
C(34)-C(29)-C(30)-C(31)	-58.8(3)
C(29)-C(30)-C(31)-C(37)	-60.0(4)
C(29)-C(30)-C(31)-C(32)	60.3(4)
C(37)-C(31)-C(32)-C(33)	57.0(4)
C(30)-C(31)-C(32)-C(33)	-62.0(4)
C(31)-C(32)-C(33)-C(35)	-57.4(3)
C(31)-C(32)-C(33)-C(34)	61.7(3)
C(28)-C(29)-C(34)-C(33)	-179.8(2)
C(38)-C(29)-C(34)-C(33)	-60.1(3)
C(30)-C(29)-C(34)-C(33)	59.0(3)
C(35)-C(33)-C(34)-C(29)	60.7(3)
C(32)-C(33)-C(34)-C(29)	-60.1(3)
C(32)-C(33)-C(35)-C(36)	57.7(3)
C(34)-C(33)-C(35)-C(36)	-61.6(3)
C(33)-C(35)-C(36)-C(37)	-57.2(4)
C(33)-C(35)-C(36)-C(38)	61.4(4)
C(32)-C(31)-C(37)-C(36)	-57.6(4)
C(30)-C(31)-C(37)-C(36)	61.7(4)
C(35)-C(36)-C(37)-C(31)	57.4(4)
C(38)-C(36)-C(37)-C(31)	-61.5(4)
C(28)-C(29)-C(38)-C(36)	-179.7(3)

C(30)-C(29)-C(38)-C(36)-59.4(C(34)-
C(29)-C(38)-C(36) 59.5(3)
C(37)-C(36)-C(38)-C(29) 59.6(4)
C(35)-C(36)-C(38)-C(29)-60.2(4)
O(4)-C(39)-C(40)-C(46) 60.5(4)
O(3)-C(39)-C(40)-C(46) -119.2(3)
O(4)-C(39)-C(40)-C(45) -178.7(4)
O(3)-C(39)-C(40)-C(45) 1.6(4)
O(4)-C(39)-C(40)-C(41) -57.0(4)
O(3)-C(39)-C(40)-C(41) 123.3(3)
C(46)-C(40)-C(41)-C(42) 58.1(4)
C(45)-C(40)-C(41)-C(42)-60.1(4)
C(39)-C(40)-C(41)-C(42)175.5(3)
C(40)-C(41)-C(42)-C(49)-59.0(4)
C(40)-C(41)-C(42)-C(43) 60.6(5)
C(49)-C(42)-C(43)-C(44) 58.7(4)
C(41)-C(42)-C(43)-C(44)-60.8(5)
C(42)-C(43)-C(44)-C(48)-58.3(5)
C(42)-C(43)-C(44)-C(45) 61.2(5)
C(46)-C(40)-C(45)-C(44)-58.2(5)
C(41)-C(40)-C(45)-C(44) 59.0(5)
C(39)-C(40)-C(45)-C(44)-178.0(4)
C(43)-C(44)-C(45)-C(40)-60.3(5)
C(48)-C(44)-C(45)-C(40) 59.6(5)
C(45)-C(40)-C(46)-C(47) 58.3(4)
C(41)-C(40)-C(46)-C(47)-59.3(4)
C(39)-C(40)-C(46)-C(47)-178.6(3)
C(40)-C(46)-C(47)-C(49) 61.3(4)
C(40)-C(46)-C(47)-C(48)-59.6(5)
C(49)-C(47)-C(48)-C(44)-58.4(5)
C(46)-C(47)-C(48)-C(44) 61.3(5)
C(43)-C(44)-C(48)-C(47) 58.2(5)
C(45)-C(44)-C(48)-C(47)-61.9(5)
C(48)-C(47)-C(49)-C(42) 58.6(4)
C(46)-C(47)-C(49)-C(42)-60.9(4)
C(43)-C(42)-C(49)-C(47)-58.4(4)
C(41)-C(42)-C(49)-C(47) 60.2(4)
O(2)-C(28)-O(1)-Ru(1) 1.4(2)
C(29)-C(28)-O(1)-Ru(1) -179.0(2)
O(1)-C(28)-O(2)-Ru(1) -1.4(2)
C(29)-C(28)-O(2)-Ru(1) 178.9(2)
O(4)-C(39)-O(3)-Ru(1) -6.6(5)
C(40)-C(39)-O(3)-Ru(1)173.13(18)
C(8)-C(7)-P(1)-C(13) -173.1(2)
C(12)-C(7)-P(1)-C(13) 2.1(3)
C(8)-C(7)-P(1)-C(1) 81.2(2)
C(12)-C(7)-P(1)-C(1) -103.7(2)
C(8)-C(7)-P(1)-Ru(1) -46.2(2)
C(12)-C(7)-P(1)-Ru(1) 129.0(2)
C(14)-C(13)-P(1)-C(7) 69.7(2)
C(14)-C(13)-P(1)-C(1) 178.3(2)
C(14)-C(13)-P(1)-Ru(1) -53.6(2)
C(6)-C(1)-P(1)-C(7) 18.5(3)
C(2)-C(1)-P(1)-C(7) -165.4(2)
C(6)-C(1)-P(1)-C(13) -90.9(3)
C(2)-C(1)-P(1)-C(13) 85.2(2)
C(6)-C(1)-P(1)-Ru(1) 141.6(2)
C(2)-C(1)-P(1)-Ru(1) -42.4(3)
C(23)-C(22)-P(2)-C(15) 150.3(2)
C(27)-C(22)-P(2)-C(15) -32.9(2)
C(23)-C(22)-P(2)-C(16) 43.9(2)
C(27)-C(22)-P(2)-C(16) -139.3(2)
C(23)-C(22)-P(2)-Ru(1) -86.4(2)
C(27)-C(22)-P(2)-Ru(1) 90.5(2)
C(14)-C(15)-P(2)-C(22)-177.17(19)
C(14)-C(15)-P(2)-C(16) -69.8(2)

C(14)-C(15)-P(2)-Ru(1) 61.0(2)
C(21)-C(16)-P(2)-C(22) -135.5(2)
C(17)-C(16)-P(2)-C(22) 46.7(2)
C(21)-C(16)-P(2)-C(15) 118.8(2)
C(17)-C(16)-P(2)-C(15) -59.1(2)
C(21)-C(16)-P(2)-Ru(1) -9.3(2)
C(17)-C(16)-P(2)-Ru(1) 172.80(17)
C(39)-O(3)-Ru(1)-C(50) 19.1(2)
C(39)-O(3)-Ru(1)-O(2) -84.4(2)
C(39)-O(3)-Ru(1)-O(1) -145.0(2)
C(39)-O(3)-Ru(1)-P(1) 108.5(2)
C(39)-O(3)-Ru(1)-C(28) -114.5(2)
C(28)-O(2)-Ru(1)-C(50) -178.30(16)
C(28)-O(2)-Ru(1)-O(3) -80.67(15)
C(28)-O(2)-Ru(1)-O(1) 0.83(14)
C(28)-O(2)-Ru(1)-P(1) -5.4(3)
C(28)-O(2)-Ru(1)-P(2) 95.23(14)
C(28)-O(1)-Ru(1)-C(50) 2.3(4)
C(28)-O(1)-Ru(1)-O(3) 88.67(15)
C(28)-O(1)-Ru(1)-O(2) -0.83(14)
C(28)-O(1)-Ru(1)-P(1) 177.67(13)
C(28)-O(1)-Ru(1)-P(2) -90.22(14)
C(7)-P(1)-Ru(1)-C(50) -169.44(13)
C(13)-P(1)-Ru(1)-C(50) -48.82(13)
C(1)-P(1)-Ru(1)-C(50) 70.63(13)
C(7)-P(1)-Ru(1)-O(3) 91.88(11)
C(13)-P(1)-Ru(1)-O(3) -147.50(11)
C(1)-P(1)-Ru(1)-O(3) -28.05(11)
C(7)-P(1)-Ru(1)-O(2) 17.4(3)
C(13)-P(1)-Ru(1)-O(2) 138.1(2)
C(1)-P(1)-Ru(1)-O(2) -102.5(2)
C(7)-P(1)-Ru(1)-O(1) 11.82(11)
C(13)-P(1)-Ru(1)-O(1) 132.43(11)
C(1)-P(1)-Ru(1)-O(1) -108.12(11)
C(7)-P(1)-Ru(1)-P(2) -83.31(10)
C(13)-P(1)-Ru(1)-P(2) 37.31(10)
C(1)-P(1)-Ru(1)-P(2) 156.75(10)
C(7)-P(1)-Ru(1)-C(28) 13.51(13)
C(13)-P(1)-Ru(1)-C(28) 134.13(12)
C(1)-P(1)-Ru(1)-C(28) -106.42(13)
C(22)-P(2)-Ru(1)-C(50) -67.12(12)
C(15)-P(2)-Ru(1)-C(50) 48.67(13)
C(16)-P(2)-Ru(1)-C(50) 170.91(12)
C(22)-P(2)-Ru(1)-O(2) 36.99(10)
C(15)-P(2)-Ru(1)-O(2) 152.78(11)
C(16)-P(2)-Ru(1)-O(2) -84.98(10)
C(22)-P(2)-Ru(1)-O(1) 97.12(10)
C(15)-P(2)-Ru(1)-O(1) -147.09(11)
C(16)-P(2)-Ru(1)-O(1) -24.86(10)
C(22)-P(2)-Ru(1)-P(1) -156.16(9)
C(15)-P(2)-Ru(1)-P(1) -40.36(10)
C(16)-P(2)-Ru(1)-P(1) 81.87(9)
C(22)-P(2)-Ru(1)-C(28) 67.02(11)
C(15)-P(2)-Ru(1)-C(28) -177.19(11)
C(16)-P(2)-Ru(1)-C(28) -54.95(11)
O(1)-C(28)-Ru(1)-C(50) -179.13(15)
O(2)-C(28)-Ru(1)-C(50) 2.3(2)
O(1)-C(28)-Ru(1)-O(3) -86.07(14)
O(2)-C(28)-Ru(1)-O(3) 95.37(15)
O(1)-C(28)-Ru(1)-O(2) 178.6(2)
O(2)-C(28)-Ru(1)-O(1) -178.6(2)
O(1)-C(28)-Ru(1)-P(1) -3.25(18)
O(2)-C(28)-Ru(1)-P(1) 178.19(11)
O(1)-C(28)-Ru(1)-P(2) 92.18(13)
O(2)-C(28)-Ru(1)-P(2) -86.39(14)

Appendix

List of Abbreviations and Acronyms

acac	Acetoacetyl
BINOL	1,1'-Bi-2-naphthol
BIPHEP	2,2'-Bis(diphenylphosphino)-1,1'-bihepnyl
BIPY	2,2'-Bipyridine
cod	1,5-Cycooctadiene
COSY	Correlation Spectroscopy
cot	Cyclooctatetraene
Cy	Cyclohexyl
DBU	1,8-Diazabicycloundec-7-ene
DCE	Dichloroethane
DCM	Dichloromethane
DCyPF	1,1'-Bis(dicyclohexylphosphino)ferrocene
DFT	Density functional theory
D*i*PPF	1,1'-Bis(di-*i*-propylphosphino)ferrocene
DMB	Dimethoxybenzyl
DM-SEGPHOS	(*S*)-(–)-5,5'-Bis(diphenyphosphino)-4,4'-bi-1,3-benzodioxole
DMSO	Dimethylsulfoxide
DPPB	1,4-Bis(diphenylphosphino)butane
DPPF	1,1'-Bis(diphenylphosphino)ferrocene
DPPP	1,3-Bis(diphenylphosphino)propane
G2	Grubbs' 2nd Generation Catalyst
HG2	Hoveyda-Grubbs' 2nd Generation Catalyst

HMBC	Heteronuclear Multiple Bond Correlation
Ipc	Isopinocampheol
LUMO	Lowest Unoccupied Molecular Orbital
MeCN	Acetonitrile
Mes	Mesityl
MOM	Methoxymethyl
NHC	*N*-Heterocyclic Carbene
NOESY	Nuclear Overhauser Enhancement Spectroscopy
ORTEP	Oak Ridge Thermal Ellipsoid Plot
Phen	Phenanthroline
Pin	Pinacol
DMB	Dimethoxybenzyl
PMB	*para*-Methoxy Benzyl
PMHS	Polymethylhydrosiloxane
BINAP	2,2'-Bis(diphenylphosphino)-1,1'-binaphthyl
*p*TsOH	*para*-Toluenesulfonic Acid
SEGPHOS	5,5'-Bis(diphenylphosphino)-4,4'-bi-1,3-benzodioxole
TADDOL	α, α, α, α-tetraaryl-1,3-dioxalane-4,5-dimethanol
TBAF	Tetrabutylammonium fluoride
TBAI	Tetrabutylammonium iodide
TBS	*Tert*-Butyldimethylsilyl
TERPY	2,2':6',2"-Terpyridine
TFA	Trifluoroacetic acid
THF	Tetrahydrofuran
TRIP	Triisopropylbenzene

WALPHOS	(1*S*)-1-[(1*R*)-1-[Bis[3,5-bis(trifluoromethyl)phenyl]phsophino]-ethyl]-2-[2-(diphenylphosphino)phenyl]ferrocene
XANTPHOS	9,9-Dimethyl-4,5-bis(diphenylphosphino)xanthene

References

1. (a) Mikhailov, B. N.; Bubnov, Y. N. *Izn. Akad. Nauk SSSR, Ser. Khim.* **1964**, 1874-1875; (b) Hosomi, A.; Sakurai, H. *Tetrahedron Lett.* **1976**, *17* (16), 1295-1298.
2. Herold, T.; Hoffmann, R. W. *Angew. Chem. Int. Ed.* **1978**, *17* (10), 768-769.
3. Brown, H. C.; Jadhav, P. K. *J. Am. Chem. Soc.* **1983**, *105* (7), 2092-2093.
4. Reetz, M. T. *Pure Appl. Chem.* **1988**, *60* (11), 1607-1614.
5. Short, R. P.; Masamune, S. *J. Am. Chem. Soc.* **1989**, *111* (5), 1892-1894.
6. Corey, E. J.; Yu, C. M.; Kim, S. S. *J. Am. Chem. Soc.* **1989**, *111* (14), 5495-5496.
7. Roush, W. R.; Walts, A. E.; Hoong, L. K. *J. Am. Chem. Soc.* **1985**, *107* (26), 8186-8190.
8. Riediker, M.; Duthaler, R. O. *Angew. Chem. Int. Ed.* **1989**, *28* (4), 494-495.
9. Kinnaird, J. W. A.; Ng, P. Y.; Kubota, K.; Wang, X.; Leighton, J. L. *J. Am. Chem. Soc.* **2002**, *124* (27), 7920-7921.
10. Furuta, K.; Mouri, M.; Yamamoto, H. *Synlett* **1991**, (8), 561-562.
11. (a) Costa, A. L.; Piazza, M. G.; Tagliavini, E.; Trombini, C.; Umani-Ronchi, A. *J. Am. Chem. Soc.* **1993**, *115* (15), 7001-7002; (b) Keck, G. E.; Tarbet, K. H.; Geraci, L. S. *J. Am. Chem. Soc.* **1993**, *115* (18), 8467-8468.
12. Denmark, S. E.; Coe, D. M.; Pratt, N. E.; Griedel, B. D. *J. Org. Chem.* **1994**, *59* (21), 6161-6163.
13. Denmark, S. E.; Fu, J. *Chem. Rev.* **2003**, *103* (8), 2763-2794.
14. (a) Akiyama, T. *Chem. Rev.* **2007**, *107* (12), 5744-5758; (b) Doyle, A. G.; Jacobsen, E. N. *Chem. Rev.* **2007**, *107* (12), 5713-5743; (c) Terada, M. *Chem. Commun.* **2008**, (35), 4097-4112.
15. Overvoorde, L. M.; Grayson, M. N.; Luo, Y.; Goodman, J. M. *J. Org. Chem.* **2015**, *80* (5), 2634-2640.
16. Kim, I. S.; Ngai, M.-Y.; Krische, M. J. *J. Am. Chem. Soc.* **2008**, *130* (20), 6340-6341.
17. Hartwig, J. F.; Stanley, L. M. *Acc. Chem. Res.* **2010**, *43* (12), 1461-1475.
18. Dechert-Schmitt, A.-M. R.; Schmitt, D. C.; Krische, M. J. *Angew. Chem. Int. Ed.* **2013**, *52* (11), 3195-3198.
19. (a) Harada, T.; Sakamoto, K.; Ikemura, Y.; Oku, A. *Tetrahedron Lett.* **1988**, *29* (25), 3097-3100; (b) Hoffmann, R. W.; Kahrs, B. C. *Tetrahedron Lett.* **1996**, *37* (26), 4479-4482; (c) Hoye, T.; Kopel, L.; Ryba, T. *Synthesis* **2006**, *2006* (10), 1572-1574.
20. Rychnovsky, S. D.; Griesgraber, G.; Zeller, S.; Skalitzky, D. J. *J. Org. Chem.* **1991**, *56* (17), 5161-5169.
21. Maehr, H.; Yang, R.; Hong, L. N.; Liu, C. M.; Hatada, M. H.; Todaro, L. J. *J. Org. Chem.* **1989**, *54* (16), 3816-3819.
22. Han, S. B.; Hassan, A.; Kim, I. S.; Krische, M. J. *J. Am. Chem. Soc.* **2010**, *132* (44), 15559-15561.

23. (a) Kamiyama, T.; Umino, T.; Fujisaki, N.; Satoh, T.; Yamashita, Y.; Ohshima, S.; Watanabe, J.; Yokose, K. *J. Antibiot.* **1993**, (46), 1039; (b) Kamiyama, T.; Itezono, Y.; Umino, T.; Satoh, T.; Nakayama, N.; Yokose, K. *J. Antibiot.* **1993**, *46*, 1047; (c) Kobayashi, Y.; Czechtizky, W.; Kishi, Y. *Org. Lett.* **2003**, *5* (1), 93-96.
24. Pawlak, J.; Nakanishi, K.; Iwashita, T.; Borowski, E. *J. Org. Chem.* **1987**, *52* (13), 2896-2901.
25. (a) Satoh, T.; Yamashita, Y.; Kamiyama, T.; Arisawa, M. *Thromb. Res.* **1993**, *72*; (b) Satoh, T.; Kouns, W. C.; Yamashita, Y.; Kamiyama, T.; Steiner, B. *Biochem. J.* **1994**, *301 (Pt 3)* (3), 785-791; (c) Satoh, T.; Kouns, W. C.; Yamashita, Y.; Kamiyama, T.; Steiner, B. *Biochem. Biophys. Res. Commun.* **1994**, *204* (1), 325-332.
26. Kumpulainen, E. T. T.; Kang, B.; Krische, M. J. *Org. Lett.* **2011**, *13* (9), 2484-2487.
27. (a) Pettit, G. R.; Herald, C. L.; Doubek, D. L.; Herald, D. L.; Arnold, E.; Clardy, J. *J. Am. Chem. Soc.* **1982**, *104* (24), 6846-6848; (b) Sudek, S.; Lopanik, N. B.; Waggoner, L. E.; Hildebrand, M.; Anderson, C.; Liu, H.; Patel, A.; Sherman, D. H.; Haygood, M. G. *J. Nat. Prod.* **2007**, *70* (1), 67-74.
28. (a) Hale, K. J.; Hummersone, M. G.; Manaviazar, S.; Frigerio, M. *Nat. Prod. Rep.* **2002**, *19* (4), 413-453; (b) Kortmansky, J.; Schwartz, G. K. *Cancer Invest.* **2003**, *21* (6), 924-936.
29. (a) Etcheberrigaray, R.; Tan, M.; Dewachter, I.; Kuiperi, C.; Van der Auwera, I.; Wera, S.; Qiao, L.; Bank, B.; Nelson, T. J.; Kozikowski, A. P.; Van Leuven, F.; Alkon, D. L. *Proc. Natl. Acad. Sci. USA* **2004**, *101* (30), 11141-11146; (b) Alkon, D. L.; Sun, M. K.; Nelson, T. J. *Trends Pharmacol. Sci.* **2007**, *28* (2), 51-60.
30. Sun, M.-K.; Hongpaisan, J.; Nelson, T. J.; Alkon, D. L. *Proc. Natl. Acad. Sci. USA* **2008**, *105*.
31. (a) Alkon, D. L.; Epstein, H.; Kuzirian, A.; Bennett, M. C.; Nelson, T. J. *Proc. Natl. Acad. Sci. USA* **2005**, *2005* (102); (b) Sun, M.-K.; Alkon, D. L. *Eur. J. Pharmacol.* **2005**, *512*.
32. (a) Patman, R. L.; Bower, J. F.; Kim, I. S.; Krische, M. J. *Aldrichimica Acta* **2008**, *41*; (b) Bower, J. F.; Krische, M. J. *Top. Organomet. Chem.* **2011**, *43*.
33. Lu, Y.; Woo, S. K.; Krische, M. J. *J. Am. Chem. Soc.* **2011**, *133* (35), 13876-13879.
34. Wright, A. E.; Botelho, J. C.; Guzmán, E.; Harmody, D.; Linley, P.; McCarthy, P. J.; Pitts, T. P.; Pomponi, S. A.; Reed, J. K. *J. Nat. Prod.* **2007**, *70* (3), 412-416.
35. Yang, Z.; Zhang, B.; Zhao, G.; Yang, J.; Xie, X.; She, X. *Org. Lett.* **2011**, *13* (21), 5916-5919.
36. Sikorska, J.; Hau, A. M.; Anklin, C.; Parker-Nance, S.; Davies-Coleman, M. T.; Ishmael, J. E.; McPhail, K. L. *J. Org. Chem.* **2012**, *77* (14), 6066-6075.
37. Willwacher, J.; Fürstner, A. *Angew. Chem. Int. Ed.* **2014**, *53* (16), 4217-4221.
38. Willwacher, J.; Heggen, B.; Wirtz, C.; Thiel, W.; Fürstner, A. *Chem. Eur. J.* **2015**, *21* (29), 10416-10430.

39. Fatima, A.; Kohn, L. K.; Carvalho, J. E.; Pilli, R. A. *Bioorg. Med. Chem.* **2006**, *14* (3), 622-631.
40. Momani, F. A.; Alkofahi, A. S.; Mhaidat, N. M. *Molecules* **2011**, *16*.
41. Cardona, W.; Quinones, W.; Echeverri, F. *Molecules* **2005**, *9*.
42. Jaiswal, M.; Mishra, B.; S., M. N.; Moorthy, H. N. *Asian J. Chem.* **2007**, *19*.
43. Li, H.; Tatlock, J.; Linton, A.; Gonzalez, J.; Jewell, T.; Patel, L.; Ludlum, S.; Drowns, M.; Rahavendran, S. V.; Skor, H.; Hunter, R.; Shi, S. T.; Herlihy, K. J.; Parge, H.; Hickey, M.; Yu, X.; Chau, F.; Nonomiya, J.; Lewis, C. *J. Med. Chem.* **2009**, *52* (5), 1255-1258.
44. Wang, J.; Zhao, B.; Zhang, W.; Wu, X.; Wang, R.; Huang, Y.; Chen, D.; Park, K.; Weimer, B. C.; Shen, Y. *Bioorg. Med. Chem. Lett.* **2010**, *20* (23), 7054-7058.
45. de Souza, L. C.; dos Santos, A. F.; Sant'Ana, A. E.; de Oliveira Imbroisi, D. *Bioorg. Med. Chem.* **2004**, *12* (5), 865-869.
46. Drewes, S. E.; Horn, M. M.; Saroja Wijewardene, C. *Phytochemistry* **1996**, *41* (1), 333-334.
47. Novaes, L. F. T.; Sarotti, A. M.; Pilli, R. A. *RSC Adv.* **2015**, *5* (66), 53471-53476.
48. Novaes, L. F. T.; Sarotti, A. M.; Pilli, R. A. *J. Org. Chem.* **2015**, *80* (24), 12027-12037.
49. Cavalheiro, A. J.; Yoshida, M. *Phytochemistry* **2000**, *53* (7), 811-819.
50. (a) Yus, M.; González-Gómez, J. C.; Foubelo, F. *Chem. Rev.* **2011**, *111* (12), 7774-7854; (b) Yus, M.; Gonzalez-Gomez, J. C.; Foubelo, F. *Chem. Rev.* **2013**, *113* (7), 5595-5698; (c) Yamamoto, Y.; Asao, N. *Chem. Rev.* **1993**, *93* (6), 2207-2293; (d) Ramachandran, P. V. *Aldrichimica Acta* **2002**, *35* (1), 23-35; (e) Kennedy, J. W. J.; Hall, D. G. *Angew. Chem. Int. Ed.* **2003**, *42* (39), 4732-4739; (f) Marek, I.; Sklute, G. *Chem. Commun.* **2007**, (17), 1683-1691; (g) Hall, D. *Synlett* **2007**, *2007* (11), 1644-1655; (h) Leighton, J. L. *Aldrichimica Acta* **2010**, *43* (1), 3-12.
51. Kim, I. S.; Han, S. B.; Krische, M. J. *J. Am. Chem. Soc.* **2009**, *131* (7), 2514-2520.
52. Zbieg, J. R.; Fukuzumi, T.; Krische, M. J. *Adv. Synth. Catal.* **2010**, *352* (14-15), 2416-2420.
53. (a) Shibahara, F.; Bower, J. F.; Krische, M. J. *J. Am. Chem. Soc.* **2008**, *130* (20), 6338-6339; (b) Zbieg, J. R.; Moran, J.; Krische, M. J. *J. Am. Chem. Soc.* **2011**, *133* (27), 10582-10586.
54. Zbieg, J. R.; Yamaguchi, E.; McInturff, E. L.; Krische, M. J. *Science* **2012**, *336* (6079), 324-327.
55. McInturff, E. L.; Yamaguchi, E.; Krische, M. J. *J. Am. Chem. Soc.* **2012**, *134* (51), 20628-20631.
56. Gao, X.; Han, H.; Krische, M. J. *J. Am. Chem. Soc.* **2011**, *133* (32), 12795-12800.
57. Pal, S. *Tetrahedron* **2006**, *62* (14), 3171-3200.
58. Gao, X.; Woo, S. K.; Krische, M. J. *J. Am. Chem. Soc.* **2013**, *135* (11), 4223-4226.

59. (a) Bernet, B.; Vasella, A. *Helv. Chim. Acta* **1979**, *62* (7), 2400-2410; (b) Bernet, B.; Vasella, A. *Helv. Chim. Acta* **1984**, *67* (5), 1328-1347.
60. (a) Jordan, M. A.; Wilson, L. *Nat. Rev. Cancer* **2004**, *4* (4), 253-265; (b) Dumontet, C.; Jordan, M. A. *Nat. Rev. Drug Discov.* **2010**, *9* (10), 790-803; (c) Rohena, C. C.; Mooberry, S. L. *Nat. Prod. Rep.* **2014**, *31* (3), 335-355.
61. (a) Spector, I.; Braet, F.; Shochet, N. R.; Bubb, M. R. *Microsc. Res. Tech.* **1999**, *47* (1), 18-37; (b) Yeung, K.-S.; Paterson, I. *Angew. Chem. Int. Ed.* **2002**, *41* (24), 4632-4653; (c) Giganti, A.; Friederich, E. *Prog. Cell Cycle Res.* **2003**, *5*, 511-525; (d) Kita, M.; Kigoshi, H. *Nat. Prod. Rep.* **2015**, *32* (4), 534-542.
62. Carmely, S.; Kashman, Y. *Tetrahedron Lett.* **1985**, *26* (4), 511-514.
63. Shin, I.; Krische, M. J. *Org. Lett.* **2015**, *17* (19), 4686-4689.
64. Nakamura, R.; Tanino, K.; Miyashita, M. *Org. Lett.* **2005**, *7* (14), 2929-2932.
65. GrÄFe, U.; Schade, W.; Roth, M.; Radics, L.; Incze, M.; UjszÁSzy, K. *J. Antibiot.* **1984**, *37* (8), 836-846.
66. (a) Brooks, H. A.; Gardner, D.; Poyser, J. P.; King, T. J. *J. Antibiot.* **1984**, *37* (11), 1501-1504; (b) Kevin Ii, D. A.; Meujo, D. A.; Hamann, M. T. *Expert Opin. Drug Discov.* **2009**, *4* (2), 109-146.
67. (a) Danishefsky, S. J.; Selnick, H. G.; DeNinno, M. P.; Zelle, R. E. *J. Am. Chem. Soc.* **1987**, *109* (5), 1572-1574; (b) Danishefsky, S. J.; Selnick, H. G.; Zelle, R. E.; DeNinno, M. P. *J. Am. Chem. Soc.* **1988**, *110* (13), 4368-4378; (c) Defosseux, M.; Blanchard, N.; Meyer, C.; Cossy, J. *Org. Lett.* **2003**, *5* (22), 4037-4040; (d) Defosseux, M.; Blanchard, N.; Meyer, C.; Cossy, J. *J. Org. Chem.* **2004**, *69* (14), 4626-4647; (e) Cossy, J.; Meyer, C.; Defosseux, M.; Blanchard, N. *Pure Appl. Chem.* **2005**, *77* (7); (f) Komatsu, K.; Tanino, K.; Miyashita, M. *Angew. Chem. Int. Ed.* **2004**, *43* (33), 4341-4345; (g) Harrison, T. J.; Ho, S.; Leighton, J. L. *J. Am. Chem. Soc.* **2011**, *133* (19), 7308-7311; (h) Godin, F.; Mochirian, P.; St-Pierre, G.; Guindon, Y. *Tetrahedron* **2015**, *71* (4), 709-726.
68. Kasun, Z. A.; Gao, X.; Lipinski, R. M.; Krische, M. J. *J. Am. Chem. Soc.* **2015**, *137* (28), 8900-8903.
69. Katsuki, T.; Sharpless, K. B. *J. Am. Chem. Soc.* **1980**, *102* (18), 5974-5976.
70. Gilman, H.; Jones, R. G.; Woods, L. A. *J. Org. Chem.* **1952**, *17* (12), 1630-1634.
71. Kranenburg, M.; van der Burgt, Y. E. M.; Kamer, P. C. J.; van Leeuwen, P. W. N. M.; Goubitz, K.; Fraanje, J. *Organometallics* **1995**, *14* (6), 3081-3089.
72. Cragg, G. M.; Newman, D. J.; Snader, K. M. *J. Nat. Prod.* **1997**, *60* (1), 52-60.
73. Newman, D. J. *J. Med. Chem.* **2008**, *51* (9), 2589-2599.
74. Cragg, G. M.; Grothaus, P. G.; Newman, D. J. *Chem. Rev.* **2009**, *109* (7), 3012-3043.
75. Rohr, J. *Angew. Chem. Int. Ed.* **2000**, *39* (16), 2847-2849.
76. Sait, M.; Hugenholtz, P.; Janssen, P. H. *Environ. Microbiol.* **2002**, *4* (11), 654-666.
77. Aktar, M. W.; Sengupta, D.; Chowdhury, A. *Interdiscip. Toxicol.* **2009**, *2* (1), 1-12.

78. Steinmann, P.; Keiser, J.; Bos, R.; Tanner, M.; Utzinger, J. *Lancet Infect. Dis.* **2006**, *6* (7), 411-425.
79. Thetiot-Laurent, S. A.; Boissier, J.; Robert, A.; Meunier, B. *Angew. Chem. Int. Ed.* **2013**, *52* (31), 7936-7956.
80. Ribeiro, K. A.; de Carvalho, C. M.; Molina, M. T.; Lima, E. P.; Lopez-Montero, E.; Reys, J. R.; de Oliveira, M. B.; Pinto, A. V.; Santana, A. E.; Goulart, M. O. *Acta Trop.* **2009**, *111* (1), 44-50.
81. Pereira, A. R.; McCue, C. F.; Gerwick, W. H. *J. Nat. Prod.* **2010**, *73* (2), 217-220.
82. Hostettmann, K.; Kizu, H.; Tomimori, T. *Planta Med.* **1982**, *44* (1), 34-35.
83. (a) Rao, M. R.; Faulkner, D. J. *J. Nat. Prod.* **2002**, *65* (3), 386-388; (b) Erickson, K. L.; Gustafson, K. R.; Pannell, L. K.; Beutler, J. A.; Boyd, M. R. *J. Nat. Prod.* **2002**, *65* (9), 1303-1306.
84. Kim, H.; Hong, J. *Org. Lett.* **2010**, *12* (12), 2880-2883.
85. (a) Taylor, E. C.; LaMattina, J. L. *Tetrahedron Lett.* **1977**, *18* (24), 2077-2080; (b) Armesto, D.; Horspool, W. M.; Gallego, M. G.; Agarrabeitia, A. R. *J. Chem. Soc., Perkin Trans. 1* **1992**, (1), 163-169.
86. Shiina, I.; Kubota, M.; Oshiumi, H.; Hashizume, M. *J. Org. Chem.* **2004**, *69* (6), 1822-1830.
87. Barry, C. S.; Bushby, N.; Charmant, J. P.; Elsworth, J. D.; Harding, J. R.; Willis, C. L. *Chem. Commun.* **2005**, (40), 5097-5099.
88. Hajare, A. K.; Ravikumar, V.; Khaleel, S.; Bhuniya, D.; Reddy, D. S. *J. Org. Chem.* **2011**, *76* (3), 963-966.
89. Ball, M.; Baron, A.; Bradshaw, B.; Omori, H.; MacCormick, S.; Thomas, E. J. *Tetrahedron Lett.* **2004**, *45* (47), 8737-8740.
90. Inanaga, J.; Hirata, K.; Saeki, H.; Katsuki, T.; Yamaguchi, M. *Bull. Chem. Soc. Jpn.* **1979**, *52* (7), 1989-1993.
91. Yang, Z.; Xie, X.; Jing, P.; Zhao, G.; Zheng, J.; Zhao, C.; She, X. *Org. Biomol. Chem.* **2011**, *9* (4), 984-986.
92. Pabbaraja, S.; Satyanarayana, K.; Ganganna, B.; Yadav, J. S. *J. Org. Chem.* **2011**, *76* (6), 1922-1925.
93. Gesinski, M. R.; Rychnovsky, S. D. *J. Am. Chem. Soc.* **2011**, *133* (25), 9727-9729.
94. Sharpe, R. J.; Jennings, M. P. *J. Org. Chem.* **2011**, *76* (19), 8027-8032.
95. Gaich, T.; Baran, P. S. *J. Org. Chem.* **2010**, *75* (14), 4657-4673.
96. Dechert-Schmitt, A. M.; Schmitt, D. C.; Gao, X.; Itoh, T.; Krische, M. J. *Nat. Prod. Rep.* **2014**, *31* (4), 504-513.
97. Hendrickson, J. B. *J. Am. Chem. Soc.* **1975**, *97* (20), 5784-5800.
98. Trost, B. M. *Science* **1991**, *254* (5037), 1471-1477.
99. Wender, P. A.; Miller, B. L. *Nature* **2009**, *460* (7252), 197-201.
100. Burns, N. Z.; Baran, P. S.; Hoffmann, R. W. *Angew. Chem. Int. Ed.* **2009**, *48* (16), 2854-2867.
101. Waldeck, A. R.; Krische, M. J. *Angew. Chem. Int. Ed.* **2013**, *52* (16), 4470-4473.

102. Lu, Y.; Kim, I. S.; Hassan, A.; Del Valle, D. J.; Krische, M. J. *Angew. Chem. Int. Ed.* **2009**, *48* (27), 5018-5021.
103. Fuwa, H.; Noto, K.; Sasaki, M. *Org. Lett.* **2010**, *12* (7), 1636-1639.
104. Hong, S. H.; Wenzel, A. G.; Salguero, T. T.; Day, M. W.; Grubbs, R. H. *J. Am. Chem. Soc.* **2007**, *129* (25), 7961-7968.
105. (a) Evans, D. A.; Dart, M. J.; Duffy, J. L. *Tetrahedron Lett.* **1994**, *35* (46), 8541-8544; (b) Evans, D. A.; Allison, B. D.; Yang, M. G.; Masse, C. E. *J. Am. Chem. Soc.* **2001**, *123* (44), 10840-10852.
106. Travis, B. R.; Narayan, R. S.; Borhan, B. *J. Am. Chem. Soc.* **2002**, *124* (15), 3824-3825.
107. Gemal, A. L.; Luche, J. L. *J. Am. Chem. Soc.* **1981**, *103* (18), 5454-5459.
108. Corey, E. J.; Becker, K. R.; Varma, R. K. *J. Am. Chem. Soc.* **1972**, *94* (24), 8616-8618.
109. Srikrishna, A.; Krishnan, K. *Tetrahedron Lett.* **1989**, *30* (47), 6577-6580.
110. (a) Jang, H. Y.; Krische, M. J. *Acc. Chem. Res.* **2004**, *37* (9), 653-661; (b) Bower, J. F.; Kim, I. S.; Patman, R. L.; Krische, M. J. *Angew. Chem. Int. Ed.* **2009**, *48* (1), 34-46; (c) Hassan, A.; Krische, M. J. *Org. Process Res. Dev.* **2011**, *15* (6), 1236-1242.
111. Galan, B. R.; Kalbarczyk, K. P.; Szczepankiewicz, S.; Keister, J. B.; Diver, S. T. *Org. Lett.* **2007**, *9* (7), 1203-1206.
112. Mochly-Rosen, D.; Das, K.; Grimes, K. V. *Nat. Rev. Drug Discov.* **2012**, *11* (12), 937-957.
113. (a) Zhang, D.; Anantharam, V.; Kanthasamy, A.; Kanthasamy, A. G. *J. Pharmacol. Exp. Ther.* **2007**, *322* (3), 913-922; (b) Burguillos, M. A.; Deierborg, T.; Kavanagh, E.; Persson, A.; Hajji, N.; Garcia-Quintanilla, A.; Cano, J.; Brundin, P.; Englund, E.; Venero, J. L.; Joseph, B. *Nature* **2011**, *472* (7343), 319-324.
114. Garrido, J. L.; Godoy, J. A.; Alvarez, A.; Bronfman, M.; Inestrosa, N. C. *FASEB J.* **2002**, *16* (14), 1982-1984.
115. Inagaki, K.; Churchill, E.; Mochly-Rosen, D. *Cardiovasc. Res.* **2006**, *70* (2), 222-230.
116. Totoń, E. I., Ewa; Skrzecekowska, Karolina; Rybczyńska, Maria *Pharmacol. Rep.* **2011**, *63*, 19-29.
117. (a) Watanabe, R.; Wei, L.; Huang, J. *J. Nucl. Med.* **2011**, *52* (4), 497-500; (b) Cheng, J. Q.; Lindsley, C. W.; Cheng, G. Z.; Yang, H.; Nicosia, S. V. *Oncogene* **2005**, *24* (50), 7482-7492.
118. Schmid, T.; Jansen, A. P.; Baker, A. R.; Hegamyer, G.; Hagan, J. P.; Colburn, N. H. *Cancer Res.* **2008**, *68* (5), 1254-1260.
119. Yang, H. S.; Jansen, A. P.; Nair, R.; Shibahara, K.; Verma, A. K.; Cmarik, J. L.; Colburn, N. H. *Oncogene* **2001**, *20* (6), 669-676.
120. Yang, H. S.; Jansen, A. P.; Komar, A. A.; Zheng, X. J.; Merrick, W. C.; Costes, S.; Lockett, S. J.; Sonenberg, N.; Colburn, N. H. *Mol. Cell. Biol.* **2003**, *23* (1), 26-37.

121. Leupold, J. H.; Yang, H. S.; Colburn, N. H.; Asangani, I.; Post, S.; Allgayer, H. *Oncogene* **2007**, *26* (31), 4550-4562.
122. Nieves-Alicea, R.; Colburn, N. H.; Simeone, A. M.; Tari, A. M. *Breast Cancer Res. Treat.* **2009**, *114* (2), 203-209.
123. Dorrello, N. V.; Peschiaroli, A.; Guardavaccaro, D.; Colburn, N. H.; Sherman, N. E.; Pagano, M. *Science* **2006**, *314* (5798), 467-471.
124. Blees, J. S.; Schmid, T.; Thomas, C. L.; Baker, A. R.; Benson, L.; Evans, J. R.; Goncharova, E. I.; Colburn, N. H.; McMahon, J. B.; Henrich, C. J. *J. Biomol. Screen.* **2010**, *15* (1), 21-29.
125. Grkovic, T.; Blees, J. S.; Colburn, N. H.; Schmid, T.; Thomas, C. L.; Henrich, C. J.; McMahon, J. B.; Gustafson, K. R. *J. Nat. Prod.* **2011**, *74* (5), 1015-1020.
126. Snatzke, G. *Angew. Chem. Int. Ed.* **1968**, *7* (1), 14-25.
127. (a) Kobayashi, Y.; Tan, C. H.; Kishi, Y. *Helv. Chim. Acta* **2000**, *83* (9), 2562-2571; (b) Higashibayashi, S.; Czechtizky, W.; Kobayashi, Y.; Kishi, Y. *J. Am. Chem. Soc.* **2003**, *125* (47), 14379-14393.
128. Wang, Y.; O'Doherty, G. A. *J. Am. Chem. Soc.* **2013**, *135* (25), 9334-9337.
129. (a) Reddy, D. S.; Mohapatra, D. K. *Eur. J. Org. Chem.* **2013**, *2013* (6), 1051-1057; (b) Dias, L. C.; Kuroishi, P. K.; de Lucca, E. C., Jr. *Org. Biomol. Chem.* **2015**, *13* (12), 3575-3584; (c) Brun, E.; Bellosta, V.; Cossy, J. *J. Org. Chem.* **2015**, *80* (17), 8668-8676.
130. Hanawa, H.; Hashimoto, T.; Maruoka, K. *J. Am. Chem. Soc.* **2003**, *125* (7), 1708-1709.
131. Evans, D. A.; Gauchetprunet, J. A. *J. Org. Chem.* **1993**, *58* (9), 2446-2453.
132. Kubota, K.; Leighton, J. L. *Angew. Chem. Int. Ed.* **2003**, *42* (8), 946-948.
133. Shenvi, R. A.; O'Malley, D. P.; Baran, P. S. *Acc. Chem. Res.* **2009**, *42* (4), 530-541.
134. Lee, D.; Williamson, C. L.; Chan, L.; Taylor, M. S. *J. Am. Chem. Soc.* **2012**, *134* (19), 8260-8267.
135. (a) Dias, L. C.; de Marchi, A. A.; Ferreira, M. A.; Aguilar, A. M. *Org. Lett.* **2007**, *9* (23), 4869-4872; (b) Dias, L. C.; de Marchi, A. A.; Ferreira, M. A.; Aguilar, A. M. *J. Org. Chem.* **2008**, *73* (16), 6299-6311.
136. (a) Denmark, S. E.; Fujimori, S. *Synlett* **2001**, 1024-1029; (b) Denmark, S. E.; Fujimori, S. *Org. Lett.* **2002**, *4* (20), 3477-3480; (c) Denmark, S. E.; Fujimori, S.; Pham, S. M. *J. Org. Chem.* **2005**, *70* (26), 10823-10840.
137. Samojlowicz, C.; Bieniek, M.; Pazio, A.; Makal, A.; Wozniak, K.; Poater, A.; Cavallo, L.; Wojcik, J.; Zdanowski, K.; Grela, K. *Chemistry* **2011**, *17* (46), 12981-12993.
138. (a) Michel, B. W.; Camelio, A. M.; Cornell, C. N.; Sigman, M. S. *J. Am. Chem. Soc.* **2009**, *131* (17), 6076-6077; (b) McCombs, J. R.; Michel, B. W.; Sigman, M. S. *J. Org. Chem.* **2011**, *76* (9), 3609-3613; (c) Michel, B. W.; Steffens, L. D.; Sigman, M. S. *J. Am. Chem. Soc.* **2011**, *133* (21), 8317-8325.
139. (a) Paterson, I.; Gibson, K. R.; Oballa, R. M. *Tetrahedron Lett.* **1996**, *37* (47), 8585-8588; (b) Evans, D. A.; Coleman, P. J.; Cote, B. *J. Org. Chem.* **1997**, *62* (4),

788-789; (c) Evans, D. A.; Cote, B.; Coleman, P. J.; Connell, B. T. *J. Am. Chem. Soc.* **2003**, *125* (36), 10893-10898; (d) Stocker, B. L.; Teesdale-Spittle, P.; Hoberg, J. O. *Eur. J. Org. Chem.* **2004**, *2004* (2), 330-336.
140. Jung, M. E.; Koch, P. *Tetrahedron Lett.* **2011**, *52* (46), 6051-6054.
141. (a) Lewis, B.; Chase, C.; Fang, F.; Wilkie, G.; Schnaderbeck, M.; Zhu, X. *Synlett* **2013**, *24* (03), 323-326; (b) Chase, C.; Austad, B.; Benayoud, F.; Calkins, T.; Campagna, S.; Choi, H.-w.; Christ, W.; Costanzo, R.; Cutter, J.; Endo, A.; Fang, F.; Hu, Y.; Lewis, B.; Lewis, M.; McKenna, S.; Noland, T.; Orr, J.; Pesant, M.; Schnaderbeck, M.; Wilkie, G.; Abe, T.; Asai, N.; Asai, Y.; Kayano, A.; Kimoto, Y.; Komatsu, Y.; Kubota, M.; Kuroda, H.; Mizuno, M.; Nakamura, T.; Omae, T.; Ozeki, N.; Suzuki, T.; Takigawa, T.; Watanabe, T.; Yoshizawa, K. *Synlett* **2013**, *24* (03), 327-332; (c) Fang, F.; Austad, B.; Calkins, T.; Chase, C.; Horstmann, T.; Hu, Y.; Lewis, B.; Niu, X.; Noland, T.; Orr, J.; Schnaderbeck, M.; Zhang, H.; Asakawa, N.; Asai, N.; Chiba, H.; Hasebe, T.; Hoshino, Y.; Ishizuka, H.; Kajima, T.; Kayano, A.; Komatsu, Y.; Kubota, M.; Kuroda, H.; Miyazawa, M.; Tagami, K.; Watanabe, T. *Synlett* **2013**, *24* (03), 333-337.
142. Liang, T.; Zhang, W.; Chen, T.-Y.; Nguyen, K. D.; Krische, M. J. *J. Am. Chem. Soc.* **2015**, *137* (40), 13066-13071.
143. (a) Patman, R. L.; Chaulagain, M. R.; Williams, V. M.; Krische, M. J. *J. Am. Chem. Soc.* **2009**, *131* (6), 2066-2067; (b) Leung, J. C.; Patman, R. L.; Sam, B.; Krische, M. J. *Chem. Eur. J.* **2011**, *17* (44), 12437-12443.
144. (a) Patman, R. L.; Williams, V. M.; Bower, J. F.; Krische, M. J. *Angew. Chem. Int. Ed.* **2008**, *47* (28), 5220-5223; (b) Geary, L. M.; Leung, J. C.; Krische, M. J. *Chem. Eur. J.* **2012**, *18* (52), 16823-16827.
145. (a) Itoh, J.; Han, S. B.; Krische, M. J. *Angew. Chem. Int. Ed.* **2009**, *48* (34), 6313-6316; (b) Grant, C. D.; Krische, M. J. *Org. Lett.* **2009**, *11* (20), 4485-4487.
146. (a) Pingen, D.; Müller, C.; Vogt, D. *Angew. Chem. Int. Ed.* **2010**, *49* (44), 8130-8133; (b) Bähn, S.; Tillack, A.; Imm, S.; Mevius, K.; Michalik, D.; Hollmann, D.; Neubert, L.; Beller, M. *ChemSusChem* **2009**, *2* (6), 551-557; (c) Johnson, T. C.; Totty, W. G.; Wills, M. *Org. Lett.* **2012**, *14* (20), 5230-5233.
147. Zhang, M.; Imm, S.; Bähn, S.; Neumann, H.; Beller, M. *Angew. Chem. Int. Ed.* **2011**, *50* (47), 11197-11201.
148. (a) Chatani, N.; Tobisu, M.; Asaumi, T.; Fukumoto, Y.; Murai, S. *J. Am. Chem. Soc.* **1999**, *121* (30), 7160-7161; (b) Tobisu, M.; Chatani, N.; Asaumi, T.; Amako, K.; Ie, Y.; Fukumoto, Y.; Murai, S. *J. Am. Chem. Soc.* **2000**, *122* (51), 12663-12674.
149. Leung, J. C.; Geary, L. M.; Chen, T.-Y.; Zbieg, J. R.; Krische, M. J. *J. Am. Chem. Soc.* **2012**, *134* (38), 15700-15703.
150. Geary, L. M.; Glasspoole, B. W.; Kim, M. M.; Krische, M. J. *J. Am. Chem. Soc.* **2013**, *135* (10), 3796-3799.
151. Yamaguchi, E.; Mowat, J.; Luong, T.; Krische, M. J. *Angew. Chem. Int. Ed.* **2013**, *52* (32), 8428-8431.

152. (a) Dohi, T.; Takenaga, N.; Nakae, T.; Toyoda, Y.; Yamasaki, M.; Shiro, M.; Fujioka, H.; Maruyama, A.; Kita, Y. *J. Am. Chem. Soc.* **2013**, *135* (11), 4558-4566; (b) Uyanik, M.; Yasui, T.; Ishihara, K. *Tetrahedron* **2010**, *66* (31), 5841-5851; (c) Cox, C.; Danishefsky, S. J. *Org. Lett.* **2000**, *2* (22), 3493-3496; (d) Tamura, Y.; Yakura, T.; Haruta, J.; Kita, Y. *J. Org. Chem.* **1987**, *52* (17), 3927-3930.

153. (a) Curran, D. P.; Chen, M. H.; Spletzer, E.; Seong, C. M.; Chang, C. T. *J. Am. Chem. Soc.* **1989**, *111* (24), 8872-8878; (b) Zhang, W.; Pugh, G. *Tetrahedron Lett.* **2001**, *42* (33), 5617-5620; (c) Zhang, W. *Tetrahedron Lett.* **2000**, *41* (15), 2523-2527; (d) Merlic, C. A.; Walsh, J. C. *J. Org. Chem.* **2001**, *66* (7), 2265-2274; (e) Otsubo, K.; Inanaga, J.; Yamaguchi, M. *Tetrahedron Lett.* **1986**, *27* (47), 5763-5764; (f) Fukuzawa, S.-i.; Nakanishi, A.; Fujinami, T.; Sakai, S. *J. Chem. Soc., Chem. Commun.* **1986**, (8), 624-625; (g) Streuff, J. *Synthesis* **2013**, *45* (EFirst), 281-307.

154. (a) Mandal, A. K.; Jawalkar, D. G. *J. Org. Chem.* **1989**, *54* (10), 2364-2369; (b) Fujioka, H.; Matsuda, S.; Horai, M.; Fujii, E.; Morishita, M.; Nishiguchi, N.; Hata, K.; Kita, Y. *Chem. Eur. J.* **2007**, *13* (18), 5238-5248; (c) Faraj, H.; Claire, M.; Rondot, A.; Aumelas, A.; Auzou, G. *J. Chem. Soc., Perkin Trans. 1* **1990**, (11), 3045-3048; (d) Eipert, M.; Maichle-Mössmer, C.; Maier, M. E. *Tetrahedron* **2003**, *59* (40), 7949-7960; (e) Mandal, A. K.; Jawalkar, D. G. *Tetrahedron Lett.* **1986**, *27* (1), 99-100.

155. (a) Ye, W.; Cai, G.; Zhuang, Z.; Jia, X.; Zhai, H. *Org. Lett.* **2005**, *7* (17), 3769-3771; (b) Burstein, C.; Glorius, F. *Angew. Chem. Int. Ed.* **2004**, *43* (45), 6205-6208.

156. (a) Bigi, M. A.; Reed, S. A.; White, M. C. *Nat. Chem.* **2011**, *3* (3), 216-222; (b) Uyanik, M.; Suzuki, D.; Yasui, T.; Ishihara, K. *Angew. Chem. Int. Ed.* **2011**, *50* (23), 5331-5334.

157. (a) Choudhury, P. K.; Foubelo, F.; Yus, M. *Tetrahedron Lett.* **1998**, *39* (21), 3581-3584; (b) Csuk, R.; Glānzer, B. I.; Hu, Z.; Boese, R. *Tetrahedron* **1994**, *50* (4), 1111-1124; (c) Fouquet, E.; Gabriel, A.; Maillard, B.; Pereyre, M. *Tetrahedron Lett.* **1993**, *34* (48), 7749-7752; (d) RenĆsuk; Hua, Z.; Abdou, M.; Kratky, C. *Tetrahedron* **1991**, *47* (34), 7037-7044; (e) Machrouhi, F.; Namy, J.-L. *Tetrahedron* **1998**, *54* (37), 11111-11122; (f) Yves Michellys, P.; Pellissier, H.; Santelli, M. *Tetrahedron Lett.* **1993**, *34* (12), 1931-1934.

158. Xiong, H.; Rieke, R. D. *J. Org. Chem.* **1992**, *57* (26), 7007-7008.

159. Bartoli, A.; Rodier, F.; Commeiras, L.; Parrain, J.-L.; Chouraqui, G. *Nat. Prod. Rep.* **2011**, *28* (4), 763-782.

160. (a) Musashi, Y.; Sakaki, S. *J. Am. Chem. Soc.* **2002**, *124* (25), 7588-7603; (b) Ngai, M.-Y.; Barchuk, A.; Krische, M. J. *J. Am. Chem. Soc.* **2006**, *129* (2), 280-281.

161. Sanchez-Delgado, R. A.; Bradley, J. S.; Wilkinson, G. *J. Chem. Soc., Dalton Trans.* **1976**, (5), 399-404.

162. (a) Nishigaichi, Y.; Orimi, T.; Takuwa, A. *J. Organomet. Chem.* **2009**, *694* (24), 3837-3839; (b) Kang, S.-K.; Baik, T.-G.; Jiao, X.-H. *Synth. Commun.* **2002**, *32* (1), 75-78; (c) Gewald, R.; Kira, M.; Sakurai, H. *Synthesis* **1996**, *1996* (01), 111-115; (d) Ramachandran, P. V.; Rudd, M. T.; Burghardt, T. E.; Ram Reddy, M. V. *J. Org. Chem.* **2003**, *68* (24), 9310-9316; (e) Dhondi, P. K.; Carberry, P.; Choi, L. B.; Chisholm, J. D. *J. Org. Chem.* **2007**, *72* (25), 9590-9596; (f) Inaba, S.-i.; Rieke, R. D. *Synthesis* **1984**, *1984* (10), 844-845.
163. (a) Petrovskaia, O.; Taylor, B. M.; Hauze, D. B.; Carroll, P. J.; Joullié, M. M. *J. Org. Chem.* **2001**, *66* (23), 7666-7675; (b) Vanden Eynden, M. J.; Kunchithapatham, K.; Stambuli, J. P. *J. Org. Chem.* **2010**, *75* (24), 8542-8549; (c) Fatiadi, A. J. *Synthesis* **1978**, *1978* (03), 165-204; (d) Nieminen, V.; Taskinen, A.; Hotokka, M.; Murzin, D. Y. *J. Catal.* **2007**, *245* (1), 228-236; (e) Busygin, I.; Rosenholm, M.; Toukoniitty, E.; Murzin, D. Y.; Leino, R. *Catal. Lett.* **2007**, *117* (3-4), 91-98.
164. Stockis, A.; Hoffmann, R. *J. Am. Chem. Soc.* **1980**, *102* (9), 2952-2962.
165. Nyhlén, J.; Privalov, T.; Bäckvall, J.-E. *Chem. Eur. J.* **2009**, *15* (21), 5220-5229.
166. Hayashi, M.; Terashima, S.; Koga, K. *Tetrahedron* **1981**, *37* (16), 2797-2803.
167. Lunardi, I.; Cazetta, T.; Conceição, G. J. A.; Moran, P. J. S.; Rodrigues, J. A. R. *Adv. Synth. Catal.* **2007**, *349* (6), 925-932.
168. Dakdouki, S. C.; Villemin, D.; Bar, N. *Eur. J. Org. Chem.* **2012**, *2012* (4), 780-784.
169. de Boer, J. W.; Browne, W. R.; Harutyunyan, S. R.; Bini, L.; Tiemersma-Wegman, T. D.; Alsters, P. L.; Hage, R.; Feringa, B. L. *Chem. Commun.* **2008**, (32), 3747-3749.
170. Hlasta, D. J.; Luttinger, D.; Perrone, M. H.; Silbernagel, M. J.; Ward, S. J.; Haubrich, D. R. *J. Med. Chem.* **1987**, *30* (9), 1555-1562.
171. Chiba, S.; Zhang, L.; Ang, G. Y.; Hui, B. W.-Q. *Org. Lett.* **2010**, *12* (9), 2052-2055.
172. Autrey, R. L.; Tahk, F. C. *Tetrahedron* **1967**, *23* (2), 901-917.
173. Still, W. C.; Kahn, M.; Mitra, A. *J. Org. Chem.* **1978**, *43* (14), 2923-2925.

Vita

Andrew R. Waldeck attended Lancaster Country Day School in Lancaster, Pennsylvania. Upon graduating, he attended the University of Vermont, Burlington, Vermont, where he conducted organic chemistry research under the supervision of Dr. A. Paul Krapcho. After the receiving the degrees of Bachelor of Science in Chemistry and Bachelor of Science in Mathematics from the University of Vermont in 2010, Andrew entered the graduate program at the University of Texas at Austin to study transition metal catalyzed reaction development and the total synthesis of natural products in the laboratory of Professor Michael J. Krische.

Permanent email: andrew.r.waldeck@gmail.com

This dissertation was typed by the author.